



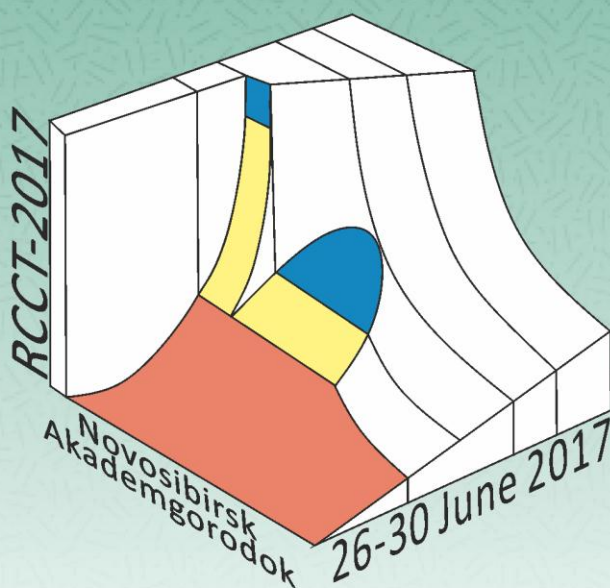
NIIC SB RAS

RCCT 2017

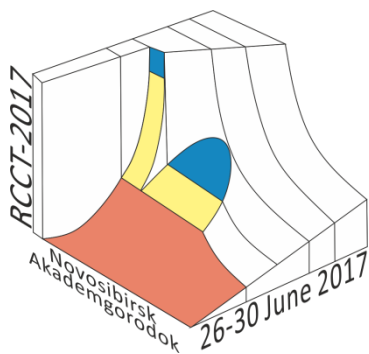
ABSTRACTS

XXI International Conference on Chemical
Thermodynamics in Russia

School-Conference on Chemical Thermodynamics
for Young Scientists



June 26-30, 2017,
Akademgorodok, Novosibirsk, Russia



**XXI International Conference
on Chemical Thermodynamics in Russia
(RCCT-2017)**

**School-Conference on Chemical Thermodynamics
for Young Scientists**

ABSTRACTS

June 26-30, 2017
Akademgorodok, Novosibirsk, Russia

Novosibirsk
2017

XXI International Conference on Chemical Thermodynamics in Russia (RCCT-2017) (June 26-30, 2017, Novosibirsk, Russia): Abstracts. – Novosibirsk: NIIC SB RAS, 2017. – 401 pp.

ISBN 978-5-90168-841-0

This book presents abstracts of the participants of the XXI International Conference on Chemical Thermodynamics in Russia (RCCT-2017). The conferences on chemical thermodynamics are among the largest conferences held in Russia since 1961. Till 1977 the conference was called "All-Union conference on calorimetry", further, till 1992 - "All-Union conference on calorimetry and chemical thermodynamics", then after a long break the tradition of holding the conference was revived in 2001.

At present the RCCT International Conferences take place every two years in various large Russian scientific centers such as Moscow, St. Petersburg, Nizhny Novgorod, Novosibirsk, Kazan, Samara and others. At present the RCCT International Conferences take place every two years in various large Russian scientific centers such as Moscow, St. Petersburg, Nizhny Novgorod, Novosibirsk, Kazan, Samara and others. Every RCCT is unique and significant event both for Russian and for world thermodynamic community as a whole. The conference traditionally covers all the aspects of chemical thermodynamics: from fundamental to applied areas, including multidisciplinary approaches and related areas of science. RCCT-2017 scientific program includes plenary and invited lectures, oral presentations, poster sessions and virtual contributions

Electronic version of the book can be found at:
<http://www.rcct2017.ru>

© NIIC SB RAS, 2017

Organizers

*Nikolaev Institute of Inorganic Chemistry,
Siberian Branch of Russian Academy of Sciences
Technopark of Novosibirsk Akademgorodok
Novosibirsk State University*



Nikolaev Institute of
Inorganic Chemistry
Siberian Branch of Russian
Academy of Sciences



N* Novosibirsk
State
University
***THE REAL SCIENCE**

Supporting organizations

*Russian Foundation for Basic Research
The Federal Agency for Scientific Organizations (FASO Russia)
Mendeleev Russian Chemical Society*



RUSSIAN
FOUNDATION
FOR BASIC
RESEARCH



FASO RUSSIA



Information support



Journal of Thermal Analysis and Calorimetry

Sponsors



NETZSCH



Organizing Committee

Co-Chairman **Anatoly I. Rusanov** (Academician of RAS, SPbSU, St. Petersburg)
Co-Chairman **Vladimir P. Fedin** (Corr-member of RAS, NIIC SB RAS, Novosibirsk)
Vice-Chairman **Konstantin S. Gavrichev** (D.Sci. (Chem.), IGIC RAS, Moscow)
Vice-Chairman **Nikolay V. Gelfond** (D.Sci. (Chem.), NIIC SB RAS, Novosibirsk)
Scientific secretary **Kseniya V. Zherikova** (PhD (Chem.), NIIC SB RAS, Novosibirsk)
Scientific secretary **Ludmila N. Zelenina** (PhD (Chem.), NIIC SB RAS, Novosibirsk)

Members of Organizing Committee

Gleb A. Abakumov, Academician of RAS, IOMC RAS, Nizhni Novgorod
Andrey S. Alikhanyan, D.Sci. (Chem.), IGIC RAS, Moscow
Mikhail F. Churbanov, Academician of RAS, ICHPS RAS, Nizhni Novgorod
Vladimir A. Durov, D.Sci. (Chem.), MSU, Moscow
Pavel P. Fedorov, D.Sci. (Chem.), GPI RAS, Moscow
Alexey A. Goryunkov, D.Sci. (Chem.), MSU, Moscow
Viktor V. Gusarov, Corr-member of RAS, SPbSTU, S.-Petersburg
Alexander B. Kaplun, D.Sci. (Tech.), IT SB RAS, Novosibirsk
Alexander V. Knyazev, D.Sci. (Chem.), NNSU, Nizhni Novgorod
Oskar I. Koifman, Corr-member of RAS, ISUCT, Ivanovo
Arkady M. Kolker, D.Sci. (Chem.), ISC RAS, Ivanovo
Oleg L. Kuskov, Corr-member of RAS, IGAC RAS, Moscow
Nikolay T. Kuznetsov, Academician of RAS, IGIC RAS, Moscow
Valery V. Lunin, Academician of RAS, MSU, Moscow
Andrey K. Lyashchenko, D.Sci. (Chem.), IGIC RAS, Moscow
Oleg V. Mikhailov, D.Sci. (Chem.), KSTU, Kazan
Vladimir M. Novotortsev, Academician of RAS, IGIC RAS, Moscow
Valentin N. Parmon, Academician of RAS, IC SB RAS, Novosibirsk
Andrey A. Pimerzin, D.Sci. (Chem.), SamSTU, Samara
Alexander K. Shchekin, Corr-member of RAS, SPbSU, S.-Petersburg
Natalia A. Smirnova, Corr-member of RAS, SPbSU, S.-Petersburg
Natalia N. Smirnova, D.Sci. (Chem.), NNSU, Nizhni Novgorod
Valentina L. Stolyarova, Corr-member of RAS, SPbSU, S.-Petersburg
Sergey V. Stankus, D.Sci. (Phys.-Math.), IT SB RAS, Novosibirsk
Alexander M. Toikka, D.Sci. (Chem.), SPbGU, Saint Petersburg
Aslan Yu. Tsivadze, Academician of RAS, IPCE RAS, Moscow
Vladimir M. Valyashko, D.Sci. (Chem.), IGIC RAS, Moscow
Alexey I. Viktorov, D.Sci. (Chem.), SPbSU, S.-Petersburg
Gennady F. Voronin, D.Sci. (Chem.), MSU, Moscow
Anatoliy G. Zakharov, D.Sci. (Chem.), ISC RAS, Ivanovo
Irina A. Zvereva, D.Sci. (Chem.), SPbSU, S.-Petersburg
Irina A. Uspenskaya D.Sci. (Chem.), MSU, Moscow
Andrey B. Yaroslavtsev, Corr-member of RAS, IGIC RAS, Moscow

Members of International Organizing Committee

Prof. Dr. Sergey P. Verevkin (Rostock, Germany)	Prof. Dr. Gabriele Sadowski (Dortmund, Germany)
Dr. Andrei Rotaru (Bucharest, Romania)	Prof. Dr. Li-Xian Sun (Guilin, China)
Dr. Juan Z. Dávalos (Madrid, Spain)	Prof. Joan Brennecke (Notre Dame, USA)
Prof. Dr. Edward Maginn (Notre Dame, USA)	Prof. Vahur Oja (Tallinn, Estonia)
Dr. Kenneth Kroenlein (Boulder, USA)	Prof. Dr. Fabrice Mutelet (Nancy, France)
Prof. John M. Simmie (Galway, Ireland)	Prof. James S. Chickos (Missouri, USA)
Prof. Dr. Christoph Schick (Rostock, Germany)	Prof. Dr. Rafiqul Gani (Kgs. Lyngby, Denmark)
Prof Joao A. P. Coutinho (Aveiro, Portugal)	Dr. Stefano Vecchio Cipriotti (Roma, Italy)
Prof. Dr. Deresh Ramjugernath (Durban, South Africa)	Prof. Dr.-Ing. Ralf Dohrn (Leverkusen, Germany)

Program Committee

Co-Chairmen: Konstantin S. Gavrichev, Nikolay V. Gelfond
Secretary: Kseniya V. Zherikova

Section 1. General problems of chemical thermodynamics

Chairman: Gennady F. Voronin
Section secretary: Ruslan E. Nikolaev
Nata I. Matskevich, Vladimir I. Belevantsev, Irina A. Uspenskaya

Section 2. Thermochemistry and databases

Chairman: Konstantin S. Gavrichev
Section secretary: Ludmila N. Zelenina
Tamara P. Chusova, Inga G. Vasilyeva, Irina A. Zvereva

Section 3. Thermodynamics of solutions and heterogeneous systems

Chairman: Arkady M. Kolker
Section secretary: Alexandr P. Ryzhikh
Konstantin A. Khaldoyanidi, Victor I. Kosyakov, Vladimir A. Shestakov

Section 4. Thermodynamics of surface phenomena and self-organization phenomena in fluid systems

Chairman: Alexander K. Shchekin
Section secretary: Ruslan E. Nikolaev
Vladimir V. Bakovets, Alexandr I. Bulavchenko

Section 5. Applied aspects of chemical thermodynamics

Chairman: Andrey A. Pimerzin
Section secretary: Alexandr P. Ryzhikh

Local Organizing Committee

Kseniya V. Zherikova	Igor Ilyin	Anatoliy Musikhin
Lyudmila M. Levchenko	Nataliya Nikolaeva	Dmitri Bonegardt
Ludmila N. Zelenina	Evgeniya Vikulova	Sergey Cherkasov
Mikhail Bespyatov	Ivan Cherniaikin	Ksenya Karakovskaya
Tatyana Kokina	Daria Kliamer	Svetlana Mosyagina
Natalia Kuratieva	Anna Nazarova	Artem Shushanyan

Contacts of Organizing Committee:

Nikolaev Institute of Inorganic Chemistry, SB RAS
3, Acad. Lavrentiev Ave.
630090 Novosibirsk, Russia
Kseniya V. Zherikova
Phone: +7(383)316-55-34
Fax: +7(383)330-94-89
E-Mail: rcct2017@yandex.ru
Website: <http://www.rcct2017.ru>



Table of content

Plenary lectures.	8
Invited lectures.	21
Lectures of the School-conference on chemical thermodynamics for young scientists.	36
Sponsor.	40
Section 1. General problems of chemical thermodynamics	
Oral presentations.	41
Poster presentations.	59
Virtual presentations.	75
Section 2. Thermochemistry and databases	
Oral presentations.	90
Poster presentations.	116
Virtual presentations.	175
Section 3. Thermodynamics of solutions and heterogeneous systems	
Oral presentations.	206
Poster presentations.	228
Virtual presentations.	258
Section 4. Thermodynamics of surface phenomena and self-organization phenomena in fluid systems	
Oral presentations.	314
Poster presentations.	329
Virtual presentations.	347
Section 5. Applied aspects of chemical thermodynamics	
Oral presentations.	357
Poster presentations.	369
Virtual presentations.	389



XXI International Conference on Chemical Thermodynamics in Russia (RCCT-2017)

26-30 June 2017, Akademgorodok, Novosibirsk

Plenary lectures



THOUGHTS ABOUT THERMODYNAMICS

Atkins P.

University of Oxford, UK

E-mail: peter.atkins001@btinternet.com

Elementary thermodynamics is so well established that there is perhaps little to discover and even less to consider when instructing our students. But is that really true? In this lecture I shall explore aspects of thermodynamics that remain interesting and which open up deep questions about this mature subject and which could lie in the back of our minds when teaching our students. There are deep questions to explore, such as why the laws of thermodynamics are valid. Why, for instance, is energy conserved? Why does entropy increase? There are fascinating analogies, such as those between temperature and time that might reveal deep truths about the fabric of reality. What happens when systems of interest are so small that fluctuations dominate the most probable values? What are the origins of the fundamental constants that characterize thermodynamics, such as Boltzmann's constant and the gas constant? Did the originators of thermodynamics introduce unnecessary complications when formulating, for instance, the concept and measurement of temperature? What are the thermodynamic properties of the electromagnetic field: how is the Sun capable of driving processes on Earth? I shall explore these thoughts: they do not really open up revisions of elementary thermodynamics, but show that by reflecting on elementary principles, deep questions arise and can stimulate how we teach and encourage our students to become questioning scientists.



APPLICATION OF LATTICE CLUSTER THEORY TO POLYMER PHASE AND INTERFACIAL BEHAVIOR

Enders S.

Institute of Technical Thermodynamics and Refrigeration Engineering, Karlsruhe Institute of Technology, D-76131 Karlsruhe, Germany

E-mail: sabine.enders@kit.edu

All occurring phase equilibria as well as the interfacial properties depend on the one side on the interactions between the molecules present and on the other hand on the architecture of the molecules. This contribution focuses on the influence of the molecular architecture on different types of phase equilibria and the properties related to the interface. The incorporation of these effects in the thermodynamic equations can be realized by the Lattice Cluster Theory (LCT) originally developed by Freed and Coworkers [e.g. 1] and applied for different substance classes reaching from pure alkanes [2] to mixtures containing linear, branched and hyperbranched polymers [e.g. 3,4].

Within the LCT the Helmholtz energy can be obtained by double series expansion in inverse coordination number and in interaction energy taking into account the molecule architecture. This situation allows us to model the liquid-liquid-equilibrium (LLE) and the solid-liquid-equilibrium (SLE) and their superposition (SLLE) [5]. Additionally, the SLE of a polymer in a solvent or a solvent mixture depends also on the semi-crystallinity of the polymer. This effect can also be taken into account in the framework of LCT [6]. In order to model the vapor-liquid equilibrium (VLE) empty lattices are placed on the lattice resulting in an equation of state (LCT-EOS).

The interphase is established between two fluid phases related to the VLE or the LLE. In this case the LCT-EOS will be combined with the density gradient theory. This allows the calculation of the interfacial tension, the interfacial profile and the relative enrichment within the interface.

The theoretical framework will be demonstrated on two examples. The first one deals with the LLE of hyperbranched polymers in one or two solvents (water and alcohols). For these calculation the LCT is combined with an extended chemical association lattice model in order to take the self-association and the cross-association into account [7]. The adjustment of the model parameters, especially the interaction energy, using the binary sub-systems permits the prediction of the ternary phase behavior.

The second example is the phase behavior of different types of polyethylene in ethylene, hexane and octane. The studied polyethylene polymers differ in the molecular weight distribution as well as in the degree of branching. The modelled phase diagrams regarding to SLE and LLE were compared with experimental data taken from the literature.

[1] J. Dudowicz, K.F. Freed, *Macromolecules*, 1991, 24: 5076-5095.

[2] K. Langenbach, S. Enders, *Fluid Phase Equilibria* 2012, 331: 58–79.

[3] K. Langenbach, D. Browarzik, J. Sailer, S. Enders, *Fluid Phase Equilibria* 2014, 363: 196-212.

[4] T. Zeiner, S. Enders, *Chem. Eng. Sci.* 2011, 66: 5244–5252.

[5] K. Langenbach, M. Fischlschweiger, S. Enders, *Molecular Physics* 2016, 114: 2712-2723.

[6] M. Fischlschweiger, S. Enders, *Macromolecules* 2014, 47: 7625–7636.

[7] T. Zeiner, C. Browarzik, D. Browarzik, S. Enders, *J. Chem. Thermodynamics* 2011, 43: 1969–1976.

UNDERSTANDING TRANSITION ENTHALPIES OF IONIC LIQUIDS AT THE MOLECULAR LEVEL

Ludwig R.¹

¹Institute of Chemistry, University of Rostock, 18051 Rostock, Germany

E-mail: ralf.ludwig@uni-rostock.de

Understanding transition enthalpies of ionic liquids is challenging. In this lecture we show that spectroscopy, quantum chemical calculations and molecular dynamics simulations allow an interpretation of these thermodynamic properties at molecular level. Here, we will address a number of relevant questions. What are the structures present in the solid state, in the liquid or in the gas phase? How are these specie characterized by the subtle balance between Coulomb interaction, hydrogen bonding and dispersion forces?

Why is the vaporization enthalpy for ethyl ammonium nitrate high but the boiling point so low? Why are the vaporization enthalpies of aprotic ionic liquids (AILs) significantly larger than those of protic ionic liquids (PILs)? How are the transition enthalpies between contact and solvent separated ion pairs governed by temperature, solvent polarity and solvent concentration? How large is the transition enthalpy which is required to shift the equilibrium from H-bonded to dispersion-driven cation-anion interaction? Does like-charge attraction affect the solid-liquid phase transition?

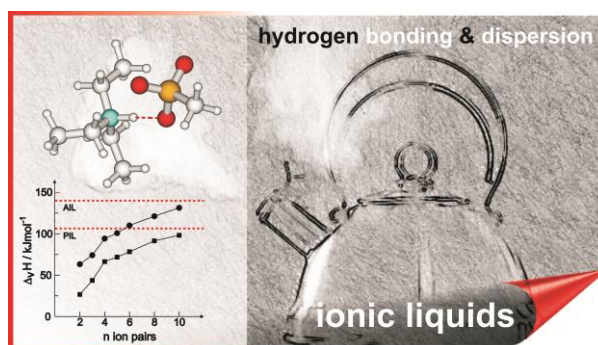
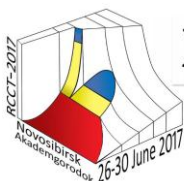


Figure 1: Vaporization enthalpies are higher for AILs than those for PILs.

References:

- [1] Emel'yanenko, V.N.; Boeck, G.; Verevkin, S.P.; Ludwig, R.; *Chem. Eur. J.*, **2014**, 20, 11640-11645.
- [2] Zaitsau, D.H.; Emel'yanenko, V.N.; Stange, P.; Schick, C.; Verevkin, S.P.; Ludwig, R.; *Angew. Chem.*, **2016**, 128, 11856-11860; *Angew. Chem. Int. Ed.*, **2016**, 55, 11682-11686.
- [3] Fumino, K.; Fossog, V.; Stange, P.; Wittler, K.; Polet, W.; Hempelmann, R.; Ludwig, R.; *ChemPhysChem* **2014**, 15, 2604-2609.
- [4] Stange, P.; Fumino, K.; Ludwig, R.; *Angew. Chem.* **2013**, 125, 3064-68; *Angew. Chem. Int. Ed.* **2013**, 52, 2990-94.
- [5] Fumino, K.; Stange, P.; Fossog, V.; Hempelmann, R.; Ludwig, R.; *Angew. Chem.* **2013**, 12667-12670; *Angew. Chem. Int. Ed.* **2013**, 52, 12439-12442.
- [6] Fumino, K.; Fossog, V.; Stange, P.; Hempelmann, R.; Ludwig, R.; *Angew. Chem.* **2015**, 127, 2792-2795; *Angew. Chem. Int. Ed.* **2015**, 54, 2792-2795.
- [7] Knorr, A., Stange, P.; Fumino, K.; Weinhold, F.; Ludwig, R.; *ChemPhysChem* **2016**, 17, 458-462.
- [8] Niemann, T.; Strate, Michalik, D.; A.; Ludwig, R.; *Angew. Chem.* **2017**, 129, 510-514; *Angew. Chem. Int. Ed.* **2017**, 56, 496-500.



SOME ASPECTS OF THERMODYNAMICS OF MIXED OXIDES ON THE BASIS OF RARE EARTH AND TRANSITION ELEMENTS

Matskevich N.I.¹, Wolf Th.², Adelman P.², Stankus S.V.³, Gelfond N.V.¹, Greaves C.⁴

¹Nikolaev Institute of Inorganic Chemistry, Siberian Branch of the Russian Academy of Sciences, 630090 Novosibirsk, Russia

²Karlsruhe Institute of Technology, Institute of Solid State Physics, D-76334 Karlsruhe, Germany

³Kutateladze Institute of Thermophysics, Siberian Branch of the Russian Academy of Sciences, 630090 Novosibirsk, Russia

⁴School of Chemistry, University of Birmingham, B15 2TT Birmingham, United Kingdom

E-mail: nata.matskevich@yandex.ru

Mixed oxides on the basis of rare earth and transition elements are important in a wide range of applications, many of which are of particular importance to today's environmental and energy problems. Examples include electrolytes and electrodes in SOFCs, oxygen sensors and membranes for purification, pigments, catalysts *etc.*

Here some aspects and trends in thermodynamics of oxides on the basis of rare earth and transition elements will be considered. Mixed oxides are widely studied in the world by calorimetry and chemical thermodynamics methods, such as high-temperature reaction calorimetry, solution calorimetry, low temperature adiabatic calorimetry, EMF method, differential scanning calorimetry, drop calorimetry *etc.*

It is impossible to mention here all the countries and world schools working in the field of thermodynamics of oxides on the basis of rare earth and transition elements. Thermodynamics of mentioned oxides are widely studied in United States of America, Canada, Germany, France, United Kingdom, Netherlands, Norway, Hungary, Russian Federation and others. It is such organizations as University of California, Karlsruhe Institute of Technology, Argonne National Laboratory, University of Amsterdam, Oslo University, Birmingham University, Moscow State University, Kurnakov Institute of General and Inorganic Chemistry RAS, Lobachevsky State University of Nizhni Novgorod, Nikolaev Institute of Inorganic Chemistry SB RAS, and others.

An example of international cooperation and successful realization to use thermodynamic methods for understanding processes in materials will be considered on the basis of HTSC materials.

Thermodynamics is successfully applied to solve materials science problems. At present the methods of chemical thermodynamics are widely used to develop and optimize the synthesis processes and technologies of materials including mixed oxides of rare earth and transition metals. Here the application of thermodynamics to synthesize phase-pure ceramic $\text{LuBa}_2\text{Cu}_3\text{O}_x$ will be considered [1]. The thermodynamic characteristics of advanced materials such as $\text{Bi}_{12.5}\text{R}_{1.5}\text{ReO}_{24.5}$ and $\text{BaCe}_{1-x}\text{R}_x\text{O}_{3-y}$ (R – rare earth element) will be reported [2-5]. The Kapustinskii rule will be involved to clear trends in lattice energy.

To assess progress in using of thermodynamics over the past twenty years for developments of some energy alternative sources, this report discusses a number of modern researchers in fields of modelling processes in systems on the basis of rare earth and transition metals oxides. In conclusion we will consider some aspects of applied problems for massive calorimeters arising from linear calorimetric systems theory such as thermometer localization *etc.*

This work is supported by Karlsruhe Institute of Technology (Germany), RFBR 16-08-00226, DFG, NATO grant "Science for Peace" and Government Task for NIIC SB RAS.

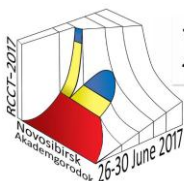
[1] Matskevich, N; Wolf, Th; Pochivalov Yu. Inorg. Chem., 2008, 47, 2581-2584.

[2] Matskevich, N; Wolf, Th; Greaves, C; Bryzgalova A. J. Alloys Comp., 2014, 582, 253-256.

[3] Matskevich, N; Wolf, Th; Greaves, C; Adelman, P. J. Chem. Thermodyn., 2015, 91, 234-239.

[4] Matskevich, N; Wolf, Th; Pischur, D; Kozlova, S. J. Therm. Anal. Calorim., 2016, 124, 1745-1748.

[5] Matskevich, N; Wolf, Th; Le Tacon, M; Adelman, P; Stankus, S; Samoshkin, D; Tkachev, E. J. Therm. Anal. Calorim., in press.



INVESTIGATIONS OF THE PROPERTIES OF SOLIDS BASED ON LOW-TEMPERATURE ADIABATIC CALORIMETRY

Naumov V.N., Bespyatov M.A., Musikhin A.E., Kuzin T.M., Chernyaikin I.S., Gelfond N.V.

Nikolaev Institute of Inorganic Chemistry, Siberian Branch of the Russian Academy of Sciences, 630090 Novosibirsk, Russia

E-mail: vn@niic.nsc.ru

A great number of publications are devoted to the study of low-temperature heat capacity of solids. This is due to its high informativity, which allows us to consider and study a wide range of properties and phenomena in solids. It can be experimentally determined with high accuracy. Heat capacity is the main thermodynamic value because it is directly related to the energy of the system. The energy of the solid and its heat capacity in the vicinity of room temperature are determined mainly by vibrations of the nuclei of atoms. These vibrations are well described in the framework of the phonon formalism taking into account their quantum-statistical distribution. This determines a decrease of the heat capacity up to zero at low temperatures and is an inherent property of all solids. Any processes taking place in phonon, electronic and magnetic subsystems of the solids are reflected in the behavior of the heat capacity with temperature changes. The heat capacity is a measure of the fluctuations of energy in the system and it is regarded as the main quantitative indicator of processes associated with the phase transitions. The ability to isolate and then analyze the behavior of these components is the basis for understanding the nature of processes that are going in solids. Already from this it follows that the method of experimental study the heat capacity at low temperatures is a powerful tool in the study of properties and phenomena in solids.

The experimental basis for considering the problems of this review is the heat capacity obtained by the adiabatic method in the range of 4–320 K. Note that the low-temperature adiabatic calorimetry, developed by Nernst and his colleagues in 1910, remains beyond competition when it comes to obtaining high-precision data on heat capacity in a wide range of low temperatures. Precise data on low-temperature heat capacity is needed in the consideration of a wide range of both applied and academic problems.

Here we will touch upon some topics that are back to back to the tasks of physical chemistry, and which cover the following questions:

- a priori idea of the heat capacity and thermodynamic functions behavior of solids (the range of expected values of the heat capacity functional behavior, the Dulong and Petit law and the Debye law);
- components of various nature and their contributions to the heat capacity of solids (phonon, electron, magnetic, etc.)
- quantum-mechanical nature of the description of low-temperature thermodynamics of solids;
- a relationship between the lattice heat capacity and the vibrational spectrum of crystal (the phonon density of states);
- a description of heat capacity and thermodynamic functions in the framework of empirical, semi-empirical and physically grounded representations;
- high-temperature expansion of heat capacity (effective sum method);
- searching for empirical and fundamental regularities between the structure characteristics of crystal and its thermodynamic behavior;
- influence the short-range and long-range order on the thermodynamics of solid;
- anisotropic and isostructural characteristics of solids and the reflection of these structural features in the heat capacity behavior;
- anomalies in the heat capacity behavior and identification of their typical thermodynamic features (Schottky anomaly, first- and second-order phase transitions and others);
- characteristic temperature (is there a characteristic energy or characteristic temperature that is uniquely determined for any solid, or is there an alternative to the Debye characteristic temperature?);
- analysis of groups or series of compounds, united by some features, within the framework of law of corresponding states;
- the possibility of calculating zero-point energy of crystal from the heat capacity data, the accuracy of determining this quantity;
- a possibility of calculating the total energy of solids;
- the development of new methods for obtaining the most important characteristics of solids based on the high-precision data on the low-temperature heat capacity.

**THERMODYNAMICS OF NONEQUILIBRIUM CHEMICAL PROCESSES.
EXAMPLES OF USE FOR SOLVING NON-STANDARD PROBLEMS IN STUDY OF
CHEMICAL TRANSFORMATIONS**

Parmon V.N.

Boreskov Institute of Catalysis, Novosibirsk State University, 630090, Novosibirsk, Russia

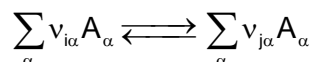
E-mail: parmon@catalysis.ru

The presentation concerns an experience in the application of a *thermodynamic form* of kinetic equations for providing joint kinetic-thermodynamic analysis of a large variety of detailed schemes of stepwise reactions. The basis of the thermodynamic form is the substitution of parameter “concentration” C_α of a substance A_α by a related value

$$\tilde{A}_\alpha = \exp\left(\frac{\mu_\alpha}{RT}\right) \equiv \gamma_\alpha C_\alpha \exp\left(\frac{\mu_\alpha^0}{RT}\right),$$

expressed via chemical potential $\mu_\alpha \equiv \mu_\alpha^0 + RT(\gamma_\alpha C_\alpha)$ of thermalized substance A_α . Here μ_α^0 is standard value of μ_α , and γ_α is the activity coefficient of substance A_α .

It is shown that in such case the rate of any elementary chemical reaction “ij”



between thermalized reactants of two reaction groups i and j can be expressed in a pseudolinear form

$$v_{ij} = \frac{d\xi_{ij}}{dt} = \varepsilon_{ij} (\tilde{n}_i - \tilde{n}_j),$$

where ξ_{ij} is the chemical variable of the reaction ij, $\tilde{n}_i \equiv \exp\left(\frac{\mu_i}{RT}\right) = \prod_\alpha \exp\left(\frac{\nu_{i\alpha} \mu_\alpha}{RT}\right) = \prod_\alpha \tilde{A}_\alpha^{\nu_{i\alpha}}$,

$\varepsilon_{ij} = \varepsilon_{ji} \equiv \frac{k_B T}{h} \exp\left(\frac{\mu_{ij}^{0\ddagger}}{RT}\right)$ is a *truncated rate constant* of the reaction. Here k_B and h are the Boltzmann

and Planck constants, T is temperature, $\mu_{ij}^{0\ddagger}$ is the *standard chemical potential* of the transition state only for the reaction.

The application of the above substitution allows dramatic simplification of expressions for the rate of stoichiometric stepwise reactions even far from their equilibria and possibility, e.g., to give correct quantitative thermodynamic criteria of the kinetic irreversibility of stoichiometric stepwise reactions as well as of their limiting (a *bottle neck*) and rate controlling steps. Occasionally, these steps appear to be not coincident for some particular cases, e.g. for catalytic transformations.

Also, the application of the thermodynamic form of kinetic equations for analyzing complex reactions schemes, at least for those linear in respect to reaction intermediates, allows to receive a simple general Horiuti-Boreskov-like expression for the rate of the stepwise reaction at its steady state occurrence and to suggest both simple Lyapunov functions which are minimized in the stepwise reaction steady state as well as a reciprocity equations which are analogous to the Onsager's ones but valid for occurrence of the parallel stepwise reactions far from the reaction equilibria. Again, the use of the thermodynamic form of kinetic equations gives a simple explanation of the well known phenomenon of *kinetic compensation effect* as a sequence of an existing *isokinetic* temperature. Some other helpful results, especially of analyzing the schemes of catalytic reactions, are demonstrated too.

1. V.N. Parmon. Thermodynamics of Non-Equilibrium Processes for Chemists with a Particular Application to Catalysis. Elsevier: Amsterdam, 2010
2. V.N. Parmon. Thermodynamics of Non-Equilibrium Processes for Chemists with Applications to Chemical Kinetics, Catalysis, Material Science and Biology. (the second edition in Russian), Dolgoprudnyi: Intellekt, 2015
3. V. N. Parmon. Kinetic compensation effects: a long term mystery and the reality. A simple kinetic consideration. Reaction Kinetics, Mechanisms and Catalysis, 2016, Volume 118, Issue 1, pp 165–178



ACHIEVEMENTS AND CHALLENGES IN EXPERIMENTAL AND STATISTICAL THERMODYNAMICS OF ORGANIC COMPOUNDS

Pimerzin A.A.

Samara State Technical University, Samara, 443100, Russia

pimrzin@samgtu.ru

Experimental results are extremely important for thermodynamics and thermochemistry, due to the fact that experiment is the only reference point for verifying calculations and the consistency of information obtained from various sources. Traditional thermochemical and thermodynamic methods of research operate with high purity individual compounds. Moreover, the accuracy of the result is directly arise from the purity level of chemicals. Obviously, the requirement for high-purity substances imposes meaningful constraints on authenticity of the obtaining data.

The combination of traditional methods and techniques without mentioned limitations (for example, the method of studying chemical equilibrium) makes it possible to broaden the set of studied compounds, especially for chemicals, which are difficult to obtain in high-purity samples. The suggested simultaneous approach proved effective for various classes of organic compounds. Several examples are given in the report.

The development of molecular modeling and quantum-chemical calculations opens the door to multiple opportunities for prediction the thermodynamic properties of polyatomic organic compounds. However, today these opportunities are not always fully used. The accuracy of the result of calculation depends on several factors that must be performed if we are looking forward to a positive outcome. First and foremost, it is the observance of the assumptions underlying the statistical calculations of thermodynamic properties of compounds. Among them

- The principle of independence of the different types of motion and the additivity of their contributions to thermodynamic functions;
- Approximation of "rigid rotator - harmonic oscillator".

However, the complex structure of polyatomic molecules, the conformational heterogeneity of the compounds, the appearance of intramolecular degrees of freedom with high-amplitude movement, unharmonic character of the vibrational frequencies are very often do not fit into the framework of the established assumptions.

This research analyzes the reasons for the differences between the forecast of the thermodynamic properties (entropy, enthalpy, heat capacity) and experiment. The analysis was performed on the example of the thermodynamic properties of aliphatic, alicyclic, aromatic hydrocarbons, alkylphenols, alkylhalogenbenzenes and its reactions.

Some of the raised issues have been decided. For other ones the methods, which allow detecting their emergence and making estimation, have been proposed. For some problems have yet to find a solution.



DEVELOPMENT OF EXPERIMENTAL EQUIPMENT AND MODELS FOR THERMODYNAMIC DATA

Ramjugernath D.

Thermodynamics Research Unit, School of Engineering, University of KwaZulu-Natal, Durban, South Africa

E-mail: ramjuger@ukzn.ac.za

Phase equilibrium and thermophysical property data, e.g. vapour-liquid equilibria, liquid-liquid equilibria, solid-liquid equilibria, hydrate equilibria, critical properties, vapour pressures, liquid viscosities, infinite dilution activity coefficients, etc, are essential for the design, simulation and optimization of chemical processes and plants. The experimental measurement of some of these properties can be challenging, which results in experimental data for these properties either not being available or available for limited numbers of compounds and/or systems. This requires the subsequent development of correlative and predictive models.

Over the last 30 years, the Thermodynamics Research Unit at the University of KwaZulu-Natal has built a reputation for the development of equipment for the measurement of phase equilibrium data and thermophysical properties. In the last 15 years, we have also undertaken the development of various correlative and predictive models for thermophysical properties. We have a strong belief in the complementarity of experimental and computational studies, and have endeavored to develop both aspects.

In this presentation, some of the experimental equipment developed in our laboratories for phase equilibria, vapour pressure measurements, determination of infinite dilution activity coefficients, critical property measurement, pressure-temperature-volume measurements, heat capacity, etc, will be discussed.

With regard to the development of correlations and predictive models for thermophysical properties, a range of group contribution (GC), and quantitative structure property relationship (QSPR) models, which have been developed, will be presented and discussed. Models have been developed for vapour pressure, boiling points, critical properties, liquid viscosity, liquid thermal conductivity, thermal decomposition temperatures, electrical conductivity, sublimation and vaporization enthalpies, saturated liquid speeds of sound, standard molar chemical exergies, refractive indices, and freezing points. In addition, for ionic liquids, models and correlations were developed for heat capacity, surface tension, infinite dilution activity coefficients, and critical temperature. The computational methods used have enabled large databases to be utilized for thermophysical property development, which affords greater applicability of models developed. Novel algorithms developed for the determination of model parameters will also be briefly discussed.



THERMOPHYSICAL PROPERTIES OF THERMALLY LABILE COMPOUNDS

Abdelaziz A.^{1,2}, Zaitsau D.H.^{2,3,4}, Chua Y.Z.^{1,2}, Verevkin S.P.^{2,3}, Schick C.^{1,2,5}

¹ University of Rostock, Institute of Physics, 18051 Rostock, Germany

² University of Rostock, Faculty of Interdisciplinary Research, Competence Centre CALOR, 18051 Rostock, Germany

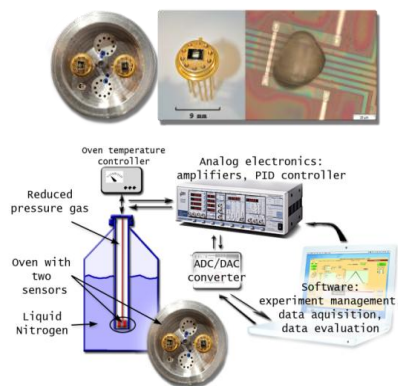
³ University of Rostock, Institute of Chemistry, 18051 Rostock, Germany

⁴ Samara State Technical University, 443100 Samara, Russian Federation

⁵ Kazan Federal University, Kazan 420008, Russian Federation

E-mail: christoph.schick@uni-rostock.de

How to obtain reliable thermophysical properties from thermally labile compounds, e.g. biomolecules or ionic liquids? In general, one has to stay at temperatures where decomposition is negligible during the time of the measurement. If possible, one can stay at sufficiently low temperatures avoiding decomposition. However, often this strategy is not applicable because the effect of interest does not occur at such low temperatures or the rate is so low that it is very hard to get any signal from the process under investigation. Typical examples for such situation are the melting of biomolecules, e.g. dry proteins, or vaporization of ionic liquids or sublimation of biomolecules. Then, the only way to obtain reliable data is by speeding up the process under investigation in order to avoid the decomposition, which is usually slower. For example, only if the complete heating-cooling cycle to observe the melting of dry proteins is so fast that decomposition at the highest temperatures is negligible, there is a chance to get melting temperature and heat of fusion of the high temperature transition. Fast scanning calorimetry (FSC) [1-3] offers a possibility to realize experiments on millisecond time scales and with that to overturn chemical decomposition in many materials. The general principle of FSC with heating and cooling rates up to 10^6 K/s will be introduced and applications to the melting of proteins [4, 5] and other biomolecules will be discussed. The focus will be on the vaporization of ionic liquids [6, 7] and the sublimation of biomolecules.



Funktional Materials Rostock e.V.



Mettler Toledo

Photographs of available fast scanning calorimeters

References:

- [1] C. Schick, V. Mathot, Fast Scanning Calorimetry, Springer, 2016.
- [2] E. Zhuravlev, C. Schick, Fast scanning power compensated differential scanning nano-calorimeter: 1. The device, Thermochim. Acta 505 (2010) 1-13.
- [3] E. Zhuravlev, C. Schick, Fast scanning power compensated differential scanning nano-calorimeter: 2. Heat capacity analysis, Thermochim. Acta 505 (2010) 14-21.
- [4] P. Cebe, X. Hu, D.L. Kaplan, E. Zhuravlev, A. Wurm, D. Arbeiter, C. Schick, Beating the Heat - Fast Scanning Melts Silk Beta Sheet Crystals, Scientific Reports 3 (2013) 1-7.
- [5] P. Cebe, B.P. Partlow, D.L. Kaplan, A. Wurm, E. Zhuravlev, C. Schick, Using flash DSC for determining the liquid state heat capacity of silk fibroin, Thermochim. Acta 615 (2015) 8-14.
- [6] M. Ahrenberg, M. Brinckmann, J.W.P. Schmelzer, M. Beck, C. Schmidt, O.H. Keßler, U. Kragl, S.P. Verevkin, C. Schick, Determination of volatility of ionic liquids at the nanoscale by means of ultra-fast scanning calorimetry, Physical Chemistry Chemical Physics 16 (2014) 2971-2980.
- [7] M. Ahrenberg, M. Beck, C. Neise, U. Kragl, S.P. Verevkin, C. Schick, Vapor pressure of ionic liquids at low temperatures from AC-chip-calorimetry, Physical Chemistry Chemical Physics 18 (2016) 21381-21390.



DENSITY FUNCTIONAL THEORY OF SIZE-DEPENDENT EFFECTS IN THERMODYNAMICS OF DROPLETS ON NEUTRAL AND CHARGED NANOPARTICLES

Shchekin A.K., Lebedeva T.S.

Department of Statistical Physics, Faculty of Physics, St. Petersburg State University, 199034 St. Petersburg, Russia

E-mail: akshch@list.ru

Size-dependent effects in thermodynamics of droplet formation on wettable uncharged and charged solid particles are related to the nonuniformity of the droplet provided by overlapping surface layers the solid core – liquid film and the liquid film – vapor. The overlapping can be thermodynamically described in terms of competition between the capillary and the disjoining pressure as contributions to the chemical potential of a condensate molecule in the droplet which can phenomenologically be taken the same as for flat thin liquid films [1,2]. The disjoining pressure is created by molecular forces in small volumes and can be modified by presence of long-range electrical forces.

In the case of uncharged solid cores, the attempts to compute the disjoining pressure in the droplet on a molecular level were undertaken more than ten years ago by Napari and Laaksonen [3] and by Bykov and Zeng [4,5] with the help of the nonlocal density functional theory (DFT) for fluids with the Lennard-Jones molecular potential. Here we would like to extend the study by consideration of the effect of molecular interactions of the condensate molecules with the solid core jointly with the effect of central electric field in the case of charged core. A similar problem had been formulated for ion-induced nucleation by Kitamura and Onuki [6], and we made a development of it recently for condensation cores of molecular size [7,8]. However, the situation in the case of nanosized and larger condensation cores has its own specificity. It is associated with increasing the disjoining pressure with the size of the core and its possible interplay with the electric field of a charged core. Increasing the size of the cores also establishes limits for complete wetting and affects the work of wetting.

We report here the results of numerical study of the size-dependent effects for the chemical potential, disjoining pressure and work of droplet formation of a small droplet with solid insoluble core. The study has been performed within the square-gradient DFT [9]. The Lennard-Jones fluid with the Carnahan-Starling model for the hard-sphere contribution to intermolecular interaction in liquid and vapor phases and interfaces has been used for description of the fluid condensate. The intermolecular forces between the solid core and condensate molecules have been taken into account with the help of the Lennard-Jones part of the total molecular potential of the core. The influence of the electric charge of the particle has been considered under assumption of the central Coulomb potential in the fluid with the dielectric permittivity depending on local condensate density. The condensate density profiles and equimolecular radii for equilibrium droplets at different values of the condensate chemical potential have been computed in the cases of an uncharged solid core with the molecular potential, a charged core without molecular potential, and a core with joint action of the Coulomb and molecular potentials. The capillary and disjoining pressures in the droplet and electrostatic contributions to the condensate chemical potential have been found and compared with the predictions of classical thermodynamics and thermodynamics of mesoscopic droplets [1,2]. With the help of the found dependence of the condensate chemical potential in droplet on the droplet size, the energetic characteristics of nucleation on uncharged and charged particles have been computed as functions of vapor supersaturation and core size.

This work was supported by Russian Fond for Basic Research grant 16-03-00281 mol-a.

- [1] F.M. Kuni, A.K. Shchekin, A.I. Rusanov, B. Widom, *Adv. Colloid Interface Sci.* 65, 71, 1996.
- [2] A.K. Shchekin, T.S. Podguzova, *Atmospheric Research* 101, 493, 2011.
- [3] I. Napari, A. Laaksonen, *J. Chem. Phys.* 119, 10363, 2003.
- [4] T.V. Bykov, X.C. Zeng, *J. Chem. Phys.* 117, 1851, 2002.
- [5] T.V. Bykov, X.C. Zeng, *J. Chem. Phys.* 125, 144515, 2006.
- [6] H. Kitamura, A. Onuki, *J. Chem. Phys.* 123, 124513, 2005.
- [7] A.K. Shchekin, T.S. Lebedeva, D.V. Tatyanyenko, *Colloid J.* 78, 553, 2016.
- [8] A.K. Shchekin, T.S. Lebedeva, D.V. Tatyanyenko, *Fluid Phase Equilib.* 424, 162, 2016.
- [9] A.K. Shchekin, T.S. Lebedeva, *J. Chem. Phys.*, 2017.

**THERMODYNAMICS AND VAPORIZATION
OF BINARY AND MULTICOMPONENT CERAMICS BASED ON HAFNIA**Stolyarova V.L.

Institute of Chemistry, Saint Petersburg State University, 199034 Saint Petersburg, Russia

E-mail: v.stolyarova@spbu.ru

Progress in developing of high-temperature refractory ceramics significantly depends on the volatilities of their components. One of the most promising materials from this point of view are the ceramics based on hafnia that may be considered as having low volatility as well as high thermal and chemical stability. That is the reason of the wide application of these ceramics used in the various fields of high-temperature processing such as space, nuclear and optical industries. As well known information on thermodynamic properties and vaporization properties of the materials considered is the key question for obtaining advanced ceramics with the required properties that may be used up to the temperatures 3000 K. The most powerful tool for these purposes is the high-temperature Knudsen effusion mass spectrometric method [1]. The review on the available experimental data in the binary and ternary systems containing hafnia [1-10] found by this approach is presented. The results obtained are summarized in Table 1. The question on the reliability of these values is examined. The available data on thermodynamic properties and vaporization processes of hafnia containing systems are discussed in connection with the acid-base concept [1]. It is found that the relative changes of thermodynamic properties and volatility of these systems are in agreement with the main statements of this theory. The opportunities for the prediction of thermodynamic properties of the systems containing hafnia using the sub-regular solution model are considered.

This study was carried out based on the financial support by RFBR according to the project N 16-03-00940.

Table 1. Data on vaporization processes and thermodynamic properties of ceramics based on hafnia obtained using Knudsen effusion mass spectrometric method [1-10].

System under study	Temperature range (K)	Composition of vapor	References
HfO ₂ -Y ₂ O ₃	2000-2900	YO, HfO, HfO ₂ , O	[1-4]
HfO ₂ -ZrO ₂	2300-2800	ZrO, ZrO ₂ , HfO, HfO ₂ , O	[1-4]
HfO ₂ -Sc ₂ O ₃	2600	ScO, HfO, HfO ₂ , O	[5]
HfO ₂ -Nd ₂ O ₃	2000-2750	NdO, HfO, HfO ₂ , O	[6]
HfO ₂ -Gd ₂ O ₃	2000-2750	GdO, HfO, HfO ₂ , O	[6,7]
HfO ₂ -ZrO ₂ -Y ₂ O ₃	2690-2925	YO, ZrO, ZrO ₂ , HfO, HfO ₂ , O	[8,9]
HfO ₂ -Y ₂ O ₃ -Gd ₂ O ₃	2500	GdO, YO, HfO, HfO ₂ , O	[10]

[1] Stolyarova, V. Russ. Chem. Rev., 2016, 85, 60-80.

[2] Belov, A. Thesis, Leningrad, AN SSSR, 1981, 20.

[3] Marushkin, K; Alikhanyan, A. Zhurnal Neorganicheskoi Khimii, 1991, 36, 2637-2642.

[4] Kablov, E; Folomeikin, Yu; Stolyarova, V; Lopatin, S. Doklady Physical Chemistry, 2015, 463, 150-153.

[5] Semenov, G; Kuligina, L; Teterin, G; Menchuk, E; Shkol'nikov, T. Soviet progress in chemistry, 1986, 52, 1-3.

[6] Sevastyanov, V; Simonenko, E; Simonenko, N; Stolyarova, V; Lopatin, S; Kuznetsov, N. Eur. J. Inorg. Chem., 2013, 2013, 4636-4644.

[7] Kablov, E; Stolyarova, V; Lopatin, S; Vorozhtcov, V; Karachevtsev, F; Folomeikin, Yu. Rapid Commun. Mass Spectrom., 2017, 31, 538-546.

[8] Belov, A; Semenov, G. Neorganicheskie materialy, 1989, 25, 994-997.

[9] Sevastyanov, V; Simonenko, E; Simonenko, N; Stolyarova, V; Lopatin, S; Kuznetsov, N. Materials Chem. and Phys., 2015, 153, 78-87.

[10] Stolyarova, V; Lopatin, S; Vorozhtcov, V; Karachevtsev, F. Khimiya tverdogo tela i funktsionalnyye materialy-2016, XI seminar "Termodinamika i materialovedenie", Ekaterinburg, 2016, 289.



THERMODYNAMICS OF HYDROCARBON + CO₂ MIXTURES

Sanchez-Vicente Y.¹, Tay W.¹, Al Ghafri S.², Trusler M.¹

¹*Department of Chemical Engineering, Imperial College London, London SW7 2AZ, UK*

²*Fluid Science & Resources Division, School of Mechanical & Chemical Engineering, The University of Western Australia, Crawley, Australia*

E-mail: m.trusler@imperial.ac.uk

Mixtures of hydrocarbons and carbon dioxide are important in numerous technologies, including both CO₂-enhanced oil recovery and CO₂ sequestration in depleted hydrocarbon reservoirs. For the design and optimization of these processes, it is necessary to have reliable knowledge of the thermophysical properties. In the examples cited, the fluids enter a domain of high temperatures and high pressure and, while general behaviors are largely understood, quantitative measures of the thermophysical properties in these regimes are lacking in terms of scope and reliability. Furthermore, available models lack validation at high temperatures and high-pressures. The objectives of the present work were to provide reliable and comprehensive multi-property experimental data for a selection of binary mixtures, and to use those data to test the performance of predictive thermodynamic models.

In this study, measurements have been made of the phase behavior and saturated-phase densities along the bubble- and dew-curve, including the critical region, at temperatures up to 448 K. Additionally, the compressed liquid densities and speed of sound have been measured at pressures up to 70 MPa and 400 MPa, respectively, at temperatures up to 473 K. The binary systems studied include (CO₂ + heptane) and (CO₂ + toluene). Some of these properties (including also viscosity) have been measured for a number of other (CO₂ + hydrocarbon) systems. The experimental work was carried out using bespoke equipment developed in our laboratory and emphasis was placed on the assessment of uncertainty. The experimental data provide a comprehensive basis for testing predictive equations of state in high-temperature, high-pressure regions where little data beyond the phase boundaries were previously available.

The models considered in detail are the Predictive Peng-Robinson equations of state (PPR-78) and the SAFT- γ Mie equation of state. Both of these models use group contribution approaches to estimate key parameters. In the PPR-78 model, pure-component terms are obtained from the critical properties and the acentric factor, while all binary interaction parameters are obtained from the group-contribution scheme of Jaubert and co-workers [1,2]. The SAFT- γ Mie equation of state is based on the SAFT approach for segments that interact through the generalized Mie potential. In this model, all interaction terms (both like and unlike) are obtained from group parameters tables [3,4]. These parameter tables were developed primarily by fitting pure-component vapor pressure and saturated liquid densities for a wide range of systems. However, in the case of molecules such as CO₂ that are themselves defined as a single group, binary vapor-liquid equilibrium data were also used to obtain unlike group interaction parameters [4].

The results indicate that both models account reasonably well for the phase boundaries and the critical locus. However, the saturated-phase densities are generally predicted much better by SAFT- γ Mie than by PPR-78. Despite its superior genesis, SAFT- γ Mie was found to perform little better than the PPR-78 model for the prediction of compressed-liquid densities, although it gave much better results than PPR-78 for the speed of sound. It seems likely that improvements in the parameterization of SAFT- γ Mie are possible, leading to better results for mixtures of the type investigated. The inclusion of density and sound-speed data in the parameter regression would be helpful in reducing unfavorable correlations between parameters.

[1] Jaubert JN; Mutelet F; *Fluid Phase Equilib.* 2004, 224, 285-304.

[2] Vitu S; Privat R; Jaubert JN; Mutelet F. *J Supercrit Fluids.* 2008, 45, 1-26.

[3] Papaioannou V; Lafitte T; Avendano C; Adjiman CS; Jackson G; Muller EA; Galindo, A. *J Chem Phys.* 2014, 140, 054107.

[4] Papaioannou V; Calado F; Lafitte T; Dufal S; Sadeqzadeh M; Jackson G; Adjiman CS; Galindo, A. *Fluid Phase Equilib.* 2016, 416, 104-19.



XXI International Conference on Chemical Thermodynamics in Russia (RCCT-2017)

26-30 June 2017, Akademgorodok, Novosibirsk

Invited lectures



**THERMODYNAMIC STUDIES BY KNUDSEN EFFUSION MASS SPECTROMETRY:
FROM “HIGH TEMPERATURE MOLECULES” TO LOW TEMPERATURE
EVAPORATION/DECOMPOSITION OF ORGANIC AND HYBRID MATERIALS**

Ciccioli A.

Department of Chemistry, Sapienza – University of Rome, 00185 Rome, Italy

E-mail: andrea.ciccioli@uniroma1.it

High temperature Knudsen Effusion Mass Spectrometry (HT-KEMS) has been for about 60 years one of the most powerful techniques to investigate the vaporization behaviour of a wide range of chemical systems and to derive a wealth of related thermodynamic properties. The author's laboratory at Sapienza - University of Rome, founded by Giovanni De Maria, led subsequently by Giovanni Balducci and currently by Guido Gigli, has a fifty-year-long tradition in this kind of studies.

The author will give here an overview of the recent work performed in his laboratory, going from the investigation of new molecular species in high temperature vapours of inorganic systems to the study of thermal stability and evaporation properties of organic and hybrid materials which are currently considered with interest for potential technological applications.

With regard to high temperature molecules, a combined HT-KEMS and computational study of the series of AuM diatomics (with M = first row transition metal) will be presented. Transition metals are known to exhibit a varied and complex chemical behaviour related to their peculiar electronic structure, in particular to the close-lying *ns* and $(n-1)d$ orbitals, giving rise to a multitude of inorganic and metallorganic species with various bonding properties. On the experimental side, the production and characterization of these species in the gas phase is often difficult, what makes the current information on dissociation/atomization energy rather scanty, and error bars of available data larger than main block species. From the theoretical point of view, the aforementioned complex electronic structure is responsible for the difficulties encountered in the theoretical description of these species, which remain challenging even for the most advanced quantum chemistry techniques. It is thus not surprising that the traditionally accepted “chemical accuracy” of ± 1 kcal/mol in the theoretical evaluation of energetic properties is a target still hard to achieve and indeed a *ad hoc* loosed “transition metal chemical accuracy” of ± 3 kcal/mol was proposed for transition metal species. Here, we show how our integrated approach [1] based on the combination of HT-KEMS measurements performed with various molecular source configurations and a highly correlated computational technique such as CCSD(T) resulted in a satisfactory assessment of dissociation energies of the entire AuM series.

In the last years, additional lines of research were tackled in the author's laboratory, oriented to the study of the evaporation behaviour and thermodynamic properties of organic and hybrid materials by HT-KEMS (actually...not so HT in this case). In particular, the study of aprotic ionic liquids [2] and alkylammonium lead halide perovskites [3] was undertaken in collaboration with colleagues at Sapienza, namely S. Vecchio Cipriotti, B. Brunetti, A. Latini, A. Lapi. These classes of substances received much attention in the past decade for their potential applications in various field of chemical and energy conversion technologies. In the second part of the lecture recent work on these systems is overviewed. Special emphasis will be given to the unique capability of KEMS of ascertaining the presence of different evaporation/decomposition processes which can take place simultaneously and to the investigation of factors affecting their relative importance. Evidences of the occurrence of kinetically hindered decomposition processes will be shown. A comparison with the results obtained by other tensimetric techniques retrieved from the literature or carried out by us will be also presented.

[1] Carta, V.; Ciccioli, A.; Gigli, G. *J. Chem. Phys.*, 2014, 140(6), 064305.

[2] Brunetti, B.; Ciccioli, A.; Gigli, G.; Lapi, A.; Misceo, N.; Tanzi, L.; Vecchio Cipriotti, S. *Phys. Chem. Chem. Phys.*, 2014, 16(29), 15653-15661.

[3] Brunetti, B.; Cavallo C.; Ciccioli, A.; Gigli, G.; Latini, A. *Sci. Rep.*, 2016, 22(6), 31896.

FUNDAMENTAL FEW-PARAMETER EQUATION OF STATE FOR CALCULATION OF THERMODYNAMIC PROPERTIES OF SUBSTANCES AT UP TO 200 MPa

Kaplun A.B.¹, Meshalkin A.B.¹, Bezverkhiiy P.P.².

¹Kutateladze Institute of Thermophysics SB RAS, 630090, Novosibirsk, Russia

²Nikolaev Institute of Inorganic Chemistry SB RAS, 630090, Novosibirsk, Russia

E-mail: kaplun@itp.nsc.ru

There is the opinion that in connection with development of computer technology almost all problems of description of the thermodynamic surface can be solved using the formal multi-parameter equations containing many tens or even hundreds of empirical coefficients. It is difficult to accept this point of view because these equations have a number of known fundamental disadvantages. In particular, the critical conditions are not usually satisfied in these equations.

We have previously determined the preferred form of EoS involving the differential equations of thermodynamics, and it is shown that the “right” equation for the compressibility factor $Z = PV/RT$ and Helmholtz equation for the reduced function should include only the density function as a component. A new step potential was offered, which was used to obtain the equation for accurate calculation of the second virial coefficient in the entire temperature range under study, including the second virial coefficient for helium and water. It was found out that on the whole thermodynamic fluid – gas surface, including in the areas bounded by bimodal with spinodal, the isochoric heat capacity is significantly positive, and derivative $(\partial P/\partial V)_S$ remains significantly negative.

In the developed few-parameter equations, for the first time it becomes possible to satisfy strictly the classical critical conditions with no loss in accuracy in description of original P - V - T data. With the help of differential equations of thermodynamics, the regular equations for precision calculations of caloric characteristics and speed of sound (Ar, N₂, CO₂, etc.) were derived from the thermal equations of state without involvement of data on the caloric properties. The few-parameter single equation of state in the form of reduced Helmholtz function (“fundamental” EoS) for precise description of the thermodynamic properties of normal substances in the gas, liquid or fluid state contains typically up to 10 individual adjustable coefficients. It describes the thermodynamic properties of normal substances at pressures of up to 200 MPa with high accuracy and within the initial thermal and caloric data. Comparison of calculated sound velocities with table “reference” data for CO₂ is presented in the figure as an example.

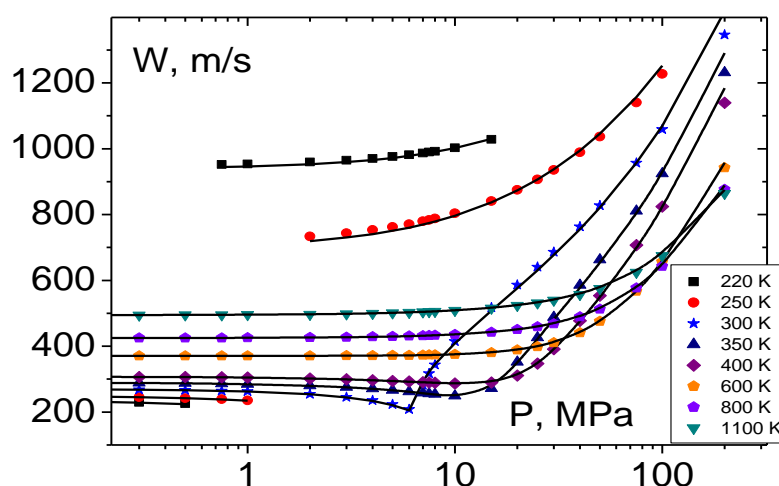


Figure 1. Comparison of calculated sound velocities (lines) for CO₂ with table data of [R. Span, W. Wagner, 1996] on isotherms, in the form of pressure functions.

Acknowledgements. This work was supported by RFBR grants 15-08-01072-a and 15-08-03443-a.



THERMODYNAMISTS AND OTHER CRAZY PEOPLE

Kleiber, M.

²*thyssenkrupp Industrial Solutions AG, 65812 Bad Soden, Germany*

E-mail: michael.kleiber@thyssenkrupp.com

Thermal separation processes and thermodynamics are strongly related, and process specialists and thermodynamists often work close together to get an adequate modeling of processes. However, there are a lot of misunderstandings between the validity of a process model and the behaviour of a plant.

The presentation will address a number of difficulties in real processes where thermodynamics plays a major role, e.g.

- the removal of organic byproducts in the acetaldehyde process
- the removal of ethyl acetate from vinyl acetate monomer
- the boiling point of biodiesel with ethanol impurities
- the ammonia – water separation
- the THF-water separation (with reservation)
- the PO purification (with reservation)
- the water removal from trioxane
- the inertization with nitrogen coming from cylinders

All these cases have in common that thermodynamics finally proved to be capable to describe these processes correctly, while at the beginning serious discrepancies had been observed. Common misunderstandings are the accuracy demand of thermodynamic models, the role of estimations and measurements, the target of process model and the unavoidable human factor, making people trust operational data and distrust what they do not understand.

Moreover, sometimes people even take advantage from models which are obviously inaccurate or wrong. Bad thermodynamics can justify to claim high tray efficiencies in distillation or a remarkable accuracy with a fantastic heat transition coefficient in the design of evaporators.

SOLID-LIQUID PHASE EQUILIBRIA OF ORGANIC SUBSTANCES – EXPERIMENTAL DETERMINATION AND APPLICATION

Lorenz H., Horosanskaia E., Seidel-Morgenstern A.

Max Planck Institute for Dynamics of Complex Technical Systems, D-39106 Magdeburg, Germany

E-mail: lorenz@mpi-magdeburg.mpg.de

In-depth knowledge of the fundamental solid-liquid phase equilibria is of crucial importance for design of crystallization-based separations, independent on the application media used, i.e. if crystallization from the melt or the solution phase is intended. Contrary to many inorganic systems (like alloys or mineral salts) the phase diagrams characterizing the solid-liquid phase behavior of organic substances from the fine chemicals background are mostly not or only partially known. However, in the related industries producing e.g. pharmaceuticals or food additives separation and purification of the target materials is an important task. Often it is not recognized that crystallization as a comparatively simple and cost-efficient technique (besides being commonly used in downstream processing) is also applicable for separation purposes of these substances in an earlier stage of process development. Since the crystal lattice is very sensitive to slight changes in the molecular structure, crystallization generally facilitates high purities and thus may allow for successful separation even in challenging and complex cases.

This contribution is focused on the experimental determination and application of solid-liquid phase diagrams required for design of crystallization-based separation processes exemplified on enantiomer separation and natural product purification. Therewith it addresses two limiting cases of separation problems: 1) the separation of only two but very similar substances and 2) the isolation of a specific target compound out of a multicomponent mixture.

In the presentation, after addressing the techniques used for determination of melt and solution equilibria, several examples of phase diagrams of chiral systems studied in our research group are presented and discussed with regard to potential concepts of crystallization-based separation [1, 2]. Both melt phase diagrams of the two enantiomers and ternary solubility phase diagrams of the enantiomers in a solvent are considered. Problems arising from occurrence of various solid-state forms such as polymorphs, solid solutions and solvates are encountered. Figure 1 shows exemplary melt phase diagrams of the chiral 2- and 3-chloromandelic acid systems (2-/3-CIMA, left and right).

Further, the application of solubility studies for isolation of a natural product target compound from a plant extract and/or a complex semi-synthetic mixture will be demonstrated.

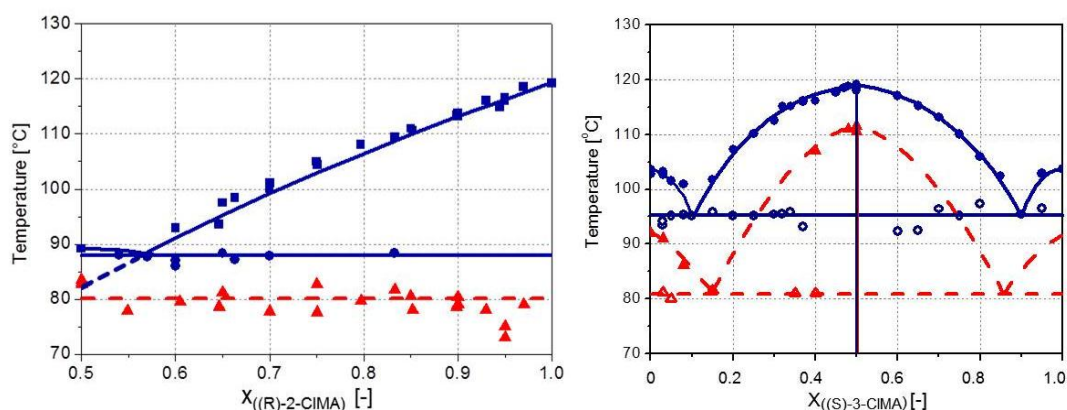


Figure 1. Melt phase diagrams of the 2- and 3-chloromandelic acid enantiomers [3, 4]. For 2-CIMA only half of the phase diagram is shown. Dashed lines specify metastable equilibria.

- [1] Lorenz, H; Seidel-Morgenstern, A. *Angew. Chem. Int. Ed.*, 2014, 53, 1218-1250.
- [2] von Langermann, J; Seidel-Morgenstern, A; Lorenz, H. *J. Chem. Eng. Data*, 2015, 60, 721-728.
- [3] Lorenz, H; von Langermann, J; Sadiq, G; Seaton, C. C; Davey, R; Seidel-Morgenstern, A. *Cryst. Growth Des.*, 2011, 11, 1549-1556.
- [4] Le Minh, T; von Langermann, J; Lorenz, H; Seidel-Morgenstern, A. *J. Pharm. Sci.*, 2010, 99, 4084- 4095.



**APPLICATION OF PRECISE CALORIMETRY IN STUDY OF MATERIALS
AND COMPOSITIONS BASED ON ORGANIC, ORGANOELEMENT
AND POLYMERIC COMPOUNDS**

Markin A.V.

Lobachevsky State University of Nizhni Novgorod, 603950 Nizhni Novgorod, Russia

E-mail: markin@calorimetry-center.ru

This work is devoted to the fundamental problem, namely the application and development of methods of chemical thermodynamics in study of materials and compositions based on organic, organoelement and polymeric compounds. Among these perspective compounds, the most thoroughly investigated representatives are metal fullerides, fullerene complexes with organoelement ligands, fullerene-containing polymers, carbosilane and liquid crystalline dendrimers with different nature of the surface layer. The discussion and conclusions are based on the results of complex precision calorimetric determination of the temperature dependences of heat capacities and characteristics of the revealed phase transitions in a wide temperature range.

In the present work, the temperature dependences of heat capacities of the above compounds in different states (amorphous, crystalline, partially crystalline, liquid crystalline) were determined in the temperature interval from 6 to 870 K by precision adiabatic vacuum calorimetry (BCT-3 with discrete heating, Termis, Moscow region, Russian Federation) and differential scanning calorimetry (DSC 204 F1 *Phoenix*, Netzsch-Gerätebau, Selb, Germany). As a result, the revealed phase, physical and relaxation transformations were detected and discussed. The analysis of the obtained complex of standard thermodynamic and thermochemical characteristics of the investigated objects, the qualitative and quantitative dependences "thermodynamic property – composition", as well as the most general trends of changes in thermodynamic properties of compounds on their structures and physical states is given in detail. The established dependences can be successfully used for the prediction of methods of synthesis of the advanced materials with the required characteristics.

This work was performed with the financial support of the Russian Foundation for Basic Research (Project № 15-03-02112).

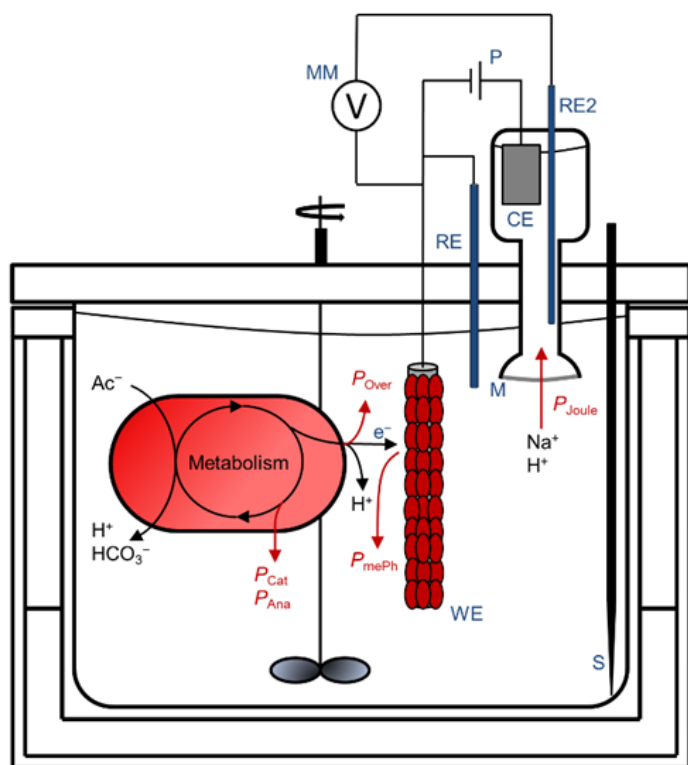
EFFICIENCY OF METABOLIC UTILIZATION OF NON-CHEMICAL ENERGY SOURCES.

Maskow T.¹

¹Department of Environmental Microbiology, WG Biocalorimetry/Ecothermodynamics, Helmholtz Centre for Environmental Research-UFZ, 04318 Leipzig, Germany
E-mail: Thomas.maskow@ufz.de

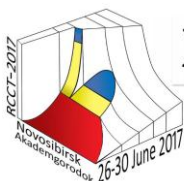
Chemoorganoheterotrophic organisms use the energy that is chemically linked to nutrients for biosynthesis, maintenance of the structures, replication and growth. The attainable growth efficiency¹ as well as the growth rates² are determined by thermodynamic rules and can be calorimetrically monitored in real time. This is of great practical importance if, for example, microorganisms are to be used as producers in the chemical industry. Interestingly, despite the impressive successes of biothermodynamics and calorimetry in the area of chemoorganoheterotrophic energy conservation, non-chemical energy sources for microbial growth (e.g. light and electricity) have been largely neglected. Here, the energy of photons and electrons allows the microbial reduction of CO₂ and make bio-reactions feasible which are thermodynamically not allowed. Potential reasons for this surprising lack of knowledge are challenges to develop the required tailor-made calorimeters and to quantify very low energy conversion efficiencies in case of photosynthesis.

For these reasons, new photocalorimeters and bioelectrocalorimeters were developed and tested. In the case of light energy, it is now possible to determine the efficiency of energy conservation as a function of light intensity and environmental conditions in real time with an accuracy which is not accessible by other methods. This was successfully confirmed for two examples: Microalgae of industrial (*Chlamydomonas reinhardtii*) and ecological (*Phaeodactylum tricornutum*) importance. In the case of electrical energy, we succeeded with our calorimeter in quantifying previously unknown energetic burden for growth on electrodes (i.e. microbial electrochemical Peltier heat).³ Scheme 1 shows exemplarily the principle of a bioelectrocalorimeter. Numerous applications of the new calorimetric techniques are conceivable.



Scheme 1: Illustration of the bioelectrocalorimeter and a simplified flow of metabolites, electrons, ions and heat during *Geobacter* biofilm growth on acetate (Ac⁻). Details are given in³.

- (1) Liu, J. S.; Vojinović, V.; Patiño, R.; Maskow, T.; von Stockar, U. *Thermochim. Acta* **2007**, *458*, 38-46.
- (2) Desmond-Le Quemener, E.; Bouchez, T. *ISME J* **2014**.
- (3) Korth, B.; Maskow, T.; Picioreanu, C.; Harnisch, F. *Energy Environ. Sci.* **2016**, *9*, 2539-2544.



THERMODYNAMIC AND THERMOPHYSICAL PROPERTIES OF BINARY MIXTURES CONTAINING AMINES OR ALCANOLAMINES

Ouaar F.¹, Feddal-Benabed B.¹, Negadi A.¹, Negadi L.^{1,2}, Mokbel I.^{3,4}, Jose J.³

¹ LATA2M, Laboratoire de Thermodynamique Appliquée et Modélisation Moléculaire, University of Tlemcen, Post Office Box 119, Tlemcen 13000 (Algeria)

² Thermodynamics Research Unit, School of Engineering, University of KwaZulu-Natal, Howard College Campus, Durban, 4041, South Africa.

³ Laboratoire Multimatériaux et Interfaces, UMR 5615, Université de Lyon, Université Claude Bernard Lyon1, 69622 Villeurbanne, France.

⁴ Université de Saint Etienne, Jean Monnet, F-42023 Saint Etienne, Université de Lyon, F-42023 Saint Etienne, France.

Abstract

Amines are an important class of compounds used in different fields of industry, they represent a particularly interesting family of molecules for the purpose of testing group-contribution models, and analyze of the intramolecular effects, especially the proximity effect.

The present work is part of a research program on thermodynamic and thermophysical properties of binary mixtures containing amines or alkanolamines.

In this paper, the vapor pressures of several aqueous solutions of amines, diamines, triamines or alkanolamines are reported. The vapor pressures were measured by means of two static devices at temperatures between (283 and 363) K. The data were correlated with the Antoine equation. From these data, excess Gibbs functions were calculated for several constant temperatures and fitted to a fourth-order Redlich-Kister equation using Barker's method.

The experimental data have been modeled using several methods such as NRTL, UNIQUAC, UNIFAC and its modifications.

Additionally, we report the experimental densities, speeds of sound, and refractive indices for four binary mixtures: DMSO + methylethanolamine (MEA), or + benzylamine, or + 3-dimethylaminol-1-propanol, or + 2-[2-(dimethylamino-ethoxy)-ethanol] measured over the entire composition range and in the temperatures range (293.15 to 323.15) K at 10 K intervals.

From these experimental data, excess molar volume, isentropic compressibility, excess isentropic compressibility, refractive index deviation, excess refractive index, molar refraction, and molar refraction deviation have been calculated over the entire composition range and at each temperature.

Excess molar volume, excess isentropic compressibility, excess speed of sound, excess refractive index, and molar refraction deviation data have been correlated using the Redlich-Kister equation. The thermodynamic properties have been discussed in terms of the nature of molecular interactions between the components of the mixture.

The experimental data have been compared to those obtained used the PSRK and VTPR equations of state.

Keywords: Amine, VLE, density, speed of sound, refractive index, models, equations of state.



DYNAMIC ASPECTS OF THERMOPHYSICAL PROCESSES IN ELECTROCERAMIC MATERIALS

Rotaru A.

¹INFLPR – National Institute for Laser, Plasma and Radiation Physics, Bvd. Atomistilor 409, Magurele, Jud. Ilfov, Bucharest, Romania

²Institute of Chemistry of the Academy of Sciences of Moldova, Str. Academiei 3, Chisinau, Republic of Moldova

³University of St Andrews, School of Chemistry, North Haugh, St Andrews, United Kingdom

⁴University of Cambridge, Department of Earth Sciences, Downing Street, Cambridge, United Kingdom

E-mail: andrei.rotaru@inflpr.ro

There is great interest in the development of new polar dielectric ceramics and multiferroic materials with new and improved properties. A family of tetragonal tungsten bronze (TTB) relaxors of composition $\text{Ba}_6\text{M}^{3+}\text{Nb}_9\text{O}_{30}$ ($\text{M}^{3+} = \text{Ga}^{3+}, \text{Sc}^{3+}$ and In^{3+} , and also their solid solutions) were studied in an attempt to understand their dielectric properties to enable design of novel polar TTB materials. A combination of electrical measurements (dielectric and impedance spectroscopy) and powder diffraction (X-ray and neutron) studies as a function of temperature was employed for characterising the dynamic dipole response in these materials. The effect of B-site doping on fundamental dipolar relaxation parameters were investigated by independently fitting the dielectric permittivity to the Vogel-Fulcher (VF) model, and the dielectric loss to Universal Dielectric Response (UDR) and Arrhenius models. These studies showed an increase in the characteristic dipole freezing temperature (T_f) with increase B-cation radius. Crystallographic data indicated a corresponding maximum in tetragonal strain at T_f , consistent with the slowing and eventual freezing of dipoles. In addition, the B1 crystallographic site was shown to be most active in terms of the dipolar response.

A more in-depth analysis of the relaxor behaviour of these materials revealed that, with the stepwise increase in the ionic radius of the M^{3+} cation on the B-site within the Sc-In solid solution series, the Vogel-Fulcher curves ($\ln f$ vs. T_m) are displaced to higher temperatures, while the degree of relaxor behaviour (frequency dependence) increases. Unfortunately, additional features appear in the dielectric spectroscopy data, dramatically affecting the Vogel-Fulcher fitting parameters. A parametric study of the reproducibility of acquisition and analysis of dielectric data was therefore carried out. The applicability of the Vogel-Fulcher expression to fit dielectric permittivity data was investigated, from the simple unrestricted (“free”) fit to a wider range of imposed values for the VF relaxation parameters that fit with high accuracy the experimental data. The reproducibility of the dielectric data and the relaxation parameters obtained by VF fitting were shown to be highly sensitive to the thermal history of samples and also the conditions during dielectric data acquisition (*i.e.*, heating/cooling rate). In contrast, UDR analysis of the dielectric loss data provided far more reproducible results, and to an extent was able to partially deconvolute the additional relaxation processes present in these materials. The exact nature of these additional relaxations is not yet fully understood.

The ferroic properties of interest are coupled with strain, which will be important in the context of stability, switching dynamics and thin film properties. Coupling of strain with the ferroelectric order parameter give rise to changes in elastic properties and these have been investigated for the ceramic sample of $\text{Ba}_6\text{GaNb}_9\text{O}_{30}$ (BGNO) by resonant ultrasound spectroscopy (RUS). Room temperature values of the shear and bulk moduli for BGNO are rather higher than for TTB’s with related composition which are orthorhombic at room temperature, consistent with suppression of the ferroelectric transition. Instead, a broad, rounded minimum in the shear modulus measured at ~ 1 MHz is accompanied by a broad rounded maximum in acoustic loss near 115 K, and signifies relaxor freezing behaviour. Elastic softening with falling temperature from room temperature, ahead of the freezing interval, is attributed to the development of dynamical polar nanoregions (PNRs), while the non-linear stiffening below ~ 115 K is consistent with a spectrum of relaxation times for freezing of the PNR microstructure.

ANALYSIS OF SOLID-SOLID TRANSITIONS VIA MELTING AND NON-MELTING

Schubnell M., Schawe Jü.

Mettler-Toledo AG, CH-8603 Schwerzenbach, Switzerland

E-mail: markus.schubnell@mt.com

Solid–solid transitions can occur through melting or without melting in between the transition. The first case designates so called monotropic transitions in which metastable modifications are involved. Solid–solid transitions without intermediate melting are referred as enantiotropic transitions and occur among stable modifications. In this contribution we show how such transitions can be analyzed by conventional DSC and fast scanning calorimetry. We also show how such data can be used to determine the respective thermodynamic potentials.

We first discuss some fundamental differences among enantiotropic and monotropic transitions. We then focus on the analysis of solid–solid transitions via melting in metals. As an example we extensively investigate such transitions in $\text{Au}_{70}\text{Cu}_{5.5}\text{Ag}_{7.5}\text{Si}_{17}$. As a result we could identify for the first time a monotropic transition in a metal (see Figure 1).

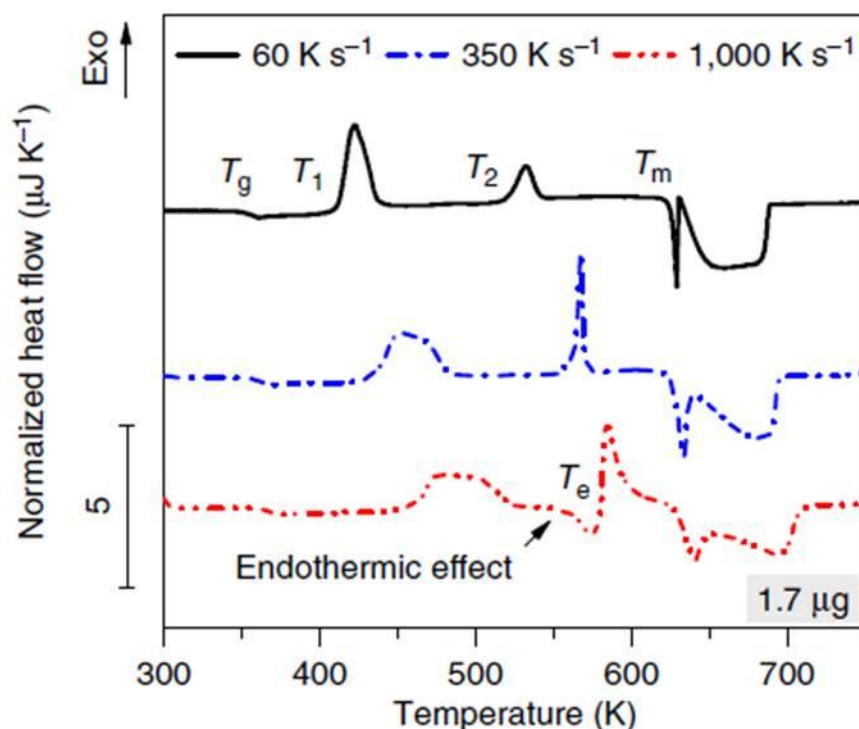
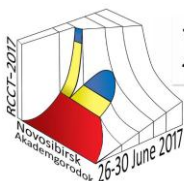


Figure 1. Transitions in amorphous $\text{Au}_{70}\text{Cu}_{5.5}\text{Ag}_{7.5}\text{Si}_{17}$ upon heating at different heating rates. The exothermic peaks after T_g are traditionally understood as crystallization (T_1) and a solid–solid transition (T_2). Melting occurs from T_m onwards (black curve, heating rate 60 K/s). If the same material is heated at 1000 K/s (red curve) it can be seen that before the supposed solid–solid transition an endothermic peak occurs at T_e . This corresponds to the melting of the crystals formed at T_1 . This indicates that the crystals formed at T_1 are metastable.

Reference

S. Pogartscher, D. Leutenegger, J. E. K. Schawe, P. J. Ugowitz, J. F. Löffler; Solid–solid phase transition via melting in metals; Nat. Commun. 7:11113 doi: 10.1038/ncomms11113 (2016)



THERMAL ANALYSIS IN MATERIALS SCIENCE

Szilágyi I. M.^{1,2,*}

¹*Budapest University of Technology and Economics, Department of Inorganic and Analytical Chemistry, H-1111 Budapest, Hungary;*

²*MTA-BME Technical Analytical Chemistry Research Group, H-1111 Budapest, Hungary;*

*E-mail: imre.szilagyi@mail.bme.hu

The lecture gives an overview and shows trends about the main fields where thermal analysis is used in materials science – based on the recent publications in the Journal of Thermal Analysis and Calorimetry, where the author works as editor-in-chief. These areas include e.g. organometallic complexes, clays, cement and concrete, glasses, alloys, salts, propellants, nanomaterials, composites, phase change materials, biomass, liquid crystals, etc.

Consecutively, selected case studies are given based on the author's experience about the application of thermal analysis in materials science. The thermal behavior of tungsten oxides, tungstates and tungsten bronzes is discussed, and the importance of their thermal treatment in light source industry, photocatalysis and gas sensing is presented. The thermal behavior of nanofibers prepared by electrospinning is shown. The use of thermal analysis in preparing various carbon nanostructures (fulleren, graphene oxide, etc) and their composites is presented.



ATOMISTIC MOLECULAR SIMULATIONS FOR ENGINEERING APPLICATIONS: METHODS, TOOLS AND RESULTS

Vrabec J. et al.

Thermodynamics and Energy Technology, University of Paderborn, Germany,
jadran.vrabec@upb.de

Molecular modeling and simulation has a sound physical basis and is a versatile approach to numerous challenges in chemical engineering. It relies on models for the molecular interactions which, once they are parameterized, contain the complete thermodynamic behavior of the considered material. This goes far beyond classical models, such as equations of state which describe e.g. thermal and caloric properties of bulk phases only. Molecular models also contain information on transport properties, the behavior of matter at interfaces, in pores, during phase changes and under many other conditions. Moreover, the spatial and temporal resolution is typically many orders of magnitudes better than in case of experimental approaches, while similar accuracies can often be reached.

The crucial ingredients are molecular models, which nowadays often rely on quantum chemical *ab initio* data, computational tools that embody simulation methods and computing power.

In this presentation, a short introduction into the development of molecular models is given [1]. Examples of their predictive capabilities for fluid phase equilibria [2] and transport properties of liquids [3] are discussed with respect to strongly non-ideal mixtures. Mutual diffusion data are particularly interesting, because most separation processes, such as distillation, absorption or extraction, are affected by diffusion in liquids. However, the experimental data base is insufficient, especially for multicomponent liquid mixtures.

Thermodynamic properties are a crucial foundation for the design and optimization of chemical engineering processes and they are generally in too short supply. While the classical experimental route is often time consuming, expensive or sometimes even impossible, predictive molecular simulation data can be generated very rapidly for a tiny fraction of the cost. To facilitate this task, the molecular simulation tool *ms2* [4] is co-developed by the author, covering a broad range of systems and properties. Being well optimized for parallel execution on modern computing infrastructure, from PC workstations over clusters to high performance computers, it can generate large thermodynamic datasets with short response times [5].

A new route to devise fundamental equations of state in the form of the Helmholtz energy is laid out for fluids for which very few experimental data are available. Experimental and simulation data are combined to hybrid datasets. On such a basis, fundamental equations of state can be parameterized also for hazardous fluids like ethylene oxide [6].

Fluid phase interfaces [7] and processes across them, like during evaporation [8] or condensation, are of fundamental importance in chemical engineering. Because of the small spatial scale, experiments on their structure and dynamics are hardly feasible. In this presentation, molecular dynamics results on the interface of liquid acetone in highly compressed nitrogen gas are discussed. Moreover, non-equilibrium simulations of the evaporation of a model fluid are shown.

[1] Deublein et al., *Mol. Sim.* **39**: 109-118 (2013)

[2] Merker et al., *AIChE J.* **59**: 2236-2250 (2013)

[3] Parez et al., *Phys. Chem. Chem. Phys.* **15**: 3985-4001 (2013)

[4] Glass et al., *Comput. Phys. Commun.* **185**: 3302-3306 (2014)

[5] Rutkai et al., *J. Chem. Eng. Data* **60**: 2895-2905 (2015)

[6] Thol et al., *Chem. Eng. Sci.* **121**: 87-99 (2015) and **134**: 887-890 (2015)

[7] Eckelsbach et al., *Phys. Chem. Chem. Phys.* **17**: 27195-27203 (2015)

[8] Lotfi et al., *Int. J. Heat Mass Transf.* **73**: 303-317 (2014)



HEAT CAPACITIES, EXCESS ENTROPIES, AND MAGNETIC PROPERTIES OF BULK AND NANO $\text{Fe}_3\text{O}_4\text{-Co}_3\text{O}_4$ AND $\text{Fe}_3\text{O}_4\text{-Mn}_3\text{O}_4$ SPINEL SOLID SOLUTIONS

Schliesser J.M.¹, Huang B.¹, Sahu S.K.², Navrotsky A.², and Woodfield B.F.¹

¹Department Of Chemistry, Brigham Young University, Provo, UT 84602, USA

²Peter A. Rock Thermochemistry Laboratory and NEAT ORU, University of California Davis, Davis, CA 95616, USA

E-mail: brian_woodfield@byu.edu

We have measured the heat capacities of several well-characterized bulk and nanophase $\text{Fe}_3\text{O}_4\text{-Co}_3\text{O}_4$ and $\text{Fe}_3\text{O}_4\text{-Mn}_3\text{O}_4$ spinel solid solution samples from which magnetic properties of transitions and third-law entropies have been determined. The magnetic transitions show several features common to effects of particle and magnetic domain sizes. From the standard molar entropies, excess entropies of mixing have been generated for these solid solutions and compared with configurational entropies determined previously by assuming appropriate cation and valence distributions. The vibrational and magnetic excess entropies for bulk materials are comparable in magnitude to the respective configurational entropies indicating that *excess* entropies of mixing must be included when analyzing entropies of mixing. The excess entropies for nanophase materials are even larger than the configurational entropies. Changes in valence, cation distribution, bonding and microstructure between the mixing ions are the likely sources of the positive excess entropies of mixing.



STRUCTURE-PROPERTY RELATIONS IN VAPORIZATION THERMODYNAMICS: MOLECULAR LIQUIDS *vs* IONIC LIQUIDS

Zaitsau D.

Chemical Department, Samara State Technical University, 443100, Samara, Russia

E-mail: ZaitsauDz@gmail.com

Molecular solvents have been used for a long time as main reaction media for synthesis: from cooking food to many stage industrial syntheses of biomolecules. The purification of the target product is the main energy consumption of the industrial synthesis. Ionic liquids (ILs) were recently proposed to be a perspective media for synthesis decreasing the purification costs. These compounds consist of the bulky organic cation and organic or inorganic counter ion. The ion interaction in ILs is suppressed by the steric repulsion of the bulky cations and leads to low melting temperature. The low melting temperature clears the ways for ILs as a synthesis media.

The liquid state of ILs is not the only their positive feature, they also possess extremely low vapor pressure, the wide electrochemical window, and the high conductivity. The great advantage of ILs is numerical degrees of structural freedom which can be applied to design the structure of IL and altering the physical properties (viscosity, density, solubility) together with polarity and aromatic and so on according to needs.

The enthalpy of vaporization is the key value for understanding the inter- and intra-molecular interaction in materials, for example through molecular simulation computation techniques. Experimental determination of the vaporization enthalpies for systems with such extremely low vapor pressure and thermal lability is a challenging task. But during the last ten years, we have come a long way *per aspera* to develop and improve the set of experimental techniques allowing determination of the vaporization enthalpy and in many cases absolute vapor pressures even for systems with low thermal stability. From the other side, plenty degrees of structural freedom in ILs spoil the approach of measuring the enthalpy of vaporization for all ILs as the number of possible ILs is too high ($\sim 10^{18}$).

The only way to solve such problem is creating the simple but reliable correlation between the ILs structure and its enthalpy of vaporization. Application of the additive approaches has shown the similarities as well as significant differences in vaporization enthalpy for molecular and ionic liquids.

Thus, for molecular systems, the additivity of the vaporization enthalpy is an ordinary case and the most observed deviations correspond to strong interactions in molecules like H-bands. But in the case of ILs strong coulomb interaction is an ordinary case and therefore deviations from the additivity are often observed.

Enthalpy of vaporization can be presented as the difference in the enthalpy of formation of liquid and gas phases. Both values are additive for molecular substances. But in the case of ILs such additivity is not obvious and should be investigated in each case.

We have analyzed the enthalpies of vaporization for series of ILs with different cations (imidazolium, pyridinium, and ammonium) and anions (halides, BF_4 , PF_6 , NTf_2 , and so on). For all systems observed the value of the vaporization enthalpy of CH_2 increment $\Delta_l^g H_m^o(\text{CH}_2)$ is significantly lower (2.3 to 4.0 $\text{kJ}\cdot\text{mol}^{-1}$) than that of alkane and other molecular compounds (4.5 to 5.0 $\text{kJ}\cdot\text{mol}^{-1}$).

Observed deviations can be assessed to the gas or liquid phase structuring. In the case of molecular compounds the decrease of the vaporization increment is observed and in most case, this corresponds to the transfer of the residual specific inter- intra-molecular interaction from the liquid into the gas phase and corresponding decrease of vaporization enthalpy.

In the case of ILs not only decrease of the vaporization increment is corresponds to the change in the structure of the liquid phase.



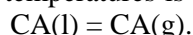
**COMPETITION BETWEEN VAPORIZATION AND
DECOMPOSITION OF IONIC LIQUIDS.
AN UNSOLVED PROBLEM REGARDING THEIR THERMAL STABILITIES**

Vecchio Cipriotti S.

Dipartimento S.B.A.I., Sapienza University of Rome, 00161 Rome, Italy

E-mail: stefano.vecchio@uniroma1.it

Ionic liquids (ILs) have received much attention in the last ten years, due to their remarkable properties, and among them their high thermal stability and low volatility. In spite of their claimed low volatility, the vapor pressure of several ILs is low, but still measurable at temperatures lower than those where decomposition takes place. In some studies, it was assumed *a priori* that the only (or largely prevailing) process taking place under heating at moderate temperatures is the simple vaporization to single, integer ion pairs CA:



However, in some cases vaporization and thermal degradation may simultaneously occur at different extent, depending on the nature of the IL as well as on the experimental condition used. At this regard, many efforts were directed to the development of experimental procedures aimed at performing measurements in temperature ranges as low as possible. This requirement is especially important for ionic liquids that are known to be more sensitive to thermal degradation, due to the existence of preferential decomposition pathways. Since thermal degradation is likely to lead to the formation of volatile products, it may bring about serious errors in vapor pressure measurements performed with techniques where the nature of the species present in the vapor phase cannot be ascertained.

A multi-technique approach was recently undertaken to tackle this delicate issue, which combines classic Knudsen cell thermogravimetry (KEML, Knudsen Effusion Mass Loss), simultaneous thermogravimetry and differential thermal analysis (TG-DTA), and Knudsen cell mass spectrometry (KEMS) measurements [1]. The latter technique, in particular, enables one to get information on the nature of the gaseous species existing in the saturated vapors, although fragmentation processes may complicate the task. Recently, monocationic and dicationic alkylimidazolium ionic liquids were investigated [2], and the results suggested that decomposition starts to occur at temperatures remarkably lower than those determined as onset by TG. In particular, while our measurements confirm the high stability of monocationic alkylimidazolium NTf₂, we have evidence that the higher stability of the corresponding dicationic species claimed in the recent literature [3] is at least overestimated. Indeed, although dicationic ionic liquid with NTf₂ anion exhibits significantly lower vapor pressures than the corresponding monocationic ones, thermal decomposition in the liquid phase seems to occur at lower temperatures. The very low stabilities of monocationic chloride and iodide were also confirmed from the analysis of KEMS spectra and from the low reproducibility of KEML results carried out by varying the diameter of the effusion hole. On continuing this research, we have explored in this study the role of some operative conditions in affecting the competition between thermal decomposition and vaporization of 3-butyl-1-methylimidazolium hexafluorophosphate ([C₄mim][PF₆]) by carrying out TG/DTA experiments under two different inert gas atmospheres (in open surface), according to a procedure reported in literature [4], thus confirming that under the conditions used the extent of decomposition cannot be neglected. Furthermore, effusing experiments with both KEML and KEMS techniques were performed on [C₄mim][PF₆] with the aim to ascertain how factors like the material of the crucibles and the diameter of the effusing hole may play a role on the competition between evaporation and decomposition processes that can take place simultaneously [5]. The most important findings are presented here, and critically discussed.

[1] Brunetti, B.; Ciccioli, A.; Gigli, G.; Lapi, A.; Misceo, N.; Tanzi, L.; Vecchio Cipriotti, S. *Phys. Chem. Chem. Phys.*, 2014, 16(29), 15653-15661.

[2] Brunetti, B.; Ciccioli, A.; Gigli, G.; Lapi, A.; Vecchio Cipriotti, S. *XX International Conference on Chemical Thermodynamics in Russia (RCCT 2015)*, Nizhni Novgorod, (Russia), June 22-26, 2015.

[3] Shirota, H.; Mandai, T.; Fukazawa, H; Kato T. *J. Chem. Eng. Data, Chem.*, 2011, 56, 2453-2459.

[4] Heym, F.; Etzold, B.J.M.; Kern, C.; Jess, A. *Green Chem.* 2011, 13, 1453-1466.

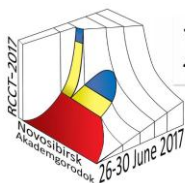
[5] Volpe, V.; Brunetti, B.; Gigli, G.; Lapi, A.; Vecchio Cipriotti, S.; Ciccioli, A. *J. Phys. Chem. B*, *submitted*, 2017.



XXI International Conference on Chemical Thermodynamics in Russia (RCCT-2017)

26-30 June 2017, Akademgorodok, Novosibirsk

Lectures of the School-conference on chemical thermodynamics for young scientists



CONCEPT ABOUT A BODY PATH AS A BASIS IN THE ANALYSIS OF BARO-, THERMO-, VOLUMO- AND A CALORIMETRY APPLICATIONS IN CHEMICAL THERMODYNAMICS

Belevantsev V.I.¹, Ryzhikh A.P.^{1,2}

¹Nikolaev Institute of Inorganic Chemistry, Siberian Branch of the Russian Academy of Sciences, 630090 Novosibirsk, Russia

²Novosibirsk State Pedagogical University, 630126 Novosibirsk, Russia

E-mail: ryzhikh@niic.nsc.ru

In works [1, 2] (made on the basis of earlier generalizations [3]) is strictly shown that the full interpretation of colligative properties of solutions is impossible without directly addressing the specifics of the detailed components in comparison with the initial (independent according to Gibbs [4, p.68-69]) and to the principle of universal behavior of matter in diffuse state (following van't Hoff [5]). The purpose of our report - analysis and addition to the consequences with emphasis on the first [4, p. 9-39 (I)] of the three interrelated steps of the Gibbs to the chemical thermodynamics. This step is the main and fundamental as for the formation of the second [4, p. 40-60 (II)] and third [4, p. 61-118, 140-146, 152-186 (III)], and for the modern ideas about chemical forms and detailed components [1, 2, 6]. The basis of these ideas are problem-oriented generalizations, including in the framework of the classical chain composition – structure – properties. This applies not only to liquids and gases (fluids following the Gibbs), but also solids (e.g., in the analysis of solid solutions or defect structures in solids). Detailing of arbitrarily chosen phase (a portion of gas, liquid or solid) states in terms of the "body path" on the basis of the fundamental equation ($dU = \delta Q - \delta A = TdS - PdV$) lead to the equivalences presented in table.

Table 1. The consequences of the expansions of the elementary heats.

I	(S, V)	$C_{V/S} = (\delta Q/dS)_V \equiv \delta Q_{V/S} / dS = (\partial U/\partial S)_V = T = (\partial H/\partial S)_P$
II	(T, V)	$C_V \equiv C_{V/T} = (\delta Q/dT)_V \equiv \delta Q_{V/T} / dT = T(\partial S/\partial T)_V = (\partial U/\partial T)_V$
		$l_T \equiv C_{T/V} = (\delta Q/dV)_T \equiv \delta Q_{T/V} / dV = T(\partial S/\partial V)_T = (\partial U/\partial V)_T + P = T(\partial P/\partial T)_V = -T(\partial V/\partial T)_P / (\partial V/\partial P)_T = T(\alpha/\chi)$
III	(P, V)	$C_{V/P} = (\delta Q/dP)_V \equiv \delta Q_{V/P} / dP = T(\partial S/\partial P)_V = (\partial U/\partial P)_V$
		$C_{P/V} = (\delta Q/dV)_P \equiv \delta Q_{P/V} / dV = T(\partial S/\partial V)_P = (\partial U/\partial V)_P + P$
VI	(T, P)	$C_P \equiv C_{P/T} = (\delta Q/dT)_P \equiv \delta Q_{P/T} / dT = T(\partial S/\partial T)_P = (\partial U/\partial T)_P + P(\partial V/\partial T)_P = (\partial H/\partial T)_P = C_V + T(V\alpha^2/\chi)$
		$h_T \equiv C_{T/P} = (\delta Q/dP)_T \equiv \delta Q_{T/P} / dP = T(\partial S/\partial P)_T = (\partial U/\partial P)_T + P(\partial V/\partial P)_T = -T(\partial V/\partial T)_P = -TV\alpha$

Similarly, one can enter and consider the notion on “work capacity” as well.

[1] Belevantsev, VI; Ryzhikh, AP. Russ. J. Phys. Chem. A. 2011, 85, 747-750.

[2] Belevantsev, VI; Ryzhikh, AP. Russ. J. Gen. Chem., 2014, 84, 979-985.

[3] Belevantsev, VI. J. Struct. Chem., 1998, 39, 224-229.

[4] Gibbs J.W. Thermodynamika. Statisticheskay mekhanika.- M.: Nauka, 1982. 584 p..

[5] Van't Hoff J.H. Chimicheskoe ravnovesie.- M., 1902. P. 2-30, 85-100.

[6] Belevantsev, VI; Ryzhikh, AP; Terekhova, IS; Villeval'd, GV. Russ. J. Gen. Chem., 2015, 85, 1558-1564.



MODERN MEASUREMENTS, CURVE FITTING, AND ANALYSIS OF HEAT CAPACITY DATA

Woodfield B.F.¹

¹*Department Of Chemistry, Brigham Young University, Provo, UT 84602, USA*

E-mail: brian_woodfield@byu.edu

Since the beginning of the twentieth century, specific heat measurements have been a useful tool for studying the physical and thermodynamic properties of materials. While the specific heat and other thermodynamic properties of many compounds are already known, specific heat measurements continue to provide new insights into the properties of modern materials, and these insights help us to think about materials in new ways. Unlike the vibrational information provided by methods such as Raman or infrared spectroscopy, specific heat measurements make no distinction between the vibrational, magnetic, or electronic energies in a system, thus the specific heat provides a complete measure of all the energy states in a system. Furthermore, the specific heat also provides a measure of the absolute entropy and enthalpy increment of materials, which can be used in conjunction with enthalpies of formation to calculate the free energy landscape.

Specific heat is a bulk property, yet the low-temperature specific heat is extremely sensitive to electronic, magnetic and structural changes present in a system as well as to sample impurities down to the part per million range depending on the impurity. For these reasons, specific heat measurements are a useful tool in understanding the chemistry and physics of systems, since from thermodynamics and quantum theory, it is possible to extract information on the lattice vibrations, electronic contributions, magnetic properties, and a variety of other phenomena. Thus, the specific heat is a unique and powerful tool to provide a window into understanding the intrinsic properties of materials. While the specific heat may have been in use for over a century, measurement and analysis techniques continue to evolve to keep the specific heat relevant in modern chemistry and physics.

In this talk we will provide an overview of currently available measurement techniques for the specific heat, the importance of temperature scales, curve fitting techniques to extract theoretical parameters, and we will end by putting it all together to discuss some interesting material systems where the specific heat has provided unique insights into the materials available in no other way. Truly, the specific heat is a technique that can do it all.



THERMODYNAMICS AND KINETICS OF THE DIRECTED SYNTHESIS OF SEMICONDUCTOR MATERIALS

Zlomanov V.P., Gaskov A.M., Kotin P.A.

Lomonosov Moscow State University, Department of chemistry, 119991 Moscow, Russia

E-mail: zlomanov1@mail.ru

Semiconductor materials are substances with specified functional properties, which have a strong dependence on external influences such as temperature, illumination, electric and magnetic fields, hydrostatic pressure. In turn, this dependence is determined by a) composition - the nature and concentration of the particles forming the substance, b) their interaction energy ΔG , c) structure - the order in their spatial arrangement, and finally d) size. The transformation of matter includes a set of chemical reactions that result in changes to one or more characteristics of a substance. Thermodynamics and kinetics of such reactions are in consideration.

In characterizing the composition of complex substances, it is necessary to include not only the stoichiometry and impurity content, and the related concentration of intrinsic and impurity defects. In this regard, the classification of defects, their formation processes, methods of management of the defect composition. The distribution of intrinsic and impurity defects in a substance is random. In this regard, the statistical criteria of homogeneity of a pure substance are discussed.

The interaction energy $\Delta G = \Delta H - T\Delta S$ of the particles includes enthalpy (ΔH) and entropy (ΔS) components. The first of them characterizes ordinary chemical bond associated with the electron density distribution, and the second - topological, or "non-chemical" bond.

An important characteristic of substance is the particle size. In the nanometer range (1-100 nm) the surface and bulk energies are comparable, and it becomes possible the formation of new physical and chemical properties of nanoparticles. In addition, when the commensurability of the geometric dimensions of nanoparticles with a wavelength de Broglie of electrons observed quantum-size effect. It is associated with the quantization energy of the charge carriers, which movement is limited in one, two, or three directions.

The size and shape of nanoparticles significantly affect their functional characteristics. In this connection, some peculiarities of the preparation and the morphology control of nanocrystals are considered. For the synthesis of anisotropic nanocrystals are the most common methods of colloidal chemistry using high-boiling organic solvents. Conditions of synthesis - temperature, pH, type of stabilizer and solvent, the addition of specific inhibitors of growth of specific faces, and the use of external influences (microwave or laser radiation) can allow to control the size and shape of nanocrystals.



SPONSOR

INTRODUCTION TO THEMYS, THE INNOVATIVE THERMAL ANALYSIS PLATFORM

Fabrice BANCEL¹, Rémi ANDRE¹

¹SETARAM Instrumentation, 7 rue de l'Oratoire, 69300 CALUIRE, FRANCE

E-mail: bancel@setaram.com

As it was recently published, new and suitable experimental data are necessary for accurate materials thermodynamics. In order to fit with the needs of the field, the new **THEMYS thermal analysis platform** was designed, based on the feedback from experimentalists, with the objectives of enhancing the **control of experimental conditions** and the **instrument versatility**, and improving the **results quality** and **ease of use**. These features and experimental data will be detailed during the presentation.

THEMYS (RT – 1750°C) provides accurate **control of the furnace atmosphere**, with different options including mass flow controllers, gas switching and blending devices, vacuum pumps and gauges. They all have in common an intelligent software control system for changing sequentially the gases types, flowrates, or blend ratios during the experiment or sample pretreatment. Primary, forced primary or secondary **vacuum options** are available with a selection of adapted vacuum pumps with pre-programmed procedures for stepwise sample evacuation.

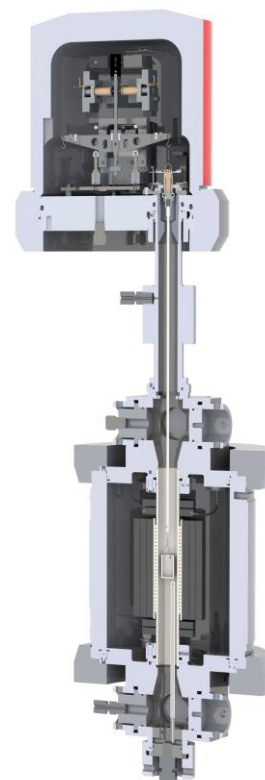
Three optional balance models based on the hang-down design are offered. The **HIGH SENSITIVITY balance** is designed for the accurate study of very small mass variations. It has the best noise level, the best limit of detection and the best isothermal drift. **HIGH CAPACITY** has a +/- 3000 mg mass variation range which makes it perfect for experiments that lead to the full decomposition of large samples, like it is required with heterogeneous materials. The **HIGH VERSATILITY balance** is equipped with the AUTO-TARE system. It virtually avoids the need to manually equilibrate the balance between tests. It is perfect to get the full potential of the THEMYS platform modularity, when it is necessary to change frequently samples types, crucibles, or other experimental conditions.

THEMYS HP TGA is a robust, flexible high pressure version based on the vertical hang-down principle and operating on a temperature and pressure range **up to 1200 °C and 150 bar**.

THEMYS is designed for **Evolved Gas Analysis** by coupling to the main gas analysis techniques: mass spectrometry, FTIR spectrometry, gas chromatography, and combinations of these. Moreover, the THEMYS furnace allows for **in-situ analyses** with two 4-ports parts placed at its top and bottom. Up to 8 extra sensors can be connected: humidity, oxygen or other measurement could be achieved.

Daily operation like balance opening, balance beam locking are made easier with tool-free operating systems. Thermocouple change has become handier than ever with the **TWIST AND LOCK** system: it is fast, does not require tools, and the thermocouple's temperature range is detected automatically.

[1] Ipsier, H. J. Phase Equilib. Diffus. (2017) 38: 1.



THEMYS Thermal Analysis platform



Section 1.

General problems of chemical thermodynamics

Oral presentations



HEAT AND WORK OF THE CHEMICAL SYSTEMS

Bazhin N.M.^{1,2}

¹Voevodsky Institute of Chemical Kinetics and Combustion, Siberian Branch of the Russian Academy of Sciences, 630090 Novosibirsk, Russia, ²Novosibirsk State University, 630090 Novosibirsk, Russia

E-mail: bazhin8999@kinetics.nsc.ru

The most common point of view on the work of the reversible chemical systems is that the reversible work at a constant temperature and pressure is carried out by the Gibbs energy $w'_{\text{useful}} = \Delta G = \Delta H - T\Delta S$, where ΔG , ΔH and ΔS are change in reaction Gibbs function, enthalpy and entropy. However, there is another opinion. Analysis of ideal gas expansion in vacuum shows that the Gibbs energy is not conserved. Therefore, the Gibbs energy is not true energy. Nevertheless, useful work is equal to the Gibbs energy change.

Let us consider for simplicity the reaction with $\Delta H < 0$ and $\Delta S > 0$. In that case ΔH and $-T\Delta S$ have the negative signs. It is generally recognized that the work in volume $-T\Delta S$ is performed by thermostat heat. Tools for the work production have a high specialization: they can consume energy only one type. Consequently, the energy in volume ΔH must be dragged as heat from the thermostat. Despite the existence of two members in ΔG , the only source of energy for work production is heat of the thermostat $w'_{\text{useful}} = \Delta G(\text{система}) = \Delta H(w, \text{термостат})$. Chemical energy of the system (ΔH) is not used for the production of the work and is released as heat. Violation of the second law does not exist as simultaneously the reaction takes place in the system. In some systems it is possible receive heat and work separately, ie receive double volume of energy.

The paper is considered the heat generation and work on concrete examples, namely mechanical, osmotic, galvanic and living systems

Production of mechanical energy has been demonstrated by van't Hoff in 1884 on the system, which is called now as the van't Hoff equilibrium box (VHEB). The coal oxidation reaction is considered in our work with VHEB. Mechanical energy is the result of heat consumption from thermostat with pistons and cylinders. VHEB separately produces mechanical energy in the volume ΔG and heat in the volume ΔH . The Pressure Retarded Osmosis (PRO) system was used for osmotic work demonstration. It was shown that the reversible mixing of fresh and salt water produces the cooling of the mixed solutions. Cooling of the resulting solutions in a reversible double dilution is approximately 0.1 °C. The dragged heat is spent for mixed solution formation under pressure $p < \Pi$ (osmotic pressure). Subsequently, the resulting solution is routed to a turbine to produce electrical energy. PRO system is the most "green" way to produce energy: energy is generated by cooling the environment, and after the use of the produced energy it is returned to the environment in the form of heat.

The mechanism of electrical energy formation in electrochemical cells is demonstrated on the example of concentration element consisting of two zinc electrodes. Electrical energy is created by the cooling in a cell. The cooling of the electrodes is produced during motion of zinc ions against the electric field from metal zinc into bulk of solution for equilibrium restoration disturbed by current. Similarly works galvanic cell, consisting, for example, copper and zinc electrodes. Chemical energy of reaction is released as heat.

The energy transformation in living systems is discussed.

Conclusion.

1. Gibbs energy is not energy. Gibbs energy should be called as a Gibbs function (There is no contradiction with the IUPAC).
2. The reversible work at constant temperature and pressure is equal the Gibbs function change, but work is produced only due to the heat of the thermostat: $w'_{\text{useful}} = \Delta G(\text{system}) = \Delta H(w, \text{thermostat})$.

There are no violations of the second law as simultaneously chemical reaction takes place.

3. The chemical energy, equal ΔH , evolves only in the form of heat and is not used to produce the work.
4. Some chemical systems can produce double amount of energy: $\Delta H + \Delta G$.



MODELING OF HEAT CAPACITY CURVES

Gavrichev K.S., Golushina L.N.

Kurnakov Institute of General and Inorganic Chemistry of the Russian Academy of Sciences, 119991 Moscow, Russia

E-mail: gavrich@igic.ras.ru

Modeling of temperature dependences of the heat capacity plays an important role in chemical thermodynamics and solid-state physics for the evaluation of a thermodynamic functions and some important parameters of a solid body. Modeling of heat capacity and mathematical description of heat capacity data should be distinguished. The main objectives of mathematical description of heat capacity curve are to minimize the deviation of experimental data from the smoothed values and to interpolate $C_p(T)$ data for selected temperature in the studied range. In mathematical description of $C_p(T)$ dependence by spline approximation or polynomials the extrapolation can lead to large errors. The exception, perhaps, is the equation of Maier-Kelley [1] for the description of the heat capacity at high temperatures. An important property of the modelled $C_p(T)$ curves is the use of physical principles, that allows the extrapolation of the temperature dependence beyond the investigated temperature range.

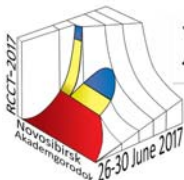
Among the existing models of heat capacity the most applicable are Einstein [2], Debye [3], Kieffer [4], Blackman [5], Tarasov [6] models, in which the heat capacity is correlated with the spectral characteristics. In the relatively recent works the model of Komada-Westrum [7] can be noted, in which, in addition to the characteristic temperature, authors used the mass of the molecules. Heat capacities of complex compounds are satisfactorily described by the additive scheme, in which the different contributions are calculated according to the above mentioned models for each type of motion in the molecule [8]. The latest efforts in the heat capacity modeling were conducted with the application of fractal approach [9, 10]. Additive scheme allows, in some cases, to solve satisfactorily the inverse problem – estimation of the spectral characteristics based on the temperature dependence of heat capacity. Shape of the heat capacity contribution due to rotational degrees of freedom can be, depending on the magnitude of the energy barrier, changed from Sigma-shaped to curve with a gentle maximum. Form of contribution associated with the splitting of the energy levels, can also have a different view. The extraction of contributions in additive scheme proceeds successively with increasing the characteristic temperatures (frequencies) of the individual contributions.

Acknowledgements

This study was carried out by the partial support of RFBR 15-03-04388 (for RE zirconates) and State assignment on fundamental researches of IGIC RAS (0088-2014-0003) (for RE phosphates and vanadates).

References.

1. Maier C.G., Kelley K.K. // *Journal of American Chemical Society*. 1932. V.54. P.3243.
2. Einstein A. // *Annalen der Physik*. 1907. B.22. T.180.
3. Debye P. // *Annalen der Physik*. 1912. B.39. T.789.
4. Kieffer S.W. // *Review of Geophysics and Space Physics*. 1979. V.17. P.35.
5. Blackman M. *Specific Heat of Solids*. In *Handbuch der Physik*, B.: Springer, 1955. V.7. Pt.1. P.325.
6. Tarasov V.V. // *Russian Journal of Physical Chemistry*. 1950. V.24. №1. P.111.
7. Westrum E.F., Komada N. // *Thermochimica Acta*, 1986, v.109, p.11.
8. Sakamoto Y. // *Journal of Sciences of Hiroshima University*. 1954. V.17A. No.3. P.397.
9. Yakubov T.S. // *Doklady AN SSSR*. 1990. V.310. P.145.
10. V.B. Lazarev et al. // *Thermochimica Acta*. 1995. V.269/270. P.109.

**THERMODYNAMICS AND KINETICS OF THE NANO-SCALE STAGES OF THE CRYSTAL NUCLEATION FROM LIQUID PHASE**

Kidyarov B.I.

Rzhanov Institute of Semiconductor Physics, Siberian Branch of the Russian Academy of Sciences, 630090 Novosibirsk, Russia
E-mail: kidyarov@isp.nsc.ru

The many experimental data on nano-scale stage of the nucleation kinetics from liquid phase can be explained only by the theory of multi-barrier processes of non steady-state nucleation [1]. The simple stationary nucleation can be also possible in real super-cooled liquid at some condition. But it is observed as rule non steady state nucleation with monotonously increased, or decreased rate of nucleation ($J(t)$), and with maximum / minimum $J(t)$ at definite time [2]. The possible mechanism and thermodynamics of the one-step (one barrier), or two step (two barrier) process of nano-nucleus formation is also discussed early in our works [3-4]. It is shown experimentally, that multi-stage nucleation process has been stipulated mainly by the solid state phase transition into nano-nucleus, and into nano- liquids [2, 5]. Besides it is possible formation of the initial liquid-crystalline nucleus, Fig.1 [6]. It is shown that clear experimental index of the nucleation type is a distribution function of the waiting times for nucleus appearance [1-2, 7].

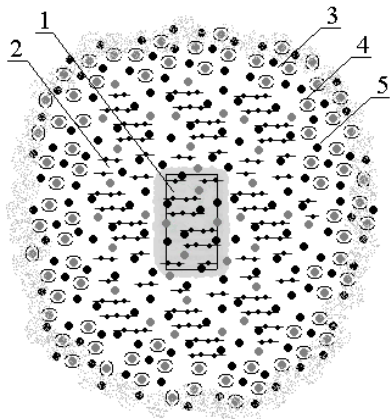


Figure 1. 2-D –Scheme of the initial BaB_2O_4 nucleus: 1) Crystal kernel. 2) Inside smectic cover. 3) Outside fractal nematic cover. 4-5) The BaB_2O_4 atoms.

The data on the mechanism and kinetics of the crystal formation from aqueous solution more 150 inorganic salts allows to suppose the general design of the perfect crystal growth technology from aqueous solution [8-9].

Knowledge of the crystal nucleation mechanism and kinetics into dispersion of aqueous-petroleum solution of gas-hydrate is very useful also for control its crystallization at petroleum extract, and its transportation [7].

[1] Aleksandrov L.N., and Kidyarov B.I. Kinetic theory of three-barrier processes of non steady-state nucleation at phase transformation // *Physica Status Solidi (a)*. 1976. **36**, №2, 403 - 410.

[2] Kidyarov B.I. Crystal formation mechanism from the liquid phase at process nano-stage // In: *Physical and chemical aspects into cluster, nano-structures, and nano-materials formation*. Proceedings of the Tver' University. Eds. V.M. Samsonov, N.Yu. Sdonyakov. 2014. V.6. Tver'. P.155 - 161. (In Russian).

[3] Kidyarov B.I. Thermodynamics of crystalline nano- nucleus formation from liquid phase // *Journal of Structural Chemistry*.

New York, Springer. 2004. Vol.45, Supplement 1, S31-S35.

[4] Kidyarov B.I. Crystal formation mechanism and kinetics into liquid phase // *Condensed matter and interface boundary*. 2009. – V.11, № 4. – P. 314-317. (In Russian).

[5] Leiman V.I. Nano-phase formation and dimensional effects into the nano-particle properties inside glasses. Dr. Science dissertation. Sankt Petersburg. 2006. - 33 p. (In Russian).

[6] Tsvetkov E.G., Kidyarov B.I. Nano-scale stages of crystal-genesis from liquid phase // *Notes of the Russian mineralogical society*. 2007. 136, special issue.P.66-76. (In Russian).

[7] Stoparev A.S. Gas hydrates into petroleum suspensions. Dr. Ph. Thesis. 2016. Niichem. Novosibirsk. (In Russian).

[8] Kidyarov B.I. Nucleation kinetics and technology design for crystal growth from aqueous solution // *Journal of the Korean Crystal Growth and Crystal Technology*. 2003. Vol.13, № 2 51-55

[9] Kidyarov B.I. Structural and physical regularity in the mechanism and kinetics of piezoelectric and ferroelectric crystal formation from liquid phase // *Physics of the Solid State*. 2009. V.51, № 7. P.1435 - 1439.



CFE vs. DKM: COMPARING KINETICALLY CONSTRAINED GIBBS ENERGY MODELS WITH MECHANISTIC REACTION RATE MODELS

Koukkari P.S., De Paiva, E.J.M.²

¹*Technical Research Centre of Finland, Sustainable energy and chemical technologies, 02044 VTT Finland*

²*Universidade Federal do Parana, Curitiba - Brazil*

E-mail: pertti.koukkari@vtt.fi

In process and materials chemistry, digitalization with computational methods has been a long-time continuing process. The methodology based on numerical methods in mechanistic reaction kinetics as well as for fluid phase thermodynamics applying equations of state is well established. During the last two decades, however, thermodynamic multiphase technology based on the minimization of Gibbs free energy has made progress in modelling both reactive flows and processing functional materials. Recent advancements also include introduction of such new Gibbs'ian algorithms, which facilitate calculation of time-dependent dynamic changes in multi-phase systems [1,2].

Comparison between detailed kinetic mechanisms and multiphase thermochemical techniques has yet seldom, if at all, been available. The present work describes a fundamental analysis between constrained Gibbs free energy calculation (with one constrained kinetic reaction rate) and detailed kinetic mechanism of 67 reversible reactions, as performed for the industrially interesting Titanium(IV)Chloride oxidation process [3]. The results show close agreement between the two different techniques when the time-dependent formation of the prominent chloride and oxychloride species in the gas phase are accounted. Range of applicability of the alternative simulation techniques will be shortly discussed.

[1] Koukkari, P.; Laukkanen, I.; Liukkonen, S., *Fluid Phase Equilibria*, (1997) No: 136, 345 - 362 .

[2] Pajarre, R., Koukkari, P. & Kangas, P., (2016), *Chem. Eng. Sci.* 146, 244-258.

[3] West, R.H., (2008), *Modelling the Chloride Process for Titanium Dioxide Synthesis*, Ph.D. thesis, University of Cambridge, U.K.



INFORMATIVITY OF VARIOUS DATA IN THE COMPUTER ASSESSMENT OF THE BINARY SYSTEMS

Kuznetsov V.N., Kareva M.A., Kabanova E.G.

Chemistry Department, Moscow State University, 119991 Moscow, Russia

E-mail:vnk@general.chem.msu.ru

Computer assessment, or optimization of data, is generally accepted as a way to get most precise and consistent values of thermodynamic functions. This procedure enables one to generalize all measurements of equilibrium properties including various thermodynamic data and (when possible) phase equilibria.

The Au-Pd binary system [1] contains two stable phases namely liquid and fcc solid solution. There are two investigations of liquidus-solidus lines as well as three calorimetric studies and two measurements of partial properties of components for fcc solution and a study of the liquid phase.

In the course of computer assessment of the system the possibility of obtaining several solutions which provide close description of data was noticed [2]. The present work is devoted to analysis of the reasons of such ambiguity.

At first stage all the data were analyzed using so-called *jackknife*, or *cross-validation* technique [3]. It consists in a series of calculations, at every of which one piece of data was omitted. The results of calculations should reasonably restore omitted data.

To estimate the uncertainty of results we performed singular analysis of the hessian of sum of squared normalized residues of final approximation. This enabled us to find the confidence region of model parameters as suggested by [4]. Analysis of “partial” hessians restricted to the results of separate experimental works permits us to find informativeness of every work, *i.e.* its account to restriction of the acceptable region of parameter space. This also enables us to estimate systematic trends in every piece of data, which may be due to either systematic errors of data or to incomplete adequacy of models.

The results of the present approach are compared with other procedures of assessment of data with possible systematic errors, *f.e.* with so-called linear error model suggested by Rudnyi [3].

[1] Au-Pd (Gold-Palladium), in: Landolt-Boernstein, New Series, v. IV/5, p. 1-4

[2] Kareva M.A., Kabanova E.G., Kuznetsov V.N., XX International Conference on Chemical Thermodynamics in Russia (RCCT-2015): Abstracts. Nizhni Novgorod, 2015, p. 260

[3] Efron B. The Jackknife, the Bootstrap and Other Resampling Plans, Philadelphia, SIAM, 1982. Russ. Transl.: Efron B., in: Non-Traditional Techniques of Multi-Dimensional Statistics, Moscow, “Finansy i Statistika”, 1986, p. 48-150

[4] Bard Y., Nonlinear parameter estimation, Acad. Press, N.Y., 1974 Russ. Transl.: Moscow, “Statistics”, 1979

[5] Rudnyi E.B., Chemometrics and Intelligent Laboratory Systems 34 (1996) 41-54.



EQUATION OF STATE OF MATTER AT EXTREME CONDITIONS

Lomonosov I.V.¹

¹*Institute of Problems of Chemical Physics RAS, 142432 Chernogolovka, Russia*
E-mail: ivl143@yandex.ru

The equation of state (EOS), governing the functional dependence among the parameters that characterize the state of a substance, is the main quantitative characteristic of a substance, which makes it possible to apply the general formal body of thermodynamics and dynamics of continuous media (mathematical physics) to describe different physical objects and processes of a highly diverse nature. The mass, momentum, and energy conservation laws reflect the totality of processes in the surrounding environment in the most general form, while the equation of state (EOS) introduces into this general formalism the concrete quantitative characteristic of precisely the given (concrete) state of a substance: gas, liquid, solid, electromagnetic or quark-gluon plasma, or nuclear matter radiation. That is why interest in the EOS of matter has always been keen, not only from the standpoint of numerous pragmatic (technical and energy) applications but also from the viewpoint of understanding and describing processes and phenomena under extremely high energy densities.

EOS governs the system of gas dynamic equations and defines significantly accuracy and reliability of results of numerical modeling. In practice, it is required for numerical modeling of physical processes arising under conditions of extreme energy densities. In this report we'll give examples of different EOS, discuss the progress in experimental study of material's properties at high pressure, high temperature and in theoretical methods as well.

In spite of a significant progress achieved on construction of EOS in solid, liquid and plasma state with the use of the most sophisticated "first-principle" theoretical approaches (classic and quantum methods of self-consistent field, diagram technique, computer's Monte-Carlo and molecular dynamics methods) the disadvantage of these theories is their regional character. The range of an applicability of each theory is local and, rigorously speaking, no one of them allows to provide for a correct theoretical calculation of thermodynamic properties of matter on the whole phase plane from the cold crystal to liquid and hot plasmas. The principal problem here is the necessity to take into account correctly the strong collective interparticle interaction in disordered media, which meets especial difficulties in the region occupied by dense disordered non-ideal plasmas. In this case experimental data at high pressures, high temperatures are of peculiar significance, because they serve as reference points for theories and semi-empirical models. Data obtained with the use of dynamic methods are of the importance from the practical point of view. Shock-wave methods allow to study a broad range of the phase diagram from compressed hot condensed phase to dense strongly coupled plasma and quasi-gas states. Available experimental data on the shock compression of solid and porous metals as well as isentropic expansion embrace to nine orders with respect to pressure and four to density. We'll describe experiments on static and shock compression, isentropic expansion of shocked substances, electrical explosion of conductors, different theoretical approaches of calculating material's properties in solid, liquid and plasma states.

Wide-range multi-phase EOS for metals of most practical interest will be reported as well as results of numerical modeling of processes at extreme conditions. This EOS fully assigns the free energy thermodynamic potential for metals over entire phase diagram region of practical interest. It accounts for solid, liquid, plasma states as well as two-phase regions of melting and evaporation. Some coefficients in EOS, included in the analytical expressions, are constants characteristic for each metal (atomic weight and charge, density at normal conditions and other) and are found from tabular data, while the rest serve as fitting parameters and their values are found from the optimum description for the available experimental and theoretical data and providing for correct asymptotes to calculations on the base of Debay-Huckel and Thomas-Fermi theories. To construct EOS, used was following information at high pressures, high temperatures: measurements of isothermal compressibility in diamond anvil cells, data on sound velocity and density in liquid metals at atmospheric pressure, electrical explosion of conductors measurements, registration of shock compressibility for solid and porous samples in incident and reflected shock waves, impedance measurements of a shock compressibility under condition of an underground nuclear explosion, data on isentropic expansion of shocked metals, calculations by Debay-Huckel and Thomas-Fermi models, evaluations of the critical point.



THERMODYNAMIC MODEL FOR MIXED-SOLVENT ELECTROLYTE SYSTEMS

Maksimov A.I., Kovalenko N.A., Uspenskaya I.A.

Chemistry Department, Lomonosov Moscow State University, 119991 Moscow, Russia

E-mail: ai.maksimov@td.chem.msu.ru

Electrolyte solutions are widely used in different industrial processes. The knowledge of thermodynamic properties and phase equilibria in the aqueous and mixed-solvent electrolyte systems is needed for the separation processes, hydrometallurgy, water treatment, distillation, desalination and many others. These applications require thermodynamic models covering a wide range of pressures, temperatures and concentrations from pure solvents to fused electrolytes. Therefore, the development of models of electrolyte solutions is a very important task.

In this work a new thermodynamic model (electrolyte Generalized Local Composition Model, eGLCM) describing phase equilibria and thermodynamic properties of the mixed-solvent electrolyte solutions was developed. The nonideality of solutions was taken into account with the help of three contributions to the excess Gibbs energy of the system which have different physical nature. Long-range electrostatic interactions are described with the modified Pitzer-Debye-Huckel equation [1]. Dependence of the solution density and dielectric constant from the temperature and solution composition are taken into consideration. Middle-range term looks like polynomial Pitzer term and accounts for the interactions including charged particles, which were not considered in the long-range term. Short-range contribution includes interactions between all species and described with the generalized local composition model [2]. This model generalizes well-known local composition models such as UNIQUAC, Wilson and Tsuboka – Katayama and showed its applicability for the non-electrolyte systems.

Developed model allows to calculate contribution to the excess Gibbs energy not only from the pure solvents and ions but also from different species. It makes possible to model a wide range of chemical equilibria: ion pairing, association, formation of complexes, hydrolysis of metal ions, etc.

The model represents phase and chemical equilibria, thermal and volumetric properties in mixed-solvent electrolyte systems. The applicability of the model was tested using experimental data on vapor-liquid, solid-liquid and liquid-liquid equilibria, activities, heats of dilution and mixing, and densities. Testing systems included water – organic solvent systems (water – tributyl phosphate, water – 2-butanol) with complex dependence of the mutual solubility of the components, which cannot be described with the existing thermodynamic models. Fully miscible system water – nitric acid was modeled in the concentration range from water to pure electrolyte with and without accounting of the undissociated acid. As an example of the systems with the limited solubility of the electrolyte water – rare earth nitrates systems were used. To test the predictive ability of the model extraction system water – tributyl phosphate – nitric acid – neodymium nitrate – samarium nitrate was used.

Suggested model describes thermodynamic properties and phase equilibria in the aqueous and mixed-solvent electrolyte systems over the entire concentration range from pure solvents to saturated solutions or fused electrolytes. For all types of systems it describes experimental data physically and accurately. It forms a good basis for the modeling of the industrial chemical processes including electrolytes.

This research work was financially supported by RFBR according to the research project No. 16-33-01038 mol_a and by the URALCHEM Holding.

[1] Pitzer, K.; Simonson, J. J. *Phys. Chem.*, 1986, 90, 3005-3009.

[2] Maksimov, A.; Kovalenko, N. *J. Chem. Eng. Data*, 2016, 61, 4222-4228.

**THERMOCHEMISTRY OF SOME AZIDOCONTAINING COMPOUNDS.
5. ENERGY OF REORGANIZATION OF AZIDO - AND AZORADICALS**Miroshnichenko E. A.¹, Pashchenko L.L.², Kon'kova T.S.¹¹Semenov Institute of Chemical Physics RAS, Kosygin str. 4, Moscow, 119991, Russia,²Department of Chemistry, Lomonosov Moscow State University, Leninskie Gory 1-3, 119991, Russiae-mail: eamir02@mail.ru

Azidocontaining compounds are important industrial chemicals with a broad range of applications. This class of compounds is widely used in the synthesis of many diverse products. Some compounds are highly explosive. To investigate the stability and performance of these chemicals, knowledge of the enthalpy of formation ($\Delta_f H^\circ_{298}$) is an essential requirement. Other thermochemical properties, such as enthalpies of vaporization ($\Delta_{\text{vap}} H^\circ_{298}$) and energies of reorganization of azido-radicals are needed for the characterization of the chemical degradation pathways of their compounds. Despite the extensive studies of azido containing compounds, available thermochemical experimental information is often scarce and frequently shows significant discrepancy among published results.

In this work the enthalpies of formation, $\Delta_f H^\circ_{(\text{cond})}$, and vaporization $\Delta_{\text{vap}} H^\circ$, of five azidocontaining compounds are determined, a namely phenylazide **I** ($\text{C}_6\text{H}_5\text{N}_3$), benzylazide **II** ($\text{C}_6\text{H}_5\text{CH}_2\text{N}_3$), three-phenyl-methylazide **III** (C_6H_5)₃ CN_3 , three-nitromethylazide **IV** (NO_2)₃ CN_3 и 1-azido-1,1-dinitroethane **V** $\text{CH}_3(\text{NO}_2)_2\text{CN}_3$. Using experimentally obtained values of $\Delta_f H^\circ_{(\text{cond})}$ and $\Delta_{\text{vap}} H^\circ$ the standard enthalpies of formation in gas phase are calculated. The bond dissociation energies, D , C – N are calculated (Table 1).

Using fundamental equations of the chemical physics [1], the calculation scheme by a method by “a double difference” of the energies of reorganization of molecules fragments into radicals is offered. The new calculation method is offered to determine the energies of reorganization of molecule fragment N_3 into radical N_3 . Significant thermochemical characteristics of azidocontaining compounds are given in Table 1.

Table 1. Thermochemical characteristics of azido-compounds ($\text{kJ} \cdot \text{mol}^{-1}$)

	$\Delta_f H^\circ_{(\text{cond})}$	$\Delta_{\text{vap}} H^\circ$	$\Delta_f H^\circ_{\text{g}}$	D
I (l)	345.2 ± 2.5	44.8 ± 0.8	389.9 ± 3.4	362.3
II (l)	368.2 ± 1.2	48.1 ± 0.4	416.3 ± 1.7	205.8
III (cr)	486.2 ± 1.2	120.5 ± 1.2	606.7 ± 2.5	199.6
IV (l)	306.3 ± 5.4	46.0 ± 2.1	352.3 ± 6.2	286.6
V (l)	196.6 ± 2.9	56.5 ± 0.8	253.1 ± 3.8	270.3

[1] Semenov N.N. About some problems of chemical kinetics and reaction ability, Moscow:

Acad. Sci., SSSR. 1958. 686 p. [2] Orlov Y.D., Y.A. Lebedev, I.S. Saifullin. 2001. Thermokhimija organicheskikh svobodnykh radikalov [Thermochemistry of organic free radicals]. Moscow: Nauka. 304 p. (In Russian). [3] Pedley J.B., Nailor R.D., Kirby C.P. Thermochemical data of organic compounds. L. – N.Y.: Chapman and Hall, 1986. 792 p. [4] Luo Y. Comprehensive Handbook of Chemical Bond Energies, CRC Press, Boca Raton- London-New York, 2007, p.1655.

Reorganization energies of azido-radicals and bond dissociation energies, D , are calculated ($\text{kJ} \cdot \text{mol}^{-1}$). The new calculation method for determination of the energy of reorganization of azido - radical gives a way to calculate ($\text{kJ} \cdot \text{mol}^{-1}$): the enthalpy of formation of radical ($\text{N}=\text{NC}_6\text{H}_5$) · 275.7, bond dissociation energy $\text{C}_6\text{H}_5 - (\text{N}=\text{NC}_6\text{H}_5)$ 207.5, median thermochemical bond energies E (C – N) 362.3, E (N = N) 489.1, ΣEN_3 1004.2, $\Sigma \text{EN}=\text{NC}_6\text{H}_5$ 5904.5. Reorganization energies of radicals, ε , ($\text{kJ} \cdot \text{mol}^{-1}$) are calculated, a namely ($\text{N}=\text{NC}_6\text{H}_5$) · - 154.8, which is near to energy of reorganization of acetylene radicals, ~ 160 $\text{kJ} \cdot \text{mol}^{-1}$; $\text{C}_6\text{H}_5\text{CH}_2$ · -40.5; $(\text{C}_6\text{H}_5)_3\text{C}$ · -85.4; $(\text{NO}_2)_3\text{C}$ · -16.3 and $\text{CH}_3(\text{NO}_2)_2\text{C}$ · -8. 5. Bond dissociation energies, D , which listed in Table 1 and in calculation process of reorganization energy of azido-radical are obtained from the enthalpies of formation of compounds I – V and literature data [2 – 4]. Obtained ours data of reorganization energies of azido- and azo-radicals and bond dissociation energies are needed for energy calculations of the kinetics of the reactions involving azido-containing compounds.



THE METHOD OF CALCULATING THE THERMODYNAMIC PROPERTIES OF NATURAL CLAY MINERALS WITH THE USE OF CHEMICAL COMPOSITION

Oshchepkova A.V.^{1,2}, Bychinskii V.A.^{1,2}, Chudnenko K.V.¹

¹ A.P. Vinogradov Institute of Geochemistry, Siberian Branch of the Russian Academy of Sciences, 664033 Irkutsk, Russia

² Irkutsk State University, 664001 Irkutsk, Russia

E-mail: oshchepkova-anasta@mail.ru

A detailed study of crystal-chemical properties of clay minerals is constrained by difficulties related to their complex structure and large number of isomorphic impurities. One way to solve this problem is physical-chemical modeling. This paper presents the results of a study of the most common representatives of clay minerals - montmorillonite. A large number of works devoted to the study of composition, structure and various properties of natural and modified montmorillonite was published. However, due to the complexity of the composition and high dispersion of montmorillonite, the experimental study thermodynamic properties of montmorillonite is limited.

The article [2] presents the results of studies of the chemical composition and thermodynamic properties of natural montmorillonite. We used their data as a test to verify the accuracy of the method we are developed. Our method allows us to calculate the mineral composition and the thermodynamic properties. It describes complex natural clay minerals with the use of solid-solution models and determine the thermodynamic properties of these minerals by dual decisions using the method of free energy minimization implemented in a universal program complex (PC) "Selector" [1].

Source data is the chemical composition of montmorillonite from three fields represented in [2]. To a given chemical composition 0.5 moles of water (H₂O) is added for balancing ions contained in interlayer spaces. The montmorillonite solid solution equilibrium with an aqueous solution is calculated using software "Selector". We have previously shown the competence modeling natural clay formations in the solid solution model of montmorillonite, including 24 minals [3]. Aggregated conventional stoichiometric formula of clay minerals are calculated based on the obtained equilibrium solutions. Number of the chemical element *i* in the summary formula: $e_i = \sum_j (a_{ij} \cdot x_j) / X_a$, where a_{ij} - minal stoichiometry coefficient *j* for the solid solution of the chemical element *i*, x_j - minal moles *j*, X_a - molar amount of solid solution phase, $j = 1, L, L$ - minals amount in solid solution. Chemical potentials of the independent components (u_i) are estimated basing on dual-making mathematical programming problems. It allows us to calculate the free energy of formation of montmorillonite as a $\sum_i e_i \cdot u_i$ (table. 1).

Table 1. Comparison of the calculated data from the source [2]

No	Data	stoichiometric formula	$-\Delta_f G^\circ$ (298 K) (kJ/mol)	aqueous solution components
1	Calculated	$\text{Na}_{0.3}\text{Mg}_{0.3}\text{Al}_{1.9}\text{Si}_{3.8}\text{O}_{10}(\text{OH})_{2.5}$	3293	$\text{Ca}^{+2}, \text{H}_4\text{SiO}_4, \text{Mg}(\text{OH})_2$
	Initial	$\text{Na}_{0.3}\text{Ca}_{0.1}\text{Mg}_{0.4}\text{Al}_{1.7}\text{Si}_{3.9}\text{O}_{10}(\text{OH})_2$	5677.6 ± 7.6	
2	Calculated	$\text{Na}_{0.4}\text{K}_{0.1}\text{Ca}_{0.1}\text{Mg}_{0.2}\text{Fe}_{0.2}\text{Al}_{2.0}\text{Si}_{3.5}\text{O}_{10}(\text{OH})_2$	5961.89	$\text{H}_4\text{SiO}_4, \text{Mg}(\text{OH})_2$
	Initial	$\text{Na}_{0.4}\text{K}_{0.1}\text{Ca}_{0.1}\text{Mg}_{0.3}\text{Al}_{1.6}\text{Fe}_{0.1}\text{Si}_{3.9}\text{O}_{10}(\text{OH})_2$	5614.3 ± 7.0	
3	Calculated	$\text{K}_{0.1}\text{Ca}_{0.1}\text{Mg}_{0.9}\text{Al}_{1.9}\text{Fe}_{0.1}\text{Si}_{3.6}\text{O}_{10}(\text{OH})_{3.0}$	9953.58	$\text{Ca}^{+2}, \text{H}_4\text{SiO}_4, \text{K}^+, \text{Mg}(\text{OH})_2$
	Initial	$\text{K}_{0.1}\text{Ca}_{0.2}\text{Mg}_{0.8}\text{Al}_{1.6}\text{Fe}_{0.1}\text{Si}_{3.7}\text{O}_{10}(\text{OH})_2$	5719 ± 11	

The table shows that we can estimate structural formula and thermodynamic properties clay minerals using the method proposed. Probably variations in the calculated values are due to the imperfection model of solid solutions at this stage. A part of calcium and magnesium go into the aqueous solution in our model. This problem has to be solved by including new minals containing calcium and magnesium. It will increase the accuracy of the calculations.

This work was supported by the Russian Foundation for Basic Research (grant № 16-35-00266) and the Irkutsk State University (individual research grant № 091-16-225).

[1] Chudnenko K.V Thermodynamic modeling in geochemistry: theory, algorithms, software, applications. Novosibirsk: "Geo", 2010. - 287 p.

[2] Ogorodova L.P, Kiseleva I.A., Melchakova L.V. et al. Geochemistry, 2013, 6, 541-551.

[3] Oshchepkova A.V., Kuzmin M.I., Bychinskii V.A. et al. Reports of the Academy of Sciences, 2015, 461, 4, 447-450.



UNDERSTANDING NONIDEAL MIXING OF PROTIC IONIC LIQUIDS: MD SIMULATIONS AND LATTICE MODELS

Paschek, D.¹, Golub, B.¹, Ondo, D.², Ludwig, R.¹

¹*Institute of Chemistry, University of Rostock, 18051 Rostock, Germany*

²*Department of Physical Chemistry, University of Chemistry and Technology, 166 28 Prague 6, Czech Republic*

E-mail: dietmar.paschek@uni-rostock.de

We report results of molecular dynamics (MD) simulations characterizing the hydrogen-bonding in mixtures of two different protic ionic liquids sharing the same cation: Triethylammonium-Methylsulfonate (TEAMS) and Triethylammonium-Triflate (TEATF). The Triethylammonium-cation acts as a hydrogen-bond donor, being able to donate a single hydrogen bond. Both, the Methylsulfonate- and the Triflate-anions can act as hydrogen-bond acceptors, which can accept multiple hydrogen bonds via their respective SO₃-groups. In addition, replacing a Methyl-group in the Methylsulfonate by a Trifluoromethyl-group in the Triflate significantly weakens the strength of a hydrogen bond from an adjacent Triethylammonium cation to the oxygen-site in the SO₃-group of the anion. Our MD simulations indicate that these subtle differences in hydrogen-bond strength significantly affect the formation of differently sized hydrogen-bonded aggregates in these mixtures as a function of the mixture-composition. Moreover, the reported hydrogen-bonded cluster sizes can be predicted and explained by a simple combinatorial lattice model, based on the approximate coordination number of the ions, and using statistical weights that mostly account for the fact that each anion can only accept three hydrogen bonds. Based on the simple lattice model, we introduce a lattice mixture model for mixtures of protic ionic liquids, including the effect of hydrogen bonding redistribution. We show the observed non-ideal negative mixing energies as a function of the mixture composition can be solely explained by hydrogen-bond redistribution.

[1] Paschek D; Golub, B; Ludwig, R. *Phys. Chem. Chem. Phys.*, 2015, 17, 8431-8440.

[2] Fumino, K; Bónsa, A-M; Golub, B; Paschek, D; Ludwig, R. *ChemPhysChem*, 2015, 299-304.

TERNARY GAS-GAS-LIQUID MIXTURES DIFFUSION IN MESOPOROUS MATERIALS: INSIGHTS FROM COMPUTER SIMULATION

Sizova A.A., Ivanova E.A., Sizov V.V., Brodskaya E.N.

Institute of Chemistry, St. Petersburg State University, 198504 St.Petersburg, Russia

E-mail: shapovalovaaa@mail.ru

Diffusion of gases and liquids in porous media is the foundation of a wide variety of important industrial processes and natural phenomena, such as heterogeneous catalysis, adsorptive separation and purification, fuel element engineering, waste disposal, natural gas recovery, and soil aeration. Therefore, the development of efficient tools for the description, prediction and quantitative modeling of diffusion of mixtures in materials of various origins remains a field of active research for many decades. The application of theoretical approaches to the diffusion in complex systems adsorbed in realistic porous materials meets serious problems. At the same time, atomistic computer simulations are playing an increasingly important role in the studies of transport phenomena in porous media, since they allow one to use significantly more complex and detailed models than any classical theory. It is especially important to describe diffusion in multi-component mixtures, for which the data on single-component diffusion have only limited value, since the dynamic behavior of the adsorbed mixture cannot be reliably deduced from simple relations. Thus, direct simulation of gas mixture diffusion is the most suitable approach.

The goal of this work was to elucidate the effects of pore loading and modificative liquids on diffusivity of adsorbed gas mixture in hydrophilic and hydrophobic environments. With this aim in view, self-diffusion of CH_4/CO_2 mixture in SBA-15 mesoporous silica and CMK-5 mesoporous carbon in the presence of preadsorbed water and acetonitrile was investigated. Dry adsorbent was used as a reference system. Mobility in these systems was examined at 298 K by means of molecular dynamics simulation. Various adsorbed gas mixture compositions and amounts of modificative liquids were considered. Compositions of adsorbate were obtained previously by Monte Carlo simulations of adsorption from equimolar CH_4/CO_2 mixture at pressures up to 70 atm. Since CMK-5 and SBA-15 materials are known to have complex structure (meso- and micropores in SBA-15, mesopores and interpore space in CMK-5), diffusion coefficients of fluids were calculated separately for different types of pores.

Several types of diffusion behavior under varying pressure were observed, including non-monotonic dependence with a maximum, monotonic decrease, and apparent lack of pressure dependence (for example, see Fig. 1). In the presence of preadsorbed liquids gas diffusion coefficients can be both higher or lower than in unmodified adsorbents.

Comparison of thermodynamic and transport selectivity of adsorbents to carbon dioxide provides an opportunity to achieve the optimal conditions for gas mixtures separation.

This work was supported by the Russian Foundation for Basic Research (grant no. 16-33-00919 MOL_A).

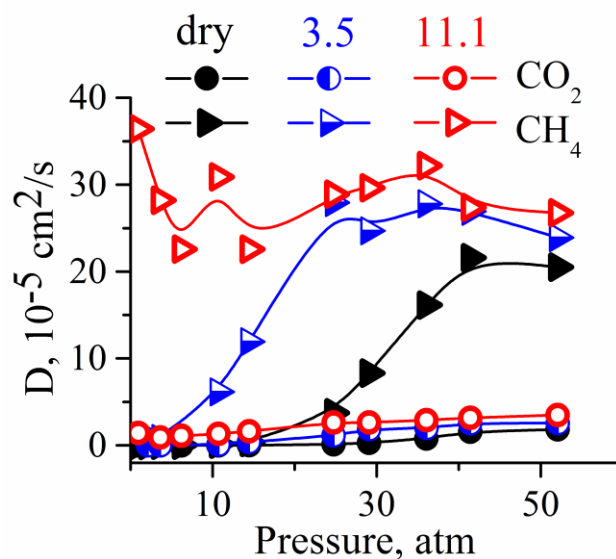


Figure 1. Diffusion coefficients of carbon dioxide and methane adsorbed in SBA-15 with different water contents (3.5 and 11.1 mmol/g) at 298 K



THE PROBLEM OF INTERNAL ROTATION IN THERMODYNAMICS

Turovtsev V.V.^{1,2}, Kaplunov I.A.², Orlov Yu.D.²

¹*Tver State Medical University, 170100, Tver, Russia*

²*Tver State University, 170100, Tver, Russia*

E-mail: turtsma@tversu.ru

The exact calculation of the thermodynamic properties of non-rigid polyatomic compounds is complicated by the fact that one needs to make a review of the whole set of conformers, which probability of the existence depends on the temperature and the energy barriers. Besides, the lower the energy threshold or higher temperature of the calculated property is, the worse the standard model "rigid rotator-harmonic oscillator" works. Here it is necessary taken into account of the large amplitude movement contributions in an explicit form, and this requires a solution of the Schrödinger equation for such movements.

Previously we have found the solution of one-dimensional torsion Schrödinger equation in the complex arithmetic with periodic potential of the general form of plane-wave basis set [1], and in the basis set of Mathieu functions [2]. In presented work, an analytic expression for the torsion state density probability was obtained based on the solution [1]. This allowed to compute the probability p of states in the potential wells, and to introduce a quantitative measure of the localization/delocalization phenomenon for the state. Introduced criterion makes possibility to unique assign of the energy levels to specific potential well or indicate the probability of referring state to the specific conformer. The value p is also a generalization form of the rotational symmetry number in problems of symmetric and asymmetric internal rotation. Criterion allows to make more rigorously calculating of the individual conformer contribution in the thermodynamic properties, their mole fractions and the entropy of mixing for non-rigid polyatomic compounds at high temperatures and/or low barriers on the potential energy surface.

The work was performed in the Tver State University under the support of Russian Ministry of Education in the framework of the state task for scientific activity.

[1] Turovtsev, V. V.; Belotserkovskii, A. V.; Orlov, Yu. D. *Optics and Spectroscopy*, 2014, 117, 710–712.

[2] Turovtsev, V. V.; Orlov, Yu. D.; Tsirulev, A. N. *Optics and Spectroscopy*, 2015, 119, 2, 191-194.



UP-TO-DATE INFRARED THERMOGRAPHY AS A HIGHLY INFORMATIVE DIAGNOSTIC TECHNOLOGY SUCCESSFULLY APPLIED TO THERMODYNAMIC STUDIES

Boris G. Vainer^{1,2}

¹Rzhanov Institute of Semiconductor Physics, Siberian Branch of the Russian Academy of Sciences, 630090 Novosibirsk, Russia

²Novosibirsk State University, 630090 Novosibirsk, Russia

E-mail: BGV@isp.nsc.ru

Focal plane array (FPA)-based infrared thermography (IRT) is a well-accepted diagnostic technique fruitfully used in industry, biomedicine, etc. It is also a popular research instrument of modern experimental science [1]. At the same time, just a scanty amount of contributions, devoted to the use of this method in chemical sciences, including thermodynamic lines of inquiry, is presently known. Among them, it is worth mentioning the successful application of IRT to some catalysis research problems reported in [2].

In the present review, we start with a short introduction to the basics of IRT and then we progress to multifarious scientific applications of this method with the main attention focused on physicochemical problems. The reported experimental results are based on the most interesting original investigations conducted by the author and his colleagues during the last decade.

It was shown in [1, 3] that the last-generation IRT is capable of giving temperature indications for adsorption/desorption phenomena with the sensitivity of hundredth parts of a gas molecular monolayer adsorbed on a solid surface. Here, the thermal signal is emerged owing to the first-order phase transition heat release or absorption. The pronounced "thermal flame" ("thermal fire") phenomenon is exhibited and quantitatively represented on the uneven surfaces of a set of organic materials (fabrics) at room temperature. This thermal effect ranged within an order of magnitude.

Silica gel and zeolite samples placed into a cylindrical quartz adsorber were investigated in details during the air drying process. The movement of a heat wave inside the adsorber was first observed and quantitatively characterized. The thermodynamic processes accompanying vacuum swing adsorption cycles were studied thoroughly at the variable adsorption time/desorption time ratio [4].

A special setup combining the FPA-based infrared camera and fast laser ellipsometer within a single system was created to investigate the initial stages of adsorption/desorption and catalytic thermal processes progressing on solid surfaces, as soon as these surfaces are attacked by gas molecules. The obtained combined results [5, 6] are also demonstrated in the present review.

The sorption-enhanced infrared thermography (SEIRT) original method based on the real-time physicochemical thermodynamics concept is a new trend in respiratory investigations in humans and animals [6, 7]. Recent achievements in this biomedical area are also demonstrated.

It is convincingly shown in the present review that the up-to-date IRT may be successfully involved as a highly informative diagnostic technology meant to solve numerous thermodynamic problems in physics and chemistry.

This work was supported by the Russian Foundation for Basic Research (Grant No. 15-02-07680).

[1] Vainer, B.G. *J. Phys. D: Appl. Phys.*, 2008, 41, 065102.

[2] Loskyll, J.; Stoewe, K.; Maier, W.F. *ACS Comb. Sci.* 2012, 14, 295-303.

[3] Vainer, B.G. *QIRT J.*, 2008, 5, 175-193.

[4] Mel'gunov, M.S.; Ayupov, A.B.; Fenelonov V.B.; Vainer B.G. *Adsorption*, 2013, 19, 835-840.

[5] Vainer, B.G.; Guzev, A.A.; Mogilnikov, K.P.; Romanov, S.I.; Shvets, V.A. *Proc. QIRT-2014 Conf.* Available at QIRT Open Archives: <http://qirt.gel.ulaval.ca/archives/qirt2014/QIRT2014.html>.

[6] Vainer, B.G. *Appl. Opt.*, 2016, 55, D95-D100.

[7] Vainer, B.G. In: *Development Prospects of Science and Education, Intern. Scientific-Pract. Conf., February 28, 2015. Proceedings*. Part 8. Tambov: Consulting company Ucom Ltd, 2015, pp. 32–34. DOI: 10.17117/2015.02.28.08 (in Rus.)

MOLECULAR DYNAMICS SIMULATIONS OF IONIC SURFACTANT SOLUTIONS: DIFFUSION, AGGREGATION AND STRUCTURE

Volkov N.A., Shchekin A.K., Tuzov N.V.

Department of Statistical Physics, Faculty of Physics, Saint Petersburg State University, 198504 Saint Petersburg, Russia

E-mail: nikolay.volkov@spbu.ru

The real micellar solutions contain aggregates with different aggregation numbers [1]. These aggregates are very difficult to distinguish and, hence, to study separately by experimental methods such as, e.g., dynamic light scattering and nuclear-magnetic resonance. At the same time, the methods of molecular modeling allow one to study in detail the transport, formation and structure of separate aggregates with arbitrary aggregation numbers. We report the results of molecular modeling of aggregation in the sodium dodecyl sulphate (SDS) aqueous solutions [2, 3, 4]. Both salt-free solutions with different SDS concentrations and those containing sodium chloride and calcium chloride additives have been studied. The all-atom molecular dynamics simulations have been performed within CHARMM36 force field using MDynaMix software package [5]. Formation of one or several aggregates have been observed in the molecular dynamics runs at several surfactant concentrations (see Fig.1). Aggregation kinetics has been investigated, and the characteristic sizes of the aggregates have been

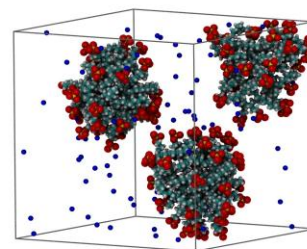


Figure 1. Snapshot of the system with 96 SDS and 9600 water molecules (water molecules are not shown).

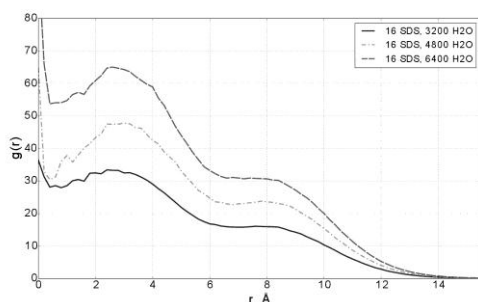


Figure 2. The RDF of terminal carbon atoms C_{12} relative to the aggregate's center of mass for the systems with 16 SDS molecules and 3200, 4800, 6400 water molecules.

on the total surfactant concentration as well as the dependence of size and diffusivity of an aggregate/micelle on its aggregation number (16, 32, 48, 64) at fixed total surfactant concentration. By finding the mean force potential, the degrees of counterion binding for the aggregates having different aggregation numbers have been estimated. The potentials of mean force for the interaction of sodium and calcium counterions with an aggregate having the aggregation number $n = 32$ show that only calcium ions can be strongly bound to such an aggregate.

The research has been performed using the resources of the Computing Center of St.Petersburg State University Research park. The work has been supported by Russian Science Foundation (grant 14-13-00112).

- [1] Shchekin, A.K.; Babintsev, I.A.; Adzhemyan, L.Ts.; Volkov, N.A. RSC Adv., 2014, 4, 51722-51733.
- [2] Volkov, N.A.; Divinskiy, B.B.; Vorontsov-Velyaminov, P.N.; Shchekin, A.K. Colloids and Surfaces A: Physicochem. Eng. Aspects, 2015, 480, 165-170.
- [3] Volkov, N.A.; Tuzov, N.V.; Shchekin, A.K. Fluid Phase Equilibr., 2016, 424, 114-121.
- [4] Volkov, N.A.; Tuzov, N.V.; Shchekin, A.K. Colloid Journal, 2017, 79, No. 2, 181-189.
- [5] Lyubartsev, A.P.; Laaksonen, A. Comp. Phys. Commun., 2000, 128, 565-589.

CPFIT PROGRAM FOR APPROXIMATION OF THERMODYNAMIC FUNCTIONS OF ZEOLITES

Voskov A.L., Voronin G.F.

¹Department of Chemistry, Lomonosov Moscow State University, 119991, Moscow, Russia

E-mail: alvoskov@gmail.com

Modeling of heat capacities and other thermodynamic functions of substances including zeolites and other aluminosilicates is an actual problem. The most common models are based on polynomials. Their main drawbacks are impossibility to use one dependence at the whole temperature range and to make extrapolations.

CpFit program approximates experimental heat capacity, enthalpy and entropy using Einstein-Planck functions sum from [1]:

$$C_p(T) = \sum_i \alpha_i C_E\left(\frac{\theta_i}{T}\right); \frac{C_E(x)}{R} = \frac{3x^2 e^x}{(e^x - 1)^2} \quad (1)$$

where α_i and θ_i are adjusted model parameters. This model allows to describe thermodynamic functions of zeolites (and another classes of compounds) in the whole temperature range using one set of functions and parameters. The used model also allows to make physically correct extrapolations to lower and higher temperatures. An example of approximation of $C_p(T)$ experimental data from [2] for natrolite $\text{Na}_2\text{Al}_2\text{Si}_3\text{O}_{10} \cdot 2\text{H}_2\text{O}$ is given at Figure 1.

The CpFit program uses the non-linear constrained least squares method for finding optimal values of model parameters. Levenberg-Marquardt algorithm (levmar library [3]) is used for this optimization. Constraints prevent obtaining of physically incorrect negative values of the model parameters.

The sum of squares is:

$$RSS(\vec{\alpha}, \vec{\theta}) = \sum_{i=1}^m \omega_{C_p,i}^2 (C_{p,i}^{\text{exp}} - C_{p,i}^{\text{calc}})^2 + \sum_{j=1}^n \omega_{H,j}^2 (H_j^{\text{exp}} - H_j^{\text{calc}})^2 + \sum_{k=1}^l \omega_{S,k}^2 (S_k^{\text{exp}} - S_k^{\text{calc}})^2 \quad (2)$$

where ω are statistical weights, exp and calc – experimental and calculated values respectively, C_p is heat capacity, $H = H - H(0)$ is enthalpy, $S = S - S(0)$ is entropy. It should be noted that $C_{p,i}^{\text{calc}} = C_p^{\text{calc}}(T_i, \vec{\alpha}, \vec{\theta})$, $H_j^{\text{calc}} = H^{\text{calc}}(T_j, \vec{\alpha}, \vec{\theta})$ and $S_k^{\text{calc}} = S^{\text{calc}}(T_k, \vec{\alpha}, \vec{\theta})$, i.e. heat capacity, enthalpy and entropy are described by the same set of parameters. H^{calc} and S^{calc} are obtained by integration of eq. 1.

The CpFit program has the next important features:

- Automatic selection of the number of terms in the eq. 1 using statistical criteria.
- Support of arbitrary custom terms that can be used in the case of second-order phase transitions.

It is planned to use CpFit for creation of self-consistent database of zeolites thermodynamic properties. Demo-version of the CpFit program can be obtained at the web-site of the Laboratory of Chemical thermodynamics of Lomonosov Moscow State University: <http://td.chem.msu.ru/en/>.

This work was financially supported by the Russian Foundation for Basic Research (Project No. 16-03-00677-a)

[1] Voronin G.F., Kutsenok I.B. J. Chem. Eng. Data, 2013, 58(7), 2083-2094

[2] Johnson G.K., Flotow H.E., O'Hare P.A.G. // Amer. Mineralog., 1983, 68, 1134-1145

[3] Lourakis M.I.A. <http://www.ics.forth.gr/~lourakis/levmar/>

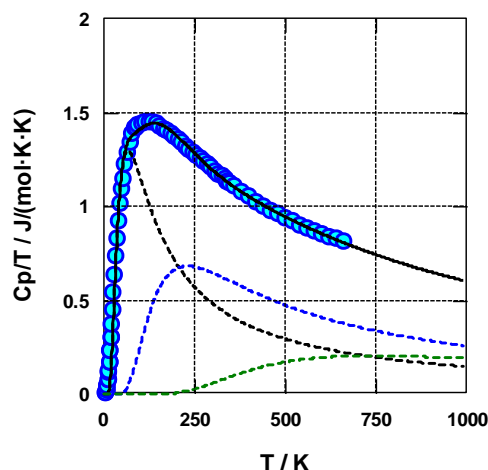


Figure 1. Approximation of C_p data for natrolite (solid line and circles). Dashed lines – terms of eq. 1.



CONSTRUCTION OF TRAJECTORIES OF IRREVERSIBLE PROCESS BASED ON PROPOSITIONS OF EQUILIBRIUM THERMODYNAMICS

Boris M. Kaganovich¹, Maxim S. Zarodnyuk¹, Sergey V. Yakshin¹

¹ Melentiev Energy Systems Institute, Siberian Branch of the Russian Academy of Sciences, 664033 Irkutsk, Russia

E-mail: thermo@isem.irk.ru, max@isem.irk.ru, s.yakshin@isem.irk.ru,

The paper proposes the model of extreme intermediate states (MEIS) to construct trajectories [1]. MEIS allows a set of possible motion results to be determined without defining the paths to attain them. Addition of the kinetic constraints to the model significantly improves the computation accuracy [2]. Admissibility of equilibrium modeling of the irreversible processes was provided by two different methods. The first consisted in refusal of the unified equation of the trajectory and in transition to its step-by-step construction. The second was based on the statement of the problem solved in one-dimensional, always potential, space of variables. With the step-by-step increase of optimal results of solutions the steps were taken to be finite, but so small that the assumption on the stationarity of motion and invariability of its laws was valid. Hence, it became possible to solve intrastep problems using the principles of extremality of conservative systems and to reduce the intrastep problems to searching for an extreme equilibrium state. This fact allowed the intrastep modeling with the help of MEIS and the increase of the results of intrastep computations by the dynamic programming method [3, 4]. One of the main advantages of the proposed approach is the possibility for a versatile analysis of the specific features of individual steps of the computational process. Consideration of changes in the equations of modeled processes and conditions of the system interaction with the environment becomes admissible. Dynamic programming also allows the modeling of systems with the functions: of discrete type, containing discontinuity points, and those which can not be described analytically. It turns out possible to study self-organization and degradation phenomena, and to solve problems of technological process control. Comparative advantages of the graphical approach are related with the simultaneous use of the advantages of thermodynamic and one-dimensional spaces of variables. In the thermodynamic space the regions of feasible solutions are invariant manifolds, which is explained by the monotony of the characteristic functions. The potentiality and equilibrium are always observed in the one-dimensional space. According to the accepted approach the space is represented by a closed circuit or a tree. The circuit branches show individual stages of the studied process. The extremality principles of conservative systems are observed for branches and steps, when the step-by-step approach is applied to construction of trajectories. Therefore, the equilibrium thermodynamic modeling of trajectories becomes feasible.

Admissibility of this modeling was tested by the examples: optimization of the coal combustion process control; calculation of nonstationary operation condition of a heating network which includes the stage of hydraulic shock and pipe fracture on one of its sections; assessment of the impact of a large-scale wind power plant on conversion of pollutant emissions into the atmosphere by the conditional hydraulic circuit and some others. The examples showed the possibility for sufficiently accurate representation of the features of real phenomena based on the thermodynamic description. Surely, the extension of the field of thermodynamics applications does not eliminate the need of kinetic modeling. The increase in complexity of solved scientific problems requires a more extensive set of different models to be created for their comprehensive analysis. However, the role of thermodynamic models based on simple and universal prerequisites with the improvement of computer technology must continuously increase.

[1] Gorban A.N., Kaganovich B.M., Filippov S.P., Keiko A.V., Shamansky V.A., Shirkalin I.A. Thermodynamic Equilibria and Extrema. Analysis of Attainability Regions and Partial Equilibria. – Springer. 2006 – 282 p.

[2] Kaganovich B.M., Keiko A.V., Shamansky V.A. Equilibrium Thermodynamic Modeling of Dissipative Macroscopic Systems // Advances in Chemical Engineering. Vol. 39. Thermodynamics and kinetics of complex systems. Chapter 1 – Elsevier, 2010. – P. 1–74.

[3] Kaganovich B.M., Keiko A.V., Shamansky V.A., Zarodnyuk M.S. On the Interrelations Between Kinetics and Thermodynamics as the Theories of Trajectories and States // Chemical Kinetics. – Rijeka: Intech, 2012. – P. 31–60.

[4] Kaganovich B.M. Equilibrium Thermodynamics. Problems and Perspectives. Second edition. – Saarbrücken: LAP Lambert Academic Publishing, 2015. – 240 p.



TERMINOLOGICAL PROBLEMS OF PHYSICO-CHEMICAL ANALYSIS

Zlomanov V.P.¹, Danilov V.P.²

¹ *Lomonosov Moscow State University, Department of chemistry, 119991 Moscow, Russia*

² *Kurnakov Institute of general and inorganic chemistry of RAN, 119991 Moscow, Russia*

E-mail: zlomanov1@mail.ru

Physico-chemical analysis is a branch of chemistry considering the interrelations "composition – structure - properties" of substances. The basic terms of physico-chemical analysis formed in the last century. Currently, in scientific literature there are many new, not always successful and not always understandable terms. Ordering terminology, clarification and interpretation of the terms was carried out by the terminological Commission, composed of academician N.T. Kuznetsov (Chairman), Professor V. P. Danilov, Professor Zlomanov V.P., Professor Garkushin I.K., Professor Drobot D.V., Professor Il'in, K.K., Professor Kudryashova O.S., Professor Mazunin S.A., Professor Fedorov P.P. As a result of the work of the Commission prepared and published a collection of "Basic terms of physico - chemical analysis». The basis for the development of terminology based on the General principles and methods for constructing systems of scientific and technical terms developed by the Committee of technical terminology of the RAN (USSR). The proposed collection includes the most important terms of physico-chemical analysis, which are used in modern educational and scientific literature. The collection is intended for professionals working in the field of chemistry, chemical engineering, materials science, Geochemistry and other related disciplines applying the methods and approaches of physical-chemical analysis.



Section 1.

General problems of chemical thermodynamics

Poster presentations

REVERSIBLE RECONSTRUCTION PHASE TRANSITION $c(4 \times 4) - (1 \times 3)$ ON THE (001) InSb SURFACE

Bakarov A.K., Mansurov V.G., Galitsyn Yu.G., Zhuravlev K.S.

Rzhanov Institute of Semiconductor Physics, Siberian Branch of the Russian Academy of Sciences, 630090 Novosibirsk, Russia

E-mail: mansurov@isp.nsc.ru

The (001) surface of InSb substrate is the most common growth surface for the homo and hetero-epitaxial structures on base of InSb, GaSb, AlSb. On the surface (001)InSb a number of surface reconstructions appears depending on both of the Sb pressure and of the substrate temperature. During variation of these parameters (P_{Sb}, T) reversible phase transitions take place. In the present work surface structures were studied using reflection high energy electron diffraction (RHEED). The $c(4 \times 4) \leftrightarrow (1 \times 3)$ reconstruction transition was investigated in details. Note, that the $c(4 \times 4)$ reconstruction corresponds to Sb-rich surface, and increasing of the substrate temperature or decreasing of Sb pressure lead to decreasing of Sb-coverage because of Sb desorption. As result a new asymmetric (1×3) reconstruction appears, see Fig.1.a,b.. The intensity of fractional spot (0 3/2) of the $c(4 \times 4)$ structure was measured during the variation of antimony flux at different substrate temperatures. At the substrate temperatures of $T < 400$ °C, hysteresis loop of fractional spot intensity appeared during the forward and reverse Sb flux variation, testifying that $c(4 \times 4) \leftrightarrow (1 \times 3)$ transition is discontinuous first order phase transition (Fig.2). At the temperatures $T > 400$ °C, hysteresis loop was not observed, that corresponds to continuous phase transition. We believe that this phase transition is analogous to the van der Waals gas \leftrightarrow liquid transition. We have developed a model to describe $c(4 \times 4) \leftrightarrow (1 \times 3)$ transition in the framework of the lattice gas approximation. This model takes into account the complex nature of indirect interactions that result in the effective attraction between lattice gas cells forming surface reconstruction.

$$\ln \left[\frac{P}{P_0} \right] = \frac{\mu + \varepsilon}{kT} = \ln \left[\frac{\Theta}{1 - \Theta} \right] + \left[\frac{E_i \Theta}{kT} - \frac{U/kT}{1 + \exp[(V - U \cdot \Theta)/kT]} \right]$$

where Θ denotes the surface coverage by Sb; P – is the Sb_2 pressure; μ is the chemical potential of $c(4 \times 4)$ lattice gas cell, ε is the vertical energy of this cell interaction with the surface, the parameters U, V, E_i are related to the lateral interaction in lattice gas.

The reasonable agreement between the calculated and experimental curves was achieved for the following value of parameters: $U = -0.32$ eV, $V = 0.12$ eV, and $E_i = 0.16$ eV, and the experimental values of Sb_2 pressure normalized by factor $P_0 = 7 \times 10^{-6}$ Torr. For the used parameters the critical temperature $T_c = 415$ °C was found. Hence, at temperatures $T < T_c$ the discontinuous phase transition occurs, and at $T > T_c$ continuous phase transition takes place.

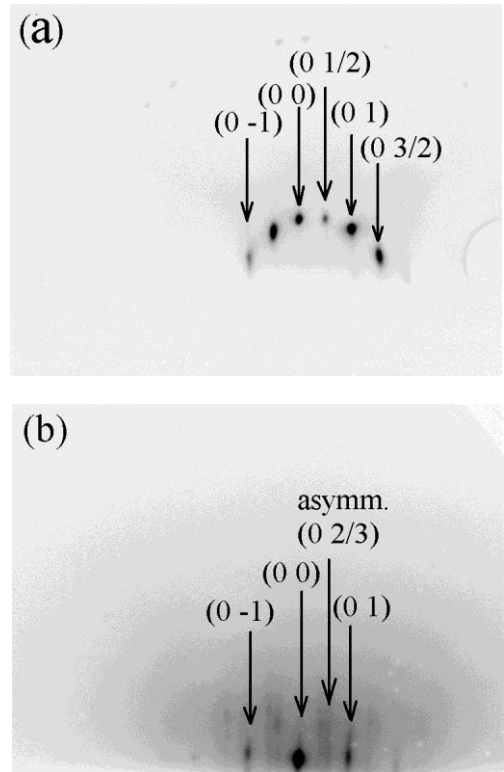


Figure 1. RHEED patterns of (001)InSb reconstructions
a) $c(4 \times 4)$; b) asymmetric (1×3).

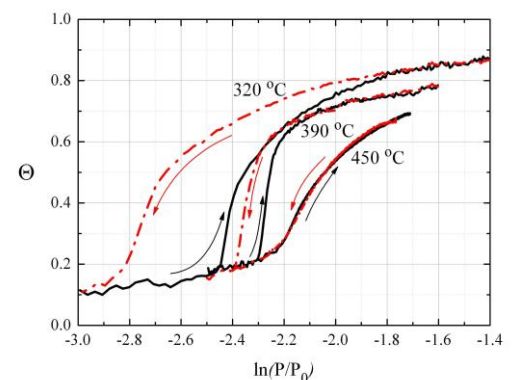


Figure 2. Fractional (0 3/2) spot intensity evolution at different temperatures.

HEAT CAPACITY AND THERMODYNAMIC PROPERTIES OF NEODYMIUM-STRONTIUM TUNGSTATE

Taimassova Sh.T.¹, Zhakupov R.M.^{1,2}, Bissengaliyeva M.R.¹, Gogol D.B.¹, Balbekova B.K.¹

¹Institute of Problems of Complex Development of Mineral Resources, 100019 Karaganda, Kazakhstan

²Lobachevsky State University of Nizhni Novgorod, 603950 Nizhni Novgorod, Russian Federation

E-mail: mirabis@ipkon.kz

Neodymium-strontium tungstate of the stoichiometric composition, SrNd_2WO_7 , is a complex oxide consisting of alkaline earth, rare earth and transition metals. This paper presents the results of measurements of the low-temperature heat capacity of a synthesized compound as well as evaluation of its thermodynamic functions. A sample of the compound was synthesized from oxides and salts of the initial elements by the "sol-gel" method using polyvinyl alcohol at the temperature of annealing up to 1150°C. The crystal structure corresponds to the monoclinic system with space group $P112_1/b$. The substance obtained is isostructural one and it corresponds in its structure to compounds BaLa_2WO_7 and SrLa_2WO_7 described earlier in [1]. The unit cell parameters of the compound after refinement of the X-ray pattern profile were equal to $a = 8.6795 \text{ \AA}$, $b = 12.4454 \text{ \AA}$, $c = 5.7107 \text{ \AA}$, $\gamma = 105.355^\circ$.

Measurements of the heat capacity in helium area were carried out on a low-temperature thermophysical installation produced by «Termax» [2] (the weighed sample was 0.9648 g). Three series of experimental data over the temperature ranges of 4.5-25 K, 4.5-40 K, and 35-80 K were obtained. On the heat capacity curve of the compound below 15 K we registered an abnormal behavior, corresponding to the end of the phase transition of II type, the maximum peak of which was located at about 4 K.

To calculate the lattice component of the heat capacity and compute the anomalous component, we used the equations proposed in [3]. To describe the anomalous component of the heat capacity and extrapolate it to absolute zero the Schottky equation was used. On the basis of the dependence obtained the changes

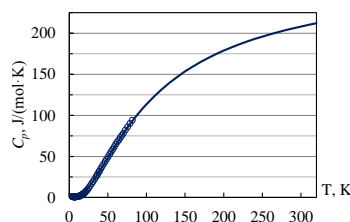


Figure 2. Extrapolated heat capacity of SrNd_2WO_7 .

of enthalpy and entropy in the observed transition were evaluated. The appearance of this anomaly is most likely due to the presence of magnetic moments of Nd^{3+} ions in the crystal structure of the compound [4].

For extrapolation of the heat capacity in the area above the temperature of liquid nitrogen and evaluation of the thermodynamic functions of the compound we used the equation for approximation of the heat capacity proposed in [5]. This equation correctly describes the heat capacity of the compound in the studied temperature range by means of two parameters reflecting the asymptotic behavior of the heat capacity at high and low temperatures.

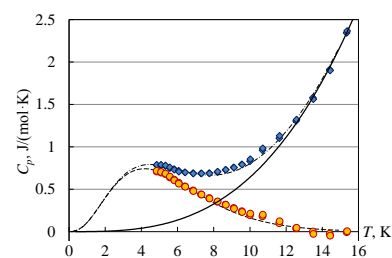


Figure 1. Total (---), lattice (—) and anomalous (— · —) heat capacities of SrNd_2WO_7 .

Table 1. Evaluative values of the thermodynamic functions of compound SrNd_2WO_7 .

T (K)	$C_p(T)$ (J/(mol·K))	$S^\circ(T)$ (J/(mol·K))	$H^\circ(T) - H^\circ(0)$ (kJ/mol)	$G^\circ(T)$ (J/(mol·K))
10	0.852	1.956	0.007	1.290
50	48.68	24.05	0.803	7.980
100	113.5	79.25	4.973	29.51
200	178.8	181.3	20.08	80.95
298.15	207.7	258.8	39.20	127.3

[1] Fu, W; IJdo, D; Bontenbal, A. J. Solid State Chem., 2013, 201, 128-132.

[2] Bissengaliyeva, M; Gogol, D; Taymasova, S; Bekturganov, N. J. Chem. Eng. Data, 2011, 56, 195-204.

[3] Melia, T; Merrifield, R. J. Inorg. Nucl. Chem. 1970, 32, 2573-2579.

[4] Şabikoğlu, I.; Paralı, L.; et al. Prog. Nat. Sci. Mater. Int. 2015, 25, 215-221

[5] Bespyatov, M; Naumov, V. Bull. Kazan Technol. University. 2010, No.6, 33-36.



THE ORDER PARAMETER APPROACH TO THERMODYNAMICS OF NANO-OBJECTS

Chernyshev A.P.

¹*Institute of Solid State Chemistry and Mechanochemistry, SB RAS, 630128, Novosibirsk, Russia*

²*Novosibirsk State Technical University, 630073, Novosibirsk, Russia*

E-mail: alfred.chernyshev@solid.nsc.ru

Nanomaterials are of interest because they allow the use of the unique properties of nanoparticles, nanowires, thin films and other nano-objects in existing materials and are promising components for new materials with unique properties. The latest advances in new synthetic nanomaterials confirm that nanomaterials can retain characteristics of the original building blocks, i.e. nano-objects. In turn, thermodynamical methods in the study and prediction of the properties of nano-objects allow us to consider and systematize the large groups of nanomaterials. In present study, most nano-objects are isolated nanoparticles, nanowires, or thin films on inert substrates, where the interface interaction can be neglected. A theoretical investigation on the size dependence of the surface energy is performed for nanoparticles with the characteristic size less than 10 nm. In addition, some thermodynamics problems are solved for solid–liquid and order–disorder transitions. The mean-field approximation is used to solve these problems. The consideration of the size effect on the thermodynamics functions is carried out by the introduction of the order parameter (η).

The order parameter definition based on the Lindemann criterion is of the form $\eta = \sigma^2 / \sigma_m^2$. Here σ^2 and σ_m^2 are the mean square displacements of atoms from their equilibrium positions at any fixed temperature and at the melting point respectively. The Gibbs free energy (G) of nano-objects is presented by the Ginzburg-Landau functional $G = \int \left[\frac{J}{2} (\nabla \eta)^2 + g(\eta) \right] d^3x$, where $\eta = \eta(x)$ and $g(\eta)$ is the Gibbs energy density and J is a constant.

The surface tension is defined as the excess of the appropriate thermodynamics potential of a nano-object after subtracting that of the homogeneous bulk phase occupying the same volume. Therefore, the specific surface energy (g_s) of the nano-object at constant pressure and temperature can be presented as $g_s = (G - G_{\text{bulk}}) / A$. Here A is the surface area of the nano-object. It is obtained in the present study that the surface energy of thin films increases with decrease in their thickness passing its maximum meaning. A further decrease in the solid film thickness leads to a monotonic decrease in the surface energy. A qualitative explanation of this effect is following. In the present study, it is shown that the existence of the nano-object surface leads to change of the order parameter in the whole volume of the nano-object. It means that the bulk atoms of nano-objects have increased their energy. Per the definition of the specific surface energy, this phenomenon leads to the increase of the surface energy. If the size of nano-objects less than 10 nm approximately, the gradient of the order parameter begins to decrease with the decrease of the nano-objects size. It causes the simultaneous decrease of g_s .

In the framework of the mean-field theory, the surface melting of nano-objects is considered. It is revealed that there exists a critical size of nanoparticles (r_c) at which the surface melting does not occur before the nanoparticle melting. The value of r_c depends on the vibrational component of the melting entropy and the shape of nanoparticles. Surprisingly that there exist nanoparticles, the surface of which melts only at the melting point.

The mean-field theory is used to study the self-diffusion coefficients of nano-objects. If the size of nano-objects is less than 10 nm approximately, there is a mixing of bulk and surface diffusion paths in them. This diffusion property makes the mean-field approach useful for studying diffusion in nano-objects. It is known that the diffusion coefficient of the metal at a temperature of its melting point is almost independent of the pressure. For most metals, the diffusion coefficient decreases with increasing pressure. At the same time the melting temperature is increased that leads to a constant value of the diffusivity at the same homologous temperature for a given metal. For bulk diffusion, this relation is described by the rule of van Liempt. In terms of the mean field approach, this rule is adapted to the nanoscale. The adaptation gives the van Liempt rule $\Delta H(\eta) = K(\eta)RT_m(\eta)$, where $K(\eta)$, R and T_m are the analytical function of η , the gas constant and the melting temperature of nano-object respectively. It follows from this rule that the activation enthalpy of diffusion ($\Delta H(\eta)$) decreases with decreasing the order parameter of nano-objects. Therefore, the maximum of diffusivity is expected in the disorder state of nano-objects.

THE ENTROPY CHANGE IN THE ASSOCIATION INTO DIMERS OF MIXTURES OF HARD SPHERES WITH DIFFERENT DIAMETERS

Davydov A.G., Tkachev N.K.

Institute of High-Temperature Electrochemistry, Ural Branch of the Russian Academy of Sciences, 620137 Ekaterinburg, Russia
E-mail: alex_davydov@mail.ru

The consequences of the statistical-thermodynamic model to calculate the chemical equilibrium in the case of the dimerization of species of different sizes. The dimer supposed to be a rigid dumbbell is formed by the partial overlapping of hard spheres of another diameters. We have analyzed the dimerization equilibrium deviations from the ideal, depending on the ratio of diameters of reacting particles of different size and degree of overlap in the molecule. It was found that the excess entropy shows more pronounced ordering with the increasing differences in the monomer diameters, but with less fusion.

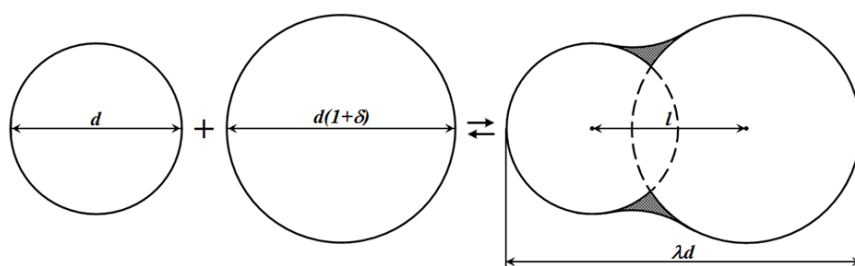


Figure 1. Model for the accounting of excluded volume effects at formation of dumbbell dimeric molecules with partial fusion of particles.

We offer a description of features of the dimerization of two hard spheres fluids with different diameters in the chemical association into dumbbell molecule depending on the degree of monomer overlapping. The consequences of the simplest model to account for the excluded volume effects within the van-der-waals type theory. It was carried out a more accurate description using Mansoori-Carnahan-Starling (MCS) approach to the hard sphere mixtures of different diameters, but with the effective packing fraction depending on form factor of the mixture. Dimeric molecules can be characterized by non-sphericity factor $\alpha = \frac{R_{AB} S_{AB}}{3V_{AB}}$, where R_{AB} is the radius of curvature, S_{AB} is the area and V_{AB} is the volume of dimer [1].

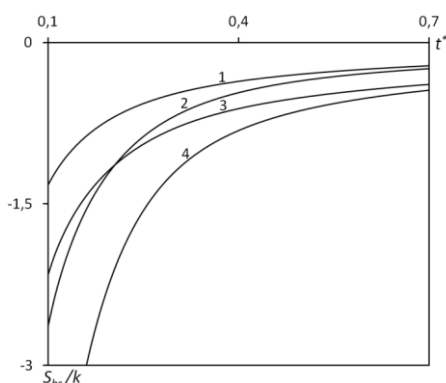


Figure 2. Temperature dependences of a hard-sphere contribution to the entropy: 1 – $\lambda=1.2$, $\delta=0$; 2 – $\lambda=1.9$, $\delta=0$; 3 – $\lambda=1.9$, $\delta=0.7$; 4 – $\lambda=2.6$, $\delta=0.7$.

The behavior of the packing fraction depends on the size difference of monomers and their overlapping in the molecule. It is shown that the stronger the fusion of monomers the greater the displacement of the chemical equilibrium from ideality. Conversely, at slight fusion the negative deviations take place. However, these negative deviations are much smaller.

Fig. 2 shows the results of calculations of the excess entropy as a function of the reduced temperature. This dependence of the excluded volume effect contribution into the entropy of dimerizing fluid mixture are always negative. It can be readily seen that the larger difference in diameters the stronger ordering in the reacting mixtures takes place.

This work was supported by the Russian Foundation for Basic Research (15-03-01588).

- [1] Largo J., Solana J.R. Phys. Rev., 1998, 58, 2251-2258.
[2] Tkachev N.K., Zinatullina A.R. Rus. J. Phys. Chem. A, 2013, 87, 1457-1462.
[3] Tkachev N.K. Rasplavy (in Russian), 2014, 87-92.

MOLECULAR DYNAMICS SIMULATION OF GAS DIFFUSION IN CMK-5 MATERIAL IN THE PRESENCE OF ACETONITRILE

Ivanova E.A., Sizova A.A., Sizov V.V., Brodskaya E.N.

Institute of Chemistry, St. Petersburg State University, 198504 St.Petersburg, Russia

E-mail: elena_130596@inbox.ru

Adsorptive separation of gaseous mixtures has been steadily gaining popularity over the last two decades. The use of porous solids for separation and purification of gases is a particularly promising approach for important industrial mixtures such as biogas (CO_2/CH_4) and flue gas (CO_2/N_2). To improve the existing separation technics the detailed knowledge of thermodynamic and transport properties of adsorbate is necessary.

In this work, the diffusion of gases in the mesoporous carbonaceous CMK-5 material in the presence of acetonitrile was investigated. The simulations were performed using molecular dynamics method in canonical ensemble at temperature of 298 K. The diffusion of pure gases and CO_2/N_2 and CO_2/CH_4 mixtures of various compositions was considered in this study. The amount of preadsorbed acetonitrile in the pores was for 0%, 6% and 20 mass.% (Fig. 1). Molecular dynamics simulations were carried out using Gromacs v.5.0.4 software package.

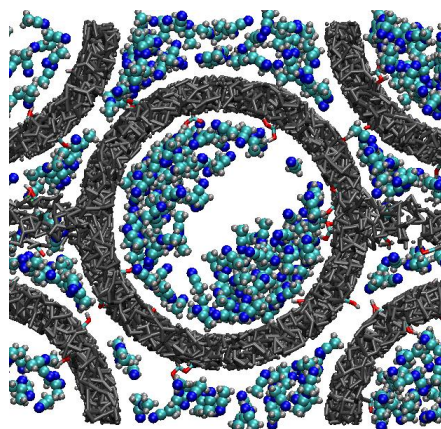


Figure 1. Structure of CMK-5 material with preadsorbed acetonitrile (20 mass.%).

Gas diffusivity is found to depend on adsorbate local structure. Molecules located near the surface of the adsorbent are characterized by very low diffusion coefficients. Displacement of molecules towards the pore center enhances their mobility. The growth of fluid density in the pore center can lead to the decrease of gas diffusivity. In the presence of acetonitrile in CMK-5 at low and medium gas content the adsorbate mobility became higher than in dry material. At high adsorbate densities the presence of acetonitrile molecules, which significantly reduce the available pore volume, restricts diffusion of gases.

This work was supported by the Russian Foundation for Basic Research (grant no. 16-33-00919 MOL_A).

RECONSTRUCTION OF A SINGLE FEW-PARAMETRICAL EQUATION FOR CALCULATING THE VISCOSITY COEFFICIENT. ARGON

A.B. Kaplun, A.B. Meshalkin, O.S. Dutova, and E.P. Raschektaeva
Kutateladze Institute of Thermophysics SB RAS, Lavrentiev Av. 1, Novosibirsk, 630090, Russia.
 E-mail: kaplun@itp.nsc.ru

Using previously determined [1] unambiguous dependence of excessive viscosity $\Delta\eta = \eta(T, \rho) - \eta_{en}(T)$ on the density of interaction energy $\Delta U/V$ [1], where $\Delta U = U_{ig} - U(T, \rho)$, which is satisfied in the zone of liquid phase and dense gas, a single few-parametrical (4 parameters) equation for calculating the viscosity coefficient of liquid, gas and fluid was obtained. This equation accurately describes experimental and tabular data on the viscosity of argon. Internal energy $U(T, \rho)$ was calculated using the new single few-parametrical equation of state to calculate the thermodynamic properties of liquid, gas and fluid [2]. The detailed analysis revealed that the maximal systematic deviations of calculated values of viscosity from the original tabular and experimental data in [1] are in the region of transition from the rarefied to mildly dense gas. It is believed that in the transition region, where it is necessary to consider the dependence of viscosity coefficient on density, both momentum transfer mechanisms are used: momentum transfer by collisions and momentum transfer due to intermolecular interaction (the “field” mechanism). Since the field mechanism of momentum transfer becomes prevalent with an increase in the internal energy density, and the mixed mechanism of momentum transfer can be neglected, the equation describing viscosity by the mixed mechanism should be supplemented by some crossover function, which should provide the transition from one mechanism of momentum transfer at the shear flow to another. To estimate the total contribution of the collision and field mechanisms of momentum transfer to the viscosity coefficient, we have described the total contribution of these mechanisms to the viscosity as the RMS value of both these contributions. The equation for calculating the excessive viscosity of argon in the range of the “mixed” momentum transfer mechanism at the shear flow was derived. Different versions of approximation of excessive viscosity dependence on the density of interaction energy were compared, and the optimal version of this dependence was determined. A simple single few-parametrical equation for describing the viscosity coefficient of argon in a wide range of the state parameters was derived (Fig. 1). It is shown that the calculated values of viscosity agree with the experimental and tabular data within the experimental error (Fig. 2). It was found out that this equation for calculating the viscosity coefficient of liquid and gas allows reliable extrapolation beyond the studied area.

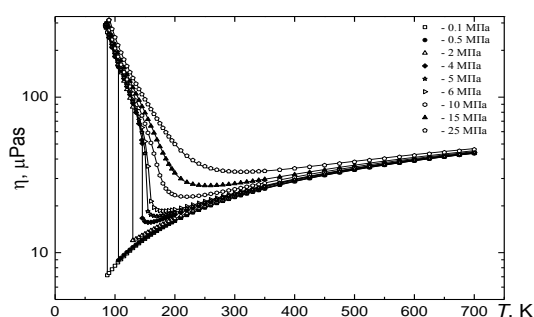


Figure 1. Comparison of calculated values of argon viscosity (lines) with tabular (symbols) data for the densities from 0 to ρ_{tr} .

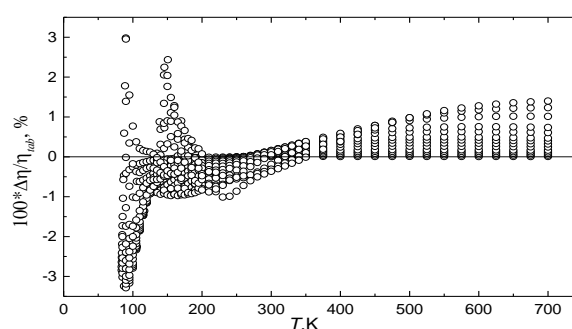


Figure 2. Relative deviations of calculated viscosity values $\Delta\eta/\eta$, % from the tabular data (Lemmon, 2004) for argon depending on the temperature in the pressure range of up to 25 MPa.

The work was partially supported by the Russian Foundation for Basic Research, grant No.15-08-01072.

[1] A.B. Kaplun, *High Temperatures*, 1989, **27**, No.5, 884-888.

[2] A.B. Kaplun; A.B. Meshalkin, *Thermophysics and Aeromechanics*, 2017, in print.



**TERMODINAMIC PROPERTIES OF SOLUTIONS IN THE
D2EHPA – O-XYLENE – DI-(2-ETHYLHEXYL)PHOSPHATE LANTHANIDE
SYSTEM**

Kurdakova S.V.^{1,2}, Kovalenko N.A.², Zapolskih T.V.², Genkin V.M.², Uspenskaya I.A.²

¹ Department of Materials Science, *M.V. Lomonosov Moscow State University. Leninskiye Gory. 1, str. 3, 119991 Moscow, Russia*

² Chemistry Department, *M.V. Lomonosov Moscow State University. Leninskiye Gory. 1, str. 3, 119991 Moscow, Russia*

E-mail: s.kurdakova@gmail.com

Rare earth elements (REE) and their compounds are in demand in a wide and rapidly expanding range of applications. In some cases, a single rare earth element is required. Since REE have similar chemical properties, separation and purification of lanthanides are based on multistage and laborious processes. Liquid phase extraction is an efficient method to purify these elements. Di-(2-ethylhexyl) phosphoric acid (D2EHPA) is one of the most perspective extractants for this purpose. REE are extracted into the organic phase in the form of lanthanide di-(2-ethylhexyl) phosphate complexes (LnA_3). The extraction process may be complicated by occurrence of the third phase, which is formed as a result of precipitation of LnA_3 complexes [1]. In thermodynamic terms it means the loss of liquid phase stability, so thermodynamic properties of the ternary solutions D2EHPA – LnA_3 – diluent are necessary for the solving of “a third phase problem”. This information is required too as input data for the thermodynamic modeling of REE separation and purification by extraction. To the best of our knowledge, there are no experimental investigations of such systems thermodynamics and solubility of LnA_3 was studied only partially [2].

The purpose of this work is to measure the solubility of LnA_3 in D2EHPA and mixed solvent D2EHPA – *o*-xylene and to study thermodynamic properties of the D2EHPA – LnA_3 – *o*-xylene solutions. Di-(2-ethylhexyl)phosphate lanthanides (LnA_3 , Ln = Nd, Sm, Eu, Gd) were synthesized according to the technique from Trifonov [3]. X-ray powder diffraction (XRD), infrared spectroscopy (FTIR), simultaneous thermal analysis coupled with mass-spectrometry of evolved gases (STA–MS) were used to identify the products. The ratio Ln/P was determined by scanning electron microscopy with energy-dispersive analyzer (SEM–EDX).

The vapor–liquid equilibria in the ternary systems D2EHPA – LnA_3 (Ln = Nd, Sm, Eu, Gd) – *o*-xylene were investigated in the temperature range of 283.15–308.15 K using an installation described in detail in [4].

Densities of solutions were measured by VIP-2MP density meter (Termex) at 298 ± 0.05 K.

The solubility of LnA_3 (Ln = Nd, Sm, Eu, Gd) in pure D2EHPA in the temperature range of 283.15–323.15 K and in the mixed solvent D2EHPA–*o*-xylene at 298.15 K was obtained. The decreasing solubility of di-(2-ethylhexyl) phosphate lanthanide in D2EHPA was observed with increasing atomic number of lanthanide. It was revealed that solubility of LnA_3 (Ln is light and middle REE) depends on the composition of mixed solvent; the difference among solubility of complexes with various Ln in mixtures enriched with D2EHPA significantly larger than for mixtures enriched with diluent (at 93 % *o*-xylene in D2EHPA this difference the does not exceed the measurement error).

The work is performed at User Facility Center of M.V. Lomonosov Moscow State University under financial support of URALCHEM.

[1] Testard, F; Bauduin, P; Berthon L. *Ion Exch. Solvent Extr.*, 2010, 19, 381-428.

[2] Proyayev, V.V; Yedinakova, V; Martsokha, S.B. *Radiochim.*, 1991, 33, 65-70.

[3] Trifonov, Y.I; Legin, E.K; Suglobov, D.N. *Radiochim.*, 1985, 27, 422-429.

[4] Kovalenko, N.A; Pustovgar, E.A; Uspenskaya, I.A. *J. Chem. Eng. Data*, 2013, 58, 159-166.



QUANTUM-CHEMICAL SIMULATIONS OF COLOUR CENTERS IN MBE A_3B_5 COMPATIBLE SYSTEMS

Lyamkina A.A.¹, Anikeeva V.E.², Moshchenko S.P.¹

¹*A.V. Rzhanov Institute of Semiconductor Physics, Siberian Branch of the Russian Academy of Sciences, 630090 Novosibirsk, Russia*

²*Novosibirsk State University, 630090 Novosibirsk, Russia*
E-mail: lyamkina@isp.nsc.ru

Solid state quantum emitters represent an important building block for advanced nano-devices as they allow for operations with single photons required for quantum cryptography and quantum computing. The most promising candidates include colour centers in diamond [1] and semiconductor quantum dots [2]. While the former has a benefit of operations at the room temperature as well as a number of attractive spectroscopic features, it is less technologically advanced as diamond is rather difficult to process. The latter provides the access to the well developed semiconductor technology that allows producing structures with integrated monolithically embedded mirrors and resonators etc. Electrical pumping allows for greatly scaling down devices with semiconductor quantum dots but they have a significantly limited range of working temperatures. Therefore, a convenient platform that combines both advantages would be of great interest for a wide range of applications.

Here, we start from the semiconductor platform where first a technologically compatible dielectric with a wide band gap would be needed to realize colour centers. Aluminum oxide could be considered as such a dielectric as it can be formed after the oxidation of aluminum arsenide layers. This oxidation is a routine procedure that is widely used for processing structures fabricated by technology of molecular beam epitaxy (MBE). It is applied to form oxide apertures of Al_xO_y in structures for vertical-cavity surface-emitting lasers and can be carried out with a high precision [3]. Moreover, Al_2O_3 has a chromium-based colour center $Al_2O_3:Cr$ that is well known as ruby and could be technologically produced with either implantation of Cr ions or corresponding doping of semiconductor layers followed by diffusion. Ion implantation method normally requires subsequent high-temperature annealing for formation of bright colour centers [4]. This procedure might not be compatible with GaAs postprocessing, so chromium diffusion from the substrate to AlAs layers followed by the selective oxidation should be primarily considered. As AlAs layers can be grown on substrates of gallium arsenide, the proposed scheme would directly combine all the advantages of the GaAs technology with ruby-like colour centers. Thus, quantum emitters can be readily coupled to semiconductor nanostructures and provide a highly versatile hybrid system.

While this scheme is obviously compatible with MBE technology, its experimental implementation is complicated and requires careful elaboration of structure parameters and growth/annealing conditions. In this work we focus on theoretical investigation of chromium impurities in GaAs, AlAs and their diffusion in layered structures. We carry out density-functional calculations and determine the formation energy of an impurity and its migration barriers. Based on these results, we analyze MBE accessible mechanisms and factors that could facilitate chromium migration and the formation of colour centers (growth temperatures, the ratio of III/V fluxes to enable an optimal spectrum of intrinsic defects in matrix).

The work was supported by RFBR via grant 16-37-60075. AAL acknowledges the financial support via RF president scholarship (SP-3014.2016.3).

- [1] Rogers, L.J.; Jahnke, K.D.; Teraji, T.; Marseglia, L.; Mueller, C.; Naydenov, B.; Schauffert, H.; Kranz, C.; Isoya, J.; McGuinness, L.P. and Jelezko, F. *Nat. Comm.*, 2014, 5, 4739.
- [2] Bimberg, D.; Pohl, Udo W. *Mat. today*, 2011, 14, 388–397.
- [3] Germann, T.D.; Hofmann, W.; Nadochiy, A.M.; Schulze, J.-H.; Mutig, A.; Strittmatter, A. and Bimberg, D. *Optics Express*, 2012, 20(5), 5099-5107.
- [4] Ahn, Y.-K.; Seo, J.-G.; Park, J.-W. *J. of Cr. Growth*, 2011, 326, 45–49.

GRAPHENE-LIKE AlN LAYER FORMATION AND PHASE TRANSITION INTO WURTZITE PHASE ON THE Si(111) SURFACE BY AMMONIA MBE

Mansurov V.G., Galitsyn Yu.G., Malin T.V., Zhuravlev K.S.

Rzhanov Institute of Semiconductor Physics, Siberian Branch of the Russian Academy of Sciences, 630090 Novosibirsk, Russia

E-mail: mansurov@isp.nsc.ru

After the discovery of graphene, graphene-like materials attracted an extraordinary amount of interest from both the fundamental science and industry because of their unusual physical and chemical properties and high specific surface areas.

In this work, for the first time, a graphene-like AlN (g-AlN) layer on a (111)Si substrate has been fabricated in ammonia molecular beam epitaxy (MBE) and investigated by RHEED (Fig.1) and TEM. A flat g-AlN layer with a thickness of a few monolayers was formed by the deposition of Al atoms onto a highly ordered SiN-(8×8) surface prepared on the atomically flat (111)Si substrate under an ammonia flux. An unusual (4×4) structure on the Si surface was found. The exact coincidence of the fundamental (0 1) AlN streak and the fractional-order (0 5/4) beam the (4×4) RHEED structure of (111)Si surface allows us to measure precisely the in-plane lattice parameters of g-AlN. The g-AlN lattice constant of 3.08 Å is found in a good agreement with the *ab initio* calculations performed recently [1]. We have carried out precise measurements of the in-plane AlN lattice constant under the Al and NH₃ fluxes supplied onto the surface either separately or simultaneously. The evolution of the in-plane lattice constant during the process of formation of g-AlN is shown in Fig.2

The wurtzite phase of the III-nitrides are polar materials and characterized by strong polarization (i.e. strong charges appears on the surfaces) spontaneously appeared in the nitrides, but polarization is absent in graphit-like structures. Phase transition from g-AlN phase to w-AlN phase at thickness of 24 ML is predicted from *ab initio* calculations [2]. The transition at thickness of 6 ML is found experimentally in this work. For this case the driving force of the phase transition is the interlayer Van-der-Waals interaction resulting in transformation from the plain structure based on sp² hybridization orbitals to 3D structure on base of sp³ orbitals (Fig.3). This phase transition is experimentally observed here for the first time (see Fig.1 and Fig.2).

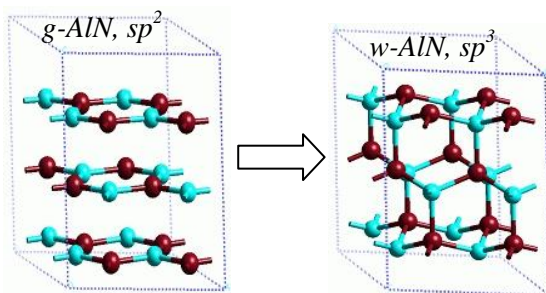


Figure 3. Structure transformation – new type of the Van-der-Waals phase transition

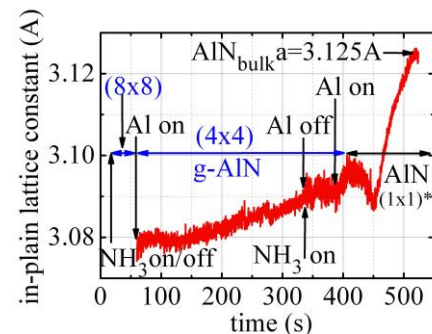
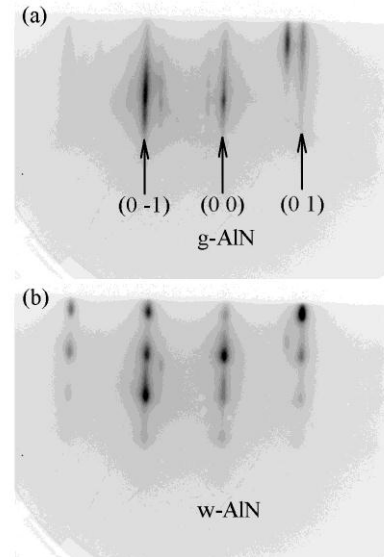


Figure 2. In-plane lattice parameter behavior during AlN formation process. Sharp transition g-AlN to w-AlN is visible

This work was supported by RFBR (grants 17-52-45108, 17-02-00947).

[1] Şahin, H., Cahangirov, S., Topsakal, M., Bekaroglu, E., Akturk, E., Senger, R.T., Ciraci, S. Phys. Rev. B, 80 (2009), p. 155453

[2] Freeman, C.L., Claeysens, F., Allan, N.L., Harding, J.H. Phys. Rev. Lett., 96 (2006) 066102



THERMODYNAMIC FEASIBILITY ANALYSIS – A SUITABLE TOOL FOR SYSTEMS BIOLOGY

Kohrt, H.¹, Held, C.², Verevkin, S.³, Maskow, T.¹

¹Department of Environmental Microbiology, WG Biocalorimetry/Ecothermodynamics, Helmholtz Centre for Environmental Research-UFZ, 04318 Leipzig, Germany

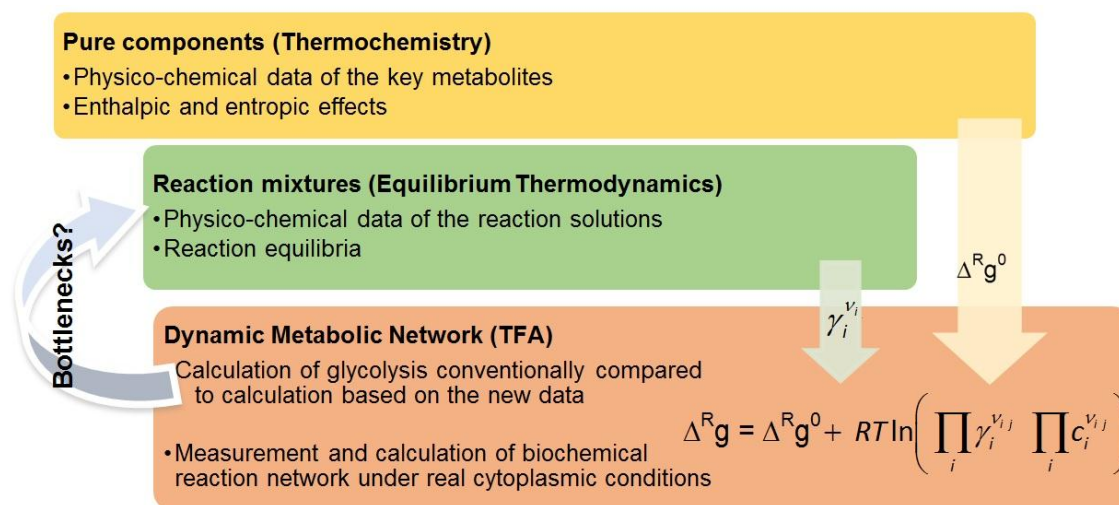
²Laboratory of Thermodynamics, Department of Biochemical and Chemical Engineering, Technische Universität Dortmund, 44227 Dortmund, Germany

³Institute of Chemistry, Department of Physical Chemistry, University of Rostock, 18051 Rostock, Germany
E-mail: Thomas.maskow@ufz.de

Metabolic Flux Analysis (MFA) is a powerful tool of systems biology in describing the functioning of an entire cell. MFA by applying mass balances as well as kinetic relations results unfortunately in huge undetermined equation systems. Thermodynamics might help in reducing solution space by eliminating solutions that fulfill mass balances but violate second law of thermodynamics. For this reason an algorithm called Thermodynamic Feasibility Analysis (TFA) has already been tested on well-known glycolysis pathway.¹ Unfortunately, even glycolysis pathway has been estimated thermodynamically unfeasible. Neglecting activity coefficients, poor thermodynamic basic data as well as neglecting the influence of special conditions in the cytosol of the cell (e.g. macromolecular crowding, ionic strength etc.) have been detected as possible reasons of the unexpected outcome.²

Within the algorithm of TFA, Δ_{gR} is calculated for each single reaction of a certain metabolic pathway as well as for combinations of consecutive reactions using the measured concentration range of the metabolites. Reactions that will reveal a positive value of Δ_{gR} will be considered as thermodynamically unfeasible and designated as localized bottlenecks. Combinations of consecutive reactions with a positive value of Δ_{gR} for the total reaction result in so called distributed bottlenecks. Both, the occurrence of localized and distributed bottlenecks, will make a given metabolic pathway unfeasible.

In the current work, the applicability of TFA on glycolysis will be explored using state of the art thermodynamic data and models. Three areas will be researched (Fig. 1). First, physical and thermochemical basic data of selected pure metabolites will be determined. Second, the reaction equilibria of these metabolites under real cytoplasmic conditions (e.g. ionic strength, molecular crowding) are determined and modelled with e-PC-SAFT. Finally, the pure component data as well as the reaction data are applied to a dynamic metabolic network. This project will help to clarify the potential role of thermodynamics to enlighten complex intra-cellular metabolic networks.



(1) Maskow, T.; von Stockar, U. *Biotechnol. Bioeng.* **2005**, *92*, 223-230.

(2) von Stockar, U.; Maskow, T.; Vojinovic, V. *Thermodynamic Analysis of Metabolic Pathways*; EPFL Press Distributed by CRC Press., 2013.



ADDITIONS TO THE TECHNIQUES OF DATA ANALYSIS FOR POLYTHERMIC PROCESSES INDIVIDUAL SUBSTANCE – SATURATED VAPOR

Belevantsev V.I.¹, Ryzhikh A.P.^{1,2}

¹Nikolaev Institute of Inorganic Chemistry, Siberian Branch of the Russian Academy of Sciences, 630090 Novosibirsk, Russia

²Novosibirsk State Pedagogical University, 630126 Novosibirsk, Russia

E-mail: ryzhikh@niic.nsc.ru

The purpose of the report is to analyze (on the base precision of information about the system: water – saturated steam in the interval 0.01–200°C of P,T -line their coexistence [1]) fundamental relationship between effects from the Clausius-Clapeyron equation and additions from the van't Hoff equation. On this basis we provide a generalized method of analysis P,T,\tilde{V} -data on equilibria of this class ($A_{\text{cond}} \leftrightarrow (A)_{\text{gas}}$). As is known, the Clausius-Clapeyron equation is usually represented as:

$$(dP/dT)_{\text{coex}} = \Delta_r \tilde{H} / (T \cdot \Delta_r \tilde{V}), \quad (1)$$

showing the relationship between derivative of the $P = \varphi(T)$ function on P,T -line coexistence of the considered phases and their specific enthalpies and volumes. Analysis of equation (1) (based on ideas borrowed from previous works [2, 3]) have given rise to three dimensionless complexes:

$$(d \ln P / d \ln T)_{\text{coex}} = T \Delta_r \tilde{S} / (P \Delta_r \tilde{V}) = \Delta_r \tilde{H} / (P \Delta_r \tilde{V}). \quad (2)$$

A consequence from (2) in the most constructive form:

$$(d \ln P / d \ln T)_{\text{coex}} \cdot (P \Delta_r \tilde{V}) = T \Delta_r \tilde{S} = \Delta_r \tilde{H}, \quad (3)$$

gives access from P,T,\tilde{V} -data on the two phases to the thermodynamic characteristics of the reaction ($\Delta_r \tilde{H}$, $\Delta_r \tilde{S}$, $\Delta_r \tilde{C}_p$). The implementation of the method is possible on the basis of the OLS-approximations of P,T -data in the form of polynomials $\ln P_{\text{init}} \cong \varphi_k(X_k) = \ln P_{\text{k calc}}$, where X_k is the T^*/T , or $(T-T^*)/T$, or $\ln(T/T^*)$. For the selected dataset (for H_2O) either X_k choice the cubic polynomials with a common center $T^*=373.15$ K were adequate. Moreover, it is the third ($X_3 = \ln(T/T^*)$) provided the best results and direct access to the connection (3) using:

$$(d \ln P / d \ln T)_{\text{coex}} \sim d \ln P / d X_3 = 13.31939 - 17.18166 \cdot X_3 + 11.88606 \cdot (X_3)^2. \quad (4)$$

For possible detailing of the hydrogen oxide (as a gross component) state in the saturated steam one should turn to the fundamental van't Hoff equation. For the solving problems of this class it is rational to submit the equation in the form:

$$d \ln K_{C^*}^{\ominus} / d \ln T |_{\text{coex}} = (\Delta_r \tilde{H} - P \Delta_r \tilde{V}) / RT. \quad (5)$$

Here in our case $K_{C^*}^{\ominus} = C^*(\text{mol/l})/1^*(\text{mol/l})$ [4] – the equilibrium constant in terms of molar concentration of the hydrogen oxide. The data array [1] made it possible to introduce approximations $P \Delta_r \tilde{V} \cong P \tilde{V}_g$ and $\ln K_{C^*}^{\ominus} \cong \ln(C^*/\gamma^*)$ (where $\gamma^* = RT/P \tilde{V}_g = C^* RT/P$), used to identify the consequences of (5) to support the hypothesis [5] on significant dimerization ($C^* = C_{H_2O} + 2C_{(H_2O)_2}$) on the interval 100–200°C. In the interval of 0.01–20°C deviation of the $P \tilde{V}_g$ product calculated in the ideal-gas version is not beyond mistakes, and 25–90°C segment was used to estimate the regression parameters describe significant deviations from the ideality of monomer ($\gamma^* \cong \gamma^0$, where $\gamma^0 \cong C_{H_2O} RT/P$). The results for the interval 100–200°C confirmed the validity of the dimerization hypothesis and assessed the proportion of the hydrogen oxide in dimer state about 6% by the end of the interval.

[1] Moscow Power Engineering Institute: Mathcad Calculation Server.

http://twf.mpei.ac.ru/MCS/Worksheets/PhyRefBook/13_2.xmcd.

[2] Belevantsev, VI; Malkova, VI.; Ryzhikh, AP. Russ. J. Phys. Chem. A. 2010, 84, 134-136.

[3] Belevantsev, VI; Ryzhikh, AP; Zherikova, KV; Morozova, NB. J. Therm. Anal. Calorim. 2014, 115, 1851-1856.

[4] Belevantsev, VI. Russ. J. Phys. Chem. A. 2002, 76, 524-529.

[5] Vigasin, AA. Zhurn. Strukt. Chimii. 1983, 24, 116-141.



THE EFFECT OF WATER AND AQUEOUS-ORGANIC MEDIUMS ON COMPLEX FORMATION OF SOME d-, f-METAL IONS WITH NITROGEN-CONTAINING ORGANIC LIGANDS

Uali A., Amerkhanova Sh.K., Shlyapov R.M., Abdiken F.S.
Buketov Karaganda State University, 100028, Karaganda, Kazakhstan
E-mail: amerkhanova_sh@mail.ru, ualieva.84@mail.ru

Nowadays researches relating to the modification of biologically active compounds by metals have been taken a great relevance since the majority of compounds possessing biological activity contain atoms of N, S, and O as a part of cyclic compounds, and d-, f-metals ions are the most effective modifiers in this case. Investigations of the complexing ability of methionine (Met) and DL-tryptophan with Y (III) ions in the aqueous solutions, 4-hydroxybenzoylhydrazide (1), and N-2-(2-hydroxybenzoyl)hydrazinocarbonthioylbenzamide (2) [1] in water-1,4-dioxane medium, as well as hydrazide of N-morpholinylacetic acid (3) in water-EtOH medium with Nd (III), and La (III) ions in a wide range of ionic strength ($0.1 \div 1$), temperature ($298 \div 318$ K) and concentration of the organic solvent ($10 \div 90$ vol.%) have been carried out.

pH-Metric measurements were carried out on the device pH-meter 827 Lab (Metrohm). It has been found that the pKa value (1) varies parabolically with an increase in the amount of dioxane, and pKa equals to 2.85 at a ratio of water - 1,4-dioxane (50:50 vol.%) corresponding to mole fraction of dioxane 0.17. In this concentration interval, 1,4-dioxane is in the form of individual molecules in the cavities formed by the water molecules and there is a maximum of pKa at a ratio of water - 1,4-dioxane is 10:90 vol. %. Formation of coarsely dispersed emulsion of water (500 - 600 molecules) is typical for this concentration interval [1]. It is shown that the pKa (2) reaches the maximum (6.67) at mole fraction of dioxane 0.17 (50:50 vol. %). pKa (3) has the maximum value (8.50) at mole fraction of EtOH 0.24 (50:50 vol. %), and pKa equals to 2.54 at mole fraction of EtOH 0.73. This is caused by a change of permittivity and electron-acceptor ability of EtOH expressed by E_T^N .

These changes are due to the selective solvation of hydrophilic substituents of the ligand by water molecules and non-polar aromatic groups by molecules of dioxane and EtOH. Consequently, the donor ability of solvent by Gutman (DN) varies in a series of dioxane 16.39 and EtOH 20.69, and affects the acid-base properties of the ligand. Therefore, it has been considered the influence of the donor numbers of water and water-organic solvent at a ratio (50:50 vol. %) on the value of thermal effect of the complex formation. It is revealed that $\Delta_f H_{298}^\circ$ of complexes in systems investigated are as follows: Y(III) ion - Met, Y (III) ion - Trp are (-369.48) kJ/mole and (-120.91) kJ/mole, respectively, Nd (III) ion - (1) is 275.30 kJ/mole, Nd (III) ion - (2) is equal to -102.99 kJ/mole, Nd (III) ion - (3) is equal to 8.22 kJ/mole, and La (III) ion - (2) is -72.98 kJ/mole.

It has been shown that DL-tryptophan demonstrates low activity toward Y (III) ions, which is explained by the steric effect of the radical, namely, low availability of the nitrogen atom of indole ring. In the case of methionine, the presence of sulfur atom in the chain increases the probability of binding the metal ion. This is due to the influence of the donor ability of the solvent on the solvation energy of cations ($-\Delta G_{sol}^\circ$), thus the latter is 6.70 kJ/mole for Y (III) ion in water, 6.20 kJ/mole for Nd (III) ion in dioxane, 6.28 kJ/mole for Nd (III) ion in EtOH, and 5.75 kJ/mole for La (III) ion in dioxane, which is correlated with the values of the heats of complexation. Thus, the influence of water and aqueous-organic mediums on the strength of the bond metal-ligand and complex is due to the change of the ability of the ligand to dissociate and solvation energy of the cation, which will determine the biological activity of the organic ligand.

[1] Lischenko, A.S., Tanasyuk, D.A., Yermakov, V.I.// Rus. J. of Journal Adv. in Chem. and Chem. Tech., 2015, 29, 6, 27-29.



MOLECULAR DYNAMICS AND CONTINUUM ELECTROSTATIC METHOD TO COMPUTE pKa's AND IONIZATION DEGREES OF IONIZABLE GROUPS AND FRACTIONS OF HISTIDINE TAUTOMERS OF PROTEINS AS FUNCTION OF pH

Vorobjev Yu. N.^{1,2,3*}, Scheraga H. A.³ and Vila J. A.^{3,4}

¹ Institute of Chemical Biology and Fundamental Medicine of the Siberian Branch of the Russian Academy of Science, Novosibirsk 630090, Russia;

² Novosibirsk State University, Novosibirsk 630090, Russia;

³ Baker Laboratory of Chemistry and Chemical Biology, Cornell University, Ithaca, NY 14853-1301; ⁴IMASL-CONICET, Universidad Nacional de San Luis, Avenida Italia 1556, 5700 San Luis, Argentina.

*E-mail: ynvorob@niboch.nsc.ru

A computational method, to predict the pKa values of the ionizable residues Asp, Glu, His, Tyr and Lys of proteins, is presented here. Calculation of the electrostatic free-energy of the proteins is based on an efficient version of a continuum dielectric electrostatic model. The conformational flexibility of the protein is taken into account by carrying out molecular dynamics simulations of 10 ns in implicit water. The accuracy of the proposed method of calculation of pKa values is estimated from a test set of experimental pKa data for 297 ionizable residues from 34 proteins. The pKa-prediction test shows that, on average, 57%, 86% and 95% of all predictions have an error lower than 0.5, 1.0 and 1.5 pKa units, respectively. This work contributes to our general understanding of the importance of protein flexibility for an accurate computation of pKa, providing critical insight about the significance of the multiple neutral states of acid and histidine residues for pKa-prediction, and may spur significant progress in our effort to develop a fast and accurate electrostatic-based method for pKa-predictions of proteins as a function of pH.

The study the accuracy of the prediction of the tautomeric fractions of the imidazole ring of each of the 6 histidine residues from *Loligo vulgaris* (pdb id 1E1A), a 314 residues protein. The average tautomeric fractions of the His was compute by using an approach that includes, but is not limited to, molecular dynamic simulations coupled with calculations of the ionization states for all 94 ionizable residues of the protein 1E1A in water at pH 6.5 and 300 K. The results of the analysis on protein 1E1A indicate that the averaged calculated fractions of histidine tautomers, namely for the N^{δ1}-H and N^{ε2}-H forms, respectively, are in good agreement, within ~11%, with the prediction of an NMR-based methodology[1,2]. Computer program is available by request from professor Y.V., <http://bison.niboch.nsc.ru/fambe.html>

This research was supported by grants from the Russian Academy of Science, grants 15-04-00387-a, Molecular and cell biology #6.11, RSF-14-14-00063, RSF #16-14-10038 and also by grants from the National Institutes of Health (GM-14312), the National Science Foundation (MCB10-19767) (HAS), PIP-112-2011-0100030 from CONICET-Argentina, Project 3-2212 from UNSL-Argentina, and PICT-2014-0556 from ANPCyT-Argentina (JAV).

[1] Vorobjev, Y.N.; Vila, J.H.; Scheraga, H.A. *J. Phys. Chem.* 2008, 112, 11122-11136.

[2] Vila, J.A.; Arnautova, Y.A.; Vorobjev, Y.N., Scheraga, H.A. *Proc Natl Acad Sci USA.* 2011, 108, 5602-5607.

**THERMODYNAMIC DATABASE OF ZEOLITES**Voronin G.F., Kutsenok I.B., Voskov A.L.*Lomonosov Moscow State University, Chemistry Department, 119991 Moscow, Russia*

E-mail: ibk@td.chem.msu.ru

A database on the thermodynamic properties of zeolites has been created. It contains the published results of raw experimental measurements of heat capacities, entropies and enthalpies for 43 zeolites of different composition at different temperatures and molar volumes at 298.15 K in addition to literature references. It is about 1/3 higher than the number of zeolites that have been discussed in known published analytical reviews and databases on thermodynamic properties of these substances. The database software is able to detect violations of electroneutrality condition in zeolite formulae, change the formulae recording format and corresponding numerical values of zeolites' properties. For example, it allows to calculate the thermodynamic properties per one silicon-oxygen tetrahedron (so-called TO₂-format) as well as to choose data that meet specified conditions (chemical composition, set of thermodynamic properties of interest, temperature range) and to include or exclude peculiarities of thermodynamic functions associated with the λ -transformations.

To analyze the quality of available data and for their subsequent use, the temperature dependences of $C_p(T)$, $S(T) - S(0)$, $H(T) - H(0)$, $G(T) - H(0)$ thermodynamic functions have been approximated by linear combinations of harmonic oscillators functions (Planck-Einstein functions). For example, the approximation expression for the molar isobaric heat capacity is

$$C_p(T) = \sum_{i=1}^m \alpha_i C_E(\theta_i/T),$$

where $C_E(x) = 3Rx^2 \exp(x) / [\exp(x) - 1]^2$ is the molar heat capacity of the 3D harmonic oscillator in the Planck-Einstein model; α_i and θ_i are the approximation parameters found by the least squares method; m is the number of summands that is usually between 3 and 9. Similar formulae with the same approximation parameters set were used for approximating other thermodynamic functions listed above. All other details of this approximation method were described in [1]. For most zeolites under consideration, the results of the isobaric specific heat measurements at temperatures below 10 K are available. That is why the applied calculation method leads to consistent values of heat capacities, entropy and enthalpy. It allows to quantitatively estimate the uncertainties of these thermodynamic values as well. Data in the database are presented as self-consistent thermodynamic functions with a single set of parameters for each substance. The database contains information about the thermodynamic properties of zeolites consisted of Na, K, Ca, Mg, Sr, Ba, Fe, Al, Si oxides and H₂O.

Using values available in the database, a new method of approximating the known and predicting unknown thermodynamic properties of zeolites based on their chemical composition has been proposed. This new method could be called as a functional contributions method. The difference between the new proposed method and existing methods of group contributions is as follows. Existing method for evaluating the thermodynamic properties of aluminosilicates that are widely used at the present time are based on so-called additive group schemes. In these schemes the property of interest can be calculated by summing up the group contributions of each chemical element (or oxide) composing a compound multiplied by the amount of the element (oxide) in the compound. Thus, each group contribution is characterized by a single numeric parameter. Our approach assumes that the contribution of each zeolite component to the corresponding thermodynamic properties can be expressed as a function of the component composition of the compound. Furthermore, the new method uses the features of the component composition of zeolites that are not typical for other aluminosilicates. For example, for this reason, the contributions of aluminum or its oxide to the thermodynamic properties of the zeolite are not allocated. This approach in combinations with the method of approximating the temperature dependencies of thermodynamic functions described above provides more reliable and accurate estimates of the thermodynamic properties of zeolites.

This work is supported by RFBR (grant 16-03-00677a)

[1] Voronin, G.F.; Kutsenok I.B. *J. Chem. Eng. Data*, 2013, 58, 2083-2094.



ANALYTICAL DETERMINATION OF THE STATISTIC SUM AND THE BOLTZMANN DISTRIBUTION

V.P. Malyshev, Yu.S. Zubrina, A.M. Makasheva
 Chemical and metallurgical institute, Karaganda, Kazakhstan
 eia_hmi@mail.ru

On the basis of the coefficient of proportionality of discrete and continuous eponymous distributions developed by the authors [1] analyzes of the statistic sum in the Boltzmann distribution was fulfilled

$$P_i = \frac{N_i}{N} = e^{-\frac{\varepsilon_i}{kT}} / \sum_{i=1}^{\infty} e^{-\frac{\varepsilon_i}{kT}}$$

on proportionality with improper integral of function with an arbitrary combination of temperature and interval of variation of particle energy $\Delta\varepsilon$. Convergence of the row on the basis of the integral sing Cauchy and Maclaurin and equal proportionality of row and improper integral of eponymous function in each unit interval of variation row and of eponymous function was installed

$$K = \frac{\int_{x=n-1}^{x=n} e^{-(x-1)\Delta\varepsilon/kT} dx}{e^{-(n-1)\Delta\varepsilon/kT}} = \frac{kT}{\Delta\varepsilon} \left(e^{\frac{\Delta\varepsilon}{kT}} - 1 \right).$$

This allows us to express the full statistic sum through this coefficient and a specific value of the improper integral

$$\int_0^{\infty} e^{-(x-1)\Delta\varepsilon/kT} dx = \frac{kT}{\Delta\varepsilon} e^{\frac{\Delta\varepsilon}{kT}}$$

in the form of the calculation formula

$$\sum_{n=1}^{\infty} e^{-(n-1)\Delta\varepsilon/kT} = \frac{1}{K} \int_0^{\infty} e^{-(x-1)\Delta\varepsilon/kT} dx = \frac{e^{\frac{\Delta\varepsilon}{kT}}}{e^{\frac{\Delta\varepsilon}{kT}} - 1}.$$

Accordingly, the Boltzmann distribution, we need for calculate the entropy of the formula $H = -\sum_{i=1}^{\infty} P_i \ln P_i$, gets more specific expression

$$P_i = e^{-\frac{i\Delta\varepsilon}{kT}} \left(\frac{\Delta\varepsilon}{e^{\frac{\Delta\varepsilon}{kT}} - 1} \right).$$

Thus it is possible any combination $\Delta\varepsilon$ and T , including as a functional connection $\Delta\varepsilon = f(T)$, since the output of obtained relationships treated isothermal distribution for the specified step of varying (quantization) energy. It is also possible numerical solution of inverse problems to identify $\Delta\varepsilon$ through known distribution of P_i for any temperature.

References

1. V.P. Malyshev, A.M. Makasheva, Yu.S. Zubrina. On the relationship and proportionality of discrete and continuous dependences // Reports of the National academy of sciences of the Republic of Kazakhstan. – 2016. – №1. – p. 49-56.



Section 1.

General problems of chemical thermodynamics

Virtual presentations

THERMODYNAMIC AND SURFACE PROPERTIES OF MOLYBDENUM

Akhmedov E.N.

Institute for Geothermal Research, Dagestan Scientific Centre of the Russian Academy of Sciences,
 Shamilya str. 39^d, 367030 Makhachkala, Russia
 E-mail: a.e.n@rambler.ru

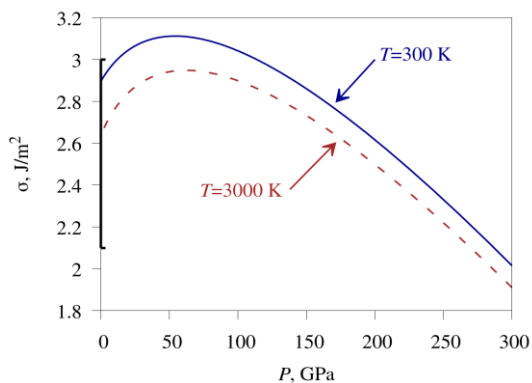


Figure 1. Isotherms of function $\sigma(100)$ (J/m^2) dependence on pressure P (GPa).

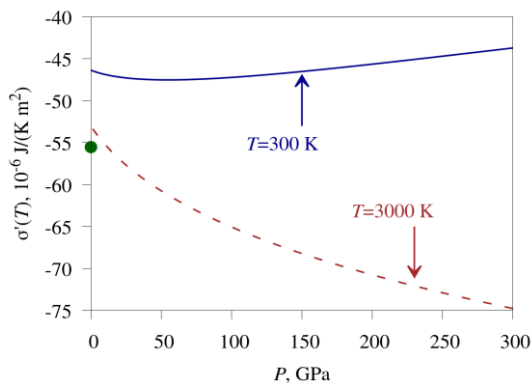


Figure 2. Isotherms of function $\sigma'(T)$ ($10^{-6} \text{ J}/(\text{K m}^2)$) dependence on pressure P (GPa).

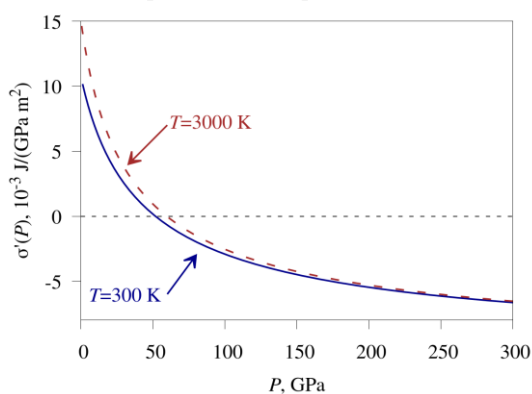


Figure 3. Baric dependence of function $\sigma'(P)$ along isotherm ($10^{-3} \text{ J}/(\text{GPa m}^2)$).

Understanding of the surface energy dependence on the pressure and temperature $\sigma(P, T)$ is necessary both for the calculations of crystal nucleation thermodynamics and for the study of crack formation in different P - T -conditions. Besides, the $\sigma(P, T)$ dependence for molybdenum has not been studied yet and there is no published data about it.

Using method proposed in [1] we obtained pair interatomic Mie-Lenard-Jones potential parameters and thermal equation of state $P(T, V/V_0)$ for a molybdenum crystal with bcc structure. Here T – temperature, V/V_0 – relative volume, V_0 – volume of the crystal for $P = 0$ and $T = 0$ K. Calculation of the isotherms $T = 300$ and 3000 K up to $P = 300$ GPa showed good agreement with the experimental data.

Using method proposed in [2] we have calculated specific surface energy (per unit area) of the face (100): $\sigma(100)$ and it's isochoric derivative with respect to temperature $\sigma'(T) = (\partial\sigma/\partial T)_V$ depending on the relative volume V/V_0 along indicated isotherms. This allowed us to obtain the baric dependence of the functions σ , $\sigma'(T)$ and $\sigma'(P) = (\partial\sigma/\partial P)_T$ along isotherms 300 and 3000 K.

Fig. 1 shows the isotherms of the pressure dependence of the surface energy of the face (100): solid curve – 300 K, dashed curve – 3000 K. Along vertical axis shown the scatter range, that is known from [2], of the surface energy at atmospheric pressure: $\sigma(100) = 2.1 - 3.0$ [J/m^2]. From the fig. 1 it is evident that our values are in this scatter range.

Fig. 2 shows isotherms of the pressure dependence of the isochoric derivative of the surface energy of the face (100) on temperature: solid curve – 300 K, dashed curve – 3000 K.

Point on the vertical axis is the estimate from [2], obtained by the other method for $P = 0$ and molybdenum melting temperature ($T_m(P=0) = 2890$ K): $\sigma'(T) = -55.5 \times 10^{-6} \text{ J}/(\text{K m}^2)$.

Fig. 3 shows baric dependences for $\sigma'(P)$ obtained by numerical differentiation by pressure along the isotherms: solid curve – 300 K, dashed curve – 3000 K.

The reported study was funded by RFBR according to the research project № 16-03-00041-a and the Program of the Presidium of the Russian Academy of Sciences (program № I.11P(1)).

[1] Magomedov M.N. Change in the Thermophysical Properties of BCC Iron during Isothermal Compression, Technical Physics, 2015, **60**, 11, 1619–1625.

[2] Magomedov M.N. Study of Interatomic Interaction, Vacancy Formation and Self-Diffusing in Crystals, Fizmatlit, Moscow, 2010. (In Russian)



THERMODYNAMIC MODEL OF THE POLAR SOLVENTS SORPTION BY GRAPHITE OXIDE

N.V. Avramenko, A.T. Rebrikova, L.O. Usoltseva, E.A. Shilyaeva, N.I. Ivanova, A.M. Parfenova,
V.M. Senyavin, M.V. Korobov

Department of Chemistry, Moscow State University, 119991, Leninskie gory, 1-3, Moscow, Russia

E-mail: natali@td.chem.msu.ru

In the present study the intercalation of graphite oxide (GO) with water and typical polar organic solvents was quantitatively characterized and described theoretically using general thermodynamic approach. Sorption of polar solvents CH_3OH , $\text{C}_4\text{H}_8\text{O}$ (THF), CH_3CN , $\text{C}_3\text{H}_7\text{NO}$ (DMF), $\text{C}_2\text{H}_6\text{OS}$ (DMSO), $\text{C}_5\text{H}_6\text{NO}$ (NMP) and water was quantitatively evaluated for Hummers (H-GO) and Brodie (B-GO) graphite oxides at $T = 298 \text{ K}$ and at melting temperature (T_m) of the solvents. Sorption measurements at $T = 298 \pm 0,5 \text{ K}$ were performed by isopiestic (ISP) method. Equilibration of GO with H_2O and organic solvents vapors in the thermostated desiccator persisted until the mass of GO saturated with the solvent became constant (5–10 days). Amount of sorbed solvent was also evaluated at the temperature point of solvent melting using DSC heating traces (5 K/min). Water sorption isotherms for H-GO and H-GOM were obtained by ISP and for H-GO additionally by dynamic desorption method. Thermodynamic approach was used to account for Hummers and Brodie graphite oxides sorption/swelling in polar organic solvents and water. This is a complex process sensitive to the way of material preparation and to the pre-history of the samples studied. Even if complete equilibrium in these systems is likely not achievable in our experiments, it was demonstrated that thermodynamic considerations can be used to describe characteristic temperature and pressure behavior of graphite oxide/solvent systems. The swollen materials were considered to be solid solvates of graphite oxides and the two distinct types of their temperature behavior were explained within the concept of narrow or wide homogeneity ranges of the corresponding solvates. One and the same thermodynamic routine were used to account for temperature and pressure maximums of sorption/swelling at the points of phase transitions of the solvents.

Thermodynamic equations allowed to explain “maximums” of swelling/sorption in the binary systems H-GO – solvent at T_m . The specific relation between the values of enthalpies of sorption and melting leads to the change of sign in enthalpies of sorption at T_m and causes maximal swelling/sorption. The same thermodynamic explanation was given for the “maximum” on the swelling vs. pressure dependence in B-GO and H-GO – H_2O systems at pressure of phase transition “liquid water-ice VI”. The sorption of all studied solvents was found to be stronger for Hummers compared to Brodie graphite oxide and for all studied systems to be higher at lower temperature. The last-mentioned result opens up possibilities to separate grapheme oxide sheets by swelling at temperatures below ambient. Sorption of all studied solvents by Brodie graphite oxide is remarkably similar if expressed in volumetric units (cm^3/g) thus demonstrating that at equilibrium sorption into graphite oxide structure is controlled by limitations of available inter-layer volumes (lattice expansion) rather than by the number of available adsorption sites which would be the case if molar uptakes were similar.

This work was supported by the RFBR grant 15-03-02168.

SURFACE PROPERTIES OF THE TUNGSTEN CRYSTAL

Gazanova N.Sh.

*Institute for Geothermal Problems of the Dagestan Scientific Center of RAS, 367003 Makhachkala, Russia
E-mail: dyuzva@gmail.com*

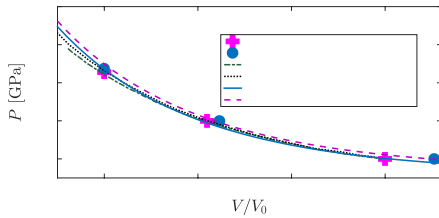


Figure 1. Isotherms of the tungsten equation of state.

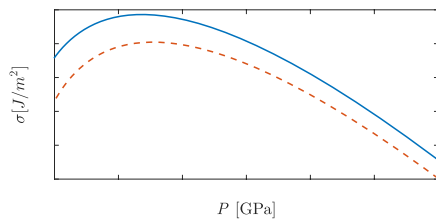


Figure 2. Specific surface energy of the (100) face for BCC-W.

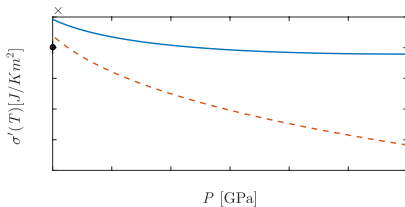


Figure 3. Temperature derivative of the surface energy.

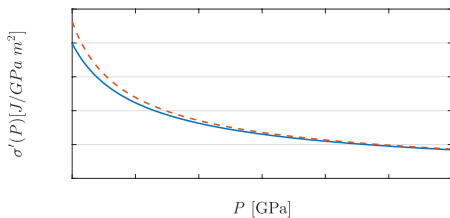


Figure 4. Pressure derivative of the surface energy.

Experimental study of the tungsten surface energy is extremely difficult. Therefore, there are numerous attempts to estimate the specific (per unit area) surface energy (σ). But all those methods do not provide information about the temperature (T) and pressure (P) dependences of the σ function.

In this paper we have calculated the surface properties of tungsten at the pressure $P = 0 - 300$ GPa along the isotherms: $T = 300$ and 3000 K. In the calculations we used the method proposed in [1], where the interatomic interaction is described by a pair potential Mie-Lennard-Jones: $\varphi(r) = D[a(r_0/r)^b - b(r_0/r)^a]/(b - a)$. Here D and r_0 – potential depth and minimum coordinate, $b > a$ – the numerical parameters. For BCC-W we have calculated (here k_B – Boltzmann constant):

$$r_0 = 2.7365 \cdot 10^{-10} \text{ m}, D/k_B = 25608.93 \text{ K}, a = 3.97, b = 6.28.$$

We have calculated the equation of state (Figure 1) and it have a good agreement with experimental data and data obtained by other authors. Figures 2 – 4 show pressure dependence calculated by the method proposed in [1, 2], for the following BCC-W surface properties:

1. σ – surface energy of the (100) face, which is shown on Figure 2, was calculated according to the following aquation:

$$\sigma = -\frac{k_n \cdot D \cdot R^2}{12\alpha^{2/3} \cdot r_0^2} \left[U(R) + \frac{18\gamma}{(b+2)} \frac{k_B \Theta_E}{D k_n} E_w \left(\frac{\Theta_E}{T} \right) \right],$$

here k_n – first coordination number, $c = [6k_p V/(\pi N)]^{1/3}$ – the distance between the centers of neighboring atoms, k_p – structure packing coefficient, $R = r_0/c$, $\alpha = \pi/(6 k_p)$, Θ_E – Einstein temperature, γ – Grüneisen parameter,

$$U(R) = \frac{aR^b - bR^a}{b - a}, \quad E_w(y) = 0.5 + \frac{1}{[\exp(y) - 1]}.$$

Figures shows the dependences along the isotherms: $T = 300$ K – solid curves, $T = 3000$ K dashed curves.

The calculated dependence is in a good agreement with the estimates of other authors obtained for $P = 0$, which lie in the interval [2]: $\sigma(P=0) = 2.61 - 4.64$ [J/m²].

2. $\sigma'(T) = (\partial\sigma/\partial T)_V$ – the temperature derivative of the σ function which is shown on Figure 3. Point on the Figure 3 – data from [2] where $P = 0$: $\sigma'(T) = -5.49$ [10^{-5} J/(K m²)].

3. $\sigma'(P) = (\partial\sigma/\partial P)_T$ – the pressure derivative of the σ function, which was obtained by numerical differentiation by pressure.

The baric dependence of this function is presented on Figure 4.

The reported study was funded by RFBR according to the research project № 16-03-00041-a and the Program of the Presidium of the Russian Academy of Sciences (program № I.11P(1)).

[1] Magomedov M.N. Change in the Thermophysical Properties of BCC Iron during Isothermal Compression, Technical Physics 2015, **60**, 11, 1619–1625.

[2] Magomedov M.N. Study of Interatomic Interaction, Vacancy Formation and Self-Diffusing in Crystals, Fizmatlit, Moscow, 2010. (In Russian)



SOLVATION FREE ENERGY OF PHENOLIC COMPOUNDS IN SUPERCRITICAL CARBON DIOXIDE

Gurina D.L.^{1,2}, Odintsova E.G.¹, Antipova M.L.¹, Petrenko V.E.¹, Golubev V.A.¹

¹G.A. Krestov Institute of Solution Chemistry of the Russian Academy of Sciences, 153045 Ivanovo, Russia

²Ivanovo Fire and Rescue Academy, 153040 Ivanovo, Russia

E-mail: gdl@isc-ras.ru

The solvation free energy (SFE) represents a very important characteristic for the thermodynamical description of a solution. When it comes to describing the properties of supercritical (SC) solutions, it is actual to use computer simulation methods which allow to obtain the data in a wide range of state parameters. It is well known that SC CO₂ is environmentally friendly, nontoxic, inflammable and cheap solvent. However, polar compounds are low soluble in it. To solve this problem small amounts of polar cosolvents are used. The calculation of cosolvent-induced solubility enhancement (CISE) from the SFE of the solutes in pure and modified SC media is a good way to preliminarily qualitatively estimate and compare the influence of the cosolvents on the solubility of the various compounds without expensive experiment.

In the present work, we will focus our attention on seven phenolic compounds varying in the number and type of ring substituents: 3,4,5-trihydroxybenzoic acid (gallic acid, GA), 3,4-dihydroxybenzoic acid (protocatechuic acid, PCA), and 4-hydroxy-3,5-dimethoxybenzoic acid (syringic acid, SA), p-hydroxybenzoic acid (p-HBA), methyl-3,4,5-trihydroxybenzoate (methyl gallate, MG), 3,4-dihydroxybenzaldehyde (protocatechuic aldehyde, PAL), (E)-3-(4-hydroxyphenyl)-2-propenoic acid (p-coumaric acid, p-CA) and 3-(3,4-dihydroxyphenyl)-2-propenoic acid (caffeic acid, CFA). In addition to the fundamental interest, these compounds are also of practical importance due to a wide range of their pharmacological properties.

Classical molecular dynamics (MD) simulations were performed using Gromacs-5.0.7 [1] software package. A cubic cell with periodic boundary conditions contained one molecule of solute, 10328 CO₂ and 320 cosolvent molecules or 10008 CO₂ and 640 cosolvent molecules (corresponded to 0.03 or 0.06 mole fraction of cosolvent: methanol or acetone). Calculations of SFEs were carried out by Bennett's acceptance ratio (BAR) method [2]. For each SFE calculation we performed a series of 11 independent NPT-MD simulations differing from each other by the value of a coupling parameter λ . The coupling parameter λ is changed from 0 to 1 with a step of 0.1 which characterizes fully decoupled and coupled solute-solvent interaction, correspondingly. Stochastic leap-frog integrator with 2 fs time step was used. Constant pressure was maintained by Parrinello-Rahman barostat with the compressibility of fluid $7.8 \cdot 10^{-4}$ bar⁻¹. For each simulation of the BAR series equilibration in NPT ensemble (T=323 K and P=20 MPa, T=328 K and P=21 MPa) was performed during 200 ps (initial configurations of ternary systems were taken from NVT MD simulations). The product simulation time was 2 ns.

It was shown that the free energy of solvation of GA, PCA, SA, MG, PAL, p-CA and CFA is correlated with the average number of hydrogen bonds (HBs) formed by the compounds with methanol and acetone in SC CO₂. Based on the SFE and CISE values we can conclude that using methanol as cosolvent can lead to an increase of the phenolic compounds solubility greater than using acetone. Moreover, the more number of hydrogen bonds is formed by the solute with cosolvent molecules, the greater the solubility increase can be achieved. The more the number of functional groups in a molecule of solute is capable to form HBs with the cosolvent, the more sensitive its solubility will be to the addition of polar cosolvent. Namely, in SC CO₂ modified by 0.06 mole fraction of methanol, GA, PCA, p-CA and CFA are able to form up to 2.8 HBs with cosolvent that leads to solubility enhancement of the acids almost by three orders of magnitude comparing with the pure fluid. At the same time, SA is able to form up to 1.6 HBs in the solution of the same methanol concentration resulting in an increase in SA solubility of fifteen times as much only. In the case of acetone, the solubility is increased several tens of times as much for GA, PCA, MG, PAL, p-CA, CFA and four times as much for SA.

This research was supported by the Russian Foundation for Basic Research (grant No. 16-33-00126 and No. 16-33-60060)

[1] Hess, B.; Kutzner, C.; van der Spoel, D.; Lindahl, E., *J. Chem. Theory Comput.*, 2008, 4, 435-447.

[2] Bennett, C. H., *J. Comput. Phys.*, 1976, 22, 245-268.

DEVELOPMENT OF THE ELECTRONIC DATABASE OF THE HALOGENATED FREE RADICAL ENTHALPY OF FORMATION

A. Kotomkin¹, N. Rusakova¹, V. Turovtsev^{1,2}, Yu. Orlov¹

¹ Department of general physics, Physics Faculty, Tver State University, Sadovy Per., 35, Tver, Russia,

² Department of Physics, Mathematics and Medical Informatics, Tver State Medical University, Sovetskaya Str. 4, Tver, Russia

E-mail: prospectpobedy@mail.ru

Halogen-organic compounds have a great significance in the biologic systems, natural and technological processes. Herewith, the halogenated free radical is an important intermediate stage in the synthesis of these compounds. The energy and thermodynamic properties of free radicals determine their stability and reactivity. One of the main thermodynamic properties is an enthalpy of formation.

Electronic databases are modern support tool in science and technological researches. The lack of the thermodynamic property database of halogen containing radicals violate the development of many scientific and technological directions.

We have constructed a relational database of the thermodynamic property of organic free radicals containing halogen atoms – fluorine, chlorine, bromine and iodine. The database was developed by Microsoft Access database management system. In addition to storing of data, database procedures allow to search and to choose objects and related information.

The objects of database are free hydrocarbon halogenated radicals described by gross formulations, structural formulas, names and patterns, radical groups, kind of halogen atom, groups containing double or triple chemical bond, cycles or aromatic cycle.

Each hydrocarbon radical is characterized by enthalpy of formation (in kJ/mole) and references. Database contains 112 free organic halogen-containing radicals, characterized by 212 values of the enthalpy of formation from 51 sources.

Figure 1. The interface of database.

**PROPERTIES OF THE ISOTOPICALLY PURE DIAMONDS
FROM C-12 AND C-13 AT COMPRESSION**

Magomedov M.N.

*Institute for Geothermal Research, Dagestan Scientific Centre of the Russian Academy of Sciences,
Shamilya str. 39a, 367030 Makhachkala, Russia
E-mail: mahmag4@mail.ru*

In this paper were obtained the state equation and the baric dependencies of thermodynamic properties for the diamond with the mass of the atom $m = 12$ a.m.u. and for diamond with $m = 13$ a.m.u. In the calculations was used the method proposed in [1], where the interatomic interaction in diamond is described by pairwise potential Mie-Lennard-Jones: $\varphi(r) = D[a(r_0/r)^b - b(r_0/r)^a]/(b - a)$. Here D and r_0 are the depth and coordinate of the potential minimum, and $b > a$ are the numerical parameters.

For diamond with ^{12}C the next values were obtained (here k_B is the Boltzmann constant) [1]:

$$r_0 = 0.1545 \text{ nm}, \quad D/k_B = 97821.72 \text{ K}, \quad a = 2.05, \quad b = 3.79.$$

At the transition from diamond with ^{12}C to diamond with ^{13}C the value of r_0 is reducing, and the depth of the pairwise interatomic potential is rises to the values that were determined from experiments [2]:

$$r_0^* = r_0(^{13}\text{C})/r_0(^{12}\text{C}) = 0.99985, \quad D^* = D(^{13}\text{C})/D(^{12}\text{C}) = 1.00323.$$

The following properties of diamond with ^{12}C and ^{13}C were calculated: the state equation $P(V, T)$, Debye temperature Θ and its derivative with respect to pressure along an isotherm ($\Theta'(P) = (\partial\Theta/\partial P)_T$), the first ($\gamma = -[\partial\ln(\Theta)/\partial\ln(V)]_T$), the second ($q = [\partial\ln(\gamma)/\partial\ln(V)]_T$) and the third ($z = -[\partial\ln(q)/\partial\ln(V)]_T$) Grüneisen parameters, the bulk modulus $B_T = -[\partial P/\partial\ln(V)]_T$ and $B'(P)$, the thermal expansion coefficient ($\alpha_p = [\partial\ln(V)/\partial T]_p$) and $\alpha_p'(P)$, the isochoric (C_v) and the isobaric (C_p) heat capacity, $C_v'(P)$ and $C_p'(P)$, $\alpha_p \cdot B_T = (\partial P/\partial T)_v$, σ is the specific (per unit area) surface energy of the (100) face, $\sigma'(T)$ and $\sigma'(P)$.

Calculations performed at temperature $T = 300$ K for pressures up to $P = 10000$ kbar = 10 Mbar = 1000 GPa = 1 TPa, showed following results:

1. The $P(V)$ curve for ^{13}C lies slightly lower than for ^{12}C . For example, if $V = 3.4 \text{ cm}^3/\text{mol}$:
 $P(^{12}\text{C}) = 76.64 \text{ kbar}, \quad P(^{13}\text{C}) = 72.65 \text{ kbar}.$
2. Dependencies of $\Theta(P)$, $q(P)$ and $z(P)$ are increasing with pressure, and for the diamond with ^{13}C these dependencies lie lower than for the diamond with ^{12}C .
3. Dependencies of $\gamma(P)$, $B'(P)$, $\alpha_p(P)$, $C_v(P)$, $C_p(P)$ and $\alpha_p(P) \cdot B_T(P)$ are decreasing with pressure, and for the diamond with ^{13}C these dependencies lie higher than for diamond with ^{12}C .
4. Relations of $\Theta(^{12}\text{C})/\Theta(^{13}\text{C})$ and $\gamma(^{12}\text{C})/\gamma(^{13}\text{C})$ are decreasing with increasing pressure $P(^{12}\text{C})$, and these dependences with the validity coefficient R_c are approximated by the following functions:
 $\Theta(^{12}\text{C})/\Theta(^{13}\text{C}) = 1.03851 + (2.52681 \times 10^{-4}) \exp(-P[\text{kbar}]/5820.32), \quad R_c = 0.9963,$
 $\gamma(^{12}\text{C})/\gamma(^{13}\text{C}) = 0.999536 + (2.39967 \times 10^{-4}) \exp(-P[\text{kbar}]/5785.2), \quad R_c = 0.9925.$
5. Function of $B_T(P)$ increases with pressure, and for the diamond with ^{13}C this dependence lies higher than for diamond with ^{12}C .
6. Dependence of $\Theta'(P)$ decreases with pressure, and for the diamond with ^{13}C this dependence lies lower than for diamond with ^{12}C .
7. Functions of $\alpha_p'(P)$, $C_v'(P)$ and $C_p'(P)$ are negative, their absolute values decrease with pressure, and for these functions the isotopic dependence is not detected.
8. Dependence of $\sigma(P)$ with increasing pressure increases to the maximum at P_{\max} and then decreases, and becoming negative. The specific surface energy for diamond with ^{13}C is always greater than for the diamond with ^{12}C : at $P = 0$ is shown in [2]: $\sigma_0(^{13}\text{C})/\sigma_0(^{12}\text{C}) \cong D^*/(r_0^*)^2$.
9. Function of $\sigma'(T)$ is negative, its absolute value decreases with pressure, and the magnitude of $|\sigma'(T)|$ for diamond with ^{13}C is greater than for diamond with ^{12}C .
10. Function of $\sigma'(P)$ decreases with pressure, passing at P_{\max} to negative area, and isotope dependence of this function on the interval $P = 0 - 10$ Mbar was not detected.

The reported study was funded by RFBR according to the research project № 16-03-00041-a and the Program of the Presidium of the Russian Academy of Sciences (program № I.11P(1)).

[1] Magomedov M.N. Izvestiya VUZov: Khimiya i Khimicheskaya Tekhnologiya, 2016, **59**, 9, 57-61.

[2] Magomedov M.N. Russian Journal of Physical Chemistry A, 2006, **80**, 2, 210-213.

THE STATE EQUATION FOR NANOCRYSTAL

Magomedov M.N.

*Institute for Geothermal Research, Daghestan Scientific Centre of the Russian Academy of Sciences,
Shamilya Av. 39a, 367030 Makhachkala, Russia
E-mail: mahmag4@mail.ru*

On the basis of the three-phase model of simple matter [1, 2] and the RP-model of the nanocrystal [3] the expression for the Helmholtz free energy was derived and the state equation $P(v/v_0)$ for the nanocrystal, in which there are vacancies in the lattice and the delocalized (i.e. diffusing) atoms was calculated. It was assumed that the atoms interact via the pairwise potential of the Mie-Lennard-Jones:

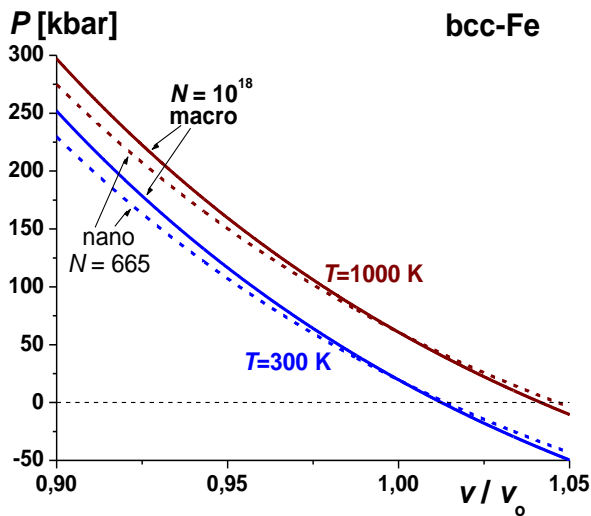


Figure 1. The state equations for macrocrystal (solid lines) and for nanocrystal (dashed lines).

$$\varphi(r) = \frac{D}{(b-a)} \left[a \left(\frac{r_0}{r} \right)^b - b \left(\frac{r_0}{r} \right)^a \right].$$

Here D and r_0 are the depth and the coordinate of the potential minimum, $b > a > 1$ are the numerical parameters.

Calculations were performed for iron with body-centered cubic (BCC) structure along the two isotherms: for low ($T/\Theta < 1$): $T = 300$ K, and for high ($T/\Theta > 1$) temperature: $T = 1000$ K. Parameters of the Mi-Lennard-Jones potential for BCC-Fe defined in [4] are:

$$r_0 = 2.4775 \cdot 10^{-10} \text{ m}, \quad D/k_B = 12576.7 \text{ K}, \\ a = 2.95, \quad b = 8.26.$$

Based on these parameters, the normal specific volume, the Debye temperature and the first Gruneisen parameter at $v/v_0 = 1$ are: $v_0 = [\pi/(6k_p)]r_0^3 = 7.0494 \text{ cm}^3/\text{mole}$, $\Theta(1) = 408.073 \text{ K}$, $\gamma(1) = 1.702$. Here k_B is the Boltzmann constant, k_p is the structure packing coefficient (for BCC structure $k_p = 0.6802$).

Figure 1 shows the isomorphic-isomeric (with the same shape and a constant number of atoms N in the crystal) dependence of pressure versus the normalized volume (v/v_0) in a cubic nanocrystal of BCC iron. Comparison of the calculated in this way dependence of $P(v/v_0)$ with the experimental data for the macrocrystal of BCC-Fe was performed in [4]. In Figure 1 the solid curves are obtained for macrocrystal (at $N = 1.3 \times 10^{18}$), and the dashed curves – for nanocrystal at $N = 665$. Two curves that lie below are the isotherms at $T = 300$ K, the two above curves – isotherm at $T = 1000$ K. The decrease in pressure upon compression of the nanocrystal (compared to macrocrystal) indicates a decrease of the modulus of elasticity for the nanocrystal. From the Figure 1 it is seen that at a certain value of relative volume $(v/v_0)_0$ the dependencies of $P(v/v_0)$ for the nanocrystal and for the macrocrystal are intersecting. Thus, at $(v/v_0)_0$ the surface pressure becomes zero: $P_{sf}(v/v_0)_0 = 0$. At $v/v_0 < (v/v_0)_0$ the surface pressure compresses the nanocrystal ($P_{sf} > 0$), and at $v/v_0 > (v/v_0)_0$ the surface pressure stretches nanocrystal: $P_{sf} < 0$. The value of $(v/v_0)_0$ decreases at the isomorphic-isomeric growth of temperature T , at the isomorphic-isothermal decrease of the atoms number N , and at the isomeric-isothermal deviation of the nanocrystal shape from the most stable shape (for RP-model the most stable shape is a cube).

It is shown that the most perfect nanocrystals will be formed either at low static pressures P and at low temperatures T or at high static pressures and at any temperatures.

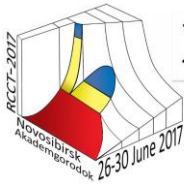
The reported study was funded by RFBR according to the research project № 16-03-00041-a and the Program of the Presidium of the Russian Academy of Sciences (program № I.11P(1)).

[1] Magomedov M.N. Nanotechnologies in Russia, 2014, **9**, 5-6, 293-304.

[2] Magomedov M.N. The Physics of Metals and Metallography, 2013, **114**, 3, 207-216.

[3] Magomedov M.N. Nanotechnologies in Russia, 2015, **10**, 1-2, 89-99.

[4] Magomedov M.N. Technical Physics, 2015, **60**, 11, 1619-1625.



ABOUT THE GENERALIZATION OF THERMODYNAMICS IN FRACTIONAL ORDER DERIVATIVES

Magomedov R.A.¹, Meilanov R.R.¹, Akhmedov E.N.¹, Beybalaev V.D.^{1,2}, and Aliverdiev A.A.^{1,2}

¹ Institute for Geothermal Research, Daghestan Scientific Center of the Russian Academy of Sciences, 367030, Shamilya Str. 39A, Makhachkala, Russia

² Dagestan State University, 367025, Gadjeva Str. 43A, Makhachkala, Russia
E-mail: ramazan_magomedov@rambler.ru

The study of non-equilibrium processes in terms of the principle of local non-equilibrium requires to consider memory effects (non-locality in time) and spatial correlations (coordinate non-locality) and the development of innovative analysis methods. Some of these methods are based on the mathematical apparatus of fractional derivatives. [1] In the case of the equilibrium thermodynamics the transition to fractional derivatives on the thermodynamic parameters (temperature, volume) also contributes to the theory a new parameter α – the rate of derivative of fractional order – with nontrivial physical sense, that implicitly takes into account the non-locality of the collision integral, thereby leading to the expansion of the area of applicability of the one-parameter family equations of state to fractal equation of state. In the continuation to our recent works [2, 3] we present the generalization of thermodynamics in formalism of fractional derivatives with the calculation of the one-parametric “fractal” state equation with second virial coefficient (B) for noble gases:

$$P = \rho RT \left\{ 1 + \rho B + (1 - \alpha) \cdot \left[\ln \left(\frac{eM}{\rho N_A} \left[\frac{mkT}{2\pi\hbar^2} \right]^{3/2} \right) + \psi(1) - \psi(2 - \alpha) - \rho B \right] \right\}. \quad (1)$$

Here P is the pressure, $\psi(x)$ is a ψ -function of the number x , ρ is the density, T is the temperature, k is a Boltzmann constant, N_A is the Avogadro's number, R is the universal gas constant, a and b are Van-der-Waals constants ($B(T) = b - \frac{a}{kT}$), M is the molar mass, m is the mass of atom, e is the exponent, \hbar is the Plank constant. On a base of (1) we can find the compressibility factor (z) and the isochoric heat capacity (C_V):

$$z = 1 + \rho B + (1 - \alpha) \cdot \left[\ln \left(\frac{eM}{\rho N_A} \left[\frac{mkT}{2\pi\hbar^2} \right]^{3/2} \right) + \psi(1) - \psi(2 - \alpha) - \rho B \right]$$

$$C_V = \frac{R}{\tilde{A}(2 - \alpha)} \left\{ \frac{3}{2} - \frac{27P_c b^2}{N_A T} + (1 - \alpha) \left[\ln \left[\frac{e\dot{l}}{\rho N_A} \left(\frac{mkT}{2\pi\hbar^2} \right)^{3/2} \right] - \frac{3}{2} - \rho b \left(1 - \frac{27P_c b}{N_A T} \right) \right] \right\}$$

The results of our calculations are in satisfactory agreement with the experimentally measured data. In addition, it is possible to extrapolate the equation of state to the extreme thermodynamic parameters, where experiments are difficult or impossible. Thus, the thermodynamics of fractional calculus, containing a traditional thermodynamics (which is based on the principle of local equilibrium) as a special case, is expanding its scope, encompassing the processes under fulfillment of the principle of local non-equilibrium.

The work was partially supported by RFBR (16-08-00067a). A.A. is also grateful to COST (Action MP1208).

[1] Meilanov, R.P.; Shabanova M.R.; Akhmedov, E.N. Chaos Soliton. Fract., 2015, **75**, 29-33

[2] Meilanov, R.P.; Magomedov, R.A. J. Eng. Phys. Thermophys., 2014, **87**(6), 1521-1531

[3] Magomedov, R.A.; Meilanov, R.P.; Akhmedov E.N.; Aliverdiev, A.A. J. of Physics: Conference Series, 2016, **774**, 012025



SIMULATION ACTIVITY COEFFICIENTS OF LANTHANUM IN FUSED LA(GA-IN)/3LiCl-2KCl SYSTEM

Novoselova A.V.^{1,2}, Smolenski V.V.^{1,2}, Luk'yanova Ya.M.³

¹Institute of High-Temperature Electrochemistry UB RAS, 20 Akademicheskaya St., 620137, Ekaterinburg, Russia

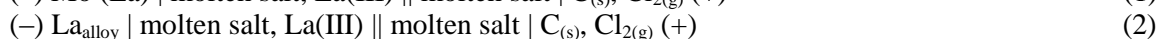
²Department of Rare Metals and Nanomaterials, Institute of Physics and Technology, Ural Federal University, 19 Mira St., 620002, Ekaterinburg, Russia

³JSC "State Scientific Centre-Research Institute of Atomic Reactors", 433510, Dimitrovgrad, Russia

E-mail: alena_novoselova@list.ru

Pyrochemical separation processes in molten salt media have been proposed as a promising option in the future nuclear fuel cycle. The major steps of these processes include the electrorefining or reductive extraction of the recovering actinides in molten chloride/liquid metal systems and for recovery of minor actinides from spent fuel or high level radioactive liquid wastes.

The experiments were carried out at 723–823 K under dry argon atmosphere in an electrochemical cell with a three electrode setup. The electrochemical measurements were performed employing an AUTOLAB 302N potentiostat controlled by NOVA 1.11 software. The following galvanic cells were used for measuring the electrode potentials of the $E_{La(III)/La}^*$ (1) and alloys $E_{La(Ga-In)}^{**}$ (2):



$$\log \gamma_{U(Cd)} = \frac{3F}{2.303RT} (E_{La(III)/La}^* - E_{La(Ga-In)}^{**}) \quad (3)$$

Newton interpolation polynomial expression was obtained to develop three-dimensional $\log \gamma_{La} - C_{(Ga-In)} - T$ graph on the basis of the functional dependence of the apparent electrode potentials of metals and alloys, Ga–In mixture compositions, and temperature. Universal mathematical Maple 17 software was used for this purpose. Three-dimensional graph is presented in Fig. 1. The following expression describes the three-dimensional graph:

$$\log \gamma_{\beta-La(Ga-In)} = (-13333 + 61.644C - 0.308C^2) / T + 4.72 - 0.03728C + 0,00016C^2$$

where C is the concentration of indium in (Ga–In) alloy, wt.%; T is an absolute temperature, K.

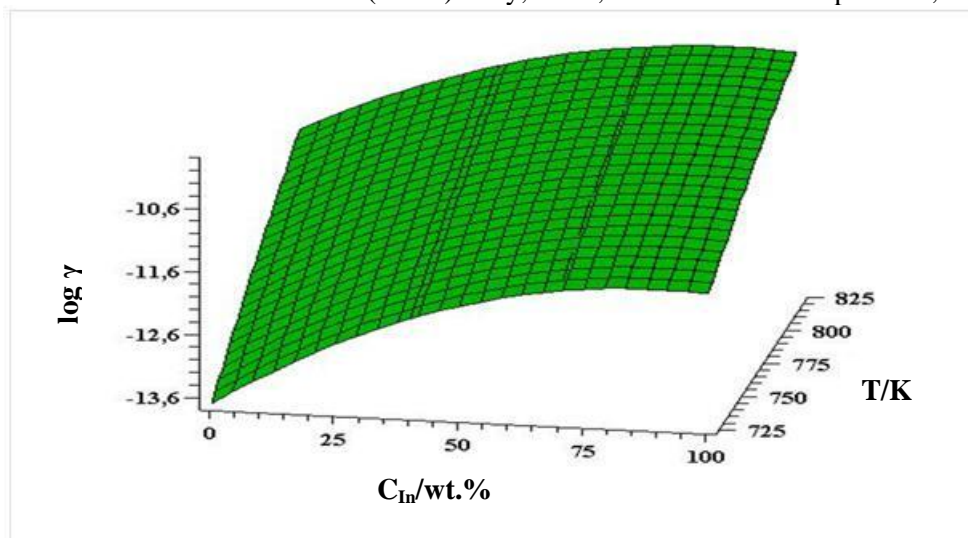


Figure 1. Three-dimensional $\log \gamma_{La(Ga-In)} - C - T$ graph in fused $La(Ga-In)/3LiCl-2KCl$ system.

The small values of activity coefficients show on strong interaction between lanthanum and liquid alloy. The increasing temperature shifts the system towards more ideal behavior.



LOW-PARAMETRICAL EQUATION OF STATE AS A COMPROMISE BETWEEN PHYSICAL CLARITY AND MATHEMATICAL ACCURACY

Petrik G.G.

Institute for Geothermal Research DSC of the Russian Academy of Sciences, 367030 Makhachkala, Russia

E-mail: galina_petrik@mail.ru

In 2015 celebrated 105 years of the Nobel prize, which J. D. van der Waals received with the phrase for "advances in the theory of equations of state" (EOS). His famous EOS became the ancestor of many independent empirical modifications. In this information field two trends were designated long ago, each of which has followers. One can be considered searching of physical clarity. Another – searching of a mathematical accuracy. The first are low-parametrical, and the second – multiconstant EOS (in the form of polynoms where the number of subracing parameters can be 100 and more). As for the low-parametrical equations, "a little" now can mean and 10, and 15 parameters. It is apparent that they also are subracing and it is hardly worth looking for in them physical sense.

At the same time prime the EOS in which physical clarity is combined with mathematical accuracy is still the purpose for many researchers. Including for the author. Therefore, considering that EOS parameters have to make physical sense, we allocate in separate group equations for which there is a hope to solve this problem - truly low-parametrical the EOS with number of parameters from 2 to 5. (And not obligatory it is a vdw-type EOS). Let's note two aspects of the interest remaining to them. Apparently, it is practical engineering interest to the EOS as to the instrument of calculation i.e. as mathematical model. Fundamental interest in them as physical model as to means of an approximation to the reasonable forecast and the description of properties of substances from concrete molecules is not less obvious.

In that case special attention has to be paid to the molecular models which are the cornerstone of the corresponding equations. Especially as the main reproach in the vdw-type EOS address – their loose coupling with microlevel. (As the counterexample is given virial EOS which coefficients are expressed through intermolecular interactions – pair, threefold, etc.). Practically it is limited to the fact that many authors shift "responsibility for physics" to van der Waals, claiming that use the same model.

For many years in literature up to EOS the huge calculated material demanding carrying out the intellectual analysis is saved up. Answers to many questions and new knowledge have to become result. However traces of such analysis in literature are almost not visible.

At the same time, it is apparent that establishment of communications a vdw-type EOS with models of a molecular scale has to help with development optimum low-parametrical EOS. We are convinced that a significance of "know-how" (i.e. EOS form) will only amplify with deepening "know-why" – i.e. the found its communication with molecular model.

In this direction conducts the systems approach realized by us for the most prime molecular model - interacting point centers (unlike more composite model of rigid spheres of van der Waals) (see the website www.csmos.ru – our main works). Last year the emphasis on the analysis of the cognitive problems which collected in this area was placed. New results, being applied to known a vdw-type EOS, allowed to give physically reasonable answers to a number of the fundamental issues. Many untied a vdw-type EOS, considered as empirical correlations of properties, can be considered as terms of one physically reasonable family of the equations. At the same time all deposits and parameters make sense, the bound to manifestation of forces operating between model "molecules". For the first time the hierarchy of parameters, being managing directors for separate levels of modeling is built (a separate molecule from atoms; couple of molecules – coordinates of singular points of potential and force curve intermolecular interaction; transition from them to critical parameters of model "substance"; thermodynamic level – the operating EOS parameters determined by a set of the efficient sizes of the point centers [1] – similarly new, entered by us earlier informationfilled characteristic of model "molecule" [2]).

[1] Petrik, G. Monitoring. Science and Technology. 2016, 3, 58-71 (rus.)

[2] Petrik, G; Todorovsky, B. J. Phys.Chem.1988, 62, 12, 3257-3264 (rus)

THE CONSTRUCTION AND ANALYSIS OF NONEQUILIBRIUM PHASE DIAGRAMS OF LOW MOLECULAR WEIGHT ORGANIC COMPOUNDS

A.Ye. Pokyntelytsia, O.A. Pokyntelytsia, N.V. Shchebetovskaya

Faculty of Physics and Physical Materials Science, Donbas National Academy of Civil Engineering and Architecture,
Derzhavina Str.2, 86123 Makiivka, Ukraine

E-mail: lnk0013@gmail.com

We provide long-term monitoring of known equilibrium phase diagrams of binary systems, based on low-molecular organic compounds such as naphthalene-diphenyl, naphthalene-dibenzyl, diphenyl-dibenzyl, o-terphenyl-dibenzyl, o-terphenyl-diphenyl, o-terphenyl-naphthalene, o-terphenyl-m-terphenyl, m-terphenyl-diphenyl, m-terphenyl-naphthalene, etc., in order to find ways to build relevant non-equilibrium phase diagrams using thermal analysis. As an example, Fig. shows the equilibrium and the non-equilibrium phase diagram of the diphenyl-naphthalene system.

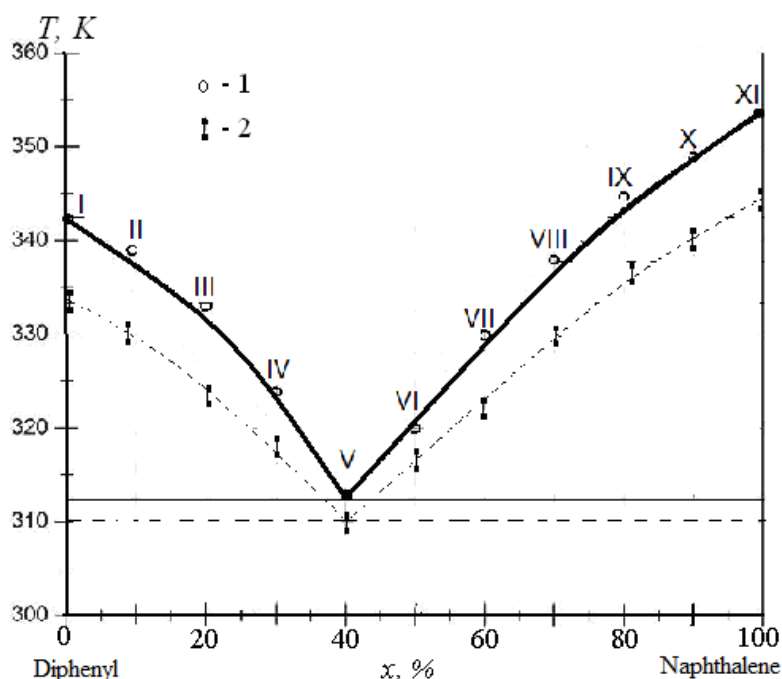


Figure. Equilibrium and nonequilibrium phase diagrams in the diphenyl-naphthalene system

Further analysis allows to establish a pattern of precrystallization undercooling temperature variation referring to liquidus temperature. The resulting undercooling values are used to calculate various nucleation and mass crystallization parameters (Gibbs energy variation, enthalpy of phase transitions, critical nucleus size, nucleation energy, etc.). The mathematical model of the liquidus temperature variation depending on concentration is being developed for enhancing calculation of eutectic temperature and eutectic compositions.

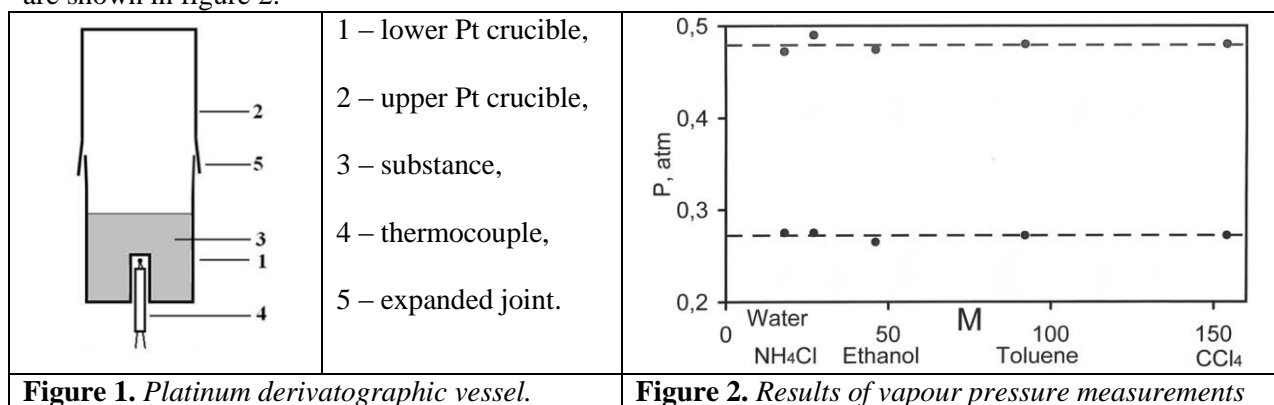
THERMODYNAMICS OF VAPORIZATION AND DECOMPOSITION PROCESSES OBTAINED WITH DERIVATOGRAPHIC METHOD

Polyachenok O.G., Branovitskaya N.V., Polyachenok L.D.
 Mogilev State University of Food Technologies, 212027 Belarus, Mogilev, Schmidt str., 3
 E-mail: polyachenok@mogilev.by

Precise measurements of vapour pressure over pure substances as well as over complexes, i.e. over salt hydrates, are often used to determine thermodynamics of different molecules and substances. Several tensimetric methods are usually used to obtain the reliable data [1–3]. However precision of the water vapour pressure measurements over salt hydrates is often limited by hydrolysis reactions, low rate of equilibration, formation of metastable, highly disperse or amorphous phases. But for practical use of such thermodynamic results and for preliminary technological calculations it is often enough to have approximate data.

The latter can be obtained in particular using the derivatographic method [3] and a known either estimated value of standard entropy change of the process studied. As is seen in figure 4 [3], there is a good conformity between the differential line fast deviation and the mass loss fast deviation near the boiling temperature at 1 atm. We have used until now the differential curve deviation (the beginning of its linear section), and this method proved to be very useful to obtain dissociation pressures of different metal salt hydrates and their enthalpies of dehydration [4–6]. But at higher temperatures electrical interference begins to decrease sensitivity of the differential thermocouple, therefore we have examined the possibility of vapour pressure evaluation using the mass loss line deviation.

We have found that the mass loss line can give information not only concerning the boiling temperature at 1 atm, but there can be found for each used derivatographic vessel 1–2 points, corresponding to somewhat lower vapour pressures. This proved to be especially useful for sodium fluorosilicate dissociation pressure measurement, since its eutectic melts at the pressure near 1 atm and distorts the results. The used platinum vessel is shown in figure 1. The obtained results for some standard substances with different molar mass are shown in figure 2.



[1] Suvorov, A.V. Thermodynamic Chemistry of Vaporous State, 1970, Chimia, Leningrad.
 [2] Polyachenok, O.G; Dudkina, E.N; Branovitskaya, N.V; Polyachenok, L.D. Thermochim. Acta, 2008, 467, 44–53.
 [3] Polyachenok, O.G; Dudkina, E.N; Polyachenok, L.D. J. Chem. Thermodyn., 2009, 41,74–79.
 [4] Dudkina, E.N. Synthesis and thermal stability of some metal chlorides lowest hydrates, Diss. Abstract, 2009, Minsk.
 [5] Polyachenok, O.G; Ogorodnikova, T.G; Voitenko, S.I; Dudkina, E.N; Polyachenok, L.D. XX Mendeleev Congress on general and applied chemistry (Ekaterinburg), 2016, Abstracts, V.3, 213.
 [6] Polyachenok, O.G; Ogorodnikova, T.G; Voitenko, S.I; Dudkina, E.N; Polyachenok, L.D. XX International Conference on Chemical Thermodynamics in Russia (Nizhni Novgorod), 2015, Abstracts, 158.



PHASE AND CHEMICAL EQUILIBRIA IN SOME SYSTEMS WITH ESTER SYNTHESIS REACTION

Toikka A.M., Samarov A.A., Toikka M.A., Tsvetov N.S.

Department of Chemical Thermodynamics and Kinetics, Institute of Chemistry, Saint Petersburg State University, Universitetskii prospect 26, Saint Petersburg, 198504, Russia
E-mail: a.toikka@spbu.ru

Investigations of the phase and chemical equilibria in the reacting liquid systems cover a wide range of problems related to both experimental determination of thermodynamic properties and various aspects of the basic analysis of coupled (equilibrium and non-equilibrium) processes in these systems. In the case of fluid reacting systems one should consider the systems with vapor – liquid equilibrium (VLE), liquid – liquid equilibrium (LLE) and vapor – liquid – liquid equilibrium (VLLE). These systems represent the most important classes of the systems with simultaneous phase and chemical processes. Nevertheless the experimental information on the binary and ternary systems is very poor and the main data sets are connected with quaternary systems. Our recent review [1] includes mostly systems with esterification and trans-esterification reactions. Previously other review on VLE in reacting systems [2] covered the systems with ester synthesis reactions as a most important and common class. Usually in the case of reacting heterogeneous systems authors consider two cases: i. simultaneous phase and chemical equilibria, ii. phase equilibria in the system with nonequilibrium chemical reaction. In the last case we can consider the slow reaction or the system with “frozen” reaction (e.g. without catalyst). All this indirectly reflects the diversity of the problems associated with the study of processes occurring in heterogeneous reacting systems.

The main goal of our presentation is the analysis of new available experimental data concerning the VLE, LLE and VLLE in multicomponent reacting system. Here we restricted ourselves to the case of the ester synthesis reactions. We consider also the case of non-equilibrium chemical reactions but the most of examples concern the simultaneous phase and chemical equilibria. The systems with esterification reaction are of well-known practical interest, e.g. for the design of reactive distillation or extraction processes. Unfortunately because of this engineering significance many papers include rather limited data volume which is not sufficient for basic thermodynamic analysis. Accordingly only the detailed new data on physicochemical properties, phase transitions and chemical processes will be considered. The main objects of presentation will be following:

- some complicated and unusual diagrams of simultaneous phase and chemical equilibria;
- the problems of reaction kinetics in heterogeneous media;
- the problem of distinguishing of thermal effects of mixing and reactions;
- some experimental aspects of the study of simultaneous equilibria and coupled processes.

In conclusion we will present some practical applications of thermodynamic theory of heterogeneous reacting systems for chemical engineering tasks.

Acknowledgement: Alexander Toikka and Nikita Tsvetov acknowledge Russian Foundation for Basic Research for the grant 15-03-02131. Authors are also grateful to co-workers from the Department of Chemical Thermodynamics and Kinetics of SPbSU: Maya Trofimova, Alexandra Golikova, Irina Letyanina and Oleg Pervukhin for fruitful discussions.

[1] A.M. Toikka, A.A. Samarov, M.A. Toikka. Phase and chemical equilibria in multicomponent fluid systems with a chemical reaction // Russian Chemical Reviews. 2015. V. 84. № 4. P. 378-392.

[2] A.M. Toikka, M.A. Toikka, Yu.A. Pisarenko, L.A. Serafimov. Vapor-liquid equilibria in systems with esterification reaction // Theor. Found. Chem. Eng. 2009. V. 43, No. 2. P. 129-142.

QUANTUM-CHEMICAL SIMULATION OF THERMODYNAMIC PARAMETERS OF SOLVATION OF BENZOCAINE AND ITS GLYCOSYLATED DERIVATIVE IN SOLVENTS

Volkova T.G.¹, Talanova I.O.²

¹Ivanovo State University, 153025 Ivanovo, Russia

²Ivanovo State Medical Academy, 153012 Ivanovo, Russia

E-mail: tgvolkova@yandex.ru

The medium influence should be taken into account under quantum-chemical calculations of the structural, energetic and electronic characteristics in condensed phase. Solvent, polymer or crystal serves as medium. The different kinds of interaction between solvated species and solvent, i.e. solvation are the most important for chemists. From the point of view of continuum approaches, including the polarized continuum model (PCM), the solvent is a structureless continuous medium, that polarized by solvated species. It is characterized by a scalar permittivity.

The simulation of benzocaine and its glycosylated analogue (ethyl ester of p-(N- α -D-glucopyranoside)aminobenzoic acid) (figure) in aqueous and chloroform mediums has been carried out. The calculations were carried out by B3LYP/6-31G (p,d) method using PCM model (PC GAMESS7.1) [1].

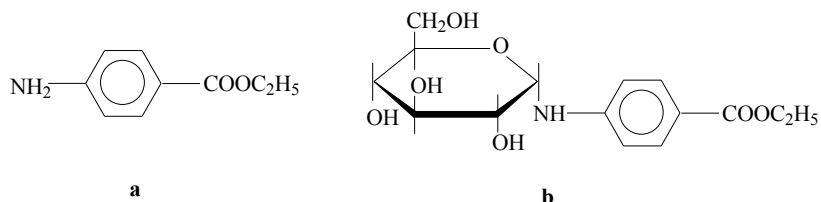


Figure. Benzocaine (a) and ethyl ester of p-(N- α -D-glucopyranoside)aminobenzoic acid (b)

Table. The energy of solvation and thermodynamic characteristics of dissolution of the benzocaine and ethyl ester of p-(N- α -D-glucopyranoside)aminobenzoic acid

Compound	E_s (kcal/mol)	ΔH_s (kcal/mol)	ΔS_s (kcal/mol K ⁻¹)	ΔG_s (kcal/mol)
solvent H ₂ O				
a	-10.93	0.24	2.95	-0.63
b	-24.18	1.69	23.59	-5.07
solvent CHCl ₃				
a	-7.15	-0.91	-0.47	-0.40
b	-14.15	3.39	22.79	-4.06

From a thermodynamic point of view, formation of solution passes spontaneously ($\Delta G_s < 0$), and the dissolution of substances occurs with a small endothermic effect ($\Delta H_s > 0$), except for benzocaine in chloroform. Therefore, the positive value of entropy change ($\Delta S_s > 0$) is a condition of dissolution process. The simulation results of the studied compounds in aqueous solution are in good agreement with the data of comparative analysis of their lipophilic properties [2]. It confirms the conclusion that benzocaine modified by glucose residue leads to increase of its solubility in water. Simulation of compounds being studied in chloroform medium gives contradictory results. It is known that benzocaine is weakly soluble in water but its solubility in chloroform is sufficiently high. At the same time the glucose practically is not soluble in chloroform [3].

However, the solvation energy of benzocaine in chloroform is smaller than in water. According to simulation the benzocaine modified by glucose residue is highly soluble both in aqueous and in chloroform solutions, i.e. thermodynamic characteristics of both dissolution processes have similar values. But it is not consistent with experimental data.

[1] Granovsky A.A. PCGAMESS version 7.1, <http://classic.chem.msu.su/gran/gamess/index.html>

[2] Volkova, T.G.; Talanova, I.O.; Ryzhakov, A.M.; Tsarkova, A.I. Book of abstracts 2nd Russian Conference on Medicinal Chemistry (MedChem 2015) July 5-10, 2015, Novosibirsk, Russia, 306.

[3] Handbook for the pharmacist, 2nd ed., Rev., ed. by A. I. Tenzaloy, Medicine, Moscow, 1981.



Section 2.

Thermochemistry and databases

Oral presentations



GEOMETRIC FOUNDATION OF THERMODYNAMICALLY STABLE (GENERAL) TYPES OF ATOMIC INORGANIC STRUCTURES

Borisov S.V., Pervukhina N.V., Magarill S.A.

Nikolaev Institute of Inorganic Chemistry, Siberian Branch of the Russian Academy of Sciences, 630090 Novosibirsk, Russia

E-mail: borisov@niic.nsc.ru

The crystalline state, the long-range order in the atomic arrangement, was established experimentally to be created by locating atoms on the families of the parallel equidistant planes [1, 2]. This results in the translational symmetry to decrease the general number of degrees of freedom for atoms as material particles up to the unit cell volume. The releasing energy is evolved as the crystallization heat. A further decrease in the kinetic energy occurs on the formation of the symmetry bonds in the atomic arrangement in the unit cell volume. At length, the quantitative criterion is derived to characterize the given crystal structure, namely, the ratio of atomic degrees of freedom to their number in the primitive unit cell, (S). The smaller S , the more stable is the structure. The number of the atomic degrees of freedom in the cell is the number of variable basic atomic coordinates unfixed by the symmetry elements [3].

The other criterion to estimate the structure stability is the minimal volume in the unit cell, V^* , which forms the unit cell of the volume V_0 being multiplied by the symmetry operations.

Its value is calculated by the formula $V^*=V_0/M$, where M is the multiplicity of the symmetry space group of the structure. The final balance effect of the atomic arrangement to provide the structure stability is characterized by V^* . The smaller this value, the more stable is the structure.

The general tendency for any condensed substance state is the tendency to the closest packing added by the fifth Pauling rule for crystals, namely, the tend to the minimal variety of the structure fragments [4, 5]. Among the diversity of the known crystal structures, common structure types stand out as peculiar geometric standards to crystallize various atomic compositions. The crystallographic method [6] and the proposed criteria provide comparing the energetically stable atomic constructions.

In the diamond structure (symmetry group $Fd\bar{3}m$, $M=192$, $z=8$, $a=3,567\text{\AA}$, $V=45,5\text{\AA}^3$), the carbon atoms are located in the particular positions with $S=0$, and $V^*=45,5/192=0,24\text{\AA}^3$ is, probably, the least value for crystals. For comparison, in the graphite structure ($P6_3/mmc$, $M=24$, $z=4$, $a=2,464\text{\AA}$, $c=6,711\text{\AA}$, $V=35,29\text{\AA}^3$) with $S=0$ and $V^*=1,48\text{\AA}^3$, this criterion is six times more. Owing to the higher symmetry, the metastable diamond is competitive in the crystallization process with graphite if there are conditions to form suitable-sized nuclei. Close to the diamond is the popular structure type of spinel, ($Fd\bar{3}m$, $M=192$, $z=8$, $a=8,075\text{\AA}$, $V=526,5\text{\AA}^3$), in which the anions have one degree of freedom, $S=1/14\approx 0,071$, $V^*=2,75\text{\AA}^3$, with located cation positions. These criteria increase for complex atomic compositions, for instance, the apatite structure type, $S\approx 0,26$; $V^*=44\text{\AA}^3$, tourmalines, $S\approx 0,62$; $V^*=88\text{\AA}^3$, a.o. [7].

The results obtained show a tendency for spatial structure parameters to decrease in number in popular (stable) types, geometric standards with different atomic sorts in the located positions, sometimes 2 or 3 sorts in one position.

[1] Borisov S.V., Magarill S.A., Pervukhina N.V. Russ. Chem. Rev. 2015, 84, 393-421.

[2] Borisov S.V. J. Struct. Chem. 1992, 33, 123-129.

[3] Borisov S.V. J. Struct. Chem. 1995, 36, 1156-1157.

[4] Pauling L. J. Am. Chem.Soc. 1929, 51, N 1010, 26.

[5] Borisov S.V., Pervukhina N.V., Magarill S.A. Structural Chemistry. 2016, 27,1673-1683.

[6] Borisov S.V., Magarill S.A., Pervukhina N.V. Crystallography Reports. 2011, 56, 935-940.

[7] Borisov S.V., Magarill S.A., Pervukhina N.V. J. Struct. Chem. 2017 (in press).

THERMAL PROPERTIES OF VOLATILE PALLADIUM (II) COMPLEXES WITH SCHIFF BASES

Cherkasov S.A.^{1,2}, Vikulova E.S.¹, Nikolaeva N.S.¹, Sysoev S.V.¹, Trubin S.V.¹, Morozova N.B.¹

¹Nikolaev Institute of Inorganic Chemistry, Siberian Branch of the Russian Academy of Sciences, 630090 Novosibirsk, Russia

²Novosibirsk State University, 630090 Novosibirsk, Russia

E-mail: cherkasov-s_95@mail.ru

Complexes of palladium (II) with tetradentate Schiff bases are widely used as catalysts for organic synthesis, as well as organic diodes and optical sensors [1-3]. However, similar to other transition metal complexes, the usage of this type of complexes as precursors for obtaining palladium-containing functional films by chemical vapor deposition (MOCVD) is promising. The precursors used in MOCVD should possess the certain thermochemical requirements, the main ones is high volatility and stability. Among the known palladium complexes with tetradentate Schiff bases, the most preferred for the use in MOCVD seems to be Pd(acacen) (acacen²⁻ - N,N'-(ethylene)-bis(acetylacetoniminato)) because of the smallest molecular weight. It is shown by the example of similar copper (II) complexes that the insertion of additional carbon atoms and methyl substituents in diamine bridge increases the volatility of the produced compounds [4]. In this regard, the investigation of the influence of ligand structure on the thermal properties of palladium (II) complexes with tetradentate Schiff bases is of interest.

Thus, the aim of this work is the synthesis and study of the thermal properties in a series of Pd(acacen), Pd(acacpda), Pd(acacmpda) (acacpda²⁻ = N,N'-(propylene)-bis(acetylacetoniminato), acacmpda²⁻ = N,N'-(2,2-dimethylpropylene)-bis(acetylacetoniminato)) (Fig. 1). Complexes Pd(acacpda), Pd(acacmpda) were obtained for the first time. All the compounds were synthesized by the interaction of Pd(CH₃CN)Cl₂, H₂L (L = acacen²⁻, acacpda²⁻, acacmpda²⁻) in acetonitrile and NaOH, and characterized by the methods of elemental analysis, IR-spectroscopy, mass-spectroscopy and X-ray diffraction. It was shown by the TGA method that all the obtained compounds quantitatively pass into the gas phase in the temperature range 200-325°C. The temperature dependences of saturated vapor pressure were measured by Knudsen's effusion method for Pd(acacen) and flow method for Pd(acacpda), Pd(acacmpda), and the thermodynamic parameters of sublimation processes were calculated for all the complexes (Tab. 1). The data obtained for palladium (II) complexes allow us to conclude that the volatility increases in the order of Pd(acacen) - Pd(acacpda) - Pd(acacmpda).

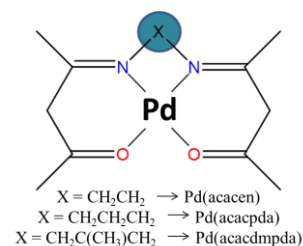


Figure 1. General structure formula for palladium (II) complexes.

Table 1. Thermodynamic parameters of sublimation for palladium (II) complexes.

Compound	ΔT , K	N	$\ln(P/P_0) = A - B/T$		$\Delta_{\text{sub}}H$, kJ/mol	$\Delta_{\text{sub}}S^\circ$, J/(mol*K)
			A	B		
Pd(acacen)	370 – 458	8	22.24	14550	121±1	185±3
Pd(acacpda)	423 – 453	11	25.34	15994	133±4	210±9
Pd(acacmpda)	432 – 479	25	26.23	16238	135±1	218±3

This work was supported by the Russian Scientific Foundation grant № 15-13-10014.

- [1] Phan, N; Brown, D; Adams, H. J. Chem. Soc., 2004, 9, 1348.
 [2] Liu, P; Feng, X; He, R. Tetrahedron, 2010, 66, 631.
 [3] Borisov, S; Saf, R; Fischer, R. Inorg. Chem., 2012, 52, 1206.
 [4] Dorovskikh, S; Kuratieva, N; Tkachev, S. J. Struct. Chem., 2014, 55, 1067.

THERMODYNAMIC PROHIBITION OR KINETIC RESTRICTIONS? EFFECT OF PRESSURE ON TWO POLYMORPHS OF TOLAZAMIDE

Fedorov A.Yu.^{1,2}, Rychkov D.A.^{1,2}, Losev E.A.^{1,2}, Zakharov B.A.^{1,2}, Stare J.³, Boldyreva E.V.¹

¹Institute of Solid State Chemistry and Mechanochemistry SB RAS, 630128 Novosibirsk, Russia

²Novosibirsk State University, 630090 Novosibirsk, Russia

³National Institute of Chemistry, SI-1000 Ljubljana, Slovenia

E-mail: alexfed97@yandex.ru

The same molecules can form different periodic structures – polymorphs – depending on crystallization conditions. At any given temperature and pressure, only one polymorph is thermodynamically stable. However, other polymorphs can crystallize either instead of the stable form, or concomitantly with it due to the kinetic control of nucleation and nuclei growth.

Hydrostatic compression is a powerful instrument for obtaining new polymorphs with essential properties. Various factors, such as compression-decompression protocol, the rate of pressure increase, the presence of nuclei of other phases, the nature of the pressure-transmitting fluid can have a significant influence on the formation of new structures. Studying the effect of pressure on polymorphism is very useful for physical chemists as well as for crystallographers since it helps to gain a better insight into causes and mechanisms of phase transformations in solids.

Two polymorphs of tolazamide – antidiabetic drug – provide a shining example of kinetic control of polymorphic transformations at ambient pressure [1]. When crystallized from solution, the nuclei of the two polymorphs, I and II, seem to be formed almost simultaneously, then the crystals of Form II grow much faster than those of Form I. However, if the crystals of polymorph II are stored in solution, they eventually recrystallize into polymorph I. The irreversible II to I transformation has also been detected in the solid state by single-crystal and powder X-ray diffraction and thermomicroscopy upon heating.

Besides that, the two polymorphs differ radically in molecular packing and, slightly, in densities. Therefore, one could expect that pressure could favor the II to I transformation in the crystals of tolazamide, or, if nucleation in the solid state is hindered, a recrystallization of polymorph II into polymorph I when pressure is increased.

The aim of this study was to follow the effect of pressure on both forms of tolazamide in different fluids (dissolving or not dissolving the crystals) using single-crystal X-ray diffraction and DFT methods. Neither of the two polymorphs transforms into another at least up to 6 GPa in pentane-isopentane mixture but there is a partial II to I recrystallization in methanol at 0.1 GPa. Solid state DFT-D3 calculations of internal energies and enthalpies of both polymorphs across a wide pressure range were performed, as well as estimation of minimal energy barrier between two forms of tolazamide. This comprehensive study helps to answer what experimental results are related to – thermodynamic prohibition of transformations or kinetic restrictions on them.

This work was supported by Russian Science Foundation (project 14-13-00834).

[1] Boldyreva E.V. *et al.* Chemistry - A European Journal, 2015, 21 (43), 15395-15404.

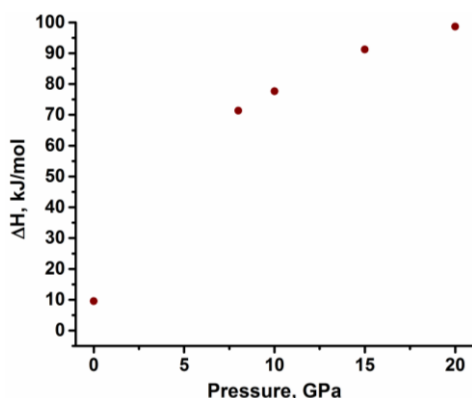


Figure 1. Calculated enthalpy difference of Form II and Form I versus pressure.

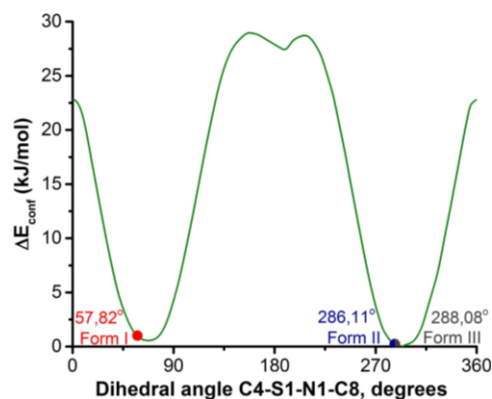


Figure 2. Conformational landscape of tolazamide C4-S1-N1-C8 dihedral angle

THERMODYNAMICS OF UNUSUAL COORDINATION OF LEWIS BASES TO 1,2,5-CHALCOGENADIAZOLES: EXPERIMENT AND THEORY

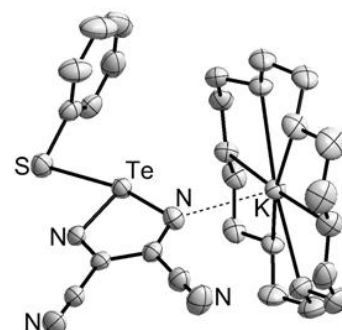
 Gorbunov D.E.^{1,2}, Gritsan N.P.^{1,2}, Semenov N.A.³, Shakhova M.V.^{1,2}, Zibarev A.V.^{1,3}
¹Novosibirsk State University, 630090 Novosibirsk, Russia

²Voevodsky Institute of Chemical Kinetics and Combustion, Siberian Branch of the Russian Academy of Sciences, 630090 Novosibirsk, Russia

³Vorozhtsov Institute of Organic Chemistry, Siberian Branch of the Russian Academy of Sciences, 630090 Novosibirsk, Russia
 E-mail: gritsan@kinetics.nsc.ru

1,2,5-Chalcogenadiazoles (chalcogen: S, Se, Te) and their fused derivatives are of considerable interest for chemistry and materials science. Their distinctive feature is a positive electron affinity, and both the full and partial electron transfer from their donors to 1,2,5-chalcogenadiazoles as the acceptors are possible. In the case of partial electron transfer depending on the donor charge (an anion or a neutral molecule), both the anionic and neutral charge-transfer (CT) complexes have been obtained [1-3].

According to the X-ray diffraction data, the E-A⁻ (E = Se, Te; A = F, Cl, Br, I, SCN, SeCN, SPh, SePh) coordinate bond is always longer than the sum of the covalent radii (by 0.1 – 0.7 Å) but shorter than the sum of the van der Waals radii (by 0.7 – 1.4 Å) of the atoms forming the bond (e.g. S-Te, Fig. 1). Telluradiazole **1** and its Se-analog **2** are characterized by an intense absorption band in the near-UV region. The coordination of anions leads to a substantial shift of the long-wavelength band to the visible spectral region. The substantial change in the electronic absorption spectra upon the coordination made it possible to study the thermodynamics of complex formation (Table 1). Only the low limit of the equilibrium constant and, correspondingly, the upper limit of the free



Gibbs energy of complex formation was estimated for very strong complexes. Table 1 demonstrates that calculations using B97-D3 functional with account of dispersion interactions reproduce well experimental results. The free energy of solvation of anions A⁻ is considerably higher than that of the larger coordination products. Therefore, taking into account the solvent in quantum chemical calculations results in a substantial destabilization of the coordination products compared to the gas phase. The same factor causes a higher destabilization of the coordination products in polar solvents compared to nonpolar solvents.

According to the gas-phase DFT calculations, the E-A⁻ bond energy varies in a wide range, from ~105 kJ·mol⁻¹ comparable to the energy of weak covalent bonds to ~360 kJ·mol⁻¹ comparable to the C-C bond energy in organic compounds. Results of the comprehensive computational studies on the nature of the bonding interactions and the influence of the chemical nature of the reagents on the properties of adducts will be discussed.

Acknowledgement. This work was supported in part by RFBR (grant 15-03-03242).

Table 1. Experimental Gibbs free energies of complex formation and values calculated at the B97-D3/def2-TZVP (with ECP for Te and I) level using COSMO model to account the solvation.

Compound	Solvent	$-\Delta_r G_{exp}^0(298\text{ K})$ (kJ/mol)	$-\Delta_r G_{calc}^0(298\text{ K})$ (kJ/mol)
[1 -SCN] ⁻	MeCN	15.3 ± 0.1	18.3
[1 -SeCN] ⁻	MeCN	15.9 ± 0.5	16.0
[1 -F] ⁻	CH ₂ Cl ₂	>50	138.7
[1 -SPh] ⁻	CH ₂ Cl ₂	>50	59.9
[2 -SPh] ⁻	THF	27.7 ± 0.4	27.7
	MeCN	19.7 ± 0.4	–

[1] Semenov, N.A.; Lonchakov, A.V.; Pushkarevsky, N.A.; et al. *Organometallics*, 2014, 33, 4302-4314.

[2] Semenov, N.A.; Lonchakov, A.V.; Gritsan, N.P.; et al. *Russ. Chem. Bull.*, 2015, 64, 499-510.

[3] Chulanova, E.A.; Pritchina, E.A.; Malaspina, L.A.; et al. *Chem. Eur. J.*, 2017, 23, 852-864.

INTERACTIONS OF MeTMPyP₄ METALLOPORPHYRINS WITH NUCLEOSIDE DIPHOSPHATES

Ivanov M.A., Sizov V.V., Dzhuzha A.U., Sidorova K.S., Kudrev A.G.

Saint Petersburg State University, Institute of Chemistry, 198504, Russia, Saint-Petersburg, Peterhof, Universitetskii pr. 26

E-mail: mikhail.ivanov.1995@gmail.com

TMPyP₄ (also known as 5,10,15,20-tetrakis(N-methylpyridinium-4-yl)-21H,23H-porphyrin) and its metallic derivatives (MeTMPyP₄, Me = Zn, Cd, Eu, Cu, Fe, Au) are one of the most widely used ligands to form complexes with G₄-quadruplexes (G₄-DNA). These ligands may bind strongly and selectively to G₄-DNA, thus they may be used as precursors of new anticancer drugs and G₄-DNA fluorescent probes. Despite the intensive recent research, the nature of binding of MeTMPyP₄ with G₄-DNA requires further clarification.

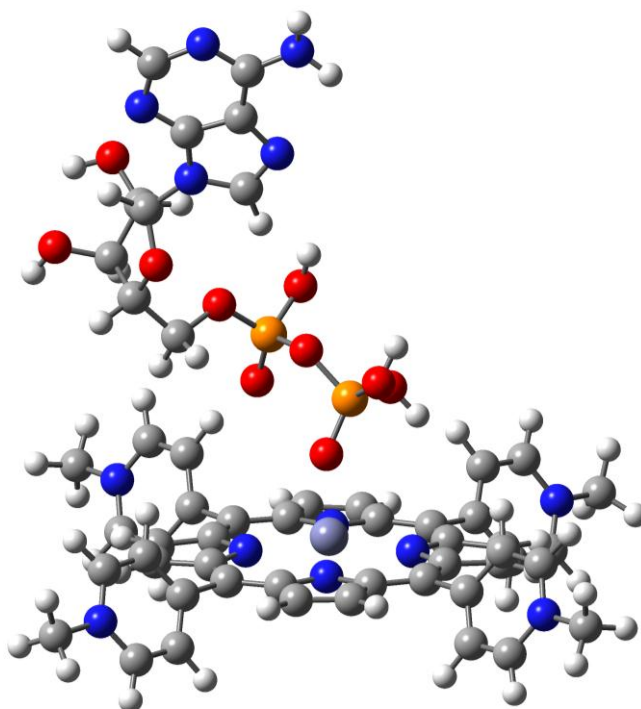


Figure 1. One of possible coordination modes for the ZnTMPyP₄ – ADP complex

In the present work, nucleoside diphosphates are selected as models for G₄-DNA active sites, and the interactions of MeTMPyP₄ with nucleoside diphosphates are studied both theoretically and experimentally. Quantum chemical DFT calculations were carried out to obtain structural and thermodynamic properties of MeTMPyP₄ and its complexes with nucleoside diphosphates (see Figure 1). Comparison of energy changes upon nucleoside diphosphate coordination allows one to identify the most favorable coordination modes. Time-dependent DFT studies were performed for free MeTMPyP₄ and optimized complexes with nucleoside diphosphates to confirm the validity of electronic structure calculations by comparing the computed UV-visible absorption spectra with experimental data. The results obtained in this work may provide insight into the nature of preferential binding sites of G₄-DNA with MeTMPyP₄.

The calculations were performed using the facilities provided by the Computational Resource Center (Research Park, Saint Petersburg State University).



INTERPLAY OF HIGHLY ACCURATE QUANTUM CHEMICAL COMPUTATIONS AND THERMAL ANALYSIS TECHNIQUES IN THE STUDY OF THERMOCHEMISTRY OF ENERGETIC MATERIALS

Kiselev V.G.^{1,2,3}, Muravyev N.V.³, Monogarov K.A.³, Pivkina A.N.³

¹Novosibirsk State University, 630090 Novosibirsk, Russia

²Institute of Chemical Kinetics and Combustion, SB RAS, 630090 Novosibirsk, Russia

³Semenov Institute of Chemical Physics RAS, 4, Kosygin Str., 119991 Moscow, Russia

E-mail: vitaly.kiselev@kinetics.nsc.ru

Thermochemistry, kinetics, and mechanism of thermal decomposition of energetic materials (EM) are crucial for understanding their performance, compatibility, and storage properties. However, the direct experimental measurements of both thermochemistry and kinetics are often hindered by very complex nature of numerous fast physical and chemical processes simultaneously occurring during thermal decomposition of high-energy species. Modern highly accurate quantum chemical calculations are very powerful and promising complementary tool to experiment for the determination of thermodynamics, rate constants of elementary reactions, and chemical mechanism of thermolysis. In the present contribution, we show two typical applications of quantum chemistry in combination with experimental thermal analysis techniques for particular problems of thermochemistry and kinetics of EM.

First, we proposed the convenient and facile procedure to determine thermochemistry of EM, viz., the solid-state formation enthalpies. The latter values are obtained as combinations of theoretically calculated gas-phase formation enthalpies and sublimation enthalpies extracted from thermogravimetric (TGA) experiments with the aid of the Langmuir equation. The highly accurate quantum chemical methods allow for the mean accuracy comparable to experimental one (~1-2 kcal/mol). In turn, the mass loss measurements are performed under vacuum conditions to avoid thermal decomposition of EM. Comparison with available combustion calorimetry values for well-studied high-energy species justifies the high accuracy of our procedure. With the aid of this technique, we resolved the existing discrepancies in the formation enthalpies of several important EM (e.g., FOX-7) [1] and proposed the lacking values for a series of energetic nitroesters and heterocyclic species.

Quantum chemical calculations are also a very convenient tool for understanding the detailed chemical mechanism of thermolysis of EM. As a typical example, we studied thermal decomposition of tetranitroacetimidic acid (TNAA), a new chlorine-free oxidizer first reported in 2014. TGA and differential scanning calorimetry (DSC) experimental techniques at atmospheric, vacuum, and elevated pressures were used to obtain kinetics of the whole decomposition process. Computations, in turn, allowed for understanding tiny details of mechanism: viz., the important role of tautomeric equilibria was revealed, and several closely lying radical (C-NO₂ bond scission) and molecular (N₂O elimination) channels occurring in various tautomers turned out to be dominating primary decomposition reactions [2]. The theoretically predicted activation energies (~39 kcal/mol) are in perfect agreement with experimental values.

Acknowledgement. This work was supported by Russian Science Foundation (grant 16-13-10155).

[1] N.V. Muravyev, A.N. Pivkina, V.G. Kiselev, Comment on “Studies on Thermodynamic Properties of FOX-7 and Its Five Closed-Loop Derivatives”. *J. Chem. & Eng. Data* 2017, 62, 575–576. DOI: 10.1021/acs.jced.6b00483.

[2] V.G. Kiselev, N.V. Muravyev, K.A. Monogarov, A.F. Asachenko, M.S. Nechaev, I.V. Fomenkov, A.N. Pivkina, N.P. Gritsan, Thermochemistry, Tautomerism, and Thermal Decomposition of Tetranitroacetimidic Acid (TNAA): New Insights from Thermal Analysis and High-Level *ab initio* Calculations *J. Phys. Chem. B.* 2017, submitted.



PREDICTION OF THERMODYNAMIC PROPERTIES OF VAPORIZATION FOR ALKANES

Krasnykh E.L., Portnova S.V., Safronov S.P.
 Samara State Technical University, Samara, 443100 Russia
 E-mail: kinterm@samgtu.ru

Pressure of saturated vapors of a substance can be determined with the following equation established by integrating Clausius-Clapeyron equation

$$R \cdot \ln(p) = A_f + \frac{B_f}{T} + \Delta_l^g C_p^o \cdot \ln\left(\frac{T}{298.15}\right) \quad (1)$$

where p – a pressure of saturated vapor of a compound; A_f , B_f – coefficients, $\Delta_l^g C_p^o$ – change of heat capacity of “liquid-vapor” transition.

B_f coefficient can be calculated on the basis of vaporization enthalpy with the following equation

$$B_f = -\Delta_{ucn} H^o(298,2) + \Delta_l^g C_p^o \cdot 298,2 \quad (2)$$

Thus, in order to predict the pressures of saturated vapors it is needed to predict the vaporization enthalpies, the change of heat capacity of “liquid-gas” transition and A_f coefficient which comprises entropy constituent and the change of $\Delta_l^g C_p^o$ under the temperature.

Earlier, in the work [1] we proposed a method for prediction the enthalpies of vaporization of alkanes and in the work [2] – a method for prediction the change of heat capacity of “liquid-vapor” transition on the basis of modified Randić indices.

The calculation of $\Delta_{vap} H^o(298,2)$ $\Delta_l^g C_p^o$ is performed by the following linear equations

$$\Delta H_{vap}^o(298,2) = A \cdot \chi^{0-3} + B \quad (3)$$

$$\Delta_l^g C_p^o = C \cdot \chi^{*0-3} + D \quad (4)$$

χ^{0-3} - total molecular connectivity index determined by the method described in the work [1].

Thus, there is a possibility to co-optimize the equations mentioned above to obtain values of carbon groups descriptors. In order to perform co-calculation of saturated vapor pressures, the vaporization enthalpies and the changes of “liquid-gas” transition we optimized the following equations system where A , B , C , D , A_f , B_f coefficients are the functions of total molecular index and consequently are the functions of values of carbon groups descriptors.

A system of the equations for optimization

Control parameters of optimization

$$\Delta H_{vap}^o(298,2) = A \cdot \chi^{0-3} + B \quad \sum (\Delta H_{vap}^o(298,2)_{exp} - \Delta H_{vap}^o(298,2)_{calc})^2 \longrightarrow \min$$

$$\Delta_l^g C_p^o = C \cdot \chi^{*0-3} + D \quad \sum (\Delta_l^g C_p^o_{exp} - \Delta_l^g C_p^o_{calc})^2 \longrightarrow \min$$

$$R \cdot \ln(p) = A_f + \frac{B_f}{T} + \Delta_{sc}^n C_p^o \cdot \ln\left(\frac{T}{298.15}\right) \quad \sum (p_{exp} - p_{calc})^2 \longrightarrow \min$$

The following literature data were used as test series: the dependencies of saturated vapors pressures on temperature – for 21 alkanes; the vaporization enthalpies – for 21 alkanes; the change of heat capacity of “liquid-vapor” transition – for 12 alkanes.

As a result of processing the following values of descriptors were obtained: CH₃ – 1.1791; CH₂ – 1.2797; CH – 1.7028; C – 4.2683, and also the following linear equations for calculation of necessary characteristics:

$$\Delta H_{vap}^o(298,2) = 0,8715 \cdot \chi^{0-3} - 0,73; \quad \Delta_l^g C_p^o = -1,2567 \cdot \chi^{*0-3} - 6,79$$

$$A_f = 2,5288 \cdot \chi^{0-3} + 146,75; \quad B_f = -\Delta_{ucn} H^o(298,2) + \Delta_{sc}^n C_p^o \cdot 298,2$$

Values of pressures of saturated vapors were determined with the equation

$$R \cdot \ln(p) = A_f + \frac{B_f}{T} + \Delta_{sc}^n C_p^o \cdot \ln\left(\frac{T}{298.15}\right), \text{ and values of normal temperatures of boiling with the same}$$

equation at $P=101325$ Pa.

This work was supported by the Russian Foundation for Basic Research, project no. 16-08-00383 a.

[1] Krasnykh E.L. J. of Struc. Chem., 2008, 49, 6, 986-993.

[2] Krasnykh E.L.; Portnova S.V. J. of Struc. Chem., 2017, 58, 4, 753-758.

THERMAL PROPERTIES OF AMMONIUM HEXAFLUOROSILICATE

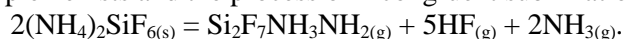
Laptash N.M.¹, Sysoev S.V.², Kozlova S.G.²

¹Institute of Chemistry, Far Eastern Branch of the Russian Academy of Sciences, 690022 Vladivostok, Russia

²Nikolaev Institute of Inorganic Chemistry, Siberian Branch of the Russian Academy of Sciences, 630090 Novosibirsk, Russia

E-mail: laptash@ich.dvo.ru

Recently, researches have drawn their attention to ammonium hexafluorosilicate $[(\text{NH}_4)_2\text{SiF}_6]$, which has a variety of possible uses ranging from medicine to electronics. It is effective in preventing dental caries from progressing, does not change tooth color and seems to be a promising desensitizing agent with low or no cytotoxicity *in vitro*. Dealumination with $(\text{NH}_4)_2\text{SiF}_6$ is an appropriate technique to prepare zeolitic catalysts. The $(\text{NH}_4)_2\text{SiF}_6$ layer could be an efficient host for light emitting silicon particles. $(\text{NH}_4)_2\text{SiF}_6$ is a key compound in the fluoride processing of raw materials. Natural silicon-containing raw materials (quartz and silicates of different structure and compositions) are fluorinated with ammonium hydrogen difluoride (NH_4HF_2) producing double fluoride salt $(\text{NH}_4)_3\text{SiF}_7 = (\text{NH}_4)_2\text{SiF}_6 \cdot \text{NH}_4\text{F} = (\text{NH}_4)_3[\text{SiF}_6]\text{F}$, whose thermal decomposition is accompanied by sublimation of $(\text{NH}_4)_2\text{SiF}_6$ [1]. The history of $(\text{NH}_4)_2\text{SiF}_6$ goes back more than 200 years [2] but its thermal behavior is under discussion till now. Davy [2] mentioned that the compound “just perceptibly reddens litmus paper and appears to sublime unaltered when heated”. Marignac described cubic [3] and hexagonal [4] forms of $(\text{NH}_4)_2\text{SiF}_6$ volatilized without melting. The more accepted statement is that the compound decomposes with the formation of five gas molecules: $(\text{NH}_4)_2\text{SiF}_6(\text{s}) = \text{SiF}_4(\text{g}) + 2\text{NH}_3(\text{g}) + 2\text{HF}(\text{g})$ [5]. However, our tensimetric investigations show that it decomposes with the formation of four gas molecules as it follows from the temperature dependence of saturated and unsaturated vapor pressure measured by the static method and calculated from the data of flow method. The data of the two methods are enabled to determine the average molar mass of the gas phase. Thermodynamic parameters of the sublimation process are the following: $\Delta H^\circ_{298} = 95.2 \pm 1$ kJ/mol, $\Delta S^\circ_{298} = 176.4 \pm 2$ J/(mol·K). The mass-fragment of 223 was detected in the mass-spectrum of the $(\text{NH}_4)_2\text{SiF}_6$, the decomposition product was isolated with the help of elementary silicon. This means that only dinuclear silicon complex exists and the process of incongruent sublimation can be expressed as:



Our density functional theoretical calculations (DFT, carried out on the basis of spin-restricted method implemented in the code ADF2013) of this dinuclear complex, give the only viable structural model consisting of two corner-sharing polyhedra (octahedron and tetrahedron) joined by the NH_2 group (Figure 1).

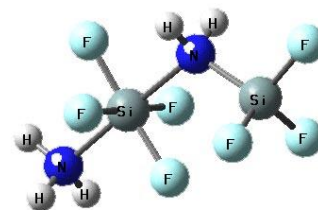


Figure 1. Siliceous dinuclear complex with NH_2 -bridged octahedron and tetrahedron.

[1] Laptash, N.M.; Kurilenko L.N., RU Patent 2306546, 2007.

[2] J. Davy, Phil. Trans., R. Soc. London, 1812, 102, 352–369.

[3] Marignac M.C., Ann. Mines, 1859, 15, 221–290.

[4] Marignac, M.C. Ann. Chim. Phys. 1860, 60 (3), 257–307.

[5] Abdel Rehim, A.M. J. Therm. Anal. 1997, 48, 177–202.

THERMODYNAMIC PROPERTIES OF DIATOMIC ARGON COMPOUNDS

Maltsev M.A.^{1,2}, Morozov I.V.^{1,2}, Osina E.L.¹

¹Joint Institute for High Temperatures of Russian Academy of Sciences, 125412 Moscow, Russia

²Moscow Institute of Physics and Technology, 141701 Dolgoprudny, Russia

E-mail: maksim.malcev@phystech.edu

The compounds containing the ions of argon play essential role in the mass spectrometry with argon plasma sources such as laser ablation inductively coupled plasma mass spectrometry (LA-ICP-MS). Thermodynamic properties of such molecules are required to estimate their abundance in the plasma source and distortions of the spectrometry results due to an overlap of desired signals and the signals from argide ions [1]. However, there is a lack of information about such properties in the literature. In this work we report the calculations of the partition function and thermodynamic properties of the compounds of argon with 3d metals (argide ions) ArCo^+ , ArV^+ , the dimeric ion of argon (Ar_2^+) and the dimer Ar_2 . We use the method based on resolving the one-dimensional Schrödinger equation with a given interatomic potential and finding the energy spectra of the diatomic molecule [2,3]. First the LEVEL code (version 8.2) [4] is used to compute discrete eigenvalues of the rotationless energies and vibronic constants. Then rovibronic energy spectrum is calculated that takes into account rotation of the diatomic molecule. Calculation of the internal partition function requires accurate data for the interatomic potential at low lying electronic states. Therefore a special attention is paid to evaluation of various forms of the potentials that fit spectroscopic data.

In order to compute the partition function for the compounds of argon with 3d metals we use the potential suggested by D. Bellert and W.H. Breckenridge [5]. The results are compared with much simpler Morse potential and the Harmonic Oscillator – Rigid Rotator mode (see Fig. 1). Totally 15 electronic states of ArV^+ and 12 electronic states of ArCo^+ are taken into account.

For the dimeric ion of argon we use both the Morse potential and the modified Morse potential fitting them to the experimental data [6]. Totally 5 molecular terms are considered. It is found the use of more complicated potentials results in a difference up to 10% for the partition function at the upper temperature boundary 20000K compared to the simple Morse potential.

The results are used to extend the IVTANTHERMO database on thermodynamic properties of individual substances that is being developed in JIHT RAS.

$$Q_{\text{vib-rot}} = \sum_{v,J} (2J+1) e^{-(E(v,J) - E(0,0))/kT}$$

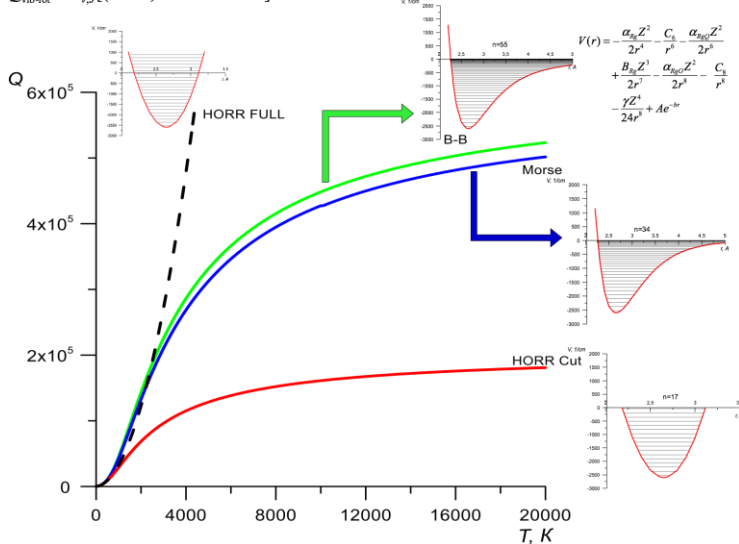


Figure 1. Partition function for different rovibronic interaction potential for VAr^+

[1] Witte, T.M.; Houk, R.S. Spectrochimica Acta Part B, 2004, 69, 25-31.

[2] Maltsev, M.A.; Kulikov, I.V.; Morozov I.V. Journal of Physics: Conference Series, 774, 12023

[3] Gurvich, L.V.; Bergman, G.A.; Veys, I.V. Thermodynamic Properties of Individual Substances. Vol. 4, parts 1 and 2. Moscow, 1984.

[4] Le Roy R.J., Level code, <http://leroy.uwaterloo.ca/programs/>

[5] Bellert, D.; Breckenridge, W.H. Chem. Rev., 2002, 1595-1622.

[6] Michels, H.H.; Hobbs, R.H.; Wright, L.A. The Journal of Chemical Physics, 1978, 69, 5151-5162.

CHEMICAL KINETICS AND THERMODYNAMICS OF THE AlN CRYSTALLINE PHASE FORMATION ON SAPPHIRE SUBSTRATE IN AMMONIA MBE

Milakhin D.S., Malin T.V., Mansurov V.G., Galitsyn Y.G., Zhuravlev K.S.

A.V. Rzhanov Institute of Semiconductor Physics of the Siberian Branch of the Russian Academy of Science, pr. Lavrentieva 13, Novosibirsk 630090, Russia
E-mail: denironman@mail.ru

To date III-nitrides are successfully grown on foreign substrates (Al_2O_3 , Si, SiC et al). Special substrate surface treatment (nitridation) and thin AlN film as a buffer layer are frequently used on sapphire or silicon substrate to improve crystal quality of subsequent epitaxial III-nitrides layers in both molecular beam epitaxy (MBE) and MOCVD growth. However, there is still no agreement according to the mechanisms of AlN phase formation. In the present work the early stages of the AlN crystal formation on the (0001) Al_2O_3 surface during nitridation in ammonia MBE have been investigated as functions of substrate temperature and NH_3 pressure by reflection high energy electron diffraction (RHEED). A kinetic scheme of surface reactions is developed and thermodynamic aspects of the process are discussed. A nitridation experiments can be divided in two types: exposing of substrate surface under fixed NH_3 flux, varying the substrate temperature in the range of 850-1050 °C, and the AlN formation under different ammonia fluxes in range of 12.5-400 sccm at constant temperature.

The investigation of the temperature dependence of AlN formation rate reveals a complicated character of the process. Two different temperature dependences of the AlN formation rate are found: strong temperature dependence at $T < 940$ °C, and the formation rate is not dependent on the temperature at range $T > 940$ °C. Hence, at $T < 940$ °C chemical reactions do limit the formation rate, but at $T > 940$ the process is determined by a surface phase transition in AlN lattice gas. The kinetic scheme of the surface reactions AlN formation is developed. The values of kinetic constants for the surface processes (i.e. activations barriers and pre-exponential factors) are determined. Good agreement of numerically calculated kinetics curves with experimental curves was achieved (Fig.1).

The lattice gas model, as it's described in Refs. [1,2], seems to be very helpful to describe the AlN formation at comparatively high temperature range. Obviously, at the beginning stages of the nitridation some separate elementary AlN cells appear on the sapphire surface, their concentration increases with ammonia exposition time. An ensemble of the cells constitutes a lattice gas. There is a lateral interaction between the AlN cells, hence, a phase transition from the lattice gas to a condensed phase occurs. Good agreement (Fig. 2) of the calculated isotherm with experimental curve at $T = 1020$ °C is found for the following parameters of lateral interaction: $E_i = -0.725$ eV is the pairwise lateral repulsive energy between neighboring filled AlN cells, $U = -0.725$ eV is a stabilization energy (energy gain with AlN cell formation), $V = 0.09$ eV is an energy loss for the formation of intermediate lattice gas cell. The critical temperature of $T_c = 795$ °C is determined by the parameters of lateral interaction. The experimental temperatures are higher than T_c , hence the observed phase transition is a continuous phase transition, i.e. there is no interphase boundary between the lattice gas and condensed phase.

This work was funded by RFBR and Government of the Novosibirsk region according to the research project № 17-42-543091 and by RFBR № 17-32-80019, 17-02-00947.

[1] A. Zangwill, Physics at Surfaces, Cambridge University Press 1988, 278.

[2] Yu. G. Galitsyn; A. A. Lyamkina; S. P. Moshchenko et al., in: Self-assembly of Nanostructures, edited by S. Belucci, The INFN Lectures, Springer, 2012, 3, chap. 3.

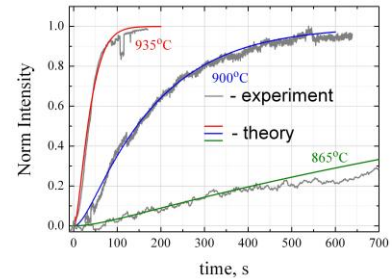


Figure 1. Kinetic curves of AlN formation.

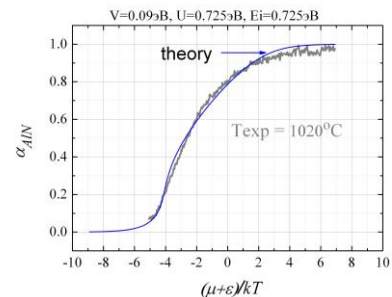


Figure 2. Phase transition isotherm.



THERMODYNAMIC DATABASE FOR PURE SUBSTANCES IVTANTHERMO-ONLINE

Belov G.V.^{1,2}, Dyachkov S.A.^{1,3}, Levashov P.R.^{1,3}, Lomonosov I.V.^{1,4}, Minakov D.V.^{1,3}, Morozov I.V.^{1,3},
Smirnov V.N.^{1,3}

¹Joint Institute for High Temperatures of Russian Academy of Sciences, 125412 Moscow, Russia

²Department of Chemistry, Lomonosov Moscow State University, 119991 Moscow, Russia

³Moscow Institute of Physics and Technology, 141700 Dolgoprudny, Moscow Region, Russia

⁴Institute of Problems of Chemical Physics of the Russian Academy of Sciences, 142432 Chernogolovka, Moscow Region, Russia

E-mail: morozov@ihed.ras.ru

Thermodynamic databases play an essential role in a wide range of applications such as rocket engine engineering, nuclear power, chemical technology, metallurgy, resource usage, waste recycling, etc. The IVTANTHERMO information system [1,2] has made a significant contribution to the accumulation of thermodynamic data. It was created in the department of chemical thermodynamics that was founded in 1966 in the Institute of High Temperatures of the Academy of Sciences of the USSR. Nowadays the development is continued in the Department for Thermophysical Data of JIHT RAS.

The IVTANTHERMO information system includes the database which contains more than 3400 substances, formed of 96 chemical elements, as well as supplementary software for analysis of experimental results, data fitting, calculation and estimation of thermodynamical functions and thermochemistry quantities. Due to its long history the technologies used for the database and software development became out of date and have to be upgraded.

In this report we present a new version of the above mentioned information system called “IVTANTHERMO-Online”. It has a new extensible database design, user-friendly web interface with client-server architecture and a number of features for online and offline data processing. The new system enables to handle multiple versions of each block of data, to store additional information for users and experts (such as comments, bibliography, experimental data, molecular structure, etc.), to present data in multiple forms, to attach calculation services and link with other databases. The substances can be searched using their names, formula, atomic composition or CAS numbers (see Fig. 1). The supplemented software includes the modules for calculation of chemical composition and data fitting.

This work was funded by the State Atomic Energy Corporation ROSATOM, contract No. H.4x.44.9Б.16.1012.

[1] Gurvich, L.V.; Bergman, G.A.; Veyts, I.V. Thermodynamic Properties of Individual Substances. Moscow, 1984.

[2] Belov, G.V.; Iorish, V.S.; Yungman V.S. CALPHAD, 1999, 23, No. 2, 173-180.

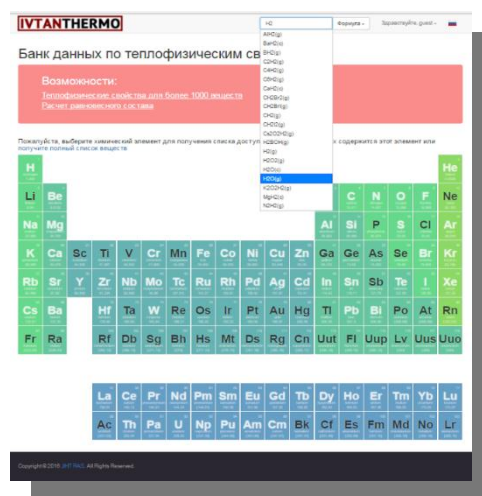


Figure 1. Main page of the IVTANTHERMO-Online web site.

**METHOD FOR DETERMINATION ENTHALPY OF PHASE TRANSITIONS OF ORGANIC COMPOUNDS BASED ON SOLUTION CALORIMETRY**

Nagrimanov R.N., Solomonov B.N.

Alexander Butlerov Institute of Chemistry, Kazan federal university, 420111, Kazan, Russia

E-mail: rnagrimanov@gmail.com

Thermochemical properties of liquid-gas or solid-gas phase transitions are necessary to carry out the synthesis of these substances. The traditional way for evaluation of these values includes experimental studies of processes of transition from the condensed state to the gas phase usually at elevated temperatures. This procedure is not universal and has some well-known problems, which were discussed in [1].

In this work, we propose the solution calorimetry approach to the determination of the enthalpies of phase transitions directly at 298 K. This approach is based on the well-known relationship between the enthalpy of the phase transition of compound A_i at 298 K and the enthalpy of solution ($\Delta_{\text{soln}} H^{A_i/S}$) and solvation ($\Delta_{\text{solv}} H^{A_i/S}$) of compound A_i in solvent S at 298 K:

$$\Delta_{\text{cr(l)}}^g H^{A_i/S} (298 \text{ K}) = \Delta_{\text{soln}} H^{A_i/S} (298 \text{ K}) - \Delta_{\text{solv}} H^{A_i/S} (298 \text{ K}) \quad (1)$$

Solution enthalpy can be measured experimentally. Solvation enthalpy can be calculated. In this work the calculated data of enthalpies of solvation of aromatic compounds were calculated. Based on experimental solution enthalpies of solute A_i in various solvents and the calculated enthalpies of solvation (eq. (1)) were obtained the enthalpies of vaporization and sublimation of aromatic compounds with different substitutes. The comparison of the obtained results with literature data on phase transitions enthalpies shows that solution enthalpies at 298 K can be used for calculation of the vaporization and sublimation enthalpies at 298 K.

The comparison between experimental and literature solution enthalpies in benzene at 298 K and fusion enthalpies at melting temperature showed, that these values are approximately equal. In the presence of polymorphic phase transitions in the range of from 298 K to a melting temperature is necessary to add them to the enthalpy of fusion:

$$\Delta_{\text{soln}} H^{A_i/C_6H_6} (298 \text{ K}) \approx \Delta_{\text{cr}}^1 H^{A_i} (T_{\text{fus}}) + \sum \Delta_{\text{cr I}}^{\text{cr II}} H^{A_i} (T) \quad (2)$$

In accordance with the eqs. (1) and (2) the sublimation enthalpy of A_i at 298 K can be determined by the fusion enthalpy of A_i at the melting temperature and enthalpy of solvation of A_i in benzene according to the following equation:

$$\Delta_{\text{cr(l)}}^g H^{A_i/S} (298 \text{ K}) = \Delta_{\text{cr}}^1 H^{A_i} (T_{\text{fus}}) + \sum \Delta_{\text{cr I}}^{\text{cr II}} H^{A_i} (T) - \Delta_{\text{solv}} H^{A_i/S} (298 \text{ K}) \quad (3)$$

In this work the limits of applicability of this equation were studied.

This work has been performed according to the Russian Government Program of Competitive Growth of Kazan Federal University and Russian Foundation for Basic Research No. 15-03-07475.

[1] Verevkin, SP. *Experimental Thermodynamics*, Elsevier, 2005, 5-30.

HIGH-TEMPERATURE PHASE TRANSITION IN AGGAGES₄ BY MEANS OF STATIC VAPOR PRESSURE MEASUREMENT

Nikolaev R.E., Vasilyeva I.G.

Nikolaev Institute of Inorganic Chemistry, Siberian Branch of the Russian Academy of Sciences, 630090 Novosibirsk, Russia

E-mail: nikolaev@niic.nsc.ru

AgGaGeS₄ (AGGS) is the most promising infrared nonlinear optical material but inclusions as scattering centers lowering optical quality are often observed in crystals grown from melt by Bridgman-Stockbarger method. Therefore, the mechanism of the scattering centers formation became the main aim of the study using well-characterized starting crystals and a most promising static method with quartz membrane-gauge manometers. Being very sensitive to phase transitions, this method was able to determine precisely the homogeneous $p_{\text{partial}}-T-x$ space in the vicinity of the stoichiometric AGGS of the system AgGaS₂ – GeS₂ and to fix temperatures of transitions from one to other phase regions, see Fig. Interpretation of the $p(T)_{x=\text{const}}$ and $p(T, x)$ dependences measured resulted in detection of a polymorphic transition AgGaGeS₄ ↔ AgGaGeS₄' at temperature of $819 \pm 2^\circ\text{C}$. The effect of the presence of amorphous (colloidal) particles of GeS₂ distributed regularly in the AGGS crystals was detected first and understanding of their origin gave a good idea how to eliminate them. The effectiveness of the static method in detection and explanation of unusual phenomenon is considered.

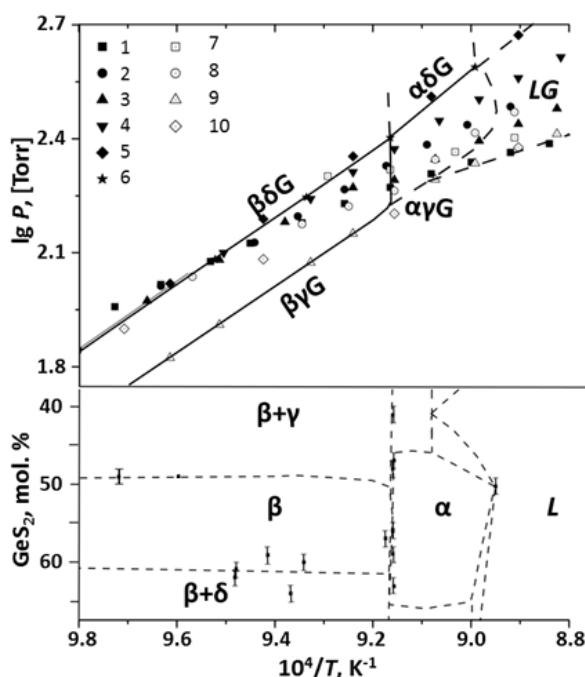


Figure. P - T and T - x projections of the GeS₂-AgGaS₂ diagram: α - and β - AgGaGeS₄; γ - AgGaS₂;

δ – GeS₂; L – liquid; G - $2\text{GeS}_{2(\text{Gas})} \rightarrow 2\text{GeS}_{(\text{Gas})} + \text{S}_{2(\text{Gas})}$.

We thank indeed V.V. Badikov and L.I. Isaenko for the preparation of crystals.

QUANTUM-CHEMICAL MODELING OF TITANIUM MONOXIDE NANOPARTICLES WITH STRUCTURAL VACANCIES

Popov I.S., Rempel A.A., Enyashin A.N.

Institute of Solid State Chemistry, Ural Branch of the Russian Academy of Sciences, 620990 Yekaterinburg, Russia

E-mail: popov@ihim.uran.ru

Properties of substances can be changed when going from the bulk to the nanocrystalline state. Crystal structure of cubic titanium monoxide (TiO) is characterized by the presence of vacancies in both sublattices of Ti and O. So far, it is unknown whether the equilibrium concentration of vacancies in TiO changes upon transition from the bulk to nanoparticles. Here, the influence of the size factor on the equilibrium concentration of vacancies in TiO and its impact on the electronic properties of TiO are investigated in the framework of the density functional tight binding method (DFTB).

Bulk TiO crystal and cubic nanoparticles of stoichiometric composition were chosen as the models. Initial compositions of prototypic nanoparticles corresponded to $\text{Ti}_{32}\text{O}_{32}$, $\text{Ti}_{108}\text{O}_{108}$ и $\text{Ti}_{256}\text{O}_{256}$. Vacancies were introduced into both sublattices randomly and in equimolar concentrations, ranging from 0 to 25%.

The optimized lattice constant a of the perfect crystal was equal to 448.3 pm. The value of a decreases with increase of vacancies' concentration. In contrast to the perfect crystal, all nanoparticles with and without vacancies, as well as the crystals with vacancies, are characterized by a dispersion of the interatomic bonds lengths after a full geometry optimization. Surface reconstruction and a significant contraction of the small size nanoparticles are observed. Ti atoms on surface are immersed to a greater depth than the O atoms on surface.

The magnitude of the density of states (DOS) at the Fermi level is critically affected by the presence of vacancies or surface. The Fermi level on the DOS for the perfect and defect-free crystal is located on the shoulder of the $\text{Ti}3d$ band, which is energetically unfavorable. The rise of surface in the case of nanoparticles leads to a significant reduction of DOS at the Fermi level. The latter is hosted in a DOS local minimum. Therefore, the role of surface in modulation of electronic properties of TiO coincides with the role of the vacancies introduced into the perfect crystal, as revealed in the past.

The formation energies of the crystal and nanoparticles, depending on the content of vacancies, are depicted in Figure 1. Crystal and nanoparticles exhibit a different behavior. Nanoparticle $\text{Ti}_{256}\text{O}_{256}$ with vacancies does not possess an increased stability like the crystal. Obviously, the surface relaxations at the nanoparticle play the same role as vacancies do in the crystal. Smaller nanoparticles have an energy minimum shifted with decrease in size toward the higher concentrations of vacancies. This can be probably explained due to the fact that, such nanoparticles have a significant part of surface atoms. Thus, the introduction of vacancies into the model is almost always accompanied by the surface atoms removal. In conclusion, the surface of TiO nanoparticles plays the same role in stabilization of TiO composition as structural vacancies in the crystal. Therefore, the bulk of TiO nanoparticles should have a smaller amount of vacancies, than the crystal.

The work was done with the financial support of the Russian Science Foundation (project № 14-23-00025).

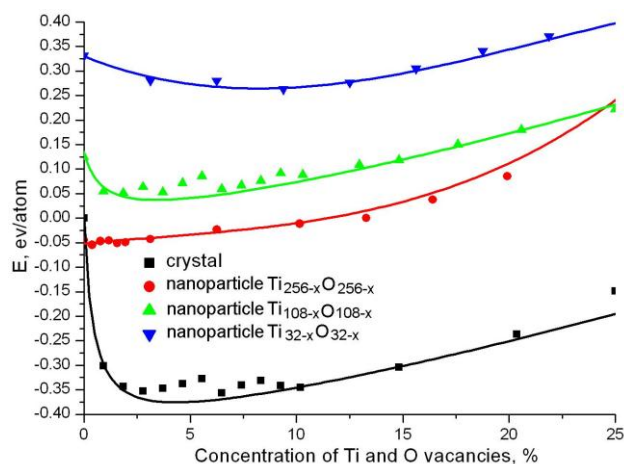


Figure 1. Dependence of the formation energies for TiO crystal and TiO nanoparticles (relative to defect-free crystal TiO) on the concentration of vacancies.

PRESSURE-DRIVEN PHASE TRANSITION MECHANISMS REVEALED BY QUANTUM CHEMISTRY: L-SERINE POLYMORPHS

Rychkov D.A.^{1,2}, Stare J.³, Boldyreva E.V.²

¹Novosibirsk State University, 630090 Novosibirsk, Russia

²Institute of Solid State Chemistry and Mechanochemistry SB RAS, 630128 Novosibirsk, Russia

³National Institute of Chemistry, SI-1000 Ljubljana, Slovenia

E-mail: rychkov.dennis@gmail.com

Polymorphism of organic compounds is widely and constantly discussed topics in chemistry. Formation of new three-dimensional periodic structure of the same compound, which co-exists with thermodynamically stable form, is well-known but still amazing phenomenon. Even more interesting is to obtain new polymorphs at different P-T conditions. Nevertheless, the questions about thermodynamic stability of different polymorphs, the reasons for phase transition and about exact mechanism – are still opened for the most organic systems.

L-serine polymorphism under pressure was studied experimentally in a number of works, showing two reversible phase transitions at pressures 5 GPa and 8 GPa [1–5]. Moreover, different opinions on reasons for phase transition at molecular level were suggested [3, 5]. As one can understand, standard DSC techniques could not be applied at such pressures. In this work we applied state-of-the-art DFT techniques to unveil the question of phase transitions in L-serine system under pressure. Combined solid state and gas phase calculations help to explain and correlate enthalpies of different polymorphs with certain molecular behavior in their crystal structures.

The study has shown that at a macroscopic level (Fig.1) phase transitions are led by decrease in the volume of the crystal unit cell (contributing to the enthalpy change, but not the internal crystal energy). At a microscopic level (Fig.2) we suggest that hydrogen bond “overstrain” leads to a jump-wise phase transition with substantial experimental hysteresis, while no such overstrain was found for the “normal type” phase transition. The predicted pressures for the phase transitions deduced by the minimum enthalpy criterion are in a very good agreement with the observed ones.

By delivering unambiguous explanations not provided by previous studies and probably not accessible to experiment, this work demonstrates the predictive and explanatory power of quantum chemistry in conjunction with thermodynamics, confirming its indispensable role in structural studies.

This work was supported by Russian Science Foundation (project 14-13- 00834).

- [1] E. N. Kolesnik, S. V. Goryainov and E. V. Boldyreva, *Dokl. Phys. Chem.*, 2005, **404**, 169–172.
- [2] S. A. Moggach, D. R. Allan, C. A. Morrison, S. Parsons and L. Sawyer, *Acta Crystallogr. Sect. B Struct. Sci.*, 2005, **61**, 58–68.
- [3] E. V. Boldyreva, H. Sowa, Y. V. Seryotkin, T. N. Drebuschak, H. Ahsbahs, V. Chernyshev and V. Dmitriev, *Chem. Phys. Lett.*, 2006, **429**, 474–478.
- [4] T. N. Drebuschak, H. Sowa, Y. V. Seryotkin, E. V. Boldyreva and H. Ahsbahs, *Acta Crystallogr. Sect. E Struct. Reports Online*, 2006, **62**, o4052–o4054.
- [5] P. A. Wood, D. Francis, W. G. Marshall, S. A. Moggach, S. Parsons, E. Pidcock and A. L. Rohl, *CrystEngComm*, 2008, **10**, 1154.

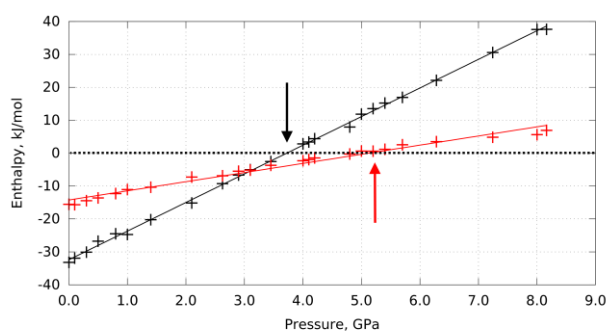


Figure 1. Calculated enthalpy difference of Form I and II (black) and Form II and III (red) versus pressure.

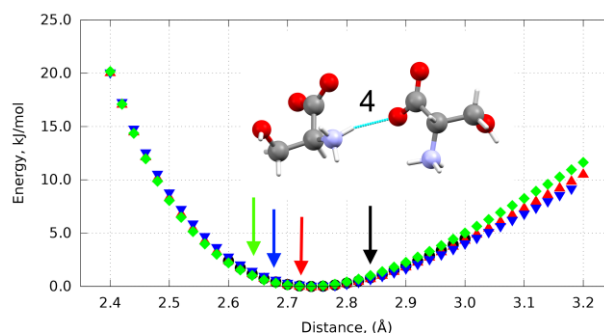


Figure 2. Energy wells of pair-wise intermolecular interactions along H-bond #4 (a) at different pressures

**STUDY OF ORTHOTANTHALATES OF YTTRIUM AND GADOLINIUM. HEAT CAPACITY AND THERMAL STABILITY.**

Ryumin M.A.¹, Sazonov E.G.², Guskov V.N.¹, Nikiforova G.E.¹, Khoroshilov A.V.¹, Golushina L.N.¹, Gavrichev K.S.¹

¹Kurnakov Institute of General and Inorganic Chemistry of the Russian Academy of Sciences, 119991 Moscow, Russia

²LLC Technological systems for Protective Coatings, 142172 Shcherbinka, Moscow region, Russia

E-mail: Ryumin@igic.ras.ru

Orthotantalates of rare earth elements, $RETaO_4$, a double oxides melting congruently above than 2300 K, are of interest for various applications, both as an individual compound and as a component of high-temperature functional materials [1]. The chemical and biological inertness of RE orthotantalates makes it a potential diagnostic of X-ray contrast medium [2].

The purpose of this work was to measure experimentally the isobaric heat capacity of yttrium and gadolinium orthotantalate in the temperature range from 9 to 340 K using adiabatic calorimetry and to study the thermal stability of different structural modifications up to the temperature of 1673 K.

Orthotantalates of RE were synthesized by method of the inverse sedimentation of their components ($RECl_3$, $REBr_3$, $TaCl_5$) in aqua-alcohol solution by the addition of ammonia. The percentages of tantalum and RE in the solutions were determined gravimetrically. The dry precipitate ($T = 378$ K, $t = 72$ h) was thoroughly ground and sequentially annealed at temperatures of 673, 1073, and 1473 K for $YTaO_4$ and 673, 873, 1073, 1273, 1473 и 1673 K for $GdTaO_4$ for 4 h. After each anneal, the material was characterized by X-ray diffraction. After final crystallization $RETaO_4$ had a monoclinic crystal structure: M'-fergusonite type (P2/a) - $YTaO_4$ and M-fergusonite type (I2/a) - $GdTaO_4$.

M' - $YTaO_4$ was formed at 1073 K and stable up to 1473 K. M' - $GdTaO_4$ was formed at 1073 K but at temperature at 1273 K the phase transition into M- $GdTaO_4$ proceeds. Single phase of M- $GdTaO_4$ is formed at 1673 K.

Heat capacity at low temperatures was measured in a BKT-3 automatic adiabatic calorimeter using liquid helium and nitrogen as cryogenic liquids. The high-temperature heat capacity was measured in platinum crucibles by the differential scanning calorimetry in NETZSCH STA 449 F1 Jupiter.

The temperature dependence of a heat capacity of these orthotantalates hasn't any pronounced anomalies. In the temperature range of 0–9 K, the heat capacity values were obtained using the Debye model under the assumption that the function $C_p/T = f(T^2)$ is linear and can be represented by the equation $C_p/T = 0.00025T^2$.

The high-temperature heat capacity of M - $GdTaO_4$ in the area 323-1323 K is well described by Maier-Kelly's equation: C_p (J/(mol·K)) = 125.2954 + 0.014366T - 1236596T⁻². The recommended heat capacity values and the thermodynamic functions calculated from spline coefficients are presented in table 1.

Table 1. Thermodynamic functions of orthotantalates

Compound	$C_p^\circ(298.15\text{ K})$ (J/(mol·K))	$S^\circ(298\text{ K})$ (J/(mol·K))	$H^\circ(298.15\text{ K})-H^\circ(0\text{ K})$ (kJ/mol)	$\Phi^\circ(298\text{ K})$ (J/(mol·K))
M' - $YTaO_4$	115.1 ± 0.4	115.6 ± 0.4	19.10 ± 0.04	51.5 ± 0.6
M- $GdTaO_4$	113.9 ± 0.5	121.7 ± 0.5	19.46 ± 0.08	56.4 ± 0.3

This research was performed using the equipment of the JRC PMR IGIC RAS. This study was financially supported by the Russian Science Foundation.

[1] Rozhdestvenskii F.A., Zuev M.G., and Fotiev A.A. Tantalaty trekhvalentnykh metallov (Trivalent Metal Tantalates), Moscow: Nauka. 1986.

[2] Molchanov V.V., Zuev M.G., Plyasova L.M., and Bogdanov S.V. Inorg. Mater., 2004, 40, (1), 73–79.

CALORIC PROPERTIES OF LIQUID BISMUTH

Savchenko I.V., Yatsuk O.S., Stankus S.V.

Kutateladze Institute of Thermophysics, Siberian Branch of the Russian Academy of Sciences, 630090 Novosibirsk, Russia
 E-mail: savchenko@itp.nsc.ru

Caloric properties of bismuth were investigated in a large number of works. A literature review on this subject until 1966 was given in the well-known and authoritative handbooks [1, 2]. Caloric properties of liquid bismuth recommended in [2] were based on the results of heat capacity measurements [3], which were carried out from the melting temperature to 800 K. In this work a sharp decrease of bismuth heat capacity (C_p) near melting point was observed, as well as the behavior of a well-studied tin. Temperature dependence of C_p [2] at higher temperatures was estimated similarly to tin $C_p(T)$. However, in 1975 the article [4] was published, where heat capacity of liquid bismuth was measured up to 950 K, and it was shown that above 800 K the heat capacity started to grow and this increasing is not completed at maximum temperature of experiments (Fig. 1). The aim of this work was to obtain new accurate experimental data on the caloric properties of liquid bismuth over a wide temperature range. Experiments were performed using isothermal drop calorimeter. Its installation and measurement procedure are detail described in [5]. The error of enthalpy measurement was determined in experiments with reference substance ($\alpha\text{-Al}_2\text{O}_3$) and did not exceed 0.2%. Bismuth samples had a purity not less than 99.95 wt.%. As is evident from Fig. 1, the obtained experimental data are in good agreement with the results [4]. The temperature dependence of the heat capacity has double extremum in the temperature range of 750 - 1000 K.

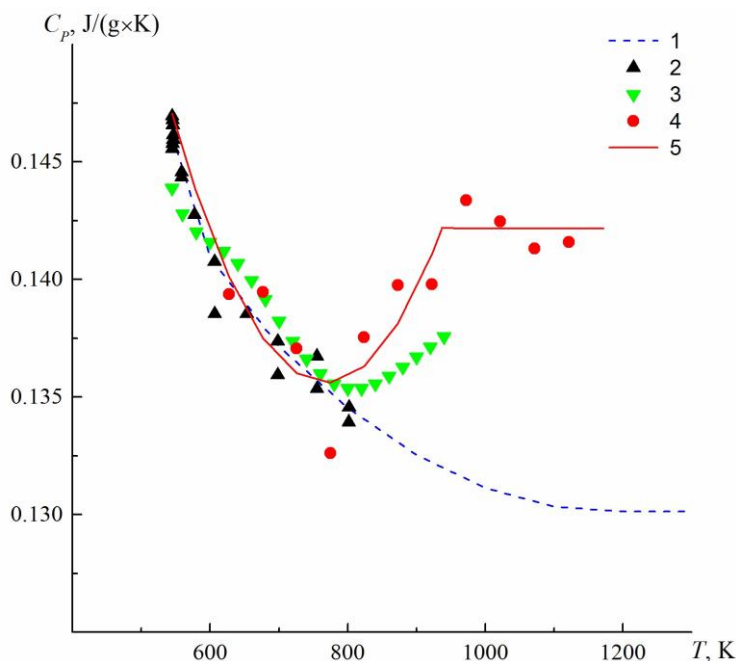


Figure 1. Heat capacity of liquid bismuth. 1 – [2], 2 – [3], 3 – [4], 4 – our measurements, 5 – our recommendations.

The study was supported by the grant of the Russian Science Foundation (Project No. 16-19-10023).

- [1] Touloukian Y.S., Buyco E.H. Thermophysical Properties of Matter - The TPRC Data Series. Volume 4. Specific Heat - Metallic Elements and Alloys. 1971. – 832 p.
- [2] Hultgren R., Desai R.D., Hawkins D.T., et.al. Selected values of thermodynamic properties of elements. Ohio, Amer. Soc. Metals, 1973. – 636 p.
- [3] Bell, H., & Hultgren, R. (1970). Heat capacity of liquid bismuth. - Report Number: UCRL-19673
- [4] Gronvold F. Heat Capacity and Thermodynamic Properties of Bismuth in the Range 300 to 950 K. Fusion Characteristics. Acta Chemica Scandinavica A29, 1975, p. 945-955.
- [5] Stankus S.V., Savchenko I.V., Yatsuk O.S. High temperature drop calorimeter for studying of substances and materials in the solid and liquid states. Instruments and Experimental Techniques, № 3, 2017.

PHASE TRANSFORMATIONS OF PROTONATED PEROVKITE TYPE LAYERED OXIDES $HLnTiO_4$ ($Ln = La, Nd$) DURING THERMOLYSIS PROCESS

Silyukov O.I., Abdulaeva L.D., Burovikhina A.A., Rodionov I.A.

Institute of Chemistry, Saint Petersburg State University, 198504, Saint Petersburg, Russia

E-mail: oleg.silyukov@spbu.ru

Layered perovskite-like oxides are solid crystalline substances formed by two-dimensional nanosized perovskite slabs interleaved with cations or cationic structural units. Until present time perovskite-like compounds are actively studied as materials with wide range of important physical and chemical properties such as super-conductivity, colossal magnetoresistance, ferroelectricity, catalytic and photocatalytic activity, thermochemical and electrochemical properties. In recent years there has been a constant interest in using the soft chemistry methods for the development of new layered perovskite-like compounds with specified physicochemical properties as well as design of these materials based on perovskite structure.

In the present work the phase transitions during the thermolysis process of protonated $HLnTiO_4$ ($Ln = La, Nd$) related to the Ruddlesden–Popper perovskite-type phases were studied in order to investigate the intermediate stages of metastable $Ln_2\Box Ti_2O_7$ oxides formation and their further evolution to stable compounds. Photocatalytic activity of initial, intermediate and final compounds was measured in order to demonstrate how the occurring topotactic phase transformations affect the physic-chemical properties of compounds under investigation.

$HLnTiO_4$ compounds were found to form partially hydrated $Ln_2Ti_2O_7 \cdot xH_2O$ during thermal dehydration as well as the defect oxides $Ln_2\Box Ti_2O_7$ as final products. Further heating of defect $Ln_2\Box Ti_2O_7$ substances leads to the pyrochlore-type oxides $Ln_2Ti_2O_7(p)$, with subsequent transformation to stable layered 110-type perovskites $Ln_2Ti_2O_7$ (Fig.1). The occurring structure transformations lead to an increase of photocatalytic activity in the order of $HLnTiO_4 < Ln_2Ti_2O_7 \cdot yH_2O < Ln_2\Box Ti_2O_7 < Ln_2Ti_2O_7(p) < Ln_2Ti_2O_7$ in the reaction of hydrogen evolution from aqueous isopropanol solution.

Structure change upon heating

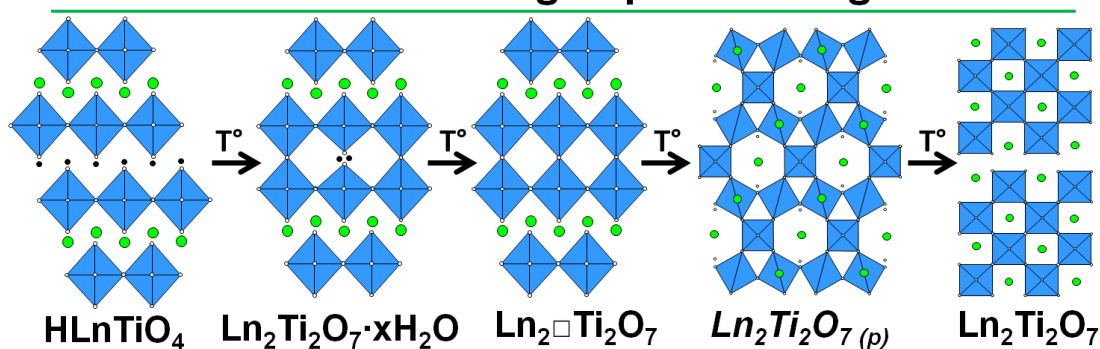


Figure 1. Structure change upon heating.

Acknowledgement This research was supported by Russian Foundation for Basic Research (grants № 16-33-00240 и № 16-33-60082).). Authors also are grateful to Saint Petersburg State University Research Park: Center of Thermal Analysis and Calorimetry, Research Centre for X-ray Diffraction Studies, Center for chemical analysis and materials research, Interdisciplinary Resource Center for Nanotechnology.

METHODS OF APPROXIMATION OF EXPERIMENTAL DATA ON THERMODYNAMIC PROPERTIES OF INDIVIDUAL SUBSTANCES

Sineva M.A.¹, Aristova N.M.¹, Belov G.V.^{1,2}, Morozov I.V.^{1,3}, Borisov P.G.^{1,3}

¹Joint Institute for High Temperatures of Russian Academy of Sciences, 125412 Moscow, Russia

²Department of Chemistry, Lomonosov Moscow State University, 119991 Moscow, Russia

³Moscow Institute of Electronics and Mathematics, Higher School of Economics, 123458 Moscow, Russia

E-mail: maria.a.sineva@gmail.com

The modern methods of theoretical research in power engineering, chemical industry, material design, resource usage, waste recycling, etc. often require thermodynamic modeling. It involves systematic experimental and theoretical studies of new classes of substances, continuous accumulation of the data with critical analysis of their reliability, followed by systematization in the form of reference books and databases. The latter type of data presentation makes it useful for scientists and engineers working in different fields of science and technology. The major element of thermodynamic model is the information on thermodynamic properties of individual substances [1]. In this work various methods for approximating dependences of the thermodynamic functions on temperature are overviewed [2-5]. A problem of creating and development of a unified data base is formulated.

A new computer code ‘EnthalpyFit’ with graphical user interface (see Fig. 1) is proposed for analyzing experimental results for the enthalpy increment and heat capacity. The enthalpy increment data can be fitted using the well-known Shomate method with variable polynomial degree. Input data accuracy can be specified for data sets or individual data points. The Shomate approximation results can be used at the next step where experimental heat capacity data is analyzed and fitted with an almost arbitrary polynomial. In this way the enthalpy increment data and the heat capacity data can be processed simultaneously.

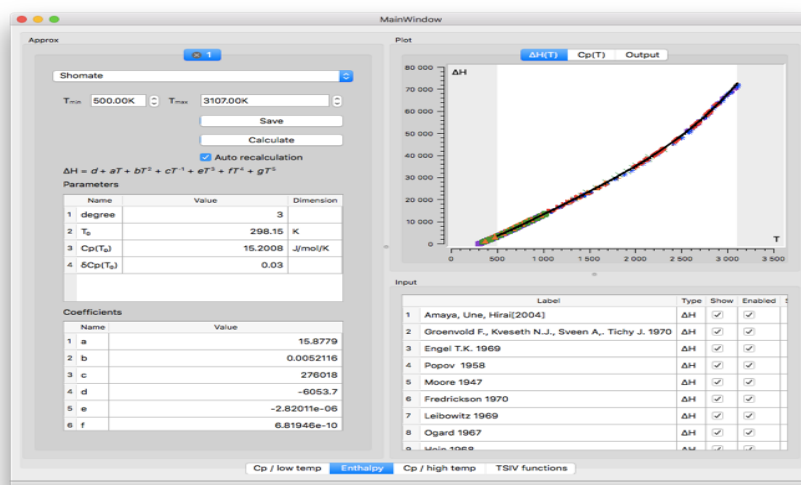


Figure 1. User interface of the ‘EnthalpyFit’ code

The proposed algorithm was used for revising the UO_2 thermodynamic functions published previously in [1] with respect to a new experimental data obtained since 1982.

[1] Gurvich L.V., Bergman G.A., Veyts I.V. Thermodynamic Properties of Individual Substances. Vol. 4, parts 1 and 2. Moscow, 1984.

[2] V.A. Bychinskii, A.A. Tupitsyn, A.V. Mukhetdinova, K.V. Chudnenko, S.V. Fomichev, V.A. Krenev, Method of Approximation of Dependence of Isobaric Heat Capacity on Temperature, Russian Journal of Inorganic Chemistry. — 58(12) (2013) 1511-1517.

[3] Bychinskii V.A., Tupitsyn A.A., Mukhetdinova A.V., Chudnenko K.V., Fomichev S.V., Krenev V.A., Russian Journal of Inorganic Chemistry. — 2013. — Vol. 58, № 12. — P. 1511-1517

[4] Coufal O., Computer Physics Communications. — 2013. — Vol. 184. — C. 194-200.

[5] I. Puidomènech, J.A. Rard, A.V. Plyasunov, I. Grenthe., OECD Nuclear Energy Agency. — 1999. — C. 4.

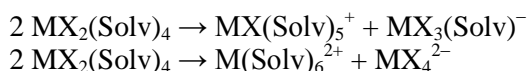
TRANSITION METAL SOLVATE COMPLEXES IN WATER/ORGANIC MEDIA: A DFT COMPUTATIONAL STUDY

Sizov V.V., Domnin A.V., Skripkin M.Yu.

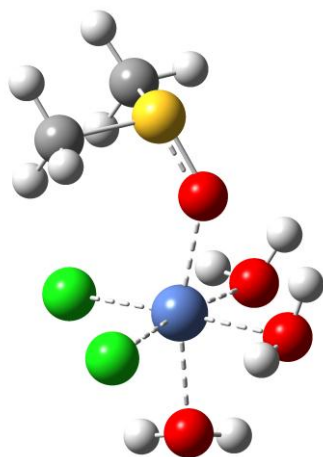
Institute of Chemistry, Saint Petersburg State University Saint Petersburg, Russia

E-mail: sizovvv@mail.ru

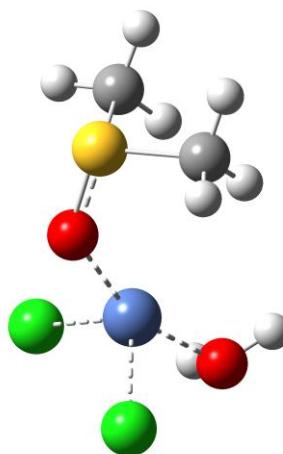
The goal of the present work is to study the stability of octahedral solvate complexes in relation to coordination disproportionation reactions, such as



where M is transition metal ion, X is the counterion (typically, a halide ion), and Solv denotes coordinated solvent molecules. These reactions can play an important role in the equilibrium between various solvated forms of transition metal ions and significantly influence on the formation of solid phases from concentrated solutions. Experimental studies have shown that the feasibility of the above reactions depends on the nature of the metal and counterions. The nature of the solvent is another important factor, since competitive solvation in mixed water/organic solvents can strongly affect the composition and relative stability of solvate complexes.



*Optimized structure of the
[NiCl₂(H₂O)₃(DMSO)] complex
with six-coordinated Ni(II)*



*Optimized structure of the
[NiCl₂(H₂O)(DMSO)] complex
with four-coordinated Ni(II)*

In this work DFT (Density Functional Theory) calculations were carried out to obtain structural and thermodynamic parameters for a series of transition metal complexes with M = Ni, Co, Cu, Cd; X=Cl⁻, Br⁻; Solv = H₂O, DMSO, DMF with four-, five- and six-coordinated metal atoms. Such complexes can be formed in water/organic mixed solvents of corresponding transition metal salts. DFT calculations were carried out using the B3LYP hybrid functional and triple-zeta-level basis set; effective core potential was used for cadmium atoms. Media effects were taken into account in the framework of polarizable continuum model. All structures were fully optimized without geometry constraints and verified by vibrational analysis. Thermodynamic data obtained for the optimized structures were used to evaluate the favorability of various coordination disproportionation reactions for the complexes considered in this study.

The calculations were performed using the facilities provided by the Computational Resource Center (Research Park, Saint Petersburg State University).



THERMODYNAMIC INVESTIGATION OF ORGANIC DERIVATIVES Sb(V) OF Ph_3SbX_2 TYPE

Smirnova N.N., Lyakaev D.V., Markin A.V.

Lobachevsky State University of Nizhni Novgorod 603950 Nizhni Novgorod, Russia

E-mail: smirnova@ichem.unn.ru

The synthesis and investigation of structures and physicochemical properties of organometallic compounds, particularly highly coordinated antimony compounds are actual and used with great importance. It is cause of structure's variety and catalytic effect of these compounds. There are antimony complexes with good cytotoxicity and antitumor activities. Some organoantimony (V) derivatives tend to be significant antimicrobial against human tumor cell lines and often higher than other earlier known agent. A huge number of organic antimony compounds have been applied to polymerization as catalyzers and reagents.

The present research reports a complex study of the heat capacity organic derivatives of pentavalent antimony Ph_3SbX_2 , where X are organic ligands. By methods of adiabatic vacuum calorimetry (AVC) and differential scanning calorimetry (DSC) the temperature dependence of the heat capacity compounds under study were determined in the wide temperature range.

Heat capacity of samples was measured over the range of 6–300 K in a BKT-3.0 fully automatic adiabatic vacuum calorimeter with liquid helium and nitrogen used as cooling agents. The measurements were carry out with an error not exceeding $\pm 2\%$ at $T = (5 \text{ to } 15) \text{ K}$, $\pm 0.5\%$ between 15 and 40 K and $\pm 0.2\%$ in the range from 40 to 300 K. The phase transition temperatures are measured within about $\pm 0.01 \text{ K}$ and the enthalpies of transformations with the error of $\pm 0.2\%$.

Thermal behavior of samples in the range from 300 K to decomposition temperatures was investigated with the differential scanning calorimeter DSC204F1 Germany, Netzsch Gerätebau. The determined values correspond to an error of $\pm 0.5 \text{ K}$ in temperature and $\pm 1\%$ in the enthalpy of transition.

The phase transitions were identified, and their thermodynamic characteristics were defined and analyzed with according to composition and structure. As a result of this study the interpretation of ligands influence was made. For some compounds from investigative rank the transition from glassy to over-cooled state was revealed.

The thermal stability of the compounds under study was determined by the method of thermogravimetric analysis. It was done using thermal microbalance TG209F1, Germany, Netzsch Gerätebau.

The complex of standard thermodynamic functions (heat capacity, enthalpy, entropy, and Gibbs energy) was calculated over the range from $T \rightarrow 0$ to the onset decomposition temperatures for the compounds. The energy of combustion, standard enthalpy of combustion, formation enthalpy, formation entropy, Gibbs energy of formation of substances in the crystalline state at $T = 298.15 \text{ K}$ were calculated.

Multifractal treatment of low-temperature heat capacity was made as a result the topological structure of the compound was established and the chain-layered structure topology of the compounds under study was defined. Debye characteristic temperatures were calculated and structure hardness of samples was evaluated.

As results of this study the dependences of thermodynamic properties vs composition were established. They allow us to predict the thermophysical properties for compounds of this class.



***IN SITU* X-RAY STUDY OF PHASE TRANSITIONS IN THIN LAYERS OF METAL PHTHALOCYANINES**

Sukhikh A.S.^{1,2}, Basova T.V.^{1,2}, Gromilov S.A.^{1,2}

¹Nikolaev Institute of Inorganic Chemistry, 630090 Novosibirsk, Russia

²Novosibirsk State University, 630090 Novosibirsk, Russia

E-mail: a_sukhikh@niic.nsc.ru

X-ray diffraction characterization of phase transitions in thin layers of transition metals phthalocyanines (TMF) is a major challenge for researchers. The difficulty of obtaining single crystals with quality high enough for x-ray structural analysis or single-phase polycrystalline product for powder diffraction leads to the fact that currently only a small number of the most stable TMF phases have been studied. Data on metastable phases are often of poor quality or non-existent.

Difficulty of *in situ* studies of phase transitions in TMF thin (less than 100 nm) polycrystalline layers (i.e. the form in which they are of greatest interest) is mainly due to the low intensity of diffraction reflections. The obtaining of diffraction pattern of acceptable quality even in grazing beam geometry requires a long acquisition time and / or use of high-power X-ray sources (rotating anode tube, synchrotron radiation). Another problem is associated with TMF having the tendency to form oriented layers on substrate surface. Uninformative diffraction patterns of these samples have usually only the orders of reflections from the selected crystallographic plane. In this paper, these problems are solved by implementing pseudo-“grazing beam” (2D Grazing Incidence X-ray Diffraction, 2D GIXD) geometry on the basis of serial diffractometer, equipped with a microfocus tube, two-dimensional CCD-detector and thermal attachment.

Additional diffraction spots (other than reflections from selected plane) can be observed on 2D GIXD patterns. In general, such pattern allows one to: evaluate the degree of orientation of the crystallites relative to the substrate surface (length of the reflex arc), measure interplanar distances (d) and measure the angles between the crystal faces (φ), all by using single frame with 60 s acquisition time. Combining the data about d and φ gives us the ability to correctly carry out indexing and determine the unit cell parameters. Such information allows one to reliably interpret the phase transformations occurring in TMF oriented thin layers, in our case when heating sample substrate.

In this paper we describe a series of phase transitions in oriented thin layers of substituted TMF (Co, Pd, Zn, V, etc.).

The work was supported by the Russian Science Foundation (Project № 15-13-10014).



THERMAL ANALYSIS AND CALORIMETRY FOR MATERIALS SCIENCE IN SAINT PETERSBURG STATE UNIVERSITY

Zvereva I.A., Tsvetov N.S.

Centre "Thermogravimetric and Calorimetric Research", Saint Petersburg State University, St. Petersburg, Russia
E-mail: irina.zvereva@spbu.ru

The presentation is devoted to results obtained by methods of thermal analysis and calorimetry in different areas of Materials Science also Chemistry, Physics, Biology, Geology in Saint Petersburg State University during last three years. Brief review will be done on the description of the opportunities for different methods of thermal analysis and calorimetry and a park of equipment of Centre "Thermogravimetric and Calorimetric Research".

Thermogravimetry and simultaneous thermal analysis (TG +DSC) coupled with mass-spectrometry or FTIR-spectroscopy for gas evolution (TG 209 F1 Libra Netzsch with TENSOR 27 Bruker and STA 449 F1 Jupiter Netzsch with QMS 403 CF Aeolos) were attractively used for the investigation of formation and thermal stability of a number of new functional materials, nanomaterials and composite materials (ceramics with magnetic and electric properties, synthetic zeolites for different application, catalysts, organic-inorganic composites, membranes). New complex methodology was proposed for the investigation of ion-exchange and intercalation which take place for layered structures in water medium and impact on properties of layered materials, for example on photocatalytic activity in reactions of water splitting with hydrogen producing or dyes degradation for water purification.

As supplementary method to prove thermal behaviour and to show changes in the macrostructure during heating the optical thermomicroscopy (Axio Scope A1 Carl Zeiss with thermostable Linkam TS1500) was implemented for different materials even for samples of oil shale.

Using the differential scanning calorimetry (DSC 204 F1 Phoenix Netzsch including device with μ -sensor of high precision, μ DSC 3 EVO SETARAM) new results on phase transitions were obtained for wide range of materials: solids and liquids, constructional materials, photovoltaics, ion liquids, pharmaceuticals, composites with minor content of functional components. Important information on photoinduced processes in polymers and composites could be obtained by investigation under UV-irradiation (DSC 204 F1 Phoenix Netzsch coupled with OmniCure S200).

Thermal expansion and thermal behavior in wide temperature range have been investigated for ceramics, polymers and solids including shape memory materials as TiNi alloy using TMA 402 F1 Hyperion Netzsch.

Calorimetry of mixing (C 80 SETARAM and TAM III Instruments) was used for obtained of data on excess molar enthalpies including binary and ternary mixture in liquid-liquid or liquid-solid systems with components of different nature.

Isothermal titration calorimetry (Nano ITC 2G TA Instruments) has ensured new data on interactions and thermodynamic properties of proteins, DNA and new complex compounds,

Some of data which will be presented have been published in leading international journals including Journal of Thermal Analysis and Calorimetry.

THERMOCHEMISTRY OF LiBC_2 CRYSTALS WITH $\text{B} = \text{In, Ga}$; $\text{C} = \text{S, Se, Te}$

Vasilyeva I.G.

 Nikolaev Institute of Inorganic Chemistry, Siberian Branch of the Russian Academy of Sciences, 630090 Novosibirsk, Russia
 E-mail: kamarz@niic.nsc.ru

The family of the Li-containing ternary LiBC_2 compounds is very attractive due to their unique non-linear optical properties. These applications demand to grow bulk homogeneous single crystals of a high optical quality with strictly stoichiometric composition. Traditionally, the Bridgman-Stockbarger technique is used for the crystal growing although this process has peculiarities associated with enhanced volatility of chalcogen and chemical activity of the Li-containing vapor and melt. In this case synthesis of initial charge and crystal growing met with difficulties which may be minimized if the basic thermodynamic and thermochemical data of a high degree of reliability are available for LiBC_2 . Such measurements for materials active in the gaseous and liquid states are unpopular and attempts to perform them are limited in number. We have an achievement in development of experimental approaches and techniques for measuring precisely vapor pressure and melting temperature using a high-speed thermal analysis operated at high, middle or low buffer-gas pressure (P_G) and being very attractive for the goals [1-2]. This thermal analysis is capable to measure precisely as melting point (T_m) suppressing kinetically evaporation of volatile component by high-pressure buffer gas and short heating as well as the vapor pressure under solid and chemical active liquid phases (P_V) by the boiling point (T_b) isobaric procedure without contamination from the Mo crucible material, Fig. 1. Today, the study of thermal behavior of solid and liquid states for the LiBC_2 materials have become challenging and with this technique there is a high chance to attain desired thermochemical data.

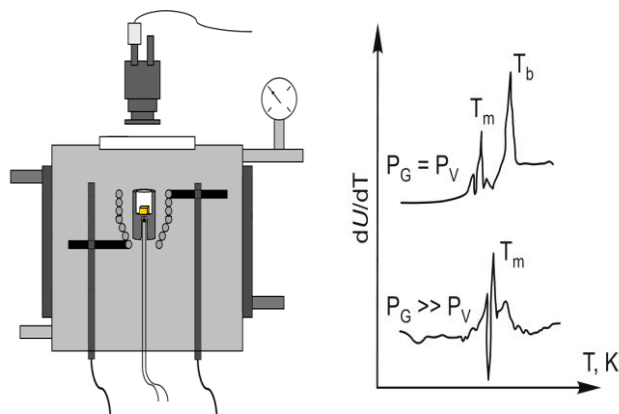


Fig.1. Apparatus recording radiation of heated sample as dU/dT - T function with the IR photodiode through optical microscope

Varied types of experiments were developed to suggest the most probable composition and structure of the overheated melts of LiBC_2 . First, the changes of the p - T functions measured near melting, at the fusion moment and for overheated melts gave information on proper transitions of solid and liquid phases LiBC_2 . Second, new and important details on origin of the transitions were added by studying kinetics of these processes by TGA-DTA and microscopic analysis of frozen melts. Third, the changes of chemical bonds at melting of LiBC_2 were considered based on the changes of those observed at melting individual components Li_2C and B_2C_3 of the compounds. Finally, the correlation was found between pre-crystallization phenomena and optical properties of the crystals LiBC_2 growing from the melt and the recommendation is given on the most optimal temperature - time regime of the process.

It is a pleasure to thank Dr. L. Isaenko and P. Krinitsin for crystal preparation.

[1] Ya. Gibner, I. Vasilyeva, J. Therm. Anal. 1998, 53, 151-160, patent SU 1806358 A3 1992.

[2] I. Vasilyeva, R. Nikolaev, J. Alloys Compd. 2008, 452, 94-98.



THERMODYNAMIC STUDY OF PHASE EQUILIBRIA AND SYNTHESIS OF INTERMEDIATE PHASES IN THE SYSTEMS $MSe_{2-\delta}$ – $MSe_{1.5}$ ($M = La-Nd, Y, Sm, Gd, Dy, Ho$)

Zelenina L.N.^{1,2}, Chusova T.P.¹, Vasilyeva I.G.¹

¹Nikolaev Institute of Inorganic Chemistry, Siberian Branch of the Russian Academy of Sciences, 630090 Novosibirsk, Russia

²Novosibirsk State University, 630090 Novosibirsk, Russia

E-mail: zelenina@niic.nsc.ru

Rare-earth polyselenides are promising for the creation of functional materials with effective optical, magnetic and thermoelectric properties. A characteristic feature of these compounds with MSe_x composition ($1.5 < x < 2.0$) is the ability of selenium atoms to create a low-dimensional structure in anion sublattice. This ability appears in a rich variety of superstructures whose period grows with decrease of x . The displacement of the selenium atoms in new positions of superstructures leads to charge density wave formation and to the emergence of electronic-structural transitions. For experimental investigation of their properties the high-quality crystals of rare-earth polyselenides are needed. These crystals are difficult to obtain without knowledge of the thermodynamic parameters (p_{Se} - T - x) which define the conditions of their growth.

The initial samples for investigation were the single crystals of higher La–Nd, Y, Sm, Gd, Dy, Ho polyselenides with the compositions MSe_2 ($M = La-Nd$), $SmSe_{1.9}$, $YSe_{1.8}$, $MSe_{1.875}$ ($M = Gd, Dy$) and $HoSe_{1.85}$. Selenium vapour pressure over samples studied has been measured by static method with quartz membrane-gauge manometers. Limiting errors in values of pressure, temperature and solid phase composition were 0.5 Torr, 1 K and 0.01 formula units, accordingly. The measurements have been realized in the wide intervals of temperature ($673 \leq T/K \leq 1400$), pressure ($1 \leq p/\text{Torr} \leq 760$) and composition ($1.5 \leq x/f. u. \leq 2.0$).

The aim of this work is to clarify the compositions and homogeneity regions of intermediate phases in the systems $MSe_{2-\delta}$ – $MSe_{1.5}$ ($M = La-Nd, Sm, Y, Gd, Dy, Ho$), to obtain a set of standard thermodynamic functions of these phases and to calculate the optimal growth conditions for intermediate phases by thermodynamic modeling.

As a result of this work the homogeneity regions of intermediate phases and their compositions are defined, the thermodynamic characteristics of dissociation processes of rare-earth polyselenides are obtained and their standard thermodynamic functions ($\Delta_f H^\circ_{298}$, S°_{298} , $\Delta_f G^\circ_{298}$) are calculated [1-3]. The composition of intermediate phases in the systems under study is described by the general formula $M_n Se_{2n-1}$ ($n = 3, 4, 5, 7, 8, 10, 20$), the majority of these compositions have been found for the first time in our research.

Based on these results the thermodynamic modeling of MSe_x crystal growth conditions by transport reactions with iodine has been performed. The calculation of equilibrium is based on the minimization of the total Gibbs energy of the system under study. As a result of the calculation the temperature intervals of intermediate phases existence without impurity of other condensed phases are obtained as a function of the atomic concentrations of iodine, selenium and rare-earth metal.

The calculated conditions of synthesis have been reproduced in the closed quartz reactors and the crystals of intermediate rare-earth polyselenides are grown.

[1] Zelenina L.N., Chusova T.P., Vasilyeva I.G. J. Therm. Anal. Calor., 2010, 101, 59-62.

[2] Zelenina L.N., Chusova T.P., Vasilyeva I.G. J. Chem. Thermodyn., 2013, 57, 101-107.

[3] Zelenina L.N., Chusova T.P., Vasilyeva I.G. J. Chem. Thermodyn., 2015, 90, 122-128.



Section 2.

Thermochemistry and databases

Poster presentations

LOW-TEMPERATURE THERMODYNAMIC PROPERTIES OF Pd(C₁₁H₁₉O₂)₂

Bespyatov M.A., Cherniaikin I.S., Zharkova G.I., Naumov V.N., Morozova N.B., Gelfond N.V.

Nikolaev Institute of Inorganic Chemistry, Siberian Branch of the Russian Academy of Sciences, 630090 Novosibirsk, Russia

E-mail: bespyatov@niic.nsc.ru

Palladium films are widely used in a variety of applications in electronics and catalysis. For example, they can be applied as metal contacts in nanoelectronics or as materials for energy storage. Method of deposition from the gas phase (or chemical vapor deposition – CVD) - is one of the widely used methods of manufacturing films and palladium membrane. Beta-diketonates of palladium are perspective complexes for their use as precursors in CVD-technology. Optimization of processes requires a detailed information on the various physicochemical properties of precursors, including the thermodynamic properties. The results of experimental research of Pd(C₁₁H₁₉O₂)₂ heat capacity in the temperature range from (6 to 306) K are presented in this work. The data obtained were used to calculate its thermodynamic functions (entropy, enthalpy, reduced Gibbs energy).

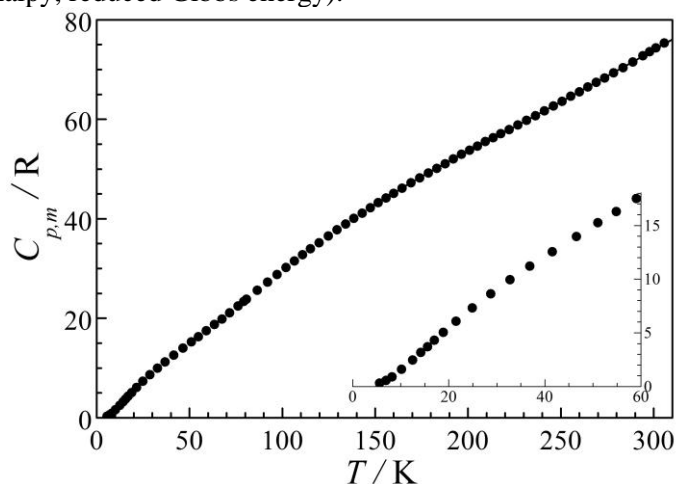


Figure 1. Experimental heat capacity for Pd(C₁₁H₁₉O₂)₂ in the range of 6 K to 306 K

Bis(2,2,6,6-tetramethylheptan-3,5-dionato)palladium(II) Pd(C₁₁H₁₉O₂)₂ has been produced by the procedure described in detail in [1]. After synthesis, the product was additionally purified by means of double sublimation in a vacuum gradient furnace at $p = 7$ Pa and $T = (463-473)$ K. Purity of the final compound is not lower than 99.8%. According to the X-ray phase analysis, the compound is single-phase; the structure of the obtained crystals corresponds to the Pd(C₁₁H₁₉O₂)₂ structure determined in the paper [2]. The calculated X-ray density, according to the data of the paper [2], is 2.51 g/cm³. The sample of Pd(C₁₁H₁₉O₂)₂ at room temperature is orange crystalline powder with a typical crystallite size of ~0.2 mm. The melting temperature of the sample determined on a Kofler bench is 496 K which agrees with the data presented in [1].

The heat capacity $C_{p,m}(T)$ of the sample Pd(C₁₁H₁₉O₂)₂ was measured in the range (6 to 306) K by the adiabatic method on the installation described in reference [3]. A sample of 4.281 g was loaded into the calorimetric ampoule. The molar mass used in the calculation of the molar heat capacity was determined from the formula Pd(C₁₁H₁₉O₂)₂ as 472.96 g·mol⁻¹. The analysis of the functional dependence of the heat capacity has not revealed any thermal anomaly in its behavior. The smoothed $C_{p,m}(T)$ dependence over the temperature range 6–306 K was used to calculate the thermodynamic functions, including entropy $\Delta_0^T S_m^\circ$, enthalpy $\Delta_0^T H_m^\circ$, and reduced Gibbs energy $\Phi_m^\circ(T)$. The value of the absolute entropy was used to calculate the entropy of formation of Pd(C₁₁H₁₉O₂)₂ at $T=298.15$ K.

[1] Zharkova, G.I.; Igumenov, I.K.; Tkachev, S.V.; Zemskov, S.V. *Koord. Khim.*, 1988, 14, 67–74.

[2] Baker, G.J.; Raynor, J.B.; Smits, J.M.M.; Beurskens, P.T.; Vergoossen, H.; Keijzers, C.P. *J.Chem.Soc., Dalton Trans.*, 1986, 2655-2662.

[3] Naumov, V.N.; Nogteva, V.V. *Instrum. Exp. Tech.*, 1985, 28, 1194-1199.

LOW-TEMPERATURE HEAT CAPACITY OF HOLMIUM SELENIDE (2:3)

Bespyatov M.A., Musikhin A.E., Naumov V.N., Zelenina L.N., Nikolaev R.E., Naumov N.G.
 Nikolaev Institute of Inorganic Chemistry, Siberian Branch of the Russian Academy of Sciences, 630090 Novosibirsk, Russia
 E-mail: bespyatov@niic.nsc.ru

Chalcogenides of rare-earth metals are promising materials for practical applications in thermoelectric energy converters, in laser technology, in precision metallurgy and in other fields of engineering. At the same time, many properties of these compounds, including thermodynamic ones, have not been studied sufficiently. In this work presented the results of an experimental study of the heat capacity of Ho_2Se_3 at low temperatures.

Holmium selenide (2:3) was obtained by a direct reaction of holmium metal (99.9%) with elemental selenium (5N) in sealed quartz ampoules. The synthesis was carried out at 1200 K and then the sample was homogenized at 1050 K for one week. Sample single-phase was confirmed by the X-ray powder diffraction method. Ho_2Se_3 crystallizes in an orthorhombic Sc_2S_3 -type structure. The octahedral symmetry for the Ho^{3+} showed only an insignificant distortion and the crystal field was taken as cubic [1].

The heat capacity $C_{p,m}(T)$ of Ho_2Se_3 was measured in an adiabatic vacuum calorimeter [2] in the range 4.75–302.60 K (Fig. 1). The sample of Ho_2Se_3 of 5.1255 g (in a vacuum) was loaded into the calorimetric ampoule. The molar mass used in the calculation of the molar heat capacity was determined from the formula Ho_2Se_3 as $566.74 \text{ g}\cdot\text{mol}^{-1}$.

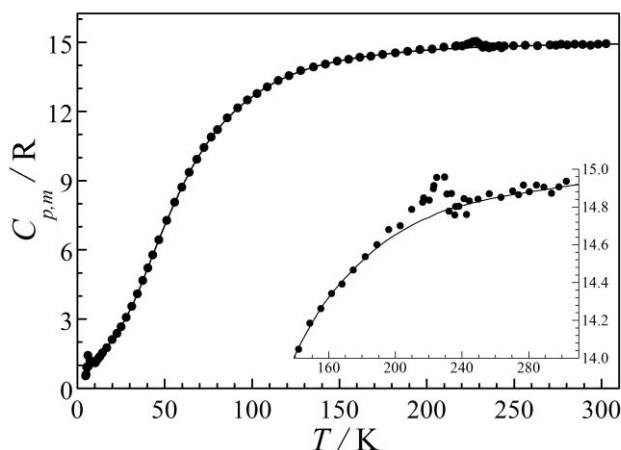


Figure 1. Experimental heat capacity for Ho_2Se_3 in the range of 4.75–302.60 K.

In the experimental heat capacity observed two anomalies which points to the phase transitions of the complex. The heat capacity has a maximum at $T_N \approx 6 \text{ K}$ associated with the antiferromagnetic ordering in the system at the Neel temperature T_N [3]. The nature of the second anomaly at $T_c \approx 228 \text{ K}$ is not known. The contributions of anomalous component ΔS_{tr} into entropy are $(2.2 \pm 0.2) \text{ J}\cdot\text{mol}^{-1}\cdot\text{K}^{-1}$ and $(0.15 \pm 0.03) \text{ J}\cdot\text{mol}^{-1}\cdot\text{K}^{-1}$. In addition, the heat capacity of Ho_2Se_3 showed a continuing excess heat capacity consistent with a Schottky anomaly from energy levels lying roughly 2 to 200 cm^{-1} above the ground state. The ground term of the Ho^{3+} ion, $^5\text{I}_8$, splits in a regular crystal field into seven sublevels: one singlet, two doublets, and four triplets [3].

The smoothed $C_{p,m}(T)$ dependence over the temperature range 5–303 K was used to calculate the thermodynamic functions, including entropy $\Delta_0^T S_m^\circ$, enthalpy $\Delta_0^T H_m^\circ$, and reduced Gibbs energy $\Phi_m^\circ(T)$.

[1] Pawlak, L.; Duczmal, M.; Pokrzywnicki, S. Crystalline Electric Field Effects in f-Electron Magnetism, 1982, 473-478.

[2] Naumov, V.N.; Nogteva, V.V. Instrum. Exp. Tech., 1985, 28, 1194-1199.

[3] Lashkarev, G.V.; Fedorchenko, V.P.; Obolonchik, V.A.; Skripka, I.P. Powder Metall. Met. Ceram., 1976, 15, 394-396.

CALCULATION OF CO₂ THERMODYNAMIC PROPERTIES USING THE NEW COMBINED EQUATION OF STATE WITH A SMALL NUMBER OF ADJUSTABLE CONSTANTS

Kaplun A.B.¹, Meshalkin A.B.¹, Bezverkhy P.P.², Martynets V.G.²

¹Kutateladze Institute of Thermophysics, Siberian Branch of the Russian Academy of Sciences, 630090 Novosibirsk, Russia

²Nikolaev Institute of Inorganic Chemistry, Siberian Branch of the Russian Academy of Sciences, 630090 Novosibirsk, Russia

E-mail: ppb@niic.nsc.ru

Earlier to describe *PVT*- surface we used a regular equation of state (EOS) with a small number of adjustable constants, the range of their applicability is limited by the liquid density at the triple point. In this regard, we have developed a new EOS which has no a density (pressure) limit, and may be used to describe the thermodynamic properties of normal substances up to the liquid density on the melting curve (i.e., at pressures p up to (200 ... 400) MPa)). This equation has the form:

$$\frac{p_{reg}}{p_c} = \frac{t\omega}{z_c} \left\{ 1 + [A_4 ex_2 + A_6 (ex_4 - 3/t)] \omega \left(1 - \frac{\omega}{(1-z_c\omega)^2} \right) \varphi(\omega) + A_2 \omega/t + A_3 ex_1 \omega + A_4 ex_3 \omega + A_5 ex_6 \omega^2 \left(2 - \frac{\omega}{(1-z_c\omega)^2} \right) \varphi(\omega) \right. \\ \left. - A_7 \frac{z_c \omega}{1-z_c \omega} + A_8 \omega \frac{1+z_c \omega}{(1-z_c \omega)^3} + A_9 \omega^2 \frac{2+z_c \omega}{(1-z_c \omega)^4} + A_{10} \omega^3 \frac{3+z_c \omega}{(1-z_c \omega)^5} - 3A_{11} \omega^3 \exp(-\omega^3) \right\}$$

where $t = T/T_c$, $ex_2 = e^{1/t} - 1 - 1/t$; $ex_1 = e^{-1/t} - 1$; $ex_3 = e^{-3/t} - 1$; $ex_4 = e^{3/t} - 1$; $ex_6 = e^{6/t} - 6/t$;

$\varphi(\omega) = \exp(-\omega/(1-z_c\omega))$, T_c is the critical temperature, $\omega = \rho/\rho_c$ is the reduced density. The equation (1) contains 11 fitting empirical coefficients. Three of them (A_3, A_5, A_{11}) are calculated from the values of the remaining adjustable A_n so that the three conditions are satisfied at a critical point. Here calculation results are presented as an example for deviations of density from experimental values using a EOS (1) in a p, T range up to 200 MPa and 1100 K and at densities between 0 and density on the crystallization line.

The values of the A_n in eq. (1) were obtained by the least squares method with minimal deviation of p_{calc} from the original table data p_{tab} [1] received from EOS containing 164 fitting coefficients. Discrepancies for ρ_{calc} (EOS (1)) along isotherms (fig. 1) do not exceed the error of table and experimental data in the field of regular behavior of CO₂. Calculations showed that the obtained values of the caloric properties of CO₂ and the speed of sound in the regular region are consistent with standard tabular data [1] mostly within experimental error. But the use of only a regular EOS (1) does not allow correctly the calculation of the heat capacity and the speed of sound in the critical region.

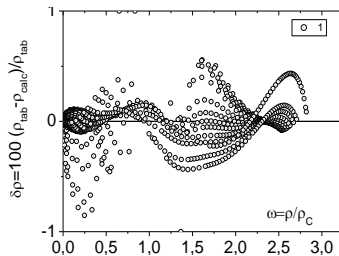


Figure 1. Calculated ρ - values of CO₂ in comparison with the tabulated data [1]. $1 -$

For the calculation of the thermodynamic properties near the critical point of CO₂ we proposed a combined EOS (CES) $p/p_c = (1-Y) p_{reg}/p_c + Y p_{scal}/p_c$, involving regular part p_{reg} (1), asymmetric scaling part p_{scal} [2] and a new crossover function $Y = \omega[(1 - \omega/\omega_c)^2/(1 - 1/\omega_c)^2] \operatorname{erfc}(\sqrt{\lambda} \cdot |\tau|) \exp(-\mu(\Delta\rho)^2)$, here $\tau = (T-T_c)/T_c$, $\omega_c = \rho_{tr}/\rho_c$, $\Delta\rho = \omega - 1$, ρ_{tr} is the liquid density

at triple point, λ и μ are adjustable constants, $\operatorname{erfc}(\sqrt{\lambda} \cdot |\tau|)$ is the Laplace error function. The scaled (singular) part of CES p_{scal} contains the values of p_c, ρ_c, T_c and adjustable constant $q, k, M-a_p, C_1, b$, where q is a fitting binodal coefficient in the formula $\Delta\rho = \pm (-\tau/q)^\beta + B_1(-\tau)^{1-\alpha}$, $B_1 = -bk \cdot 2.531412\gamma\beta/q^{2\beta}$, k is the coefficient in the asymptotic relation of compressibility $p_c K_T = \tau^{-\gamma}/k$ along critical isochore, b, a_p are asymmetry constants, γ, β, α are critical exponents taken for the 3-dimensional Ising model [2]. In total, the CES is contains 18 adjustable constants. The new CES applied to the calculation of thermodynamic properties of CO₂ in the ranges $0 < \rho/\rho_c < 2$, $217 \text{ K} < T < 430 \text{ K}$, $0 < p \leq 50 \text{ MPa}$ including the critical region. The $P\rho T$ data description was reached with the mean square error of $\pm 0.63\%$. We calculated the heat capacity C_v, C_p , and the speed of sound on isochores, isotherms in the critical region and along binodal within error of 5%. It was made a comparison with the known reference data [1].

This work was supported by RFBR grant 15-08-01072-a and by RFBR grant 15-08-03443-a.

[1] Span, R., Wagner, W. J. Phys. Chem. Ref. Data, 1996, 25, 1509-1596.

[2] Bezverkhy, P.P., Martynets, V.G. High Temp. – High Press., 2016, 45, №2, 145-154



THERMAL PROPERTIES of IRIIDIUM(I) CYCLOPENTADIENYL COMPLEXES WITH CYCLOOCTADIENE

Bonegardt D.V.^{1,2}, Ilyin I.Y.¹, S.V. Trubin¹, Morozova N.B.¹

¹Nikolaev Institute of Inorganic Chemistry, Siberian Branch of the Russian Academy of Sciences, 630090 Novosibirsk, Russia

²Novosibirsk State University, 630090, Pirogova str., 2, Russia

E-mail: bonegardt@yandex.ru

Iridium based film materials are widely used in various fields of science and technology, as barrier layers of the ferroelectric memory (FRAM) electrodes; high capacity coatings of pacemaker electrodes; electrical stimulators of eye retina etc. Iridium is a refractory metal ($T_{\text{melt.}} = 2466 \text{ }^\circ\text{C}$) with high oxidation resistance which makes it an excellent protective material. One of the most promising technique to produce iridium based coatings is Metal-Organic Chemical Vapor Deposition (MOCVD). This method allows one to make uniform coatings with required characteristics on complex shape substrates at relatively low temperatures. An important problem is to find new MOCVD precursors, possessing a certain set of properties: high volatility, chemical stability, low decomposition temperature. It is also necessary to expand the range of precursors used to satisfy any requirements of the experiments: different aggregate states, various temperatures of the gas phase transition and decomposition, etc.

Thermodynamic data obtained for synthesized compounds, allow one to predict their behavior in the MOCVD process, to choose the temperature modes of deposition processes, as well as to prognosticate the behavior of previously unknown precursor.

In this work, we synthesized and investigated cyclopentadienyl complexes of iridium(I) with cyclooctadiene [IrCodCp^{Et}] (**1**) and [IrCodCp*] (**2**) (Cod - cyclooctadiene, Cp^{Et} - ethylcyclopentadiene, Cp* -pentamethylcyclopentadiene) by a set of methods (IR, CHN, NMR). The crystal structure was solved for complex **2** by single-crystal XRD method. Thermal properties of the complexes in condensed phase were investigated by thermogravimetry and differential thermal analysis.

For each compound the P/T dependencies of the saturated vapor pressure were measured by Knudsen method (Figure 1) and the thermodynamic parameters of vaporization processes were calculated (Table 1). As we expected, complex **2** is less volatile than complex **1** ($P = 0.005 \text{ Torr}$: $T = 353 \text{ K}$ (**2**) > $T 331 \text{ K}$ (**1**)).

In addition, iridium coatings were prepared and analyzed using synthesized compounds as MOCVD precursors.

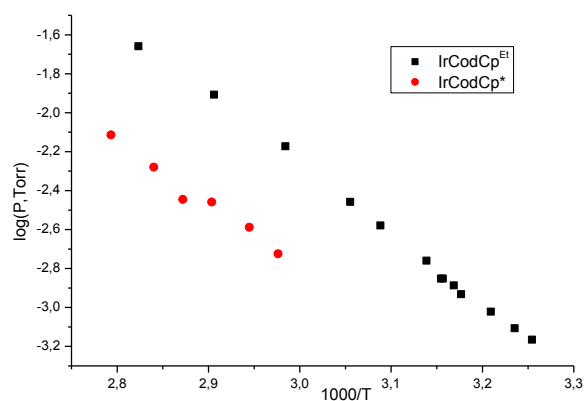


Figure 1. P/T dependencies of the saturated vapor pressure for iridium complexes

Table 1. Thermal behavior of the iridium complexes.

Compound	Process	$\lg(P, \text{Torr}) = -A/(T, \text{K}) + B$		ΔH_T , kJ/mol	$\Delta S^\circ_{T^*}$, J/mol·K	Δt , $^\circ\text{C}$
		A	B			
[IrCodCp ^{Et}] (1)	Evap.	3617	8.6	69.2±0.9	109.1±2.9	32-81
[IrCodCp*] (2)	Sub.	3177	6.7	60.8±4.8	73.8±13.8	63-85

The work was financially supported by RFBR and Fund "NIR", Project 17-33-80100 mol_ev_a.



PHASE FORMATION AND THERMAL PROPERTIES OF GLASS-FORMING Cu-Zr-Ti ALLOYS

Bykov V.A., Yagodin D.A., Kulikova T.V.

Institute of Metallurgy, Ural Branch of Russian Academy of Sciences, 620016 Amundsena 101, Ekaterinburg, Russia
E-mail: wildrobert@gmail.com

The Cu-Zr system has a unique glass-forming ability and is therefore the basis for creating bulk amorphous metal alloys. The binary equiatomic alloy $\text{Cu}_{50}\text{Zr}_{50}$ in addition to the formation of bulk amorphous demonstrates the effects of shape memory. In this regard, the study of the effect of titanium on the thermal properties of the alloy $\text{Cu}_{50}\text{Zr}_{50}$ and the characteristics of martensitic transformations are an urgent task. It was shown earlier [1] that amorphous samples can be obtained in the composition range of $\text{Cu}_{50}\text{Zr}_{50-x}\text{Ti}_x$ ($x = 0-8$ at. %), which determined the choice of these compositions.

In the present study we investigated the temperature dependence of the thermal diffusivity alloys $\text{Cu}_{50}\text{Zr}_{50-x}\text{Ti}_x$ ($x = 0 - 8$ at.%) by the laser flash method on Netzsch LFA 457 instrument (Germany) under vacuum with a residual pressure of 0.1 MPa in the temperature range of $T = 300-1100$ K. It should be noted that with increasing titanium content the thermal diffusivity linearly decreases in the temperature range from 500 to 1100 K. In the temperature range from 300 to 500 K, the nonlinear dependence of the concentration curves of thermal diffusivity is observed. This is due to the presence of a martensitic phase and its influence on the behavior of thermal diffusivity. According to X-ray phase analysis, the amount of martensitic CuZr phase decreases with increasing titanium content, but low thermal diffusivity values for all $\text{Cu}_{50}\text{Zr}_{50-x}\text{Ti}_x$ ($x = 0, 2, 4, 6, 8$ at.%) are retained. Extremely low values of the thermophysical properties of Cu-Zr and Cu-Zr-Ti alloys, which are uncharacteristic for metallic systems, are due to the features of the electronic structure and the presence of various crystal structure defects in these objects.

It was found that the addition of titanium in the binary alloy $\text{Cu}_{50}\text{Zr}_{50}$ significantly lowers the martensitic transformation of temperature region. For the ternary alloy $\text{Cu}_{50}\text{Zr}_{42}\text{Ti}_8$, the transition start temperature is 327 K and it is smaller by 230 K than for the equiatomic alloy.

Thus, the high-temperature studies of thermal diffusivity and structural transformations in $\text{Cu}_{50}\text{Zr}_{50}$ and $\text{Cu}_{50}\text{Zr}_{50-x}\text{Ti}_x$ ($x = 0-8$ at.%) were carried out under controlled heating conditions. The sequence and type of reactions during thermal exposure to Cu-Zr-Ti alloys were established in a wide temperature range.

This work was supported by the Russian Scientific Foundation (Grant No RNF14-13-00676) and RFBR (Grant No 16-02-00835)

[1] Inoue A., Zhang W., Zhang T., Kurosaka K., *Acta Mater.*, 2001, 49.



UNIVERSAL BEHAVIOR OF THE LOW-TEMPERATURE THERMODYNAMIC PROPERTIES OF DIPIVALOYLMETHANATES OF METALS

Cherniaikin I.S., Bespyatov M.A., Naumov V.N.

*Nikolaev Institute of Inorganic Chemistry, Siberian Branch of the Russian Academy of Sciences,
3, Acad. Lavrentiev Ave., Novosibirsk, 630090, Russia
E-mail: cherny@niic.nsc.ru*

Dipivaloylmethanates of metals as well as other beta-diketonates have a high vapor pressure at rather low temperatures. This allows them to be used as precursors in CVD and MOCVD processes. Many properties of these compounds, including thermodynamic properties, have not been sufficiently studied. The acquisition, study, and accumulation of experimental data on thermodynamic properties are significantly behind the practical requirements. In this case, the low-temperature thermodynamic properties are necessary for studying the nature of volatility, equilibrium conditions for crystal-gas systems, and other properties of compounds. The possibility of calculating the thermodynamic characteristics of complex objects through theoretical modeling is currently limited due to the lack of data on many force constants and reliable data on the parameters of the interatomic interaction potential. Therefore, it is necessary not only to determine the thermodynamic properties of specific substances experimentally, but also to search some empirical and semiempirical relationships for the estimation and approximately calculation of these properties.

In the present work, we analyzed all our experimental data on the low-temperature heat capacity for metal dipivaloylmethanates ($\text{Al}(\text{C}_{11}\text{H}_{19}\text{O}_2)_3$ [1], $\text{Fe}(\text{C}_{11}\text{H}_{19}\text{O}_2)_3$ [2], $\text{Co}(\text{C}_{11}\text{H}_{19}\text{O}_2)_3$ [3], $[\text{Eu}(\text{C}_{11}\text{H}_{19}\text{O}_2)_3]_2$ [4], $\text{Ru}(\text{C}_{11}\text{H}_{19}\text{O}_2)_3$ [5], $\text{Y}(\text{C}_{11}\text{H}_{19}\text{O}_2)_3$ [6], $\text{Zr}(\text{C}_{11}\text{H}_{19}\text{O}_2)_4$ [7], $\text{Pd}(\text{C}_{11}\text{H}_{19}\text{O}_2)_2$) in order to reveal the laws governing the behavior of thermodynamic properties and the relationship between such properties and the structural characteristics of these materials. For the dipivaloylmethanates of metals, a correlation was found between the heat capacity and the effective molecular volume. This correlation reflects the intensity of intermolecular interactions. It is shown, that for the beta-diketonates of metals with identical ligands in a wide temperature range, a universal heat capacity behavior is observed. The explanation of the discovered regularities in the series of isolines is connected with the identical organization structure in the short range ordering, which, in turn, determines the coincidence of the vibrational spectra of objects in the high frequency range. A simple equation was proposed that makes it possible to describe the behavior of the heat capacity in the compounds under study over a wide range of temperatures. The results obtained can be used to calculate the thermodynamic properties of objects that have not been studied, for which structural data are known.

- [1] Bespyatov, M.A.; Chernyaikin, I.S.; Naumov, V.N.; Stabnikov, P.A.; Gelfond, N.V. *Thermochimica Acta*, V. 596, 2014, P. 40–41.
- [2] Bespyatov, M.A.; Chernyaikin, I.S.; Naumov, V.N.; Stabnikov, P.A. // 9th seminar SO RAN – UrO RAN «Termodinamika i materialovedenie», Novosibirsk, 30 June – 4 July, 2014, P. 46.
- [3] Bespyatov, M.A.; Chernyaikin, I.S.; Naumov, V.N.; Dorovskikh, S.I.; Gelfond, N.V.; Morozova, N.B. XX International Conference on Chemical Thermodynamic in Russia (RCCT 2015), Nizhniy Novgorod, June 22–26, 2015, P. 88.
- [4] Chernyaikin, I.S.; Bespyatov, M.A.; Naumov, V.N.; Stabnikov, P.A.; Tsygankova, A.R.; Gelfond, N.V. XX International Conference on Chemical Thermodynamic in Russia (RCCT 2015), Nizhniy Novgorod, June 22–26, 2015, P. 97.
- [5] Kuzin, T.M.; Sysoev, S.V.; Bespyatov, M.A.; Naumov, V.N.; Gelfond, N.V.; Morozova, N.B. XX International Conference on Chemical Thermodynamic in Russia (RCCT 2015), Nizhniy Novgorod, June 22–26, 2015, P. 133
- [6] Bespyatov, M.A.; Chernyaikin, I.S.; Naumov, V.N.; Stabnikov, P.A.; Gelfond, N.V. 10th Vserossiyski simpozium s mezhdunarodnym uchastiem « Termodinamika i materialovedenie », Saint Petersburg, 07 – 11 September 2015, P. 63.
- [7] Bespyatov, M.A.; Cherniaikin, I.S.; Zherikova, K.V.; Naumov, V.N.; Igumenov, I.K.; Gelfond, N.V.; Morozova, N.B. *J. Chem. Thermodynamics* 110 (2017) 171–174.



HEAT CAPACITY AND THERMODYNAMIC PROPERTIES OF THE TITANATES $R_2Ti_2O_7$ (R = Sm, Er)

Chumilina L.G., Golubeva E.O.

Department of Physical and Inorganic Chemistry, Siberian Federal University, 79 Svobodny pr., 660041 Krasnoyarsk, Russia
E-mail: lubov89@mail.ru

The titanates $R_2Ti_2O_7$ (R = rare earth element) crystallize in pyrochlore structure. These compounds have interesting catalytic, magnetic and optical properties, therefore these materials are finding a widely application as electrolytes and electrodes in oxide solid fuel cells, oxygen partial-pressure sensors, catalysts and their carrying agents [1]. Many research papers are devoted to $R_2Ti_2O_7$, but their thermodynamic properties are underexplored. However, thermodynamic investigations are necessary for the development of a theory about the interaction of the components in the substances and to guide the selection of the optimal conditions for their synthesis and application. Thus, the aim of this work was a heat capacity of $R_2Ti_2O_7$ (R = Sm, Er) measurement and thermodynamic functions calculation.

The titanates $Sm_2Ti_2O_7$ and $Er_2Ti_2O_7$ were prepared by a solid-phase reaction from TiO_2 and R_2O_3 (R = Sm, Er). Stoichiometric mixtures of the reactants were ground in an agate mortar, pelletized and heated at 1773 K in air for 20 h with four intermediate grindings and pressings. Compositions of the samples were controlled by X-ray phase analysis (PANalytical X'Pert Pro MPD). The heat capacity was measured by differential scanning calorimetry (NETZSCH STA 449 C Jupiter).

Figure 1 shows the temperature dependence of the heat capacity of the rare earth titanates $R_2Ti_2O_7$ (R = Sm, Er). The experimental data $C_p = f(T)$ ($J mol^{-1}K^{-1}$) in the temperature range 343 – 1000 K were described by the classical equation of Mayer–Kelli

- for $Sm_2Ti_2O_7$:

$$C_p = (267.2 \pm 0.5) + (28.1 \pm 0.5) \cdot 10^{-3}T - (34.6 \pm 0.5) \cdot 10^5 T^{-2}; \quad (1)$$

- for $Er_2Ti_2O_7$:

$$C_p = (258.3 \pm 0.4) + (18.6 \pm 0.4) \cdot 10^{-3}T - (28.7 \pm 0.4) \cdot 10^5 T^{-2} \quad (2)$$

The equations (1), (2) allowed us to calculate the thermodynamic properties (the enthalpy change, the entropy change, and the reduced Gibbs energy) of these rare earth titanates.

[1] Lyashenkova, L. P., Belov, D. A., Shcherbakova, L. G. Inorganic Materials, 2008, Vol. 44, № 12, P. 1349–1353.

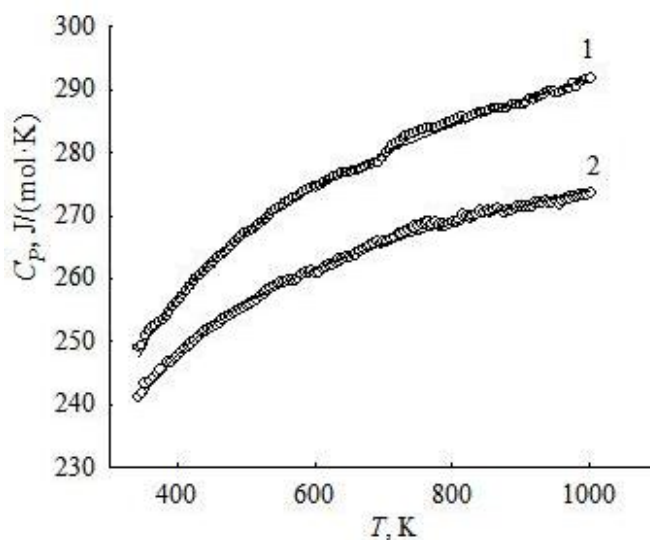


Figure 1: The temperature dependence of the heat capacity of the rare earth titanates:
1 - $Sm_2Ti_2O_7$; 2 - $Er_2Ti_2O_7$

THERMODYNAMIC STUDY OF Bi(III) POLYBROMIDES

Chusova T.P.¹, Zelenina L.N.^{1,2}, Gorokh I.D.², Adonin S.A.^{1,2}

¹Nikolaev Institute of Inorganic Chemistry, Siberian Branch of the Russian Academy of Sciences, 630090 Novosibirsk, Russia

²Novosibirsk State University, 630090 Novosibirsk, Russia

E-mail: chu@niic.nsc.ru

Bismuth halide complexes are of interest due to the variety of attractive physical properties of these compounds: luminescence, photochromism, semiconductor properties, etc. Recently, a family of polybromide complexes containing $\{\text{Br}\}^n$ units was introduced [1-2]. Among them, there are compounds containing pyridinium-type cations and anions of the same structural type (Fig. 1): $(\text{N-MePy})_3[\text{Bi}_2\text{Br}_9]\text{Br}_2$ and $(\text{PyH})_3[\text{Bi}_2\text{Br}_9]\text{Br}_2$ (**1** and **2**). Preliminary studies reveal [1] that these complexes demonstrate remarkable thermal stability. On this reason an additional study of their thermodynamic properties are needed.

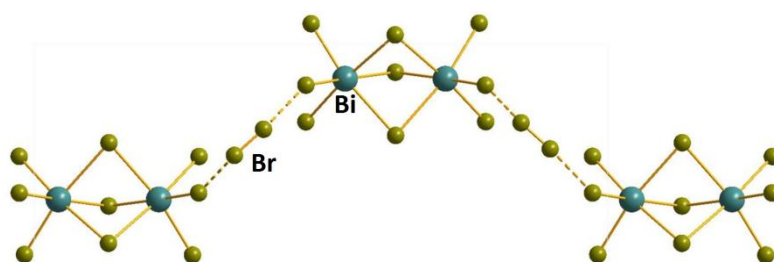


Figure 1. Structure of the anionic part in **1** and **2**.

Thermal behavior of these new complexes has been investigated by static method with glass (pyrex) membrane-gauge manometers [3]. The limiting uncertainties in measurement of pressure, temperature and solid phase composition on this set-up were 0.5 Torr, 0.5 K and 0.01 formula units, accordingly. The experiments have been carried out in the wide intervals of temperature ($313 \leq T/\text{K} \leq 533$) and pressure ($0.1 \leq p/\text{Torr} \leq 760$).

As a result of thermodynamic study of these complexes the fields of their thermal stability were established, the temperature dependences of bromine vapor pressure were obtained, the thermodynamic characteristics of evaporation processes ($\Delta_r H_T$, $\Delta_r S_T$) were calculated and the conclusions about the nature of interaction between bromine molecules and a matrix are made.

[1] Adonin S.A., Gorokh I.D., Abramov P.A., Plyusnin P.E., Sokolov M.N., Fedin V.P. Dalton Trans. 2016, 45, 3691.

[2] Adonin S.A., Perekalin D.S., Gorokh I.D., Samsonenko D.G., Sokolov M.N., Fedin V.P. RSC Adv. 2016, 6, 62011.

[3] Zelenina L.N., Chusova T.P., Sapchenko S.A., Ukraintseva E.A., Samsonenko D.G., Fedin V.P. J. Chem. Thermodyn., 2013, 67, 128-133.



THERMAL DECOMPOSITION AND VOLATILITY OF IONIC LIQUIDS INVESTIGATED BY EFFUSION-BASED TECHNIQUES AT DIFFERENT EFFUSION RATES: THE CASE OF BMImPF₆

Ciccioli A., Brunetti, B., Gigli G., Lapi A. Vecchio Cipriotti S.
Department of Chemistry, Sapienza – University of Rome, 00185 Rome, Italy
Department S.B.A.I., Sapienza – University of Rome, 00161 Rome, Italy
E-mail: andrea.ciccioli@uniroma1.it, stefano.vecchio@uniroma1.it

The exceptionally low volatility compared to common molecular organic liquids is probably the most distinctive properties of ionic liquids (ILs), making these substances attractive as potential substitutes of volatile solvents in many applications. As a consequence, the determination of vapor pressure of ILs was the subject of considerable efforts in recent years. One of the main problems with vapor pressure measurements of ILs is that, though thermally stable compared to molecular solvents, they can start to decompose at the same temperatures where their vapor pressure become measurable. This prevented vapor pressure of several ILs from being measured and might limit the accuracy of a number of data presently available in the literature. The use of mass spectrometry-based vaporization techniques [1] can be of great help in such cases, because information on the composition of the vapor can be obtained from mass spectra.

1-butyl-3-methylimidazolium hexafluorophosphate (BMImPF₆) is one of the most common aprotic ILs with an imidazolium cation. More than one decade ago, Kabo and co-workers [2] reported on Knudsen Effusion thermogravimetric experiments that they claimed to provide results unsuitable for deriving vapor pressure and evaporation enthalpy, due to the occurrence of thermal decomposition phenomena. No further vaporization study on this IL was carried out since then until few months ago, when Verevkin and co-workers [3] succeeded in measuring the vapor pressure of this compound by a quartz crystal microbalance (QCM) technique, down to very low temperatures where decomposition phenomena are supposed to be much reduced.

In this work, the vaporization of BMImPF₆ is reconsidered and new measurements are performed, using both the Knudsen Effusion Mass Loss and Knudsen Effusion Mass Spectrometry (KEMML and KEMS, respectively) techniques, with the specific aim to investigate the occurrence of decomposition and the factors affecting its competition with simple evaporation. To this end, effusion cells of different materials and with different orifice size (from 0.2 mm to 3 mm in diameter) were employed. Specific effusion fluxes measured by KEMML and mass spectra patterns resulted to depend significantly on the effusion orifice size. The analysis of mass spectra provided a clear evidence of the occurrence, besides the simple evaporation BMImPF₆(l) = BMImPF₆(g), of thermal decomposition processes giving 1-ethylimidazole as the most abundant decomposition product.

The KEMS technique enabled us to monitor the evaporation process and to measure the partial pressures of the gaseous ion pair BMImPF₆(g) as a function of temperature. By exploiting the thermal functions available in the literature both in the gaseous and in the liquid phase, an experimental value for the evaporation enthalpy of BMImPF₆ was derived by the third-law analysis of partial pressures, which resulted in good agreement with the second-law value recently obtained from QCM measurements [3] and with a few among the various molecular dynamics studies available in the literature.

[1] Brunetti, B.; Ciccioli, A.; Gigli, G.; Lapi, A.; Misceo, N.; Tanzi, L.; Vecchio Cipriotti, S. *Phys. Chem. Chem. Phys.*, 2014, 16, 15653-15661.

[2] Zaitsau, D.H.; Paulechka, Y.U.; Kabo, G.J. *J. Phys. Chem. A* 2006, 110, 11602-11604.

[3] Zaitsau D.H., Yermalayeu A.V., Emel'yanenko V.N., Butler S², Schubert T., Verevkin S.P., *J Phys Chem B.*, 2016, 120, 7949-7957.

[4] Volpe, V.; Brunetti, B.; Gigli, G.; Lapi, A.; Vecchio Cipriotti, S.; Ciccioli, A. *J. Phys. Chem. B*, submitted, 2017.



SEEKING POLYMORPHIC TRANSITIONS: THERMAL STUDY OF TOLAZAMIDE

Fedorov A.Yu.^{1,2}, Rychkov D.A.^{1,2}, Losev E.A.^{1,2}, Zakharov B.A.^{1,2}, Boldyreva E.V.¹

¹*Institute of Solid State Chemistry and Mechanochemistry SB RAS, 630128 Novosibirsk, Russia*

²*Novosibirsk State University, 630090 Novosibirsk, Russia*

E-mail: alexfed97@yandex.ru

Polymorphism of pharmacologically active compounds plays an important role in producing drugs. Various polymorphs having different bioavailability, it is necessary to take into account all possible ways of their transformations into each other. To understand the reasons of these transitions, all their thermodynamic and kinetic aspects should be followed.

Seeking stable polymorphs of pharmaceutical compounds with required properties is an actual task for science and industry. In recent years it has become more popular to use extreme conditions for obtaining new polymorphs. Pressure and temperature are powerful thermodynamic parameters and under operating by them it is possible to crystallize new structures.

However, whilst researchers today are coming close to predicting the stable structure of a given compound, they still cannot answer why some compounds are polymorphic, or which of the predicted forms can be realized experimentally, and how. Thermal study of polymorphs is very helpful in order to gain better insight into the various factors that control the formation of organic crystal structures and their transformations. Such information will ultimately allow a better prediction of solid-form landscapes and polymorphism.

Tolazamide, an oral blood glucose lowering drug of the sulfonylurea class, has two polymorphs with significantly different molecular packing. When crystallized from solution at ambient conditions, the nuclei of the two polymorphs, I and II, seem to be formed almost simultaneously, then the crystals of Form II grow much faster than those of Form I [1]. However, if the crystals of polymorph II are stored in solution, they are prone to dissolution and subsequent solvent-assisted transformation into Form I. Thus, in agreement with Ostwald's rule-of-stages, one could suppose from these observations that Form I must be the thermodynamically stable form under ambient conditions, and that the crystallization of Form II depends strongly on kinetic factors. These conclusions made it interesting to follow the crystals of the polymorphs on cooling and heating.

The aim of this study was to investigate the behavior of tolazamide polymorphs under non-ambient temperature conditions. Samples of both tolazamide forms were followed in a wide temperature range from 100 K to melting point of compound. All experiments were accompanied by single-crystal X-ray diffraction. Detail analysis of hydrogen bonds and stacking contacts were made at different temperature points.

This work was supported by Russian Science Foundation (project 14-13-00834)

[1] Boldyreva E.V. *et al.* Chemistry - A European Journal, 2015, 21 (43), 15395-15404.

HIGH TEMPERATURE HEAT CAPACITY OF $\text{LaLnZr}_2\text{O}_7$ SOLID SOLUTIONS

Gagarin P.G., Khoroshilov A.V., Guskov V.N. Gavrichev K.S.

Kurnakov Institute of General and Inorganic Chemistry of the Russian Academy of Sciences 31 Leninsky prospect, Moscow 119991, Russia

E-mail: Gagarin@igic.ras.ru

Zirconates of lanthanoids, $\text{Ln}_2\text{Zr}_2\text{O}_7$, intensively studied because of a set of useful physical properties, along with the absence of phase transitions in a wide temperature range and can be used as the core components for high-temperature materials [1]. Relatively low thermal conductivity of these zirconates makes them promising as thermal barrier coatings (TBC) [2]. Moreover, zirconates are used as a solid electrolytes for solid oxide fuel cells (SOFCs) [3], catalysts [4, 5], and a starting materials for scintillators [6]. It was found that the coefficient of thermal conductivity of solid solution $\text{LaSmZr}_2\text{O}_7$ is lower than that of lanthanum zirconate $\text{La}_2\text{Zr}_2\text{O}_7$ and it gives the opportunity to develop new materials for the TBC ceramic with low thermal conductivity, high durability and reliability at high temperatures.

The aim of this study was to study the thermal behavior of pyrochlore solid solutions of zirconate lanthanides and to measure of the high-temperature heat capacity in the temperature range 300 -1400 K by Differential Scanning Calorimetry using Netzsch STA 449 F1 Jupiter.

Samples of Ln zirconates with the pyrochlore structure (space group $\text{Fd}\bar{3}\text{m}$) were synthesized from high-purity reagents by inverse sedimentation followed by drying at 90°C for 72 hours and calcination at 1400°C and characterized by XRD techniques using the powder diffractometer Bruker Advance D8, and XPS-analysis. Annealing at 1400°C yielded crystallites with size >100 nm, whereas after annealing at temperatures $\leq 1200^\circ\text{C}$ the samples remained nanoscale fluorite structure (<20 nm) regardless of the time of annealing. DSC measurements confirmed the absence of phase transitions in the studied temperature range. Parameters of the pyrochlore crystal lattice unit cell of the synthesized solid solutions are given in the second column of the Table 1. Heat capacity curves obtained by DSC were described by Maier-Kelly equation $C_p = a + b \times T + c/T^2$ in the range of 300-1400 K. The coefficients of this equation for studied $\text{LaLnZr}_2\text{O}_7$ solid solutions are presented in columns 3-5.

Table 1. The parameters of the crystal lattice of solid solutions and coefficients of Maier-Kelly equation.

1	2	3	4	5
$\text{LaLnZr}_2\text{O}_7$	$a, \text{Å}$	a	b	c
$\text{LaNdZr}_2\text{O}_7$	10.727	248.8164832	0.03761945733	-2708356.743
$\text{LaSmZr}_2\text{O}_7$	10.6966	275.1609184	0.01248451526	-4799732.104
$\text{LaGdZr}_2\text{O}_7$	10.665	263.0728914	0.0235921491	-4313576.11
$\text{LaDyZr}_2\text{O}_7$	10.6455	250.5077335	0.0358372819	-2899003.117

The work was supported by the Russian Foundation for Basic Research (15-03-04388A).

[1] Arsen'ev P.A., Glushkova V.B., Evdokimov A.A. et al. Rare-Earth compounds. Zirconates, hafnates, niobates, tantalates, antimonites. M.: Nauka, 1985. 261 p. (in Russian).

[2] Fergus J.W. Zirconia and pyrochlore oxides for thermal barrier coatings in gas turbine engines.// Metallurgical and Mater. Trans. E. 2014. V. 1A P. 118-129.

[3] Kumar M, Arul Raj I, Pattabiraman R. $\text{Y}_2\text{Zr}_2\text{O}_7$ (YZ)-pyrochlore based oxide as an electrolyte material for intermediate temperature solid oxide fuel cells (ITSOFCs) – influence of Mn addition on YZ. Mater Chem Phys 2008;108:102–8.

[4] Korf SJ, Koopmans HJA, Lippens BC, Burggraaf AJ, Gellings PJ. Electrical and catalytic properties of some oxides with the fluorite or pyrochlore structure. CO oxidation on some compounds derived from $\text{Gd}_2\text{Zr}_2\text{O}_7$. J Chem Soc Faraday Trans 1 1987;83:1485–91.

[5] Uno M, Kosuga A, Okui M, Horisaka K, Muta H, Kurosaki K, et al. Photoelectrochemical study of lanthanide zirconium oxides, $\text{Ln}_2\text{Zr}_2\text{O}_7$ (Ln = La, Ce, Nd and Sm). J Alloys Compd 2006;420:291–7.

[6] Chaudhry A, Canning A, Boutchko R, Weber MJ, Grnbech-Jensen N, Derenzo SE. First-principles studies of Ce-doped $\text{RE}_2\text{M}_2\text{O}_7$ (RE = Y, La; M = Ti, Zr, Hf): a class of non-scintillators. J Appl Phys 2011;109:083708.



CORRELATION OF PHASE COMPOSITION WITH THERMAL AND TRANSPORT PROPERTIES FOR SYSTEM BASED ON RUBIDIUM MONO - AND DIHYDROGEN PHOSPHATES

Gaidamaka A.A., Ponomareva V.G, Bagryantseva I.N.

Institute of Solid State Chemistry and Mechanochemistry, Siberian Branch of the Russian Academy of Sciences, 630128

Novosibirsk, Russia

Novosibirsk State University, 630090 Novosibirsk, Russia

E-mail: a.gaidamaka@g.nsu.ru

Solid acids $M_nH_m(AO_4)_p$ ($M =$ alkali metal, $A = P, S, Se$) are a new generation of proton conductors. These compounds have high proton conductivity at the intermediate temperature range (130-250°C). Solid acids are perspective electrolytes for membranes of the intermediate temperature fuel cells. They are of interest from both practical and fundamental points of view.

The family of solid acids is actively investigated since a phenomenon of superprotonic conductivity was found in $CsHSO_4$. The conductivity at room temperature is low but it exhibits a sharp increase by heating. The structural mechanism of this phenomenon was explained by the concept of dynamically disordered network of hydrogen bonds. According to this mechanism, both positions of the H-bond centers and orientations of these bonds are dynamically disordered. In the low temperature range the phase which represents an ordered network of hydrogen bonds the conductivity is defined by defects such as proton vacancies at the site, and an interstitial proton. The conductivity is low due to the low concentration of defects. High temperature phase is disordered. As a result, the fast proton diffusion and low activation energy take place. The mechanism of proton transport consists of two stadiums: rotation of oxoanions and migration of the proton. Conductivity of phases with a disordered network of hydrogen bonds is defined by symmetry of crystal structure and doesn't depend on defects.

CsH_2PO_4 has the highest conductivity among the solid acids ($\sigma \sim 6 \cdot 10^{-2} \Omega^{-1}cm^{-1}$). A number of researches has been done to determine an influence of homogeneous doping on the transport properties of this compound. The investigation of $(1-x)CsH_2PO_4 - x Cs_2HPO_4 \cdot 2H_2O$ gave interesting results: compositions showed high conductivity, a new $Cs_3(HPO_4)(H_2PO_4) \cdot 2H_2O$ phase was found. Due to isotypical crystal structure of cesium and rubidium dihydrogen phosphates one can suggest an existence of highly conductive phases in equivalent system based on rubidium. RbH_2PO_4 is known to exhibit a superprotonic phase transition with conductivity increase by several orders of magnitude.

The aim of our work is the investigation of phase composition, thermal and transport properties of $(1-x)RbH_2PO_4 - xRb_2HPO_4 \cdot 2H_2O$ ($x = 0-1$) system. $Rb_2HPO_4 \cdot 2H_2O$ was prepared by slow evaporation of aqueous solution containing Rb_2CO_3 and H_3PO_4 in 1:1 molar ratio. Samples $(1-x)RbH_2PO_4 - x Rb_2HPO_4 \cdot 2H_2O$ ($x = 0.1-0.67$) were prepared by solid state synthesis. The properties of $(1-x) RbH_2PO_4 - x Rb_2HPO_4 \cdot 2H_2O$ have been investigated with the help of DSC, XRD and impedance measurements. X-ray powder diffraction data (XRD) for $x=0.25$ corresponds to $Rb_5H_7(PO_4)_4$. For all other samples XRD data represents a mixture of two phases: $Rb_5H_7(PO_4)_4$ and one of starting compounds (RbH_2PO_4 for $x= 0.1, 0.2$ or $Rb_2HPO_4 \cdot 2H_2O$ for $x = 0.33, 0.5, 0.67$, respectively). Crystalline structure of $Rb_5H_7(PO_4)_4$ is known but positions of protons haven't been determined. The other properties of this compound haven't been studied before. Growth of single crystal, refinement of the structure and investigation of transport and thermal properties of $Rb_5H_7(PO_4)_4$ is one of the goals of our research. IR-spectra of all samples represent a superposition of bands from two substances according to phase composition of sample. Appearance of some specific bands in 3000-1500 cm^{-1} range is evidence for existence strong hydrogen bonds. Thermal properties of starting and resulting compounds have been investigated via thermogravimetry and differential thermal analysis. Proton conductivity of $Rb_2HPO_4 \cdot 2H_2O$ has been measured for the first time. The electrotransport properties were determined and analyzed for all compositions at different temperatures.

Obtained results are strongly different from those for $(1-x) CsH_2PO_4 - x Cs_2HPO_4 \cdot 2H_2O$ system. The additional measurements of conductivity under humidified N_2 flow conditions should be carried out to investigate transport properties of the title system in details.



CALORIMETRIC STUDY OF DERIVATIVES WITH HYDROXY AMINO ACIDS CATION

Gheorghe D.¹, Contineanu I.¹, Neacsu A.¹, Teodorescu F.², Tanasescu S.¹

¹"Ilie Murgulescu" Institute of Physical Chemistry of the Romanian Academy, Splaiul Independentei 202, Bucharest, Romania

²"C. D. Nenitescu" Center of Organic Chemistry of the Romanian Academy, Splaiul Independentei 202B, Bucharest, Romania

E-mail: gheorghedanny2@gmail.com

Two inorganic derivatives of L- α -threonine and ethyl ester L-serine, namely ThrNO₃ and SerC₂NO₃ were synthesized and studied by combustion and differential scanning calorimetry. The enthalpies of combustion and formation of the two nitrates in the condensed state were determined for the first time. The thermal behavior in the temperature range of 200 to 600 K was observed and the melting/decomposition temperatures together the corresponding enthalpies of transitions were evidenced. The obtained data highlighted the influence of cation nature on the thermodynamic properties as a result of intra- and intermolecular interactions, and showed the increasing of the stability of the derivatives compared with that of the corresponding amino acids.

The UV-vis spectral study was carried out to test the optical transmitting property. Additional polarimetric measurements which confirmed the chiral nature of the two nitrates were performed.

The results could be used for a better explanation of the behavior and stability when these inorganic derivatives are involved in different biological processes, as well as in the view of ionic liquids or NLO (non-linear optical) applications.

Acknowledgement This contribution was carried out within the research programme - Chemical Thermodynamics of the "Ilie Murgulescu" Institute of Physical Chemistry, financed by the Romanian Academy. The support of the EU (ERDF) and Romanian Government under the project INFRANANOCHEM Nr. 19/01.03.2009 and of the project NanoReg2, Nr. 646221/2015 in the frame of the Horizon 2020 Framework Program of the European Union is acknowledged.



THERMAL EFFECTS OF HYDROXYAPATITE SYNTHESIZED IN GELATINE MATRIX

Golovanova O.A., Zaits A.V

*Department of Inorganic Chemistry Omsk F. M. Dostoevsky State University, 644077 Omsk, Prospekt Mira 55A, Russia
E-mail: Golovanoa2000@mail.ru*

Materials based on hydroxyapatite $\text{Ca}_{10}(\text{PO}_4)_6(\text{OH})_2$ (HA) are analogs of the mineral component of the bone tissue and considered as those most promising to be applied in bone defect replacement. The materials' bioactivity is believed to be determined by their chemical composition, crystal morphology, and surface properties. It is known that the main components of bone are type I collagen (~ 20%), a mineral phase (~ 60%), water (~ 9%) and non-collagenous proteins (~ 3%), the rest being polysaccharides and lipids. The organic part of bone is composed of collagen fibers and proteins, such as osteocalcin, osteonectin and fibronectin. Gelatin is a natural polymer formed through hydrolysis of collagen. In contrast to the latter, it is more stable and exhibits less antigenicity, thereby can be effectively used as a calcium phosphate based organic matrix biomaterial. Gelatin contains biologically active functional amino acid groups, and it is an advanced material for bone regeneration, including its combination with hydroxyapatite. The SBF (Simulated Body Fluid) was used as a model solution of extracellular fluid. A solid phase was prepared by precipitation from aqueous solutions; the starting components of the system were CaCl_2 , MgCl_2 , K_2HPO_4 , NaHCO_3 , Na_2SO_4 , NaCl solutions and 3 wt.% gelatin. Thermal effects were studied by isothermal thermogravimetric analysis. Hydroxyapatite samples synthesized in the presence of gelatin were placed in dry ceramic crucibles. Then the samples were placed in a muffle furnace and kept for 2 h. The calcination temperature was varied from 200 to 800°C by increment of 200°C. After that, the crucibles were allowed to cool to room temperature, and then they were weighed on an analytical balance. The XRD results showed that the samples synthesized in SBF under varying concentration of gelatin were single-phase and represented hydroxyapatite. The X-ray diffraction patterns of the HA samples subjected to heat treatment show peak splitting at 400°C. In our opinion, this is caused by degradation of the gelatin components (amino acids), and thereby release of the carbonate component that has been partially released in the form of carbon dioxide, and partially entered the calcium phosphate structure. At 600°C and 800°C, the intensity of peak splitting did not increase and remained at the same level. This is most likely due to the fact that no orbitals are left vacant to bind carbonate ions in calcium phosphate as compared to that in case of unsubstituted hydroxyapatite. The analysis of the IR-spectra identified the bands that determine the HA structure: 1040–1080 (ν_3), 960, 840 (ν_2), 602, 574 (ν_4) and 473 (ν_2) cm^{-1} corresponding to the phosphate group vibrations, a broad band at 3440–3570 cm^{-1} related to deformation vibrations of the OH^- -groups and valent vibrations of the adsorbed water. Carbonate ions are observed to localize in the phosphate ion lattice position with the corresponding absorption bands of the C–O deformation vibrations of the CO_3^{2-} ion bonds at 875 cm^{-1} and valent vibrations at 1415–1481 cm^{-1} in the IR-spectra. The band of deformation vibrations of the C = C bond is in the region of 1658 cm^{-1} .

The results of FT-IR spectroscopy showed that the spectrogram of the samples not subjected to heat treatment is identical to that of the samples heated at 200°C. During the analysis, several overlapping spectra were observed: in the region from 2700 cm^{-1} to 3800 cm^{-1} , which, apart from the -OH water vibrations, include vibrations of the amino groups, and methyl and methylene groups. In addition, $-\text{H}_2$ groups overlap the carboxyl groups in the region of 1400 cm^{-1} . At 400°C, the peak significantly decreases in the region of 3500 cm^{-1} that indicates removal of water from the structure and degradation of amino acids, and methyl and methylene groups. The shape of the carboxyl group doublet in the region of 1415–1466 cm^{-1} changed as well that can be confirmed by the removal of the $-\text{CH}_2$ group from the prepared sample. When the temperature rises to 600°C, the intensity of the C=C band (1658 cm^{-1}) is not observed, and the intensity of the C-O band (1420–1466 cm^{-1}) decreases that indicates the start of the carbonate component destruction. In addition, the O-H band (3569 cm^{-1}) reduces, which is also indicative of the start of the hydroxyapatite destruction. At 800°C, the spectrogram shows further reduction of the O-H band (3569 cm^{-1}) and C-O band (1420–1466 cm^{-1}).

This research was supported in part by the Russian Foundation for Basic Research (grant No. 15-29-04839 ofi_m).

THERMODYNAMIC FUNCTIONS OF THULIUM ORTHOPHOSPHATE TmPO_4 IN THE RANGE OF 0–1350 K

Gurevich V.M.¹, Gavrichev K.S.², Ryumin M.A.², Tyurin A.V.²

¹Vernadsky Institute of Geochemistry and Analytical Chemistry of Russian Academy of Sciences, 119991 Moscow, Russia

²Kurnakov Institute of General and Inorganic Chemistry of the Russian Academy of Sciences, 119991 Moscow, Russia

E-mail: gurevichvm@mail.ru

TmPO_4 heat capacity was measured in the temperatures intervals 11–346.05 and 304.6–1344.6 K by adiabatic and differential scanning calorimetries, respectively (Figure 1). Based on these data temperature dependencies of heat capacity, entropy, enthalpy change, and relative Gibbs energy of TmPO_4 were determined in the range of 10–1344 K.

The Gibbs free energy of formation from elements $\Delta_f G^0(298.15 \text{ K}, \text{TmPO}_4)$ was estimated (table 1), and the value of a Shottky's anomalous contribution $C_{an}(T)$ in heat capacity of TmPO_4 was calculated. Thulium orthophosphate was synthesized by a ceramic route using procedures described in [1]. The synthesized sample was examined by X-ray diffraction analysis to compare it with literature data.

All reflections are characteristic of TmPO_4 [2].

Rare-earth zircons (in particular REE vanadates and phosphates) are paramagnetic

at room temperatures, but at very low temperatures (in the range of 0–3.5 K) ones are transformed from the paramagnetic state to antiferromagnetic one. Since this transition is out of the measured temperature interval, the value of the absolute entropy at $T=298.15 \text{ K}$ was calculated based on the following equation: $S^0(298.15 \text{ K}) = [S^0(298.15 \text{ K}) - S^0(10 \text{ K})] + R \ln 2 = (122.18 + 5.76) \text{ J K}^{-1} \text{ mol}^{-1} = 127.9 \text{ J K}^{-1} \text{ mol}^{-1}$. Values of lattice contributions in the thermodynamic functions given in table 1 were considered negligible below 10 K.

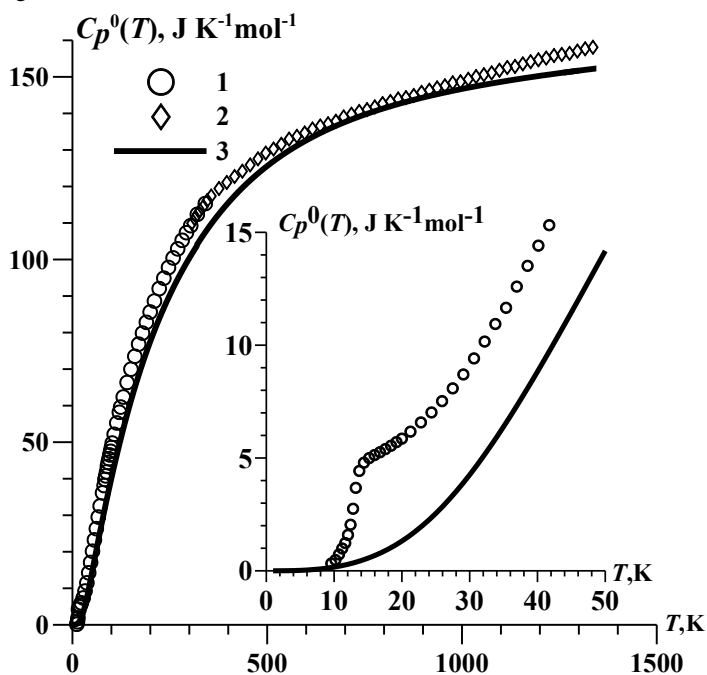


Figure 1. Experimental points of $C_p^0(T)$ of TmPO_4 determined by the adiabatic (1) and DSC (2) method; (3) – dependence of $C_p^0(T)$ of LuPO_4 [1, 3].

Table 1. Thermodynamic functions of TmPO_4 at $T=298.15 \text{ K}$.

$\Delta_f H^0(298.15 \text{ K}), \text{kJ mol}^{-1}$	-1964.7 ± 4.7 [2]
$\Delta_f G^0(298.15 \text{ K}), \text{kJ mol}^{-1}$	-1846 ± 5
$\Delta_f S^0(298.15 \text{ K}), \text{J K}^{-1} \text{ mol}^{-1}$	-397.2 ± 0.3
$C_p^0(298.15 \text{ K}), \text{J K}^{-1} \text{ mol}^{-1}$	108.89 ± 0.06
$S^0(298.15 \text{ K}), \text{J K}^{-1} \text{ mol}^{-1}$	127.9 ± 0.6
$H^0(298.15 \text{ K}) - H^0(0), \text{kJ mol}^{-1}$	18.84 ± 0.02
$\Phi^0(298.15 \text{ K}), \text{J K}^{-1} \text{ mol}^{-1}$	64.7 ± 0.6

[1] K.S. Gavrichev, et al. // Thermochim. Acta 2006. V.448. P.63–65.

[2] S.Ushakov, et al. // J. Mater. Res. 2001. V.16. P.2623–2633.

[3] G.E. Nikiforova et al. // Inorg. Mat.. 2012. V.48. No 8. P.841–844.

This work was supported by RFFI project № 15-05-01161

The equipment of the Joint Research Centre of IGIC was used to carry out this investigation.

SYNTHESIS AND THERMODYNAMIC PROPERTIES OF $Tb_2Sn_2O_7$ AND $Dy_2Sn_2O_7$

Irtugo L.A., Denisova L.T.

*Institute of Non-Ferrous Metals and Materials Science, Siberian Federal University,
pr. imeni Gazety "Krasnoyarskii rabochii" 95, Krasnoyarsk, 660025 Russia*

E-mail: irtugo@rambler.ru

Even though there is unabated interest in the $Ln_2Sn_2O_7$ ($Ln = La-Lu$) pyrochlore oxides, many of their properties have not been studied in sufficient detail yet. Such materials are terbium and deuterium stannates. Data on the high-temperature heat capacity, thermodynamic properties and Raman spectra of $Tb_2Sn_2O_7$ and $Dy_2Sn_2O_7$ are not available in the literature.

The objectives of this work were to study the high temperature heat capacity of $Tb_2Sn_2O_7$ and $Dy_2Sn_2O_7$ and to determine their thermodynamic properties on the basis of these data, and to measure their Raman spectra.

The terbium and deuterium stannates were synthesized by the solid-phase reaction method. Stoichiometric mixtures of Dy_2O_3 or Tb_2O_3 (reagent grade) and SnO_2 (analytical grade) were ground in an agate mortar and pressed into pellets, which were then fired in air at 1473 K for 200 h, with intermediate grindings and pressing every 20 h.

The phase composition of the samples prepared by this way was determined by X-ray diffraction on a PANalytical X'Pert Pro MPD diffractometer with $CuK\alpha$ radiation. The lattice parameters of $Tb_2Sn_2O_7$ and $Dy_2Sn_2O_7$ were determined by profile fitting with derivative difference minimization. The results obtained at room temperature for $Tb_2Sn_2O_7$ (sp. gr. $Fd3m$, $a = 10.4287(1)$ Å, $V = 1134.20(3)$ Å³) and $Dy_2Sn_2O_7$ (sp. gr. $Fd3m$, $a = 10.4010(1)$ Å, $V = 1125.20(3)$ Å³) are in reasonable agreement with previous data.

Raman spectra were measured on a Thermo Nicolet Almega dispersive Raman spectrometer at a spatial resolution of 2.5 cm^{-1} . As a coherent light source a diode laser ($\lambda = 785$ nm) was used. The samples had the form of pressed polycrystalline powders. Figure 1 shows the Raman spectra of the $Tb_2Sn_2O_7$ and $Dy_2Sn_2O_7$ polycrystals prepared in this study. Comparison of the measured Raman spectra with spectra of other rare-earth stannates demonstrates that there are no significant distinctions in peak positions.

The heat capacity C_p was measured in platinum crucibles by differential scanning calorimetry with an STA 449 C Jupiter (NETZSCH) in air atmosphere within the temperature interval 360-1000 K at heating rates of 20 K/min for the base, sapphire (reference), and sample. The samples had the form of pressed polycrystalline powders.

The experimental data were analyzed using the Netzsch Proteus Thermal Analysis software package and Systat Sigma Plot 12 graphing software.

The values of C_p grow regularly with increasing temperature for both stannates, with no extrema in the $C_p(T)$ curve.

The heat capacity data obtained in the temperature range studied are well represented by the equation

$$C_p = a + bT + cT^{-2} \quad (\text{J/mol}\cdot\text{K}):$$

$$C_{p, Tb_2Sn_2O_7} = (244.2 \pm 0.7) + (52.2 \pm 0.8) \times 10^{-3} T - (18.0 \pm 0.8) \times 10^5 T^{-2} \quad (1)$$

$$C_{p, Dy_2Sn_2O_7} = (238.5 \pm 0.4) + (71.9 \pm 1.2) \times 10^{-3} T - (2.4 \pm 0.1) \times 10^5 T^{-2} \quad (2)$$

The correlation coefficients were determined for equations (1) and (2) to be 0.9993 and 0.9992, respectively. Using the temperature-dependent heat capacity data for $Tb_2Sn_2O_7$ and $Dy_2Sn_2O_7$ in combination with well-known thermodynamic relations, were determined the enthalpy $H^\circ(T) - H^\circ(360 \text{ K})$, entropy $S^\circ(T) - S^\circ(360 \text{ K})$ and Gibbs reduced energy $\Phi^\circ(T)$.

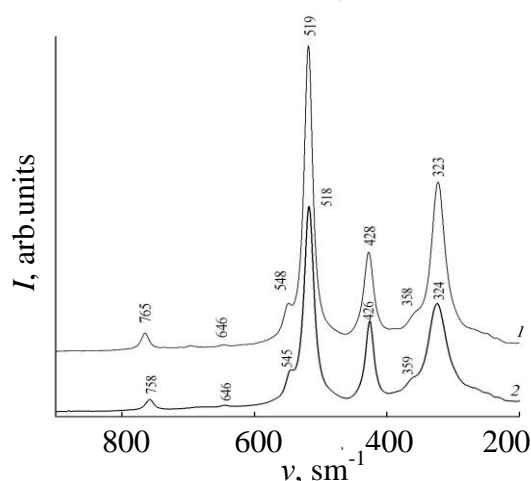


Figure 1. Raman spectra of polycrystals $Dy_2Sn_2O_7$ (1), $Tb_2Sn_2O_7$ (2).



THERMODYNAMICS OF FORMATION OF METHYLAMMONIUM LEAD HALIDES HYBRID PEROVSKITES

Ivanov I.L., Steparuk A.S., Bolyachkina M.S., Tsvetkov D.S., Safronov A.P., Zuev A.Yu.
Ural Federal University, Institute of Natural Sciences and Mathematics, 620002 Ekaterinburg, Mira str., 19, Russia
E-mail: ivan.ivanov@urfu.ru

The problem of green power generation is one of the most important today. The solar power is one of the promising solutions of this problem. Hybrid perovskite-type methylammonium lead halides have received a lot of attention in recent years due to high solar energy conversion efficiencies obtained in solar cells based on these materials. Since the time of the first demonstration [1] the photovoltaic devices based on the hybrid perovskites $\text{CH}_3\text{NH}_3\text{PbX}_3$ ($\text{X}=\text{Cl}, \text{Br}, \text{I}$) have shown huge progress in terms of solar energy conversion efficiency reaching currently 20.1% [2]. However, despite very promising achievements the fundamental chemistry and physics of hybrid organic-inorganic (HOIP) perovskites is far to be completely understood. This is particularly true for thermodynamic properties of HOIP perovskites $\text{CH}_3\text{NH}_3\text{PbX}_3$ ($\text{X}=\text{Cl}, \text{Br}, \text{I}$). Their heat capacity, C_p , as well as standard entropy as a function of temperature in the range of 13-365 K was published as early as 1990 by Onoda-Yamamuro et al. [3]. At the same time up to now there is no reliable data on the standard enthalpy of formation of these materials. Recently, there have been published two works [4, 5] dealing with solution calorimetry [4] and equilibrium vapor pressure [5] measurements aiming to provide the necessary thermodynamic data. Unfortunately the results obtained by Nagabhushana et al. [4] and Brunetti et al. [5] are not consistent with each other. The main goal of the current work was to provide the data by means of solution calorimetry measurements using carefully prepared samples.

Enthalpies of solution of hybrid perovskites $\text{CH}_3\text{NH}_3\text{PbX}_3$ ($\text{X}=\text{Cl}, \text{Br}, \text{I}$) in DMSO were measured using solution calorimetry. Standard enthalpies and Gibbs free energies of formation of $\text{CH}_3\text{NH}_3\text{PbX}_3$ ($\text{X}=\text{Cl}, \text{Br}, \text{I}$) hybrid perovskites from halides as well as from elements at 298 K were calculated on the basis of experimental data obtained and compared with the data available in literature. Entropy contribution was shown to play a major role in the stability of hybrid organic-inorganic perovskites with respect to their decomposition on constituent halides.

This work was supported by the Russian Foundation for Basic Research (Grant No. 16-33-60120).

- [1] Kojima A., Teshima K., Shirai Y., Miyasaka T., *J. Am. Chem. Soc.*, 2009, 131, 6050-6051.
- [2] Green M. A., Emery K., Hishikawa Y., Warta W., Dunlop E. D., *Prog. Photovolt: Res. Appl.*, 2016, 24, 3-11.
- [3] Onoda-Yamamuro N., Matsuo T., Suga H., *J. Phys. Chem. Solids*, 1990, 51, 1383-1395.
- [4] Nagabhushana G. P., Shivaramaiah R., Navrotsky A., *PNAS.*, 2016, 113, 7717-7721.
- [5] Brunetti B., Cavallo C., Ciccioli A., Gigli G., Latini A., *Scientific reports.*, 2016, 6, 31896.

THE PROGRAM FOR THE ANALYSIS OF THE THERMODYNAMIC CHARACTERISTICS OF BIOLOGICAL FLUIDS

Izmaylov R.R.^{1,2}, Golovanova O.A.²

¹Institute of Hydrocarbon Processing, Siberian Branch of the Russian Academy of Sciences, 644040, Omsk, Russia

²Omsk F.M. Dostoevsky State University, 644077, Omsk, Russia

E-mail: r.r.izmailov@gmail.com

Modern materials used in orthopedics and traumatology should be similar to the natural tissues of the human body. Thus, it is important to include the ions in the structure of calcium phosphates, which contain in biological fluids. This can be achieved by using the method of biomimetic synthesis of calcium phosphates from model solutions of biological fluids: simulated body fluid (SBF), saliva, plaque fluid, etc. However, the processes of crystallization of calcium phosphate in multicomponent solutions are very difficult for studying. Changes in the ionic composition of biological fluids strongly affect to the stoichiometry of phosphates and their structural and morphological characteristics. Therefore, a program (ThermodynamicsSetup) was developed to obtain preliminary information on synthesis products and the possibility of its control. In this program it is possible to calculate the basic thermodynamic parameters (Gibbs energy, supersaturation index) of the formation of insoluble compounds from a solution simulating the ionic composition of biological fluids. In the dialog box, you can vary the pH, ionic strength, supersaturation of calcium ions and phosphate ions and others.

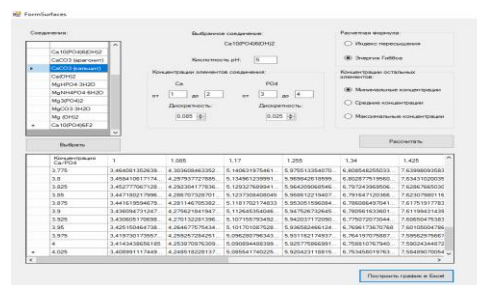


Figure 1. Dialog window of the program.

The model is based on the following parameters:

- The electrostatic interaction was calculated from the ionic strength of the solution. The microelements and organic composition of biological solutions are not taken into account in the studied system.
- The prototype of a biological fluid corresponds to the inorganic composition, temperature and pH for the average physiological values of an adult.
- The theoretical possibility of the formation characteristic of the mineral phases, which hypothetically can form in the studied modeling solutions, is the reference values of solubility product K_s .
- The conditional solubility of hardly soluble compounds is calculated taking into account the hydrolysis of ions.
- Participation of cations in hydrolysis reactions at hydroxy complexes formation is a negligible result of their low stability (Ca^{2+} , Mg^{2+}) and complexing ability (Na^+ , K^+). Therefore, their mole fractions equal to one.
- The possibility of insoluble compounds formation was evaluated by the values of the supersaturation index (SI) and Gibbs energy (ΔG) of crystallization, characterizing the possibility of the formation of sparingly soluble compounds in model systems.
- Physical and chemical processes are in equilibrium and occur in the simulated solutions at a constant temperature (25°)

**THERMAL PROPERTIES OF IRIDIUM (I) VOLATILE COMPLEXES WITH CARBONYLS AND BETA-DIKETONES**Karakovskaya K.I.^{1,2}, Vikulova E.S.¹, Ilyin I.Yu¹, Zelenina L.N.^{1,2}, Sysoev S.V.¹, Morozova N.B.¹¹Nikolaev Institute of Inorganic Chemistry, Siberian Branch of the Russian Academy of Sciences, 630090 Novosibirsk, Russia²Novosibirsk State University, 630090 Novosibirsk, Russia

E-mail: red_garden@mail.ru

Nowadays Ir-containing coatings possess a number of important applications including refractory protecting layers for different materials, biocompatible electrochemical layers of neuro- and cardioelectrodes, etc. Metal-Organic Chemical Vapor Deposition (MOCVD) and related methods are ones of the most preferable techniques to obtain the coatings with targeted characteristics on the objects with complex shapes such as components of medical electrodes. The modern trend in MOCVD precursors field is combine extremely high volatility with required stability in condensed and gas phases and specific reactivity [1]. In the case of iridium complexes, this purpose could be achieved by using of carbonyl ligands. On the other hand, β -diketonate ligands are widely used for volatile precursors as they provide the opportunity to manage thermal properties of the complexes formed by changing of terminal substituents.

The aim of the present work is to investigate the influence of ligands on the thermal properties of Ir(I) complexes with both types of ligands indicated: $[\text{Ir}(\text{CO})_2(\text{L})]$, where L = β -diketonate, $\text{R}^1\text{C}(\text{O})\text{CHC}(\text{O})\text{R}^2$: $\text{R}^1 = \text{CF}_3$, $\text{R}^2 = \text{Me}$ (tfac) **1**, CF_3 (hfac) **2**; tBu (ptac) **3**, Ph (btfac) **4**, $\text{R}^1 = \text{R}^2 = \text{tBu}$ (thd) **5**, Me (acac) **6**.

The targeted compounds were synthesized at inert atmosphere by passing a CO flow through a hexane solution of corresponding cyclooctadiene-1,5 complexes $[\text{Ir}(\text{cod})(\text{L})]$ with 75-95% yields. Compounds **3-5** were obtained for the first time. All complexes synthesized were characterized by elemental analysis, IR- and ^1H and $^{13}\text{C}\{^1\text{H}\}$ NMR spectroscopy and powder X-Ray diffraction (XRD). Crystal structures of compounds **1-5** were determined by single-crystal X-Ray Diffraction (XRD).

Thermal properties of complexes in condensed phase were investigated by Thermogravimetry (TG/DTA) and Differential Scanning Calorimetry (DSC). TG/DTA investigation was carried out using thermobalances Netzsch TG 209 F1 Iris (He, 20 mL·min⁻¹, 10 K·min⁻¹, sample mass 9-11 mg). For all compounds, mass loss occurs in single step and residual mass is less than 1.0% indicating the complete evaporation. The following volatility row has been established on the base of 50% mass loss temperature: L = hfac **2** (388 K) > tfac **1** (408 K) > ptac **4** (431 K) > acac **6** (444 K) \approx thd **5** (448 K) > btfac **4** (481 K). So, influence of terminal substituents are mostly the same as that for parent $[\text{Ir}(\text{cod})(\text{L})]$ series, namely, the increase and decrease of volatility as a result of introducing of CF_3 and Ph groups, respectively [2]. The feature of the carbonyl series seems to be the close volatility for complexes with both Me- and tBu -substituents in β -diketonate (compounds **5** and **6**). DSC investigation was performed using a Setaram DSC 111 calorimeter (0.5–1.0 K·min⁻¹; sample mass 13–25 mg). The results obtained are presented in the Table 1. All compounds exhibit no any phase transitions up to melting.

For some complexes, the temperature dependences of saturated vapor pressure were measured by flow (transmission) method and thermodynamic parameters of sublimation were calculated.

The data obtained are useful to choose the optimal MOCVD experimental parameters for each precursor.

Table 1. Thermodynamic parameters of melting of $[\text{Ir}(\text{CO})_2(\text{L})]$ complexes

L	$T_{\text{melt.}}$, K	$\Delta_{\text{melt.}}H_{T_{\text{melt.}}}$, kJ·mol ⁻¹	$\Delta_{\text{melt.}}S_{T_{\text{melt.}}}$, J·(mol·K) ⁻¹
hfac 2	400.0 \pm 0.5	22.2 \pm 0.3	55.6 \pm 0.4
ptac 3	432.0 \pm 0.5	27.6 \pm 0.4	63.8 \pm 0.5
btfac 4	389.9 \pm 0.5	23.4 \pm 0.3	60.0 \pm 0.5
thd 5	387.5 \pm 0.5	23.2 \pm 0.2	53.7 \pm 0.5

[1] Koponen, S.E., Gordon, P.G., Barry, S.T. Polyhedron, 2016, 108, 59–66.

[2] Vikulova, E.S., Ilyin, I.Y., Karakovskaya, K.I. et al. J. Coord. Chem., 2016, 69, 2281–2290.

The work was partially financially supported by the Council on the Grants from the President of the Russian Federation (SP-3215.2016.4).

CRYSTAL HARDNESS, HEAT AND MELTING TEMPERATURE AS INDICES OF THE CHEMICAL BOND STRENGTH

Kidyarov B.I.

Rzhanov Institute of Semiconductor Physics, Siberian Branch of the Russian Academy of Sciences, 630090 Novosibirsk, Russia
E-mail: kidyarov@isp.nsc.ru

The crystal hardness (H_s), heat (ΔH_m), and melting temperature (T_m) are dependent on the chemical bond strength, and they are some indices (indicators) of its value [1]. Besides, the hard oxide materials, including minerals, have many applications in technique as abrasive, precious stones, refractory, building and instrument-making materials [2]. The hardness is also the simplest diagnostic property at mineral characterization [3]. At present, the hard and refractory oxide crystals are the main materials at creation of some powerful solid state laser systems [4]. For this goal, the crystalline laser elements must be high heat-conducting materials [4]. So, the knowledge of the quantitative relation between the values of hardness, thermal conductivity (k), heat and melting temperature is necessary at search and selection of different oxide crystals for many applications [5].

The properties of crystalline phases are determined by nature of chemical bonds, and the interrelationship between these properties has multifactor character [1, 5]. But, the full correlation between the two physical properties is as rule the indistinct function, and the set of $\{H_s - T_m\}$ is also fuzzy [5]. Nevertheless, the knowledge of the boundary of these fuzzy sets, and their taxonomy is necessary undoubtedly to a priori prediction of material properties. Besides, the more detail understanding of interrelationship «composition–structure–property» of multi-component crystals is needed for the development of modern physics and material science [5].

Fig.1 presents the dependence of the upper envelope $\{H_s - T_m\}$ (points 1, solid line), and a set of $\{\Delta H_m - T_m\}$ data (points 2). The dotted–line is the upper boundary for hard oxide crystals with $H_s = 9$ Mohs. Nevertheless from the clear point scattering, it is seen that the most values of the hardness H_s , and the melting heat are positioned in interval $T_m = 1463\text{--}2243$ K. Namely, the most refractory oxide crystals have not the high hardness (for ThO_2 : $T_m = 3573$ K, but $H_s = 6.5$ Mohs). The maximum of the hardness is observed for cubic $\text{Zn}_4\text{B}_6\text{O}_{13}$ crystal ($T_m > 1473$ K), rhombic mineral alumotantit, AlTaO_4 ($T_m = 1973$ K)), rhombohedral mineral sapphire Al_2O_3 ($T_m = 2320$ K), and the same for $\alpha\text{-Ga}_2\text{O}_3$ crystal ($T_m = 1973$ K), mineral escolait, Cr_2O_3 ($T_m = 2573$ K), hexagonal mineral bromellit BeO ($T_m = 2843$ K).

So, in general the values of hardness, heat and melting temperature may be as some indicators of oxide bond strength, but the full conformity is not observed.

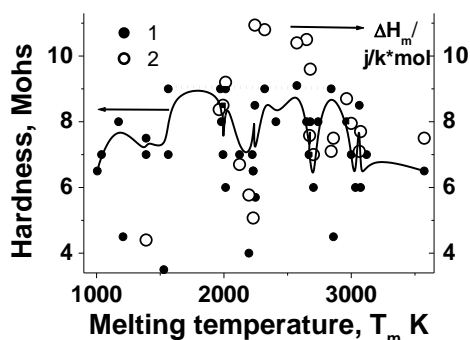


Figure 1. Correlation between the $\{H_s - T_m\}$, and $\{\Delta H_m - T_m\}$ data set for simple and binary oxide crystals, curve 1 and point 2 respectively.

34006, Proceedings, in 7 Volumes. V.5. Novosibirsk, NGTU, 2014. P.64-67.

[1] Bokii G.B. Crystal-chemistry. Moscow: Nauka.1971. (In Russian).

[2] Marfunin. A.S. Introduction in the mineral physics. Moscow. Nedra. 1974. (In Russian).

[3] Feklichev. V.G. Diagnostic constants of minerals. Handbook. Moscow: Nedra. 1989. (In Russian).

[4] Kaminskii A.A. Crystalline Lasers: Physical processes and operating schemes. Boca Raton, CRC Press, 1996.

[5] Kidyarov B.I., Makukha V.K. Interrelationship «structure-hardness-fusibility» for oxide crystals // 12th International conference on actual problems of electronics instrument engineering (APEIE)-

HEAT CAPACITY AND THERMODYNAMIC FUNCTIONS OF MgGa_2O_4 – MgFe_2O_4 SPINELS

Kondrat'eva O.N., Tyurin A.V., Nikiforova G.E., Khoroshilov A.V., Ketsko V.A., Gavrichev K.S.

Kurnakov Institute of General and Inorganic Chemistry, Russian Academy of Sciences, 119991 Moscow, Russia

E-mail: ol.kondratieva@gmail.com

The MgFe_2O_4 – MgGa_2O_4 system is considerable interest both scientifically and technologically. Magnesium ferrite has been widely used in high-density recording media, heterogeneous catalysis, and sensors. In addition, due to its high biocompatibility, MgFe_2O_4 can be used as magnetic material for cancer therapy and as a drug delivery system. On the other hand, MgGa_2O_4 ceramics are promising candidate materials for millimeter-wave devices such as filters, resonators and antennas. Recently [1] the thin film heterostructures for magnetoelectronic devices based on MgGa_2O_4 and MgFe_2O_4 solid solutions were grown. To describe correctly the processes occurring at the interface during its crystallization the thermodynamic data for this system in a wide temperature range are required. These applications provide some motivation for the thermodynamic study of the MgFe_2O_4 – MgGa_2O_4 system.

The samples were prepared by sol-gel auto-combustion synthesis technique described elsewhere [1]. The characterization of the samples were performed using X-ray diffraction (Bruker D 8 Advance diffractometer, $\text{CuK}\alpha_1$ -radiation, $\lambda = 1.5406 \text{ \AA}$, LYNXEYE detector, reflection geometry) and inductively coupled plasma-mass spectrometry (Agilent 7500ce spectrometer, Agilent Technologies, USA). The final purity of all the samples was established to be $>99.0\%$.

The heat capacities of the samples were measured using adiabatic vacuum calorimeter BKT-3 ("Termis", Russia) in the temperature range from 7 to 348 K. The relative standard uncertainties for the heat capacity measurements ($\text{J K}^{-1} \text{ mol}^{-1}$) were $u_r(C_p) = 0.02$ at $T < 15 \text{ K}$, $u_r(C_p) = 0.005$ in the temperature range from 15 to 40 K, and $u_r(C_p) = 0.002$ between 40 and 350 K. A simultaneous thermal analyzer STA 449 F1 Jupiter® (NETZSCH-Gerätebau, Germany) was used to measure heat capacities of $\text{MgFe}_{2-x}\text{Ga}_x\text{O}_4$ ($x = 0.4, 0.8$ and 2) in the temperature range from 320 to 800 K. The relative standard uncertainty for the experimental heat capacity values was $u_r(C_p) = 0.03$.

The experimental heat capacity data obtained by adiabatic calorimetry were smoothed using a linear combination of Debye and Einstein functions. The calculation procedure has been described in detail [2]. The experimental heat capacity values obtained by DSC were fitted using a polynomial functions. The coefficients of polynomial functions were determined by the linear least squares method.

The standard thermodynamic functions of $\text{MgFe}_{2-x}\text{Ga}_x\text{O}_4$ ($x = 0.4, 0.8$ and 2) from 0 to 800 K were calculated. Experimental and smoothed heat capacity data are plotted in Fig. 1. The Debye characteristic temperatures of $\text{MgFe}_{2-x}\text{Ga}_x\text{O}_4$ ($x = 0.4, 0.8$ and 2) were also evaluated from heat capacity data and from elastic constants (for MgGa_2O_4).

Hump-like heat capacity anomaly, which may be associated with magnetic ordering, was detected below 50 K (inset in Fig. 1). A further study of the magnetic properties of gallium-substituted magnesium ferrites would allow one to understand the origin of the observed anomaly.

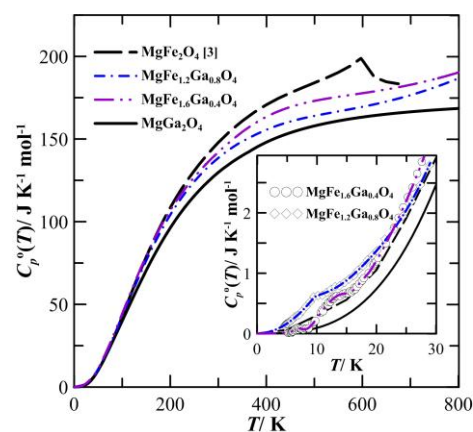


Figure 1. The heat capacities of the MgGa_2O_4 – MgFe_2O_4 system.

[1] Nipan, G.D.; Stognij, A.I.; Ketsko, V.A. Russ. Chem. Rev., 2012, 81, 458-475.

[2] Gurevich, V.M.; Gorbunov, V.E.; Gavrichev, K.S.; et al. Geochem. Int., 1999, 37, 367-377.

[3] Turkin, A.I.; Drebuschak, V.A.; Kovalevskaya, Y.A.; et al. J. Therm. Anal. Calorim., 2008, 92, 717-721.

This work was supported by the Russian Foundation for Basic Research (Project No. 16-29-0524). The experimental work was performed using the equipment of the Joint Research Centre of IGIC RAS.

**THERMODYNAMIC PROPERTIES OF AMMONIUM METHANESULFONATE**

Kosova D.A., Zagribelnyy B.A., Druzhinina A.I., Tiflova L.A., Monaenkova A.S.

Department of Chemistry, Lomonosov MSU, GSP-1, 1-3 Leninskiye Gory, 119991, Moscow, Russia

E-mail: dakosova@gmail.com

Methanesulfonic acid has some valuable properties such as thermal stability, low toxicity, and degradability by microorganisms. This substance and its salts are widely applied in various industries. However, information on properties of the methanesulfonates is presented fragmentary in the literature. In the present work we focused on the investigation of the thermodynamic properties of ammonium methanesulfonate ($\text{NH}_4\text{SO}_3\text{CH}_3$).

The aims of the present study were (1) experimental investigation of the $\text{NH}_4\text{SO}_3\text{CH}_3$ isobaric molar heat capacity ($C_{p,m}$) in a wide range of temperatures; (2) approximation of the data on $C_{p,m}$ by combination of Einstein functions; (3) determination of the enthalpy of $\text{NH}_4\text{SO}_3\text{CH}_3$ dissolution in water; (4) calculation of the main thermodynamic functions of $\text{NH}_4\text{SO}_3\text{CH}_3$ ($G^\circ(T)-H^\circ(0)$, $H^\circ(T)-H^\circ(0)$, $S^\circ(T)-S^\circ(0)$) and thermodynamic functions of formation on the basis of experimental data.

The heat capacity of the $\text{NH}_4\text{SO}_3\text{CH}_3$ was measured with the help of an automated vacuum adiabatic calorimeter in the temperature range from 8 to 350 K. Liquid helium and nitrogen were applied as refrigerants. Detailed description of the device configuration and calorimetric technique were done by Varushenko et al. [1]. The calorimeter was tested with high-pure Cu (99.995 weight %). Maximum deviations of experimental data from literature data were not exceeded 1.5 % in the range 8–80 K and 0.3 % above 80 K. Reproducibility of the results was confirmed by triple repetition of the experiments. The measurements of the enthalpy of $\text{NH}_4\text{SO}_3\text{CH}_3$ dissolution in water were performed at $T = 298.15$ K in sealed swinging calorimeter with an isothermal jacket, similar to that described in [2]. The calorimeter was tested several times by the dissolution of KCl in water.

A linear combination of Einstein functions (Eq. (1)) was applied to approximate the results of the heat capacity measurements. Thermodynamic foundation of the $C_{p,m}$ vs. T description by these functions was discussed in detail in [3]. It should be noted that α_i and θ_i are variable parameters, which, in this case, do not have a strict physical meaning. Experimental data over the entire temperature range can be fitted to Eq. (1) by a single set of parameters. The thermal contributions to the entropy and enthalpy at any given temperature T (Eqs.(2) and (3), respectively) can be calculated analytically, i.e., the question of agreement of the thermodynamic data is solved:

$$C_{p,m}(T) = 3R \sum_i \alpha_i \frac{\left(\frac{\theta_i}{T}\right)^2 e^{\frac{\theta_i}{T}}}{\left(e^{\frac{\theta_i}{T}} - 1\right)^2} \quad (1),$$

$$(S_m^\circ(T) - S_m^\circ(0)) = 3R \sum_i \alpha_i \left(\frac{(\theta_i/T)}{e^{\theta_i/T} - 1} - \ln(1 - e^{-\theta_i/T}) \right) \quad (2),$$

$$(H_m^\circ(T) - H_m^\circ(0)) = 3RT \sum_i \alpha_i \frac{(\theta_i/T)}{e^{\theta_i/T} - 1} \quad (3).$$

Unknown parameters α_i and θ_i of Eq. (1) were determined by the solution of the system of the nonlinear equations by the method of least squares using software «Cpfit» developed in the Laboratory of Chemical Thermodynamics of Lomonosov MSU. The relative deviations between experimental and calculated heat capacity were applied as an objective function.

[1] R.M. Varushchenko, A.I. Druzhinina, E.L. Sorkin, J. Chem. Thermodynamics, 1997, 29, 623 – 637.

[2] A.S. Monayenkova, S.A. Lezhava, A.A. Popova, L. A. Tiphlova, J. Chem. Thermodynamics, 2001, 33, 1679–1686.

[3] G.F. Voronin, I.B. Kutsenok. J. Chem. Eng. Data, 2013, 58, 2083–2094.

This work was performed by financial support of RFBR № 16-33-00958.



SATURATED VAPOR PRESSURES AND VAPORIZATION ENTHALPIES OF TRIMETHYLOLPROPANE ESTERS

Aleksandrov A.Yu., Krasnykh E.L., Druginina Y.A.

Samara State Technical University, Samara, 443100 Russia

E-mail: kinterm@samgtu.ru

Trimethylolpropane esters are widely used in industry for production of paints, synthetic oils and lubricants. Nevertheless, development of technologies and production of trimethylolpropane ethers, which can be used as plasticizers, require data on saturated vapors pressures and vaporization enthalpies. This work uses transfer method that determines saturated vapors pressures and vaporization enthalpies of trimethylolpropane triesters with C₂-C₆ acids of different structure.

Samples of trimethylolpropane esters were obtained with azeotropic etherification in the presence of benzene (when synthesizing trimethylolpropane triacetate) and toluene (when synthesizing the other samples) and phosphorus acid as a catalyzer [1]. The purity of samples obtained was at least 99.5% (GLC).

Saturated vapor pressures were determined with the transfer method (transpiration). When processing saturated vapor pressures we used Clausius-Clapeyron equation integrated in the range from p_{aw} to p to get the equation:

$$R \cdot \ln\left(\frac{p}{p_{aw}}\right) = A_f - \frac{B_f}{T} + \Delta_i^s C_p^o \cdot \ln\left(\frac{T}{T_{aw}}\right), \quad (1)$$

where p – vapors pressure at T; p_{aw} – vapors pressure at average research temperature T_{aw}; A_f and B_f – empirical coefficients obtained through processing of p-T-data with the least squares method; Δ_{ic}ⁿ C_p^o – difference between heat capacity of gas and liquid phases, determined with method suggested in [2].

The value of vaporization enthalpy Δ_{vap}H_m^o at 298.2 K was calculated with an equation (2):

$$\Delta_{vap}H_m^o(298.2) = -B_f + \Delta_i^s C_p^o \cdot 298.2 \quad (2)$$

The results of vaporization enthalpy calculation are shown in a table 1.

Table 1. Vaporization enthalpies (kJ/mol) of trimethylolpropane triesters.

TPM ester	n	I ₂₅₀ [1]	T-range, K	Δ _i ^s C _p ^o , J/(mol*K)	Δ _{vap} H _m ^o exp. (298.15 K)	Δ _{vap} H _m ^o calc. (298.15 K)
Triacetate	2	1542.6	318.6-344.6	-136.9	88.0±0.7	90.0
Tripropionate	3	1790.6				100.9
Tributyrate	4	2036.5	328.6-363.5	-162.4	114.0±1.1	107.8
Trivaleriat	5	2298.6	347.4-371.2	-178.4	119.8±1.6	119.2
Tricapronate	6	2575.5	355.2-372.0	-195.1	133.4±6.4	132.0
Tri-iso-butyrate	-	1913.7	318.6-363.2	-156.2	99.3±0.8	103.5
Tri-iso-valeriat	-	2163.1	339.3-369.0	-172.3	111.5±1.2	114.8
Tripivalates	-	1985.8	316.5-354.3	-161.7	105.2±1.3	107.4

On the basis of data obtained we determined the dependencies of vaporization enthalpies on number of carbon atoms in a molecule of linear substituents (n,C) and on retention indexes (I₂₅₀).

The following equations were established:

$$\Delta_{vap}H_m^o(298.2) = 11.04 * n, C + 67.04 \quad (R^2=0.98) \quad (3)$$

$$\Delta_{vap}H_m^o(298.2) = 0.044 * I_{250} + 18.6 \quad (R^2=0.95) \quad (4)$$

Furthermore, the assessment of author's QSPR-method [3] was done to ensure possibility of TPM esters prediction. The results, shown in the table 1, demonstrate a good predictive capability of the method.

This work was supported by the Russian Foundation for Basic Research, project no. 16-08-00383 a.

[1] Krasnykh E.L.; Aleksandrov A.Yu.; Sokolova A.A.; Rus. J. of Phys. Chem. A, 2017, 91, 2, 398–402.

[2] Krasnykh E.L.; Portnova S.V. J. of Struc. Chem., 2017, 58,4, 753-758, 2017.

[3] Krasnykh E.L.; Portnova S.V. J. of Struc. Chem., 2016, 57, 3, 437-445.



ONLINE DATABASE ON MATERIALS PROPERTIES AT EXTREME CONDITIONS

Lomonosov I.V.^{1,2}, Khishchenko K.V.², Levashov P.R.^{1,2}, Minakov D.V.²

¹*Institute of Problems of Chemical Physics RAS, 142432 Chernogolovka, Russia*

²*Joint Institute for High Temperatures RAS, 127412 Moscow, Russia*

E-mail: ivl143@yandex.ru

Shock-wave and related dynamic material response data serve for calibrating, validating, and improving material models over very broad regions of the pressure-temperature-density phase space. The required information includes thermodynamic and mechanical properties of materials under conditions of shock wave and other dynamic loadings, selected related quantities of interest, and the meta-data that describes the provenance of the measurements and material models. Measurements of principal, reflected and porous Hugoniot and determinations of release isentrope parameters cover a broad range of the phase diagram. These experimental points embrace nine orders with respect to pressure and five orders with respect to density. All of the data are unique, have their own history and present a result of complicated expensive experiments. We have collected about 20000 experimental points on shock compression, adiabatic expansion, measurements of sound velocities behind the shock front and free-surface-velocity profiles for more than 650 substances. The database with graphical user interface containing experimental data and typical 1D computational experimental setups has been worked out. One can search the information in the database and obtain the experimental points in tabular or plain text formats directly via the Internet using common browsers. It is also possible to draw the experimental points on graphs in comparison with different approximations and results of equation-of-state calculations. One can present the results of calculations in text or graphical forms and compare them with any experimental data available in the database.

The database uses client-server architecture. The access is granted by user account thru local network or Internet. The client can use any Internet browser and any platform, such as workstation or network gadget. The server part includes www Apache and PostgreSQL servers. The client request comes from www to SQL server thru program interface written with the use of PHP and Perl tools. The query result is output via the interface from the server to the SQL- www-server of the user and then in the form of tables or graphs. Free software is used. Database includes the administrative module providing for user's access, implementing and editing of data as well as connecting of calculation modules; service functions with user interface and a calculation module for modeling shock-wave processes.

This work was performed under the auspices of the ROSATOM State Atomic Energy Corporation under Contract No. H4x.44.90.13.1112.



STANDARD ENTHALPY OF FORMATION OF L –THREONINE

Lukyanova V.A.¹, Pimenova S.M.¹, Druzhinina A.I.¹, Gimadeev A.A.², Sagadeev E.V.²

¹Department of Chemistry, Lomonosov Moscow State University, Leninskie Gory 1, bl.3, Moscow, 119991, Russia

²Physical and Colloid Chemistry Department, Kazan National Research Technological University, Karl Marx street 68, Kazan, 420015, Russia

E-mail: lukyanova@phys.chem.msu.ru

L-threonine (C₄H₉NO₃, L-Thr) is one of the most important irreplaceable amino acids, which plays a great role in human life. L-Thr is involved in the natural synthesis of protein and enzymes, supports normal functioning of the Central nervous, immune and cardio-vascular systems and has other useful properties. Thermodynamic data are necessary for the understanding of protein biosynthesis. The literature review showed that between the experimental values of the enthalpy of L-Thr formation the maximum difference is more 30 kJ·mol⁻¹ [1, 2]. This work is devoted to clarify the enthalpy of formation of L-Thr.

The commercial sample of L-Thr was obtained from Matrix Company. The content of the basic substance in the original sample constituted 0.993 mass.%. It was purified by twice of precipitation from a saturated aqueous solution (deionized water, "MilliQ") with excess of isopropanol (LiCrosolv, LC-MS grade); precipitated crystals of L-Thr were first dried in vacuum (~2.6 Pa) and then in a desiccator over phosphorus oxide. According to elemental analysis, found (mass.%): C (40.2±0.2), H (7.7± 0.3) and N (11.8± 0.3). The content of elements in the purified sample is consistent with the theoretical values in limits of error (mass%) : C (40.33), H (7.62) and N (7.62). This corresponds to a purity better than (0.998 ±0.002 mass.%).

The combustion energy of crystalline L-Thr was determined in a static-bomb isoperibolic calorimeter. The temperature rise ~1K was measured by means of a copper resistance thermometer and a bridge scheme. About 0.5g of L-Thr was pressed into tablet, sealed into a Terylene-film bag and burned together with a tablet of benzoic acid at initial $T = 298.15\text{K}$ and $p = 3.04\text{MPa}$. 2 ml of distilled water was placed into the bomb to dissolve the NO₂ (g), formed in the experience. The products of the combustion were analyzed for CO₂ (g), HNO₃ (aq) and the absence of CO (g); a traces of soot were detected in separate experiments.

The mean value specific energy of combustion, $\Delta_c u^\circ(\text{cr}) = (-17506.7 \pm 4.7) \text{ J/g}$, was obtained on the basis of nine experiments. The molar energy of combustion, $\Delta_c U_m^\circ = (-2085.4 \pm 0.7) \text{ kJ/mol}$ refers to following reaction of combustion: C₄H₉NO₃(cr) + 4.75 O₂(g) = 4 CO₂(g) + 4.5 H₂O(l) + 0.5 N₂(g). The enthalpies of combustion, $\Delta_c H_m^\circ(\text{cr})$ kJ/mol, and formation, $\Delta_f H_m^\circ(\text{cr,g})$ kJ/mol, of L-Thr in crystalline and gaseous states found in this work and the literature data are given in Table 1.

Table 1. Standard enthalpy of combustion and formation of L-Thr at $T = 298.15 \text{ K}$

$\Delta_c H_m^\circ(\text{cr})$, kJ/mol	$\Delta_f H_m^\circ(\text{cr})$, kJ/mol	$\Delta_f H_m^\circ(\text{g})^*$, kJ/mol	Reference
-2086.0 ± 0.6	-774.3 ± 0.8	-613.3 ± 7.0	This work
-2053.1 ± 0.84	-807.2 ± 0.9	-646.2 ± 7.1	Tsuzuki et al. (1958) [1,3]
-2084.6 ± 1.1	-776.3 ± 1.1	-615.3 ± 7.1	Wu et al. (1993) [2,3]
-2071.3 ± 3.1	-790.0 ± 3.1	-629.0 ± 7.6	Contineanu et al. (2013) [4]

*the value of $\Delta_f H_m^\circ(\text{g})$ was calculated using enthalpy of sublimation, $\Delta_s H_m^\circ = 161 \pm 7 \text{ kJ/mol}$, from [5].

Our results are consistent with the data of [2] and significant differ from the data [1, 4]. The works [1, 4] have a number of drawbacks. The values of $\Delta_c H_m^\circ(\text{cr})$ and $\Delta_f H_m^\circ(\text{cr})$ of [2] is listed in [3], but the original article [2] is not available for the analysis of experimental results. The results obtained in this study for the enthalpy of combustion and enthalpy of formation of L-Thr are recommend regarded as the most reliable.

[1] Tsuzuki, T; Harper, D; et al. J. Phys. Chem., 1958, 62, 1594–1595.

[2] Wu, D; Zhu, Y; et al. J. Wuhan Univ. (Natl. Sci. Ed.), 1993, 78–82.

[3] <<http://webbook.nist.gov/chemistry/>>.

[4] Contineanu, I; Neacsu, A; et al. Thermochemica Acta, 2013, 563, 1–5.

[5] Tyunina, V; Krasnov, A; et al. J. Chem. Thermodyn., 2016, 98, 62–70.



THERMODYNAMIC PROPERTIES OF $\text{Ph}_4\text{SbOC(O)CCPh}$

Lyakaev D.V.¹, Markin A.V.¹, Smirnova N.N.¹, Sharutin V.V.², Sharutina O.V.²

¹Lobachevsky State University, 603950 Nizhny Novgorod, Russia

²South Ural State University National Research, 454080 Chelyabinsk, Russia

E-mail: lyakaev94@mail.ru

Nowadays there is wide variety of organic derivatives of metals with different properties. Among them, antimony complexes have been reported with good cytotoxicity and antitumor activities. Physicochemical characteristics of this type compounds, especially influential key quantities, are essential as fundamental data and for estimating the thermal processes with these compounds participation.

In the present work for the first time the temperature dependence of the heat capacity of $\text{Ph}_4\text{SbOC(O)CCPh}$ was determined in the range of 5–480 K by methods of adiabatic vacuum calorimetry (AVC) and differential scanning calorimetry (DSC).

The heat capacity of sample was measured over the range of 6–300 K by a BKT-3.0 fully automatic adiabatic vacuum calorimeter with liquid helium and nitrogen used as cooling agents, the range from 300 K to 480 K with the differential scanning calorimeter DSC204F1 Germany, Netzsch Gerätebau.

The fusion of the compound under study was established over the range of 420–450 K, and its thermodynamic characteristics (enthalpy, entropy and temperature range) were defined and analyzed. The interpretation of ligands influence was made. Also the purity of sample was evaluated.

Using thermal microbalance TG209F1, Germany, Netzsch Gerätebau, the thermal stability of the compound was identified.

The complex of standard thermodynamic functions (heat capacity, enthalpy, entropy, and Gibbs energy) was given for the various physical states in the range from $T \rightarrow 0$ to 450 K. The energy of combustion, standard enthalpy of combustion, formation enthalpy, formation entropy, Gibbs energy of formation of a substance in the crystalline state at $T = 298.15$ K were calculated. Comparison of thermodynamic properties was made for the derivative of antimony studied in the present work, Ph_5Sb and $\text{Ph}_4\text{Sb}(\text{OC(O)C}_{10}\text{H}_{15})$

Multifractal treatment of low-temperature heat capacity was made as a result the topological structure of the compound was established. The comparison of structure of understudied and others organoantimony compounds was made.



THERMODYNAMIC PROPERTIES OF C₇₀ FULLERIDES WITH ORGANOELEMENT FRAGMENTS

Samosudova Ya.S., Ogurtsov T.G., Markin A.V., Smirnova N.N., Lyakaev D.V.

Lobachevsky State University of Nizhni Novgorod, 603950 Nizhni Novgorod, Russia

E-mail: sayanina@yandex.ru

From the first synthesis of fullerene C₆₀ and C₇₀ in microquantities, numerous studies on fullerenes and their functional derivatives that exhibit potentially valuable properties have been undertaken. So, donor-acceptor complexes of fullerenes in which the latter plays the role of relatively strong acceptors are actively used as materials with unusual optical, magnetic and electrical conductivity properties. The complexes with aromatic hydrocarbons as donor partners were synthesized more often and their physico-chemical properties have been studied. As a result of these investigations for some bis-(η⁶-arene)chromium fullerides the low-temperature dimerization of anion-radicals of the fullerene was detected.

Nevertheless, there have been no data in literature about heat capacity and thermodynamic properties of fullerene C₇₀ functional derivatives with organoelement fragments. They are however, necessary as fundamental data for new functional derivatives of C₇₀ to understand the nature of low-temperature dimerization of fullerene fragments as well as to detect the influence of organoelement groups on the «hardness» and the stability of bonds between fullerene fragments in the low-temperature dimeric phase of (C₇₀)₂. Therefore the goal of this work is a calorimetric investigation the temperature dependences of the heat capacity of crystalline *bis*-(η⁶-diphenyl)chromium fulleride [(η⁶-Ph₂)₂Cr]^{•+}[C₇₀]^{•-} and *bis*-(η⁶-trimethylbenzene) chromium fulleride [(η⁶-[1,3,5-trimethylbenzene](#))₂Cr]^{•+}[C₇₀]^{•-} between $T = (6 \text{ and } 350) \text{ K}$ by the method of precision adiabatic calorimetry.

A reversible relaxation glassy transformation (a G-type transition) was observed for fulleride [(η⁶-Ph₂)₂Cr]^{•+}[C₇₀]^{•-} in the range from $T = (12 \text{ to } 30) \text{ K}$ and its thermodynamic characteristics were estimated. The nature of this transition is associated with disordered defrost rotational motions of the phenyl groups in *bis*-(η⁶-diphenyl)chromium fulleride C₇₀.

The standard thermodynamic functions, namely, the heat capacity $C_p^0(T)$, enthalpy $H^\circ(T) - H^\circ(0)$, entropy $S^\circ(T) - S^\circ(0)$ and potential Φ_m° , for the range from $T \rightarrow 0 \text{ K}$ to 350 K and the standard entropies of formation of fullerides have been calculated. The thermodynamic characteristics of the investigated samples have been compared with the data for studied earlier

This work was performed with the financial support of the Russian Foundation for Basic Research (Projects No. 16-33-00713 mol_a).



THERMODYNAMIC PROPERTIES OF POLYMETHYLSILSESQUIOXANE NANOGELS

Sologubov S.S.¹, Sarmini Yu.A.¹, Markin A.V.¹, Smirnova N.N.¹, Muzafarov A.M.^{2,3}

¹Lobachevsky State University of Nizhni Novgorod, 603950 Nizhni Novgorod, Russia

²Nesmeyanov Institute of Organoelement Compounds of Russian Academy of Sciences, 119991 Moscow, Russia

³Enikolopov Institute of Synthetic Polymeric Materials of Russian Academy of Sciences, 117393 Moscow, Russia

E-mail: s.slg90@gmail.com

Nanogels are nanosized hydrogel particles with three-dimensional networks formed by physically or chemically cross-linked polymer chains. In recent years, they have attracted more attention because of their high stability, biocompatibility, and adjustable chemical and mechanical properties. These unique properties provide great opportunities for the use of nanogels in biomedical applications, such as tissue engineering, diagnostics, and, most importantly, as nanocarriers in drug delivery.

The investigation of standard thermodynamic properties of nanogels in a wide temperature range by precision calorimetry allows us to reveal and analyze practically important dependences of thermodynamic properties on their composition and structure.

In the present work, the temperature dependences of heat capacities of two polymethylsilsesquioxane (PMSSO) nanogels were measured for the first time in the temperature range from 6 to 350 K by precision adiabatic vacuum calorimetry. The glass transition was detected for both investigated samples in the above temperature interval, and thermodynamic characteristics of the revealed transformation were determined and analyzed. The standard thermodynamic functions, namely, heat capacity $C_p^\circ(T)$, enthalpy $[H^\circ(T) - H^\circ(0)]$, entropy $[S^\circ(T) - S^\circ(0)]$, and the Gibbs energy $[G^\circ(T) - H^\circ(0)]$ were calculated for the range from $T \rightarrow 0$ to 350 K, and the standard entropies of formation $\Delta_f S^\circ$ at $T = 298.15$ K were also determined for nanogels under study.

The obtained thermodynamic characteristics of the investigated nanogels were compared with the data for corresponding dendrimers. As a result, some conclusions were made, and the physicochemical discussion of the structural organization of nanogel systems was proposed. The structural characteristics and composition of nanogels were used for these conclusions.

This work was performed with the financial support of the Russian Foundation for Basic Research (Projects №№ 15-03-02112, 16-33-00713).



ELECTRONIC STRUCTURE OF [NiSalen] DERIVATIVES MODIFIED BY NITROXYL RADICALS

Mashkovtsev D.N., Hrom S.I., Levin O.V., Sizov V.V.

Institute of Chemistry, Saint Petersburg State University Saint Petersburg, Russia

E-mail: mashkovtcev.dn@gmail.com

The performance of electrodes in batteries, supercapacitors and electrochemical sensors can be improved via modification by conducting polymer films, e.g., films composed of polymeric transition metal complexes. Complexes based on derivatives of Salen ligand provide a versatile tool for construction of polymeric systems with desired electrochemical properties.

In this work the properties of hypothetical derivatives of [NiSalen] are studied by quantum chemical calculations. The goal of this work is to compare the redox properties of a series of [NiSalEn]-based species with free-radical substituents and to select the most promising candidate compounds for synthesis and further experimental studies in the context of asymmetric catalysis, antibacterial drug design, improved materials for Li-ion batteries, etc. Quantum chemical calculations are carried out for monomer and dimer complexes using density functional theory. The analysis of the properties is focused on the redistribution of electron density upon oxidation/reduction of the complexes and the energetic effects of these processes. Electron density in complexes is described via density distribution plots and effective charges of fragments, while the energy effects upon oxidation are characterized by energy (or free energy) changes and effective reduction potentials, which can be directly compared to the experimental measurements. Using these techniques, one can identify the contribution of different fragments of the complex to withdrawal of electrons, which provides the necessary information on structure-property relationship and serves as the foundation for targeted optimization of electrochemical properties.

The calculations were performed using the facilities provided by the Computational Resource Center (Research Park, Saint Petersburg State University).

This work is supported by the Russian Science Foundation (grant # 16-13-00038).

**THERMOCHEMISTRY OF BISMUTH-COBALT OXIDE DOPED BY ERBIUM**

Matskevich N.I.¹, Wolf Th.², Adelman P.², Fuchs D.², Semerikova A.¹, Vyazovkin I.¹, Matskevich M.¹, Anyfrieva O.¹

¹Nikolaev Institute of Inorganic Chemistry, Siberian Branch of the Russian Academy of Sciences, 630090 Novosibirsk, Russia

²Karlsruhe Institute of Technology, Institute of Solid State Physics, D-76334 Karlsruhe, Germany

E-mail: nata.matskevich@yandex.ru

Compounds on the basis of bismuth oxide are widely used for gas monitoring and combustion control, in metallurgy, petrology, chemical kinetics, in solid state electrolyte fuel cells *etc.* As was established in a number of papers the bismuth oxide conductivity is two orders of magnitude greater than that of yttrium-stabilized zirconia at the same temperatures. The delta form of bismuth oxide shows the highest value of conductivity. The problem is that the δ - Bi_2O_3 phase exists in a narrow temperature range (1000-1100 K). A lot of papers are devoted to the problem of delta form of bismuth oxide stabilization. The attempts to stabilize the bismuth oxide by adding rhenium and rare earth elements were taken in papers [1-2]. The phases obtained [1-2] are related to cubic δ - Bi_2O_3 but have low-temperature oxide ion conductivities that are significantly higher than previously reported for δ - Bi_2O_3 phases and comparable to those of BIMEVOX materials.

In the present study, we measured the dissolution enthalpy, calculated enthalpy of formation and thermodynamic stability of the $\text{Bi}_{2.67}\text{Er}_{0.33}\text{CoO}_x$ phase. In addition, we calculated the lattice energy in two ways according to the Kapustinskii rule and compared this value with the lattice energy calculated by the Born-Haber cycle using our experimental data. Moreover we measured the magnetic properties of $\text{Bi}_{2.67}\text{Er}_{0.33}\text{CoO}_x$ in the temperature range of 2-300 K.

The compound with composition $\text{Bi}_{2.67}\text{Er}_{0.33}\text{CoO}_{5.83}$ was synthesized from bismuth oxide (Bi_2O_3), erbium oxide (Er_2O_3) and cobalt (II, III) oxide (Co_3O_4). Synthesis was performed by solid state reaction. X-ray analysis showed that the phase was pure. Phase was indexed in monoclinic structure (P 2/m space group). Thermochemical cycle was constructed in such a way that investigated compound ($\text{Bi}_{2.67}\text{Er}_{0.33}\text{CoO}_{5.83}$) was dissolved in 1 mol dm^{-3} HCl. We also dissolved Bi_2O_3 in 1 mol dm^{-3} HCl. The thermochemical cycle allows us to calculate the standard formation enthalpy for $\text{Bi}_{2.67}\text{Er}_{0.33}\text{CoO}_{5.83}$. The dissolving experiments were carried out in solution calorimetry with isothermal jacket [1-2].

On the basis of measured experimental and literature data we calculated the standard formation enthalpy for compound $\text{Bi}_{2.67}\text{Er}_{0.33}\text{CoO}_{5.83}$. Further it was interesting to calculate the thermodynamic stability for $\text{Bi}_{2.67}\text{Er}_{0.33}\text{CoO}_{5.83}$ in respect to decomposition to binary oxides (Bi_2O_3 , Er_2O_3 , Co_3O_4). Using obtained standard formation enthalpy measured by us and standard formation enthalpies for binary oxides taken from literature we calculated the formation enthalpy for $\text{Bi}_{2.67}\text{Er}_{0.33}\text{CoO}_{5.83}$ from binary oxides. We established that compound $\text{Bi}_{2.67}\text{Er}_{0.33}\text{CoO}_{5.83}$ is thermodynamically stable in respect to decomposition to binary oxides.

For investigated compound $\text{Bi}_{2.67}\text{Er}_{0.33}\text{CoO}_{5.83}$ we estimated the lattice energy by two ways using Kapustinskii rule. After calculation we compare the calculated values for lattice energy with lattice energy obtained by us from Born-Gaber cycle on the basis of experimentally measured standard formation enthalpy. Comparison of experimental lattice energy with lattice energy calculated using Kapustinskii rule allows one to conclude that in an accuracy of 1% the values are in a good agreement.

Since the compound is new and not investigated, we also carried out the measurement of magnetic characteristics. The magnetic properties of the samples were studied using a superconducting quantum interference device (Quantum Design MPMS XL). Field-cooled measurements were taken at field strength of 0.1 T in the temperature range $2 \text{ K} \leq T \leq 300 \text{ K}$. The magnetization of sample shows Curie-like temperature dependence down to 2 K. Obviously the sample seems to be paramagnetic down to 2 K.

This work is supported by Karlsruhe Institute of Technology (Germany) and Government Task for NIIC SB RAS.

[1] Matskevich, N; Wolf, Th; Greaves, C; Bryzgalova A. J. *Alloys Comp.*, 2014, 582, 253-256.

[2] Matskevich, N; Wolf, Th; Greaves, C; Adelman, P. *J. Chem. Thermodyn.*, 2015, 91, 234-239.

**THERMOCHEMICAL STUDY OF THE ENTHALPIES OF FORMATION AND REORGANIZATION OF SOME BIPHENYL AND DIPHENYL OXIDE RADICALS**Pashchenko L.L.¹, Miroschnichenko E. A.², Kon'kova T.S.²¹Department of Chemistry, Lomonosov Moscow State University, Lewinski Gory 1, bl.3, Moscow, 119991, Russia²Semenov Institute of Chemical Physics RAS, Kosygin str. 4, Moscow, 119991, RussiaE-mail: eamir02@mail.ru

Aromatic compounds, including 4-nitrobiphenyl and others, are important industrial chemicals with a broad range of applications. This class of compounds is widely used in the synthesis of many diverse products, including drugs, dyes, polymers, pesticides and explosives. Some aromatic nitro compounds are highly explosive, especially when the compound contains more than one nitro group. To investigate the stability and performance of these chemicals, the knowledge of the enthalpy of formation ($\Delta_f H^{\circ}_{298}$) is an essential requirement. Other thermo-chemical properties, such as enthalpy of vaporization ($\Delta_{\text{vap}} H^{\circ}_{298}$) and enthalpy of sublimation ($\Delta_{\text{sub}} H^{\circ}_{298}$), are needed for the characterization of the chemical degradation pathways of aromatic nitro and oxide compounds.

Despite the extensive studies of aromatic nitro compounds and diphenyl oxide, available thermo-chemical experimental information is often scarce and frequently shows significant discrepancy among published results. The enthalpies of formation of 4-nitrobiphenyl and 1, 1'-biphenyl were calculated using their enthalpies of sublimation. In this work, the standard $\Delta_{\text{sub}} H^{\circ}_{298}$ were determined on micro-calorimeter Calvet over the temperature range from 323 to 373 K with an estimated accuracy of < 1 per cent. We have used these experimental results for correlating the enthalpies of sublimation of 4-nitrobiphenyl and 1, 1'-biphenyl with the temperature in order to test internal consistency of the experimental data. The average values of the standard enthalpies of vaporization were adjusted to 298.15 K.

On the base of "double the difference" method the novel scheme for formation enthalpies of aromatic radicals calculations have been suggested. Using fundamental equations of the chemical physics, the new calculation method is offered to determine the energies of reorganization of molecules fragments into radicals. Formation enthalpies of radicals a namely biphenyl, diphenyl-oxide and phenyl-oxide are determined, using their enthalpies of formation in gas state [1]. Restructuring energies of these radicals and bond dissociation energies are calculated (kJ mol^{-1}): phenyl 0; piridyl-4-yl 0; piridyl-3-yl 4; piridyl-2-yl 33; biphenyl-4-yl 0; diphenyl-oxide-4-yl 0; $\text{C}_6\text{H}_5\text{O}^{\bullet}$ -100.8 и $\text{C}_6\text{H}_5\text{C}^{\bullet}\text{H}_2$ -40.2. Restructuring energy of phenyl radical gives way to calculate for the first time median thermo-chemical energies of bonds in benzene: $E(\text{C}-\text{H}) = 472, 8 \text{ kJ}\cdot\text{mol}^{-1}$ and $E(\text{C}-\text{C}) = 448, 1 \text{ kJ}\cdot\text{mol}^{-1}$. Energies of bonds in pyridine $E(\text{C}-\text{H})$ and $E(\text{C}-\text{C})$ are same as in benzene, and energies of bonds, $E(\text{C}-\text{N}) = 424, 5 \text{ kJ mol}^{-1}$.

Table 1. Power properties of biphenyls and enthalpy of formation of biphenyl-4-yl, $\text{kJ}\cdot\text{mol}^{-1}$

Compound	$\Delta_f H^{\circ}_{(g)}(298.15\text{K})$	$\Delta_f H_{\text{BP}}(\text{NO}_2)$	$\Delta_f H_{\text{BP}}(\text{H})$	$\Delta_{\text{vap}} H_{\text{exp}}(298.15\text{K})$
Biphenyl (BP)	179.9 ± 2.9	432.6	–	81.5 ± 0.8
4-nitroBP	154.4 ± 7.1	–	425.9	108.4 ± 0.9
4-methylBP	143.3 ± 1.3	429.7	429.7	69.7 ± 0.7
4-iso-propylBP	97.2 ± 2.5	430.1	430.1	76.6 ± 0.5
4-tert-butylBP	72.0 ± 2.8	431.8	431.8	79.6 ± 0.8

[1] Druzhinina, A.I.; Pimenova, S.M.; Tarasnov, S.V.; Nesterova, T.N.; Varushchenko, R.M. J. Chem. Thermodyn., 2015, 87, 69-74.



SUBLIMATION THERMODYNAMICS OF COBALT (II) PIVALATE COMPLEXES

Morozova E.A., Malkerova I.P., Kiskin M.A., Alikhanyan A.S.

N. S. Kurnakov Institute of General and Inorganic Chemistry, Russian Academy of Sciences, 117234 Moscow, Russia

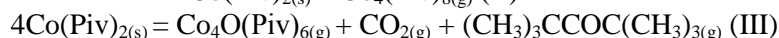
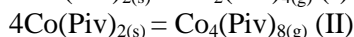
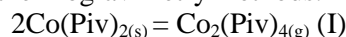
E-mail: cathrine_15@mail.ru

Two cobalt (II) pivalate complexes [CoPiv₂] and [Co₄OPiv₆] (Piv = (CH₃)₃CCOO) were studied by Knudsen Effusion Mass Spectrometry method on a MS 1301 spectrometer having a 50-1000 amu mass range, using 60-70 eV ionizing electrons. The complexes were vaporized from a Knudsen cell. The ratio (surface of evaporation)/(surface of effusion) hole was about 600. The cell temperature was measured with a Pt/Pt(Rh) thermal couple (±1 K).

Complex [CoPiv₂] was prepared according the technique described in the article [1]. The [Co₄OPiv₆] was synthesized by interaction between cobalt hydroxide and pivalic acid. The obtained blue-violet precipitate was filtered on a Buchner funnel and sublimed at dynamic vacuum ~ 1.33 Pa at T = 420 K. The C, H contents were determined by conventional elemental analysis. Anal. Calcd.: %C 41.96, %H 6.29; Found: %C 40.96, %H 6.44.

The mass-spectrum and the thermodynamic characteristics of investigated compounds are represented in Table 1 and 2.

They show that the saturated vapor over solid [CoPiv₂] consists mainly of dimeric species, small amount of tetrameric ones but also oxopivalate was detected in vapor too. Thus the complex sublimes congruently reactions I-III) and the sublimation process is accompanied by thermal decomposition (reaction III). Such behavior corresponds to the results of thermolysis study of this complex obtained in [1] by using the differential scanning calorimetry and thermogravimetry methods.



Partial thermal decomposition of [CoPiv₂] during sublimation should be taken into account by use of this compound in MOCVD.

The [Co₄OPiv₆] sublimes congruently without decomposition (reaction IV).



Table 1. Intensities of main ion currents (relative units) in mass spectra [Co₂Piv₄] and [Co₄OPiv₆].

[CoPiv ₂] (U _{ion} = 68 eV; T = 587 K)		[Co ₄ OPiv ₆] (U _{ion} = 60 eV; T = 423 K)	
[Co ₂ Piv ₃] ⁺	100	[Co ₄ OPiv ₅] ⁺	100
[Co ₂ Piv ₂] ⁺	14.8	[Co ₄ OPiv ₆] ⁺	15.7
[Co ₂ Piv] ⁺	3.3	[Co ₄ OPiv ₄] ⁺	5.7
[CoPiv] ⁺	22.1	[Co ₄ OPiv ₃] ⁺	7.9
[Co ₄ OPiv ₅] ⁺	3.4	[(Co ₄ OPiv ₃ -(C(CH ₃) ₃)] ⁺	85.6
[(Co ₄ OPiv ₃ -(C(CH ₃) ₃)] ⁺	4.3	[Co] ⁺	20.7
[Co] ⁺	36.1		
* low-intensity ions (less than 0.002) from [Co ₄ Piv ₈] molecule were registered			

Table 2. Temperature dependencies of saturated vapor pressures of [Co₂Piv₄] and [Co₄OPiv₆].

Complex	A ^[a]	B ^[a]	T range (K)	Δ _s H ^o _T (kJ/mol)
[CoPiv ₂]	8638 ± 534	14.61 ± 0.15	423 - 588	165.1 ± 10.2
[Co ₄ OPiv ₆]	9376 ± 450	21.64 ± 0.15	403 - 448	179.2 ± 8.6

$$^{[a]} \lg P (\text{Pa}) = -A/T + B$$

[1] Fomina, I; Aleksandrov, G; Dobrokhotova, Zh. Russ. Chem. Bull., 2006, 55, 1909-1919.

THE STANDARD ENTHALPY OF FORMATION OF COPPER (I) PIVALATE. THE EVALUATION TECHNIQUE

Morozova E.A., Dobrokhotova Zh.V., Alikhanyan A.S.

N. S. Kurnakov Institute of General and Inorganic Chemistry, Russian Academy of Sciences, 117234 Moscow, Russia

E-mail: cathrine_15@mail.ru

In present work the technique of evaluation of the standard enthalpy of formation was developed for carboxylate complexes by use of differential scanning calorimetry (DSC) method.

Previously [1,2] the heterogeneous synthesis of anhydrous pivalates was suggested that involves in heating of binary system $[n(\text{CH}_3)_3\text{CCOOAg} + \text{M}; \text{M} - \text{metal}]$ in the temperature interval 400-550 K. That way copper (I) pivalate was obtained and characterized [3]. The study of temperature dependence of heat flow for the system by DSC (fig.1) allowed us to determine the enthalpy of the reaction $(\text{CH}_3)_3\text{CCOOAg}_{(s)} + \text{Cu}_{(s)} = (\text{CH}_3)_3\text{CCOOCu}_{(s)} + \text{Ag}_{(s)}$, $\Delta_f H_{298,15}^\circ = -39.6 \pm 5.2 \text{ kJ mol}^{-1}$. The observed two endothermic effects relate to phase transitions in silver pivalate [4].

Using the enthalpy of silver pivalate $(\text{CH}_3)_3\text{CCOOAg}_{(s)}$ formation, measured earlier [5], the value of standard enthalpy of copper (I) pivalate formation was estimated: $\Delta_f H_{298,15}^\circ [(\text{CH}_3)_3\text{CCOOCu}_{(s)}] = -506.5 \pm 7.6 \text{ kJ mol}^{-1}$.

The thermal behavior of the system was studied on DSC

204 F1 NETZSCH in aluminium cells and thermogravimetry analysis on TG 209 F1 NETZSCH in alundum crucibles. Samples were heated under dry argon (20 ml min^{-1}) with a rate of 5 deg min^{-1} , which was the same in all experiments. The accuracy of determination of the temperature of anomalies and the heat effects in the thermograms was $\pm 1^\circ$ and $\pm 10 \%$, respectively. Manipulation of data was carried out according to standards ISO 11357-1, ISO 11357-2, ISO 11358, ASTM E 1269-95 using NETZSCH Proteus Thermal Analysis.

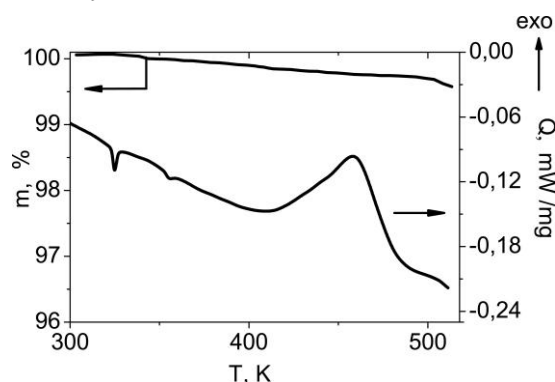


Figure 1. Temperature dependences of the weight change and heat flow for $[(\text{CH}_3)_3\text{CCOOAg} + \text{Cu}]$ system

[1] Didenko, K; Alikhanyan, A. XVI Int. Conf. Chem. Thermodyn. Russ. (RCCT 2007), Suzdal, 2007, 4/S-368.

[2] Kamkin, N; Kayumova, D; Yaryshev, N. Russ. J. Inorg. Chem., 2012, 57, 1308-1312.

[3] Alikhanyan, A; Didenko, K; Girichev, G. Struct. Chem., 2011, 22, 401-409.

[4] Morozova, E; Dobrokhotova, Zh; Churakov, A. Int. Conf. Therm. Anal. Calorim. Russ., 2016, 606-608.

[5] Lukyanova, V; Papina, T; Didenko, K. J. Therm. Anal. Calorim., 2008, 92, 743-746.

**VOLATILE COMPLEXES OF RARE-EARTH METALS AND ZIRCONIUM:
SYNTHESIS, THERMAL AND STRUCTURAL PROPERTIES**Mosyagina S.A.^{1,2}, Zherikova K.V.², Stabnikov P.A.², Kuratieva N.V.², Trubin S.V.²¹Novosibirsk State University, 630090 Novosibirsk, Russia²Nikolaev Institute of Inorganic Chemistry, Siberian Branch of the Russian Academy of Sciences, 630090 Novosibirsk, Russia

E-mail: masianiaapaser@mail.ru

In present time beta-diketonates of rare-earth elements and zirconium are used as precursors for obtaining different films and coatings by metal organic chemical vapor deposition (MOCVD). Physico-chemical properties of these materials allow their usage, for example, as high-*k* dielectric, optic and optoelectronic coatings in microelectronics and in fuel cells. One of the actively developing areas is the production of thermal barrier coatings based on zirconium dioxide doped by rare-earth metals – promised material of new generation gas turbines for the purpose of energy supply. However, it is necessary for technological purposes to develop synthetic procedures for precursors that make it possible to obtain pure compounds at ordinary conditions in lab-scale quantities with high yields (at least 70%). Such methods were developed by us for obtaining yttrium(III), neodymium(III), samarium(III), and zirconium(IV) dipivaloylmethanates (dpm). From the point of successful MOCVD process, the information on the structural and thermal properties of the precursors already known in the literature as well as new, perhaps, more appropriate ones is also needed. Since the thermal barrier coatings used in gas turbines consist of zirconium dioxide doped by rare-earth metals it seems to be effective to investigate also the thermal properties of the precursors' mixtures. As a result, new crystal structures of Sc(ptac)₃ (ptac = pivaloyltrifluoroacetato-), Sc(ptac)₃·EtOH, Sc(acac)₃ (acac = acetylacetonato-), Sc(tfac)₃ (tfac = trifluoroacetylacetonato-), [Y(ptac)₃]₂, Y(ptac)₃(H₂O)₂, Y(dpm)₃·en (en = ethylenediamine), [Nd(dpm)₃]₂, [Sm(dpm)₃]₂ were studied; the information on melting temperatures, vapor pressures and condensed phase behaviors was obtained for yttrium(III), neodymium(III), samarium(III) and zirconium(IV) dipivaloylmethanates and their mixtures as well as for yttrium(III) dipivaloylmethanate derivatives with ethylenediamine, tetramethylethylenediamine (tmeda) and bipyridyl (bipy) by using TG/DTA and Knudsen effusion method with mass-spectrometric registration of the gas phase composition (fig. 1).

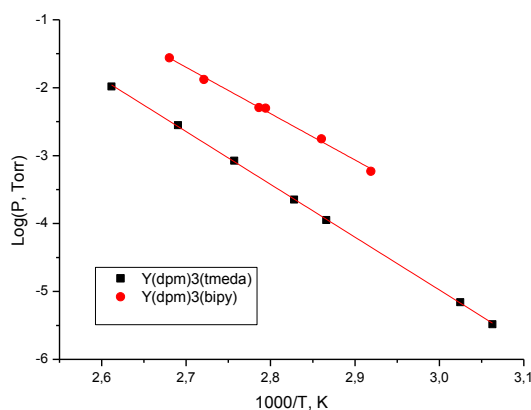


Figure 1. *p-T dependences of compounds with diimines*

Acknowledgment: This work was supported by RSF № 16-19-10325; authors are grateful to A.V. Korol'kov and N.V. Pervukhina for X-ray diffraction research, and P.E. Plusnin for thermogravimetric research.

THERMODYNAMIC PROPERTIES: HEAT CAPACITY, ENTROPY AND ENTHALPY OF BARIUM TUNGSTATE UP TO 304 K

Naumov V.N.¹, Musikhin A.E.¹, Bespyatov M.A.¹, Shlegel V.N.¹, Safonova O.E.²

¹Nikolaev Institute of Inorganic Chemistry, Siberian Branch of the Russian Academy of Sciences, 630090 Novosibirsk, Russia

²V.S. Sobolev Institute of Geology and Mineralogy, Siberian Branch of the Russian Academy of Sciences, 630090 Novosibirsk, Russia
E-mail: musikhin@niic.nsc.ru

Currently, the single crystals of molybdates and tungstates are the subject of extensive research due to their unique optical properties, which determine a number of their practical applications. Among them, great interest is attracted by barium tungstate, which is the most promising universal Raman-active crystal. It is used, for example, to create solid-state lasers. Many properties of this compound have already been investigated, including the experimental heat capacity in the 122–322 K range [1]. However, reliable data on its thermodynamic properties below 122 K are not represented in the literature. In this work we show the results of calculating thermodynamic properties of BaWO₄ in the 5.7–304 K range and some other of its characteristics based on experimentally obtained heat capacity.

The single-crystal sample of BaWO₄ was obtained by the Czochralski method under conditions of low temperature gradients. Barium tungstate belongs to the scheelite (CaWO₄) structural type and has an *I4₁/a* space group. The results of our structural analysis agree with the data shown in [2] very well.

The heat capacity $C_{p,m}(T)$ of the sample BaWO₄ in the 5.7–304 K range was measured by the adiabatic method. The methodology and setup using for heat capacity study fully comply with described in [3]. The sample weight was 51.490 g; the molar mass was 385.18 g·mol⁻¹. The analysis of the functional dependence of the heat capacity has not revealed any thermal anomaly in its behavior.

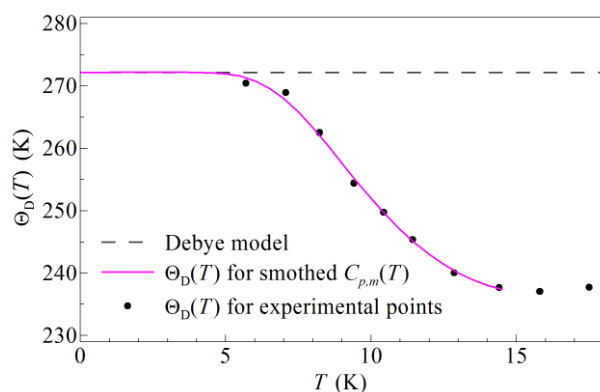


Figure 1. Debye temperature $\Theta_D(T)$ of BaWO₄ (experimental and smoothed data).

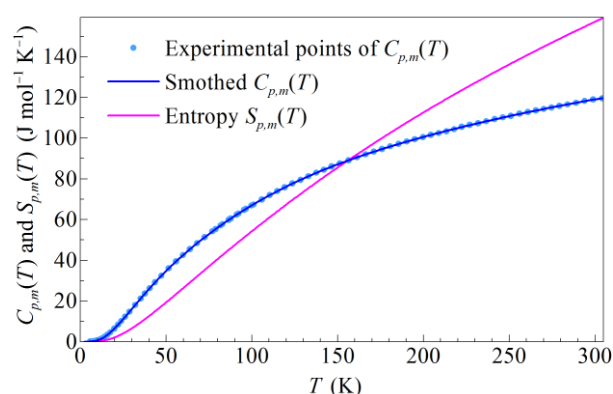


Figure 2. Heat capacity and entropy of BaWO₄.

For describing the BaWO₄ heat capacity near zero and extrapolating it to zero temperatures, we used the physically grounded approach described in [3]. In so doing, we assumed that the heat capacity of BaWO₄ had no anomalous contributions below 5.7 K. In the framework of this approach, the characteristic Debye temperature at zero was determined with high accuracy as 272.2 K. Fig. 1 shows the dependence of the Debye temperature $\Theta_D(T)$ near zero for BaWO₄ and for the Debye model. The area of validity of the Debye limit law (0–4.5 K), as well as the wider range of applicability (0–15 K) of the approach, which we used to describe the heat capacity, is clearly visible in the figure. Above 15 K, the experimental values of the heat capacity were smoothed using the method described in [3]. The smoothed $C_{p,m}(T)$ dependence over the temperature range 0–306 K was used to calculate the thermodynamic functions, including entropy, enthalpy and Gibbs free energy. The results are shown in Fig. 2.

This work was supported by the RFBR (research project No. 16-32-00884).

[1] Suda, J.; Zverev, P.G. *Vib. Spectrosc.*, 2012, 62, 85–91.

[2] JCPDS Diffraction File Card No. 43-0646.

[3] Musikhin, A.E.; Naumov, V.N.; Bespyatov, M.A.; Ivannikova, N.V. *J. Alloy. Compd.*, 2015, 639, 145–148.

LOW-TEMPERATURE HEAT CAPACITY OF SODIUM DIMOLYBDATE

Musikhin A.E., Naumov V.N., Bespyatov M.A., Ivannikova N.V., Grigor'eva V.D.

Nikolaev Institute of Inorganic Chemistry, Siberian Branch of the Russian Academy of Sciences, 630090 Novosibirsk, Russia

E-mail: musikhin@niic.nsc.ru

In this work, we present the results of experimental study of low-temperature heat capacity of sodium dimolybdate single crystal. The relevance of this functional material study is due to its unique optical properties. This material is used for a variety of optical systems, as well as a cryogenic phonon scintillation detector of high energy particles. Many properties of this compound have already been investigated, but reliable data on its low-temperature heat capacity are not presented.

The single-crystal sample of $\text{Na}_2\text{Mo}_2\text{O}_7$ was obtained by the Czochralski method under conditions of low temperature gradients. Obtained $\text{Na}_2\text{Mo}_2\text{O}_7$ crystal belongs to the base-centered orthorhombic type of structure with a space group of $Cmca$. Its density is $3.73 \text{ g}\cdot\text{cm}^{-3}$, unit cell dimensions are $a = 0.7170 \text{ nm}$, $b = 1.1836 \text{ nm}$ and $c = 1.4707 \text{ nm}$. The results of our structural analysis fully comply with the data shown in Ref. [1].

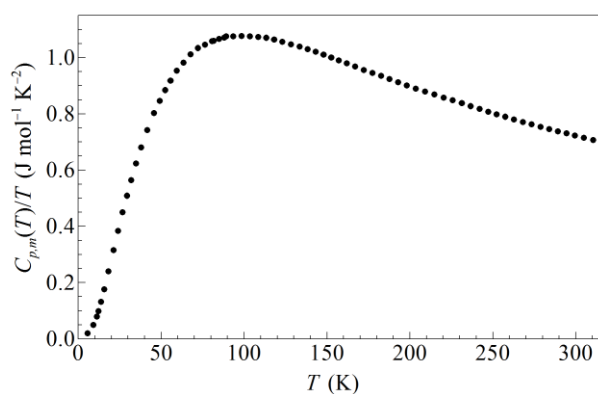


Figure 1. Experimental heat capacity of $\text{Na}_2\text{Mo}_2\text{O}_7$ in coordinates $C_{p,m}(T)/T$ versus T in the 6–310 K range.

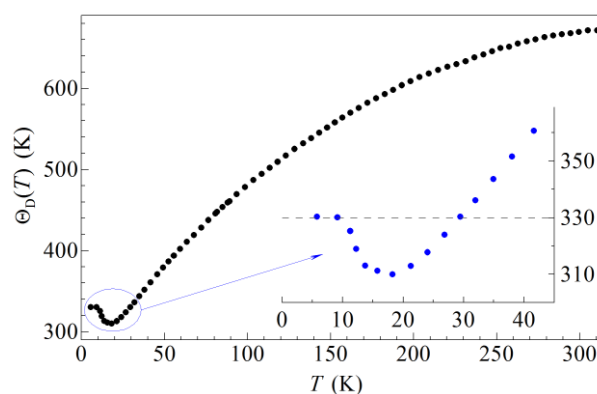


Figure 2. Debye temperature $\Theta_D(T)$ of $\text{Na}_2\text{Mo}_2\text{O}_7$ calculated from experimental heat capacity.

The heat capacity $C_{p,m}(T)$ of the sample $\text{Na}_2\text{Mo}_2\text{O}_7$ in the temperature range from 6 to 310 K was measured by the adiabatic method on the setup described in [2]. The single crystal was fragmented into smaller parts, which were placed in the calorimetric ampoule. The methodology of filling an ampoule with a substance, as well as with the heat exchange gas (helium), was described in [2]. The sample weight was 16.276 g. The molar mass used in the calculation of the molar heat capacity was determined from the formula $\text{Na}_2\text{Mo}_2\text{O}_7$ as $349.86 \text{ g}\cdot\text{mol}^{-1}$. The heat capacity has been measured in 75 points of the temperature range 6–310 K. Relative standard uncertainty of the heat capacity was 1% in the 6–20 K range; 0.3% in the 20–80 K range; and 0.15% in the 80–310 K range. The obtained experimental data in coordinates $C_{p,m}(T)/T$ versus T are shown in Fig. 1.

We calculated the Debye temperature dependence $\Theta_D(T)$ (Fig. 2) based on experimental heat capacity. The characteristic Debye temperature at zero was about 330 K, as shown by the first two experimental points. As can be seen in Figs. 1 and 2, the obtained results give no indications for the existence of any special features in heat capacity behavior associated with phase transitions.

This work was supported by the RFBR (research project No. 16-32-00884).

[1] Seleborg, M. Acta Chem. Scand., 1967, 21, 499–504.

[2] Naumov, V.N.; Nogteva, V.V. Instrum. Exp. Tech., 1985, 28, 1194–1199.



IMPACT OF THE INTERNAL POTENTIAL ENERGY ON THE THERMODYNAMIC STABILITY OF UNSUPPORTED SILVER CLUSTERS

Myasnichenko V.S.^{1,2}, Sdobnyakov N.Yu.

¹Tver State University, Sadovii per., 35, 170002 Tver, Russia

²Altai State Technical University, Lenina 46, 656038, Barnaul, Russia

E-mail: virtson@gmail.com

Potential-energy ‘landscapes’ (or surfaces, PES) play a key role in the analysis of structure, dynamics, and thermodynamics in molecular science. Atomic clusters can be valuable benchmark systems for developing and applying a wide variety of methodology and models [1]. For example, the structure of clusters has often been invoked when considering the local structure of bulk liquids and glasses. Most of the atoms are on the surface, and atomic-scale properties such as the lower coordination number of surface atoms are critical.

The work deals with the results of molecular-dynamic simulation of the atomistic structure's free energy and stability in silver clusters, using many-body tight-binding interatomic potential [2]. It is derived from Gupta's expression for the cohesive energy of a bulk material [3] and is generated by fitting experimental data to a pair potential containing repulsive pair and attractive many-body terms.

Surface effects have a huge impact on the stability of clusters at 0K. Focusing only on the stable structure or structures for each N (see Fig; 1) is useful to understand the structural evolution of clusters because, all other things being equal, lower-energy structures have greater equilibrium populations. However the population of an isomer structure is not solely determined by its potential (binding) energy.

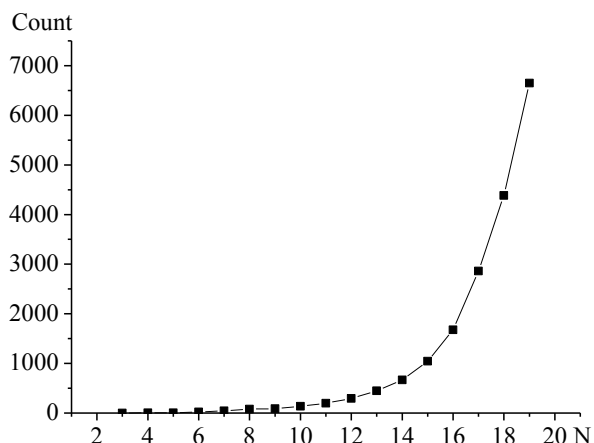


Figure 1. Size dependence of stable structures number for Ag clusters.

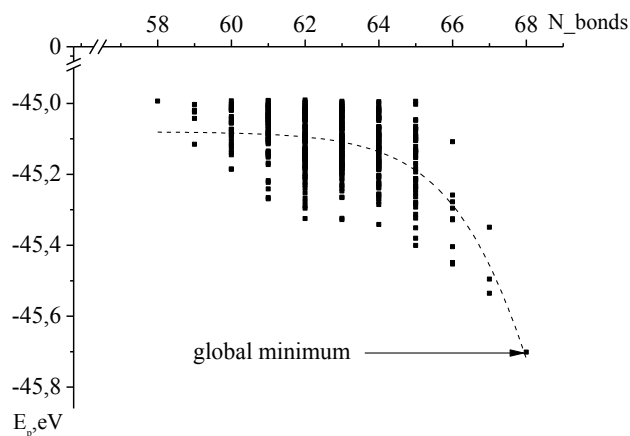


Figure 2. Dependence of the summary potential energy in Ag₁₉ clusters (top 500) from the total bonds number on the first coordination sphere.

In [4] we modeled the simulated relationship between the structure and thermal stability of copper clusters in the size range of 38-100 atoms. Were established some contenders for the «magic» nanoclusters, which meet the most stable states.

Results of the new MD experiments show that the range of the thermodynamic stability of one selected structure depends not only on the absolute value of its internal potential energy (see Fig. 2), but also on the location of this point relative to other local minima on the PES.

The work was supported by Russian foundation for basic research (grant No 17-53-04010).

[1] Wales, D.J. *Energy Landscapes*. Cambridge University Press (2003).

[2] Cleri, F., Rosato, V. *Physical Review B*. **48** (1993) 22.

[3] Gupta, R. J. *Phys. Rev. B*. **23** (1981) 6265.

[4] Myasnichenko, V.S., Ershov, P.N., Sdobnyakov, N.Yu., Sokolov, D.N. Physical and chemical aspects of the study of clusters, nanostructures and nanomaterials. **6** (2015) 345.



ON THE POSSIBILITY OF CALCULATING THE TOTAL ENERGY OF SOLIDS

Naumov V.N., Musikhin A.E.

Nikolaev Institute of Inorganic Chemistry, Siberian Branch of the Russian Academy of Sciences, 630090 Novosibirsk, Russia
E-mail: vn@niic.nsc.ru

It is known that the vibrations of nuclei determine the main energy component of a solid, which prevails over other components (electronic, magnetic, etc.). These vibrations are described well within the phonon formalism. The basic characteristic, which describes the degree of filling of the energy states of crystal vibrational spectrum, is the phonon density of states. Full quantitative information on the density of states makes it possible to obtain energy, heat capacity, entropy and other thermodynamic functions in the entire region of solid phase existence. The phonon density of states at zero temperatures makes it possible to calculate the zero-point energy of a crystal lattice. Zero-point vibrations of the atoms of a condensed medium do not disappear when the normal thermal vibrations practically "freeze". Knowledge of zero-point energy allows us to calculate the total energy of a solids for both isobaric and isochoric states.

In this report we demonstrate the possibility of calculating the total energy of a solids, using our method of phonon density of states reconstruction from experimental low-temperature heat capacity [1,2]. The original method of numerical solution of this inverse problem allows us to calculate the $g(\omega)$ dependence with correct description of its shape and correct proportion of the number of vibrational modes in different frequency intervals. Such description gives a high accuracy of the $g(\omega)$ first moments finding, allows us to calculate the zero-point energy and opens the possibility of obtaining the total internal energy of a solids.

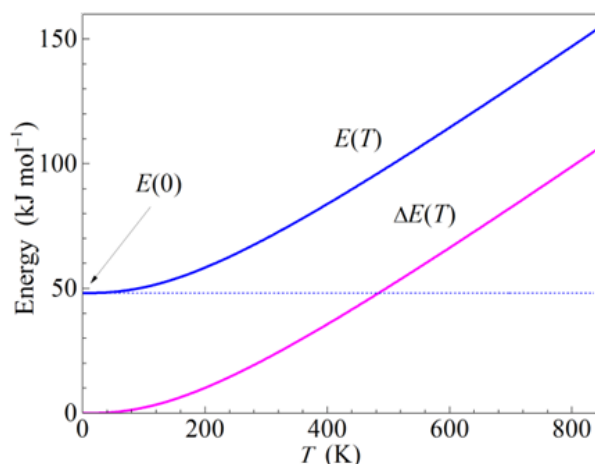


Figure 1. Total internal energy $E(T)$, thermal energy $\Delta E(T)$ and zero-point energy $E(0)$ of Li_2MoO_4 .

When calculating the phonon density of states $g(\omega)$, the zero approximation $g_0(\omega)$ that correctly describes the behavior of $g(\omega)$ at low and cut-off frequencies is first selected. Such zero approximation describes well the asymptotic behavior of heat capacity (at $T \rightarrow 0$ and $T \rightarrow \infty$), but the description for medium temperatures is not satisfactory. Further, the zero approximation is refined by an iterative process, where the number of vibration modes is redistributed over frequencies. By changing the shape of $g_0(\omega)$, such redistribution of vibration modes ultimately reduces the difference between the calculated and experimental heat capacities in the middle temperature region. The iterative process continues until the difference in heat capacities drops below the pre-specified value equal to the uncertainty of the experimental heat capacity. It should be noted that in the course of calculating the density of states $g(\omega)$ the first

moment μ_1 of obtained solutions quickly converges to its true value irrespective of the initial approximation and does not vary essentially in the course of further refinement of the spectrum $g(\omega)$ shape. Such tendency of μ_1 to the true value in the course of finding the solution determines high accuracy of its calculation [2]. The analysis shows that the calculated heat capacity curve as a whole rotates relative to the experimental heat capacity if the current value of μ_1 is greater (or less) than its true value. The uncertainty of the first moment determination is comparable to the experimental heat capacity uncertainty [2]. An example of calculating the total internal energy of Li_2MoO_4 is shown in Fig. 1.

This work was supported by the RFBR (research project No. 16-32-00884).

[1] Naumov, V.N.; Musikhin, A.E. Phys. B, 2015, 476, 41–49.

[2] Naumov, V.N.; Musikhin, A.E. Comput. Mater. Sci., 2017, 130, 257–267.

[3] Musikhin, A.E.; Naumov, V.N.; Bespyatov, M.A.; Ivannikova, N.V. J. Alloy. Compd. 2015, 639, 145–148.



THERMAL STUDY OF METAL-ORGANIC PRECURSORS $Zr(thd)_4$ AND $Y(thd)_3$

Nazarova A.A.¹, Zelenina L.N.^{1,2}, Chusova T.P.¹, Zherikova K.V.¹, Gelfond N.V.¹, Igumenov I.K.¹

¹Nikolaev Institute of Inorganic Chemistry, Siberian Branch of the Russian Academy of Sciences, 630090 Novosibirsk, Russia

²Novosibirsk State University, 630090 Novosibirsk, Russia

E-mail: nazarova@niic.nsc.ru

ZrO₂ based materials are of interest due to their combined mechanical, chemical and electrical properties. They were used as solid electrolyte in gas sensors, fuel cells, and insulators in microelectronic devices. The other applications of ZrO₂ films include protective coatings, thermal barrier coatings and solid oxide fuel cells (SOFC). The volatile zirconium precursors for metall-organic chemical vapour deposition (MOCVD) applications combined with other metal precursors for developing mixed metal oxide or composite thin films yttria stabilized zirconia (YSZ) will have still more technological applications than the pure ZrO₂ thin films. Among the different techniques for the development of thin films, MOCVD offers a conformal coverage, better growth-rate and control of composition for desired applications. The study of thermal properties of volatile Zr- and Y-complexes is needed for the most success of their MOCVD application.

This work is devoted to thermochemical study of $Zr(thd)_4$ (tetrakis(2,2,6,6-tetramethyl-3,5-heptanedionato)zirconium(IV)) and $Y(thd)_3$ (tris(2,2,6,6-tetramethyl-3,5-heptanedionato)yttrium(III)) which were synthesized by method described in [1] and characterized by elemental analysis, ¹H-NMR-spectroscopy and X-Ray diffraction. The results of analyses confirmed the homogeneity of the samples and their compliance with the chemical formula $ZrC_{44}O_8H_{76}$ and $YC_{33}O_6H_{57}$. Their thermal properties were investigated by DSC and static method.

The method of differential scanning calorimetry (SETARAM 111) was used to determine the thermodynamic characteristics of phase transitions (T_{tr} , $\Delta_{tr}H_{Tr}$, $\Delta_{tr}S^{\circ}_{Tr}$). These experiments were performed in vacuum with heating rate 0.5–1.0 K·min⁻¹. The uncertainties in the heat effect measurements were less than 1.5% [2]. $Zr(thd)_4$ samples exhibited two solid phase transitions (at 439 and 446 K) and melting at 609 K while $Y(thd)_3$ samples had only one transition (melting at 449 K).

The temperature dependences of saturated and unsaturated vapor pressure were measured by a static method with quartz membrane-gauge manometers in the temperature interval 382–520 K. The pressure and temperature measurement errors were less than 40 Pa and 0.5 K, accordingly [3]. As a result of this study the thermal stability of investigated compounds was established, the temperature dependences of pressure for sublimation and vaporization processes were obtained and the enthalpies and entropies of sublimation and vaporization were calculated.

The data on volatilities, saturated vapour and phase transitions allowed us to choose the most optimum conditions for carrying out MOCVD processes.

Acknowledgment: This work was supported by RSF № 16-19-10325.

[1] Zherikova K.V., Baidina I.A., Morozova N.B., Kuratieva N.V., Igumenov I.K. J. Struct. Chem., 49 2008, 49, 1098–1103.

[2] Zherikova K.V., Zelenina L.N., Chusova T.P., Gelfond N.V., Morozova N.B. J. Chem. Thermodyn., 2016, 101, 162–167.

[3] Zherikova K.V., Zelenina L.N., Morozova N.B., Chusova T.P. J. Therm. Anal. Calor., **2012**, **108**, **1325-1329**.



CALORIMETRIC STUDY OF PHASE TRANSFORMATION KINETICS IN THE $K_2SO_4 - ZnSO_4$ GLASSES

Nepomiluev A.M.¹, Reznitskikh O.G.², Zemlyanoi K.G.³

¹The Ural Scientific Research Institute of Metrology FGUP "UNIIM", 620000 Ekaterinburg, Russia

²Institute of High-Temperature Electrochemistry of the UB RAS, 620990 Ekaterinburg, Russia,

³Urals Federal University named after the first President of Russia B.N.Yeltsin, Ekaterinburg, Russia

E-mail: nepoan@mail.ru

Vitrification of $K_2SO_4-ZnSO_4$ binary system and some properties of glasses have been studied in [1]. The kinetics of phase transformations in the system is not studied enough. The present work is devoted to the kinetics of the glass transition and crystallisation of $(100-x) K_2SO_4-xZnSO_4$ ($x = 30-80$ mol.%) glasses. The thermal behaviour of the glasses was investigated by the DSC204F1 calorimeter. Pieces of glass (15-20 mg) were heated in aluminium crucibles at a rate of 5, 10, 20, 40 K/min. The T_g glass transition temperatures, the T_x peak onset temperature, T_c peak temperature, the $\Delta_{tr}C_p$ heat capacity change under glass transition temperature and $\Delta_{tr}H$ heat of phase transformations was directly determined from the DSC curves by Proteus computer program. To determine the E_g activation energy of structural relaxation of the glasses in the glass transition range methods reported in [2,3] were used. The E_c activation energy of crystallisation, K_0 frequency factor and n Avrami exponent, characterised the kinetics and mechanism of crystallisation were determined by the method reported in [4]. The values obtained are shown in Table 1 and 2. The dependence of E_g and E_c values on the glass composition indicates significant changes in its structure, associated with changes in the degree of SO_4^{2-} group symmetry, and as a result, the packing density of cations and anions in the glass. Crystallisation mechanism also depends on the glass composition; however, mechanisms of three-dimensional nucleation and crystal growth are predominant.

Table 1. Values of T_g , T_x , T_c , $\Delta_{tr}C_p$, $\Delta_{tr}H$ for $(100-x)K_2SO_4-xZnSO_4$ glasses at heating rate 10 K/min.

x (mol.%)	T_g (K)	$-\Delta_{tr}C_p$ (J/(g·K))	T_x (K)	T_c (K)	$\Delta_{tr}H$ (J/g)
80	508.3	0.47	565.4, 635.5, 661.3	575.1, 644.8, 666.2	62.2, 23.5, 1.1
70	494.6	0.40	550.9, 587.4, 611.2	558.9, 606.8, 625.1	57.5, 26.6, 12.3
60	490.3	0.39	552.4, 631.5	565.2, 649.3	75.9, 17.7
55	510.5	0.73	549.0	561.3	90.8
50	524.7	0.74	566.4	580.1	98.6
40	522.4	0.74	551.7	559.0	72.0
30	520.8	0.35	552.8	559.4	45.4

Table 2. E_g , E_c , K_0 values and n Avrami exponent for $(100-x)K_2SO_4-xZnSO_4$ glasses.

x (mol.%)	E_g (kJ/mol)		E_c (kJ/mol)			K_0 (s ⁻¹)			n		
	[2]	[3]	E_1	E_2	E_3	$(K_0)_1$	$(K_0)_2$	$(K_0)_3$	n_1	n_2	n_3
80	513.2	504.8	234.4	238.5	323.6	$7.1 \cdot 10^{19}$	$6.1 \cdot 10^{17}$	$6.3 \cdot 10^{23}$	3.5	4.0	4.8
70	484.5	476.3	234.8	253.5	153.8	$3.3 \cdot 10^{20}$	$2.6 \cdot 10^{20}$	$2.0 \cdot 10^{11}$	3.2	1.3	3.3
60	416.2	408.0		167.5			$1.1 \cdot 10^{14}$			2.7	
55	713.1	704.6		279.6			$1.9 \cdot 10^{23}$			2.8	
50	395.4	386.7		184.1			$1.3 \cdot 10^{15}$			2.8	
40	456.0	447.7		157.1			$1.7 \cdot 10^{13}$			3.0	
30	607.3	598.6		157.6			2.010^{13}			3.0	

[1] Narasimhan P.S.L; Rao K.J. J. Non-Cryst. Solids, 1978, 27, 225-246.

[2] Moynihan C.T.; Eastal A.J.; Wilder J.; Tucker J. J. Phys. Chem., 1974, 78, 2673-2677.

[3] Kissinger H.E. J. Res. Nat. Bur. Stand., 1956, 57, 217-221.

[4] Augus J.A.; Bennet J.D. J. Thermal. Anal., 1978, 13, 283-292.



HEAT CAPACITY OF PRASEODYMIUM ORTHOPHOSPHATE WITH DIFFERENT PARTICLE SIZE

Nikiforova G.E., Bryukhanova K.I., Khoroshilov A.V., Gavrichev K.S.

Kurnakov Institute of General and Inorganic Chemistry of the Russian Academy of Sciences, 119991 Moscow, Russia

E-mail: gen@igic.ras.ru

Praseodymium orthophosphate belongs to the family of compounds with a monazite structure, which are characterized by a high melting point, chemical inertness and very low solubility in water. Monazites are considered as interesting high-temperature ceramics and could find application in the disposal of radioactive waste, in transportation technology, as luminescent materials, scintillators or catalysts. In spite of the wide field of applications, there is a lack of knowledge of the thermodynamic properties of PrPO_4 . The low-temperature heat capacity of crystal [1] and micro-sized [2] praseodymium orthophosphate was investigated by adiabatic and relaxation calorimetries. But only theoretical high-temperature heat capacity of PrPO_4 was estimated as the sum of a lattice component and an electronic excess contribution, calculated from crystal field energies of PrPO_4 [3].

Functional properties of nanoscale crystals are significantly different from those of single crystals and micro-particles powders. The difference in the heat capacity of nanosize and bulk particles substances is mainly due to surface energy contribution. The nanoparticles' surface has a large number of structural defects, and water, presenting on the nanocrystals' surface as an impurity, poses a great problem for experimental study of the nanoscale substances' thermodynamic properties.

Rare earth orthophosphates with different particle size and morphology can be obtained, depending on the synthesis method [4]. PrPO_4 samples were synthesized using a hydrothermal treatment. The size and morphology of the particles formed was determined using scanning electron microscopy (SEM). It was shown that nano-size particles had the shape of whiskers, with a diameter of 30 nm and a length of up to 1,500 nm. The surface specific area of nanowhiskers was measured using the BET model was $15.7 \text{ m}^2\text{g}^{-1}$ (as compared to $3.3 \text{ m}^2\text{g}^{-1}$ for isometric microcrystalline PrPO_4). The absence of sorbed water on the nanoparticles' surface and the thermal stability of PrPO_4 were proved by means of a DSC/TG analysis.

The heat capacity measurements for the nano- PrPO_4 whiskers, conducted using relaxation calorimetry (RC) in the temperature range from 1.93 to 29.86 K, revealed a negligible difference in the data for nanoscale and bulk praseodymium orthophosphate at very low temperatures. Nanowhiskers, in contrast to bulk crystals, have preferential crystal growth direction. Therefore, one would expect another crystal-field effect on the Pr^{3+} ion. However, the close resemblance of the heat capacity data for isometric microcrystalline praseodymium orthophosphates (with bulk particles) and nano- PrPO_4 whiskers suggests that significant changes in energy levels, corresponding to the Schottky anomaly, do not occur.

High-temperature heat capacities of praseodymium orthophosphate with different particle size were measured by DSC. No change of a shape and size of particles caused by the heating to temperature of 1200 K were revealed. The difference in heat capacities of the bulk- and nano- PrPO_4 reaches $20 \text{ JK}^{-1}\text{mol}^{-1}$ (near 12%) at 900 K. The surface energy contribution to heat capacity was estimated.

The influence of a size factor on heat capacity, characteristic temperature Θ_D and thermodynamic functions, calculated from $C_p(T)$ dependences (entropy and enthalpy change), was evaluated.

This study was carried out using the equipment of the Joint Research Centre of IGIC RAS and was funded by grant #0088-2014-0003.

[1] Bauer, J. D., Hirsch, A., Bayarjargal, L. et al. *Chem. Phys. Lett.*, 2016, 654, 97–102.

[2] Gavrichev, K. S., Gurevich, V. M., Ryumin, M. A. et al. *Geochem. Int.*, 2016, 54, 362–368.

[3] Popa, K., Konings, R. J. M. *Termochim. Acta*, 2006, 445, 49–52.

[4] Bryukhanova, K. I., Nikiforova, G. E., Gavrichev, K. S., *Nanosys.: Phys., Chem., Math.*, 2016, 7, 451–458.



VAPOR PRESSURE OF PERFLUOROOCXYLBROMIDE AND THE ADDITIVITY SCHEME OF CALCULATION OF VAPORIZATION ENTHALPIES FOR PFOC

Pashchenko L. L., Druzhinina A.I.

¹Department of Chemistry, Lomonosov Moscow State University, Leninskie Gory 1, bl.3, Moscow, 119991, Russia
E-mail: lara.paschenko@gmail.com

Perfluoroorganic compounds (PFOC) are promising as components of aqueous emulsions artificial hemoconcealer, currently used in medical practice. In this work the temperature dependence of the saturated vapor pressure, p_s , of perfluorooctylbromide, $C_8F_{17}Br$, was determined for the first time by comparative ebulliometry over the moderate “atmospheric” pressure range from 8.4 to 101.6 kPa. The apparatus has been used for the determinations of the vapor pressure in the temperature range from 298 to 461 K. Temperature (T) measurements are carried out by means of platinum resistance thermometers ($R \sim 100 \Omega$) at 20 fixed pressures maintained automatically by a mercury-contact manometer. The total errors of the temperature - pressure measurements were evaluated as $S_t = \leq 1 \cdot 10^{-2} K$ and $S_p = 13 \div 26 Pa$, respectively. The experimental values ($p_s T$) were fitted by the semi-empirical equation which was derived by integration of the Clausius - Clapeyron equation. The standard vaporization enthalpy, $\Delta_{vap}H^0$, and the vapor pressure at the temperature of human body were estimated, a namely $47.7 \pm 0.3 kJ \cdot mol^{-1}$ and 13.8 Pa, respectively. Densities of $C_8F_{17}Br$ have been measured by picnometrical method in the small temperature range from 293 to 343 K with an accuracy $\leq 1 \cdot 10^{-4} g \cdot cm^{-3}$.

A second-order group additive scheme has been applied using full-matrix [1], least-squares method (LSM) to predict the vaporization enthalpies of PFOC compounds. To decrease the differences between the experimental and estimated values, we apply more extended parameterization, which considers next to nearest-neighbor interaction in the molecule. The enthalpies of vaporization are calculated from the formula

$$\Delta_{vap}H^0 = \sum_{i=1}^n H_i \cdot m_i$$

where m_i is the linear independent numbers of atom groups in molecule, and H_i is the group value (Table 1). The values of H_i were calculated by LSM on the basis of the enthalpies of vaporization obtained in this work and taken from the literature or from our earlier investigation for some perfluoroalkanes, perfluoroalkylcyclohexanes and *cis*- and *trans*-perfluorodecalines. The estimated values $\Delta_{vap}H_{est}^0$ for twelve PFOC are in good agreement (0.7 %) with experimental ones, $\Delta_{vap}H_{exp}^0$. The differences ($\Delta_{vap}H_{exp}^0 - \Delta_{vap}H_{est}^0$) for the three compounds, which were not included in scheme, are ranged from 0.02 to 0.08 $kJ \cdot mol^{-1}$ ($\leq 2 \%$).

Table 1 Listing of groups and group values of some perfluoroorganic compounds

Group*	Constants H_i	Group values ($kJ \cdot mol^{-1}$) for			
		Perfluoro- alkanes	Perfluoro- cyclocarbons	Perfluoro- dicyclocarbons	1-Br- (PFOC)
C-(C _F)(F) ₃	H_1	6.94 ± 0.11			
C-(C _{F2})(F) ₂	H_2	4.53 ± 0.04			
C-(C _{F3})(F)	H_3	1.33 ± 0.20			
C _c -(C _{F2})(F) ₂	H'_2		4.91 ± 0.04		
C _c -(C _{F3})(F)	H'_3		2.54 ± 0.18		
C _{c..d.} -(C _{F3})(F)	$H''_{3(trans)}$			3.08 ± 0.15	
	$H''_{3(cis)}$			3.47 ± 0.15	
Br-(C _F)(F) ₂	H_4				9.05 ± 0.15

*C_F denotes a carbon atom connected with the fluorine atom; C_c and C_{c.d.} denote a carbon atom in a monocycle and a carbon atom, which is common for two cycles, respectively.

The additive schemes can be used to obtain the enthalpies of vaporization for the substances which were not investigated experimentally.

[1] Pashchenko, L.L.; Miroshnichenko, E.A. J. Therm. Anal. Calorimetry, 2015, 120, 1375.

CONTROLLABLE THERMAL EXPANSION OF MATERIALS WITH KOSNARITE- AND LANGBEINITE-TYPE STRUCTURES

Pet'kov V.I., Dmitrienko A.S., Shipilov A.S., Alekseev A.A.
 Lobachevsky State University of Nizhni Novgorod, 603950 Nizhni Novgorod, Russia
 E-mail: petkov@inbox.ru

Compounds of mineral kosnarite ($\text{KZr}_2(\text{PO}_4)_3$) and langbeinite ($\text{K}_2\text{Mg}_2(\text{SO}_4)_3$) structural types can tailor composition to attain desired thermophysical properties such as low thermal expansion, excellent thermal shock resistance, high melting temperatures, and good creep resistance. The goal of this work is to present data on the synthesis, structure and the thermal expansion behavior of $\text{MZr}_2(\text{TO}_4)_x(\text{PO}_4)_{3-x}$ ($\text{M} = \text{Li}, \text{Na}, \text{K}, \text{Rb}, \text{Cs}; \text{T} = \text{As}, \text{V}$) solid solutions, $\text{NaFeZr}(\text{PO}_4)_2\text{SO}_4$ and $\text{Pb}_{2/3}\text{FeZr}(\text{PO}_4)_{7/3}(\text{SO}_4)_{2/3}$ of the mineral kosnarite structure and $\text{KPbMgTi}(\text{PO}_4)_3$, $\text{K}_{5/3}\text{MgE}_{4/3}(\text{PO}_4)_3$ ($\text{E} = \text{Ti}, \text{Zr}$) of the mineral langbeinite structure. All samples have been prepared by a sol-gel process and studied via X-ray diffraction, electron microprobe, IR-spectroscopy, DTA-TG methods. Thermal expansion parameters have also been determined with high and low temperature X-ray diffraction. The electron probe X-ray microanalysis results have showed that their crystallites have been uniform in composition, which coincided with the intended one to within experimental uncertainty (within 2 at %).

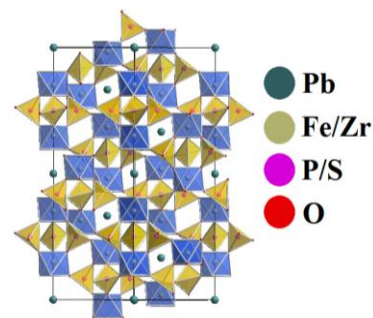


Figure Structural fragment of $\text{Pb}_{2/3}\text{FeZr}(\text{PO}_4)_{7/3}(\text{SO}_4)_{2/3}$

Basing on the yielded results, which encompass thermal expansion data, crystallographic information about structure of individual compounds and solid solutions, the meaningful selection of compounds with kosnarite (Figure) and langbeinite structure for novel materials with controllable thermal expansion has been carried out. The K-, Rb-, and Cs-containing arsenates, arsenate-phosphates, vanadate-phosphates and $\text{Pb}_{2/3}\text{FeZr}(\text{PO}_4)_{7/3}(\text{SO}_4)_{2/3}$ are the low expansion materials, $\alpha_{\text{av}} < 2 \cdot 10^{-6} \text{ K}^{-1}$; $\text{NaZr}_2(\text{AsO}_4)_3$, Li- and Na-zirconium arsenate-phosphates, vanadate-phosphates and $\text{K}_{5/3}\text{MgZr}_{4/3}(\text{PO}_4)_3$ have intermediate thermal expansion, $\alpha_{\text{av}} = (3 \div 7) \cdot 10^{-6} \text{ K}^{-1}$; $\text{LiZr}_2(\text{AsO}_4)_3$, $\text{KPbMgTi}(\text{PO}_4)_3$, $\text{K}_{5/3}\text{MgTi}_{4/3}(\text{PO}_4)_3$ are the high-expansion material, $\alpha_{\text{av}} > 7 \cdot 10^{-6} \text{ K}^{-1}$. Present results demonstrate that the change of the size of alkali metal cation, anion substitution and the varying of the solid solution composition can produce kosnarite ceramics with controlled linear thermal expansion coefficients and extremely low thermal expansion anisotropy or langbeinite ceramics with isotropic expansion (Table 1).

The reported study was partially supported by Russian Foundation for Basic Research, research project No. 15-03-00716a.

Table 1. Thermal expansion parameters of some studied compounds.

Compound	Thermal expansion coefficients, $\times 10^6 \text{ K}^{-1}$			
	α_a	α_c	α_{av}	$ \alpha_a - \alpha_c $
$\text{RbZr}_2(\text{AsO}_4)_{1.5}(\text{PO}_4)_{1.5}$	-2.3	3.6	-0.3	5.9
$\text{CsZr}_2(\text{AsO}_4)_3$	-0.3	1.7	0.4	2.0
$\text{CsZr}_2(\text{VO}_4)_{0.2}(\text{PO}_4)_{2.8}$	0.1	0.8	0.3	0.7
$\text{Pb}_{2/3}\text{FeZr}(\text{PO}_4)_{7/3}(\text{SO}_4)_{2/3}$	1.0	3.2	1.7	2.3
$\text{K}_{5/3}\text{MgZr}_{4/3}(\text{PO}_4)_3$	4.9	4.9	4.9	0



THERMODYNAMIC PROPERTIES OF THE CRYSTALLINE LEAD-CONTAINING NZP-PHOSPHATES

Asabina E.A., Mayorov P.A., Pet'kov V.I., Markin A.V., Smirnova N.N.

Lobachevsky state University of Nizhni Novgorod, 603950 Nizhni Novgorod, Russia

E-mail: petkov@inbox.ru

Crystalline $M_{0.5}Zr_2(PO_4)_3$ (M is large ion of the metal in oxidation state +2: Cd^{2+} , Ca^{2+} , Sr^{2+} , Pb^{2+} , Ba^{2+}) phosphates [1] belong to the NZP/NASICON ($NaZr_2(PO_4)_3$) compounds family, which attracts the research interest because of high stability to the extreme environmental conditions [2], such as high temperatures, water and aggressive media, radiation. These compounds are characterized by flexible crystal structure formed by PO_4 tetrahedra sharing corners with ZrO_6 octahedra, M^{2+} cations occupy framework cavities. Substitution of Zr^{4+} to M^{2+} in the framework sites leads to changing of the phosphates symmetry and physical properties.

In the present investigation, the temperature dependences of the heat capacity of the crystalline $Pb_{0.5}Zr_2(PO_4)_3$ and $PbMg_{0.5}Zr_{1.5}(PO_4)_3$ phosphates have been studied.

The compounds were synthesized by sol-gel method. The starting reactants were aqueous solutions of $Pb(NO_3)_2$, $MgCl_2$, $ZrOCl_2 \cdot 8H_2O$ and $NH_4H_2PO_4$ of chemically pure grade. The final temperature of thermal treatment was 650°C. The homogeneity and chemical compositions of the obtained polycrystalline powders were checked by electron microprobe analysis on a JSM-7600F Schottky Field Emission Scanning Electron Microscope (JEOL) equipped with microanalysis system. The samples phase purity was established by powder X-ray diffraction (XRD) at Shimadzu XRD-6000 diffractometer (CuK_{α} radiation). The amorphous impurities absence was shown by IR spectra of the samples, which were recorded on a Shimadzu FTIR 8400S spectrometer. A BCT precision automatic adiabatic calorimeter (Termis, Moscow) and a DSC 204 F1 Phoenix differential scanning calorimeter (Netzsch Gerätebau, Germany) were used to measure the isobaric heat capacities (C_p^0) of the crystalline $Pb_{0.5}Zr_2(PO_4)_3$ (7–660 K) and $PbMg_{0.5}Zr_{1.5}(PO_4)_3$ (190–660 K) phosphates.

The heat capacity of the $PbMg_{0.5}Zr_{1.5}(PO_4)_3$ phosphate was found to be gradually rising with the temperature increase, and no phase changes or thermal decompositions occurred. The $Pb_{0.5}Zr_2(PO_4)_3$ underwent reversible phase transition at T near the room temperature. The XRD data of the $Pb_{0.5}Zr_2(PO_4)_3$ (recorded at 173 and 473 K) have shown, that the nature of the transition is connected with disordering of Pb^{2+} ions in the structural cavities and corresponding increase of the phosphate structure symmetry.

At temperatures from 7 to 12 K the heat capacity of the phosphates was described by Debye function for the heat capacity.

The experimental points of C_p^0 at temperatures $T > 12$ K were fitted by means of the least-squares method using power and semilogarithmic polynomial dependences.

The phosphates heat capacities at high temperatures were estimated as $C_p^0 \rightarrow 3Rn$, where R is the gas constant, n is the number of atoms in the formulae unit. The calculated values were 436 and 449 J/(mol·K) for $Pb_{0.5}Zr_2(PO_4)_3$ and $PbMg_{0.5}Zr_{1.5}(PO_4)_3$, respectively. Experimental C_p^0 points for the studied phosphates at high temperatures were close to the above values.

The experimental data were used to calculate the standard thermodynamic functions: $[H^0(T) - H^0(0)]$, $S^0(T)$ and $[G^0(T) - H^0(0)]$ for the $Pb_{0.5}Zr_2(PO_4)_3$ phosphate. Its standard entropy of formation at 298.15 K was also estimated.

This work was supported by Russian Foundation for Basic Research (Project no. 15-03-00716).

[1] Pet'kov, V. I.; Kurazhkovskaya, V. S.; Orlova, A. I.; Spiridonova, M. L. *Crystallography Rep.*, 2002, 47, 736.

[2] Pet'kov, V. I.; Orlova, A. I. *Inorg. Mater.*, 2003, 39, 1013.

DFT STUDY OF VACANCY-INDUCED STABILIZATION OF π -SnS POLYMORPH

Popov I.S., Enyashin A.N.

Institute of Solid State Chemistry, Ural Branch of the Russian Academy of Sciences, 620990 Yekaterinburg, Russia

E-mail: popov@ihim.uran.ru

Tin monosulfide α -SnS is increasingly investigated as one of efficient materials for photovoltaics, since it is neither scarce, expensive nor toxic unlike commercially available cadmium chalcogenides. It is also a component of the popular CZTS light absorber system. Thus, a study of Sn-S phase diagram and polymorphism has an applied interest, too. Very recently, a new polymorph of tin monosulfide – so-called π -SnS – has been synthesized [1].

In this work we report the results of first quantum-chemical calculations of electronic properties and stability of π -SnS phase in comparison to the bulk α -SnS, single layer α -SnS and the bulk fcc-SnS. The role of Sn sublattice vacancies in the relative phase stability of α -SnS and π -SnS is also established.

The study is performed by means of DFT method within the framework of GGA using PBE functional as implemented in SIESTA [2]. Optimized lattice parameter of π -SnS is found equal to $a = 11.73 \text{ \AA}$ (exp. 11.7 \AA [1]). π -SnS should be a semiconductor with the indirect band gap 1.18 eV, which is also close to the value for the direct gap 1.21 eV. Both gaps are larger, than those for α -SnS (0.77 eV and 1.05 eV). New phase is only on 0.02 eV/Sn-atom less stable than common α -SnS. α -SnS monolayer adapts square-like lattice. It is a semiconductor with direct band gap 1.43 eV and with higher total energy, than the bulk α -SnS, on 0.21 eV/Sn-atom.

Introduction of vacancy in SnS sublattice leads to the increased stability of π -SnS and to the reduced stability of α -SnS (Fig. 1). π -SnS is more stable than α -SnS with the same vacancy content at a moderate concentration of Sn vacancies (less than 15%). The most stable considered crystal π -SnS has 3% of Sn vacancies. It is less stable, than α -SnS defect-free crystal, only on 0.003 eV/SnS.

X-ray diffractograms of α -SnS and π -SnS were simulated for optimized crystal cells. Single crystals of stable α -SnS and metastable π -SnS should be X-ray distinguishable and can be confidently identified. However, in the nanocrystalline state characterized by a significant broadening of the X-ray reflexes, π -SnS-modification can be "masked" by α -SnS.

Thus, the thermodynamic stability of new π -SnS polymorph is only slightly inferior to that of α -SnS. The synthesis conditions leading to the formation of vacancies within Sn sublattice can contribute to the formation of π -SnS. However, in the case of formation of nanocrystalline forms the reliable identification of π -SnS by X-ray techniques can be hindered and α -SnS can be wrongly recognized.

The work was supported by the RFBR (project № 16-03-00566).

[1] Rabkin A., Samuha S., Abutbul R.E. et al. Nano Letters, 2015, 15, 2174-2179.

[2] SIESTA software <http://departments.icmab.es/leem/siesta/>

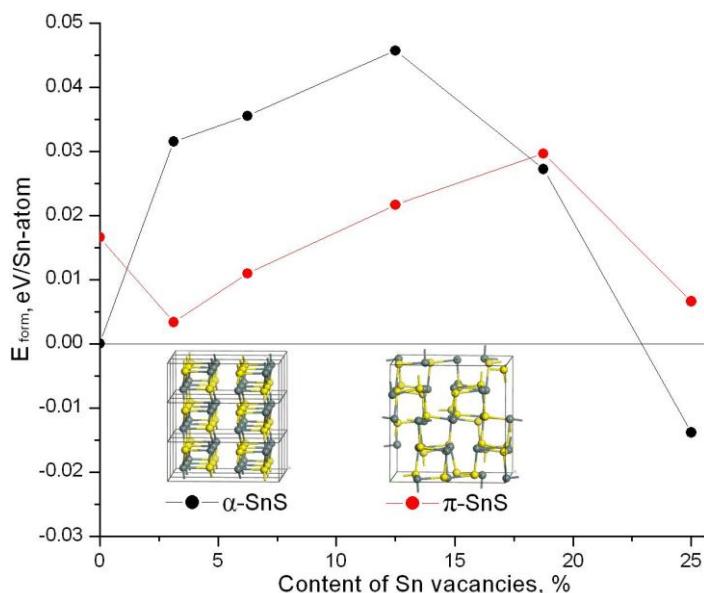


Figure 1. Formation energy of α - and π -SnS crystal polymorphs, depending on the content of Sn vacancies



THE RETENTION INDICES AND THERMODYNAMIC CHARACTERIZATION OF THE SORPTION OF LACTIC ACID ESTERS

Portnova S.V., Krasnykh E.L., Yamshchikova Y.F., Pogotovko E.M.

Samara State Technical University, Samara, 443100 Russia

E-mail: kinterm@samgtu.ru

The esters of lactic acid are monomers by polylactic acid. Methyl, ethyl, propyl, *n*-butyl, *n*-pentyl esters of lactic acid were studied in this work. The esters were prepared by esterifying lactic acid with corresponding alcohols.

The Khromatek-Analitika chromatographic software and a hardware interface based on a Kristall-2000M chromatograph were used to analyze the mixtures and to determine the retention times t_R and specific retention volumes V_g^T (cm³/g). A 100 m×0.25 mm capillary column with a bonded non-polar DB-1 phase was used in the isothermal mode. The injector temperature was 250°C and the detector temperature was 280°C. Helium was used as a carrier gas at a split ratio of 1:80. 1 μL of the mixtures obtained was injected into the chromatograph with a microsyringe.

The retention indices were calculated by the Kovats equation at four temperatures per 10 K. The experimental values of the retention indices were determined after 5–7 measurements.

The analysis of the results shows that, for all esters, the temperature dependences of the indices are linear in the studied temperature range.

The constants of an infinitely dilute solution-vapor phase equilibrium (Ostwald coefficient $k_{D,i}$, classical Henry coefficient $K_{H,i}$) were determined using the values of specific retention volumes V_g^T . The differential standard molar enthalpy ($\Delta_{sp}\bar{H}_i^o$ kJ/mol), entropy ($\Delta_{sp}\bar{S}_i^o$ J/mol·K) and internal energy change ($\Delta_{sp}\bar{U}_i^o$ kJ/mol) values were determined from the dependences of the $\ln V_{g,i}^T$ and $\ln(1/K_{H,i})$ values on the reversed temperature.

The state of the molecules of the esters in an infinitely dilute solution in the phase was characterized by means of the infinite dilution activity coefficient (the Raul activity coefficient γ_i^∞). Excess thermodynamic functions $\bar{G}_i^{E,\infty}$, $\bar{H}_i^{E,\infty}$ and $\bar{S}_i^{E,\infty}$ of mixing of the esters with phase were determined from the temperatures dependences of the γ_i^∞ values.

This work was supported by the Russian Foundation for Basic Research, project no. 17-08-00967_a.



THERMODYNAMIC AND STRUCTURAL STUDIES OF IONIC CLATHRATE HYDRATES OF TETRABUTYLAMMONIUM (TBA) CARBOXYLATES

Rodionova T.V., Terekhova I.S., Villevald G.V., Karpova T.D., Manakov A.Yu.

Nikolaev Institute of Inorganic Chemistry, Siberian Branch of the Russian Academy of Sciences, 630090 Novosibirsk, Russia

E-mail: tvr@niic.nsc.ru

The ionic clathrate hydrates of peralkylonium salts are intensely studied in the last decade as potentially applicable for various fields. The property of their water crystal framework to include small gas molecules due to the presence of vacant D cages induces interest to these compounds in terms of their usage in gas separation and gas (energy) storage. These compounds are considered as perspective phase change materials (PCMs) for cool energy storage and transportation for the following reasons: (1) they have sufficient latent heat of solid-liquid phase transition, (2) formation/decomposition temperatures at ambient pressure range from 0 °C to room temperature (dependent on the salt and its concentration), (3) they precipitate as a slurry that can be transported directly through a pipeline. The most intensively studied are the ionic clathrate hydrates of TBA halides. The ionic clathrate hydrates of TBA carboxylates are less much studied, although they are analogs. In the present work the ionic clathrate hydrates formed in TBA formate (TBAForm), TBA acetate (TBAAc), TBA propionate (TBAProp), and TBA butyrate (TBABut)*H₂O binary systems were synthesized and their compositions, melting temperatures, and enthalpies of dissociation were determined. Powder X-ray diffraction analysis revealed three hydrate structural types: tetragonal structure -I, cubic structure-I, and the structure on the base of the idealized water lattice of hexagonal structure-I. Experimentally determined thermodynamic parameters as well as the calculated values of COP (coefficient of performance) for Carnot refrigerator indicate that studied the ionic clathrate hydrates have a potential for using in air-conditioning systems and cold energy storage. For gas separation and storage the TBAForm*31.5H₂O of tetragonal structure-I is apparently the most preferable, since all D cages in the structure are vacant.

STRUCTURE-FORMING UNITS OF AMINO ACID MALEATES. THERMODYNAMIC ISSUES OF L-VALINIUM HYDROGEN MALEATE

Rychkov D.A.^{1,2}, Arkhipov S.G.^{1,2}, Boldyreva E.V.²

¹Novosibirsk State University, 630090 Novosibirsk, Russia

²Institute of Solid State Chemistry and Mechanochemistry SB RAS, 630128 Novosibirsk, Russia

E-mail: rychkov.dennis@gmail.com

Co-crystallization is a common method of modification of properties for organic crystals. Most relevant properties for pharmaceutical industry are solubility, solubility rate, bioavailability, etc. In numerous works one can find how these properties were affected with co-crystal formation.

A model system of L-valinium hydrogen maleate was chosen as an example of wide family of amino acid maleates. Deep and laborious analysis shows that there is a common crystallographic peculiarity for all these structures – $C^2_2(12)$ motif. It is present for 24 (out of total 26) maleates of amino acids – all cases, where this motif could be formed theoretically [1]. Such a remark deserves a further investigation, which can lead to a deeper understanding of co-crystals formation. Another interesting experimental phenomenon gives an assumption that $C^2_2(12)$ motif plays crucial role in co-crystal formation – difference in solubility of original compounds reaches app. 50 times, what is quite rare for such multi-component systems.

As a result of this laborious research a new salt of l-valinium hydrogen maleate was used as an example to study structure-forming units in amino acid maleates. This compound was crystallized, its structure solved from single-crystal X-ray diffraction data, and examined with a variety of methods, including XRPD, FT-IR spectroscopy and computational methods. The stability of the new salt was analyzed using density functional theory and PIXEL calculations with focus on the $C^2_2(12)$ structure forming crystallographic motif. Energies of all basic crystallographic motifs (Fig.1) were calculated and compared. Energies of original compounds and final co-crystal were estimated [2].

This research was carried out within the state assignment to ISSCM SB RAS (project 0301-2016- 0014)

- [1] S. G. Arkhipov, D. A. Rychkov, A. M. Pugachev and E. V Boldyreva, Acta Crystallogr. Sect. C Struct. Chem., 2015.
- [2] D. Rychkov, S. Arkhipov and E. Boldyreva, Acta Crystallogr. Sect. B Struct. Sci. Cryst. Eng. Mater., 2016.

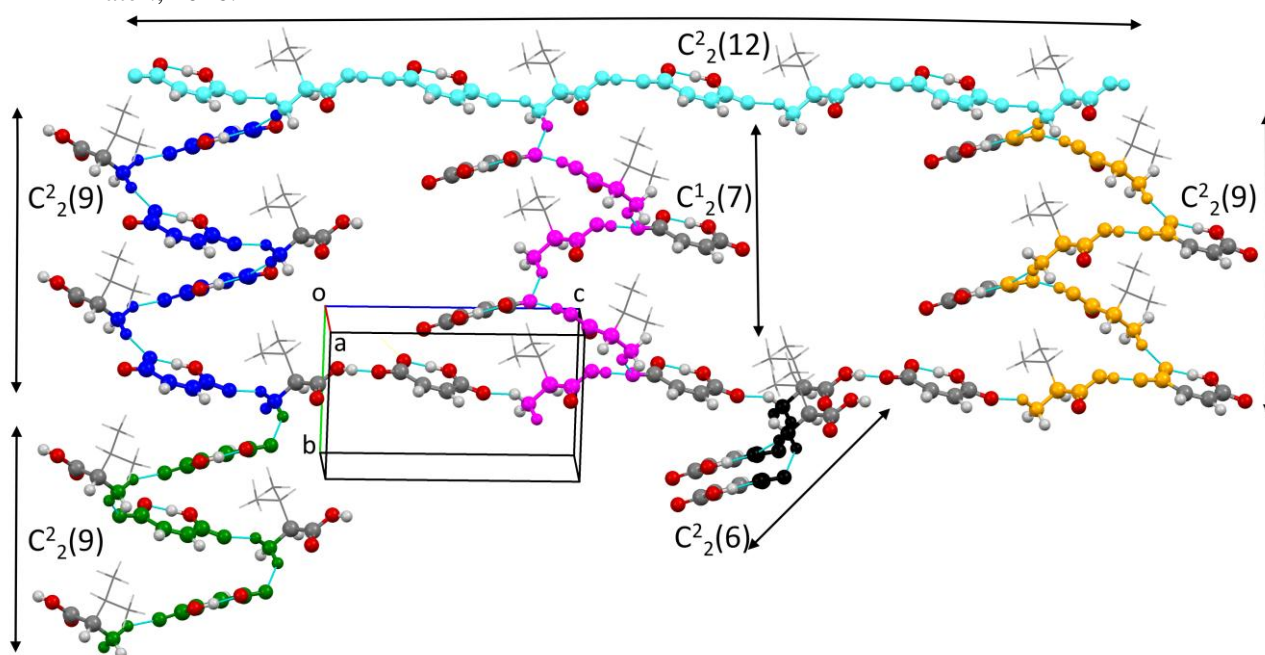


Figure 1. A fragment of the crystal structure of l-valinium hydrogen maleate showing the main structural motifs $C^2_2(12)$ in light blue, $C^2_2(6)$ in black, $C^1_2(7)$ in magenta, and three different $C^2_2(9)$ chains in green, blue and yellow



THERMOCHEMISTRY OF $\text{Sr}_2\text{MeMoO}_6$ (Me = Co, Ni)

Sereda V.V., Sednev A.L., Tsvetkov D.S., Zuev A.Yu.

Ural Federal University, Institute of Natural Sciences and Mathematics, 620010 Lenin av. 51, Yekaterinburg, Russia

E-mail: vladimir.sereda@urfu.ru

Double perovskites $\text{Sr}_2\text{MeMoO}_6$ (Me = Co, Ni) are being studied extensively over the last few decades not only due to their interesting magnetoelectric properties, but also because they are considered to be promising mixed electronic-ionic conducting (MIEC) materials for solid oxide fuel cell (SOFC) anodes. It is evident that the thermodynamic data, especially those obtained at elevated temperatures, are crucial for the prediction of stability and chemical compatibility of fuel cell components. Up to now, no such data were available for the $\text{Sr}_2\text{MeMoO}_6$ (Me = Co, Ni) oxides.

In the present study, the enthalpy increments of $\text{Sr}_2\text{MeMoO}_6$ (Me = Co, Ni) were measured in the temperature range 25-1000 °C using Setaram MHTC-96 high-temperature drop calorimeter. In order to determine the enthalpies of formation of $\text{Sr}_2\text{MeMoO}_6$ oxides, high-temperature drop solution experiments in lithium-sodium metaborate melt were performed. Small amounts (10-30 mg) of $\text{Sr}_2\text{CoMoO}_6$, $\text{Sr}_2\text{NiMoO}_6$, SrMoO_4 , SrCO_3 , CoO and NiO were dropped at least 5 times each into the 6 g of alkali borate solvent. In order to increase the speed of dissolution, it was found to be necessary to use low density samples. Thus, samples' pellets were annealed either at relatively low temperatures (700 °C for NiO , 800 °C for SrMoO_4 , etc.) or at higher temperatures with addition of poly(vinyl alcohol) (as for the $\text{Sr}_2\text{NiMoO}_6$). Solubility of each substance in the alkali borate melt was independently checked in an external oven. No more than 100 mg of substance was dissolved during each calorimeter run and the difference in heat effects between the first and the last dissolution was within the limits of experimental error. This indicates that the borate melt solutions were dilute enough during the whole experiment. Calorimeter sensitivity was calibrated during each run by dropping either high-purity sapphire or gold for drop and drop solution experiments, accordingly.

The thermochemical data of $\text{Sr}_2\text{MeMoO}_6$ (Me = Co, Ni), obtained in the present study combined with the results of the low-temperature adiabatic calorimetry measurements allowed us to derive the whole set of thermodynamic properties of $\text{Sr}_2\text{MeMoO}_6$ from 0 to 1273 K.

THERMAL STUDY OF THE FORMATION PROCESS OF PROTONATED AND INTERCALATED FORMS OF LAYERED NIOBATE $\text{KCa}_2\text{Nb}_3\text{O}_{10}$

Silyukov O.I., Burovikhina A.A., Kulish L.D., Yafarova L.V., Utkina T.D., Zvereva I.A.

Institute of Chemistry, Saint Petersburg State University, 198504, Saint Petersburg, Russia

E-mail: oleg.silyukov@spbu.ru

Complex oxides with perovskite-like crystal structures are of great interest due to their unique properties: high temperature superconductivity, colossal magnetoresistance, photocatalytic activity in water decomposition by UV irradiation, ionic conductivity, ion-exchange properties, ability to the intercalation and interlayer modification, etc. Their physicochemical properties are sensitive to the content and structure of the interlayer space that could be easily modified by the ion-exchange and intercalation reactions. In contact with water the interlayer space of alkali containing layered oxides can intercalate water molecules. The other possibility is the exchange of metal cations in the interlayer space for protons. Protonated forms of layered perovskite-like oxides appear to be solid acids associated with a number of unique physical and chemical properties. They can also be used as precursors for low temperature ion-exchange reactions.

In the present work the process of protonated and hydrated forms formation of layered three-layer Dion-Jacobson perovskite niobate $\text{KCa}_2\text{Nb}_3\text{O}_{10}$ in acidic and neutral media was investigated by thermal analysis methods. The conditions for the formation of stable forms and intermediate phases were established. The samples under study were also characterized using X-ray powder diffraction, SEM, NMR and FT-IR spectroscopy.

It was found that $\text{KCa}_2\text{Nb}_3\text{O}_{10}$ oxide is almost completely stable in neutral aqueous medium, but it undergoes hydration and protonation in acidic aqueous solutions. Thus the formation of the crystalline phase corresponding to the fully protonated derivative $\text{HCa}_2\text{Nb}_3\text{O}_{10}$ is possible while using concentration of acid higher than 1N. The protonation process is complex and includes the intermediate step of hydrated derivatives formation and also kinetics of the process depends on the concentration of acid used (Fig.1).

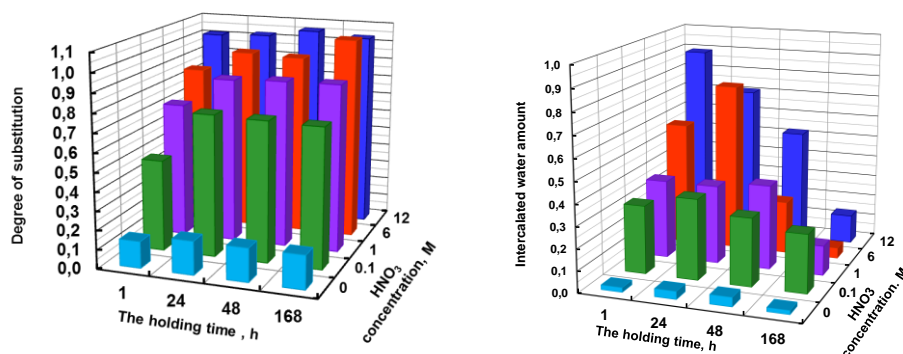


Figure 1. Amount of intercalated water and substitution degree depending on time calculated by means of TG.

Acknowledgement This research was supported by Russian Foundation for Basic Research (grants № 16-33-00240 и № 16-33-60082). Authors also are grateful to Saint Petersburg State University Research Park: Center of Thermal Analysis and Calorimetry, Research Centre for X-ray Diffraction Studies, Center for chemical analysis and materials research, Interdisciplinary Resource Center for Nanotechnology and Center for Magnetic Resonance.



THERMODYNAMIC PROPERTIES OF URANIUM DIOXIDE IN THE CONDENSED STATE

Aristova N.M.¹, Belov G.V.^{1,2}, Morozov I.V.¹, Sineva M.A.¹

¹Joint Institute for High Temperatures, Russian Academy of Sciences, Moscow, 125412 Russia

²Faculty of Chemistry, Moscow State University, Moscow, 119991 Russia

E-mail: aristo2012@yandex.ru

The appearance of the new experimental and theoretical studies of uranium dioxide requires re-counting thermodynamic functions of UO_2 that were published in reference book [1]. Refined thermodynamic functions of uranium dioxide in the crystalline and liquid states are presented in the temperature range 100 – 8000 K. The equations approximating the temperature dependence of heat capacity of the solid and liquid phases UO_2 are derived on the base of the experimental data (calorimetric measurements) available in literature in the temperature ranges 298.15 – 3130 K and 3130 – 8000 K, accordingly. The resulting equations are used to calculate the thermodynamic functions: the heat capacity, the absolute entropy, the enthalpy increments and the reduced Gibbs free energies. The resulting data is added to the database of the IVTANTHERMO software package.

The cubic modification (CaF_2 - type structure, fluorite) is assumed to be the standard state of the crystalline UO_2 at 0 – 3130 K.

The thermodynamic functions of UO_2 at $T \leq 298.15$ K are based on the high-precision measurements of low-temperature heat capacity in the range 5 – 350 K [2]. The measurements were performed using adiabatic vacuum calorimeter for two well-characterized UO_2 samples. This study indicates a very sharp transition at 30.44 K with a maximum C_p of $1636 \text{ J K}^{-1} \text{ mol}^{-1}$, which can be compared with Neel temperature. The transition antiferromagnetic – paramagnetic states was a cooperative first-order.

The high-temperature measurements of the heat capacity and of the enthalpy increments $H^\circ(T) - H^\circ(298.15 \text{ K})$ reveal an anomalous increase of the heat capacity that is particularly marked above 2000 K. In numerous literature modeling C_p involves several contributions:

$$C_p = C_{v \text{ phonon}} + C_{\text{thermal expansion}} + C_{\text{crystal field}} + C_{\text{electronic defects}} + C_{\text{pairs Frenkel}} + C_{\text{Schottky-trios}}$$

These terms are the contributions of, respectively, 1) the harmonic phonons, 2) the thermal expansion, 3) the U^{4+} crystal field, 4) thermally induced cation U^{4+} disproportionation (the electron-hole pair), 5) the disorder of the oxygen lattice as a results of Frenkel pair formation, 6) the formation of Schottky-trios vacancies.

In the present work equation of the heat capacity of the solid UO_2 in the range 298.15-3130 K was obtained by means of joint fitting of the experimental enthalpy increments and the heat capacities that are available in literature. We have fitted the heat capacity data of liquid UO_2 [3, 4] by a single polynomial equation from the melting point to 8000 K.

In conclusion the U – O binary system is certainly one of the most complex systems of the periodic table. The nature of the singularity of the heat capacity of solid UO_2 at high temperatures is still debated.

[1] Gurvich L. V., Bergman G. A., Veyts I. V. Thermodynamic Properties of Individual Substances. Volume 4. Parts One, Two. Moscow, 1984.

[2] Hunzicker J. J., Westrum E. F. J. Chem. Thermodyn., 1971, v. 3, pp. 61-76.

[3] Ronchi C., Hiernaut J. P., Selfslag R., Hyland G. J. Nucl. Sci. Eng., 1993, v. 113, pp. 1 - 19.

[4] Hiernaut J. P., Hyland G. J., Ronchi C. Int. J. Thermophysics, 1993, v. 14, № 2, pp. 259-283.

THERMODYNAMIC PROPERTIES OF POLYOXIMES BASED ON A COPOLYMER OF CARBON MONOXIDE

Aphonin P.D.¹, Smirnova N.N.¹, Markin A.V.¹, Belov G.P.², Golodkov O.N.²

¹Chemistry Department, Lobachevsky State University of Nizhni Novgorod Gagarin Av. 23/2, 603950 Nizhni Novgorod, Russia

²Institute of Problems of Chemical Physics of the Russian Academy of Sciences, pr. Akademika Semenova 1, 142432

Chernogolovka, Moscow oblast, Russia

E-mail: pavel_aphonin@live.ru

Polyoximes - class of polymeric materials, having the oxime group (= N-OH). They are valuable intermediates which can be used to produce polyamines, polyamides, chelating agents and other chemical products. Polyoximes are basis of the preparation of antioxidants, pigments, catalysts, sealants and can be used for the preparation of vaccines and immunogens synthetic antibacterial agents and as components of stable complexes of radioimmune assay diagnosis and gene therapy [1]. One way to obtain polyoximes is oximation copolymers, containing ketone group.

In this work the samples of polyoximes, obtained by oximation copolymer ethylene-carbon monoxide (1) and carbon monoxide ethylene-phenyl terpolymer (2) are investigated (Fig. 1). The samples of polyoximes were synthesized and characterized in the Institute of Problems of Chemical Physics of the Russian Academy of Sciences (Chernogolovka, Moscow region) by research group of Professor G.P. Belov. The composition of polymers was confirmed by NMR ¹H and IR spectroscopies.

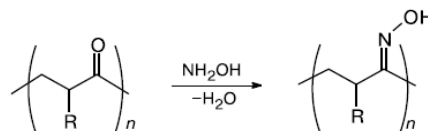


Figure 1. Polyoximes, obtained from carbon monoxide copolymer. R - H (1), Ph (2).

The temperature dependence of heat capacity $C_p^0 = f(T)$ was studied using the low-temperature adiabatic calorimeter BCT-3 in the temperature range from 6 to 350 K, and by differential scanning calorimeter DSC 204 F1 Phoenix in the temperature range from 350 K to the temperature of thermal destruction onset. As an example the $C_p^0 = f(T)$ curve of polyoxime sample (1) in the temperature range from 6 to 350 K is shown in Fig. 2. The characteristics of physical transformations on the $C_p^0 = f(T)$ curves were determined. Based on the obtained data, the standard thermodynamic functions of polyoximes ($C_p^0(T)$, $H^0(T) - H^0(0)$, $S^0(T) - S^0(0)$, $G^0(T) - H^0(0)$) were calculated in the studied temperature range.

The combustion calorimeter B-08 with a static bomb and isothermal shell was used to determine the energy of combustion. According to the data of the combustion energy of polyoximes, the combustion enthalpy and standard thermodynamic parameters of formation were calculated at $T = 298.15$ K, which allowed us to calculate standard thermodynamic characteristics of polyoximes synthesis in a wide temperature range.

The obtained values are the reference data and are of interest for further study of polyoximes for the prediction of their different properties, and for the designing processes of synthesis of this class of compounds.

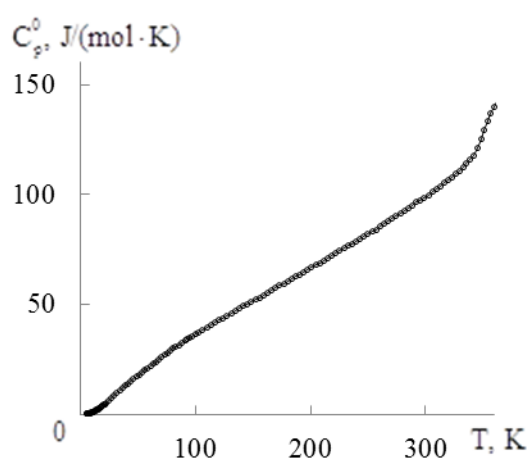


Figure 2. The temperature dependence of heat capacity of polyoxime (1) sample.

[1] Golodkov O. N. , Belov G. P. Russian Chemical Bulletin, International Edition, 2013, V. 62, N. 12, pp. 2624—2625.



COMPARISON OF THERMODYNAMIC PROPERTIES OF METHYLPREDNISOLONE AND METHYLPREDNISOLONE ACEPONATE

Stepanova O.V.^{1,2}, Knyazev A.V.¹, Smirnova N.N.¹, Samosudova Ya.S.¹, Markin A.V.¹, Knyazeva S.S.¹

¹Lobachevsky State University of Nizhni Novgorod, 603950 Nizhni Novgorod, Russia

²Joint Stock Company Chemical-Pharmaceutical Plant Akrikhin, 142450 Staraya Kupavna, Russia

E-mail: o.stepanova@akrikhin.ru

Methylprednisolone and Methylprednisolone aceponate are glucocorticoids. These pharmacologically active substances are used for treat many different inflammatory conditions like arthritis, lupus, psoriasis, ulcerative colitis, allergic disorders, gland (endocrine) disorders, and conditions that affect the skin, eyes, lungs, stomach, nervous system, or blood cells.

This work is a continuation of systematic studies of bioactive compounds. The goals of this work include calorimetric determination of the standard thermodynamic functions of the methylprednisolone and methylprednisolone aceponate with the purpose of describing biochemical and industrial processes with their participation.

The temperature dependences of heat capacity of methylprednisolone (CAS: 83-43-2) was determined in the first time [1] by precision adiabatic vacuum calorimetry in the range from 6 to 350 K. In the above temperature range the standard thermodynamic characteristics $C_p^0(T)$, $H^0(T) - H^0(0)$, $S^0(T)$,

$G^0(T) - H^0(0)$ were estimated. By the experimental data were calculated the standard thermodynamic functions for the range from $T \rightarrow 0$ to 350 K. The standard entropy of formation of methylprednisolone from simple substances was calculated at temperature $T = 298.15$ K.

The obtained thermodynamic characteristics of the investigated methylprednisolone [1] were compared with data for methylprednisolone aceponate (CAS: 86401-95-8) [2].

The heat capacity of methylprednisolone gradually increases with rising temperature and does not show any peculiarities. The heat capacity curve of methylprednisolone aceponate have an anomaly in temperature range from 102 to 140 K. The transition temperature of methylprednisolone aceponate was estimated as the temperature of maximal C_p^0 value within the temperature interval of the transition and

standard uncertainty of phase-transition temperature is 0.1 K. The standard enthalpy of phase transition is $\Delta_{tr}H^0 = 220 \pm 2$ J/mol. According to low-temperature X-ray diffraction, the observed phase transition is a second-order transition. We do not observe structural changes near the phase transition.

As a result, some conclusions were made, and the physicochemical discussion of the structural organization of these molecules was proposed.

This work was performed with the financial support of the Russian Foundation for Basic Research (Projects №№ 15-03-07475, 16-03-00288).

[1] A.V. Knyazev, V.N. Emel'yanenko, N.N. Smirnova etc., Comprehensive thermodynamic study of methylprednisolone. *J.Chem.Thermodyn.*, 2017, 107, 37-41.

[2] A.V. Knyazev, V.N. Emel'yanenko, N.N. Smirnova etc., Thermodynamic properties of methylprednisolone aceponate. *J.Chem.Thermodyn.*, 2016, 103, 244-248.



THERMODYNAMICS OF REDUCTION OF PROTONIC CONDUCTORS BASED ON DOPED BaZrO_3

Tsvetkov D.S., Ivanov I.L., Shevelev N.R., Zuev A.Yu.

Ural Federal University, Department of Physical and Inorganic Chemistry, 620000, Ekaterinburg, Russia

E-mail: Dmitry.Tsvetkov@urfu.ru

Perovskite-type oxides $\text{BaZr}_{1-x}\text{M}_x\text{O}_{3-d}$ (where M is usually a lanthanide with constant 3+ oxidation state) have received a great attention as promising protonic conducting electrolyte materials. However, they are still far to be completely understood. Their defect chemistry was studied mainly using experimental data on total conductivity and water content as a function of temperature (T) and partial pressure of oxygen ($p\text{O}_2$) and water ($p\text{H}_2\text{O}$). Unfortunately, the oxygen nonstoichiometry of variously doped zirconates $\text{BaZr}_{1-x}\text{M}_x\text{O}_{3-d}$ has not been studied so far. At the same time it should be noted that oxygen nonstoichiometry directly relating to the concentrations of various point defects is one of the most convenient properties to be analyzed using defect chemical approach. As a result the equilibrium constants of quasichemical reactions can be determined. This, in turn, allows calculating concentrations of all the defect species and analyzing defect induced properties such as total conductivity, thermoelectric power, chemical expansion, etc. Moreover, the experimental data on oxygen nonstoichiometry vs. $p\text{O}_2$ and T allow the analysis of the oxidation/reduction thermodynamics of the material. This possesses significant independent interest from both fundamental and practical point of view.

Therefore, the priority aims of the current work were (i) to measure the oxygen content in zirconates $\text{BaZr}_{1-x}\text{M}_x\text{O}_{3-d}$ (M=Y, Nd, Pr) as a function of $p\text{O}_2$ and T, (ii) to refine the defect structure of zirconates $\text{BaZr}_{1-x}\text{M}_x\text{O}_{3-d}$ doped with Y, Nd or Pr on the basis of the measured oxygen nonstoichiometry, (iii) to analyse the red-ox thermodynamics of zirconates $\text{BaZr}_{1-x}\text{M}_x\text{O}_{3-d}$ (M=Y, Nd, Pr).

Powder samples of $\text{BaZr}_{0.9}\text{M}_{0.1}\text{O}_{3-d}$ (where M=Y, Nd, Pr) were synthesized by standard ceramic technique. Stoichiometric mixture of starting materials was calcined at temperatures from 1000 to 1300 °C in air with 100 °C step for 12 h at each stage followed by mixture regrinding. The phase composition of the powder samples prepared accordingly was studied by means of X-ray diffraction (XRD) with Equinox 3000 diffractometer using Cu $K\alpha$ radiation. XRD showed no indication for the presence of a second phase.

Oxygen nonstoichiometry of zirconates $\text{BaZr}_{0.9}\text{M}_{0.1}\text{O}_{3-d}$ (where M=Y, Nd, Pr) vs. $p\text{O}_2$ and T was measured by coulometric titration technique in the ranges of T and $p\text{O}_2$ 900–1050 °C and 10^{-18} –0.21 atm, respectively.

Results obtained are discussed on the basis of the defect structure of oxides $\text{BaZr}_{0.9}\text{M}_{0.1}\text{O}_{3-d}$ (where M=Y, Nd, Pr).

This work was supported by the Russian foundation for basic research grant No. 13-03-96118.



HEAT CAPACITY AND THERMODYNAMIC PROPERTIES OF PLATINUM DISULFIDE IN THE WIDE TEMPERATURE RANGE

Tyurin A.V.¹, Chareev D.A.^{2,3}, Polotnyanko N.A.², Testov D.S.²

¹Kurnakov Institute of General and Inorganic Chemistry RAS, Moscow, Russia

²State University of Dubna, Dubna, Russia

³Institute of Experimental Mineralogy RAS, Chernogolovka, Russia

E-mail: tyurin@igic.ras.ru

From the noble metals platinum and its compounds are of particular interest to theoretical and physical chemical studies due to the unique properties and practical application in various fields, for example, in the instrument engineering and chemical industry. In nature, in addition to the native platinum there are its compounds, among them rare minerals such as cooperite (PtS) and braggite (Pt,Pd,Ni)S. Also platinum forms other sulfides, for example PtS₂, however, the phase diagram for the system S-Pt is not yet fully constructed. That is why the study of physical-chemical and thermodynamic properties of binary compounds formed by platinum sulfur is an important task for nowadays research. This work is devoted to study of the thermodynamic properties of the synthesized sample PtS₂(cr.) based on new calorimetric studies determined low-and high-temperature isobaric heat capacity.

The annealing of simple substances in stoichiometric quantities was carried out in a quartz vessel at a temperature of 850°C with one intermediate grinding. The received powder was investigated by X-ray powder diffraction on a BRUKER diffractometer (CuK_{α1}-radiation, graphite monochromator), the absence of other phases was also confirmed by the method of X-ray microanalysis.

Measurements of PtS₂ isobaric heat capacity in the low temperature range was performed using an automated adiabatic vacuum calorimeter BKT-3 (CJSC "TERMIS", Russia) with discrete energy input. The heat capacity was measured in the temperature range from 5.32 to 344.96 K (137 experimental points). Smoothing of experimental values of heat capacity was performed using spline approximation. C_p^o values below the region measurements were obtained by extrapolation to 0 K of the experimental values of heat capacity by the Debye law. On the basis of these data the standard thermodynamic functions at 298.15 K were calculated: C_p^o = 66.18±0.33 J/(mol·K), S^o = 74.51±0.39 J/(mol·K) H^o(298.15 K)-H^o(0) = 11.78±0.06 kJ/mol, Φ^o = -[G^o(298.15K)-H^o(0)]/T = 35.00±0.18 J/(mol·K). It should be noted a good agreement between the experimental and calculated values of the thermodynamic functions obtained in the present work and Westrum and authors' results in article [1].

In the high temperature range for the sample PtS₂(cr.) study we used simultaneous thermal analyzer STA 449 F1 Jupiter® ("Netzsch-Geratebau GmbH", Germany) with a platinum furnace. The using of experimental values of low-temperature heat capacity obtained in the present work, as well as the results of high temperature measurements at 345-875 K (54 experimental points) allowed one to define the coefficients of Maier-Kelley's equation. Using numerical integration at an appropriate temperature and fixed value of the entropy S^o(298.15 K) the values of thermodynamic functions for PtS₂(cr): C_p^o(T), S^o(T), H^o(T)-H^o(298.15 K) и Φ^o(T)' = -[G^o(T) -H^o(298.15 K)]/T for the interval to 875 K were calculated.

[1] Westrum, E.F., Jr.; Carlson, H.G.; Grønvold, F.; Kjekshus A. J. of Chemical Physics, 1961, **35**, 5, 1670-1676.



LOW TEMPERATURE HEAT CAPACITY AND THERMODYNAMIC FUNCTIONS OF HOLMIUM ORTHOPHOSPHATE HoPO_4

Tyurin A.V.¹, Ryumin M.A.¹, Gavrichev K.S.¹, Gurevich V.M.², Kritskaya A.P.¹

¹*Kurnakov Institute of General and Inorganic Chemistry RAS, Russia, 119991, Moscow, Leninsky pr., 31*

²*Vernadsky Institute of Geochemistry and Analytical Chemistry of RAS, ul. Kosygina 19, Moscow, 119991, Russia*

E-mail: Tyurin@igic.ras.ru

The REE orthophosphates are used as LEDs for color television and light-emitting compounds with short-duration afterglow in general. Due to the high thermal and chemical stability of these substances they can be used as materials for radioactive waste disposal.

Thermodynamic studies, currently available in the literature, are experimental data on the enthalpy of formation from elements and oxides measured by drop calorimetry in molten $3\text{Na}_2\text{O} \cdot 4\text{MoO}_3$ [1], and the calculation of thermodynamic characteristics based on the mass-spectrometric experiment [2]. Measurements of the heat capacity of holmium orthophosphate HoPO_4 below 4 K are given in [3]. The present study continues a series of studies on the thermodynamic functions of REE orthovanadates and orthophosphates aiming to obtain the reliable thermodynamic data.

Low temperature heat capacity measurements were carried out by means of BKT-3 automatic adiabatic calorimetric setup (TERMIS, Russia). The $C_p(T)$ curve fitting was made by spline-approximation using the equation of DE [4].

Schottky magnetic anomaly, associated with splitting of energy levels under the crystal field influence, was observed for heat capacity of paramagnetic rare earth orthophosphates. It should be noted that the orthophosphates of rare earth elements REPO_4 at room temperature being paramagnetic with a tetragonal zircon structure below T_N become antiferromagnets. The Neel temperature T_N is quite low: 2 - 5 K. The value of the anomaly of the specific heat reaches a maximum near the Neel point ($32.41 \text{ J K}^{-1} \text{ mol}^{-1}$ at $T = 1.391 \text{ K}$ [4]) and gives a significant contribution to the entropy of HoPO_4 .

The standard Gibbs energy of formation was calculated based on our standard entropy data for holmium orthophosphate, reference data on standard entropy of constituent elements [4] and enthalpy of HoPO_4 formation from elements [1].

This work was supported by Presidium of RAS Research Programm (Project I14P5).

[1] Ushakov, S.V.; Helean, K.B.; Navrotsky, A.; Boatner L.A. *J. Mater. Res.*, 2001, 16, 2623–2633.

[2] Rat'kovskiy, I.A.; Ashuyko, V.A.; Orlovskiy V.P. et al. *Doklady AN SSSR*, 1974, 219, 6, 1413–1415.

[3] Cooke, A.H.; Swithenby, S.J.; Wells M.R. *J. Phys. C: Solid State Phys.*, 1973, 2209–2216.

[4] Gurevich V. M.; Kuskov O.L.; Gavrichev K.S.; Tyurin A.V. *Geochemistry Int.*, 2007, 2, 206-209.

[5] <http://www.chem.msu.ru/cgi-bin/tkv.pl?show=welcome.html>.



NEW CORRELATION BETWEEN CRITICAL DENSITY AND CRITICAL TEMPERATURE

Umirzakov I.H.

Kutateladze Institute of Thermophysics, Siberian Branch of the Russian Academy of Sciences, 630090 Novosibirsk, Russia

E-mail: umirzakov@itp.nsc.ru

The following correlation

$$T_c / T_B + \rho_c / \rho_B = 0.67, \quad (1)$$

where T_c and ρ_c are critical temperature and density, T_B and ρ_B are Boyle temperature and density, was established, and it was widely used to define critical density of metals (see [1-2] and references in them). Its inaccuracy is mainly defined by inaccuracy of defining of density, because the inaccuracy of defining of temperature is by two orders of magnitude less than that of density. We have established that for 11 substances (Ar, CH₄, O₂, N₂, F₂, C₂H₄, H₂S, C₂H₆, C₃H₈, C₄H₁₀, CO₂) with known parameters T_c , ρ_B , ρ_c and T_B [3], Eq. (1) has inaccuracy 2.3%, while the inaccuracy of density is by many times smaller. Therefore one needs the correlation which is much more accurate than Eq. (1). We have established the following correlation

$$\frac{T_c}{T_B} \cdot \left(1 - \frac{T_c}{T_B}\right) + \frac{\rho_c}{\rho_B} \cdot \left(1 - \frac{\rho_c}{\rho_B}\right) = 0.4377, \quad (2)$$

which has inaccuracy 0.3%. One can define critical density from (2) using known T_c , T_B and ρ_B .

The correlations

$$\frac{T_c}{T_B} \cdot \left(1 - \frac{T_c}{T_B}\right) + \frac{p_c m}{\rho_c k T_c} \cdot \left(1 - \frac{p_c m}{\rho_c k T_c}\right) = 0.4377, \quad (3)$$

$$\frac{p_c m}{\rho_B k T_B} = \frac{T_c}{4 T_B} \cdot \left(1 - \sqrt{4 \cdot \frac{T_c}{T_B} \cdot \left(1 - \frac{T_c}{T_B}\right) - 0.7508}\right)^2,$$

$$\frac{p_c m}{\rho_B k T_B} = \frac{\rho_c^2}{2 \rho_B^2} \cdot \left(1 - \sqrt{4 \cdot \frac{\rho_c}{\rho_B} \cdot \left(1 - \frac{\rho_c}{\rho_B}\right) - 0.7508}\right),$$

where p_c is critical pressure, k is Boltzmann's constant, m is mass of molecule or atom, are also established. It is shown that using the correlations (2) and (3) one can define two of three critical parameters (T_c , p_c , ρ_c) from one of them known, if T_B and ρ_B are known.

[1] Vorob'ev V.S.; Apfelbaum E.M. High Temp., 2016, 54, 175-185.

[2] Apfelbaum E.M.; Vorob'ev V.S. J. Mol. Liq., 2016, 43, 83-87.

[3] Magalinski V.B.; Sidorenko S.N. Statistical and thermodynamic methods in approached theory of condensed condition of matter. Moscow, Nauka, 1996, 203p.



THERMODYNAMIC PHASE EQUILIBRIUM AND STABILITY AT CRITICAL POINT

Umirzakov I.H.

Kutateladze Institute of Thermophysics, Siberian Branch of the Russian Academy of Sciences, 630090 Novosibirsk, Russia
E-mail: umirzakov@itp.nsc.ru

Most of the equations of state (EOS) - the dependences of the pressure $p(T, v)$ on the temperature T and the volume per atom or molecule v , used in physics, chemistry and chemical technologies, are the analytical functions of their variables [1].

As known the critical point of liquid-vapor phase transition is defined from equations [2]

$$\left. \frac{\partial p(T, v)}{\partial v} \right|_{T_c, v_c} = 0, \quad (1)$$

$$\left. \frac{\partial^2 p(T, v)}{\partial v^2} \right|_{T_c, v_c} = 0, \quad (2)$$

where T_c and v_c are critical temperature and volume, respectively.

Usually Eqs. (1) and (2) are considered as conditions of thermodynamic stability of substance at the critical point [2].

Eq. (1) for analytical EOS was obtained from the condition of equality of liquid and vapor pressures, coexisting with each other in phase equilibrium at the same temperature, and Eq. (2) was obtained from the condition of thermodynamic stability of substance at the critical point [3].

We have shown that if the EOS is analytical function of its variables at critical point then Eq. (2) is the consequence of the equality of chemical potentials of liquid and vapor, coexisting with each other in phase equilibrium at the same temperature and pressure. So, Eqs. (1) and (2) are the consequences of the conditions of thermodynamic phase equilibrium only.

The result obtained can be very significant to study critical point of real substance.

[1] Walas S.M. Phase equilibria in chemical engineering. Butterworth publ., London, 1985.

[2] Reid R. C.; Prausnitz J. M.; Sherwood T.K. The properties of gases and liquids. McGraw-Hill, London, 1977.

[3] Landau L.D., Lifschitz E.M. Statistical physics. Pergamon, Oxford, 1980.



Section 2.

Thermochemistry and databases

Virtual presentations

ANALYSIS OF LOW-TEMPERATURE HEAT CAPACITY OF *O*-SEMIQUINIC COMPLEXES OF COBALT

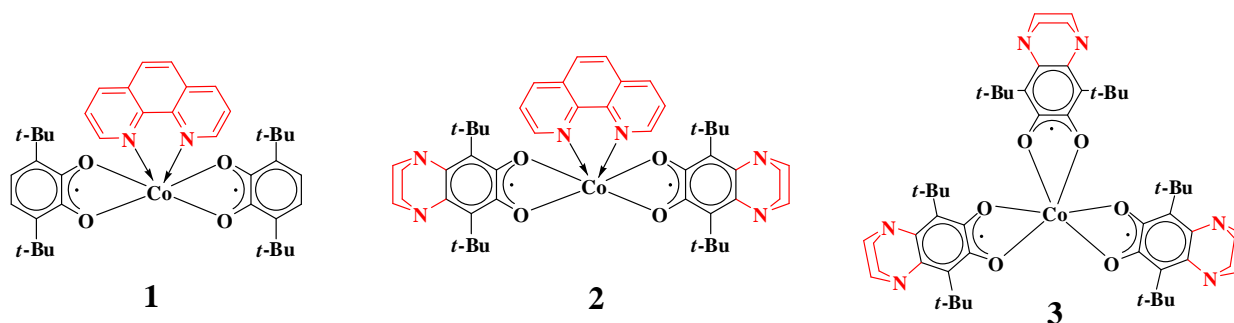
Arapova A.V.¹, Bubnov M.P.¹, Skorodumova N.A.¹, Smirnova N.N.²

¹Razuvaev Institute of Organometallic Chemistry, Russian Academy of Sciences, 603950 Nizhny Novgorod, Russia

²Lobachevsky Nizhny Novgorod University, 603950 Nizhny Novgorod, Russia

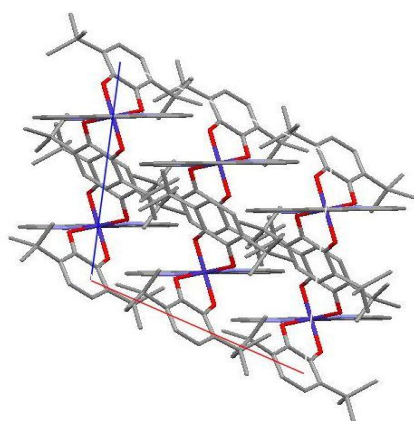
E-mail: av_arapova@mail.ru

Heat capacity of (1,10-phenanthroline)*bis*(3,6-di-*tert*-butyl-*o*-benzosemiquinone)cobalt (**1**), (1,10-phenanthroline)*bis*(4,5-(*N,N*-piperazine-1,4-di-yl)-3,6-di-*tert*-butyl-*o*-benzosemiquinone)cobalt (**2**) and *tris*(4,5-(*N,N*-piperazine-1,4-di-yl)-3,6-di-*tert*-butyl-*o*-benzosemiquinone)cobalt (**3**) represented in Figures



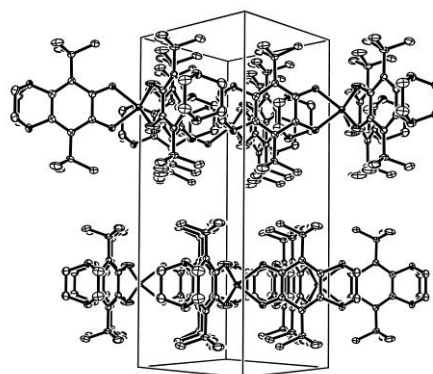
was measured by adiabatic vacuum calorimetry in the range of 7-330(350K).

Analysis of low-temperature heat capacity of investigated complexes was provided on the base of Debye theory of heat capacity of solids and its multifractal generalization [1-2]. Founded values of fractal dimension reflect chain structure of complex **1** ($D = 1.3$) and mostly layered structures of complexes **2** and **3** ($D = 1.6$ and 1.8 respectively). These calculations are confirmed by data of X-ray analysis for complexes **1** and **3**:



(1,10-phen)Co(3,6-DBSQ)₂

$D = 1.3$



Co(4,5-N,N-pipe-3,6-DBSQ)₃

$D = 1.8$

This work was supported by RFBR (grant № 16-03-00700a), Program of Presidium of RAS supporting fundamental research, Russian President grant supporting scientific schools (NSh-7916.2016.3).

[1] Yakubov, T. Doklady Chemistry, 1990, 310, 1, 145–149.

[2] Lazarev, V; Izotov, A; Gavrichev, K; Shebersheneva, O. Thermochim. Acta, 1995, 269, 109–116.

CRYSTAL STRUCTURE AND PHYSICAL-CHEMISTRY PROPERTIES OF THE Co-SUBSTITUTED FERRITE YTTRIUM

Bryuzgina A.V., Urusova A.S., Cherepanov V.A.

Department of Chemistry, Institute of Natural Sciences, Ural Federal University, Mira St. 19, 620002 Yekaterinburg, Russia

E-mail: anna.bryuzgina@mail.ru

Relevance of the work is due to the fact that at the present time the compounds with perovskite structure associated with increased interest, and the unique physical and chemical properties, such as high-temperature superconductivity, mixed electronic-ionic conductivity [1-2].

At last decade the complex oxide $YFe_{1-x}Co_xO_{3\pm\delta}$ was intensively studied to exhibit an unusual variety of magnetic properties and structural changes. Another representative of the Y – Fe – Co – O system that attracts attention of many researchers is $Y_3Fe_5O_{12-\delta}$ [3]. Investigated materials are also known to be catalytically active for the complex oxidation of hydrocarbons and as combustion catalysts, as well as being used as sensors and as solid electrolytes [4].

In this work $YFe_{1-x}Co_xO_{3\pm\delta}$ solid solutions were studied in detail.

The samples were prepared using a conventional ceramic and glycerol–nitrate techniques. $YFe_{1-x}Co_xO_{3\pm\delta}$ for the structural examination were quenched from 1373 K (cooling rate about 500 K/h) in air. X-ray diffraction of powder samples was performed at room temperature using diffractometer DRON-6 in Cu- K_α radiation ($\lambda=1.5418 \text{ \AA}$).

According to the results of X-ray diffraction analysis the homogeneity range for the $YFe_{1-x}Co_xO_{3\pm\delta}$ solid solutions at studied conditions appears within $0 \leq x \leq 0.45$. XRD pattern for all single phase samples was refined by Rietveld method within the orthorhombic structure (*sp. gr. Pnma*). (Figure 1).

The refined unit cell parameters and unit cell volumes of $YFe_{1-x}Co_xO_{3\pm\delta}$ were decreased with the increase of cobalt content probably due to larger iron radius of Fe^{3+}/Co^{4+} compared to that of Co^{3+}/Co^{4+} .

The changes of oxygen content in the single phase complex oxides were measured by TGA method (STA 409PC, Netzsch GmbH). The temperature dependence of the oxygen non-stoichiometry of $YFe_{1-x}Co_xO_{3\pm\delta}$ oxide was obtained in air. It is shown that the introduction of cobalt in iron position $YFe_{1-x}Co_xO_{3\pm\delta}$ ($0 \leq x \leq 0.45$) leads to a slight increase in the oxygen content in the samples.

The coefficients of thermal expansion (TEC) of $YFe_{1-x}Co_xO_{3\pm\delta}$ ceramics was studied within the temperature range 298 – 1373 K in air. Table 1 gives the TEC values for the complex samples $YFe_{1-x}Co_xO_{3\pm\delta}$.

Table 1. Average thermal expansion coefficients (TECs) of $YFe_{1-x}Co_xO_{3\pm\delta}$ ($0 \leq x \leq 0.45$) in air

x	temperature range, K	TEC $\times 10^{-6}$, K ⁻¹
0.00	298 - 1373	11.14
0.25	298 – 650	10.80
	650 – 1373	17.42
0.45	298 – 650	14.87
	650 – 1373	21.80

We were also studied the total electrical conductivity and Seebeck coefficient for $YFe_{1-x}Co_xO_{3\pm\delta}$.

[1] Kim J.-H., Manthiram A. J. *Electrochem. Soc.*, 2008, 155, 385-390.

[2] Zhang K., Ge L., Ran R. *Acta Materialia*, 2008, 56, 4876-4889.

[3] Aono H., Moritani K., Naohara T., Maehara T., Hirazawa H., Watanabe Y., *Mater. Letters*, 2011, 65, 1454 – 1465.

[4] Bhat M., Kaur B., Kumar R., Joy P.A., Kulkarni S.D., Bamzai K.K., Kotru P.N., Wanklyn B.M., *Nucl. Instr. & Meth. in Ph. Res.*, 2006, 243, 134–142.

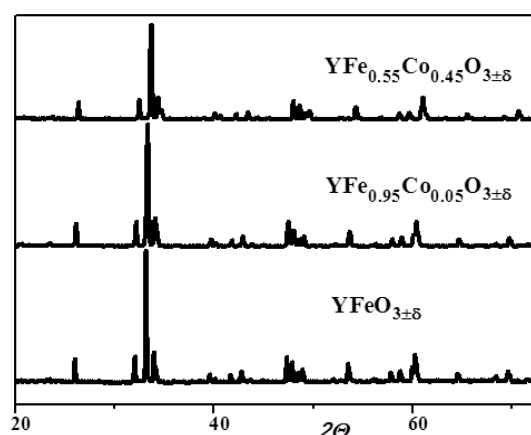


Figure 1. X-ray diffraction pattern of $YFe_{1-x}Co_xO_{3\pm\delta}$ ($0 \leq x \leq 0.45$) at 1373 K



ENTHALPY OF FORMATION OF ALLYL RADICALS

 Chernova E.M.¹, Sitnikov V.N.¹, Orlov Yu.D.¹, Turovtsev V.V.^{1,2}
¹Tver state university

²Tver state medical university

E-mail: Chernova elena_m@mail.ru

Free radicals (R^\bullet) are chemically active form of the substance. The study of the physic-chemical properties R^\bullet is complicated by their high reactivity.

The enthalpy of formation ($\Delta_f H^0$) is one of the important thermodynamic properties of substances. As a rule, $\Delta_f H^0$ can be measured with calorimetric methods, which are not suitable for studying of high reactive substances. $\Delta_f H^0(R^\bullet)$ is usually estimated from the kinetic data of the reactions with their participations using the expression:

$$D(R-X) = \Delta_f H^0(R^\bullet) + \Delta_f H^0(X) - \Delta_f H^0(RX), \quad (1)$$

where $D(R-X)$ is a bond cleavage enthalpy, $\Delta_f H^0(R^\bullet)$ is an enthalpy of formation of the radical, $\Delta_f H^0(RX)$ is an enthalpy of formation of the original molecule, $\Delta_f H^0(X)$ is an enthalpy of formation of the atom X.

Hydrogen separation from compound with multiple bonds leads to the formation of the conjugated radicals with spin density distributed on a fragment containing multiple bonds. Such conjugate radical can be represented in some canonical forms. For example, the conjugate radical $CH_3 - CH \approx CH \approx CH_2$ has the following canonical forms: $CH_3CH=CHC^\bullet H_2$ and $CH_3C^\bullet HCH=CH_2$ having the same electronic structure and, accordingly that, the same physic-chemical properties.

For the first time $\Delta_f H^0(R^\bullet)$ of five allyl radicals (Table 1) were calculated by means of expression (1), and $\Delta_f H^0(R^\bullet)$ of thirteen allyl radicals (Table 2) were defined using the electronic structure identity.

Tables 1. The enthalpies of formation of allyl radicals are calculated according to (1), kJ/mol

№	R^\bullet	$D(R-X)$ ¹	$\Delta_f H^0(RX)$ ²	$\Delta_f H^0(R^\bullet)$
1.	$E-CH_3CH=CHC^\bullet H_2$	356.8	-10.8±1.0	128.0
2.	$CH_2=C(C^\bullet H_2)C(CH_3)=CH_2$	374.9±13.0	45.1	202.0
3.	$CH_2=CHC^\bullet H(CH_2)_4CH=CH_2$	349.8	21.9	153.7
4.	$CH_3CH=CHC^\bullet H(CH_2)_4CH_3$	344.0	-92.0 -115.3 ³	34.0 10.7
5.	$CH_3CH=CHC^\bullet H(CH_2)_3CH=CHCH_3$	341.6	-21.6	112.48

¹ bond cleavage enthalpy $D(R-H)$ are derived from [1],

² enthalpy of formation of parent molecules were taken from [2],

³ it was evaluated by macroincrementation method

Table 2. The enthalpies of formation of allyl radicals are calculated according to electronic structure, kJ/mol

№	R^\bullet	$\Delta_f H^0(R^\bullet)$	№	R^\bullet	$\Delta_f H^0(R^\bullet)$
1.	$CH_3-C^\bullet H-CH=CH-CH_3$	92.0	2.	$CH_3C^\bullet HCH=CH(CH_2)_3CH_3$	29.7
3.	$C^\bullet H_2-CH=C(CH_3)-CH=CH_2$	193.7	4.	$(CH_3)_2C=CHC^\bullet HCH(CH_3)_2$	-1.4
5.	$C^\bullet H_2-CH=CH-(CH_2)_2CH_3$	89.0	6.	$C^\bullet H_2CH=CH(CH_2)_4CH=CH_2$	153.7
7.	$(CH_2=CH)_2C=CH-C^\bullet H_2$	274.0	8.	$CH_3C^\bullet HCH=CH(CH_2)_4CH_3$	34.0 10.7
9.	$C^\bullet H_2CH=CHCH=CH(CH_2)_2CH_3$	130.5	10.	$CH_3C^\bullet HCH=CH(CH_2)_3CH=CHCH_3$	112.48
11.	$C^\bullet H_2CH=CH(CH_2)_3CH=CH_2$	175.0	12.	$C^\bullet H_2CH=CH(CH_2)_{12}CH_3$	-119.5
13.	$C^\bullet H_2CH=CH(CH_2)_4CH_3$	49.8			

[1] J.-R. Luo, Comprehensive handbook of chemical bond energies, L., N.-Y.: CRC Press, Boca Raton, 2007, 1657 p.

[2] NIST Scientific and Technical Databases, version 2011. <http://webbook.nist.gov/chemistry/>

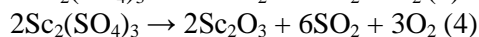
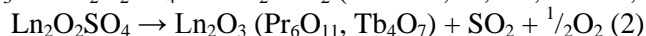
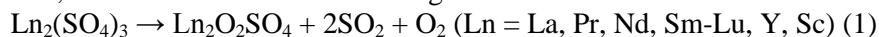
THERMODYNAMICS OF THERMAL DECOMPOSITION SULFATE RARE-EARTH ELEMENTS

Denisenko Yu.G., Osseni S.A., Basova S.A., Novikova O.A., Andreev O.V.

Tyumen State University, 625003 Tyumen, Russia

E-mail: y.g.denisenko@utmn.ru

In this work, we have studied the decomposition process of rare earth elements sulfates in an inert atmosphere by DSC, it was established the following reactions:



Adding together (1) and (2) we will get:

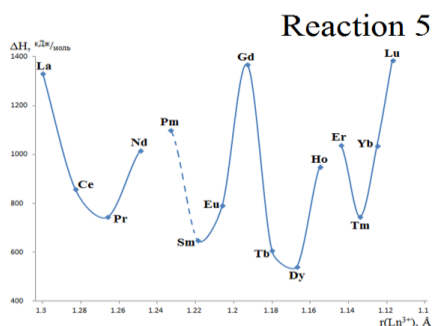
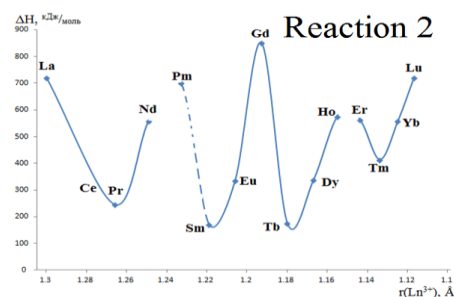
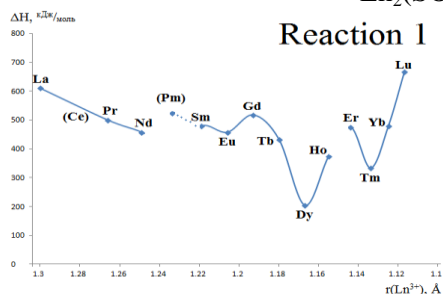
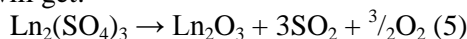


Figure 1. Relationship between enthalpy of reaction and rare earth ion radius for reaction (1), (2) and (5).

The variation of enthalpy of reactions (1) and (2) showed a tetrad effect depending on $r(\text{Ln}^{3+})$. This effect is caused by periodicity of REE electronic structure. During the decomposition, cerium and yttrium showed a different tetrad effect.

For REE from La to Eu $\Delta H_r(1)$ decreases monotonously with $r(\text{Ln}^{3+})$ and the resulting compounds: $\text{Ln}_2\text{O}_2\text{SO}_4$ of the first tetrad (La, Ce, Pr, Nd) is the most stable, which allowed a linear tetrad.

There is a clear periodicity of ΔH_r against $r(\text{Ln}^{3+})$ for the third and fourth REE tetrad. The maximum values of ΔH_r are shown for compounds of elements-electronic analogues, essentially 5d - elements La ($4f^0 5d^1 6s^2$) and Lu ($4f^{14} 5d^1 6s^2$). The small value of $r(\text{Lu}^{3+})$ characterizes the maximum value of $\Delta H_r(1)$.

The tetrad effect shows explicitly in enthalpy changing of the decomposition reaction of REE oxysulfates to oxides. Moreover, the relation is approximately equal for elements of first and third tetrad and on the other hand for elements of second and fourth tetrad.

The enthalpy minimums are recorded in the case of Pr and Tb oxysulfates, which decomposed forming mixed oxides Pr_6O_{11} and Tb_4O_7 , their formation enthalpy is significantly higher for the same sesquioxides. The tetrad effect exhibition on ΔH_r against $r(\text{Ln}^{3+})$ for reaction 5 is similar to exhibition for reaction 2, this fact points to the decisive influence of reaction 2 on the total decomposition process and also confirms the effect of the REE nature on the characteristics of their compounds reactions.

HEAT CAPACITY OF RARE-EARTH BISMUTH GERMANATES RBiGeO₅ (R - Sm, Gd, Tb, Dy)

Denisova L.T., Galiahmetova N.A.

Russia, Krasnoyarsk, Siberian federal university

E-mail: antluba@mail.ru

Synthesis of novel materials based on complex oxide compounds and improvement of existing production technologies based on studies of both phase equilibria and composition– structure–property features. In particular, this applies to complex germanates oxides RBiGeO₅ (R - rare-earth metals). For these substances, there are data on the structure [1–3], optical properties [3] and magnetic susceptibility of YbBiGeO₅ [1]. At the same time, there is a lack in information about the heat capacity and thermodynamic properties of rare-earth bismuth germanates.

The purpose of this work is to study the temperature dependence of molar heat capacity of RBiGeO₅ (R - Sm, Gd, Tb, Dy). Bulk powder samples of RBiGeO₅ were obtained by solid-state reaction of oxides R₂O₃, Bi₂O₃, and GeO₂. A stoichiometric mixture of the starting oxides was thoroughly ground in an agate mortar and then pressed into pellets. The green compacts were fired in air, first at 1003, 1073, 1123 and 1143 K for 20 h at each temperature and then at 1173 and 1223 K for 50 h at each temperature. To drive the solid state reaction to completion, the samples were reground and pressed after each heat treatment step. The phase composition of the samples thus prepared was determined by X-ray diffraction on a PANalytical X'Pert Pro MPD diffractometer (the Netherlands) with CuK α radiation. X -ray diffraction patterns were collected using a PIXcel fast detector and graphite monochromator. The lattice parameters of RBiGeO₅ were determined by profile fitting using derivative difference minimization. The data obtained are presented in Table 1. It can be seen that the present results agree well with previous data. All the compounds are isostructural and crystallized in the rhombic symmetry, space group Pbca.

Table 1. Unit cells parameters of RBiGeO₅

Parameters	SmBiGeO ₅		GdBiGeO ₅	TbBiGeO ₅		DyBiGeO ₅	
<i>a</i> , Å	5.4125(8)	5.4160(5)	5.3867(1)	5.3650(4)	5.37001(3)	5.3455(4)	5.35265(6)
<i>b</i> , Å	15.283(2)	15.2961(3)	15.2736(4)	15.241(1)	15.25895(7)	15.212(1)	15.24599(7)
<i>c</i> , Å	11.275(2)	11.2814(1)	11.1893(2)	11.1422(9)	11.14994(6)	11.0855(8)	11.09615(6)
β , град							
<i>V</i> , Å ³	932.7(3)	934.60(2)	920.59(4)	911.1(1)	913.634(8)	901.4(1)	905.52(1)
References	[3]	This work	This work	[3]	This work	[3]	This work

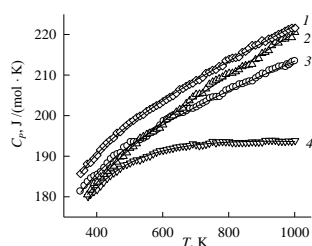


Fig. 1.

Temperature dependence of the heat capacity of RBiGeO₅ (R - Tb (1), Sm (2), Dy (3), Gd (4))

$$\text{TbBiGeO}_5: C_p = (184.14 \pm 0.34) + (39.6 \pm 0.4) \cdot 10^{-3} T - (15.15 \pm 0.36) \cdot 10^5 T^{-2}$$

$$\text{SmBiGeO}_5: C_p = (169.97 \pm 0.34) + (48.37 \pm 0.40) \cdot 10^{-3} T - (16.12 \pm 0.39) \cdot 10^5 T^{-2}$$

$$\text{DyBiGeO}_5: C_p = (183.10 \pm 0.44) + (32.0 \pm 0.5) \cdot 10^{-3} T - (16.39 \pm 0.48) \cdot 10^5 T^{-2}$$

$$\text{GdBiGeO}_5: C_p = (204.66 \pm 0.31) - (8.0 \pm 0.3) \cdot 10^{-3} T - (30.96 \pm 0.36) \cdot 10^5 T^{-2}$$

Obtained C_p data allow us to find the changes in enthalpy, entropy and reduced Gibbs energy according to the known thermodynamic equations.

[1] Cascales C., Campa J.A., Puebla E.G. et al. J. Mater. Chem., 2002, 12, 3626-3630.

[2] Cascales C., Zaldo C J. Solid State Chem., 2003, 173, 262-267.

[3] Cascales C., Zaldo C. Chem. Mater.. 2006, 18, 3742-3753.



INFLUENCE OF THE REDOX MIXTURE COMPOSITION ON THE PROCESS AND RESULTS OF COMBUSTION SYNTHESIS OF $\text{Sr}_2\text{Ni}_{0.7}\text{Mg}_{0.3}\text{MoO}_6$

Filonova E.A., Melnikova A.A., Russkikh O.V.

Institute of Natural Sciences, Ural Federal University, 620002 Yekaterinburg, Russia

E-mail: elena.filonova@urfu.ru

Solid oxide fuel cells (SOFCs) are perspective electrochemical devices that transform chemical energy into electrical power by catalytic combustion of methane. Commonly used nickel electrodes are proposed to be substituted by perovskite-type oxides due to their low cost, catalytic activity and thermochemical stability at relatively high temperatures.

Sr_2MMoO_6 (M=Mg, Ni) double perovskites are considered to be potential anode materials for SOFCs. However, the terminal compositions are unstable in a reducing ($\text{Sr}_2\text{NiMoO}_6$) and oxidation ($\text{Sr}_2\text{MgMoO}_6$) atmosphere. Intermediate compositions $\text{Sr}_2\text{Ni}_{1-x}\text{Mg}_x\text{MoO}_6$ used to improve the stability under both pO_2 -high and pO_2 -low conditions. $\text{Sr}_2\text{Ni}_{0.75}\text{Mg}_{0.25}\text{MoO}_6$ composition was characterized earlier [1].

In the present work $\text{Sr}_2\text{Ni}_{0.7}\text{Mg}_{0.3}\text{MoO}_6$ samples have been prepared by the solution combustion method employing glycine (or glycerol) as complexing agent and fuel and ammonium nitrate (AN) as trigger to promote the combustion process [2]. The temperature of combustion synthesis can be adjusted from the fuel-to-oxidisers molar ratio (φ) to the precursor solution [3]. The mass ratio between AN and glycine (or glycerol) is named R. φ and R parameters were varied between 1–3 and 0.3–1.00, respectively. The starting materials (with purity is not less than 99.5%) SrCO_3 , MgO were first dissolved with diluted nitric acid then mixed with $\text{Ni}(\text{CH}_3\text{COO})_2 \cdot 4\text{H}_2\text{O}$ and $(\text{NH}_4)_6\text{Mo}_7\text{O}_{24} \cdot 4\text{H}_2\text{O}$. The obtained solution was heated about 348 K during 12h. Then solution was evaporated at 523 K on a hot plate. Calcining the powder obtained by combustion synthesis was carried out in air in five steps with intermediate grindings: the first step at 1173 K, the second step at 1273 K and three steps at 1373 K.

In order to explore the mechanism of synthesis a temperature of combustion and composition of the exit gases were studied [3]. The composition of the exit gas was investigated by electronic gas-analyzer Testo 350XL. Maximum temperature of synthesis was measured using an infrared thermometer Testo 835.

X-ray diffraction measurements carrying out on DRON-6 diffractometer in Cu $\text{K}\alpha$ -radiation at each annealing step have been performed to determine the conditions of the synthesis single-phase materials.

Optimum conditions of $\text{Sr}_2\text{Ni}_{0.7}\text{Mg}_{0.3}\text{MoO}_6$ phase formation were presented. Only fuel-rich mixtures were effective, but carbonaceous deposits were formed when too much glycine (or glycerol) was used. In addition the use of high values of the parameters R and φ together led to a sharp increase in the combustion reaction rate. Under these conditions, the combustion step only promoted to the formation of intermediates: strontium and nickel molybdates and magnesium oxide.

[1] Filonova E.A., Dmitriev A.S., Pikalov P.S. et al. *Solid State Ionics*. 2014. V. 262. P. 365-369.

[2] Dager P.K., Chanquía C.M., Mogni L. et al. *Materials Letters*. 2015. V. 141. P. 248-251.

[3] Khaliullin Sh.M., Bamburov V.G., Zhuravlev V.D. et al. *Doklady Chemistry*. 2015. V. 461, I. 2. P. 93-95.



THE THERMODYNAMIC FUNCTIONS OF 4-METHYL-1,3-DIOXANE IN THE STATE OF AN IDEAL GAS

Garist I.V.¹, Kavaliova K.U.¹, Roganov G.N.¹, Emel'yanenko V.N.²

¹Mogilev State University of Food Technologies, 212027 Mogilev, Belarus

²Institute of Physics, University of Rostock, 18051 Rostock, Germany

E-mail: garistina@rambler.ru

The alkyl derivatives of 1,3-dioxane are widely used as solvents, plasticizers, additives for motor fuels to increase their octane number, additives to paints to prevent skinning during storage, are used in the production of plant growth regulators, medicinal preparations and etc. In large-tonnage organic synthesis the alkyl derivatives 1,3-dioxane are the initial substances for obtaining a diene hydrocarbons and intermediate products in the synthesis of heat resistant and flame retardant polymers. In addition, as the saturated oxygen-containing heterocyclic compounds, the alkyl homologues of 1,3-dioxane are steadily theoretically interesting for the development of ideas about the relationship of conformational, configurational and optical isomers of cyclic molecules.

The thermodynamic properties of substance in the state of an ideal gas to the present time is only defined for unsubstituted 1,3-dioxane [1], the properties of its alkyl derivatives by the methods of statistical thermodynamics were not evaluated.

The structural parameters of the molecule 4-methyl-1,3-dioxane are known from microwave researches and were determined from *ab initio* B3LYP (6-311++G (3df,3pd)) calculations. According to the data known from the literature, the molecule of 4-methyl-1,3-dioxane mainly adopts two unequal chair-conformations with equatorial C(e) and axial C(a) orientation of methyl group, and the two twisted boat-conformations, T(e) and T(a) are much less stable. In addition, since 4-methyl-1,3-dioxane molecule is asymmetric, thus, 4 pairs of conformational diastereomers appears. The molar ratio of conformers at equilibrium was determined on the basis of calculation B3LYP (6-311++G (3df,3pd)), their relative energies: C(e):C(a):T(e):T(a) at 298.15 and 1000 K are respectively 99.800:0.198:0.001:0.001 and 80.9:12.8:3.2:3.0 % mol. A mixture of conformational diastereomers taken into consideration.

Sets of fundamental frequencies adopted for the calculations thermodynamic functions of 4-methyl-1,3-dioxane for substance in a state of ideal gas within temperature range 298.15-1000 K were formed using known data sets of fundamental frequencies on the basis of experimental IR, Raman spectra and complemented by frequencies of the calculated B3LYP (6-311++G (3df,3pd)) spectra using different scaling factors in certain ranges of the spectrum.

A comparison vibrations (IR, Raman, range 100-1500 cm⁻¹) of 1,3-dioxane for liquid and gaseous state and the fundamental vibrations from the calculations B3LYP (6-311++G (3df,3pd)) for the gas phase, shows that a good agreement between the calculated fundamental vibrations and the experimental ones is achieved by using scaling factors in certain ranges of the spectrum: 1.0301 (for frequencies range 100-400 cm⁻¹), 1.0047 (400-1600 cm⁻¹) and 0.9582 (1600-3500 cm⁻¹).

The values of thermodynamic functions of 4-methyl-1,3-dioxane obtained for nine temperatures in the range 298.15-1000 K (J/(mol·K), ideal gas), in the table 1 they are for 298.15 and 1000 K.

Table 1. Thermodynamic functions of 4-methyl-1,3-dioxane.

T, K	C _p ^o (J/(mol·K))	S ^o (J/(mol·K))	-(ΔG _T ^o -ΔH ₀ ^o)/T (J/(mol·K))	(ΔH _T ^o -ΔH ₀ ^o)/T (J/(mol·K))
298.15	113.8	337.0	271.0	66.0
1000	299.0	586.5	408.6	177.9

[1] Dorofeeva, O.V. *Thermochimica Acta*, 1992, 200, 121-150.



HEAT CAPACITY AND THERMODYNAMIC FUNCTIONS OF NANOSIZED FERRO-CHROMO-MANGANITE $\text{NdMg}_{0.5}\text{FeCrMnO}_{6.5}$ IN THE RANGE OF 298.15-673 K

Kassenov B.K., Kassenova Sh.B., Sagintaeva Zh.I., Kuanyshbekov E.E.

Chemical-metallurgy institute named after Zh. Abishev, 100009, Karaganda, Republic of Kazakhstan

E-mail: kasenov1946@mail.ru

Until now mainly investigation are basis on ferrites, chromites and manganites, mixed ferrite- manganites and chromite-manganites of rare-earth alkali and alkaline earth metals [1, 2]. A certain interest is the combination of manganite, chromite and iron in one compound in the form of a ferro-chrome-manganite and especially getting their nanoparticles and the investigation of their thermodynamic properties.

In the connection with the above we present in this work the results of calorimetric study of the heat capacity of nano-sized ferro-chrome-manganite $\text{NdMg}_{0.5}\text{FeCrMnO}_{6.5}$, which synthesized by ceramic technology in the range of 800-1200°C from Nd_2O_3 , MgCO_3 , Fe_2O_3 , Cr_2O_3 and Mn_2O_3 . Nanoparticles of ferro-chrome-manganite have been obtained by milling on vibratory «Retsch» (Germany) of brand «MM301».

The calorimetric study of $\text{NdLiFeCrMnO}_{6.5}$ heat capacity was carried out in the range of 298.15-673 K on a device ITS-400. The table 1 shows the results of calorimetric study.

Table 1. The experimental values of $\text{NdMg}_{0.5}\text{FeCrMnO}_{6.5}$ heat capacity.

T, K	$C_{p\pm} \bar{\delta}$, J/(gK)	$C_{p\pm} \overset{\circ}{\Delta}$, J/(mol·K)	T, K	$C_{p\pm} \bar{\delta}$, J/(gK)	$C_{p\pm} \overset{\circ}{\Delta}$, J/(mol·K)
298.15	0.5411±0.0152	229±13	498	0.7611±0.0121	322±18
323	0.5661±0.0182	239±13	523	0.7296±0.0145	309±17
348	0.6641±0.0163	281±16	548	0.7651±0.0114	324±18
373	0.9108±0.0230	385±22	573	0.7800±0.0152	330±19
398	0.7566±0.0143	320±18	598	0.8165±0.0127	345±19
423	0.7978±0.0150	337±19	623	0.8753±0.0165	370±21
448	0.8183±0.0126	346±19	648	0.9413±0.0141	398±22
473	0.8594±0.0217	364±20	673	0.9934±0.0166	420±24

In the study of the heat capacity of ferro-chrome-manganite it is established that the heat capacity is racing at 373 K and 473 K, caused by to the phase transitions of II-kind. The equations of the temperature dependence $C_p^{\circ} \sim f(T)$ have derived in view of the T_{tr} .

Standard entropy $S^{\circ}(298.15)$ of ferro-chrome-manganite has been investigated by Kumok [3] using the system of ionic entropy increments.

The temperature dependence of the thermodynamic functions $S^{\circ}(T)$, $H^{\circ}(T) - H^{\circ}(298.15)$, $\Phi^{xx}(T)$ have been calculated using experimental data of $C_p^{\circ}(T)$ and the values of $S^{\circ}(298.15)$.

[1] Kassenov B.K., Mustafin E.S., Sagintaeva Zh.I., Isabaeva M.A., Davrenbekov S.Zh., Kassenova Sh.B., Abildaeva A.Zh., Journal of inorganic chemistry, 2013, 58 (2), 243-245.

[2] Kassenova Sh.B., Abildaeva A.Zh., Sagintaeva Zh.I., Davrenbekov S.Zh., Kassenov B.K., Journal of physical chemistry, 2013, 87 (5), 739-743.

[3] Kumok V.N. The problem of matching the thermodynamic characteristics evaluation methods // Direct and inverse problems of chemical thermodynamics. – Novosibirsk, 1987. – 108-123 pp.

**THERMOCHEMISTRY OF DISSOLUTION OF ARGLABIN'S ANABAZINIL DERIVATIVE C₂₅H₃₂O₃N₂ IN ETHYL ACETATE**Kassenov B.K.¹, Kassenova Sh.B.¹, Sagintaeva Zh.I.¹, Atazhanova G.A.², Adekenov S.M.²¹Chemical-metallurgy institute named after Zh. Abishev, Karaganda, Republic of Kazakhstan²JSC «International research and production holding «Phytochemistry», Karaganda, Republic of KazakhstanE-mail: kasenov1946@mail.ru

Method of solution calorimetry is used for determining the enthalpies of solution, mixing and dilution. These values are important for the development of the theory of structure and chemical thermodynamics of solutions. The enthalpy of solution was used for the calculation of the enthalpy of formation on the basis of Hess's law.

Thermochemical study of dissolution of sesquiterpene lactone anabazinil derivative of arglabin C₂₅H₃₂O₃N₂ was carried out on an automatic isothermal differential calorimeter DAC-1-1A. Checking of instrument calibration was performed by measuring the heat of solution of thrice recrystallized potassium chloride at dilutions of 1: 1600, 1: 2400, 1: 3200 (mol of salt: mol of water). The average of heat of solution of KCl in water (17860 ± 283 J/mol) is in good agreement with the recommended quantity equal to 17577 ± 34 J/mol and with the reference data for the enthalpy of dissolution of KCl at these dilutions. These thermochemical constants were processed by methods of mathematical statistics: errors of experiments and homogeneity of variances were calculated using criteria of Student and Cochran. Experimental determination of the enthalpy of anabazinil derivative of arglabin C₂₅H₃₂O₃N₂ was carried out by dissolution in ethyl acetate at dilutions of 1: 6000, 1: 12000 and 1: 24000 (mol compounds: ethyl acetate mol). The table 1 shows the results of calorimetric determination of the heat of the dissolution anabazinil derivative of arglabin in ethyl acetate at various dilutions.

Table 1. The enthalpy of dissolution of C₂₅H₃₂O₃N₂ in ethyl acetate at various dilutions (mol C₁₅H₂₀O₃ : mol 96 % ethanol), 1:6000, 1:12000 and 1:24000

mass, г	$\Delta H^m_{diss.}$, kJ/mol	mass, g	$\Delta H^m_{diss.}$, kJ/mol	mass, g	$\Delta H^m_{diss.}$, kJ/mol
1:6000		1:12000		1:24000	
0.0034	70.26	0.0017	121.46	0.0009	214.26
0.0034	70.61	0.0017	119.44	0.0009	214.71
0.0034	70.56	0.0017	120.26	0.0009	209.54
0.0034	69.80	0.0017	118.02	0.0009	210.35
0.0034	71.68	0.0017	121.53	0.0009	210.72
average $\Delta H^m_{diss.(I)} = 70.58 \pm 0.86$		average $\Delta H^m_{diss.(II)} = 120.14 \pm 1.83$		average $\Delta H^m_{diss.(III)} = 211.92 \pm 2.97$	

The results from the table 1, which depend on the basis $\Delta H^m_{pacm.} = a + b\sqrt{m}$, have been extrapolated to infinite dilution. This dependence is described by equation (kJ/mol) for anabazinil derivative of arglabin in standard (infinitely) dilute solution of ethyl acetate:

$$\Delta H^m_{diss.} \text{ C}_{25}\text{H}_{32}\text{O}_3\text{N}_2 = 342.4 - 6517.51 \sqrt{m} . \quad (1)$$

The standard enthalpy of dissolution of arglabin anabazinil derivative in standard (infinite dilution) solution of ethyl acetate is equal 342.4±0.01 kJ/mol.

**SYNTHESIS AND THERMODYNAMICS OF LEAD (II), MANGANESE (II) AND COBALT (II) CARBOXYLATE COMPLEXES**Dement'ev A.I.², Rodyakina S.N.^{1,2}, Kayumova D.B.¹, Kamkin N.N.², Yaryshev N.G.², Alikhanyan A.S.¹¹Kurnakov Institute of General and Inorganic Chemistry of the Russian Academy of Science, 119991, Moscow, Russia²Moscow State Pedagogical University Institute of biology and chemistry, 119991, Moscow, Russia

E-mail: dkayumova@gmail.com

Manganese (II), cobalt (II) oxopivalates and lead (II) pivalate were synthesized and studied by the mass-spectrometric and thermal gravimetric analysis.

The synthesis of volatile compounds of lead, cobalt and manganese was shown to be quite simple and may be conditional divided into two separate stages. The first stage is a reaction between the freshly precipitated metal hydroxide and pivalic acid with hydrated complexes formation, such as $[x \text{MPiv}_2 \cdot y \text{H}_2\text{O}]$. At the second stage the hydrated products is dried and vaporized in vacuum ($p = 1 \text{ Pa}$) in the temperature range of 150 - 300°C.

The investigations have shown that the thermal behavior of the synthesized pivalate complexes essentially depends on the vaporization conditions of the process. The synthesized complexes except the lead one are generally hydrated. Being heated under atmospheric pressure these cobalt and manganese compounds underwent deep hydrolysis and formed the corresponding metal oxide as a final product. On the other side the mass spectrometric analysis was performed in vacuum, and the thermal behavior of the hydrated complexes was completely different: a significant amount of crystallization water was removed with the minor hydrolysis leading to the volatile metal oxopivalates M_4OPiv_6 . The mass spectrometric investigations of the thermodynamic characteristics were performed on Thermo Fisher Scientific DSQII mass spectrometer with a TFS DIP direct injection probe. A long quartz capillary (microcrucible with inner diameter 0.85 mm and the length 9.0 mm) was used for evaporation and considered as analogue of Knudsen effusion cell [1]. Upon investigation of the temperature dependence of the main ionic currents intensities in the mass spectra of the saturated vapor, the standard enthalpies of sublimation of lead (II) pivalate, manganese (II) and cobalt (II) oxopivalates were calculated by the Clausius–Clapeyron equation using the least squares method. The average means of the data from three independent experiments are presented in Table 1. The enthalpies of sublimation of the cobalt and manganese oxopivalates were found at the first time, the enthalpy of sublimation of the lead pivalate $\text{Pb}(\text{Piv})_2$ was shown to correspond sufficiently published data [2].

Low values of the enthalpies, high volatility and monomolecular composition of the gas phase allow us to use these complexes as precursors for oxide films preparation and as materials for MOCVD method.

Table 1. Enthalpies of sublimation of lead pivalate, cobalt and manganese oxopivalates.

Complex	Temperature range, K	$\Delta_s H^\circ_T$, kJ/mol
PbPiv_2	350-382	113 ± 10 (103.5 ± 2.9) [2]
Co_4OPiv_6	380-425	88 ± 10
Mn_4OPiv_6	446-479	81 ± 14

[1] Kamkin N. N., Yaryshev N. G., Alikhanyan A. S., Russian Journal of Inorganic Chemistry, 2010, 55 (9), 1443–1447.

[2] Khoretonenko N.M., Rykov A.N., Korenev Y.M., Alikhanyan A.S., Malkerova I.P. Zurnal neorganiceskoj himii, 1995, 40(6), 929-932



THERMODYNAMIC PROPERTIES OF BIOLOGICALLY ACTIVE SUBSTANCES

Knyazev A.V.¹, Shipilova A.S.¹, Gusarova E.V.¹, Knyazeva S.S.¹, Smirnova N.N.¹,
Emel'yanenko V.N.², Verevkin S.P.²

¹Chemistry Department, Lobachevsky University, 603950, Nizhni Novgorod, Russia

²Institute of Physics, University of Rostock, 18051 Rostock, Germany

E-mail: knyazevav@gmail.com

Vitamins and hormones are the most important biologically active substances therefore the goals of this work include calorimetric determination of the temperature dependences of the heat capacity of riboflavin (B₂), nicotinic acid (B₃), folic acid dehydrate (B₉), cyanocobalamin(B₁₂), methylprednisolone and methylprednisolone aceponate from 6 to 350 K, definition the energies and enthalpies of combustion of B₂, B₃, B₉, B₁₂, prednisolone, hydrocortisone acetate, methylprednisolone, methylprednisolone aceponate and calculation of the standard thermodynamic functions.

To measure the heat capacities of B₂, B₃, B₉ and B₁₂, methylprednisolone and methylprednisolone aceponate in the range from 6 to 350 K a BKT-3.0 automatic precision adiabatic vacuum calorimeter with discrete heating was used. The experimental data were used to calculate standard thermodynamic functions for the range from 0 to 330 K. The heat capacity for all substances except for methylprednisolone aceponate gradually increases with rising temperature and does not show any peculiarities. The heat capacity for methylprednisolone aceponate in intervals from (7 to 102) K and from (140 to 346) K gradually increases with rising temperature and does not show any peculiarities, but from (102 to 140) K there is seen an anomalous heat capacity. The standard enthalpy of phase transition is $\Delta_{tr}H^\circ = (220 \pm 2) \text{ J}\cdot\text{mol}^{-1}$. The absolute entropies of compounds and the corresponding simple substances were used to calculate the standard entropy of formation of the compound under study at 298.15 K.

Table 1. Enthalpies of combustions and thermodynamic characteristics of formation of biologically active substances

Compound	$-\Delta_c H^\circ$ (kJ/mol)	$-\Delta_f H^\circ(298)$ (kJ/mol)	$-\Delta_f S^\circ(298)$ (J/(mol·K))	$-\Delta_f G^\circ(298)$ (kJ/mol)
Riboflavin	8116 ± 13	1432 ± 13	1961 ± 3	847 ± 14
Nicotinic acid	-	344.9 ± 0.9	503 ± 3	195 ± 2
Folic acid dihydrate	8942.8 ± 5.2	1821.0 ± 5.7	2515.5 ± 9.5	1071 ± 6
Cyanocobalamin	33459 ± 14	5017 ± 15	7281 ± 5	2846 ± 15
Prednisolone	11244.8 ± 7.6	1020.6 ± 7.6	-	-
Hydrocortisone acetate	12317.1 ± 11.6	1307.0 ± 11.6	-	-
Methylprednisolone	11898.9 ± 6.7	1045.8 ± 7.3	2141 ± 11	407 ± 8
Methylprednisolone aceponate	14304.4 ± 9.1	1465.3 ± 9.8	2592.9 ± 13.7	692 ± 10

In a calorimeter with a static bomb and an isothermal shield, the energies of combustion of the B₂, B₉, B₁₂, prednisolone, hydrocortisone acetate, methylprednisolone and methylprednisolone aceponate have been measured at 298.15 K. The enthalpies of combustion $\Delta_c H^\circ$ and the thermodynamic parameters of formation $\Delta_f H^\circ$, $\Delta_f S^\circ$, $\Delta_f G^\circ$ of the studied substances from simple substances at T = 298.15 K and p = 0.1 MPa have been calculated. Received values of standard enthalpies and entropies of formation were used to calculate the standard Gibbs function of formation at 298K (Table1) [1-5].

[1] Knyazev A.V., Smirnova N.N., Shipilova A.S., Shushunov A.N., Gusarova E.V., Knyazeva S.S., *Thermochim. Acta*, 2015, 604, 115–121.

[2] Knyazev A.V., Emel'yanenko V.N., Shipilova A.S., Lelet M.I., Gusarova E.V., Knyazeva S.S., Verevkin S.P., *J. Chem. Thermodyn.*, 2016, 100, 185–190.

[3] Knyazev A.V., Smirnova N.N., Shipilova A.S., Larina V.N., Gusarova E.V., Knyazeva S.S., *J. Therm. Anal. Calorim.*, 2016, 123, 2201–2206.

[4] Knyazev A.V., Emel'yanenko V.N., Smirnova N.N., Stepanova O.V., Shipilova A.S., Markin A.V., Samosudova Ya.S., Gusarova E.V., Knyazeva S.S., Verevkin S.P., *J. Chem. Thermodynamics*, 2016, 103, 244–248.

[5] Knyazev A.V., Emel'yanenko V.N., Smirnova N.N., Zaitsau D.H., Stepanova O.V., Shipilova A.S., Markin A.V., Gusarova E.V., Knyazeva S.S., Verevkin S.P., *J. Chem. Thermodynamics*, 2017, 107, 37–41.

THERMODYNAMIC PROPERTIES OF $\text{Bi}_3\text{NbTiO}_9$

Krashennikova O.V., Knyazev A.V., Smirnova N.N., Syrov E.V.

Chemistry Department, Lobachevsky University of Nizhni Novgorod Gagarin Av. 23/2, 603950 Nizhni Novgorod, Russia
E-mail: okkraska@gmail.com

Bismuth-containing layered perovskites, first described by Aurivillius, have recently received researchers' attention. Extensive investigations of these compounds deal with various attractive physical properties, such as high Curie temperatures and a low dielectric conductivity, superior polarization fatigue resistant characteristics. Therefore, materials based on them can be used for creation of non-volatile random access memory (FRAM). Moreover, Aurivillius phases have also found other applications as a photocatalyst working under visible light. Chemical composition of these compounds is described by the general formula $\text{A}_{m-1}\text{Bi}_2\text{B}_m\text{O}_{3m+3}$, where m is typically from 1 to 9. Their structure has been studied in detail in [1]. $\text{Bi}_3\text{NbTiO}_9$ is the member of this family with $m = 2$. Using the differential scanning calorimetry was found that this substance undergoes a phase transition at the temperature of 1173 K [1]. The study of thermodynamic properties is necessary for a quantitative description of processes occurring with the participation of Aurivillius phases, as well as predicting of the conditions of synthesis on the industrial scale. The temperature

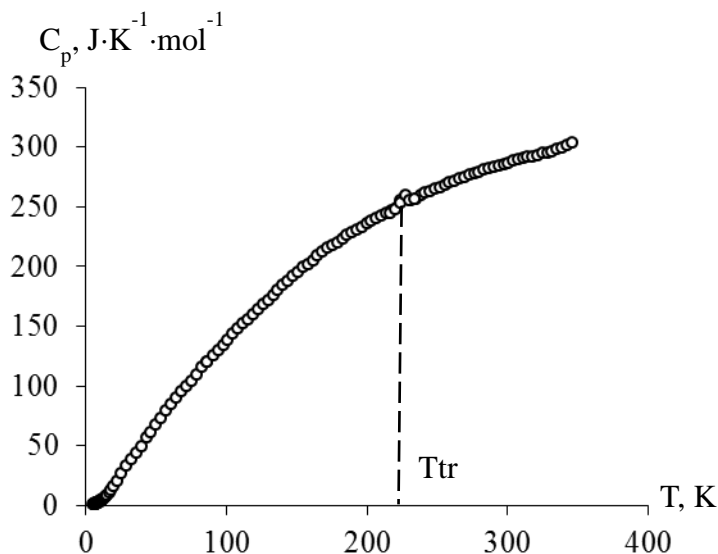


Figure 1. Temperature dependence of heat capacity of $\text{Bi}_3\text{NbTiO}_9$.

dependence of heat capacity has been measured for tribismuth niobium titanium oxide by precision adiabatic vacuum calorimetry. The experimental values of the molar heat capacity of $\text{Bi}_3\text{NbTiO}_9$, over the range from 7 to 340 K are presented in Figure 1. The heat capacity of this substance in intervals from 7 to 221 and from 230 to 340 K gradually increases with rising temperature and does not show any peculiarities, but from 221 to 230 K there is seen an anomalous heat capacity. The transition temperature of the sample under study $T_{tr} = 227 \pm 0.1$ K was estimated as the temperature of maximal heat capacity value within the temperature interval of the transition. The standard enthalpy and entropy of phase transition are $\Delta_{tr}H^\circ = 31.66 \pm 0.04$ J/mol and $\Delta_{tr}S^\circ = 0.146 \pm 0.005$ J/(mol·K). To calculate the standard thermodynamic functions of the tribismuth niobium titanium oxide, its C_p° values were extrapolated from the temperature of the measurement beginning at approximately 7 K to 0 K by graphic method. The absolute entropies of tribismuth niobium titanium oxide and the corresponding simple substances (Bi (cr), Ti (cr), Nb (cr) and O_2 (g)) were used to calculate the standard entropy of formation of the compound under study at 298.15 K; $\Delta_f S^\circ(298.15, \text{Bi}_3\text{NbTiO}_9, \text{cr}) = -817.0 \pm 0.8$ J·K⁻¹·mol⁻¹. From the experimental C_p° values in the range of 25–50 K the value of the fractal dimension D of the tribismuth titanium niobium oxide was evaluated. According to the fractal theory of the heat capacity [2], D is the most important parameter that specifies the character of heterodynamics of the substance structure. It was found that in the range of 25–50 K, $D=1.5$, $\theta_{\max} = 269.4$ K for tribismuth niobium titanium oxide. The D -value points to the chain-layered structure of $\text{Bi}_3\text{NbTiO}_9$.

[1] Knyazev, A.V.; Krashennikova, O.V.; Korokin, V. Zh. Inorganic Materials., 2014, 50, 170–178.

[2] Yakubov, T.S. Dokl. Academy of Science., 1990, 310, 145–150.

1. THERMODYNAMIC ASPECTS OF THE MOLECULAR HYDROGEN SORPTION BY *D*-SCHWARZITES

Krasnov P.O., Shkaberina G.S.
 Reshetnev Siberian State Aerospace University
 E-mail: kpo1980@gmail.com

The main characteristic of hydrogen storage material is its molecular hydrogen sorption capacity (weight fraction of hydrogen in sorbent) which was set by the USA Department of Energy (DOE) to be from 6.5% 15-20 years ago to 9.0% nowadays. Carbon nanostructures were expected to fulfill these criteria due to their large surface area which is essential for gas adsorption. Schwarzites are one of the most known nanoporous carbon structures [1-2]. These materials are strictly periodic and consist of sp^2 carbon atoms forming hexa-, hepta- and octagons with negative Gaussian curvature corresponding to the Schwarz minimal surface. For instance, *Vanderbilt* and *Tersoff* [1] in their pioneer work predicted the C_{60} counterpart with *D* (diamond-like) negative surface curvature, so-called *Buckygym*, containing 168 carbon atoms. Besides that, there are also schwarzites with *P* (primitive) and *G* (gyroid) surfaces [2].

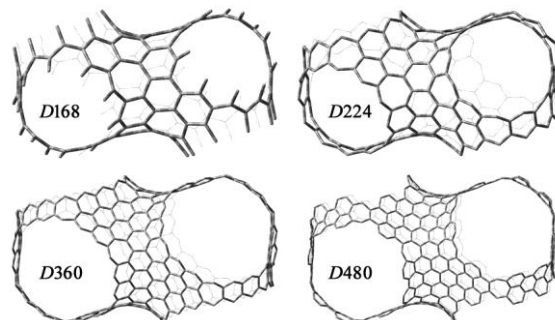


Figure 1. Schwarzites unit cells

Here we report the results of quantum-chemical investigation of molecular hydrogen sorption capacity of *D*-schwarzites containing 168, 224, 360 and 480 carbon atoms (Figure 1). All calculations were carried out in MOPAC2016 program package using semi-empirical PM6-D3 method with *Grimme* correction for dispersion interactions. The impact of temperature and external hydrogen pressure and perspectives of their usage as molecular hydrogen storage are discussed.

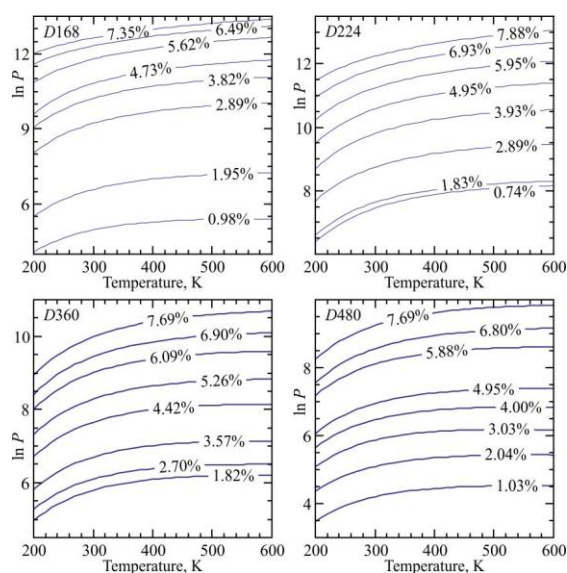


Figure 2. External hydrogen pressure (in kPa) and temperature needed for the certain hydrogen sorption capacity of schwarzites. Percents on the lines are the weight fractions of hydrogen adsorbed

Schwarzites *D168*, *D224*, *D360* and *D480* are considerably lightweight materials. Their gravimetric densities obtained using values of unit cell volume and mass are 1257, 1115, 853 and 745 kg/m^3 , respectively. High porosity of these materials and their large surface area makes them promising candidates for molecular hydrogen storage. However, the calculation shows that hydrogen weight fraction in *D168* is only ~2.89% at 200 K and 5 MPa (Figure 2) and doesn't increase much at higher pressures (3.82% at 10 MPa). Similarly, high pressure of 27, 52 and 76 MPa is needed in order to reach 5.95% hydrogen concentration in *D224* at 200, 250 and 300 K, respectively.

D360 and *D480* schwarzites were found to be more likely to adsorb hydrogen. Only 8 and 4 MPa is needed to reach 7.69% of hydrogen at 200 K, respectively. 22 and 10 MPa is required when temperature increases up to 300 K. This weight fraction is lower than that required by DOE (9%) but the difference can be eliminated by either considering other carbon structures with large interplanar distances or, for example, alkaline atoms intercalation which was proved to enhanced the energy of hydrogen adsorption.

- [1] D. Vanderbilt, J. Tersoff. Phys. Rev. Lett. 1992, 68, 511.
 [2] S.J. Townsend et al. Phys. Rev. Lett. 1992, 69, 921.

**LOW-TEMPERATURE HEAT CAPACITY AND THERMODYNAMIC FUNCTIONS OF TRIS(1,1,1,5,5,5-HEXAFLUORO 2,4-PENTANODIONATE) ALUMINUM (III)**Kuzin T.M.^{1,2}, Bespyatov M.A.¹, Gelfond N.V.¹¹Nikolaev Institute of Inorganic Chemistry, Siberian Branch of the Russian Academy of Sciences, 630090 Novosibirsk, Russia²Institute of Physics, University of Rostock, 18051 Rostock, Germany

E-mail: kuzin@niic.nsc.ru

A great interest in aluminum beta-diketonates is due to the combination of their thermal properties and practical application for the production of thin films. There are various methods for obtaining thin aluminum films. One of the most popular is the MO CVD method. In this method, beta-diketonates of aluminum act as precursors, this is due to their volatility and the ability of the compound vapors to decompose and settle on heated surfaces to form a solid phase on the support material. At the present time, various properties and characteristics of these materials have been investigated. But thermodynamic properties, which are important for optimizing the conditions for carrying out MO CVD processes, are not found in the literature. The results of experimental research of $\text{Al}(\text{C}_5\text{HF}_6\text{O}_2)_3$ heat capacity in the temperature range from (5 to 300) K are presented in this work.

The powdery tris(1,1,1,5,5,5-hexafluoro 2,4-pentanodionate) aluminum (III), $\text{Al}(\text{C}_5\text{HF}_6\text{O}_2)_3$, with a purity of 99% was supplied by Strem Chemicals, Inc. The sample of $\text{Al}(\text{C}_5\text{HF}_6\text{O}_2)_3$ at room temperature is a white crystalline powder. The melting temperature of the sample determined by DSC is 345 K. The calculated molecular weight (from the formula $\text{Al}(\text{C}_5\text{HF}_6\text{O}_2)_3$) is $648.13 \text{ g}\cdot\text{cm}^{-3}$.

Heat capacity of the $\text{Al}(\text{C}_5\text{HF}_6\text{O}_2)_3$ sample was measured by the adiabatic method on the setup described in [1] with the use of demountable calorimetric ampoule made of nickel. A demountable calorimeter ampoule and the methodology of filling an ampoule with a substance, as well as with heatexchange gas (helium), are all described in the work [2]. The temperature of the calorimeter was measured by a standard platinum resistance thermometer ($R_{100}/R_0=1.3925$). The standard uncertainty for the temperature was $u(T)=0.01 \text{ K}$. The measurement results of standard substance (benzoic acid) heat capacity which characterize a systematic error deviation from the standard data [3] by less than 1% in the range of (5-20) K, less than 0.3% in the range of (20-80) K, and less than 0.15% in the range of (80-300) K. The heat capacity has been measured at 70 points in the range of 5–300 K. At 300 K the heat capacity reaches only ~60% of limiting value and continues to increase. This is an evidence of high boundary frequency and a considerable density of modes in a high-frequency region of phonon spectrum.

We approximated the heat capacity $C_p(T)$ to zero according to the Debye law for calculating the integral thermodynamic functions. Smoothing of the experimental heat capacity was carried out by the method proposed in [4]. Entropy $S^\circ(T)$, difference of enthalpies $H^\circ(T)-H^\circ(0 \text{ K})$ and reduced Gibbs' energy $\Phi^\circ(T)$ within the range 0–300 K were obtained by numerical integration of the smoothed $C_p(T)$ dependence.

The reported study was supported by RFBR (Research project No. 16-33-01092mol_a)

[1] Naumov, V.N.; Frolova, G.I.; Nogteva, V.V.; Stabnikov, P.A.; Igumenov, I.K. Russ. J. Phys. Chem. 74, 2000, 1579-1584.

[2] Naumov, V.N.; Nogteva, V.V. Instrum. Exp. Tech., 1985, 28, 1194-1199.

[3] Rybkin, N.P.; Orlova, M.P.; Baranyuk, A.K.; Nurullaev, N.G.; Rozhnovskaya, L.N. Meas. Tech., 1974, 17, 1021-1026.

[4] Kuzin, T.M.; Bespyatov, M.A.; Naumov, V.N.; Musikhin, A.E.; Gelfond, N.V. Heat capacity and thermodynamic functions of ruthenium tris-acetylacetonate from 0 K up to the melting point.

Thermochimica Acta, 2015, 602, 49–52.



VAPORIZATION OF β -DIKETONATE COMPLEXES OF VANADYL AND SODIUM BY MASS-SPECTROMETRY

Malkerova I.P.¹, Alikhanyn A.S.¹, Makarevich A.M.², Tsymbarenko D.M.², Kuz'mina N.P.²

¹Kurnakov Institute of General and Inorganic Chemistry, Russian Academy of Sciences, Moscow

²Lomonosov Moscow State University, Moscow

e-mail: IMalkerova@gmail.com

There currently are a large number of methods for depositing film materials: magnetron sputtering, laser ablation, equilibrium thermal evaporation, and MO CVD being the main ones. The last method employs metal-organic compounds or metal complexes of organic ligands as precursors. Any of the above-listed methods requires one to know the main thermodynamic characteristics of the precursors, such as the gas-phase composition, absolute partial pressures, standard enthalpies of formation and dissociation, and their behavior over time. Volatile metal complexes of β -diketonates are considered to be the most promising precursors for the MO CVD methods. The novel mixed-ligand complex of sodium dipivaloylmeethanate with *o*-phenanthroline Na(thd)(pnen) (**I**) and vanadyl acetylacetonate VO(acac)₂ (**II**), dipivaloylmeethanate VO(thd)₂ (**III**), hexfluoracetonate VO(hfa)₂ (**IV**) can be use as a possible precursors in MO CVD synthesis of thin (K,Na)NbO₃ and VO₂ films, which are interesting materials for modern electronic engineering. The thermodynamic parameters of their vaporization are still to be under determination.

Complexes (**I**–**IV**) were studied on an MS 1301 mass-spectrometer intended for thermodynamic investigation using standard molybdenum Knudsen effusion cells. Vaporization of the Na(thd)(pnen) complex was studied in the temperature range of 380-490 K; the complexes (**II**–**IV**) – 340-410 K, 323-388 K, 313-343 K, accordingly. Analysis the mass-spectra and results of full isothermal evaporation experiments have shown, that all complexes sublime congruently without chemical decomposition in the selected temperature range. Saturated vapor of (**I**) predominantly consists of *o*-phenanthroline molecules C₁₂H₈N₂, trimeric molecules Na₃(thd)₃ and a minor amount of Na₄(thd)₄ and Na(thd)(pnen) molecules. The gas phase above β -diketonates of vanadyl complexes (**II**–**IV**) contains only monomeric molecules VO(acac)₂, VO(thd)₂ and VO(hfa)₂, accordingly. The absolute partial pressures and enthalpies of sublimation of the gas-phase components were calculated and are summarized in Table.

Table. The absolute partial pressures* and enthalpies of sublimation of β -diketonate complexes.

Compound	T, K	P, Pa	ΔT , K	$\Delta_s H^0(298 \text{ K})$ kJ/mol
Na ₃ (thd) ₃	453	$2.1 \cdot 10^{-1}$	405-460	160.8±4.9
Na ₄ (thd) ₄	453	$4.1 \cdot 10^{-3}$	405-460	168.4±6.4
VO(acac) ₂	369	$2.1 \cdot 10^{-1}$	340-410	132.3±4.3
VO(thd) ₂	330 369	$4.7 \cdot 10^{-3}$ $2.7 \cdot 10^{-1}$	325-388	126.5±10.5
VO(hfa) ₂	330	$1.8 \cdot 10^{-1}$	313-343	118.7±0.6

* $P_{\text{C}_{12}\text{H}_8\text{N}_2} = 3.9 \cdot 10^{-1} \text{ Pa}$, $P_{\text{Na}(\text{thd})(\text{pnen})} = 5.5 \cdot 10^{-4} \text{ Pa}$ (T=453 K).

Also the standard enthalpy of dissociation of gaseous Na(thd)(pnen) into Na₃(thd)₃(g) and Phen(g) was calculated as $\Delta_{\text{dis}} H^0(453 \text{ K}) = 25.3 \pm 4.2 \text{ kJ/mol}$. The $\Delta_f G^0(453 \text{ K}) = -22.0 \pm 3.5 \text{ kJ/mol}$ of formation of complex from Na(thd)(s) and Phen(l) was estimated. This value characterizes complex as a rather thermodynamically stable compound to be used to spatter the niobate films in the MO CVD method. The thermodynamic characteristics of vaporization of β -diketonates sodium and vanadyl and the simple composition of gas phase over them allows one to easily and precisely control of the composition and thickness of the resulting film material.

**THERMOPHYSICAL PROPERTIES OF COMPONENTS OF BIODIESEL AND SOME TRIGLYCERIDES**

Nikitin E.D., Bogatishcheva N.S., Popov A.P., Faizullin M.Z.

Institute of Thermal Physics, Ural Branch of the Russian Academy of Sciences, 620016 Ekaterinburg, Russia

E-mail: e-nikitin@mail.ru

Biodiesel is a renewable energy resource and has some advantages over petroleum fuels. Biodiesel is a blend of fatty acid methyl or ethyl esters and is produced through the esterification reaction from vegetable oils and animal fats which mainly consist of triglycerides. Information about the thermophysical properties of methyl (ethyl) esters of fatty acids and triglycerides is required for both the development of biodiesel production technologies and the analysis of biodiesel combustion in an engine. The paper presents the results of measuring the critical temperatures T_c , the critical pressures p_c , heat capacities C_p , and thermal diffusivities of some fatty acid methyl and ethyl esters and four saturated triglycerides.

The critical properties have been measured for the following esters:

- methyl esters of *n*-alkanoic acids $\text{CH}_3\text{C}_n\text{H}_{2n-1}\text{O}_2$ with the number of carbons $n = 6, 7, 8, 9, 10, 11, 12$, as well as oleic, linoleic, linolenic, and erucic acids;
- ethyl esters of *n*-alkanoic acids $\text{C}_2\text{H}_5\text{C}_n\text{H}_{2n-1}\text{O}_2$ with the number of carbons $n = 10, 11, 12, 14, 16, 18$.
- saturated triglycerides $\text{C}_3\text{H}_5[\text{C}_n\text{H}_{2n-1}\text{O}_2]_3$ with $n = 8, 10, 12, 14$.

The samples of the compounds studied were purchased from Alfa Aesar and Sigma-Aldrich and used without further purification. The purities of the samples were from 98.5 to 99.9 mol. %.

The critical properties of the compounds investigated have never been measured before. These compounds are thermally unstable at near-critical temperatures, so that the measurements of the critical properties have been made by the pulse-heating method developed by the authors and recognized as GSSSD technique. The pulse-heating method consists in measuring the pressure dependence of the temperature of the attainable superheat of a liquid with the help of a thin wire probe heated by electric current pulses. With increasing pressure the temperature of the attainable superheat tends to the critical temperature. The method provides little decomposition of compounds under study in the course of measuring the critical properties. The residence times were from 0.03 to 0.85 ms in various experiments. The uncertainties of the measurement of the critical parameters are $\delta T_c = 0.01T_c$ and $\delta p_c = 0.03p_c$ for ethyl and methyl esters; for triglycerides, the uncertainties are $\delta T_c = 0.015T_c$ and $\delta p_c = 0.04p_c$, where T_c is the absolute temperature. The uncertainties of the critical temperatures and pressures measured in this work are the combined expanded uncertainty at the 95% level of confidence. Equations for the calculation of the critical parameters of *n*-alkanoic acid methyl and ethyl esters have been obtained. The experimental critical properties have been compared with the values estimated by some group-contribution methods. The acentric factors of fatty acid methyl and ethyl esters have been calculated.

Heat capacities and thermal diffusivities have been measured for methyl esters of *n*-alkanoic acids with the number of carbons in the parent acid $n = 6, 7, 8, 9, 10, 11, 12$, ethyl esters of *n*-alkanoic acids with $n = 10, 11, 12, 14, 16$. The measurements have been performed for both homologous series at atmospheric pressure in the temperature range from 290 to 390 K. For saturated triglycerides with $n = 8, 10, 12, 14$, the measurements have been carried out in the temperature range from the melting point of a triglyceride to 423 K.

Heat capacity was measured with the help of a differential scanning calorimeter DSC 204 F1 *Phoenix* (Netzsch) with the uncertainty of 2%. The measurements of thermal diffusivity were taken by the laser flash technique using LFA 457 *MicroFlash* (Netzsch); the uncertainty is no more than 5%. Equations for the dependence of molar heat capacities and thermal diffusivities of the compounds studied on temperature have been obtained. For *n*-alkanoic acid ethyl esters, the dependence of molar heat capacity $C_{p,m}(298.15 \text{ K})$ on the number of carbons in the parent acid n ($n = 1-16$) is close to linear. However, thermal diffusivity as a function of n has a minimum at $n = 5$.

The study was supported by the Complex Program for Basic Research of the Ural Branch of the Russian Academy of Sciences N 15-1-2-6.

**STANDARD PARTIAL MOLAR HEAT CAPACITY AND VOLUME OF ION CADMIUM IN DIMETHYLFORMAMIDE AT 298.15 K**

Novikov A.N.¹, Dorokhin S.V.¹, Doronin Ya.I.¹, Nazarova A.Yu.¹, Vasilyov V.A.²
¹Mendeleev University of Chemical Technology, Institute in Novomoskovsk, 301665 Novomoskovsk, Russia
²Mendeleev University of Chemical Technology, 125047 Moscow, Russia
E-mail: anngic@yandex.ru

The actuality of investigation of non-aqueous solutions was caused by their wide utilization in industry, science and engineering. The solvent dimethylformamide (DMFA) chosen as the object of investigation is widely used in practice. Studies of the partial molal heat capacities \bar{C}_{p2}^0 and volumes \bar{V}_2^0 of electrolytes at infinite dilution have proved to be useful for examining ion-solvent and solvent-solvent interactions in aqueous, nonaqueous and mixed solvents. We chose cadmium iodide as objects of study that are quite soluble in DMFA. Complex formation is characteristic of the cadmium ion. For this reason, the interaction of Cd^{2+} with DMFA molecules results in the formation of bonds covalent to a substantial extent. Therefore, studies of solutions of cadmium iodide in DMFA are of certain interest.

Heat capacity C_p and density ρ of cadmium iodide solutions in DMFA at 298.15 K were experimentally investigated. For measurement of C_p a hermetic calorimeter with isothermal shell and platinum thermometer resistance as a temperature transducer were used. The error of C_p measurements was not more than $\pm 1 \cdot 10^{-3} \text{ J}(\text{g} \cdot \text{K})^{-1}$. For measurement of ρ the precision pycnometric installation (error $\pm 1 \cdot 10^{-5} \text{ g} \cdot \text{cm}^3$) was used. DMFA was dried over molecular sieves 4A and doubly distilled at low pressure. Karl Fisher titration indicated that the water content was not more than 0.01-0.02% by weight. The purity of DMFA was found to be 99.9% by weight, as determined by gas chromatographic analysis. Cadmium iodide (pure for analysis grade) was two times recrystallized from doubly distilled water and then from absolute ethanol. Recrystallized salt was dried for 3–4 h in air at 343 K and for 48 h in a vacuum at 333 K. All solutions were prepared by weight in a dry box.

On the base of the data about C_p and ρ apparent the molar heat capacities Φ_C and volumes Φ_V of cadmium iodide in DMFA were calculated. The standard partial molar heat capacity \bar{C}_{p2}^0 and volume \bar{V}_2^0 of cadmium iodide in DMFA at 298.15 K being of interest for the thermodynamics of solutions were determined by the extrapolation of concentrated dependences of Φ_C and Φ_V to the state of infinity dilution. An important problem of the theory of solutions is the search for the standard thermodynamic characteristics of separate ions. In spite of a considerable progress in experimental techniques, these values could not have been determined by direct methods. For this reason the main method is the division of the experimental standard properties of electrolytes into ionic contributions based on various assumptions. The separation of the \bar{C}_{p2}^0 and \bar{V}_2^0 values into ionic components was performed on the basis of the \bar{C}_{pi}^0 and \bar{V}_i^0 values for the iodide ion in DMFA (the values obtained via the TPTB and TATB assumption) [1,2] and using the condition of the additivity of partial molar values. The results of our calculations are presented in Table 1.

Table 1. Standard partial molar heat capacity and volume of CdI_2 and ions Cd^{2+} , Γ in DMFA at 298.15 K

	CdI_2	Γ	Cd^{2+}
$\bar{C}_{p2(i)}^0, (\text{J} \cdot (\text{mol} \cdot \text{K})^{-1})$	158±15	58 [1]	42±15
$\bar{V}_2^0, (\text{cm}^3 \cdot \text{mol}^{-1})$	65.7±0,3	24.0 [2]	17.7±0,3

1. Marcus Y., Hefter G. J.Chem. Soc. Faraday Trans., 1996, 92, 757-761.
2. Marcus Y., Hefter G. Chem. Rev., 2004, 104, 3405-3452.



**THERMODYNAMIC PROPERTIES OF NATURAL PHOSPHATE MINERAL
ANAPAITE $\text{Ca}_2\text{Fe}^{2+}(\text{PO}_4)_2 \cdot 4\text{H}_2\text{O}$**

Ogorodova L.P., Vigasina M.F., Melchakova L.V., Ksenofontov D.A., Bryzgalov I.A.

M.V. Lomonosov Moscow State University, Geological faculty

Leninskie Gory, MSU, 119234, Moscow, Russia

E-mail: logor@geol.msu.ru

Anapaite - hydrous calcium and iron phosphate was formed as a secondary mineral in oxidation zones of iron ore and also was found in sedimentary rocks with a high content of phosphorus. The investigations were performed using the natural anapaite (Kerch iron ore basin, Republic of Crimea, Russia). The mineral was characterized by modern physicochemical methods. X-ray microprobe analysis was carried out on a microanalyzer CAMEBAX SX-50 (Cameca, France). Thermal behavior of the sample was studied over the temperature range from room temperature to 1273 K on a derivatograph Q-1500 D (Hungary). IR-spectroscopic investigation was done on a Fourier spectrometer FSM-1201 (Russia). Raman spectroscopic study was carried out on a Raman microscope EnSpectr R532 (Russia). Powder X-ray analysis was performed on a diffractometer STOE-STADI MP (Germany). On the basis of sample researches it was identified as mono-mineral phase with triclinic structure - anapaite. No impurity phases were detected. The unit-cell parameters of anapaite are: $a = 6.4427$, $b = 6.808$, $c = 5.8974$ Å, $\alpha = 101.656^\circ$, $\beta = 104.235^\circ$, $\gamma = 70.760^\circ$ and $V = 234.65$ Å³. The chemical formula of the studied mineral was calculated using diagnostic data in accordance with the recommendations of the International Mineralogical Association (IMA 2015): $\text{Ca}_{1.98}\text{Fe}_{1.00}(\text{PO}_4)_{1.98} \cdot 3.96\text{H}_2\text{O}$. It was close to theoretical formula $\text{Ca}_2\text{Fe}(\text{PO}_4)_2 \cdot 4\text{H}_2\text{O}$.

The thermochemical investigation was made on a Calvet microcalorimeter (Setaram, France). The enthalpy of formation was determined by the melt solution calorimetry based on a thermochemical cycle including the dissolution of the substance and its constituent components. The dissolution was carried out by dropping the samples from room temperature into the melt-solvent with composition $2\text{PbO} \cdot \text{B}_2\text{O}_3$ at $T = 973$ K. The enthalpy increment of the substance and its solution enthalpy [$H^\circ(973 \text{ K}) - H^\circ(298 \text{ K}) + \Delta_{\text{sol}}H^\circ(973 \text{ K})$] were measured jointly. The calorimeter was calibrated using reference substance (platinum) of known enthalpy increments data [1]. The obtained value of the standard enthalpy of formation of anapaite from the elements was found to be: -4812 ± 16 kJ/mol.

No value of the standard entropy of studied mineral needed to calculate its Gibbs energy is currently available in literature. This value was evaluated on the basis of additivity employing the averaged entropy values attributable to the cations and anions in the solids (Latimer method). The data which was necessary for calculation (entropies of water, cations and anions) were taken from [2]. Using the estimated value of $S^\circ(298 \text{ K}) = 404.2$ J/(K·mol) and obtained in the present work value of $\Delta_f H^\circ(298 \text{ K})$ of anapaite the value of Gibbs energy of formation from the elements for this natural mineral was calculated as -4352 ± 16 kJ/mol. The obtained data on $\Delta_f G^\circ(298 \text{ K})$ anapaite confirm an estimate of this value (-4366.9 kJ·mol⁻¹) presented in [3].

[1] Robie R.A. and Hemingway B.S. (1995) Thermodynamic properties of minerals and related substances at 298.15 K and 1 bar (10^5 pascals) pressure and at higher temperatures. *U.S. Geol. Surv. Bull.* 1995, 2131, 461 p.

[2] Naumov G.B., Ryzhenko B.N., Khodakovskiy I.L. Reference book of thermodynamic constants (for geologists). M.: Атомиздат, 1971, 239 p.

[3] Nriagu J.O. and Dell C.I. (1974) *Amer. Mineralogist* 1974, 59, 934-946.

**THERMODYNAMIC PROPERTIES OF NATURAL Mg-Fe AMPHIBOLE - ANTHOPHYLLITE**

Ogorodova L.P., Kiseleva I.A., Vigasina M.F., Melchakova L.V., Ksenofontov D.A., Bryzgalov I.A.
M.V. Lomonosov Moscow State University, Geological faculty Leninskie Gory, MSU, 119234, Moscow, Russia
E-mail: logor@geol.msu.ru

Magnesium-iron amphiboles are rock-forming minerals of metamorphic rocks, characterized by a wide variety of chemical compositions and p - T formation conditions. The most common nature Mg-Fe amphiboles are crystallized in rhombic crystal system and form the isomorphous series: anthophyllite $\text{Mg}_2\text{Mg}_5[\text{Si}_8\text{O}_{22}](\text{OH})_2$ - ferroanthophyllite $\text{Fe}^{2+}_2\text{Fe}^{2+}_5\text{Si}_8\text{O}_{22}(\text{OH})_2$.

The sample of anthophyllite from Southwestern Pamir (Tajikistan) was selected for thermochemical study. The mineral was investigated by X-ray microprobe analysis, powder X-ray diffraction, thermal analysis and FTIR spectroscopy. The sample did not contain impurities in the noticeable amounts, and it was the monomineral phase. Chemical formula calculated on 46 charges had the form: $\text{Mg}_{2.0}(\text{Mg}_{4.8}\text{Fe}^{2+}_{0.2})[\text{Si}_{8.0}\text{O}_{22}](\text{OH})_2$.

The thermochemical study was performed on Calvet microcalorimeter (Setaram, France). The enthalpy of formation was determined by high-temperature drop solution calorimetry method using a thermochemical cycle, taking into account the dissolution of the mineral and its constituent components (oxides and magnesium hydroxide). The mineral samples were dropped from room temperature into a platinum crucible with melt-solvent $2\text{PbO}\cdot\text{B}_2\text{O}_3$ at calorimeter temperature 973 K. The measured heat effect was a sum of the heat content of substance and the enthalpy of its dissolution $\Delta H = [H^\circ(973 \text{ K}) - H^\circ(298 \text{ K}) + \Delta_{\text{sol}}H^\circ(973 \text{ K})]$. When using samples of $3\text{-}11 (\pm 2 \cdot 10^{-3})$ mg in mass and 30-35 g of solvent during the 6-8 solution experiments, the ratio of dissolved substance – melt solvent can be attributed to an infinitely dilute solution with mixing enthalpy close to zero. The calorimeter was calibrated using reference substance (Pt) of known enthalpy increments data [1].

The value of standard enthalpy of formation for the studied natural anthophyllite was calculated on the basis of the obtained calorimetric data according to the equations (1-3).



$$\Delta_{\text{r}(1)}H^\circ(298 \text{ K}) = \sum v_i \Delta H_{\text{comp},i} - \Delta H_{\text{anth.}}, \quad (2)$$

$$\Delta_f H^\circ(298 \text{ K})_{\text{anth.}} = \Delta_{\text{r}(1)}H^\circ(298 \text{ K}) + \sum v_i \Delta_f H^\circ(298 \text{ K})_{\text{comp},i}; \quad (3)$$

where v_i is stoichiometric coefficients in the equation (1-3); $\Delta H = H^\circ(973 \text{ K}) - H^\circ(298 \text{ K}) + \Delta_{\text{sol}}H^\circ(973 \text{ K})$ are thermochemical data for mineral studied and the constituent oxides and magnesium hydroxide; the values of $\Delta_f H^\circ(298 \text{ K})$ of components needed for the calculations are taken from [1]. The calculated value of the enthalpy of formation of natural anthophyllite from the elements was found to be -12021 ± 20 kJ/mol.

The enthalpy of formation of magnesium end-member of anthophyllite series was calculated using the dissolution calorimetric data for the natural mineral. The results of the measurements for studied mineral were corrected on the deviations of its composition from the ideal formula. The obtained data on the enthalpy of formation of anthophyllite $\text{Mg}_2\text{Mg}_5[\text{Si}_8\text{O}_{22}](\text{OH})_2$ was -12061 ± 20 kJ/mol. The values of standard Gibbs energies for both anthophyllite compositions were estimated as -11298 ± 20 kJ/mol ($\text{Mg}_{2.0}(\text{Mg}_{4.8}\text{Fe}^{2+}_{0.2})[\text{Si}_{8.0}\text{O}_{22}](\text{OH})_2$) and -11337 ± 20 kJ/mol ($\text{Mg}_2\text{Mg}_5[\text{Si}_8\text{O}_{22}](\text{OH})_2$).

Obtained data complement the modern base of thermodynamic constants of minerals needed for modeling the processes of their formation in different geological environments.

[1] Robie R.A. and Hemingway B.S. Thermodynamic properties of minerals and related substances at 298.15 K and 1 bar (105 pascals) pressure and at higher temperatures. U.S. Geol. Surv. Bull. 1995, 2131, 461 p.

**THERMODYNAMICS OF EVAPORATIONS PROCESSES OF YTTRIUM TRIFLUORIDE AND TRICHLORIDE**Gorokhov L.N.¹, Osina E.L.¹, Osin S.B.²¹Joint Institute for High Temperatures of RAS, Ishorskaya St., 13, Bd. 2, Moscow 125412, Russia²Lomonosov Moscow State University, Department of Chemistry, Lenin Hills, 1, Bd. 3, Moscow 119991, Russia

E-mail: j-osina@yandex.ru

The work on updating and expanding the IVTANTHERMO thermodynamic database for inorganic compounds is in progress now at the Joint Institute for High Temperatures of RAS. The work includes a new assessment of thermodynamic properties for the Rare-Earth elements (Sc, Y, Ln) and compounds. The new results on thermodynamics of yttrium trifluoride and yttrium trichloride evaporation in the form of monomer and dimer are presented in this work. The thermodynamic functions for all vapor constituents are needed for correct description of the evaporation processes of yttrium trihalides in a broad temperature range. Experimental information on the structure and spectra, which is necessary for calculation of thermodynamic functions for these molecules, is extremely scarce. The most reliable experimental data for yttrium trifluoride and trichloride were published in [1, 2]. From these data, we estimated molecular constants for YF_3 and YCl_3 gaseous species. D_{3h} planar structure was accepted for both molecules. For Y_2F_6 and Y_2Cl_6 molecules a planar bridged D_{2h} structure was accepted according to results obtained in *ab initio* computations and experimental data for Y_2Cl_6 [2]. The vibrational frequencies were selected on the basis of experimental and theoretical data available in the literature. The calculations of the thermodynamic functions were carried out using "rigid rotator - harmonic oscillator" approximation in the temperature range of 298.15K - 6000 K. Yttrium trihalides have a closed electron shell, so the calculation of the thermodynamic functions is carried out without taking into account the excited electronic states.

Yttrium trifluoride vapors mainly consist of YF_3 monomer molecules; the dimer was not detected in the vapor phase. The ratio of dimer to monomer pressures near 1400 K was evaluated in [3] as $P(d)/P(m) \leq 10^{-4}$. We used this ratio for calculation of temperature dependence of this upper bound from the equilibrium constant values of reaction $YF_3(cr,l) + YF_3(g) = Y_2F_6(g)$, $K_p = P(d)/P(m)$. In the temperature range of 1400 – 3000 K, upper bound of the $P(d)/P(m)$ value remains very low and rises from 10^{-4} only to 10^{-2} . From the experimental data for YF_3 pressure [3] we have calculated the new "Third Law" value for the monomer enthalpy of sublimation: $\Delta_s H^\circ(YF_3, cr, 0 K) = 443.5 \pm 5$ kJ/mole.

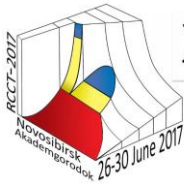
Yttrium trichloride vapors mainly consist of YCl_3 monomer molecules and some small Y_2Cl_6 dimer content: $P(d)/P(m) = 0.15$ at the temperature 1300 K [3]. The temperature dependence of this value was calculated from the equilibrium constant values for the reaction similar to that for YF_3 : $YCl_3(cr,l) + YCl_3(g) = Y_2Cl_6(g)$. In this case $P(d)/P(m)$ values rise from 0.15 to 0.21 in the temperature interval 1300 – 1600 K. Using these results, $P(d)$ and $P(m)$ values were calculated using the total pressure over yttrium trichloride from the work [4]. From the partial pressures so obtained were calculated the enthalpies of sublimation in the form of monomer and dimer: $\Delta_s H^\circ(YCl_3, cr, 0 K) = 288.9 \pm 5$ kJ/mole; $\Delta_s H^\circ(Y_2Cl_6, cr, 0 K) = 359.9 \pm 8$ kJ/mole.

[1] Akishin P.A., Naumov V.A., Tatevskiy V.M. Kristallographia, 1959, V. 4, P. 194 (in Russian).

[2] Reffy B., Marsden C. J., Hargittai M. J. Phys. Chem. A, 2003, V. 107, P. 1840.

[3] Hildenbrand D.L., Lau K.H. J. Chem. Phys., 1995, V. 102, P. 3769.

[4] Dudchik G.P., Polyachenok O.G., Novikov G.I. Z. neorgan. khimii, 1969, T. 14, C. 3165 (in Russian).



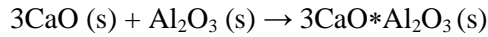
THE THERMODYNAMIC OF THE CALCIUM TRIALUMINATE FORMATION

Roxana-Diana Pașca, Firuta Goga

Department of Chemical Engineering, Faculty of Chemistry and Chemical Engineering,
Babeș-Bolyai University, Cluj-Napoca, Arany Janos str., no11, 400028, Romania

Email: roxana.pasca@ubbcluj.ro

Calcium trialuminate formation is given by the following reaction, which is quite important since calcium trialuminate is a major phase in Portland cement:



The thermodynamic data [1, 2] are given in the table below:

Compound	$C_p = f(T), \text{ cal/mol}\cdot\text{K}$			Temperature range	$C_p^{\circ}{}_{298}, \text{ cal/mol}\cdot\text{K}$	$\Delta_r H^{\circ}{}_{298}, \text{ kcal/mol}$	$S_{298}^{\circ}, \text{ cal/mol}\cdot\text{K}$
	$C_p = a + bT + \frac{c}{T^2}$						
	a	$b \cdot 10^3$	$c \cdot 10^{-5}$				
CaO (s)	11.67	1.08	-1.56	[298...1800]	10.23	-151.9	9.5
Al ₂ O ₃ (s)	27.43	3.06	-8.47	[298...1800]	18.88	-399.1	12.2
3CaO·Al ₂ O ₃ (s)	53.35	13.18	-3.36	[298...1600]	53.5	-1098.0	49.0

The affinity of the reaction can be calculated in different approximations using the equations given:

$$A = \Delta_r G_T = \Delta_r H_T - T \Delta_r S_T \quad (1); \quad \Delta_r H_T = \Delta_r H^{\circ}{}_{298} + \int_{298}^T \Delta_r C_p dT \quad (2);$$

$$\Delta_r S_T = \Delta_r S^{\circ}{}_{298} + \int_{298}^T \frac{\Delta_r C_p}{T} dT \quad (3); \quad \Delta_r G_T = \Delta_r H^{\circ}{}_{298} + \int_{298}^T \Delta_r C_p dT - T \left(\Delta_r S^{\circ}{}_{298} + \int_{298}^T \frac{\Delta_r C_p}{T} dT \right) \quad (4)$$

The results are centralized in the next table:

$\Delta_r H^{\circ}{}_{298} = -1016.6 \text{ kJ/mol}$	$\Delta_r S^{\circ}{}_{298} = 12.1 \text{ J/mol K}$	$\Delta_r G^{\circ}{}_{298} = -1020.4 \text{ kJ/mol}$	Standard conditions	
		$\Delta_r G_{1623} = -1036.2 \text{ kJ/mol}$	Ulich's First Approximation	
$\Delta_r H_{1623} = -994.8 \text{ J/mol}$	$\Delta_r S_{1623} = 40.1 \text{ J/mol K}$	$\Delta_r G_{1623} = -1060 \text{ kJ/mol}$	Ulich's Second Approximation	$\Delta_r C_{p,298}^{\circ} = 16.43 \text{ J/mol K}$
$\Delta_r H_{1623} = -1003.6 \text{ kJ/mol}$	$\Delta_r S_{1623} = -14.9 \text{ J/mol K}$	$\Delta_r G_{1623} = -902.5 \text{ kJ/mol}$	Exactly calculation	$\Delta_r C_p = -9.09 + 0.00688T + \frac{979000}{T^2} \text{ cal/mol K}$

We can see that the entropy variation is small and the Gibbs' free energy is very less affected by the temperature.

[1] M. H. Karapetianț, "Chemical Thermodynamics", Technical Edition, Bucharest, 1956.

[2] I. Ellezer, N. Ellezer, R. A. Howald, P. Viswanadham, "Thermodynamic properties of calcium aluminates, J. Phys Chem, 1981, 85 (19), 2835-2838.

**THE ENTHALPY OF DISSOLUTION OF THE PMMA SAMPLES WITH DIFFERENT HISTORIES IN PRODUCING A VARIETY OF SOLVENTS**Myalkin I.V.¹, Safonov V.M.¹, Bulgakova S.A.², Kir'yanov K.V.², Smirnova N. N.²¹Vyksa branch NUST «MISIS», Vyksa, 607030 Russia²Chemistry Research Institute of N.I.Lobachevsky State University, Nizhni Novgorod, 603950, Russia

E-mail: i.v.myalkin@gmail.com

Polymethylmethacrylate (PMMA) belongs to one of the important industrial polymers. In this paper, the thermal effects of dissolution of PMMA with different history of obtaining were determined experimentally using a micro calorimeter DAK1-1A type Calvet. PMMA synthesized as a conventional radical bulk and by controlled polymerization atom transfer, in the presence of a catalyst system dinitrile, azo-isobutyric acid (AIBN) + iron chloride (III) in dimethylformamide (DMF) and dimethyl sulfoxide (DMSO).

From the data can be seen that the stability energy of PMMA to various solvents decreases in the series: Toluene > Methyl ethyl ketone > Dichloromethane > Dimethylformamide > Ethyl acetate > Tetrahydrofuran > Deagle > o-Dichlorobenzene > Dichloromethane > Chloroform. At the same time there was a trend in enthalpy of dissolution depending on the values of the dipole moments of the considered solvent.

Table 1 Enthalpy of solution ($\Delta_{sol}H^0$) of (co)polymers in various solvents, $T = 298.15$ K

N_2 n/n	Solvent	$-\Delta_{sol}H^0(298\text{ K})$ (kJ/mol PMMA)
1	Chloroform	7.60±0.04 [1]
2	Deagle	3.20±0.06
3	Ethyl acetate	2.67±0.09
4	Dichloromethane	(4.8) [2]
5	o-Dichlorobenzene	(4.0) [2]
6	Tetrahydrofuran	2.7±0.1
7	Dimethylformamide	(2.2) [3]
8	1,2-Dichloroethane	(2.0±0.1) [4]
9	Methyl ethyl ketone	0.58±0.03
10	Toluene	0.3±0.2

[1] Effect of Supramolecular Structure on the Enthalpy of Dissolution Polymethylmethacrylate in Chloroform at 298.15 K I. V. Myalkin · S. A. Bulgakova · K. V. Kir'yanov · N. N. Smirnova Russian Journal of Physical Chemistry, 2015, Volume 89, [Issue 1](#), P. 57–60

[2] Tager, A. The heats of dissolution of polymers and packing of the molecules in different physical states / A.A. Tager, N.M. Guryanov // J. Phys. chemistry. - 1958. - T.32. - №9. - P. 1958-1962.

[3] Tager, A. The heats of dissolution of polystyrene different in molecular weight and packing density rigid chains / A.A. Tager, P. Krivokopytova. P.M. Khodorov // Dokl. USSR Academy of Sciences. - 1955. - T.10. - №4. - P. 741-743.

[4] Tager, A. Thermodynamic study of polymer systems - hydrogenated monomer / AA Tager, V.A. Kargin // colloid. Well. - 1952. - T.14. - №5. - P.367-371.

**DETERMINATION OF THERMAL EFFECTS OF CHEMICAL REACTIONS OF $\text{Ln}_2\text{O}_2\text{S}$ and Ln_2O_3 ($\text{Ln} = \text{La, Sm, Gd}$) FORMATION**Sal'nikova E. I.^{1,2}, Osseni S. A.¹, Volkova D. A.¹, Andreev O.V.¹¹Tyumen State University, 625000, Tyumen, Russia²Northern Trans-Ural State Agricultural University, 625003, Tyumen, RussiaE-mail: elenasalnikova213@gmail.com

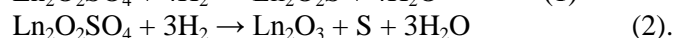
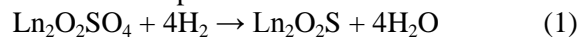
Crystal phosphors, based on rare-earth oxysulfides, are perspective laser materials. Oxysulfides of REE are studied as phosphors, biomarkers; they are used in medicine for photodynamic diagnostic.

In this work, we studied the reaction of oxysulfides and oxides formation of lanthanum, samarium and gadolinium.

Lanthanum, samarium and gadolinium oxysulfides and oxides were synthesized by using a furnace and a hydrogen generator.

Sulfates were prepared from stock oxides of REE that were dissolved in HNO_3 , nitrate solutions were poured into H_2SO_4 , and the resulting suspension was evaporated to dryness, and then treated at 600 °C until disappearance the precipitates of nitrogen and sulfur oxides. Weighed samples (10-13 g) were placed in a quartz beaker, and then into a quartz reactor tube with the feed stopper. We set the reactor into a vertical muffle furnace with "Thermolux" program. The heating temperature was setting at 500 °C. A permanent stream of hydrogen at a flow rate of 7-8 l/hr (standard state) was passed through a sample. The phase composition of the samples was determined using the method of X-ray diffraction on a DRON-7 in $\text{CuK}\alpha$ - radiation, Ni - filter.

Equations of chemical reactions were compiled:



Using data taken from [1], we calculated the thermal effects of chemical reactions (1) and (2).

Thermodynamic data are presented in table 1.

Table 1. Comparative analysis of thermal effects of $\text{Ln}_2\text{O}_2\text{S}$ and Ln_2O_3 ($\text{Ln} = \text{La, Sm, Gd}$) formation

Compound	$-\Delta_f H^\circ(298 \text{ K})$ (kJ/mol)	Compound	$-\Delta_f H^\circ(298 \text{ K})$ (kJ/mol)
$\text{La}_2\text{O}_2\text{S}$	2038±10	La_2O_3	2160±10
$\text{Sm}_2\text{O}_2\text{S}$	1949±10	Sm_2O_3	2010±10
$\text{Gd}_2\text{O}_2\text{S}$	1946±10	Gd_2O_3	2006±10

These results revealed that in the reactions of formation of oxysulfides of REE, thermal effect is higher than in the reactions of formation of their corresponding oxides.

[1] Suponitskij Y. L. Thermal chemistry of oxo compounds of REE and elements of VI group: Diss. Dr. of chem. Sciences: 02.00.04. Moscow. 2002. 248 p.

CALORIMETRIC AND MAGNETOCHEMICAL STUDIES ON SPIN-CROSSOVER IN IRON(II) COMPLEXES WITH *TRIS*(PYRAZOL-1-YL)METHANE

Shakirova O.G.¹, Pishchur D.P.², Korotaev E.V.², Lavrenova L.G.^{2,3}

¹Komsomolsk-on-Amur state technical university, 681013 Komsomolsk-on-Amur, Russia

²Nikolaev Institute of Inorganic Chemistry, Siberian Branch of the Russian Academy of Sciences, 630090 Novosibirsk, Russia

³Novosibirsk National Research State University, 630090 Novosibirsk, Russia

E-mail: ludm@niic.nsc.ru

Complex compounds of iron(II), wherein the spin state of the central atom can be affected by environmental conditions such as temperature, pressure, or light of a certain wavelength, are of current interest. Spin-crossover (SCO) in the series of complexes having a composition such as $[\text{Fe}\{\text{HC}(\text{Pz})_3\}_2]_n\text{A}_n$ (where $\text{HC}(\text{Pz})_3$ is *tris*(pyrazol-1-yl)methane, A = anion, $n = 1, 2$) is observed within the temperature range from 270 to 470 K [1]. Both abrupt and gradual SCO are inherent in them. The feature of these complexes is thermochromism, a reversible color change upon heating and cooling.

The studies on the $\mu_{\text{eff}}(T)$ dependence using a static magnetic susceptibility technique enable us to find the temperature of direct (T_c^\uparrow) and reverse (T_c^\downarrow) transitions, the value of thermal hysteresis ΔT_{SCO} , and to evaluate the SCO abruptness. The SCO in iron(II) complexes represents a phase transition, thus we systematically study thermodynamic parameters inherent in them. It is shown that the nature of the SCO mainly depends on the composition thereof.

In this work, a β -polymorph of complex $[\text{Fe}\{\text{HC}(\text{Pz})_3\}_2](\text{NO}_3)_2 \cdot \text{H}_2\text{O}$ [2] has been studied using the methods of static magnetic susceptibility and differential scanning calorimetry. The studies on the $\mu_{\text{eff}}(T)$ dependence within the range from 300 to 480 K revealed that the compound exhibits spin-crossover $^1\text{A}_1 \Leftrightarrow ^5\text{T}_2$ (Fig. 1). The direct transition occurs at $T_c^\uparrow = 430$ K, being accompanied by dehydration, the reverse one being at $T_c^\downarrow = 420$ K (1-st cycle).

$[\text{Fe}\{\text{HC}(\text{Pz})_3\}_2](\text{NO}_3)_2 \cdot \text{H}_2\text{O}$ complex exhibits thermochromism: magenta \Leftrightarrow white color changing. The thermodynamic properties of the complex have been studied using DSC (Fig. 2). The temperature dependence of the DSC signal in the heating/cooling mode exhibits an anomaly corresponding to SCO $^1\text{A}_1 \Leftrightarrow ^5\text{T}_2$, at $T_{\text{onset}}^\uparrow = 427.9$ K and $T_{\text{onset}}^\downarrow = 415.3$ K. The calculated enthalpy and entropy values of the transition are $\Delta H = 13.9 \pm 0.3$ kJ mol⁻¹, $\Delta S = 32.3 \pm 0.8$ J mol⁻¹ K⁻¹, which is in a good agreement with previous data on the thermodynamic properties of Fe(II) complexes with 1,2,4-triazoles [3].

[1] Lavrenova, L.G.; Shakirova, O.G. Eur. J. Inorg. Chem., 2013, 670-682.
 [2] Anderson, P.A.; Astley, T.; Hitchman, M.A.; Keene F.R.; Moubaraki, B.; Murrain, K. S.; Skelton, B.W.; Tiekink, E.R.T.; Toftlund, H.; White, A. H. J. Chem. Soc. Dalton Trans., 2000, 20, 3505-3512.
 [3] Berezovskii, G.A.; Pishchur D.P.; Shakirova, O. G.; Lavrenova, L. G. Rus. J. Phys. Chem. A, 2009, 83 (11), 1827-1831.

[1] Lavrenova, L.G.; Shakirova, O.G. Eur. J. Inorg. Chem., 2013, 670-682.

[2] Anderson, P.A.; Astley, T.; Hitchman, M.A.; Keene F.R.; Moubaraki, B.; Murrain, K. S.; Skelton, B.W.; Tiekink, E.R.T.; Toftlund, H.; White, A. H. J. Chem. Soc. Dalton Trans., 2000, 20, 3505-3512.

[3] Berezovskii, G.A.; Pishchur D.P.; Shakirova, O. G.; Lavrenova, L. G. Rus. J. Phys. Chem. A, 2009, 83 (11), 1827-1831.

This work was financially supported by RFBR project 16-03-00020 Bel_a.

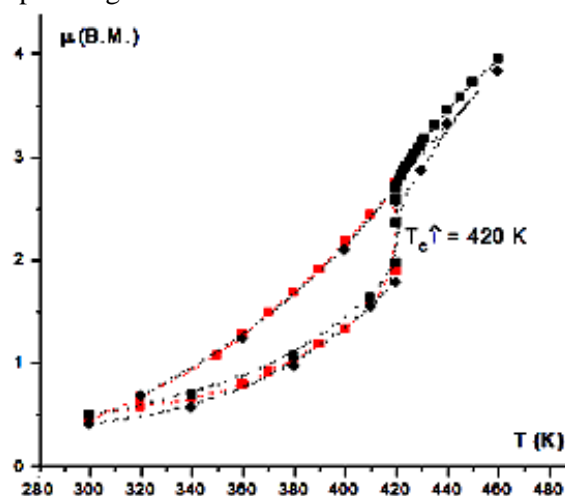


Figure 1. $\mu_{\text{eff}}(T)$ curves for the complex $[\text{Fe}\{\text{HC}(\text{Pz})_3\}_2](\text{NO}_3)_2 \cdot \text{H}_2\text{O}$.

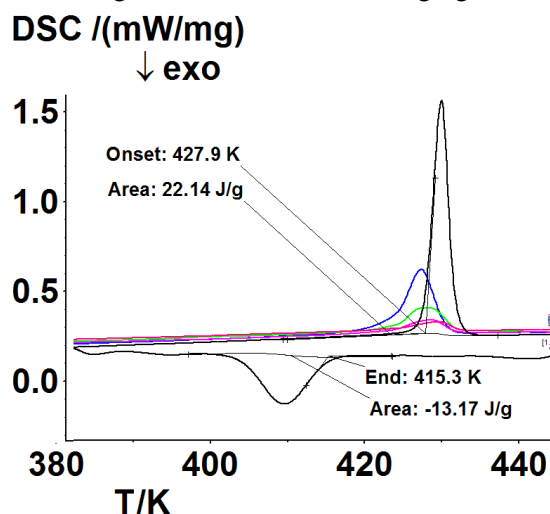


Figure 2. DSC plot for the complex $[\text{Fe}\{\text{HC}(\text{Pz})_3\}_2](\text{NO}_3)_2 \cdot \text{H}_2\text{O}$.



THE ASSOCIATION OF SPHERICAL CLUSTER POLYOXOMETALATE $\text{Mo}_{72}\text{Fe}_{30}$ WITH BIOLOGICALLY ACTIVE SUBSTANCES

Tonkushina M.O., Gagarin I.D., Ostroushko A.A.

Ural Federal University named after the first President of Russia B.N.Yeltsin, 620002, Ekaterinburg, Russia

E-mail: MargaritaTonkushina@urfu.ru

Müller's porous Keplerate type of spherical cluster polyoxometalates (POM) $\text{Mo}_{72}\text{Fe}_{30}$ are considered as promising means of the targeted delivery of biologically active substances.

It consists of oxygen polyhedra of molybdenum(VI) and iron(III): $[\text{Mo}_{72}\text{Fe}_{30}\text{O}_{252}(\text{CH}_3\text{COO})_{12}\{\text{Mo}_2\text{O}_7(\text{H}_2\text{O})\}_2\{\text{H}_2\text{Mo}_2\text{O}_8(\text{H}_2\text{O})\}(\text{H}_2\text{O})_{91}]\sim 150\text{H}_2\text{O}$ ($\text{Mo}_{72}\text{Fe}_{30}$). The structure of Keplerate type polyoxometalate stabilized by water molecules has pores and the internal cavity. Polyoxometalate can be transported by the electric field due to its ability to form polyoxoanions with different surface charge tuned by pH in aqueous solutions. We have shown that electromigration is not confined to solutions. Polyoxometalate ions can be transported by electrophoresis through the skin, too. $\text{Mo}_{72}\text{Fe}_{30}$ and its ion associates (for example, with lanthanum) can penetrate the skin of warm-blooded animals *in vitro* and *in vivo* by means of the electric field.

A distinctive feature of the discussed compounds is the lack of toxicity towards warm-blooded animals (rats), its gradual destruction promotes the removing from the body. Additional advantages are the increase of hemoglobin level in experimental animals after the introduction of $\text{Mo}_{72}\text{Fe}_{30}$ and the ability of POM to create a "depot" in the skin.

Currently one of the key problems in this area is the study of the possible association of polyoxometalate with biologically active substances of different nature. Potentially associates can be transported by electrophoresis. This work is devoted to the study of this problem.

UV/Vis spectroscopy studies have shown the formation of associates in the system of thiamine chloride- $\text{Mo}_{72}\text{Fe}_{30}$. This is evidenced by a significant increase in the optical density of solutions in the area of the characteristic absorption band of $\text{Mo}_{72}\text{Fe}_{30}$ (at 325 nm) in the presence of thiamine chloride. This change in the optical density with the increase of the ratio of B1 and POM is almost linear.

The titration of a solution of the POM by the thiamine chloride during the pH-measuring has been carried out. The decrease in pH was noted. The media became more acidic due to the deprotonation of polyoxometalate which formally is a weak acid.

Thiamine ions replace the protons of the POM. It is thought that thiamine molecules are coordinated with polyoxometalates due to the electrostatic interaction of nitrogen atom on which the positive charge is localized. The pH values were close to the range of maximum of polyoxometalate stability.

The experiments showed a significant increase in the optical density of characteristic absorption band in UV/Vis spectra $\text{Mo}_{72}\text{Fe}_{30}$ in the presence of albumin. This indicates the presence of association between proteins and polyoxometalates. Small protein albumin molecules are mainly protonated, so they are in an expanded state because of the slightly acidic media of POM solutions. It promotes their interaction with $\text{Mo}_{72}\text{Fe}_{30}$. It should be noted that the interaction of POM with proteins does not lead to the precipitate formation. Insulin molecules, whose size is comparable with polyoxometalate, also form associates with $\text{Mo}_{72}\text{Fe}_{30}$, according to electronic absorption spectra. The precipitate formation was also not observed. The interaction of protein molecules with POM, apparently, proceeds as that of thiamine: due to the hydrogen bonds.

We can assume that this association is implemented for the systems with POM-homing proteins, which are also small proteins. Further research should be aimed at the quantitative establishment of association processes of polyoxometalate with proteins depending on the conditions of the association.

The research results were obtained in the framework of the state task of the Ministry of education and science of Russia (project № 4.6653.2017), this work was supported by RFBR grant 15-03-03603, as well as the Programme of the increase of Ural Federal University competitiveness (14.594.21.0011).

[1] A. Müller, S. Sarkar, S. Q. N. Shah, H. Bögge, et al., *Angew. Chem. Int. Ed. Engl.*, 38, 3238–3241.

SUBLIMATION OF PEPTIDES: MASS SPECTRA AND ENTHALPY OF SUBLIMATION

Tyunina V.V.¹, Badelin V.G.², Tyunina E.Yu.², Krasnov A.V.¹, Girichev G.V.¹

¹Ivanovo State University of Chemistry and Technology, 153000 Ivanovo, Russia

²G.A. Krestov Institute of Solution Chemistry, Russian Academy of Sciences, 153045 Ivanovo, Russia

E-mail: isuct-studlab@mail.ru

The sublimation process of dipeptides, DL-alanyl-DL-norvaline (DL-Ala-DL-Nvl), L-alanyl-L-tryptophan (L-Ala-L-Trp), glycyl-L-alanine (Gly-L-Ala), L-alanyl-L-alanine (L-Ala-L-Ala), and DL-alanyl-DL-valine (DL-Ala-DL-Val) were investigated by Knudsen's effusion method with mass spectrometric vapor composition measurement. Magnetic mass spectrometer MI 1201 adopted for effusion experiments was used. The samples of dipeptides about 50-100 mg were placed into a molybdenum effusion cell with the ratio of vaporization surface square to effusion orifice square about 1000. The temperature of experiment was measured by tungsten-rhenium thermocouple WRe-5/20. An accuracy of temperature maintenance was ± 0.5 K. Ionization of the neutral species effusing from the Knudsen cell into the ionizing region was occurred by electron impact. The energy of the ionizing electrons was equal 50 eV. All experiments were carried out under vacuum.

Fragmentation of molecules under electron ionization was discussed. Mass spectra observed for DL-Ala-DL-Nvl and L-Ala-L-Trp are missing in literature and NIST Database. The formation of four dominant ions (m/z : 45, 72, 99, 128) is occurred for mass spectra DL-Ala-DL-Nvl. For L-Ala-L-Trp the fragment ion with m/z 130 is the most intensive ion in mass spectra. For DL-Ala-DL-Nvl the recorded ion with m/z 170 can be classified as the cyclic form ion which has a very low intensity (<1%). The sublimation of L-Ala-L-Trp is not accompanied by cyclization-dehydration in the temperature range studied. The sublimation of the peptides was studied in the following temperature ranges: 446.15-491.15 K and 458.15-485.15 K for DL-Ala-DL-Nvl and L-Ala-L-Trp, respectively.

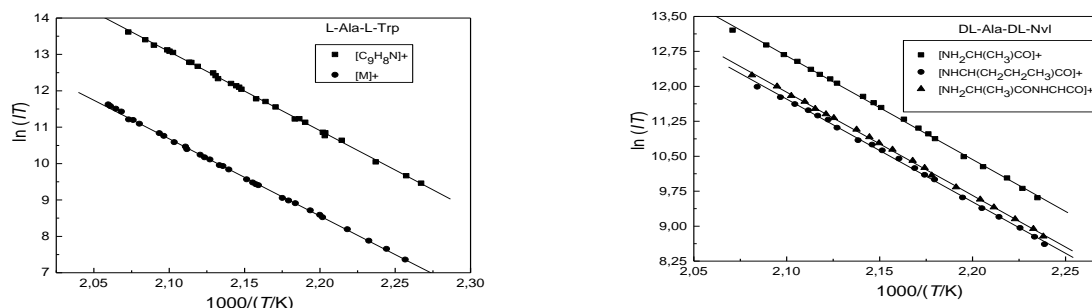


Fig. 1. The temperature dependence $\ln(IT)=f(1/T)$ of ion currents for L-Ala-L-Trp and DL-Ala-DL-Nvl.

For these compounds, the molar enthalpies of sublimation were derived from second law of thermodynamics (Fig.1). The increasing of the sublimation molar enthalpy in the series Gly-L-Ala, L-Ala-L-Ala, DL-Ala-DL-Val, L-Ala-L-Trp, and DL-Ala-DL-Nvl was accompanied by growing of aliphatic side chain and introduction of heterocyclic ring (for L-Ala-L-Trp). The sublimation enthalpy can be represented strength of the intermolecular interactions in a solid and the stability of the crystal structure. The van der Waals, dispersion, and electrostatic interaction as well as hydrogen bond formation make important contributions to the crystal packing of the peptides studied. The molecular packing densities in crystals, defined as the ratio of van der Waals volume to molecular volume of a compound, $D_{pac}=V_w/V_{mol}$, follow the order: L-Ala-L-Trp<L-Ala-L-Ala<Gly-L-Ala<DL-Ala-DL-Val<DL-Ala-DL-Nvl. We have proposed the simple correlation between the volume-specific molar enthalpies of sublimation and the molecular packing density: $\Delta_{sub}H_m^0/V_w$ ($\text{kJ}\cdot\text{mol}^{-1}\text{\AA}^{-3}$) = $(-8.685\pm 0.67) + (12.825\pm 0.89) \cdot D_{pac}$ ($r_{corr}=0.9927$, $SD=0.0164$), that make good quantitative estimation of the sublimation enthalpy of the peptides.



THE DATABASE «THERMODYNAMICS OF COMPLEX FORMATION AND SOLVATION IN BINARY SOLVENTS»

Usacheva T.R.¹, Kuz'mina K.I.¹, Cheshinskii M.A.¹, Kuz'mina I.A.¹, Sharnin V.A.^{1,2}

¹Ivanovo State University of Chemistry and Technology, General Chemical Technology Department, 153000 Ivanovo, Russia

²G.A. Krestov Institute of Solution Chemistry of the Russian Academy of Sciences, 153045 Ivanovo, Russia

E-mail: oxt@isuct.ru

The use of non-aqueous and mixed solvents in the chemical science and technology is the need to develop scientific bases for controlling the chemical processes in the liquid phase. Therefore, one of the main tasks of chemistry is to establish the general laws of thermodynamics to chemical equilibria. The complexity in solving of this problem is caused by an exceptional variety of chemical reactions in solutions, as well as the specifics of the chemical interactions in the different processes. Usually, to simplify this task, studying the effect of solvent on the same type reaction could be helpful. Such examples are complex formation reactions in different mixed solvents. That is why the estimation of the influence of mixed solvent composition on the thermodynamic solvation parameters of reagents and products (ΔG , ΔH , ΔS), and the derivation of proper relationships between their solvation parameters and those of reaction, allow one to devise predictive models for complex formation and to select the proper solvent for the synthesis of molecular complexes with predetermined thermodynamic properties (stability and energetic of complex formation reaction).

Investigation of the formation of amine, carboxylate and crown-ethers complexes with d-metal ions studied by scientists of ISUCT in binary solvents [1] revealed on the base of the solvation-thermodynamics approach several general rules governing the thermodynamic characteristics of reactions and solvation of the reagents. These rules have shown the possibility of predicting the thermodynamic parameters of the ionic complex formation reactions in different media according to a change in the solvation state of ligands.

Modern intensive development of high technologies caused by an urgent demand for quick searching of scientific information in all areas of scientific knowledge. The systematization of thermodynamic parameters of complex formation reactions in mixed solvents, obtained by researchers of ISUCT for more of 100 reaction systems [1] was realized in the database "Thermodynamics of complex formation and solvation in binary solvents" [2, 3]. It provides a quick free search of necessary thermodynamic characteristics of complex formation and solvation of reagents and the information about the used research methods. Free access to the most important commercial thermodynamic databases such as SciFinder, The IUPAC Stability Constants Database and NIST Databases is usually limited to their demo-versions, and payment for their use is not always available to researchers.

In this connection, for the convenience of generalization of results and solving the problem of systematization of accumulated experimental material using "Microsoft Access" database search system was developed. It allows carrying out the work with data (chemical formula of investigated substances, stability constants, as well as Gibbs energy, enthalpy and entropy of complex formation reactions, experimental conditions, references to the published articles). Developed software does not require a special knowledge of databases content renovation.

In addition, this database has a structure that allows adapting it to systematize data collected in different areas of basic and applied knowledge. According to this, the application of this software can expand.

This work was performed at the Research Institute of Thermodynamics and Kinetics of Chemical Processes of the ISUCT and was carried out under grant of Council on grants of the President of the Russian Federation (project 14.Z56.16.5118-MK).

[1] https://www.isuct.ru/e-publ/portal/sites/ru.e-publ.portal/files/dep/oht/works_2016.doc

[2] Usacheva, TR; Kuz'mina, KI; Cheshinskii, MA; Kuz'mina, IA; Sharnin, VA. *Izv. Vyssh. Uchebn. Zaved. Khim. Khim. Technol.*, 2016, 59, 3, 86-89.

[3] <https://www.isuct.ru/e-publ/portal/node/4258>

THERMAL ANOMALY IN $(n\text{-Bu}_4\text{N})_3[\text{M}(\text{CN})_6]$, $\text{M} = \text{Os}, \text{Ru}$ AND ITS INFLUENCE ON CRYSTAL STRUCTURE DETERMINATION

Vostrikova K. E., Pischur D. P.

Nikolaev Institute of Inorganic Chemistry, Siberian Branch of the Russian Academy of Sciences, 630090 Novosibirsk, Russia
E-mail: vosk@niic.nsc.ru

The octahedral $[\text{M}(\text{CN})_6]^{3-}$ anions represent important orbitally-degenerate magnetic building blocks with unquenched orbital momentum and their incorporation in low-dimensional molecular magnetic materials can potentially increase their magnetic anisotropy, which is important to raise a magnetization blocking temperature. In this respect, $4d$ and $5d$ counterparts of hexacyanoferrate(III), $[\text{Ru}^{\text{III}}(\text{CN})_6]^{3-}$ and $[\text{Os}^{\text{III}}(\text{CN})_6]^{3-}$ are more attractive magnetically anisotropic constituents than their iron congener due to much stronger spin-orbit coupling energy and more diffuse magnetic orbitals resulting in larger magnetic spin coupling J [1–3].

The complex $(n\text{-Bu}_4\text{N})_3[\text{Os}(\text{CN})_6]$, firstly prepared in 1968 [4], was not structurally characterized yet. We were able to prepare the both osmium and ruthenium hexacyano complexes as their n -tetra-butylammonium salts in the form of single crystals. However, the majority of attempts to investigate them by SCXRD method at low temperatures failed. In cryogenic conditions, the crystals were fissured during their installation and became non-suitable for the X-ray study.

The DSC studies have demonstrated that the polycrystalline samples of $(n\text{-Bu}_4\text{N})_3[\text{Os/Ru}(\text{CN})_6]$ displayed the thermal effects of 584 and 1252 J/mol in the temperature range of 151–162 and 153–165 K for ruthenium and osmium complex,

respectively (see Figure). This thermal anomaly is probably related to the cation disordering upon the heating, which results in a crystal symmetry lowering and the crystal cell parameters changing. It is well known that a bulky n -tetrabutylammonium cation is frequently disordered in their solid salts. Hence, upon a prompt cooling from room to liquid nitrogen temperature a sharp change in sample volume results in crystal cracking.

Considering the thermoanalysis information we succeeded to find the conditions for XRD data

collection satisfactory for crystal structure solution. The crystallographic parameters for a monoclinic crystal of $(n\text{-Bu}_4\text{N})_3[\text{Os}(\text{CN})_6] \cdot 0.5\text{H}_2\text{O}$ are: $P2_1/n$, $a = 22.8107(7)$, $b = 22.8580(3)$, $c = 22.8831(4)$ Å, $\beta = 90.6508(17)^\circ$, $V = 11931.4(7)$ Å³, $Z = 8$, $R_1 = 0.0783$, $wR_2 = 0.1761$. According to the polycrystalline XRD data ruthenium complex is isomorphous to osmium one.

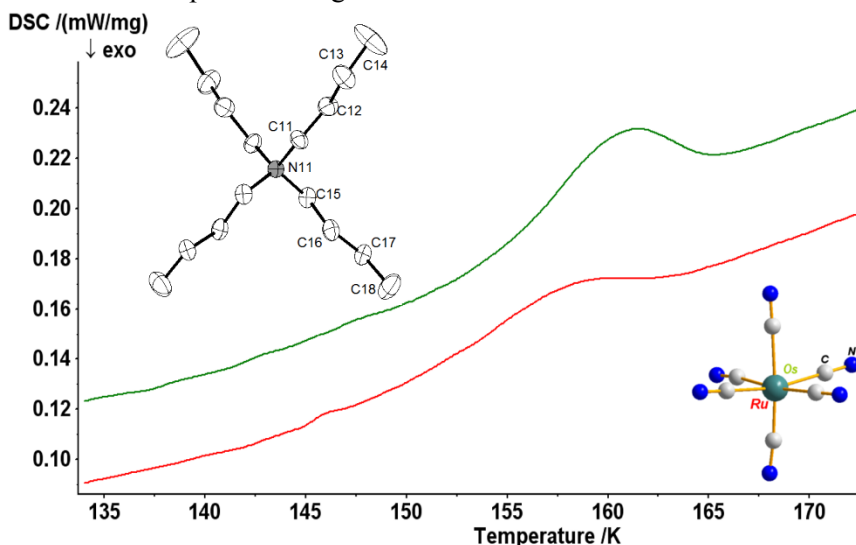


Figure. Thermal effects for Ru (red) and Os (green) complexes.

This work was supported by the Russian Foundation for Basic Research under grant number 16-03-00880.

[1] Dunbar, K. R. *Inorg. Chem.* 2012, 51, 12055.

[2] Rams, M.; Peresykina, E. V.; Mironov, V. S.; Wernsdorfer, W.; Vostrikova, K. E. *Inorg. Chem.* 2014, 53, 10291–10300.

[3] Peresykina, E.V.; Majcher, A.; Rams, M.; Vostrikova, K.E. *Chem. Commun.* 2014, 50, 7150–7153.

[4] Alexander, J. J.; Gray, H. B. *J. Am. Ceram. Soc.* 1968, 90, 4260–4271.



ONTOLOGIES AS TOOLS FOR THERMODYNAMIC DATA INTEGRATION

Erkimbaev A.O., Kobzev G.A., Trachtengerts M.S., Zitserman V.Yu.

Joint Institute for High Temperatures, Russian Academy of Sciences, Izhorskaya 13, Bldg. 2, 125412 Moscow, Russia

E-mail: adilbek@ihed.ras.ru

Last years term “ontology” has become prominent in the information technology and its application to store and sharing of scientific data and knowledge. In outline by ontology is meant the concept set represented as entity set connected with some relation. Ontology may be successfully used for such purposes as excluding ambiguity by standardization of terms; linking documents with related content by Semantic Web methods; knowledge framework required for data sharing. This stimulated activity for development of ontologies for knowledge capturing in many science areas: life science, chemistry, geoscience, etc. Recently some attempts have been taken to build special ontologies covering key thermodynamic concepts [1, 2]. As usual the encoding of the ontology using the Web Ontology Language (OWL) was preceded by the conceptualization of the domain by natural language tools [3]. Three main entities that must be determinate in context of thermodynamics are substances, properties and data. Every substance may be characterized by systematic name and its synonyms, chemical formula and may be presented in diverse phase states: gas, liquid, solid, interfacial lines (sublimation, saturation, melting), triple point etc.

The key advantage of the ontology over the vocabulary of basic terms is the existence of the associative relations adequately representing logical and physical connections between concepts. With regard to thermodynamics these relations impose the diverse limitations on the assignment of specific property to the particular substance or phase. Development of the thermodynamic ontology was followed the bottom-up strategy [3], i.e. gradual refinements of the subject field. Initial phase of the development has been constrained pure substances and strictly specified data type: value table for property as temperature function.

Integration, i.e. uniform data presentation is realized by the technology of Linked Open Data (LOD). Publishing Scientific Data as Linked Open Data provides far more possibilities in comparison with data publishing in the common “web of documents”. Linked data technology provides the connections between arbitrary things, identified from the document by URI. As to URIs (unified resources identifier) they capable to recognize arbitrary object, person or conception as contrasted to the traditional Web. The unified model of linked data is based on the RDF (resource definition framework) for the data and metadata presentation. The RDF format is composed from triples (subject-predicate-object) suitable for computer processing. The data model, thus defined, is designed so that semantic interpretation may be provided by reference to the ontologies or controlled vocabularies located in the Web. By and large the open linked data approach together with proposed ontology provides universal standard for network exchange of thermodynamic data.

[1] Erkimbaev, A; Zhizhchenko, A; Zitserman, V; Kobzev, G; Son, E; Sotnikov, A. Integration of Databases on Substance Properties: Approaches and Technologies. *Automatic Documentation and Mathematical Linguistics*, 2012, 46(4), 170.

[2] Zelenchuk, A; Prjaduhin, I; Molorodov, Yu; Fazliev, A. Applied ontology on thermophysics. Reduction problem. Selected papers of the 5th Symposium “Framework of the science information resources and systems”, p. 164. 2015, Saint Petersburg.

[3] Erkimbaev, A; Zitserman, V; Kobzev, G; Serebryakov, V; Shiolashvili, L. Data on properties of substances and materials integration evolved from ontological modeling of the domain.

Electronic libraries 2013, 16(6). (www.elbib.ru/index.phtml?page=elbib/rus/journal/2013/part6/EZKSS)



THE ERRORS INCURRED IN THE REFERENCE DATA ON HEAT OF FUSION FOR REFRACTORY METALS

Fokin L.R., Kulyamina E.Yu., Zitserman V.Yu.

Joint Institute for High Temperatures, Russian Academy of Sciences, Izhorskaya 13, Bldg. 2, 125412 Moscow, Russia

E-mail: lfokin@mail.ru

Pure substances phase transition data are critical concepts of chemical thermodynamics. When using Clapeyron–Clausius equation for melting curve calculation we run into problems of extreme unreliability (or total absence) of experimental data on heat of fusion for d-elements. The currently available tables prepared by Dinsdale A (1991) present the most authoritative source of pure element data. They have been recommended by the Scientific Group Thermodata Europe (SGTE) and included (with minor additions) into the contemporary reference editions [2, 3]. It's important to note that Dinsdale's tables widely used for the calculation of phase diagram for metals and alloys. Unfortunately we noticed some mistakes in deciding on specific values of melting enthalpy for some metals.

As an example the chromium reference value from [1] (21 kJ mol^{-1}) should be confronted with the experimental value obtained by levitation calorimetry method ($29.7 \pm 0.6 \text{ kJ mol}^{-1}$). Another interesting example of the error incurred in the reference data is related with osmium and rhenium properties. As to osmium all handbooks [1-3] present the identical values for the heat of fusion, $57.85 \text{ kJ mol}^{-1}$. This estimation as well as the analogous estimation for rhenium ($60.43 \text{ kJ mol}^{-1}$) is based on the linear correlation between melting entropy and melting point proposed by authors from IVTAN as early as 1979 [4]. Actually the correlation [4] allowed one to extrapolate the available experimental data for ruthenium and iridium to more high temperatures, T_m 3300 K for osmium and $T_m = 3453 \text{ K}$ for rhenium. At a later time a half value of heat of fusion ($34.07 \text{ kJ mol}^{-1}$) in comparison with estimation [1] has been measured. It is this figure that has been recommended by SGTE [2]. As a consequence analogous estimation of the heat of fusion for osmium may be considered as unreliable.

It turned out that high-precision data on metals surface tension produced in the USSR in the 80th helped to resolve the contradiction detected. In due time prof. B.D. Summ from the Division of colloid chemistry (MSU, Chemistry Department) has established the correlation between the surface tension at the melting point and the enthalpy of fusion for some HCP and FCC metals [5]. Such correlation makes it possible to obtain for osmium the reasonable estimation ($35\text{-}40 \text{ kJ mol}^{-1}$) of the heat of fusion. This finding is in line with the experimental value for rhenium.

We have sketched the broad outlines of the phase transition data for refractory metals. This should encourage further experiments and quantum-mechanical simulation to ensure completeness and consistency of the thermodynamic data.

[1] Dinsdale, A. SGTE data for pure elements. CALPHAD 1991, 15, 317.

[2] Thermodynamic Properties of Inorganic Substances. Landolt-Börnstein Group IV (Physical Chemistry), vol. 19. Pure Substances – Subvolume A.

Authors: Scientific Group Thermodata Europe (SGTE). Publisher: Springer Berlin/Heidelberg, 1999.

[3] CRC Handbook of Chemistry and Physics, 97th Edition W.M.-Hynes. 2016 by CRC Press.

[4] Kats, S.; Chekhovskoi, V. Enthalpies of Fusion of Metallic Elements. High Temp. - High Press. 1979, 11, 629.

[5] Summ, B. New correlations of surface tension with bulk properties of liquids. Vestn. Mosk. Un-ta. Ser. 2. Himiya. 1999, 40(6), 400.



Section 3.

Thermodynamics of solutions and heterogeneous systems

Oral presentations

**AGGREGATION BEHAVIOR OF AMINO ACID IONIC LIQUIDS (AAILs) BASED ON 1-OCTYL-3-METHYLIMIDAZOLIUM IN AQUEOUS SOLUTIONS**Alopina E.V.¹, Nikonorova A.A.², Dobryakov Yu.G.¹, Pukinsky I.B.¹, Smirnova N.A.¹¹Saint Petersburg State University, 199034 St. Petersburg, Russia²Saint Petersburg State Technological Institute, 190013 St. Petersburg, Russia

E-mail: alopina@mail.ru

Alkylimidazolium salts are considered as a special class of ionic liquids due to their unique acid–base behavior, biological significance and applications in different fields such as synthetic chemistry, biology, medicine etc. Despite their widespread applications in chemical synthesis, homogeneous catalysis, chiral solvents, electrochemistry and separation processes [1], rather restricted information is available on the aggregation of these compounds in aqueous solution. Recently the aggregation behavior of 1-alkyl-3-methylimidazolium salts (mainly halides) in aqueous solution has attracted a substantial interest [2]. However the studies of 1-alkyl-3-methylimidazolium salts having amino acid anions are relatively new and the experimental studies of their physical properties are still scarce.

In this work AAILs with L-Val, L-Lys, L-Leu, L-Ala, L-Ser as the anions and 1-methyl-3-octyl-imidazolium as the cations (Fig. 1) were successfully synthesized and characterized. The method of the synthesis elaborated by Fukumoto [3] was modified in our studies [4]. The densities of aqueous solutions of these AAILs in the concentration range 0-97 wt % were measured in the temperature range $298.15-318.15 \pm 0.05$ K. The density data have been used to calculate the molar volumes, V_m , for all the systems at several studied temperatures. The aggregation behavior of these AAILs in aqueous solutions and their physicochemical properties has been investigated using volume, conductivity, and fluorescence techniques.

The densities of the aqueous solutions with the same AAIL concentration decrease at $T=298.15$ K in the following sequence: $[C_8mim][Ser] > [C_8mim][Lys] > [C_8mim][Ala] > [C_8mim][Val] > [C_8mim][Leu]$.

The results of the conductivity measurements obtained for $[C_8mim]Cl$ and $[C_8mim]Br$ aqueous solutions in the present study are in a good agreement with those reported in literature [2, 5]. The comparison of the cmc values for $[C_8mim]Cl$, $[C_8mim]Br$ and $[C_8mim][AA]$ ($AA = Val, Lys, Leu, Ala, Ser$) solutions shows the effect of $[AA]^-$ anions on the IL micellization. The cmc of the aqueous solutions at $T=298.15$ K changes in the order: $[C_8mim]Br < [C_8mim][Ser] < [C_8mim][Ala] < [C_8mim][Leu] < [C_8mim][Lys] < [C_8mim]Cl < [C_8mim][Val]$. The values of the counterion binding parameter β increase in dependence on the nature of the ILs: $[C_8mim][Val] < [C_8mim][Lys] < [C_8mim][Leu] < [C_8mim][Ala] < [C_8mim][Ser]$. The values of ΔG_m° calculated for the AAILs are negative and give evidence that the micelle formation in aqueous solutions of the AAILs under study is a spontaneous process. These results have confirmed that amino acid anions significantly affect the thermo-physical properties of AAILs; the differences in the studied properties of the AAILs may be due to the differences in the internal interactions (hydrogen bonding, π - π interaction, van der Waals interactions, etc.) in each AAIL molecule.

The results have been used to understand the anion effects of the AAILs under study on the aggregation behavior of these AAILs and the dependence of physicochemical properties of aqueous AAIL solutions on the effect of the anions.

Acknowledgements. The work was financially supported by the Russian Science Foundation (grant 16-13-10042) and by the Russian Foundation for Basic Research (grants 16-03-00723). The NMR measurements were carried out at the Center for Magnetic Resonance, St. Petersburg State.

[1] Smirnova, N; Safonova, E. J. Phys. Chem. A, 2010, 84, 1695–1704.

[2] Jungnickel, C; Łuczak, J; Ranke, J; Fernandez, JF; Muller, A; Thoming, J. Colloids Surf. A: Physicochem. Eng. Aspects, 2008, 316, 278–284.

[3] Fukumoto, K; Yoshizawa, M; Ohno, H. J. Am. Chem. Soc., 2005, 127, 2398–2399.

[4] Alopina, E; Dobryakov, Yu; Safonova, E; Smirnova, N. Current Issues of Biological Physics and Chemistry, Russ, 2016, 2, 173-175.

[5] Bai, G.A; Lopes, M; Bastos, J. Chem. Thermodynamics, 2008, 40, 1509–1516.

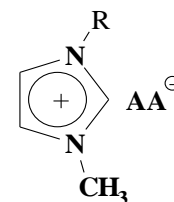


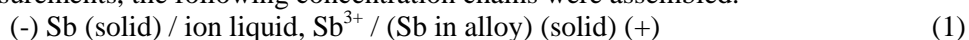
Figure 1. Structure of AAILs studied in this work. These are $[C_8mim][AA]$ molecules where $R = C_8H_{17}$ and $AA = Val, Lys, Leu, Ala, Ser$ anions.

**EMF METHOD WITH AN IONIC LIQUID IN THERMODYNAMIC STUDY OF ANTIMONY CHALCOIODIDES**Musayeva S.S.¹, Shukurova G.M.¹, Imamaliyeva S.Z.², Babanly M.B.²¹Baku State University, AZ1148, Baku, Azerbaijan²Institute of Catalysis and Inorganic Chemistry, ANAS, AZ1143, Baku, Azerbaijane-mail: babanlymb@gmail.com

Compounds of SbXI (X-S, Se, Te) type are valuable functional materials with high photosensitivity, ferroelectric, pyroelectric, pyrooptical, electrooptical, etc. properties [1]. In [2-4] we have presented the T-x-y phase diagrams of ternary systems Sb-X-I.

This work is devoted to the study of the thermodynamic properties of SbXI compounds using electromotive force (EMF) measurements.

For the EMF measurements, the following concentration chains were assembled:



in the temperature range of 300–380 K.

In the chains of type (1), a mixture of morpholine and formic acid with adding 0,5mol% anhydrous SbCl₃ was used as an electrolyte. In view of phase diagrams of the Sb-X-I systems an equilibrium alloys from three-phase SbXI-SbI₃-X areas were used as right electrodes. These equilibrium alloys were obtained by melting high purity elemental components in evacuated quartz ampoule, followed by homogenizing annealing at a temperature below the solidus at 20-30° for 500-1000 h. Equilibrium of alloys was checked by X-ray diffraction technique.

Measurements showed constancy of the EMF values within three-phase areas SbXI-SbI₃-X for each system independently of the overall composition of alloys, and that is in accordance to their phase diagrams.

Analysis of the EMF measurements showed their linearity for each three-phase area. Therefore, they were treated by the method of least squares to obtain a linear equation of the type E=a+bT.

From these equations the partial thermodynamic functions of antimony in alloys were calculated. Based on solid phase equilibrium diagrams of the studied systems the potential-forming reaction for SbXI compounds were established and their standard thermodynamic functions of formation and standard entropies were calculated (Table).

Table. The standard integral thermodynamic functions of chalcogen-iodides of stibium

Phase	$-\Delta_f G^0(298\text{K})$	$-\Delta_f H^0(298\text{K})$	$S^0(298\text{K})$ ($\text{J}\cdot\text{K}^{-1}\cdot\text{mol}^{-1}$)
	(kJ·mol ⁻¹)		
SbSI	92.4±1.7	90.7±1.3	141.1±2.9
SbSeI	80.8±1.7	78.1±1.3	154.7±2,4
SbTeI	56.6±1.7	56.4±1.3	153.8±2.5

References

- [1]. Gerzanich E.Y., Lyakhovitskaya K.A., Popovkin B.A., Fridkin V.M. In: Current topics in material science, North-Holland, 1982, 10, 55-190
- [2]. Aliyev Z.S., Musaeva S.S., Babanly D.M., Shevelkov A.V., Babanly M.B. J.Alloys Compd., 2010, 505, 450-455
- [3]. Aliev Z.S., Babanly M.B., Shevelkov A.V., Babanly D.M., Tedenac J-C. Intern.J. Material Research, 2012, 103, 3, 290-295
- [4]. Aliev Z.S., Musayeva S.S., Jafarli F.Y., Babanly M.B. Az.Chem.J., 2015, 2, 57-61

ON THE POSSIBILITY OF THE FORMATION OF A NaCl – KCl SOLID-SOLUTION CRYSTAL FROM AN AQUEOUS SOLUTION

Fedoseev V.B.^{1,2}, Shishulin A.V.¹, Titaeva E.K.¹, Fedoseeva E.N.¹

¹Lobachevsky Nizhny Novgorod State University, pr. Gagarina 23, Nizhny Novgorod, 603950 Russia

²Razuvaev Institute of Organometallic Chemistry, RAS, ul. Tropinina 49, Nizhny Novgorod, 603600 Russia

E-mail: ybfedoseev@yandex.ru

Volume reducing of a heterogeneous system is accompanied by a shift of phase equilibrium and the phase diagram deformation. It leads to a change of the mutual solubility and the emergence of resistant metastable phases that are impossible in macroscopic systems [1]. Possibility of obtaining a similar metastable phase is regarded by an example of the solid solution of the salts NaCl and KCl, with an upper critical solution temperature at 780 K. Phase transformations in small-volume system NaCl-KCl-H₂O have been simulated by means of the methods of equilibrium chemical thermodynamics [2]. The search criterion of metastable states is the minimum of Gibbs energy of the system including the surface energy of all existing phase boundaries. In small systems its contribution becomes comparable with the full system energy.

We have modelled the formation of crystals in the supersaturated solution of a spherical drop which components do not form a solid solution under normal conditions. Small volume and the amount of substance limit the number of crystals that may have arisen in the system/ Therefore the formation of one or two crystals per drop was simulated. Formed crystals are in equilibrium with the solution.

Simulation predicts the existence of metastable state, which corresponds to a solid solution of NaCl - KCl, when the degree of supersaturation exceeds ~3. The most interesting case is when only one crystal is formed in the system. In this case, the system has three equilibrium states (NaCl crystal in a supersaturated solution of KCl, KCl crystal in a supersaturated solution of NaCl, solid solution crystal NaCl - KCl). These states are shown in the figure 1, where the dark areas correspond to the Gibbs free energy minima for a drop containing one crystal. The state with two crystals of individual components of energy is much more favorable under all conditions. However, also in this case a range of conditions exists there in which the metastable state of solid solution is thermodynamically stable (local minimum of Gibbs energy).

High supersaturation of the aqueous solution is an important condition for the stability and existence of the metastable solid solution. The report presents the experimental observations that suggest the possibility of achieving the necessary degree of supersaturation in evaporating picolitre droplets.

Thermodynamic model can be applied to describe the formation of a metastable solution of different immiscible substances and other systems with an upper critical solution temperature. Those systems may be prepared using spray technology or by means of nanoreactors. The particles of metastable phases have a large stored energy, which can affect their high reactivity and catalytic ability.

The work of V. Fedoseev was supported by the Russian Science Foundation, grant no. 15-13-00137.

[1] Fedoseev V.B., Fedoseeva E.N. JETP Lett. 2013. 97(7). 408–412.

[2] Fedoseev V.B. Shishulin A.V., Titaeva E.K., Fedoseeva E.N. Phys. Solid State. 2016. 58(10). 2095–2100.

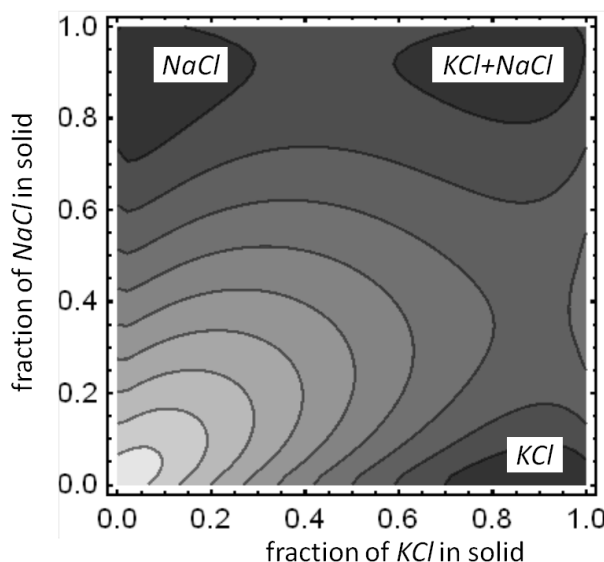


Figure 1. Gibbs energy of a spherical droplet containing one crystal surrounded by an aqueous solution.

THEORETICAL ANALYSIS OF CARBONATE HYDROXYAPATITE PRECIPITATION IN SYNOVIAL FLUID

Izmaylov R.R.^{1,2}

¹Institute of Hydrocarbon Processing, Siberian Branch of the Russian Academy of Sciences, 644040, Omsk, Russia

² Omsk F.M. Dostoevsky State University, 644077, Omsk, Russia

E-mail: r.r.izmailov@gmail.com

Calcium phosphate materials are used in medicine for the regeneration of damaged bone tissues by way of gradual replacement of the material by the newly growing bone tissue. Hydroxyapatite (HA) used for this purpose today features a slow biological resorption rate - a considerable shortcoming of the material. The resorption process can be enhanced through replacement of the phosphate and hydroxide anions in the apatite structure with carbonate groups [1]. This paper presents the method of calculating the thermodynamic parameters of Carbonate Hydroxylapatite prepared from human synovial fluid. Thermodynamic analysis of Ca-P precipitation has been reported in the following solution system (Table 1).

Table 1. Mineral composition human synovial fluid, mmol /dm³.

Ion	Concentration (mmol dm ⁻³)
Na ⁺	140
K ⁺	4.6
Mg ²⁺	1.1
Ca ²⁺	2.5
Cl ⁻	103
HCO ₃ ⁻	27
HPO ₄ ²⁻	4.38
SO ₄ ²⁻	11.40

The thermodynamic driving forces for Ca- P precipitation were calculated based on the classical equation of free energy change in supersaturated solutions.

$$\Delta G = -\frac{RT}{n} \ln(IS) = -\frac{RT}{n} \ln(A_p / K_{sp}),$$

where ΔG is the Gibbs energy per mole of ionic units that compose Ca-P in solution, R is the gas constant, T is the absolute temperature, N is the number of ion units in a Ca-P molecule, and S is the supersaturation that is defined by the ration of the activity product of ion units composing precipitates (A_p) corresponding solubility product(K_{sp}). To study the effect of concentration on the crystallization of carbonate ions of Carbonate Hydroxylapatite supersaturation index were calculated (IS) and the Gibbs energy of crystallization (ΔG), built by of stability of fields for assessing influence of several factors on the formation of KGA. Values of pH and the concentration of carbonate ions do not have a significant impact on formation of KGA.

[1] LeGeros, R.Z., Tung, M.S., Chemica Stability of Carbonate- and Fluoride-Containing Apatites, Caries Res., 1983, vol. 17, pp. 419–429.

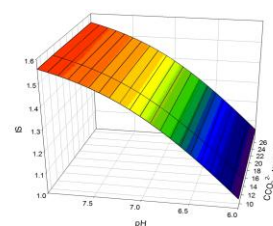


Figure 1. IS- pH- Carbonate ions for Human Synovial fluid with the initial normal saline supersaturation S = 50



PHASE DIAGRAMS OF MULTICOMPONENT SYSTEMS: CORRELATION OF THERMODYNAMICS AND TOPOLOGY

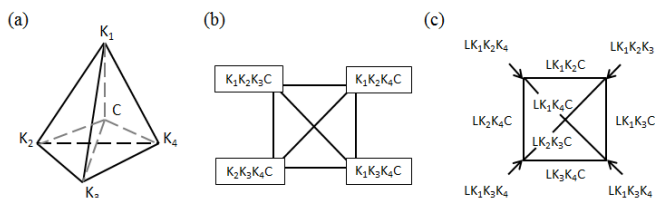
V.I. Kosyakov

NIIC SB RAN, Lavrent'ev ave. 3, Novosibirsk, 630090

kosyakov@niic.nsc.ru

Phase diagram of t -component system can be represented in the form of geometric structure in a space with dimension $t + p - 1$, where p is a number of variable parameters of the system state, which typically use a pressure P and temperature T . Each point of the p -subspace corresponds to the concentration simplex with edges of unit length. The simplex consists of regions of existence of phases and phase associations. When $p = 0$ each region corresponds to the association, containing from one to t phases. The dimension of the region equal to $t - 1$. For small variations of the thermodynamic parameters, the boundaries between the regions can move inside the simplex, so that its topology does not change. A set of phases or phase associations in the simplex changes when crossing the border between the areas of p -space. As a result, p -space consists of areas with different topologies of the concentration simplex. Simplex on the boundary is the union of simplexes that are located on different sides of this border. Changing the topology of the partition simplex may describe by the equation phase reaction. One-dimensional and zero-dimensional borders between the areas of p -space correspond to monovariant and invariant reactions, respectively.

Consider the one-dimensional p -space in which the temperature is the only coordinate. The sequence is invariant and monovariant reactions in this case is usually portrayed in the form of Sheil's diagrams. It is a graph whose vertices are labeled with the equations of the invariant reactions and edges correspond to monovariant reactions. Using Shale diagram it is possible to build topological graphs of isothermal sections or liquidus surface. When $t \leq 3$ the structure of these fragments of the diagram is described by a planar graphs, for describing the structure of four-component systems it is necessary, in general, to use non-planar graphs.



For example, in fig. (a) shows the four-component simplex of the K1-K2-K3-K4 system with quaternary compound C. Figs (b) and (c) show graphs of hypersurfaces of the liquidus and solidus. On fig. (c) vertices of the graph can correspond to different phase reactions. In addition, the special points can

exist on its edges. You can display 54 graphs with a different marking of vertexes and edges. Each graph corresponds to a specific type of the melting diagram. This example demonstrates the great variety of phase diagrams and effectiveness of the topological approach for the generation of new diagrams.

For design the set of the phase diagrams in P - T space, we need to generate consistent fragmentations of the two-dimensional subspace of parameters and concentration simplexes.

The topology describes the global structure a phase diagram and a set of diagrams with given characteristics. Topological approach suitable for the prediction of possible types of phase diagrams of multicomponent systems in the multidimensional p -space. It can be used to solve enumeration problems of phase diagrams and their topological classification. These problems are not solved in the thermodynamics methods; therefore, the topological approach is an independent section of the phase diagrams theory. However, the basis of this theory is the chemical thermodynamics. In particular, in the framework of the thermodynamics was derived the Gibbs phase rule, which is one of the fundamental equations of the topological theory of phase diagrams.

Equations of the theory of phase equilibria are local in nature. Therefore, they were used to substantiate the geometric structure of the fragments of phase diagrams, to understand the relationships between their structure and thermodynamic properties of equilibrium phases. Thermodynamic equations are widely used to calculate phase equilibrium at given P and T according to thermodynamic properties of the phases. To construct the phase diagram it is necessary to repeat these calculations in a given region of variation of parameters. Thermodynamics is also used to solve other local problems for the study of the fragments of phase diagrams and their design using physical or virtual models of the thermodynamic properties of the phases.

PHASE EQUILIBRIUM BEHAVIOR OF MIXTURES CONTAINING SUPERCRITICAL CARBON DIOXIDE NEAR CRITICAL REGION

Chiu H.Y., Chuang R.F., Lin H.M., Lee M.J.

Department of Chemical Engineering, National Taiwan University of Science & Technology, Taipei 10607, Taiwan

E-mail: mjlee@mail.ntust.edu.tw

This study employed a visual and volume-variable phase equilibrium analyzer (PEA, Figure 1 [1]) to measure the phase transition boundary data for the mixtures containing supercritical carbon dioxide over wide experimental conditions, including near critical region. The PEA was modified from a high-pressure generator which was equipped with a view window. Its internal volume can be adjusted manually to manipulate the pressure of the loaded mixture in the PEA. Using two ISCO syringe pumps to charge carbon dioxide and organic compounds, respectively, the composition of the loaded mixture is accurate to an uncertainty of 0.003 in mole fraction. The phase behavior of the loaded mixture in the PEA can be observed through the view window and the images were taken with a digital camera and displayed on an LCD. While the temperature in the PEA was controlled by a thermostatic circulated water to within 0.1 K, the pressure was monitored by a pressure transducer with a digital indicator to an uncertainty of 0.1%. After loading a mixture with known composition into the PEA, the mixture was pressurized manually to form a homogeneous phase (either liquid or vapor phase). When the temperature in the measuring cell reaches to a pre-specified value, we slowly adjusted the position of screw pump of the PEA by hand to reduce the cell's pressure until the second phase appeared and this value was recorded as a bubble or dew pressure. The experiments were conducted over a wide composition range, including near critical region. Comparing with analytic method, this synthetic technique is much easier and more efficient for determining the phase transition boundaries, especially near critical region, because we do not need to take sample from the cell and make composition analysis. Based on the phase boundary data, the isothermal K -values at a given pressure can also be calculated by interpolating the bubble-point curve ($P-x_i$) and the dew-point curve ($P-y_i$). These results provide valuable knowledges on the isothermal K -value of each component varying with pressure over wide range of condition, and more interestingly how the K -values approach to the critical point ($K_i = 1$). In this presentation, the images taken during the phase transition in different phase regions will be shown, including the phase transition around critical region. The experimental phase envelopes for several binary and pseudo-binary systems will be presented, an illustrative example of pseudo-binary system of carbon dioxide + (mixed solvents of DMSO + ethanol) as shown in Figure 2. These vapor-liquid equilibrium (VLE) data will be correlated with the Peng-Robinson equation. The comparison of correlated results with experimental values will be made.

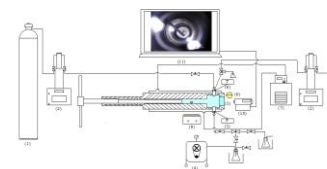


Figure 1. Schematic diagram of PEA [1]

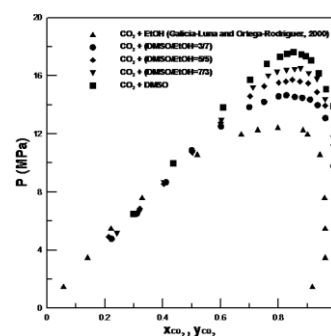


Figure 2. VLE phase boundaries for pseudo-binary system of CO_2 + (mixed DMSO + ethanol) [2]

Acknowledgement The authors gratefully acknowledged the financial support from the Ministry of Science & Technology, Taiwan, through grant no. NSC 99-2221-E011-079-MY3 and MOST 105-2221-E-011-144-MY3.

[1] Chiu, HY; Chuang, RF; Lin, HM; Lee, MJ. J. Supercrit. Fluids, 2008, 44, 273-278.

[2] Chiu, HY; Lin, HM; Lee, MJ. J. Supercrit. Fluids, 2013, 82, 146-150.



THE PHASE EQUILIBRIUM IN REFINEMENT OF MULTICOMPONENT METAL MELTS

Mikhailov G.G. Makrovets L.A.

South Ural State University, Lenin avenue, 76, Chelyabinsk, 454080, Russia

E-mail: mikhailovgg@susu.ru

Currently, the requirements for mechanical performance of both low-alloy engineering and special purpose steels have increased. The technology of steel production has changed considerably. In oxygen converters and electric furnaces, pig iron is produced, which is later brought to the right composition in ladle furnaces, degassed if necessary and cast in continuous casting machines. The modern system of refining allows us to obtain metal with the concentration of oxygen approximately 0.0001 mas.%, and sulfur within 0.002–0.003 mass.%. However, in spite of the possibility for deep deoxidation and desulphurization of non-metallic inclusions in the steel, their arrangement, form, and properties are still paid considerable attention. For them, a thermodynamic model is created for the processes going on at every stage of steel refining and alloying. Within the framework of this model, the compositions of the liquid metal and the balanced non-metallic phases are established. The thermodynamic analysis is preceded by the establishment of a database of parameters for the theory of oxide and metal melts, establishment of the heat of fusion and formation oxide compound from the components of metal melts, any by solving the equation systems for establishing the coordinates of all the equilibrium variants. The objective is to build the multidimensional surface of metal components solubility (SMCS) in the general case. The SMCS contains the composition of the metal and the equilibrium oxide phases. The SMCS is a specific diagram of steel oxygen refining. The paper discusses the results of thermodynamic modeling of steel deoxidation with magnesium, calcium, aluminum, silicon, manganese, cerium, lanthanum, yttrium, and zirconium. The results of the calculations are presented as tables and phase equilibrium diagrams.

The results obtained from the analysis of physical-chemical transformations in liquid steel allow for the solution of another set scientific problems: the establishment of the optimum composition of alloys and master alloys with the purpose of efficient use of expensive components of refining alloys. The problem of component balance in a multicomponent refining or modifier alloy needs to be solved. In this problem, the composition of the source metal, of the metal to be obtained, and the composition of the equilibrium oxide phases are given. The problem is solved by drafting balance equations. Let us assume that such balance of aluminium and silicon is to be calculated for aluminum-silicon that would allow us to obtain an alloy with easily-removed fluid impurities. The solution of the balance equation systems for iron, aluminum, silicon, and oxygen presents conclusive evidence that the composition of the deoxidizing alloy depends on the composition of the source metal. Given the change in the concentration of oxygen in the source metal from 0.2% to 0.02%, the balance of $[\text{Si, \%}]/[\text{Al, \%}]$ changes from 5 to 35, so a constant composition of master alloy cannot be established. The composition of the alloy for complex deoxidizing or modification of non-metallic inclusions is linked to the level of oxidation of the source metal. The finish refining processes should therefore be subject to strict regulations and calculations.

The work was supported by Act 211 Government of the Russian Federation, contract № 02.A03.21.0011.



THE EXPERIMENTAL AND COMPUTATIONAL DETERMINATION OF THE HENRY'S LAW CONSTANT FOR THE SOLUTIONS OF NOBLE GASES IN METHANOL, ETHANOL AND PROPAN-2-OL AT HIGH TEMPERATURES

P. A. Nikolaychuk^{1,2}, M. Linnemann¹, Y. M. Muñoz-Muñoz¹, E. Baumhögger¹, J. Vrabec¹

¹ *Kafedra analitičeskoj i fizičeskoj himii, Čeljabinskij gosudarstvennyj universitet, 454001, Chelyabinsk, Russian Federation*

² *Lehrstuhl für Thermodynamik und Energietechnik, Universität Paderborn, 33098, Paderborn, Germany*

E-mail: npa@csu.ru

Noble gases are found in a wide range of applications in medicine, environmental chemistry or lighting. The solubility and the phase behaviour of noble gases in water and organic solvents was studied rather widely, however, for many systems the available information is not complete. Particularly, data on the solubility of noble gases in primary and secondary alcohols are present only for a very limited temperature range. In the present work the experimentally determined Henry's law constant for the solutions of argon and helium in propan-2-ol at 360, 420 and 480 K, as well as the Henry's law constant for the solutions of neon, krypton, argon and xenon in methanol, ethanol and propan-2-ol at temperatures ranging from 50% to 95% of the solvent's critical temperatures are reported.

The experimental setup for the high temperature gas solubility measurements and the experimental procedure were described previously [1]. The density of argon and propan-2-ol as well as the saturated vapour pressure of pure propan-2-ol at these temperatures were calculated according to the corresponding equations of state [2, 3]. The measured Henry's law constant data are listed in Table 1.

The Henry's law constant is related to the residual chemical potential at infinite dilution that can be calculated by molecular simulation. The molecular models for noble gases [4], methanol [5] and ethanol [6] were developed previously. In this study the modified Lorentz-Berthelot rule was applied; the simulation procedure and details were described previously [7]. A state-independent binary parameter ξ was adjusted such that the differences between the simulation results, the present experimental values and the literature data were minimal; its values for the binary systems are listed in Table 2. The simulations were carried out with the *ms2* software [8]. The calculated Henry's law constant data are presented in Figure 1.

Table 1. Henry's law constants of argon and helium in propan-2-ol

T, K	$H_{\text{Ar}/2\text{-PrOH}}$, MPa	$H_{\text{He}/2\text{-PrOH}}$, MPa
360	114.0 ± 1.5	600.9 ± 43.5
420	98.5 ± 2.5	334.1 ± 13.6
480	57.6 ± 2.1	142.1 ± 6.3

Table 2. Estimated values of the binary parameter ξ in the modified Lorentz-Berthelot rule for binary systems

Component	Ne	Ar	Kr	Xe
Methanol	0.53	1	1	0.978
Ethanol	0.60	1.02	1.027	1
Propan-2-ol	1	0.964	1	0.97

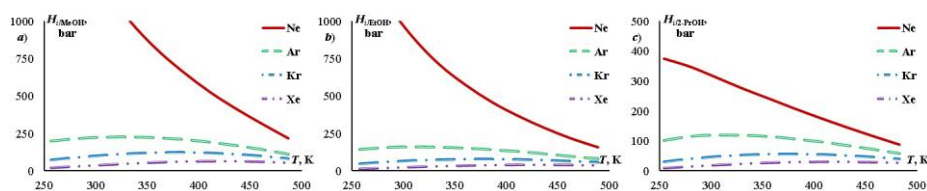


Figure 1. Henry's law constant of noble gases in a) methanol, b) ethanol, and c) propan-2-ol at temperatures between 250 and 480 K from molecular simulation

- [1] Windmann T., Linnemann M., Vrabec J., J. Chem. Eng. Data, 2014, 59(1), 28–38.
- [2] Tegeler C., Span R., Wagner W., J. Phys. Chem. Ref. Data, 1999, 28(3), 779–850.
- [3] Gross J., Sadowski G., Ind. Eng. Chem. Res., 2002, 41(22), 5510–5515.
- [4] Vrabec J., Stoll J., Hasse H., J. Phys. Chem. B., 2001, 105(48), 12126–12133.
- [5] Schnabel T., Srivastava A., Vrabec J., Hasse H., J. Phys. Chem. B, 2007, 111(33), 9871–9878.
- [6] Schnabel T., Vrabec J., Hasse H., Fluid Phase Equilib., 2005, 233(2), 134–143.
- [7] Schnabel T., Vrabec J., Hasse H., J. Mol. Liquids, 2007, 135(1–3), 170–178.
- [8] Glass C. W. et al. Comput. Phys. Commun., 2014, 185(12), 3302 – 3306.



THERMODYNAMIC STUDY OF PURE PERFLUOROORGANIC COMPOUNDS FOR BIOMEDICAL APPLICATIONS

Pashchenko L.L.¹, Druzhinina A.I.¹, Miroshnichenko E. A.²

¹ Department of Chemistry, Lomonosov Moscow State University, Moscow, 119991, Russia

² Semenov Institute of Chemical Physics RAS, Moscow, 119991, Russia

E-mail: lara.paschenko@gmail.com

The perfluoroorganic compounds (PFOC) have high chemical and thermal stabilities, perfect biological passivity and low-power intermolecular interactions (IMI). The last property permits PFOC to dissolve and to transport many quantities of gases (O₂ and CO₂), that is very important for using them as artificial blood substitutes. In this work, the thermodynamic properties were studied for seven PFOC, a namely *cis*- and *trans*- perfluorodecaline (PFD), perfluoro-N-(4-methylcyclohexyl) piperidine (PMCP), perfluorothreebutylamine (BAF-3), perfluorothreepropylamine (PAF-3), perfluorooctylbromide (PF-octylBr) и perfluorodibutyl ether (C₄F₉)₂O.

The standard vaporization enthalpies, $\Delta_{\text{vap}}H$, were determined using Wadso and Calvet calorimeters. The temperature dependences of vapor pressure, p_s , were determined, using Sventoslavsky ebulliometer. The densities, ρ , of their liquids were determined by picnometrically.

The novel method of calculation of oxygen capacity of liquid PFOC, φO_2 , based on the definition of the enthalpies of vaporization, the vapor pressures and densities in dependence on the temperature is proposed. In Table 1 given vaporization enthalpy, $\Delta_{\text{vap}}H^0$, vapor pressure, p_s , calculated oxygen capacity, φO_2 (1) and experimental oxygen capacity, φO_2 (2) for studied perfluoroorganic compounds.

Table 1. Vaporization enthalpies, vapor pressures and oxygen capacities of PFOC

Compound	PFD - <i>cis</i>	PFD - <i>trans</i>	PMCP	BAF-3	PAF-3	PF- octylBr	(C ₄ F ₉) ₂ O
$\Delta_{\text{vap}}H^0$, kJ/mol	45.5±0.5	44.8±0.5	56.6±0.2	58.9±0.8	46.9±0.3	47.7±0.3	39.3±0.4
p_s , Pa, at 37°C	15.6	17.3	0.81	1.71	14.7	13.8	82.2
φO_2 (1), cm ³ /100ml	40.3	41.1	40.0	41.9	47.4	46.6	51.2
φO_2 (2), cm ³ /100ml	40.3 ¹	42 ¹	-	40 ¹	46.5 ¹	-	51 ¹

[1] Beloyarcev, F.F.; et al. Perfluorocarbons in biology and medicine, Pushchino, 1980, 30-44.

The obtained values of oxygen capacity, φO_2 (1), of PFOC are in a good agreement with the experimental literature data, φO_2 (2), from Ref.¹ Among the studied compounds PAF-3 and (C₄F₉)₂O have the highest values of oxygen capacity.

Table 2. Vaporization enthalpies, densities of cohesion energy and molar volume of PFOC

Compound	PFD – <i>cis</i>	PFD - <i>trans</i>	PMCP	BAF-3	PAF-3	PF- octylBr	(C ₄ F ₉) ₂ O
$\Delta_{\text{vap}}H^0$, kJ/mol	45.8±0.1	44.8±0.5	61.8±0.3	60.3±0.1	46.9±0.3	47.7±0.3	40.7±0.1
$C \cdot 10^{-4}$, kJ/m ³	18.0	18.8	19.1	16.2	18.9	17.4	14.3
$V_m \cdot 10^4$, m ³ /mol	2.40	2.25	3.10	3.58	2.35	2.60	2.67

[2] Kabalnov, A.S.; et al. Colloid. J., 1986, 8(1, 2), 27-32, 393-394.

When choosing PFOC as artificial blood substitutes, the determining factors are vapor pressure at human body temperature (37°C) and stability of emulsions. Analysis of the stability of fine emulsions of PFOC in aquatic environment was conducted using data on the intermolecular interactions (IMI). A quantitative measure of the IMI in the liquid can serve as the density of cohesion energy, $C = (\Delta_{\text{vap}}H - RT) / V_m$ (V_m - molar volume, R – universal gas constant). In Table 2 given the values of the molar volumes, V_m , and densities of cohesion energy, C , for studied PFOC calculated on the basis of the experimental data. The obtained values of the density of cohesive energy PFOC are in a good agreement with the experimental literature data on reduction dispersity of their emulsions from Ref.², a namely the stability of PFOC emulsions is proportional to the increase of the density of cohesion energy, C .

REINVESTIGATION OF PD-RH PHASE DIAGRAM WITH THE USE OF METASTABLE PALLADIUM-RHODIUM NANOALLOYS

Rybinskaya A.A.¹, Shubin Yu.V.^{1,2}, Plusnin P.E.^{1,2}, Korenev S.V.^{1,2}

¹Novosibirsk State University, 630090 Novosibirsk, Russia

²Nikolaev Institute of Inorganic Chemistry, Siberian Branch of the Russian Academy of Sciences, 630090 Novosibirsk, Russia
E-mail: arybinskaya@yahoo.com

Pd-Rh nanoalloys are widely used in three-way converters (TWC) to remove harmful components (CO, NO_x and HC) from exhaust gases of gasoline engines. For high-temperature applications the assessment of the stability of the binary system “palladium-rhodium” is required. To provide that, the reinvestigation of Pd-Rh phase diagram should be done. The existing phase diagram of Pd-Rh system was plotted in 1959 [1] and no experimental data is present in literature since that time. The explanation is that investigating the system of metals having high melting temperatures ($T_{m.p.}(Pd)=1555^{\circ}C$, $T_{m.p.}(Rh)=1963^{\circ}C$) is not easy from the experimental point of view. To get reliable data, long annealing times are required, because the equilibrium is achieved very slowly in such systems.

In our work, we use two-side approach to determine the boundaries of solid solubility in that system. The key point of this strategy is that a single-phase sample of a metastable solid solution (**sol**), homogenized at high temperature or prepared in another way, with the composition falling in the two-phase region of the state diagram, and a two-phase mixture of pure components (**mix**) with the same composition should reach the same equilibrium state after sufficiently long annealing (Fig.1). Below the critical point **sol** decomposes in two equilibrium solid solutions, while **mix** affords two phases of solid solutions with characteristics identical to those of the former ones.

To prepare **sol** samples, double complex salts $[Pd(NH_3)_4][Rh(NO_2)_6]_2$ and $[Pd(NH_3)_4][Rh(NH_3)(NO_2)_5]$ were taken. The decomposition of these salts in molecular hydrogen at 300°C gives metastable solid solutions Pd_{0.6}Rh_{0.4} and Pd_{0.5}Rh_{0.5}, respectively. The method used to prepare **sol** samples has several important advantages. First, small particles are formed (according to TEM observations, average particle size is 12-20 nm). Second, the composition of **sol** samples matches with the Pd:Rh ratio in precursor compounds. And third, the composition of the solid solutions got under quick decomposition of the precursor, corresponds to two-phase area of the conventional phase diagram (Fig.1). Thus, these solid solutions may be called “metastable”. Due to small particle size, significantly less time is required for nanoalloys to reach equilibrium than that for bulk samples. Pd-Rh nanoalloy (**sol**) were used to reinvestigate the Pd-Rh phase diagram together with two-phase mixtures of Pd and Rh (**mix**) having the same Pd:Rh ratio as **sol** samples.

Mix and **sol** samples were characterized using XRD method before and after annealing. To determine the composition of the samples annealed, calibration curve was used. The lattice parameter of the solid solution Pd_xRh_{1-x} depends on its composition almost linearly (Vegard’s rule). Thus, with the help of the lattice parameter obtained after annealing, the equilibrium compositions were determined.

All the samples were annealed at 650, 750, 770, 800 and 900°C. The annealing time was 1 month for all temperatures, except of 650°C. This one required longer annealing time (2 months) to reach equilibrium.

For 650°C, the equilibrium composition found in this study was almost the same as that suggested by the conventional phase diagram [1]. For 750°C some differences were revealed: the solid state solubility was higher by 7 at.% in Rh-rich region, and by 5 at.% in Pd-rich region. For 770°C, the difference increased up to 10 at.% for Rh-rich region, and to 6 at.% for Pd-rich region. At 800°C, the solubility of Rh in Pd was found to be higher by 16 at.%, and the solubility of Pd in Rh by 9 at.%, in comparison to the solubility values proposed in [1]. At 900°C, Pd and Rh were proved to be miscible in all compositions.

Using the experimental data obtained, the refined phase diagram of Pd-Rh system was plotted. Critical temperature was shown to be lower by ~25°C than it was generally accepted (approximately 820°C instead of 845°C).

[1] Raub, E., H. Beeskov. Z. Metallk., 1959, 50, 428-431.

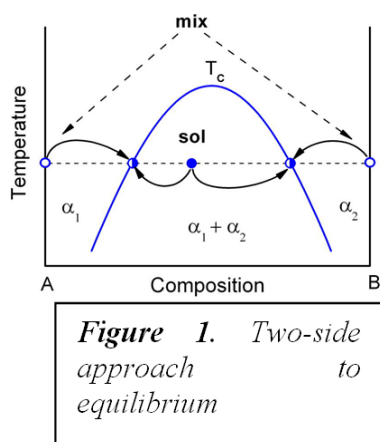


Figure 1. Two-side approach to equilibrium

HEAT CAPACITY OF HARD MAGNETIC MATERIALS BASED ON Sm-Co COMPOUNDS

Samoshkin D.A., Savchenko I.V., Stankus S.V.

Kutateladze Institute of Thermophysics, Siberian Branch of the Russian Academy of Sciences, 630090 Novosibirsk, Russia

E-mail: d.a.samoshkin@gmail.com

At the present time alloys based on rare-earth metals (REM), including REM alloys with 3d-transition metals, are one of the most interesting and promising classes of magnetic materials. Permanent magnets are an important sector of application of such alloys. The permanent magnets based on Sm-Co and Nd-Fe-B composites have the highest characteristics, such as coercive force, residual magnetic induction and maximum magnetic product. Researchers take a great interest in magnetothermal, magnetocrystalline and magnetoelastic effects discovered in the previous century in magnetic materials. However, it was noticed that there are almost absent reliable data on the caloric properties of magnetic materials, in particular on the specific heat capacity. In this connection the aim of the present work was to measure the specific heat capacity of some technically important compounds of Sm-Co system in a wide temperature range of a solid state, including the region of the magnetic phase transition, as well as to clarify the question about the influence of the residual magnetization on the heat capacity.

The specific heat coefficient was investigated by the method of the differential scanning calorimetry (DSC) using the automated experimental setup DSC 404 F1 produced by the German company NETZSCH. Measurements were carried out in the low temperature (190–375 K) and the high temperature (318–1271 K) ranges with a heating rate of 2 K/min and 10 K/min respectively in flowing argon atmosphere (20 ml/min). The experiments were performed on samples of brands YX18, YX24 and YXG22, YXG30, this is hard magnetic materials containing as a main component the crystalline phases of SmCo_5 and $\text{Sm}_2\text{Co}_{17}$ type. The specimens were the shape of cylinders 5 mm diameter and 1.5 mm thickness.

The measurement results of the heat capacity of the sample of brand YXG22 in magnetized and demagnetized states are presented in Fig. 1. As may be seen from this graph, curve of the first heating in a temperature range of 650–900 K lies 3–3.5% below than the next two heating curves. Apparently, this is caused by the demagnetization process of the sample occurring in the first heating. Wherein the sample is completely demagnetized by heating above the region of the magnetic phase transition, which is shown in the figure as a sharp maximum. Two subsequent heatings were performed for already demagnetized sample, and these heatings reproduced among themselves within the measurement error, which is estimated to be 3% for this installation. A similar situation was observed on the temperature dependence of the heat capacity for the samples of brands YX18, YX24 and YXG30.

The study was supported by the Russian Foundation for Basic Research (Project No. 15-38-20223).

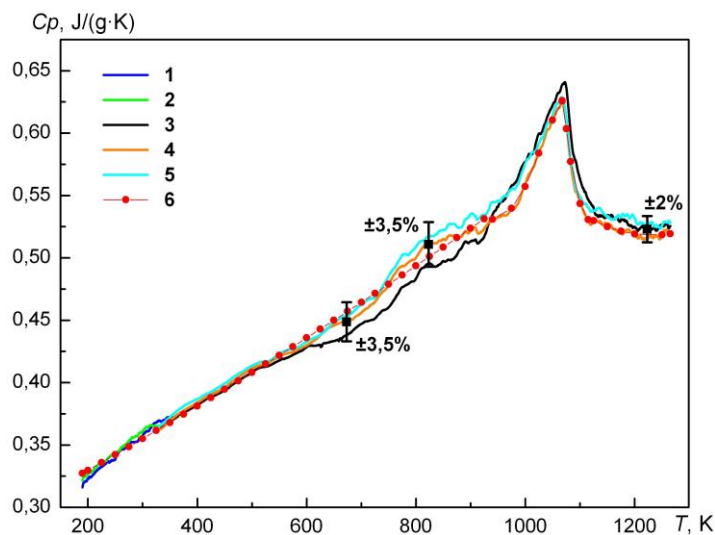


Figure 1. Heat capacity of YXG22. Temperature range 190–375 K: 1 – 1-st heating, 2 – 2-nd heating; temperature range 318–1271 K: 3 – 1-st heating, 4 – 2-nd heating, 5 – 3-rd heating; 6 – recommended data.



THERMODYNAMIC FUNCTIONS OF SOLVATION AND THE CAVITY FORMATION CONTRIBUTION

Sedov I.A.¹, Magsumov T.I.¹, Solomonov B.N.¹

¹Chemical Institute, Kazan Federal University, 420008 Kazan, Russia

E-mail: igor_sedov@inbox.ru

The concept of formation of a cavity in the solvent is commonly used in continuum solvation models, as well as in empirical equations for calculation of solvation properties. The values of the Gibbs free energy and other thermodynamic functions of the cavity formation process cannot be determined experimentally. At the same time, different theoretical approaches to calculate them may lead to significantly different results. The expression for the energy of cavity formation derived from simplistic scaled particle theory is used most frequently. More versatile and sophisticated approaches to calculation of these quantities are using computer simulations techniques.

Evaluation and comparison of the energies of cavity formation for a variety of solvents is of considerable interest. Besides the use in continuum solvation models, these values can serve as a measure of cohesive energy of solvents, and as solvent parameters in correlations describing the solvent effects on various processes and properties. The cavity-formation term is responsible for low solubility of apolar species and existence of the solvophobic effects in protic solvents. Of all solvents, only in water the thermodynamic functions of cavity formation have been extensively studied, including their dependence on the cavity size and shape, temperature, and method of calculation, while for most of the organic solvents no data have yet been obtained.

We calculated the Gibbs free energies of formation of the spherical cavities with a range of radii in various solvents containing different functional groups using Widom test particle insertion method. Nanoseconds-long molecular dynamics simulation trajectories of solvent boxes requires for calculations were obtained using OPLS-UA force field. In some cases, we also examined other force fields. Particular attention is paid to protic solvents forming intermolecular hydrogen bonds. Results are compared with literature data for some solvents [1], as well as with the scaled particle theory predictions, and assessments of the cavity formation energies basing on the values of surface tension and isothermal compressibility of solvents. Furthermore, a comparison with the empirical parameters reflecting the cost of cavity formation on the basis of solvation thermodynamics data [2] is made. It is shown that the Gibbs free energy of cavity formation grows up with increasing concentration of the hydrogen bonds in the solvent and shows no correlation with the total number of heavy atoms in a unit volume of the solvent. The key role of cavity-formation contribution in reduction of solubility of apolar compounds in self-associated solvents is demonstrated.

[1] Hofinger, S; Zerbetto, F. J. Phys. Chem. A, 2003, 107, 11253-11257.

[2] Sedov, I.; Stolov, M.; Solomonov, B. Fluid Phase Equilib., 2014, 382, 164-168.

FORM EFFECT IN PHASE TRANSITIONS IN A SMALL VOLUME Bi-Sb SYSTEM

Fedoseev V.B.^{1,2}, Shishulin A.V.¹

¹Lobachevsky Nizhny Novgorod State University, Nizhny Novgorod, Russia

²Razuvaev Institute of Organometallic Chemistry, Russian Academy of Sciences, Nizhny Novgorod, Russia

E-mail: Chichouline_Alex@live.ru

In the previous works [1,2] it is shown, that phase diagrams of small volume systems depend on their sizes and mutual position of existing phases. It is so because of the contribution of the surface that becomes comparable with the system's full energy. But when the system's volume is fixed, different geometrical shapes of nanoparticles have different surfaces of external boundaries and different surface energies. So modeling of phase equilibria dependence on the shape of the system's boundaries is an interesting problem. In this study we consider the diversity of phase diagrams, which appear as the system's external boundary's shape changes using the methods of equilibria chemical thermodynamics in a stratifying Bi-Sb system. Minima of system's Gibbs functions including the energy of all system's boundaries were taken for the equilibrium state criteria. Phase diagrams, demonstrating influence of the external boundary's shape on the composition, volume ratio of grown phases and the upper critical point of stratification, have been calculated. The shape's change has been considered by the form coefficient k_f which is equal to the ratio between the system's external boundary surface and the surface of the sphere containing the same amount of material. The geometrical configuration of the system is *core-shell*, where the core phase is spherical and doesn't touch the system's external boundary. The shape of the shell-phase's surface is set by the coefficient k_f . Change of the system's form accompanied by the increase of k_f leads to a shift or a deformation of the heterogeneity region with a decrease in the upper critical temperature of stratification (for example, see fig.) The increase of k_f leads also to a growth of the area, where the heterogeneous state is metastable.

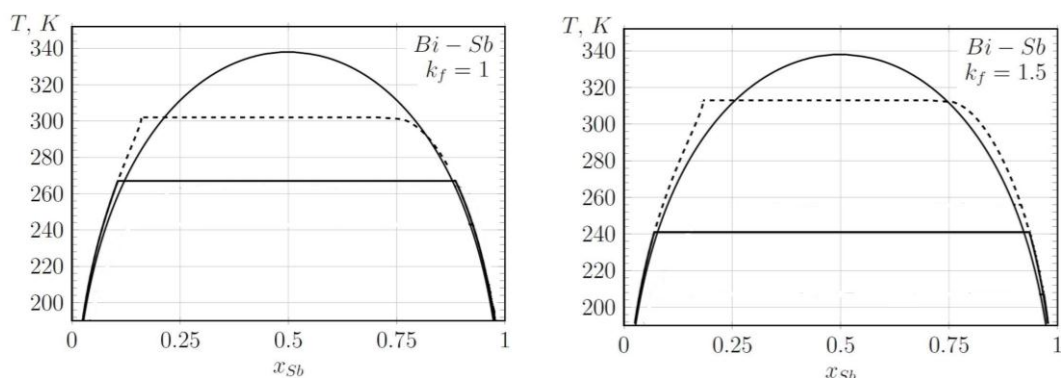


Figure 1. Phase diagrams for Bi-Sb nanoparticles as a function of their form (left image is for a spherical system ($k_f=1$), right image – for non-spherical system ($k_f=1.5$)). The couple on both pictures corresponds to the diagram for a macroscopic system. Phase diagrams for nano-systems are drawn with the solid line. The dashes outline the area, where the heterogeneous state is metastable.

These obtained results could be used in simulation of phase transitions in ultrafine-grained systems and in design of new perspective materials, for increase or decrease of alloy components' mutual solubility considerably affect the system's mechanical and physical properties.

This study was partially supported by the Russian Science Foundation (pr. 15-13-00137).

[1] Fedoseev V.B. Shishulin A.V., Titaeva E.K., Fedoseeva E.N. Phys. Solid State, 2016, 58(10), 2095–2100.

[2] Fedoseev V.B. Phys. Solid State. 2015, 57(3), 599-604.



PHASE DIAGRAM OF Co-Cu-Ni SYSTEM

Sinyova S., Starykh R., Ilatovskaya M.

Peter the Great St. Petersburg Polytechnic University

E-mail: svetlana.sinyova@gmail.com

Phase diagram of ternary Co-Cu-Ni system is very relevant for metallurgists and materials scientists. In particular, Cu-Co-Ni alloys have been proposed as the promising candidate for synthesizing magnetically heterogeneous microstructure comprising hard and soft magnetic phases, which remain distributed within the non-magnetic Cu matrix. Phase equilibria of discussed system are studied not enough, and literature data about high-temperature transformations, namely, liquidus and solidus surface projections are dated by 1914 [1] and 1938 [2] years. For this reason it was decided to study phase equilibria in Co-Cu-Ni system in detail.

The main method of research was high-temperature DSC, as this method allows us to construct the liquidus and solidus surface projection in a full range of system compositions. To perform the experiments STA analyzer Setsys evo 1750 was used, manufactured by SETARAM Instrumentation Company. The complementary methods were Scanning Electron Microscopy and Electron Probe Microanalysis (SEM/EPMA). Combination of these analytical methods enables to get the full picture of phase transformations within investigated system.

Experimental samples were prepared in the induction furnace with the use of high grade purity metals. Metals in desired ratio were vacuumised and sealed into silica tubes, then heated over the preliminary liquidus temperatures, held in a liquid state for a long time for homogenization and quenched into water. The obtained samples were investigated by DSC and SEM/EPMA methods. The total number of experimental samples was near 50.

The liquidus and solidus surface projections are the results of research. Due to peritectic reaction in boundary Co-Cu system the discussed system is characterized by miscibility gap in a solid state. The composition and temperature area of this gap as well as position of key point have been determined. Also liquidus and solidus lines have been constructed in the whole composition area of Co-Cu-Ni system.

This system is the last among ternary metallic systems that were investigated by our scientific team [3, 4]. The next step of research is study of phase equilibria and construction of the phase diagram of quaternary Co-Cu-Fe-Ni system.

Acknowledgments

This work is supported by RFBR grant № 16-38-00305\16

References

1. M. Waehlert. Studies on Copper-Nickel-Cobalt Alloys. *Osterr. Z. Berg. u. Huttenwesen*. 1914; 62: 357-361, 374-378.
2. Dannoehl, W.; Neumann, H.Ueber. On the Co-Cu-Ni Permanent Magnet Alloys. *Z. Metallkd.* 1938; 30: 217-231.
3. Sineva, S.I., Starykh, R.V., etc. The study of liquidus and solidus surfaces of the four-component system Fe-Ni-Cu-S. Part 1. Graphing of meltability in the three-component system Fe-Ni-Cu. *Rus. met. (Metally)*. 2009;. № 5: 447-453 (DOI: 10.1134/S0036029509030136)
4. Ilatovskaya M.O., Starykh R.V., Sinyova S.I. Liquidus and Solidus Surfaces in the Quaternary Fe-Cu-Co-S System. Part II: The Ternary Fe-Cu-Co System. *Met.and Mat. Trans. B.* 2015; 46B: 243-249, (<http://link.springer.com/article/10.1007/s11663-014-0202-0>)



PHASE DIAGRAM OF ETHYLENE GLYCOL - HEXAMETHYLPHOSPHORAMIDE

Solonina I.A.¹, Rodnikova M.N.¹, Kiselev M.R.², Khoroshilov A.V.¹, Sirotkin D.A.¹

¹ Institute of General and Inorganic Chemistry N.S.Kurnakova RAS, Moscow, Russia

² Institute of Physical Chemistry and Electrochemistry A.N. Frumkin RAS, Moscow, Russia

E-mail: rodnikova@igic.ras.ru

There was investigated the phase diagram of ethylene glycol system (EG) - hexamethylphosphoramide (HMPT) throughout all range of concentrations in a temperature range of +25°C – -90°C – +25°C and -150°C – +25°C by the method of DSC on installations INTERTECH DSC Q100 and METTER DSC 30 of different cooling rate / heating and rapid cooling, but slow heating.

Two exothermic peaks of crystallization were registered upon slow cooling / heating: T_{1cr.} = -58°C at cooling and T_{2cr.} = -70°C at heating. The double endothermic peak at T_{1m.} = -14°C and T_{2m.} = -9.5°C corresponds to melting system. Enthalpy change of registered processes was calculated. At low temperatures for all concentrations of the system there was remarked the falling of baseline indicating a vitrification / devitrification at T_g = -74°C. At a temperature of + 22°C there was also found the drop of baseline.

In the average concentrations of HMPT (18 mol% – 58 mol%) in the temperature range of + 25°C – -90°C thermal effects were not found out.

At rapid cooling and slow heating there were registered two endothermic melting peaks, the absence of secondary thermal effects at average concentrations, the fall of baseline at low temperatures. This is a picture of the phase diagram is the same as at the slow cooling, but at different temperatures and concentrations. Enthalpy change was calculated for registered thermal effects.

Strong hypothermia and vitrification of system were explained by stability of spatial net of the hydrogen bond in the EG and the specificity of interaction of EG with HMPT. The absence of thermal effects in the average concentrations was associated with high viscosity of the studied system due to the formation of compounds HMPT:2EG and HMPT:EG.

The resulting phase diagram was compared with the phase diagram of the system H₂O - HMPT, in which the compounds HMPA·3H₂O and clathrate HMPT·20H₂O [1] were found out. The difference was explained by the different intermolecular interactions in comparable systems and various structural characteristics of EG and H₂O.

[1] Abakumov, NA "Interparticle interaction in binary systems, solvent (H₂O) - solute (aprotic and proton dipolar organic substance)," - M. dissertation of PhD of chemistry 1982

This work was performed as part of a State Task of the Russian Academy of Sciences' Institute of General and Inorganic Chemistry in the field of basic research. It was supported by the Russian Foundation for Basic Research, project № 16-03-00897.

MAGNETIC AND STRUCTURAL PROPERTIES OF TERNARY ALLOYS IN THE CU-NI-FE, CU-CO-NI AND FE-CO-CU SYSTEMS

Starykh R.¹, Sinyova S.¹, Ilatovskaya M.¹, Tolochko O.¹, Menyshenkov V.²

¹Peter the Great St. Petersburg Polytechnic University

²Moscow Institute of Steel and Alloys

e-mail: Kafedra-cm@yandex.ru

It is well known, that combination of magnetic matrix phase and non-magnetic interstitial phase can lead to unique magnetic properties of alloys. One of such systems is Fe-Ni-Co-Cu, which is characterised by wide compositional and temperature ranges of miscibility gap. This work is devoted to study of phase diagram of the quaternary Fe-Ni-Co-Cu system and search of alloys with outstanding magnetic properties, based on the compositions of the discussed system. The research is began with determination of areas with miscibility gaps in solid state in the boundary Fe-Co-Cu, Cu-Ni-Fe и Ni-Co-Cu systems, as well as identification of their structural and magnetic properties.

Alloys were prepared in laboratory conditions with using of melting in induction furnace of proper amounts of high grade metals in preset ratio. Synthesized samples were investigated by thermal analysis, X-ray analysis, SEM/EDX analysis and oscillatory magnetometry.

It is evident, that alloys structure is closely connected with topology of phase diagrams. This fact allows managing of obtained alloys structure using proper thermal treatment. Investigation of magnetic properties also confirmed the relationship between structure and properties.

Results of research are areas of miscibility gap in solid state of the ternary Fe-Co-Cu, Cu-Ni-Fe и Ni-Co-Cu systems as well as magnetic properties – compositions relationships.

During the research compositional areas are defined, characterised by outstanding values of coercitive force and residual magnetic induction at 700°C.

As the examples of research, miscibility gaps for the Ni-Co-Cu (figure 1) and Fe-Co-Cu (figure 2) systems at room temperature are shown.

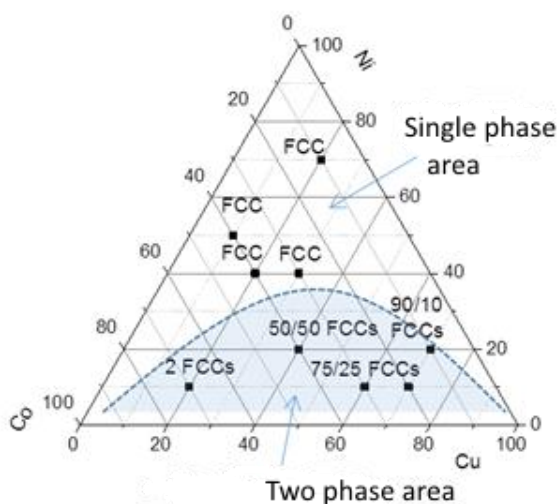


Figure 1 Miscibility gap in solid state in the Co-Cu-Ni system

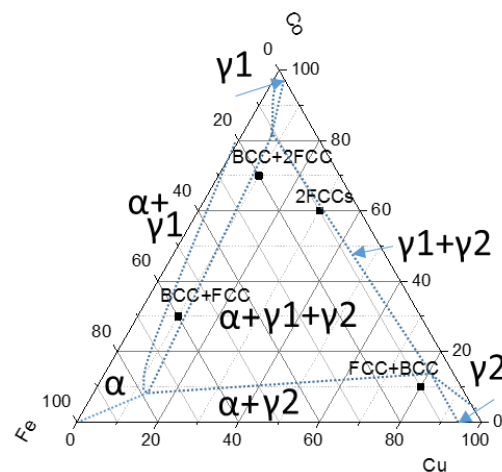


Figure 2 Miscibility gap in solid state in the Co-Cu-Fe system

Acknowledgments

This work is supported by RFBR grant № 16-03-00987\17



DIMERIZATION IN HARD-SPHERE FLUIDS: EXCLUDED VOLUME EFFECTS

Tkachev N.K.

Institute of High-Temperature Electrochemistry, Ural Branch of the Russian Academy of Sciences, 620137 Ekaterinburg, Russia
E-mail: N.Tkachev@ihte.uran.ru

Evaluating the chemical equilibrium in a non-ideal system is one of the most difficult issues in physical chemistry since the activities of the reaction participants depend on inter-molecular forces between reactant species [1]. A problem relating to dimerization can be considered to be the simplest of theoretical topics where some model pair potential of the reactant pair interactions is taken into account. However, even the consequences of the simplest hard-sphere model are still not well understood as an application of statistical thermodynamic theory to chemical reactions [2].

In this report we shall review our recent results on an attempt to apply the semi-phenomenological statistical-thermodynamic approach to dimerization in a hard sphere classical fluid. In this approach the molecular constants are assumed to be known and all pair interactions of species in the reacting mixture are included in the mean activity coefficient. The equilibrium constant remains the same as in the ideal case and the task is reduced to determining the activity coefficients which is one of the advantages of the theory. We show the physical reasons for the mass action law (MAL) deviations from ideality become much clearer when the proposed approach is used. Actually, it is necessary to determine the free energy minimum both by the number of dimers and by volume (or density) in order to obtain the mass action law and the equation of state (EOS). Moreover, the system of these two equations leads to the self-consistent determination of dimer mole fraction and density at a constant pressure and temperature. First, we implemented such an approach for the simplest case of hard-sphere dimerization in a pure fluid within the spherical shape of the dimer [1]. Some consequences for taking into account the dumbbell form in this case were considered in. In general, it was found that the form-factor allows to determined more accurately the calculation of the dimer concentration in the range of low temperatures and high pressures [2]. The model was generalized on the mixture of two different self-associating fluids and the thermodynamic description of the other dimer concentration as well as packing fraction and entropy was analyzed [3].

Another interesting topic is the dimerization in an inert solvent was investigated in [4, 5]. It was shown that an increase in the inert solvent diameter causes a dimerization equilibrium shift towards the right whenever the effect of volume shrinkage takes place due to the elementary dimerization act at low values of the dimer length (overlapping of hard spheres at the dimer formation). Density in the dimerizing fluid also decreases when the solvent size is increased and it gives the advantage of creating a spherical cavity for the dimer to appear in. However, an increase in the solvent size leads to approaching to ideality due to the density decrease. It was determined that the change of the thermal effect type from pure endothermic to alternating with the exothermic effect at moderate and high concentrations depends on the ratio of the dimerizing and the solvent species diameters.

New results on taking into consideration the form-factor of the dumbbell in case of hetero-nuclear dimerization and the evaluation of thermodynamic equilibrium as the ratio of bonded spheres of different diameters in the dimer increases will be presented as well.

This work was supported by the Russian Foundation for Basic Research (15-03-01588) and UB RAS (15-20-3-12).

- [1] Prigogine I.R., Defey R. Chemical thermodynamics. Novosibirsk, Nauka, 1966, 509 p.
- [2] Fisher M.E., Zuckerman D.M. J. Chem. Phys. 1998, **109**, 7961-7981.
- [3] Tkachev N. K., Zinatullina A. R. Rus. J. Phys. Chem. A, 2013, **87**, 1457-1462.
- [4] Tkachev N.K. Rasplavy (in Russian), 2014, 87-92.
- [5] Davydov A.G., Tkachev N.K. Rasplavy (in Russian), 2015, **5**, 22-38.
- [6] Peshkina K.G., Tkachev N.K. J.Mol.Liq., 2016, **216**, 856-861.
- [7] Peshkina K.G., Tka chev N.K. High Temperature, 2016, **54**, 300-302.



EXCESS ENTHALPIES OF TERNARY SYSTEMS CONTAINING N-PROPANOL, ACETIC ACID, N-PROPYL ACETATE AND WATER

Tsvetov N. S., Letyanina I.A., Toikka A.M.

Institute of Chemistry, St. Petersburg State University Universitetskij prospect, 26, Peterhof, 198504, Saint Petersburg, Russia
E-mail: nikita.tsvetov@spbu.ru

The study of thermodynamic properties of multicomponent liquid phase systems is an actual basic and applied problem. In contrast to binary, usually less attention is paid to multicomponent systems, and experimental data relating to them are very limited since the experiment's workflow is much more time- and effort-consuming.

Excess enthalpy of binary and multicomponent systems is key type of thermodynamic data characterizing the system. Excess enthalpy data allow to calculate many other characteristics of the systems, including prediction of liquid-vapor and liquid-liquid equilibria.

The objects of this study are three ternary systems formed by the substances which are the participants of n-propyl acetate synthesis (and hydrolysis) reaction: {n-propanol + acetic acid + water}, {n-propanol + acetic acid + n-propyl acetate} and {n-propanol + n-propyl acetate + water}. The latter system is distinguished by the existence of the miscibility gap due to the simultaneous presence of water and ether. The purpose of this work is the study of the excess enthalpies of mentioned ternary systems at $T = 313.15$ K.

The measurements of the heat of mixing (excess enthalpies) were carried out with the C80 calorimeter with membrane mixing cells manufactured by Setaram Instrumentation (France), equipped with a reversing mechanism, which ensures thorough mixing of the mixtures without making additional contributions of heat, using membrane mixing cells. The apparatus and procedure were tested by measuring of excess enthalpies for the standard system (hexane + cyclohexane), and the results were found to differ by less than 3 %. Heat of mixing is determined by adding to the preformed binary mixture a third component. Primary binary solutions were prepared by weighing so that the resulting ratios of mole fractions in the ternary system correspond to the values 1:3, 1:1 и 3:1.

The experimental data were fitted using the NRTL model equation. The comparison of results of calculations based on the set of parameters obtained from the data for the binary system only and on the set of parameters derived using both binary and ternary data was performed. As a result we propose a new set of NRTL parameters for system considered.

The experimental results will allow expanding the base of thermodynamic data for multicomponent systems and perform thermodynamic calculations based directly on experimental data, and new parameters of NRTL model.

Acknowledgements The investigations were carried out using the equipment of the Thermogravimetric and Calorimetric Research Center of SPbSU. The work was financially supported the Russian Foundation for Basic Research (Project No. 15-03-02131 and 17-03-01064).

SYMMETRY IN ENERGETICS AND ARCHITECTURE OF THE LIQUID PHASE

 Verevkin S.P.¹, Zaitsau Dz.H.¹
¹Institute of Chemistry, University of Rostock, 18059 Rostock, Germany

E-mail: sergey.verevkin@uni-rostock.de

Ionic liquids (IL) as neoteric solvents exhibit unique properties which make them suitable for replacement of common media for diverse chemical reactions as well as for materials production. Application of ILs instead of common solvents have been demonstrated to be especially effective for the synthesis of nanoparticles. A possibility of distilling a number of pure aprotic and protic ILs could be useful for separation of nanoparticles from IL-solvent. In this context, an understanding of volatility, thermal stability and vaporization thermodynamics at the molecular level, leading to reliable prediction of ILs thermochemical properties, seem to be both of practical and theoretical interest. We developed two highly sensitive methods for mass loss determination at temperatures starting from 350 K up to 800 K. The first technique is based on using a quartz crystal microbalance vacuum setup. Due to the very high sensitivity of the quartz crystal microbalance (QCM) it has become possible to measure vaporization rates at temperatures starting from 350 K [1]. The second technique is based on a fast scanning calorimetry (FSC) with scanning rates up to 1000000 K s⁻¹ in combination with an alternating current (AC) calorimeter equipped with a chip sensor, that consists of a free-standing SiNx-membrane (thickness < 1 μm) and a measuring area with lateral dimensions of the order of 1 mm. A small droplet (diameter ca. 300 μm) of an ionic liquid is vaporized isothermally from the chip sensor in a vacuum-chamber [2]. The vapor pressure in both methods is determined from the measured mass loss rates using the Langmuir equation. Both methods were successfully tested with determination of vapor pressures and the vaporization enthalpy of the archetypical ionic liquid [C₂mim][NTf₂]).

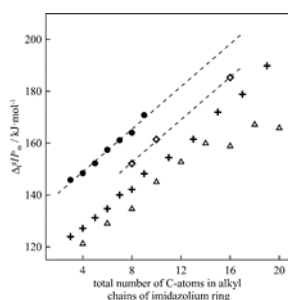


Figure 1. Dependence of the enthalpy of vaporization, $\Delta_1^g H_m^\circ$ (298 K) for imidazolium based on the total number of C-atoms in the cation alkyl chains: \diamond - [C_nC_nim][Br]; \bullet - [C_nmim][Br]; +, [C_nmim][NTf₂]; Δ - [C_nC_nim][NTf₂]

The thermodynamics of vaporization of alkyimidazolium ionic liquids containing [Br] and [NTf₂] anions was in the focus of the current study. The structure-property relationships and standard molar vaporization enthalpies $\Delta_1^g H_m^\circ$ (298 K) chain length dependence of ILs with the [Br]- and [NTf₂] anions combined with the asymmetric 1-alkyl-3-methyl-imidazolium cation [C_nmim]⁺ were compared with ILs containing the symmetric 1,3-alkylated imidazolium cation [C_nC_nIm]⁺ having the same anions. Both IL families with the asymmetric [C_nmim][Anion] and symmetric [C_nC_nim][Anion] cation have the linear trend in the $\Delta_1^g H_m^\circ$ (298 K) - alkyl-chain length (n) dependence but the trends are significantly shifted (see Figure 1) within each family. This difference could be an evidence for unusual interplay between van der Waals and Coulomb interactions in the asymmetric and symmetric ILs.

Acknowledgement: this work has been partly supported by the Government of Russian Federation (decree №220 of 9 April 2009), agreement №14.Z50.31.0038.

[1] Verevkin, S.P; Zaitsau, D.H; Emel'yanenko, V.N; Heintz, A. J. Phys. Chem. B, 2011, 115, 12889-12895.

[2] Ahrenberg, M; Brinckmann, M; Schmelzer, J.W.P; Beck, M; Schmidt, C; Keßler, O; Kragl, U; Verevkin, S.P; Schick, C. Phys. Chem. Chem. Phys. 2014, 16, 2971-2980.



THERMODYNAMIC PROPERTIES OF THE Gd_2O_3 - Y_2O_3 - HfO_2 SYSTEM AT THE TEMPERATURE 2500 K

Vorozhtcov V.A.¹, Stolyarova V.L.¹, Lopatin S.I.¹, Karachevtsev F.N.²

¹*Institute of Chemistry Saint Petersburg State University, 199034 Saint Petersburg, Russia*

²*All-Russian Research Institute of Aviation Materials, 105005 Moscow, Russia*

E-mail: st011089@student.spbu.ru

Materials based on the Gd_2O_3 - Y_2O_3 - HfO_2 system are promising for a great number of practical applications, such as enhancement of casting procedures for the gas turbine engine blades through development of new casting molds and cores, production of modern thermal barrier coatings with low thermal conductivity as well as in various fields of nuclear technology. However, these materials are synthesized or used at high temperatures at which selective vaporization of the components of the system under consideration may occur. For this reason, it is important to study vaporization processes and thermodynamic properties of the Gd_2O_3 - Y_2O_3 - HfO_2 system at high temperatures.

Twenty samples in the Gd_2O_3 - Y_2O_3 - HfO_2 system were synthesized for the present study. Chemical compositions of the samples were confirmed by X-ray fluorescence analysis. Vaporization processes and thermodynamic properties of the Gd_2O_3 - Y_2O_3 - HfO_2 system were for the first time examined over a wide concentration range by the high-temperature Knudsen effusion mass spectrometric method using a MS-1301 mass spectrometer and a tungsten twin effusion cell.

It was found that at the temperature 2500 K the main vapor species over the samples in the Gd_2O_3 - Y_2O_3 - HfO_2 system were GdO, YO and O, which corresponded to the main vapor species over pure Gd_2O_3 and Y_2O_3 . The partial pressures of the vapor species mentioned and vaporization rates of the samples in the system under study were obtained at the temperature 2500 K. These data may be used to find the samples with the lowest volatility of components to choose the most appropriate compositions for the high-temperature materials. The lowest vaporization rates were observed for the samples containing more than 50 mol. % HfO_2 as well as for the samples in which the Y_2O_3 mole fraction was at least two times higher than the Gd_2O_3 mole fraction.

The Gd_2O_3 and Y_2O_3 activities in the samples in the Gd_2O_3 - Y_2O_3 - HfO_2 system found from experimental data were used to determine the HfO_2 activities by the Gibbs-Duhem equation, the Gibbs energies of mixing and the excess Gibbs energies in the samples at 2500 K. It was shown that negative deviations from the ideal behavior took place in the Gd_2O_3 - Y_2O_3 - HfO_2 system at the temperature mentioned. Thermodynamic properties of the binary Gd_2O_3 - Y_2O_3 system were also obtained by the high-temperature mass-spectrometric method at the temperature 2630 K. The excess Gibbs energy values in the Gd_2O_3 - Y_2O_3 system illustrated negative deviations from the ideal behavior. It was found that concentration dependence of the excess Gibbs energies and Gibbs energies of mixing in this system at 2630 K may be described in terms of sub-regular solution model.

The excess Gibbs energies of the Gd_2O_3 - Y_2O_3 - HfO_2 system were calculated using approaches for determination of thermodynamic properties of ternary systems based on the data for the corresponding binary systems, such as the Kohler method, the Colinet method and the Toop method. It was shown that these semi-empirical methods are invalid for calculation of the excess Gibbs energies of the Gd_2O_3 - Y_2O_3 - HfO_2 system. The reason for this may be strong three-component interactions in the Gd_2O_3 - Y_2O_3 - HfO_2 system that are disregarded in the semi-empirical methods used. The excess Gibbs energies of the system under study may be calculated on the basis of the data for the corresponding binary systems if use is made of the Redlich-Kister equation containing a term responsible for three-component interactions in the system.

The samples in the Gd_2O_3 - Y_2O_3 - HfO_2 system were also studied by the X-ray phase analysis in a wide temperature range 298-2300 K. The main crystalline phases that were formed in the samples during storage at the temperature 2300 K were identified. The conditions for ceramic synthesis of the samples under study were recommended.

This study has been supported by the Russian Fund for Basic Research through the Project No. 16-03-00940.



NEW RELATIONSHIPS BETWEEN FUSION, SOLUTION AND SUBLIMATION ENTHALPIES OF SELF-ASSOCIATED AROMATIC COMPOUNDS

Yagofarov M. I., Nagrimanov R. N., Solomonov B. N.

Alexander Butlerov Institute of Chemistry, Kazan federal university, 420111, Kazan, Russia

E-mail: michaelyago@mail.ru

In the present work the method of determination of the sublimation enthalpies of aromatic compounds at 298.15 K from the data on their fusion enthalpies at the melting temperature, as well as on solvation enthalpies in benzene was developed. Solvation enthalpy is calculated from the additive scheme. The standard molar sublimation enthalpy of compound $(X_i)_n\text{Ar}(Y_j)_m$ with the substituents Y_j capable of self-association in the condensed phase due to hydrogen bonding due presence of both proton donor and proton acceptor (COOH, CONH₂, OH, NH₂ etc.) and the substituents X_i which do not cause self-association (Alk, Hal, NO₂, COOCH₃, CHO, COCH₃, etc.) may be expressed as follows:

$$\Delta_{\text{sub}}^{\circ} H^{(X_i)_n\text{Ar}(Y_j)_m} (298.15 \text{ K}) = \Delta_{\text{fus}}^{\circ} H^{(X_i)_n\text{Ar}(Y_j)_m} (T_{\text{fus}}) + m \cdot \Delta_{\text{vap}}^{\circ} H^{Y \rightarrow \text{H}} (298.15 \text{ K}) - \Delta_{\text{solv}}^{\circ} H^{\text{ArH}/\text{C}_6\text{H}_6} (298.15 \text{ K}) - n \cdot \Delta_{\text{solv}}^{\circ} H^{X_i \rightarrow \text{H}/\text{C}_6\text{H}_6} (298.15 \text{ K})$$

The method was examined by calculation of the sublimation enthalpies of more than 100 aromatic compounds (benzoic acids derivatives, phenols, aromatic amides, aromatic amines) and comparison with the literature data. The deviation from the results obtained from conventional methods is within an experimental error of measurement of sublimation enthalpy.

During derivation of the above equation, the relationship between fusion enthalpy at the melting temperature $\Delta_{\text{fus}}^{\circ} H(T_{\text{fus}})$ and solution enthalpy at 298.15 K $\Delta_{\text{solv}}^{\circ} H(298.15 \text{ K})$ was investigated. It was shown that the difference between the solution enthalpies of substituted phenols and their fusion enthalpies at the melting temperature is the invariant value of $7.6 \pm 1.2 \text{ kJ}\cdot\text{mol}^{-1}$ and matches with the solution enthalpies of the liquid substituted phenols at 298.15 K.

The good accuracy of the relationship between sublimation enthalpies of a wide range of aromatic compounds at 298.15 K and fusion enthalpies at the melting temperature, as well as between solution and fusion enthalpies leads to a conclusion that $\Delta_{\text{fus}}^{\circ} H(T_{\text{fus}})$ and $\Delta_{\text{fus}}^{\circ} H(298.15 \text{ K})$ values are indistinguishable within the experimental error of sublimation and fusion enthalpies determination.

Proposed relationships allow not only determining the sublimation enthalpies from the fusion enthalpies, but also give opportunity for mutual validation of the sublimation, fusion and solution enthalpies values.

[1] Yagofarov, M.I.; Nagrimanov, R.N.; Solomonov, B.N. *Thermochim. Acta*, 2016, 646, 26–31.

[2] Yagofarov, M.I.; Nagrimanov, R.N.; Solomonov, B.N. *J. Chem. Thermodyn.*, 2017, 105, 50–57.

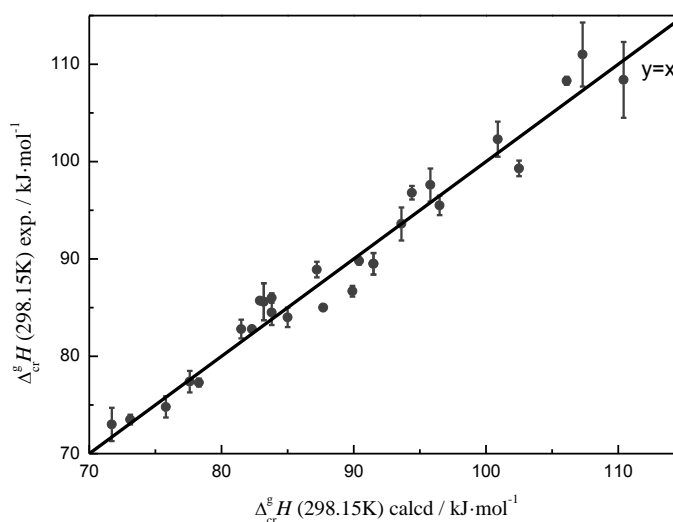


Figure 1. Comparison graph between sublimation enthalpies of substituted phenols obtained by conventional methods and calculated according to the approach proposed in this work.



Section 3.

Thermodynamics of solutions and heterogeneous systems

Poster presentations

**FEATURES OF MOLECULAR LIGHT SCATTERING AND STRUCTURE OF THE CHLOROBENZENE–*O*-DICHLOROBENZENE SOLUTIONS**

Abramovich A.I., Kargin I.D., Lanshina L.V.

Department of Chemistry, M.V. Lomonosov Moscow State University, Moscow, Russia

E-mail: a-abramovich@yandex.ru

Liquids are complex objects of study due to the lack of translational invariance and the presence of cooperative movement of a large number of particles. X-ray diffraction and neutron diffraction are utilized to study the structure of the liquids, but the data obtained with these methods is rather modest. Therefore, the methods of computer simulation and the study of various physic-chemical properties that give only indirect information about the liquid phase structure are resorted increasingly. One of the most informative methods, which is currently being applied to study liquids structure, is molecular light scattering (MLS). The classical theory of MLS allows to observe the changes in radial and orientation correlations of molecules in the local structure of liquid and to find out the nature of molecular interactions through the analysis of the concentration and temperature dependences of the MLS parameters.

The present work is a follow-up on our recent study of structure of binary solutions containing chlorine component [1-3]. Here we report a study of chlorobenzene(Chb)–*o*-dichlorobenzene(*o*-Dchb) solutions. Notably, chlorine-aggregation is an important feature of organochlorines substances. It is caused by the interaction between the chlorine atoms of several molecules by unshared pairs *np*- and free *nd*-orbitals. The universal molecular interactions (orientation, induction and dispersion) between identical or different molecules were calculated. All types of universal interactions and specific molecular interactions (chlorine–chlorine contacts and contacts of the benzene rings) in *o*-Dchb are greater than in Chb, therefore the Chb molecules can easily be integrated into *o*-Dchb structure.

The density, total light scattering coefficient R_0 , the degree of depolarization and refractive index were measured at 298 K for studied solutions. The isotropic R_{is} and anisotropic R_{an} molecular light scattering intensities, isothermal compressibility and its excess part, molar volume and its excess part were calculated. Complex nonmonotonic behavior of light scattering coefficients in response to the concentration change was found. The $R_0(x)$, $R_{is}(x)$, $R_{an}(x)$ curves pass through minimum near $x = 0.03$ and maximum near $x = 0.95$ (x – mole fractions of *o*-Dchb), which is the evidence of a substantial rearrangement of structure in solutions at concentration changes. Four intervals with different local structure were selected in concentration ranges: 0–0.03; 0.03–0.65; 0.65–0.9; 0.9–1.0 according to the molecular light scattering, excess isothermal compressibility and excess molar volume data. The solution local structure in each interval was described.

It is assumed that the first interval predominantly consists of *o*-Dchb molecules solvates with the structure of solvation shells different from the Chb structure in the volume. The second interval includes the agglomerates of molecules Chb and *o*-Dchb, the third – Chb and *o*-Dchb agglomerates and their conglomerates. The fourth interval principally consists of extended agglomerates of molecules *o*-Dchb with Chb molecules embedded in *o*-Dchb structure. Note that the maximum in binary solutions of organic liquids in the field of low concentrations (in studied system at $x(\text{Chb}) < 0.1$) was detected for the first time. This effect could be compared with the maximum of light scattering observed in diluted aqueous solutions of non-electrolytes. We hypothesize here that continuous system of chlorine-chlorine contacts acts similar to the network of hydrogen bonds in water. We believe that the features found in the system of *o*-dichlorobenzene–chlorobenzene solutions could be found in other systems which components are liquids with different structure and values (and, possibly, nature) of molecular interactions. To confirm this hypothesis, the studies of other systems with other types of interactions should be performed.

This work was financially supported by the Russian Foundation for Basic Research, project no. 16-03-00931.

[1] Lanshina. L.V., Abramovich A.I., [Rus. J. of Physical Chemistry A](#), 2008, 82, 1851-1856.

[2] Abramovich A.I., Lanshina. L.V. [Rus. J. of Physical Chemistry A](#), 2010, 84, 1147-1153.

[3] [Abramovich A.I.](#), [Alekseev E.S.](#), [Bogdan T.V.](#), [Lanshina L.V.](#) [J. of Structural Chemistry](#), 2014, 55, 651-659.



CALORIMETRIC STUDY OF HYDROGEN INTERACTION WITH MAGNETIC MATERIALS: THE CASES OF $\text{Nd}_2\text{Fe}_{17}$ AND $\text{Nd}_2\text{Fe}_{14}\text{B}$

E.Yu. Anikina¹, V.N. Verbetsky¹

¹ Lomonosov Moscow State University, Chemical Department Moscow, 119991 Russia, fax: +7 (495) 932-88-46

E-mail: anikina@hydride.chem.msu.ru

It is well known that in the production of magnetic materials Nd-Fe-B and R_2Fe_{17} -type (R=rare earth metals) the process of hydrogenation-dehydrogenation (HD) was used. However till now this process is not studied completely. Generally scientists studied magnetic properties [1-3] and influence of hydrogen on the structure of alloys. To understand better how hydrogen insertion influences physical and magnetic properties of alloys it is necessary to know of thermodynamic parameters of process of hydrogen interaction with magnet materials. Unfortunately, the works in which thermodynamic properties of HD processes done directly by calorimetric method are practically negligible. The authors in the work [4] studied hydrogen desorption from $\text{R}_2\text{Fe}_{17}\text{HX}$ (R=Nd and Dy) compounds with $x \leq 5$ using differential scanning calorimetry (DSC).

We studied the $\text{Nd}_2\text{Fe}_{17} - \text{H}_2$ and $\text{Nd}_2\text{Fe}_{14}\text{B} - \text{H}_2$ systems by means of the calorimetric method using the calorimeter Tian-Calvet type connected with a conventional Sieverts-type apparatus for gas dosed feeding. The apparatus scheme and the experimental technique were described elsewhere [5]. The initial samples of alloys were prepared by induction melting of pure metals (a purity grade is higher than 99.9%) under a pure argon atmosphere and annealing in the vacuum resistance furnace at 1100°C for 30-40 hours.

The calorimetric study of the $\text{Nd}_2\text{Fe}_{17} - \text{H}_2$ system was carried out at 300°C and $\text{Nd}_2\text{Fe}_{14}\text{B} - \text{H}_2$ system was examined by calorimetric method at 50°C. The P – C-T, $\Delta\text{H} - \text{C-T}$ and $\Delta\text{S} - \text{C-T}$ (where P – equilibrium hydrogen pressure, ΔH and ΔS – the relative partial molar enthalpy and entropy, respectively, T – temperature of reaction of hydrogen investigation with studying alloys and $\text{C}=\text{H}/\text{IMC}$) dependences were obtained for the process of hydrogen absorption and desorption. In the P – C - T isotherms there are no any plateau as it was shown in the works [6, 7]. At the same time in the plots of the $\Delta\text{H} - \text{C}$ dependences there are the some parts with constant enthalpy and entropy values. For example, in the plot of $\Delta\text{H}=\text{f}(\text{C})$ dependence for the $\text{Nd}_2\text{Fe}_{17} - \text{H}_2$ system there are plateau region $\Delta\text{H}_{\text{abs.}}=-69.3 \pm 1.3$ kJ/mol H_2 in the $0.3 < \text{C} < 0.9$ and $\Delta\text{H}_{\text{abs.}}=-35.6 \pm 1.1$ kJ/mol H_2 in the $2.3 < \text{C} < 3.7$ and $2.0 < \text{C} < 3.0$ $\Delta\text{H}_{\text{des.}}=38.7 \pm 0.8$ kJ/mol H_2 . For the $\text{Nd}_2\text{Fe}_{17} - \text{H}_2$ system such regions are $0 < \text{C} < 2.0$ $\Delta\text{H}_{\text{abs.}}=-80.5 \pm 0.9$ kJ/mol H_2 and $0.7 < \text{C} < 1.9$ $\Delta\text{H}_{\text{des.}}=79.3 \pm 0.8$ kJ/mol H_2 .

- [1] O. Isnard, S. Miraglia, M. Guillot, D. J. Appl. Phys, 1994, 76, 6035-6937.
- [2] O. Isnard, S. Miraglia, J.L. Soubeyroux. J. Magn. Magn. Mater, 1994, 137, 151-156.
- [3] C.N. Cristodoulou, T. Takeshita. J. Alloys Compd, 1993, 198, 1-24.
- [4] F. Cuevas, O. Isnard, B. Villeroy. Thermochim. Acta, 2013, 561, 14-18.
- [5] E.Yu. Anikina, V.N. Verbetsky. J. Alloys Compd, 2002, 330-332, 45-47.
- [6] H. Nahamura, K. Kurihara, T. Taksuki. J. Magn. Soc. Japan, 1991, 16, (2), 163-168.
- [7] A. Fukuno, C. Ishizaka, T. Yoneyama. J. Appl. Phys., 1991, 70, 6021-6022.

THERMODYNAMIC PROPERTIES OF DISPLACEMENT OF STRANDED OIL DEPOSITS BY FLUID

Ramazanova E.E.¹, Asadov M.M.² and Aliev E.N.¹

¹"Geotechnological Problems of Oil, Gas and Chemistry" SRI, Az1143 Baku, Azerbaijan

²Institute of Catalysis and Inorganic Chemistry ANAS, Az1143 Baku, Azerbaijan

E-mail: mirasadov@gmail.com

Technology of sub- and supercritical (SCF) CO₂-displacement of stranded oil is one of the most promising methods of deposit development [1]. The main factors determining the effectiveness of SCF CO₂ in the process of oil production, are reducing viscosity of the oil reservoir and an increase in the coefficient of volume expansion. The displacement of oil from deposits by SCF CO₂ is a complex process. Depending on the conditions of development, the oil displacement mode may occur at complete or limited miscibility of components. This process depends on the phase interaction in the condensate oil + water + CO₂ system. Parameters of critical point of a binary system are very different from the CO₂ critical parameters. For example, in a binary CO₂-H₂O system at least four phase regions, containing liquid, gas, gas hydrate and ice, are forming.

The fluid processing is considered to be a promising method for increasing production of stranded oil deposits. In the process of SCF-displacement of oil the concentration of components, such as CO₂/CH₄, varies depending on the state parameters of the layer, it is important to investigate the characteristics of the coexisting phases in the liquid-gas mixtures containing hydrocarbons. The phase equilibrium mixtures including sub- and supercritical fluid (SCF) of CO₂ and hydrocarbon are considered. The required equilibrium parameters are estimated by the properties of individual components and their binary interactions. The $p-T$ and $T-x$ phase diagrams for system state of CO₂-CH₄ are shown (Figure). The thermodynamic equations of fluid and solid phase solubility in the SCF are also shown.

Systems consisting of components of different volatility under sub- and supercritical conditions have been studied. Liquid hydrocarbon oil components (80-90% alkanes, naphthenes, aromatics) at SCF state may form with CO₂ binary mixtures of type I, where both components have similar critical parameters.

In binary mixtures containing n-alkanes the phase equilibria in a fluid state are carried out at temperatures above the critical temperature of the high-melting and high boiling component. In the $p-T$ phase diagram of binary type I mixture, the critical curve generally has a maximum pressure. In the state parameters region, above the critical curve, the low-volatile matter can be completely dissolved in the SCF. This behaviour of the critical curve is observed for the binary systems with different critical temperatures of components. Increasing the number of components for the CO₂-n-alkane systems leads to SCF heterogenization at temperatures above the critical parameters of the volatile component.

[1] Ramazanova, E.E.; Asadov, M.M. and Aliyev E.N. Technologies of extraction and use of hydrocarbons. Moscow. Gubkin Russian State University of Oil and Gas, 2014, 3, 1-3.

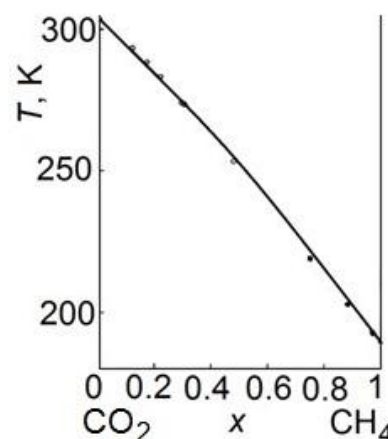


Figure 1. $T-x$ dependence CO₂-CH₄ system (points - experimental data, the curve - calculation).

THERMODYNAMICS, PHASE DIAGRAM AND TRANSPORT PHENOMENA OF THE GaS-GaSe SYSTEM

Asadov S.M. and Mammadov A.N.

Institute of Catalysis and Inorganic Chemistry ANAS, Az1143 Baku, Azerbaijan

E-mail: salim7777@gmail.com

Semiconducting single crystals have long been used as detectors of ionizing radiation in medical diagnostics instruments, customs inspection systems, dosimetric and spectrometric devices. However, the process for growing single crystals is technologically complex, requires expensive growth equipment and raw material. This ultimately determines the high cost of the product. Currently, various research groups are searching for new functional materials, which in some areas can replace conventional single crystals [1,2]. The most promising ones are gallium chalcogenide-based solid solutions. This work presents the results of a study of phase equilibrium and physical properties of GaS-GaSe-based solid solution system. Phase diagram for GaS-GaSe system has been studied by various authors before. Our calculated phase diagram for GaS-GaSe is shown in Figure. Calculated solidus and liquidus temperatures differ slightly from the experimental data. Diagram of the state for GaS-GaSe system is the type characterized by the minimum and presence of unlimited mutual solubility in the system. This is due to the proximity of the source components. The different phases are not detected in the area of $(\text{GaS})_{1-x}(\text{GaSe})_x$ solid solutions. This is consistent with thermodynamic calculations of the free energy of mixing of $(\text{GaS})_{1-x}(\text{GaSe})_x$ solid solutions. Calculation of the temperature dependence of the free energy of mixing of solid solutions was performed in 300-1200 K range.

In order to control properties of these materials we have verified GaS-GaSe phase diagram and computational modeled the liquidus and solidus curves. The Gibbs free energy change of $(\text{GaS})_{1-x}(\text{GaSe})_x$ solid solutions has been determined as functions of temperature.

The layered GaS single crystals used for our study were grown by the Bridgman method and have hexagonal structure with lattice parameters: $a = 3.58 \text{ \AA}$, $c = 15.47 \text{ \AA}$ at room temperature. The dielectric properties of the GaS single crystals were studied by a resonance technique in the frequency range $f = 5 \times 10^4$ to 3.5×10^7 Hz, using a TESLA BM 560 Q-meter. The single crystal GaS samples for dielectric measurements had the form of planar capacitors normal to the C axis of the crystals, with silver-paste electrodes. During the measurements, the samples were located in a shielded chamber. All of the ac- measurements were performed at 300 K in electric fields corresponding to Ohmic current-voltage behavior. The results demonstrate that, over the entire composition range, the measured physical properties of the solid solutions correlate with their composition. The real and imaginary parts of the complex dielectric permittivity, the dielectric loss tangent, and ac-conductivity of crystals of GaS-GaSe solid solutions have been measured as functions of frequency in the range of 50 kHz to 35 MHz. The electron-irradiated materials have also been studied.

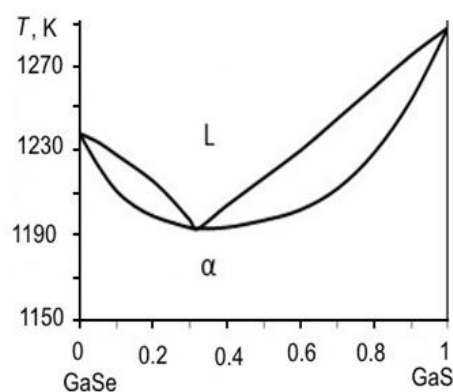


Figure . Phase diagram of the GaS-GaSe system calculated by us.

[1] Asadov M.M., Mustafaeva S.N., Mammadov A.N. et al. *Inorganic Materials*, 2015, 51(8), 843-849.

[2] Mustafaeva S.N., Asadov M.M. *Fizika B. Condensed Matter Physics*. 2014, 453, 158-160.



SOLID-PHASE EQUILIBRIA IN THE Tl-Ge-Te SYSTEM AND THERMODYNAMIC PROPERTIES OF GERMANIUM-THALLIUM TELLURIDES

Alekberova T.M.¹, Guseynov F.N.², Kuliyeva N.A.¹, Mirzoyeva R.C.¹, Babanly M.B.²

¹Baku State University, AZ1148, Baku, Azerbaijan

²Institute of Catalysis and Inorganic Chemistry, ANAS, AZ1143, Baku, Azerbaijan

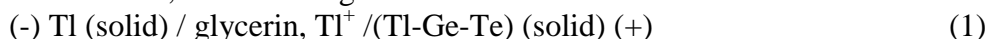
e-mail: babanlymb@gmail.com

Thallium forms following tellurides with germanium [1,2]: Tl_8GeTe_5 , Tl_2GeTe_2 , $TlGeTe_2$, Tl_2GeTe_3 , Tl_2GeTe_5 . These compounds belong to a class of promising thermoelectric materials with an abnormally low thermal conductivity [3]. For the development of synthesis methods and crystal growth of these phases requires reliable data on phase diagrams and fundamental thermodynamic properties.

This paper presents the results of the study of solid-phase equilibria in the Tl-Ge-Te system and thermodynamic properties of the aforementioned germanium-thallium tellurides.

Compounds and alloys of the title system were synthesized for studies. Syntheses were carried out by melting of high purity elemental components in evacuated quartz ampoule, followed by homogenizing annealing at 500 K for 1000 h. Individuality of the synthesized compounds and phase composition of alloys was controlled by SEM and XRD techniques.

For the EMF measurements, the following concentration chains were assembled:



The assembly of an electrochemical cell and measurements were similar to those reported elsewhere [4]. In the chains of type (1), metallic thallium was used as the left electrode, while equilibrium alloys of the Tl-Ge-Te system were exploited as the right electrode. A saturated glycerin solution of KCl with the addition of 0.1 mass % TlCl was used as an electrolyte. EMF was measured by the compensation method in the temperature range of 300–430 K.

The results of the EMF measurements of the chains (1) are consistent with the solid-state phase diagram of the system. The analysis showed the linearity of the EMF dependences upon temperature for all alloys. SEM and XRD data and the results of EMF measurements of the concentration chains of type (1) made it possible to establish a picture of solid-phase equilibria in the Tl-Ge-Te system. It was established that in the Tl_2Te -Ge-Te compositions area, this system consists of ten three-phase fields. The character of the concentration dependence of the EMF is in full accordance with the phase diagram. In each of the three-phase field an EMF values were constant regardless of the overall composition of the alloy, and the transition from one area to another EMF values changed abruptly.

Analysis of the results of EMF measurements showed their linearity for each three-phase field. Therefore, they have been treated by the least squares methods and linear equation of the type $E=a+bT$ were obtained, based on which partial thermodynamic functions of thallium in alloys were calculated. Based on the solid phase equilibria diagram potential-forming reactions for thallium-germanium tellurides were established, and their standard thermodynamic functions of formation and standard entropies were calculated.

References

- [1]. Kuliyeva N.A., Babanly M.B. Russ.J.Inorg.Chem., 1982, 27, 1531-1536.
- [2]. Touré A.A., Kra G., Eholié R. J.Less.Common Metals, 1991, 170, 199-222.
- [3]. Shevelkov A.V. Russ. Chem. Rev. 2008, 77, 1–19.
- [4]. Babanly M.B., Yusibov Y.A. Electrochemical Methods in Thermodynamics of Inorganic Systems. Baku, 2011. 305 P.



MEASUREMENT OF SOLUBILITY OF ACTIVE PHARMACEUTICAL INGREDIENTS IN WATER

Brezovska B.V., Enders S.

Institute of Technical Thermodynamics and Refrigeration Engineering, Karlsruhe Institute of Technology, D-76131 Karlsruhe, Germany

E-mail: boryana.brezovska@partner.kit.edu; sabine.enders@kit.edu

In drug formulation science, poor aqueous solubility of a drug candidate may cause many complications in the process of drug research and development. Limited water solubility and subsequent unsatisfactory dissolution rate hinder the gastrointestinal drug absorption, respectively the bioavailability of orally administered drugs, which is a prerequisite for increased therapeutic doses. Thus, effective plasma concentrations are achieved, yet a potential digestive tract toxicity risk exists. On the one hand, this is a preclinical stage related problem as long as approximately 40% NCEs (new chemical entities) fail to reach market due to their poor water solubility [1]. On the other hand, about 40% of the top 200 marketed orally administered, immediate-release drug products are categorized as practically insoluble, i.e. having solubility <100 µg/mL as defined in the US Pharmacopeia [2].

Therefore, knowledge of the thermodynamic data of aqueous solutions of drugs is a necessity for drug formulation development. Although topic importance, the experimental database for binary systems containing drug and water is still limited [3]. Hence, the aim of this work is the experimental investigation of the thermodynamic equilibrium in four drug + water systems, containing following substances of pharmaceutical interest: 2-Hydroxybenzoic acid (salicylic acid); (RS)-2-(4-(2-Methylpropyl)Phenyl) Propanoic Acid (ibuprofen); 3,7,11-Trimethyl-2,6,10-dodecatrien-1-ol (farnesol) and 1-methoxy-4-[(E)-prop-1-enyl]benzene (trans-anethole). The concentrations of the saturated aqueous solutions were measured at five temperatures in the temperature interval from 25°C to 40°C. Besides, liquid-liquid equilibrium was detected by samples in systems farnesol + water and trans-anethole + water.

- [1] D. Sharma, M. Soni, S. Kumar, G.D. Gupta, *Research Journal of Pharmacy and Technology*, 2009, 2(2), 220-224.
- [2] T. Takagi, C. Ramachandran, M. Bermejo, S. Yamashita, L.X. Yu, G.L. Amidon, *Molecular Pharmaceutics*. 2006, 3(6), 631-643.
- [3] E. Rytting, K.A. Lentz, X.Q. Chen, F. Qian, S. Venkatesh, *AAPS Journal*, 2005, 7(1), E78–E105.

THERMODYNAMIC PROPERTIES OF TERNARY AQUEOUS SOLUTIONS IN THE SYSTEM $\text{H}_2\text{O} - \text{HNO}_3 - \text{Ca}(\text{NO}_3)_2 - \text{Nd}(\text{NO}_3)_3$

Dzuban A. V.^{1,2}, Nesterov A. V.²

¹Lomonosov Moscow State University, Department of Chemistry, Russia, 119991 Moscow, GSP-1, 1-3 Leninskiye Gory

²Lomonosov Moscow State University, Department of Materials Science, Russia, 119991 Moscow, GSP-1, 1-73 Leninskiye Gory, Laboratory Building B

E-mail: dzuban@td.chem.msu.ru

Liquid-liquid extraction from multicomponent aqueous acidic solutions by an organic extraction agent has become the most common technique used for the isolation, separation and purification of rare earth elements (REEs). Nevertheless the process conditions are still adjusted on empirical basis. Thermodynamical modelling seems to be reasonable alternative for solving the problem and decreasing the number of experiments. The information on the properties of binary and ternary systems at least is required. Stock solution always contains an impurity metals (mostly, calcium) acting as salting-out agent. To the best of our knowledge, binary aqueous solutions of acids, rare earths and calcium salts are well investigated [1-4]. So, the aim of this work was studying the thermodynamic properties of ternary aqueous solutions in the system $\text{H}_2\text{O}-\text{HNO}_3-\text{Ca}(\text{NO}_3)_2-\text{RE}(\text{NO}_3)_3$ ($\text{RE} = \text{Nd}$).

Ternary system $\text{H}_2\text{O}-\text{HNO}_3-\text{Nd}(\text{NO}_3)_3$ has been previously investigated by our group [5]. Comprehensive thermodynamical modelling of $\text{H}_2\text{O}-\text{HNO}_3-\text{Ca}(\text{NO}_3)_2$ system has been made in [6]. However, Sander et al. used doubtful experimental data on solution properties at 298.15 K [7] (figure 1). We performed additional measurements of water vapor pressures in the system by transpiration method using an experimental unit developed in our group [5]. Concentration dependence of water activity in the mixed solutions of calcium and neodymium nitrates was investigated by static method of vapor pressure measurements. Again, an experimental unit designed in our lab was used [8].

Vapor pressures over 6 solutions for each system were measured at 298.15 K with the accuracy better than 1%. Obtained experimental data were described using ideal mixing formalism (Zdanovsky rule) and Pitzer model for mixed electrolytes. Ternary interaction parameters were optimized to improve the accuracy of fitting to 1%.

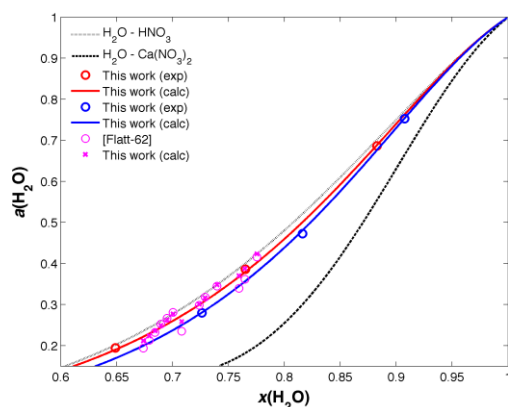


Figure 1. Water activity in the system $\text{H}_2\text{O}-\text{HNO}_3-\text{Ca}(\text{NO}_3)_2$ at 298.15 K.

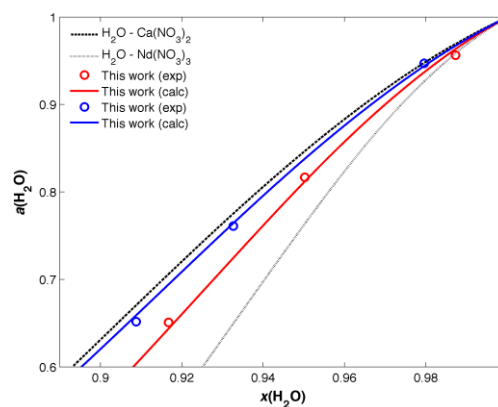


Figure 2. Water activity in the system $\text{H}_2\text{O}-\text{Ca}(\text{NO}_3)_2-\text{Nd}(\text{NO}_3)_3$ at 298.15 K.

- [1] Rard, J.A.; Miller, D.G.; Spedding, F.H. *J. Chem. Eng. Data*, 1979, 24, 348-354.
- [2] He, M.; Dong, L.; Li, B. *J. Chem. Eng. Data*, 2011, 56, 4068-4075.
- [3] Chatterjee, S; et al. *J. Chem. Eng. Data*, 2015, 60, 2974-2988.
- [4] Oakes, C.S.; Felmy, A.R.; Sterner, S.M. *J. Chem. Thermodyn.*, 2000, 32, 29-54.
- [5] Moiseev, A.E.; et al. *J. Chem. Eng. Data*, 2016, 61, 3295-3302.
- [6] Sander, B.; Rasmussen, P.; Fredenslund, A. *Chem. Eng. Sci.*, 1986, 41, 1185-1195.
- [7] Flatt, R.; Benguerel, F. *Helv. Chim. Acta*, 1962, 45, 1772-1776.
- [8] Kovalenko, N.A.; Pustovgar, E.A.; Uspenskaya, I.A. *J. Chem. Eng. Data*, 2013, 58, 159-166.



THERMODYNAMIC PARAMETERS OF THE PROTEIN THERMAL STABILITY IN THE PRESENCE OF NANOPARTICLES

Gheorghe D., Botea-Petcu A., Precupaş A., Popa V.T., Tanasescu S.

"Ilie Murgulescu" Institute of Physical Chemistry of the Romanian Academy, Bucharest, Romania

E-mail: georghedanny2@gmail.com

The aim of this study was to investigate from the energetic point of view some protein-nanoparticles systems and to evaluate the thermodynamic parameters that describe the protein stability in the presence of nanoparticles.

The effect of two of the most commonly used metal oxide nanoparticles (NPs), namely zinc oxide (ZnO) and titanium dioxide (TiO₂), on the thermal stability of bovine serum albumin (BSA) and bovine plasma fibrinogen (BPF type I-S) has been investigated. The aqueous and phosphate buffer - NPs dispersions with different concentrations were prepared and the changes in the thermal behavior of BSA and BPF (both free in solution and adsorbed to nanometer-sized oxide particles) were studied by using NanoDSC, TA Instruments equipment.

The thermodynamic parameters of the protein thermal stability represented by heat capacity change (ΔC_p), denaturation temperature (T_m), enthalpy change (ΔH_{cal}), and entropy change (ΔS) have been obtained. The effect of nanoparticle type and concentration, as well as of the pH values on the denaturation characteristics of proteins have been evidenced and the adsorption-induced changes in structural stability of the proteins have been analysed (example *Figure 1*).

Acknowledgement The support of the EU (ERDF) and Romanian Government under the project INFRANANOCHEM Nr. 19/01.03.2009 and of the project NanoReg2, Nr. 646221/2015 in the frame of the Horizon 2020 Framework Program of the European Union is acknowledged.

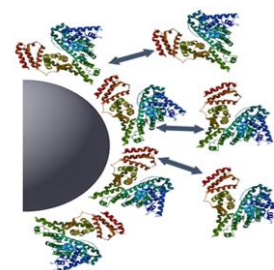


Figure 1. Model for the adsorption of BSA to NP. Free protein molecules are in fast exchange (gray arrows) with bound protein molecules.

**THERMODYNAMIC MODELING OF SOLUTION HUMAN BLOOD**

Golovanova O.A.

Department of Inorganic Chemistry Omsk F. M. Dostoevsky State University, 644077 Omsk, Prospekt Mira 55A, Russia
E-mail: Golovanoa2000@mail.ru

Environmental degradation, the increasing pace of life, and other external factors have an increasing impact on the health of city residents. Nearly every organ of the human body suffers from the adverse affects of unfavorable environment. Thus, the violation of the calcium-phosphorus metabolism in the body often leads to unwanted mineralization - the formation of tumors in many organs. Moreover, there is a constant increase in the number of diseases caused by the destruction of bone matrix (osteoporosis, arthrosis, etc.). Pathological masses can be formed in a wide variety of sites, and the cardiovascular system is one of them. Pathological cardiovascular calcification is, probably, the deadliest among other types of the pathological mineral formation. That's why researches of the Pathological Cardiovascular Deposits (PCD) possess high priority nowadays. Structure and chemical composition of PCD themselves have been already reported in a considerable amount of papers. It is common knowledge now that PCD consist of mineral and organic components. The most promising prospective in this field which can be seen today is in the model experiments. The most interesting, in our opinion, in this respect are the calcium orthophosphates with the properties of biocompatibility and bioactivity due to (crystallo-) chemical affinity to bone substance. To understand the processes associated with phase and chemical transformations of the studied salts in aqueous media, and to manipulate with them in order to obtain materials with controlled / set properties it is important to study in detail the physical and chemical nature of these processes, to identify the regularities, to define the dominant environmental parameters (pH, composition, temperature, impurities, etc.). However, the complexity of the most real processes of phase formation (joint influence on the crystallization process of the thermodynamic and kinetic factors) did not solve the problems described above only by experiment. In our opinion, the most effective in this respect are the methods of physical and chemical modeling and calculations of thermodynamic characteristics of the processes. Methods of thermodynamic modeling received broad distribution in geochemical researches for the description of processes of mineralogenesis with participation of mainly diluted solutions. The solution of a task includes use of the corresponding criterion answering to a condition of stable equilibrium of system, and thermodynamic a reasonable choice of association of minerals which can potentially be in balance with environment for this limited area of conditions. Change of standard energy of Gibbs at formation of a deposit is connected with work of solubility of slightly soluble connection by the equation:
$$\Delta G_{(M_p X_q), T}^0 = -RT \ln \frac{1}{K_s^0} = RT \ln K_s^0 \quad (1)$$
 where $\Delta G_{(M_p X_q), T}^0$ Gibbs's

standard energy, kJ/mol; R – universal gas constant (J / моль·K); T – temperature, K.

One of ways of graphic representation of balance the sediment ↔ solution (human blood) in system in which formation of almost insoluble connection from water solution proceeds is construction of "stability fields". The principle of creation of similar charts consists in establishment of functional dependence of the minimum concentration of the cation which is a part of a deposit which needs to be created for receiving supersaturation on this phase, from pH solution and concentration of anion: $pC_{M^{q+}} = f(pC_{X^{p-}}, pH)$ During the carried-out thermodynamic calculations conditions and possibility of formation of almost insoluble connections in hypothetical solution of sediment-forming ions are revealed. On the basis of the constructed charts of stability for a series of phosphates of calcium and magnesium, areas at which formation of these phases from solutions most thermodynamic is probable are defined. Thermodynamic calculation reflects possibility of formation of phases only proceeding from data on their thermodynamic stability in a standard condition and doesn't consider, in particular, the kinetic factors having impact on process of formation of a solid phase in actual practice. When carrying out model experiments analogs of phosphatic minerals were received, and also distinctions in the conditions of their education are revealed. In the system human blood deposition hydroxyapatite is thermodynamically feasible in the studied conditions.

This research was supported in part by the Russian Foundation for Basic Research (grant No. 15-29-04839 ofi_m).



THERMODYNAMIC PARAMETERS OF PROTOLYTIC AND COORDINATION EQUILIBRIA OF SOME DIAMINE COMPLEXONES

Gridchin S.N.

Ivanovo State University of Chemistry and Technology, Sheremetevskii prospekt 7, 153000 Ivanovo, Russia

E-mail: sergei_gridchin@mail.ru

The electrodeposition of a metal coating (zinc, cadmium, tin) is known to be normally used blocking out corrosion of steelwork. A promising way to enhance corrosion resistance of the protective coating is alloying its material with an iron subgroup metal (Fe, Co, Ni). At present there is a growing interest in the application of electrolytes including various ligands which form stable complexes under conditions of the electrolysis. A good combination of donor centers and their positional relationship in the molecules of alkylenediaminepolycarboxylates make these compounds useful for the galvanic baths in particular. These complexones give birth to a lot of protolytic and coordination equilibria. But it is confronted with the difficulties in understanding of the electrochemical behavior of the complexes because there appears a lot of the ionic species which are capable of being electroactive. The limited type of the reliable reference data sources for the thermodynamic properties is powerless to provide the relations between the functions of the individual chemical and electrochemical reactions in the multiconstituent systems. Comprehensive study of the electrolytes containing compounds with amino and carboxylic groups being able to form the chelate rings is the key to solving this problem.

This work presents results of calorimetric, potentiometric and spectrophotometric investigations of the acid-base interaction and zinc(II), cadmium(II), nickel(II), cobalt(II) complexation processes in aqueous solutions of some diamine-complexones related to ethylenediaminetetraacetic acid (and some amino acids as the structural analogues). Among the objects investigated are trimethylenediamine-N,N,N',N'-tetraacetic, tetramethylenediamine-N,N,N',N'-tetraacetic, hexamethylenediamine-N,N,N',N'-tetraacetic, 2-hydroxypropylene-1,3-diamine-N,N,N',N'-tetraacetic, N-(β -hydroxyethyl)ethylenediamine-N,N',N'-triacetic, ethylenediamine-N,N'-diacetic-N,N'-dipropionic, ethylenediamine-N,N'-diglutaric, glutamic, aspartic, N-(β -hydroxyethyl)imino-N,N'-diacetic acids, serine, homoserine, taurine, glycine, alanine.

Thermodynamic parameters ($\log K$, ΔG , ΔH , ΔS) for the relevant equilibria have been determined at 298.15 K and ionic strength values from 0.1 up to 1.5 M. The influence of background electrolyte character and concentration on the protolytic and coordination equilibria has been discussed. The standard thermodynamic parameters ($\log K^\circ$, ΔG° , ΔH° , ΔS°) have been evaluated for the corresponding reactions. The results obtained were compared with the reference data on related compounds investigated earlier in this laboratory under the same experimental conditions (imino-N,N'-diacetic, nitrilo-N,N,N'-triacetic, ethylenediamine-N,N,N',N'-tetraacetic, ethylenediamine-N,N'-disuccinic acids). A plausible explanation of changes in these quantities has been proposed in view of the metal ion and ligand structures (type of coordination, denticity, presence of hydrophobic and hydrophilic fragments, solvation features of the zwitter ions). As ancillary part of this study, the spatial, electronic and energy parameters for isolated molecules and ions of the mono- and diamine-complexones have been computed.

The electrodeposition of zinc, cadmium, nickel, cobalt and binary alloys of these metals from some complexone and amino acid solutions have been examined by cyclic voltammetry and polarization curve measurements in order to galvanize a 08KP steel. The influence of the competitive protolytic and coordination equilibria on the relevant processes occurred at the electrode surface was under consideration. New promising electrolytes have been suggested for plating with alloys of zinc-cobalt and zinc-nickel.

The development of the galvanic bath electrolytes was specified by the Ministry of Education and Science of the Russian Federation. The study on processes of formation and cathodic reduction of some amino acid complexes was partially supported by the Russian Foundation for Basic Research, project 14-03-00360-a. The investigation of the compounds related to ethylenediaminetetraacetic acid is the origin of project 17-03-00469-a.



THERMODYNAMICS OF COBALT(II), NICKEL(II), COPPER(II), AND ZINC(II) COMPLEXATION WITH SOME AMINO ACIDS IN AN AQUEOUS SOLUTION

Gridchin S.N.¹, Pyreu D.F.²

¹Ivanovo State University of Chemistry and Technology, Sheremetevskii prospekt 7, 153000 Ivanovo, Russia

²Ivanovo State University, Ermak 39, 153025 Ivanovo, Russia

E-mail: sergei_gridchin@mail.ru

Amino acids play a dominant role in the creation of peptide molecules, nitrogen metabolism and other important biochemical processes. Study of coordination equilibria between these vital ligands and 3d-metal ions is of particular interest to explain structural features of various ferment active centers. It offers ample scope for progress in simulation of their behaviour.

This work presents results of potentiometric, calorimetric and spectrophotometric investigation of homo- and heteroligand complex formation processes for Co^{2+} , Ni^{2+} , Cu^{2+} , Zn^{2+} ions and some amino carbonic acids in aqueous solutions. Among the objects of this investigation are serine, threonine, valine, alanine, alanyl-alanine, glycyl-glycine, glutamine, asparagine, arginine, lysine, ornithine, histidine.

The equilibrium concentration of hydrogen ions was determined by measuring the electromotive force of a glass electrode and a silver – silver chloride reference electrode using a P-363/3 potentiometer with a pH-340 pH-meter-millivoltmeter as the null-instrument. The calorimetric measurements were performed in an isothermal jacket ampoule flow-mixing calorimeter equipped with a thermistor sensor and an automatic recorder of the temperature–time curve. The unit was tested against the heat of solution of crystalline potassium chloride in water. The visible electronic spectra of the solutions investigated were recorded on Specord M-400 IENA and KFK-3 spectrophotometers. The potentiometric, calorimetric and spectrophotometric experimental data have been treated using the special software [1].

Thermodynamic parameters ($\log K$, ΔG , ΔH , ΔS) of protolytic and coordination equilibria in systems of metal + amino acid have been determined at 298.15 K and ionic strength values from 0.1 to 1.5 (KNO_3). The influence of “background” electrolyte concentration on the relevant equilibria was under consideration. The data obtained were extrapolated to the zero ionic strength. The corresponding thermodynamic quantity values have been calculated for the standard solution ($\log K^\circ$, ΔG° , ΔH° , ΔS°).

Thermodynamic parameters for addition of some amino acids to cobalt(II), nickel(II), copper(II), zinc(II) iminodiacetates and nitrilotriacetates have been evaluated at 298.15 K and an ionic strength of 0.5 (KNO_3). The $\log K$, ΔG , ΔH , ΔS values for the mixed complex formation reactions were discussed together with the corresponding thermodynamic parameters of similar formation reactions for the simple binary complexes.

The ESR method and NMR method have been used to study the heteroligand complex formation in the systems of copper(II) complexonate + amino acid and zinc(II) complexonate + amino acid, respectively. ESP spectra were recorded using a Bruker ELEXSYS II-500 spectrometer. ^1H and ^{13}C spectra were recorded on a Bruker AVANCE-500 spectrometer. The relationship between the probable coordination modes of the aminocarboxylate molecules in the mixed-ligand complex and the thermodynamic parameters obtained has been discussed.

The results have been compared with the corresponding data on related compounds (amino acids, complexones, dipeptides and diamines) investigated earlier.

This work was partially supported by the Ministry of Education and Science of the Russian Federation and the Russian Foundation for Basic Research, project 14-03-00360-a.

[1] Borodin, V.A., Vasiliev, V.P., Kozlovskii, E.V. Mathematical Problems in Chemical Thermodynamics, Novosibirsk, Nauka, 1985, 219-226.



THERMODYNAMIC INVESTIGATION OF Al-N and Ga-N SYSTEMS

Ilinykh N.I., Malkova I.A., Volgarev E.A.

¹ Ural Technical Institute of Telecommunications and Informatics, 15, Repin Str., Ekaterinburg, 620109, Russia
E-mail: ninail@bk.ru

Metal nitrides of 3-th group (AlN, GaN, BN, InN) have a great scientific and practical interest because they are perspective materials for semiconductor electronics, in particular, for the use in the semiconductor radiation sources in the short-wave region of the visible range and the near ultraviolet. Many of these compounds have high refractoriness and chemical resistance in different aggressive media, dielectric and semiconductor properties, capability to pass for superconductivity at relatively high temperatures, wear resistance, low melting points and low values of hardness [1].

Despite the fact that the experimental study of these materials is given enough attention, many of their properties and characteristics are investigated insufficiently. Therefore the theoretical investigation metal nitrides of 3-th group is important.

Presented work is devoted to the investigation of Al-N and Ga-N systems. The study was carried with the use of thermodynamic modelling methods [2]. As the software the program set TERRA was used [3].

The temperature and concentration dependences of composition and thermodynamic characteristics (enthalpy, entropy and Gibbs energy) of Al-N alloys and partial pressures of the components of the gas phase above these alloys were obtained in wide range of temperatures (300 – 3000 K) at the common pressure 10^5 Pa.

It was established, that the activities of the components have big negative deviations from Raoult's law. Concentration dependencies of integral excess Gibbs energies, entropies and enthalpies are not monotonous. These facts justify, that strong interaction between atoms of different sorts takes place.

It was shown that the partial pressures of the gas phase components can be describe by linear equations $\ln P = A+B/T$, where A and B are constant coefficients, T - temperature, K.

[1] G.V. Samsonov. *Nitrides*. Kiev, Naukova Dumka, 1969, 380 p. (in Russian).

[2] N.A. Vatolin, G.K. Moiseev, B.G. Trusov. *Thermodynamic modelling in high - temperature inorganic systems*. Metallurgia, Moscow, 1994 (in Russian).

[3] B.G. Trusov. Vestnik of Bauman Moscow State Technological University, **2** (special Issue), 240-249 (2012) (in Russian).



THERMODYNAMIC MODELING OF Ni-C-Cr-Si-B ALLOYS

Krivorogova A.S.¹, Ilinykh N.I.^{1,2}

¹ Ural Institute of the State fire service EMERCOM of Russia, 22 Mira Str., Ekaterinburg, Russia

² Ural Technical Institute of Telecommunications and Informatics, 15, Repin Str., Ekaterinburg, 620109, Russia

E-mail: ninail@bk.ru

Thermal spray processes have been widely used in the different engineering industry sectors for component protection and reclamation. Thus, thermal spray coatings are used for surface hardening, protection from exposure to high temperatures, thermal erosion and abrasive wear, corrosion protection in a variety of environments and so on. Besides that, thermal spray coatings used for restoring of geometrical dimensions and form of surface of the worn details [1-3]. As the materials for thermal spray coatings self-fluxing alloys are used [4-5]. In general, there are nickel-base or cobalt-base alloys that use boron, phosphorus, or silicon, either singly or in combination, as melting-point depressants and fluxing agents. These materials have relatively low melting points and, as a rule, require post-spray heat treatment.

For designing and optimizing processes of creation of thermal spray coatings it is necessary to improve our notions about structure of liquid alloys because heat treatment of the melt can influence greatly on properties of solidified materials. The preliminary thermodynamic estimation is necessary to predict and check the multifunctional structures of complex composition and to create the flexible coating technologies.

Present work is devoted to investigation of equilibrium composition and thermodynamic characteristics of Ni-C-Cr-Si-B alloys. Investigations were carried out using the thermodynamic modeling method [6, 8]. As a software the program complex TERRA was used [7]. The structure of solid and liquid alloys was described by the model of ideal solutions (IS) and by the model of ideal solutions of interaction products (ISIP) [6, 8]. Modeling was executed in the wide range of temperatures (300 – 2000 K) at the common pressure of $P = 10^5$ Pa in argon. Initial content of modeling systems (mass. %): 1) Ni - 79.3, C - 0.5, Cr - 15, Si - 3.2, B - 2, Ar - 1; 2) Ni - 74.3, C - 1, Cr - 17, Si - 4.1, B - 3.6, Ar - 1. According to ISIP model liquid alloy (melt) consists of Ni, C, Cr, Si, B atoms and associates corresponding to the binary compositions of Ni-C-Cr-Si-B system: Ni₃C, NiB, Ni₃B, Ni₂B, Ni₄B₃, NiSi, NiSi₂, Ni₂Si, Ni₇Si₁₃, SiC, SiB₁₄, B₄Si, B₆Si, B₄C, CrB, CrB₂, Cr₃B₄, Cr₅B₃, Cr₃C₂, Cr₇C₃, Cr₂₃C₆, CrSi, CrSi₂, Cr₃Si, Cr₅Si₃.

The temperature dependences of the integral and partial excess thermodynamic characteristics (enthalpy, entropy and Gibbs energy) and equilibrium composition of alloys were obtained.

Comparison of temperature dependences of content of alloy's components with temperature dependences of thermodynamic properties shows that there is correlation between the graphs: "fractures" on the curves are observed at the same temperatures. It can be assumed that these fractures are caused by phase transformations.

1. A. Khasui, O. Morigaki, Hard Facing and Sputtering. (Mashinostroenie, Moscow. 1985) (in Russian)
2. V.V. Kudinov, Plasma coatings (Nauka, Moscow, 1977) (in Russian)
3. R. Knight and R.W. Smith, ASM Handbook, **7**, 408 (1998)
4. R.C. Tucker, Jr. ASM Handbook, **5**, 497 (1994)
5. Frolov V.A., Poklad V.A. Svarochnoe proizvodstvo **11**, 38 (2006) (in Russian)
6. N.A. Vatolin, G.K. Moiseev, B.G. Trusov, Thermodynamic modeling in high temperature inorganic systems (Metallurgia, Moscow, 1994) (in Russian).
7. B.G. Trusov, Vestnik of Bauman Moscow State Technological University, **2** (special Issue), 240 (2012) (in Russian).
8. N.I. Ilinykh, T.V. Kulikova, G.K. Moiseev, Composition and equilibrium characteristics of metallic melts of binary systems on the basis of iron, nickel and aluminum (Publ. UB of RAS, Ekaterinburg, 2006) (in Russian).



THE STRUCTURAL INHOMOGENEITIES IN AQUEOUS SOLUTIONS OF TBA. MOLECULAR DYNAMICS STUDY

Kadtsyn E.D., Anikeenko A.V., Medvedev N.N

Voevodsky Institute of Chemical Kinetics and Combustion, SB of RAS, Novosibirsk, Russia

Novosibirsk State University, Novosibirsk, Russia

E-mail: kadtseen@mail.ru

Aqueous solutions of tert-butyl alcohol (TBA) are not homogeneous even at low concentrations. Some thermodynamic and spectroscopic properties of these solutions demonstrate extremes at 2-5 mole percent of TBA, that means the structure of the solutions undergoes drastic changes at these concentrations. One thinks that TBA molecules in solution are distributed independently below this threshold, and after, the self-association begins. However, there is no a quantitative picture of such inhomogeneities in TBA solutions on the molecular level.

We study molecular dynamics models of TBA solutions at different concentrations, and compare their structure with aqueous solutions of trimethylamine-N-oxide (TMAO, which molecule is similar to TBA one), urea (which is well incorporated in water), and systems of random spheres, which represent “an ideal solution” (a random spatial distribution of particles). All-atom molecular dynamics simulation was performed in Gromacs 5.0.7 package. Force fields were taken from [1] for TBA, from [2] for TMAO, and from [3] for urea. For water, TIP4P_2005 model was used.

Solute-solute radial distribution functions and local mole fraction reveal a strong tendency to contact between TBA molecules even at very low concentrations (0.5 mole percent). The probability of such contacts is much higher than for random spheres at the corresponding density. The same situation is in urea solutions. One can relate it with the enthalpic effect and hydrophobic interaction. On the contrary, the tendency to contact between TMAO molecules in solutions is much weaker, like in the system of random spheres. We can see it also in the distribution of volumes of Voronoi regions calculated for solute molecules in solution and for random spheres. The coincidence between TMAO solutions and the random spheres were obtained for all studied concentrations (up to 10 mole percent). TBA solutions demonstrate significant difference with random spheres. The variance of Voronoi volume distributions for TBA solutions is always larger than for random spheres. This can be related with the presence of inhomogeneities in spatial distribution of TBA in solution.

We also carried out a cluster analysis of the systems of solute molecules and random spheres. It was shown that the studied cluster characteristics for TMAO solutions are the same as for random spheres. In contrast, the solutions of TBA are different, that relates with the association process. We calculated morphology and size of the clusters, and the cluster lifetimes. The comparison of the structural characteristics of solutions with random spheres allows us to evaluate geometrical and chemical contribution to the self-association process.

[1] Caleman C. et al. *J. Chem. Theory Comput.*, 2011, 8(1), 61-74.

[2] Hölzl C. et al. *J. Chem. Phys.*, 2016, 144(14), 144104.

[3] Weerasinghe S. and Smith P. E., *J. Phys. Chem. B*, 2003, 107, 3891–3898.

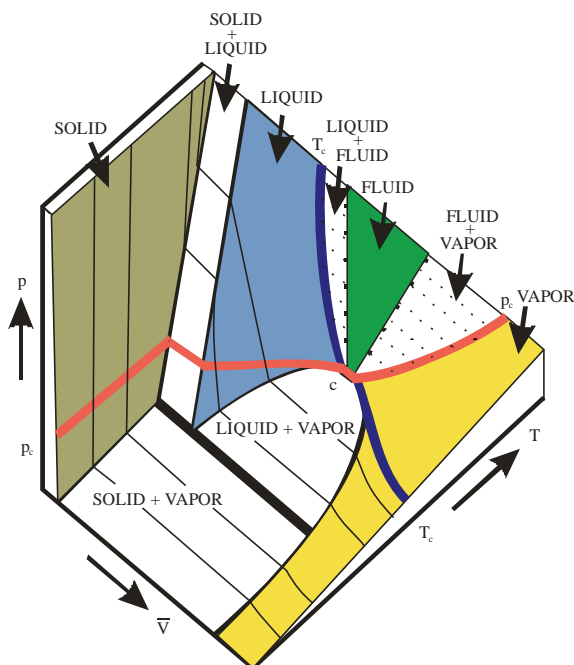
Financial support from grants RFFI (No. 15-03-03329), and grant RSCF 17-13-01059 (for cluster analysis) is gratefully acknowledged.

[3] Weerasinghe S., Smith P. E. *J. Phys. Chem. B* 107, 3891–3898 (2003)

FLUID SURFACE LOCALIZATION IN P — V — T -DIAGRAM

Khaldoyanidi K.A.

Nikolaev Institute of Inorganic Chemistry, Siberian Branch of the Russian Academy of Sciences, 630090 Novosibirsk, Russia
E-mail: khad@niic.nsc.ru



Presently similar finding was never carrying out. It concerns to the problem of fluid surface localization in the p — V — T -diagram of a one-component system. There is a widespread view that the supercritical (fluid) state of an individual substance is located both above critical isotherm and critical isobar of liquid vaporization. The well-known monograph of Vogel R. also demonstrate the p — V — T -diagram, but in this one is only the critical isotherm represented [1]. There are also a lot of diagrams and emblems of thermodynamic conferences with various attempts to imagine the fluid phase state in supercritical region of a pure individual solvent. Hence the question arises: why did not many of authors imagine in p — V — T -diagram also the curve of the critical isobar? The matter is that in this case one branch of critical isobar curve would be found on fluid surface located above the critical isotherm, and this fact requires rational explanation. In this manuscript by

the methods of Gibbs and Schreinemakers has been proved that fluid surface is located between the high-pressure branch of the critical isotherm and the high-temperature branch of the critical isobar. This conclusion was based on the fact that the subcritical isotherms and isobars must not be appeared on the supercritical surface in p — V — T -diagram. Thus, the fluid surface is localized between liquid and vapor surfaces. So far as liquid—fluid and fluid—vapor transitions cannot be observed experimentally, conodes characterizing theoretically the corresponding two coexisting phases are presented in p — V — T -diagram with dotted lines (Fig.). Also the before accepted meaning of fluid location should be corrected and qualified as erroneous as far as the fluid surface cannot be located simultaneously above all length of critical curves (isobar and isotherm) but only between parts of them. On this established fact it has been constructed the comprehensive three-axis diagram in which all surfaces of solid, liquid, fluid and vapor states of one-component system are presented. Unlike published recommendations the above presented notion may be successfully use for imagine phase diagrams of multicomponent systems in supercritical region [2]. It should be noted also that in developing high-tech by using high pressure and temperature it is desirable to have the knowledge on fluid phase localization of concrete solvents.

1. R. Vogel, Die heterogenen Gleichgewichte, Akad. Verlagsgesellschaft, Leipzig, 1959.
2. K.A. Khaldoyanidi, *Rus. J. Phys. Chem.* **80** (4) 495 (2006).
3. K. A. Khaldoyanidi, *Russ. J. Phys. Chem. A* **85** (12), 2088 (2011).
4. K. A. Khaldoyanidi, *Russ J. Inorg. Chem.* **56**, 1827 (2011).
5. K. A. Khaldoyanidi, *Russ. J. Inorg. Chem.* **58**, 1106-1112 (2013)



THE STUDY OF SOLUTION EQUILIBRIA WITH Au(III) PARTICIPATION BY CAPILLARY ZONE ELECTROPHORESIS

Kharlamova V.Yu., Mironov I.V., Kokovkin V.V.

Nikolaev Institute of Inorganic Chemistry, Siberian Branch of the Russian Academy of Sciences, 630090 Novosibirsk, Russia

E-mail: kharlamova@niic.nsc.ru

The number of methods for quantitative investigation of solution equilibrium is not too large. The vast majority of equilibrium constants were obtained by either different variants of potentiometry or spectrophotometry. Other methods are used rarely because primarily of insufficient accuracy. On the other hand, these methods frequently give additional information on forms and provide larger certainty when investigating complicated systems.

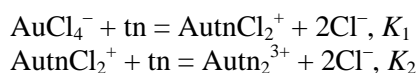
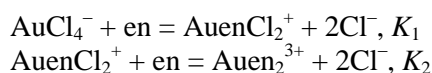
In this work, we applied capillary zone electrophoresis (CZE) in study of chloride ions substitution in AuCl_4^- on ethylenediamine (en) and 1,3-diaminopropane (tn, $\text{NH}_2-(\text{CH}_2)_3-\text{NH}_2$).

Based on separation of ionic forms in a capillary under electrical field applied, CZE is widely used for determination of simple and stable ions. However, CZE can be used for investigation of some processes with complex formation [1, 2]. The main advantages of CZE are the possibility of forms separation and determination of their characteristics, first of all, spectra and concentrations, without influence of other forms.

The objective of the work is to clarify the possibility of CZE application for investigation of systems with formation complexes and obtaining additional information on processes and forms including determination of substitution constants.

The measurements were carried out using Agilent ^{3D}CE 1600A (Agilent Technologies, USA) system with diode array detector. This system allows to detect at constant wave length and to obtain UV- and VIS-spectrum at any part of electropherogram peak.

For systems as gold(III) – ethylenediamine and gold(III) – propylenediamine, both, the substitution steps are substantially divided ($K_1 \gg K_2$) [3]



As a result, each system can be presented by two subsystems: ($\text{AuCl}_4^- + \text{AuenCl}_2^+$) and ($\text{AuenCl}_2^+ + \text{Auen}_2^{3+}$); ($\text{AuCl}_4^- + \text{AutnCl}_2^+$) and ($\text{AutnCl}_2^+ + \text{Autn}_2^{3+}$).

For the investigation of these systems by CZE, there were prepared working solutions contained two complex forms. In full agreement with this understanding at the electropherograms of equilibrated solution, there were observed two peaks.

Because in the systems with ligands substitution, the concentrations computation from calibration curves is possible only for extreme forms, for example for AuCl_4^- , the calculation of intermediate forms were made by using mass balance equations. The $[\text{H}^+]$ values were determined by means of glass electrode measurements.

Using CZE method, there was studied the substitution of chloride ions in AuCl_4^- on ethylenediamine and propylenediamine at $I = 0.05 \text{ M}$, $t = 25 \text{ }^\circ\text{C}$.

The substitution constants were determined for equilibriums: $\text{AuenCl}_2^+ + \text{en} = \text{Auen}_2^{3+} + 2 \text{Cl}^-$, $\lg K_2 = 10.4$; $\text{AuCl}_4^- + \text{tn} = \text{AutnCl}_2^+ + 2 \text{Cl}^-$, $\lg K_1 = 16.1$; $\text{AutnCl}_2^+ + \text{tn} = \text{Autn}_2^{3+} + 2 \text{Cl}^-$, $\lg K_2 = 12.0$.

The equilibrium constants obtained are in agreement with literature data and independent method.

1. Benes M., Zuskova I., Svobodova J. et al. Electrophoresis, 2012, 33, 1032.
2. Petit J., Geertsen V., Beaucaire C. et al. Journal of Chromatography A, 2009, 1216, 4113.
3. Mironov I.V., Tselodub L.D. Russ. J. Inorg. Chem., 2000, 45, 361.



THERMODYNAMICS AND TOPOLOGY OF CVD DIAGRAMS

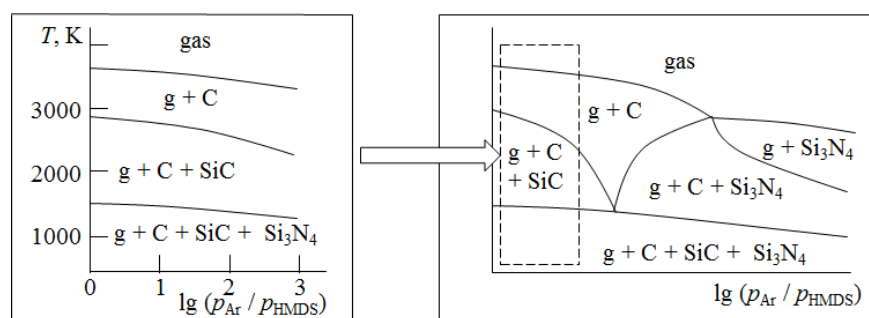
Kosyakov V.I., Shestakov V.A., Merenkov I.S., Kosinova M.L.

Nikolaev Institute of Inorganic Chemistry, Siberian Branch of the Russian Academy of Sciences, 630090 Novosibirsk, Russia
E-mail: kosyakov@niic.nsc.ru

The process of film formation by chemical vapor deposition in a flow reactor (CVD process) is performed in a multicomponent system at specified values of T and P . Gas composed from the main and auxiliary reagents and carrier gas inputs to the reactor. The film consisting of one or more condensed phases deposited as a result of chemical reactions in the gas phase and on the surface of the substrate. The a priori knowledge of the important features of the CVD process can be obtained by thermodynamic modeling. It is assumed that the chemical composition of the system coincides with the elemental composition of the input gas. Thermodynamic equilibrium between the film and the gas phase is established in the reactor. Under these assumptions, equilibrium to a CVD reactor is equivalent to the equilibrium in cylinder with a piston. CVD process is carried out in t -component system, in which the sample condition described by $(t + 1)$ values. The simulation results represent as the CVD two-dimensional diagrams, the coordinates of which are the two selected variables ξ' and ξ'' of this set of values, or their combinations. CVD diagram is calculated in the predetermined area ($\xi_1' \leq \xi' \leq \xi_2'$; $\xi_1'' \leq \xi'' \leq \xi_2''$) varying the parameters. Its relationship with the phase diagram of the chemical system is obvious. Phase diagram of the t -component system is a fragmentation of the P - T field, every point of which is associated with the concentration simplex of $(t - 1)$ dimension. It is divided into regions of stability of different phases and phase associations. For CVD processes interesting part of the diagram is the one, in which the presence of a gas g and condensed c_1, c_2, \dots phases. The dimension of the fields $f_1 = g + c_1, f_{12} = g + c_1 + c_2$ and so on is equal $t + 1$. CVD diagram is the cross section of an area of phase diagram by ξ' - ξ'' plane. It is formed from f_1, f_{12}, \dots field of different phases and phase associations deposition. Regularities of the CVD diagrams structure is determined by the features of the cross section structure of the phase diagrams of multicomponent systems. For their analysis, you can use the thermodynamic and topological approaches.

Thermodynamic modeling allows the following: (a) to determine the phase composition of the film and create CVD diagrams; (b) to determine the dependence of the chemical composition of the film on the deposition conditions; (c) to calculate the partial pressure of molecular species in the gas phase in equilibrium with the solid precipitate, and in metastable gas in the absence of a solid phase; (d) to describe the formation of a solid phase by a system of equations of heterogeneous chemical reactions; (e) to determine the equation of phase and chemical reactions on the boundaries between neighboring areas of CVD diagram; (f) to determine the conditions of formation of impurity phases.

Topological approach to the CVD diagram study is based on the construction of graphs of the phase diagrams or schemes of phase reactions. This approach allows the following: (a) to determine the ratio between the amounts of the main elements of diagrams displayed in the form of vertexes, edges, faces of the graphs; (b) to list enumerate the possible variations of CVD diagrams; (c) to classify CVD diagram according to their structure; (d) to use the results for prediction of the possible schemes of CVD diagrams based on an analysis of phase relations in specific chemical systems; (e) to use a topological approach to analyze the structure of the CVD diagrams outside the fragment constructed on the results of thermodynamic modeling; (f) to build a topological images of CVD diagrams for the system with metastable phases.



The results of calculation of CVD diagram fragment for Si-C-N-H-Ar system at $P = 1$ atm, and scheme extended fragment of the diagram.
HMDS = $(\text{CH}_3)_3\text{SiNHSi}(\text{CH}_3)_3$



THERMODYNAMIC ANALYSIS OF DNA DAMAGE RECOGNITION BY REPAIR ENZYMES

Kuznetsov N.A.^{1,2} and Fedorova O.S.^{1,2}

¹*Institute of Chemical Biology and Fundamental Medicine (ICBFM), Siberian Branch of Russian Academy of Sciences, 8 Lavrentyev Ave., Novosibirsk 630090, Russia*

²*Department of Natural Sciences, Novosibirsk State University, 2 Pirogova St., Novosibirsk 630090, Russia*
E-mail: nikita.kuznetsov@niboch.nsc.ru, fedorova@niboch.nsc.ru

Base excision repair begins by the actions of DNA glycosylases, which detect and eliminate damaged heterocyclic bases. Many types of DNA damages only slightly alter the chemical structure of DNA and have virtually no effect on the double-helical structure, because such damages are often localized in the helix inner part that makes their detection especially difficult. As a rule, such types of damages occur, on average, with the frequency of one per million nucleotides. DNA glycosylases are of very high specificity and can quickly detect damages among a huge number of undamaged nucleotides. Then apurinic/apyrimidinic endonucleases remove the remaining deoxyribose phosphate residue. The resulting one-nucleotide gap contains a hydroxyl group on the 3'-end and a phosphoric acid residue on the 5'-end. DNA polymerase joins the desired nucleotide, and DNA ligase completes the repair, restoring the deoxyribose phosphate backbone integrity.

It is still unclear how DNA repair enzymes efficiently select sparse lesions among the enormous excess of normal DNA. Understanding of the mechanism of the DNA damaged base recognition by DNA repair enzymes may be improved by elucidation of the thermodynamics of the binding and cleavage steps via determination of their Gibbs free energy (ΔG°), enthalpy (ΔH°) and entropy (ΔS°). Correlation of the thermodynamic data with the proposed sequential mechanism of damaged site binding and cleavage might result in the quantitative description of the driving forces that govern the structural adjustment of the enzyme and DNA.

In the present work, thermodynamic analysis of fast stages in the course of formation of catalytically competent states of the enzymes' interior complexes with DNA possessing damaged sites was based on results of the pre-steady-state kinetic studies. These data were obtained by recording the fluorescence of proteins and DNA and were of help for more detailed comprehension of the mechanism of detection of damaged bases and AP sites by DNA glycosylases and AP endonucleases responsible for the key function of elimination of damaged nucleotides and recovery of the native structure of DNA. Data obtained for DNA glycosylases Fpg and hOGG1 and for AP endonuclease APE1 indicate an important feature of the damage site recognition. Since the lesions of bases are small in volume and the bases themselves are localized inside the double helix, they are detected by these enzymes due to a successive compactization of structures of protein–nucleic acid complexes, which is necessary for increasing the number of intermolecular contacts. Such change in the structure of enzymes and DNA requires additional energy consumption, which is compensated by an increase in entropy of the system as a result of release of water molecules from the area of contacts.

This work was supported by the Federal Agency of Scientific Organizations (project 6.11 of the Russian Academy of Sciences in the “Molecular and Cellular Biology” program) and by the Russian Foundation for Basic Research (projects Nos. 16-04-00037 and 15-04-00467). The part of the work including analysis of experimental data for human 8-oxoguanine DNA glycosylase was supported by the Russian Scientific Foundation (project No. 14-14-00063). The part of the work including analysis of experimental data obtained for human AP endonuclease was supported by the Russian Scientific Foundation (project No. 16-14-10038).



**ACOUSTIC, VOLUMETRIC, COMPRESSIBILITY AND REFRACTIVITY
PROPERTIES OF BINARY MIXTURES CONTAINING METHYL ISOBUTYL
KETONE AT SEVERAL TEMPERATURES**

Faiza Ouair¹, Amina Negadi¹, Latifa Negadi^{1,2}, Ilham Mokbel^{3,4}, Jacques Jose³

¹ LATA2M, Laboratoire de Thermodynamique Appliquée et Modélisation Moléculaire, University of Tlemcen, Post Office Box 119, Tlemcen 13000 (Algeria)

² Thermodynamics Research Unit, School of Engineering, University of KwaZulu-Natal, Howard College Campus, Durban, 4041, South Africa.

³ Laboratoire Multimatériaux et Interfaces, UMR 5615, Université de Lyon, Université Claude Bernard Lyon1, 69622 Villeurbanne, France.

⁴ Université de Saint Etienne, Jean Monnet, F-42023 Saint Etienne, Université de Lyon, F-42023 Saint Etienne, France.

Abstract

With the steadily increasing energy consumption contributing to the depletion of fossil resources, the insecurity of energy supply and global warming, renewable energy resources emitting less CO₂ become popular alternatives to substitute fossil fuels, especially in the transportation sector which is responsible for a large part of the global CO₂ emissions.

Among many energy alternatives, biofuels, hydrogen, natural gas and syngas may likely emerge as the four strategically important sustainable fuel sources in the foreseeable future. Within these four, biofuels are the most environment friendly energy source. Hence, biofuels are being explored to replace fossil fuels. They are favorable choice of fuel consumption due to their renewability, biodegradability and generating acceptable quality exhaust gases. Biofuels are referred to liquid, gas and solid fuels predominantly produced from biomass. A variety of fuels can be produced from biomass such as ethanol, methanol, biodiesel, Fischer-Tropsch diesel, hydrogen and methane.

The present work is a continuation of a research program concerning the investigation of the thermodynamic properties of binary mixtures containing solvents derived from biomass.

In this paper, we report the experimental densities, speeds of sound, and refractive indices for four binary mixtures: (MIBK + DMSO), (MIBK + Acetone), (MIBK + Acetonitrile), or (MIBK + Cyclohexane) measured over the entire composition range and in the temperatures range (283.15 to 313.15) K at 10 K intervals. To our knowledge, there are no other published data that are available in the literature for the investigated systems.

From these experimental data, excess molar volume, isentropic compressibility, excess isentropic compressibility, refractive index deviation, excess refractive index, molar refraction, and molar refraction deviation have been calculated over the entire composition range and at each temperature.

Excess molar volume, excess isentropic compressibility, excess speed of sound, excess refractive index, and molar refraction deviation data have been correlated using the Redlich–Kister equation. The thermodynamic properties have been discussed in terms of the nature of molecular interactions between the components of the mixture.

Additionally, the VTPR and PSRK equations of state have been used to calculate the investigated properties.

Keywords: MIBK, density, speed of sound, refractive index; biomass.

MIXING ENTHALPY OF Ag-Sn SYSTEM AT 1150 °C

Oleinik K.I., Bykov A.S., Pastukhov E. A.

Institute of Metallurgy, Ural Branch of the Russian Academy of Sciences, 620016 Ekaterinburg, Russia

E-mail: 1007o1007@gmail.com

This paper presents thermodynamic results of Ag-Sn alloys mixing at 1150 °C. The need for binary data on mixing enthalpy ΔH_{mix} had appeared in the process of calorimetric study of the ternary system Ag-Cu-Sn known as the promising lead-free solder.

The mixing enthalpies of Ag-Sn system were measured by drop calorimetry method at 1150 °C using SETARAM MHTC thermal analyzer. All the tests were conducted in the dynamic protective atmosphere of argon 99.999 with the gas flow rate of 10 ml/min. The calorimeter's sensitivity calibration was done using pure metals (Ag, Sn) and standard leucosapphire samples and consisted of two stages. Initial calibration was performed by repeated dropping of Ag or Sn samples into analytical crucible in the process of gradual accumulation of the respective 1st component before alloy formation beginning. The final calibration took place after alloy formation and involved several additions of the sapphire pieces on the surface of as-prepared liquid alloy. It was shown in [4] that the use of two-stage calibration procedure improves significantly the convergence of two branches of ΔH_{mix} isotherm plotted from the pure component towards each other. The experimental results were approximated with analytical function using quasi-chemical modification of subregular solutions model (quasi-chemical model of Sharkey et. al. [5]) postulating the presence of both pair and triple interactions in solution. The measured compositional dependence of ΔH_{mix} is substantially asymmetric like the reference data, but, on the contrary, it doesn't change the sign and keeps negative value in the whole range of concentrations, as shown in Fig.1. The most noticeable exothermic interactions are observed in the compositional area between 10 and 30 at.% of Sn. This fact correlates well with the presence of several intermetallic compounds in the Ag-rich part of Ag-Sn system phase diagram.

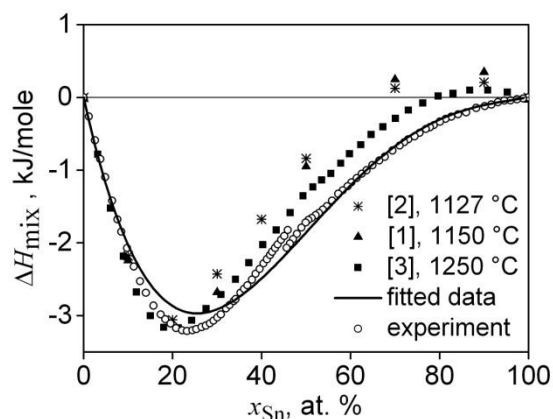


Fig. 1. Experimental and fitted values of mixing enthalpy at 1150 °C along with the available reference data [1-3].

The work was carried out within the State Assignment (Project No 0396-2015-0079) using shared equipment of the "Ural-M" Centre.

The work was carried out within the State Assignment (Project No 0396-2015-0079) using shared equipment of the "Ural-M" Centre.

References:

- [1] Kubaschewski O., Alcock C.B. Metallurgical thermochemistry. Moscow: Metallurgia, 1982. (In Rus.).
- [2] Hultgren R., Orr R.L., Anderson P.D., Kelley K.K. Selected Values of Thermodynamic Properties of Metals and Alloys. John Wiley & Sons. New York, 1963.
- [3] Flandorfer H., Luef C., Saeed U. On the temperature dependence of the enthalpies of mixing in liquid binary (Ag, Cu, Ni)-Sn alloys. J. Non-Cryst. Solids. 2008, vol. 354, p.p. 2953-2972.
- [4] Bykov A.S., Filippov V.V., Pastukhov E.A. Drop Calorimetry of Alloy Formation in the System Cu-Ag. Proceedings of XIV International Conference on Thermal Analysis and Calorimetry in Russia. Saint Petersburg: Publishing House of the Polytechnical University, 2013, p.p. 356-358. (In Rus.).
- [5] Sharkey R. L, Pool M. J., Hoch M. Thermodynamic Modeling of Binary and Ternary Metallic Solutions. Metall. Mater. Trans. B. 1971, vol. 2, p.p. 3039-3049.



INVESTIGATION OF THE SOLID – LIQUID PHASE EQUILIBRIA IN THE WATER MAGNESIUM – METHANSULFONATE SYSTEM

D.I. Provotorov, D.A. Kosova, I.A. Uspenskaya

Department of Chemistry, Lomonosov MSU, 119991, Moscow, Russia

E-mail: provotorov.d.i@gmail.com

Investigation of the properties of methanesulfonic acid's salts and systems based on them is of interest from the fundamental point of view. Information on properties of these salts is given partially in the literature, in spite of widely using of methanesulfonic acid and its inorganic derivatives in various industries [1,2]. In particular it is important to research properties of magnesium methanesulfonate and corresponding water-salt system because of geochemistry. Recently researchers have found sodium, potassium, magnesium and calcium methanesulfonates and their hydrates in ice cores of Antarctica [3]. The properties of ice and the ice crystal inclusions can be used to reconstruct the climate changes or ocean composition during the ice cores formation. Thermodynamic modeling allows to predict the most likely mineral structure of geological objects according to its elemental composition or to determine the conditions of formation of any mineral association observed in nature (geothermobarometry). It is desirable to know stability parameters of the individual substances and the data on phase equilibria in the binary systems for correct thermodynamic modeling of the systems of various dimensions.

The aims of this work were (1) estimation of the magnesium methanesulfonate ($\text{Mg}(\text{SO}_3\text{CH}_3)_2$) and its hydrates thermal stability; (2) determination of its phase transition parameters (temperatures and enthalpies); (3) investigation of the phase equilibria in the $\text{H}_2\text{O} - \text{Mg}(\text{SO}_3\text{CH}_3)_2$ system.

With the help of thermogravimetry (TGA) thermal stability of $\text{Mg}(\text{SO}_3\text{CH}_3)_2$ and its hydrates was evaluated in a flow of dry air. Phase transition parameters of the substances formed in the $\text{H}_2\text{O} - \text{Mg}(\text{SO}_3\text{CH}_3)_2$ system were estimated by differential scanning calorimetry (DSC). Liquidus and solidus coordinates in the system $\text{H}_2\text{O} - \text{Mg}(\text{SO}_3\text{CH}_3)_2$ were determined in a wide range of concentrations by means of DSC. Solubility of $\text{Mg}(\text{SO}_3\text{CH}_3)_2$ hydrates was determined by complexometric titration of saturated solutions. All obtained data would be used further for the construction and validation of the thermodynamic models of the solid and liquid phases in the $\text{H}_2\text{O} - \text{Mg}(\text{SO}_3\text{CH}_3)_2$ system.

[1] P.K. Leung, C. Ponce-de- León, , C.T.J. Low, A.A. Shah, F.C. Walsh, J. Power Sources, 196 (2011), 5174-5185

[2] G.Nikiforidis, W. A. Daoud, Electrochim. Acta, 141 (2014), 255-262

[3] T. Sakurai, H. Ohno, F. E. Genceli, S. Horikawa, Y. Iizuka, T. Uchida, T. Hondoh, J. Glaciol, Vol. 56 (2010), 837–842

This work was performed by financial support of RFBR № 16-33-00958



THERMODYNAMICS OF $\text{REPO}_4\text{-REVO}_4$ (RE= La, Gd, Y) SOLID SOLUTIONS

Ryumin M.A., Tyurin A.V., Kritskaya A.P., Nikiforova G.E., Gavrichev K.S.

Kurnakov Institute of General and Inorganic Chemistry of the Russian Academy of Sciences, 119991 Moscow, Russia

E-mail: Ryumin@igic.ras.ru

Rare earth orthophosphates and orthovanadates are of interest for the synthesis of functional materials that would have high chemical and thermal stability. In particular, they are promising as luminophors and luminophor matrices, active environment of solid state lasers, thermal barrier materials, and also for the utilization of radioactive wastes, as they can form rather extensive solid solutions.

Anionic or cationic substitutions making the solid solution composition more complex provide a flexible variation and improvement of required properties. However, the monazite and xenotime structures typical for these species, although being allied, considerably hinder the prediction of formation of solid solutions with a certain degree of substitution despite. Studies of the fundamental thermodynamic properties of some representatives of these classes of compounds can enable one to determine the existence regions of solid solutions by computational methods and to expand the existing notions of the structure types themselves.

The reagents used in this study were $\text{NH}_4\text{H}_2\text{PO}_4$ and NH_4VO_3 of pure for analysis grade and RE_2O_3 of chemically pure grade. To synthesize $\text{RE}(\text{VO}_4)_{1-x}(\text{PO}_4)_x$ (RE=La, Gd, Y) solid solutions, a mixture of the initial reagents in stoichiometric amounts was mechanically homogenized in acetone. The resulting mixture was annealed for 48 h at 1373 K, which was attained in 24 h.

Continuous solid solution in the lanthanum and yttrium system was obtained using solid state synthesis at 1000°C. Single phase $\text{Gd}(\text{VO}_4)_{1-x}(\text{PO}_4)_x$ solid solution samples ($x = 0, 0.05, 0.15, 0.25, 0.5, 0.55,$ and 0.6) with xenotime structure were synthesized, but the samples with a phosphate content of 0.65, 0.75, 0.85, and 0.95 wt % were not single phases. The calculated values of unit cell parameters for the synthesized compounds and the plots of their dependences on the degree of substitution confirm that their variations obey the Vegard law.

The heat capacity of solid solutions was studied as a function of temperature in the region of 6–350 K using a BKT 3 adiabatic vacuum calorimeter. Experimental heat capacities curve were smoothed with the use of spline approximation or polynomial approximation. The thermodynamic functions (entropy $S^0(T)$, enthalpy change $H^0(T) - H^0(0)$, and reduced Gibbs energy $\Phi^0(T)$) were calculated from smoothed heat capacities.

On the heat capacities curves in lanthanum and yttrium system $\text{RE}(\text{VO}_4)_{1-x}(\text{PO}_4)_x$ (RE=La, Y, $x=0.25, 0.5, 0.75$) has no anomalies but heat capacity curve in Gd ($x=0.50$) system has magnetic anomalies at the lowest temperatures. Analyzing the heat capacity, entropy and enthalpy change of the tested solid solutions at 298.15 K and standard pressure as dependent on the substitution level of vanadate for phosphate ion, we observed a deviation from the linear values calculated by the Neumann–Kopp rule in some compositions, this deviation exceeds the experimental error. Thus, it is possible to state a deviation of the studied solid solutions from ideal.

This study was supported by the Presidium of the Russian Academy of Sciences through program no. I14P-5 using the facilities of the Shared facilities Center of the Kurnakov Institute of General and Inorganic Chemistry.

PHASE EQUILIBRIA IN THE Cu–Ce–La–O SYSTEM UNDER THE CONDITIONS OF METAL MELT EXISTENCE

Samoilova O.V.¹, Makrovets L.A.¹

¹South Ural State University, 454080 Chelyabinsk, Russia

E-mail: samoylova_o@mail.ru

Cu–Ce–La–O system has an interest for the technological processes of production copper and copper-based alloys because it is possible to obtaining a deep deoxidized molten copper using cerium and lanthanum elements as reducing agents.

The method of constructing of the surface of components solubility in a metal melt was used for thermodynamic modeling of phase equilibria, which are realizing in the Cu–Ce–La–O system under conditions of existence of the molten metal. This method allows either construction the isotherms of oxygen solubility in molten metal in the investigated system, or to relate the micro-changes in composition of the metal melt with qualitative changes in the composition of the reaction products. The thermodynamic characteristics of deoxidation molten copper by cerium and lanthanum process were first evaluated with the help of modeling. These characteristics include the equilibrium constants of reactions occurring with the components of the metal melt in the Cu–Ce–La–O system, parameters of the first order interaction for the investigated system and the coefficients activity of the oxide melt components of the Cu_2O – CeO_2 – Ce_2O_3 – La_2O_3 system.

The surface of components solubility in a metal melt in the system Cu–Ce–La–O at the temperature of 1200°C is shown in Fig. 1. In the area I liquid metal is in equilibrium with the pure solid cuprous oxide Cu_2O ; in area II – it is with the oxide melt (O.m.) variable composition (Cu_2O , CeO_2 , Ce_2O_3 , La_2O_3); in the area III – it is with a solid solution $|\text{CeO}_2, \text{La}_2\text{O}_3|_{\text{ss}}$; in IV - with pure ceria solid Ce_2O_3 .

According to modeling, mechanism of complex deoxidation is typical for the system Cu–Ce–La–O. It should also be noted that cerium and lanthanum are strong deoxidizers and they can reduce the concentration of oxygen in the molten copper to extremely small values.

The reported study was funded by the Russian Foundation for Basic Research according to the research project № 16-mol_a_dk. 38-60144

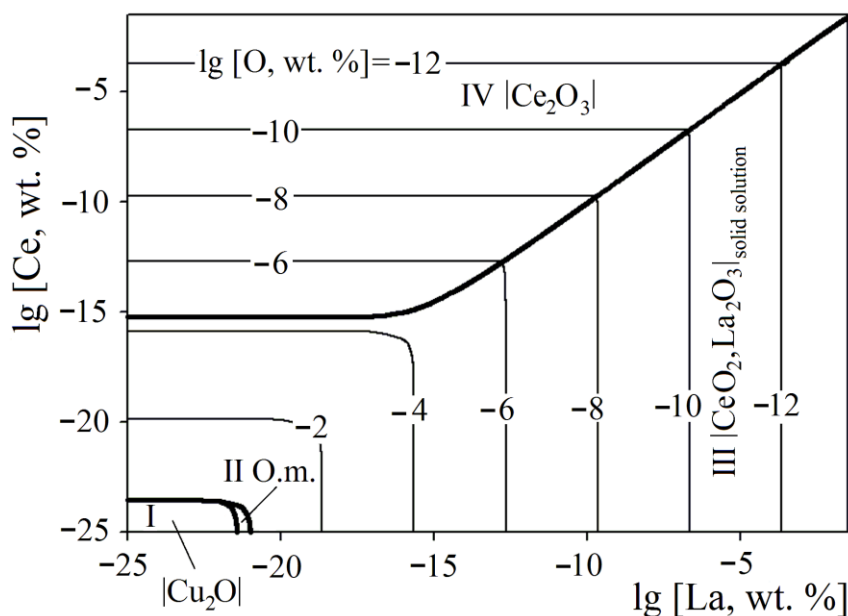


Figure 1. The surface of components solubility in a metal melt in the system Cu–Ce–La–O at the temperature of 1200°C.

THERMODYNAMIC MODELING OF PHASE EQUILIBRIA IN THE Cu–Mn–Bi SYSTEM

Samoilova O.V.¹, Zaiceva O.V.², Igizianova A.Y.²

¹South Ural State University, 454080 Chelyabinsk, Russia

²Zlatoust Branch of South Ural State University, 456209 Zlatoust, Russia

E-mail: samoylova_o@mail.ru

Cu–Mn–Bi system is an interest as a basis for the creation of new classes of bronzes with ferromagnetic properties. Magnetic properties to these alloys should be given by MnBi inclusion. Such compounds are formed by the interaction of the alloys components at melting and are uniformly distributed in bronze ingots after crystallization.

It should be noted that information about the phase diagram of this system do not occurs in the literature. The aim of this work is to carry out the thermodynamic modeling of phase equilibria in the Cu–Mn–Bi system in order to construction polythermal sections of the phase diagram of the investigated system and to determine the conditions of allocation MnBi compound particles during crystallization.

The CALPHAD method was used in the process of the thermodynamic description of phase equilibriums in the Cu–Mn–Bi system under conditions of a liquid metal existence, as well as after crystallization.

The software package FactSage (version 7.0) was used for thermodynamic modeling. For the calculating polythermal sections of the studied system (as well as for modeling of the Cu–Mn, Cu–Bi, Mn–Bi double metallic systems diagrams) we used the data from SGTE2011 databases (as amended in 2013), SGPS.

Analyzing the results of simulation (an example is shown in Fig. 1), it can be concluded that the compound MnBi can be obtained by crystallization of a melt of copper and by further cooling the obtained solid solution at a certain temperature (for an alloy Cu–5wt.% Mn–1 wt.% Bi, this temperature is 600°C).

The reported study was funded by the Russian Foundation for Basic Research according to the research project № 16-08-00133 a.

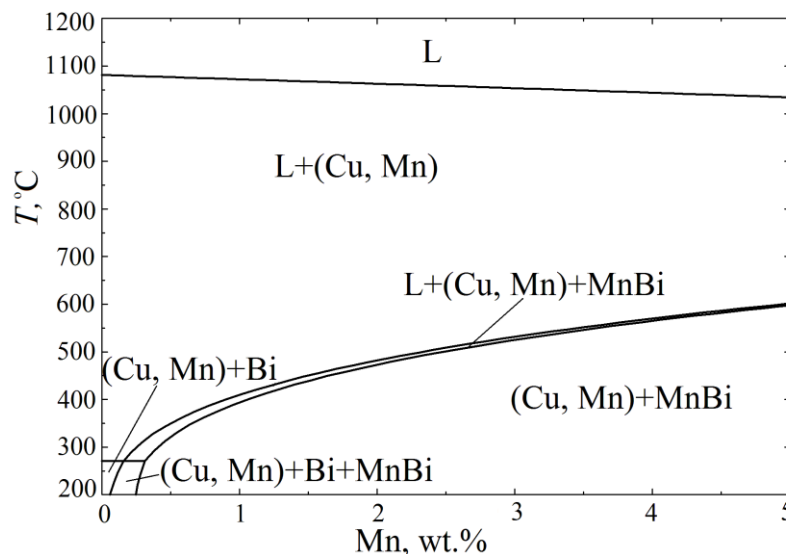


Figure 1. The polythermal section of the phase diagram of the Cu–Mn–Bi system. The bismuth concentration is 1 wt. %; (Cu, Mn) – solid solution of manganese in the copper.



THERMOPHYSICAL PROPERTIES OF ALTERNATIVE FUELS AND HEAT TRANSFER FLUIDS HIGH PRESSURES AND OVER A WIDE RANGE OF TEMPERATURES

Suleymanli Kh.¹, Huseynova G.¹, Savchenko I.², Safarov J.T.^{1,3},
Bashirov M.M.¹, Shahverdiyev A.N.¹, Hassel E.P.³

¹Department of Heat Energy, Azerbaijan Technical University, AZ-1073 Baku, Azerbaijan

²Kutateladze Institute of Thermophysics, Siberian Branch of the RAS, 630090, Novosibirsk, Russian Federation

³Institute of Technical Thermodynamics, University of Rostock, D-18059 Rostock, Germany

The various ecological, environmental problems of last decades, also the increasing role of alternative renewable fuels are deciding the production of a sustainable fuel supply. They can be successful use as a fuel in an internal combustion engine and can demonstrate to work in vehicles with gasoline engines without modification. One important development resulting from scientific investigations over the last decades is fuel evaporation within the combustion chamber by common rail injection systems which employ more than 100 MPa pressure and this injection pressure is constantly going up. In a near future, injection systems can be designed for higher pressures up to 400 MPa. Number of injections at such high pressures per cycle can be expanding and the time of one injection process can be reduced. That is why it is so important to have reliable knowledge of thermophysical properties of the fuel under high pressures. Study of basic thermophysical properties (density, vapor pressure, viscosity, speed of sound, heat capacity etc.) of fuels and their blends with alcohols would allow modeling, understanding, and optimizing the processes in an internal combustion engine.

Ionic liquids (ILs) during the last years have been used in catalysis, separation process, electrochemistry etc. because of good physical and chemical properties, such as small vapor pressure, a wide liquid range and relatively favorable viscosity and density characteristics. They are ideal substances for using as heat transfer fluids in absorption refrigeration and heat pump systems, because they have very low vapor pressure and good solubility with different natural solvents (refrigerants) such as aliphatic alcohols. The using of such binary mixtures of ILs with organic solvents in such systems needs the thermophysical properties of pure components and mixtures, VLE data, activity coefficients etc.

In this work, we will present the (p, ρ, T) properties, heat capacity, viscosity vapor pressure, speed of sound of diesel fuel or various imidazolium base ILs blends or mixtures with aliphatic alcohols (methanol, ethanol and 1-butanol) up to $p = 200$ MPa and over a temperature range $T = (263.15$ to $468.15)$ K. Investigations covering such an extended p, T -range were performed the first time for these ILs. The (p, ρ, T) properties were carried out using a specially adapted high pressure – high temperature Anton Paar DMA HPM vibration-tube densimeter with an estimated relative combined standard uncertainty of $\Delta\rho/\rho = \pm (0.01$ to $0.08)$ % in density.

The ambient or saturated pressure investigations were carried out using the following installations:

- The density values $\rho(p_0$ or $p_s, T)$ using the Anton Paar DMA 5000M, DSA 5000M and DMA HPM vibration tube densimeters.
- Vapor pressure values P/Pa using the two high-accuracy static experimental set ups.
- The dynamic viscosity $\eta(p_0, T)$ using an Anton Paar SVM 3000 Stabinger Viscometer and Anton Paar Rheometer MCR 302.
- The constant pressure specific heat capacity $c_p(p_0, T)$ using the Pyris 1 DSC Differential Scanning Calorimeter.
- The speed of sound values $u(p_0, T)$ using the Anton Paar DSA 5000M vibration tube densimeter and sound velocity meter.

An equation of state was established using parameters based on the new results to calculate the isothermal compressibility κ_T , isobaric thermal expansibility α_p , thermal pressure coefficient γ , internal pressure π , specific heat capacities at constant pressure c_p and at constant volume c_v , speed of sound u , and isentropic exponent κ_s for of investigated mixtures at $T=(263.15$ to $468.15)$ K and pressures up to $p = 200$ MPa.

CORROSION OF ALLOYS OF THE Cu-Zr-O SYSTEM IN NaCl SOLUTION

Sharlay E.V., Samoylova O.V., Shunaylov A.V.

South Ural State University (National Research University), 454080 Chelyabinsk, Russia

E-mail: sharlayev@rambler.ru

The copper alloyed by zirconium dioxide with concentration of Zr to 0,15 wt % possess the improved strength characteristics, conditions of formation of the similar strengthened materials were studied [1]. It gave the possibility to receive the copper alloys with the content of zirconium 0,05 ... 0,15 wt % in practice.

This work represents a research of a corrosion and an electrochemistry features of the received exemplars. The electrochemical behavior of copper-zirconium system' alloys was studied with use of a cyclic voltammetry with the anodic-cathodic linear sweep of potential. The classic three-electrode cell was used. Working electrodes (2 mm×5 mm), chloride-silver reference electrode and a graphitized counter electrode were plunged into 0,5 M NaCl solution. The example of the received voltammograms is shown in the figure 1.

According to the obtained data, the alloy's zirconium is actively dissolved whereas copper is oxidized to Cu₂O and CuO which form the thick passivating film on a work surface. Comparison of electrochemical activity of alloys and pure copper testifies to a larger corrosion resistance of the studied alloys.

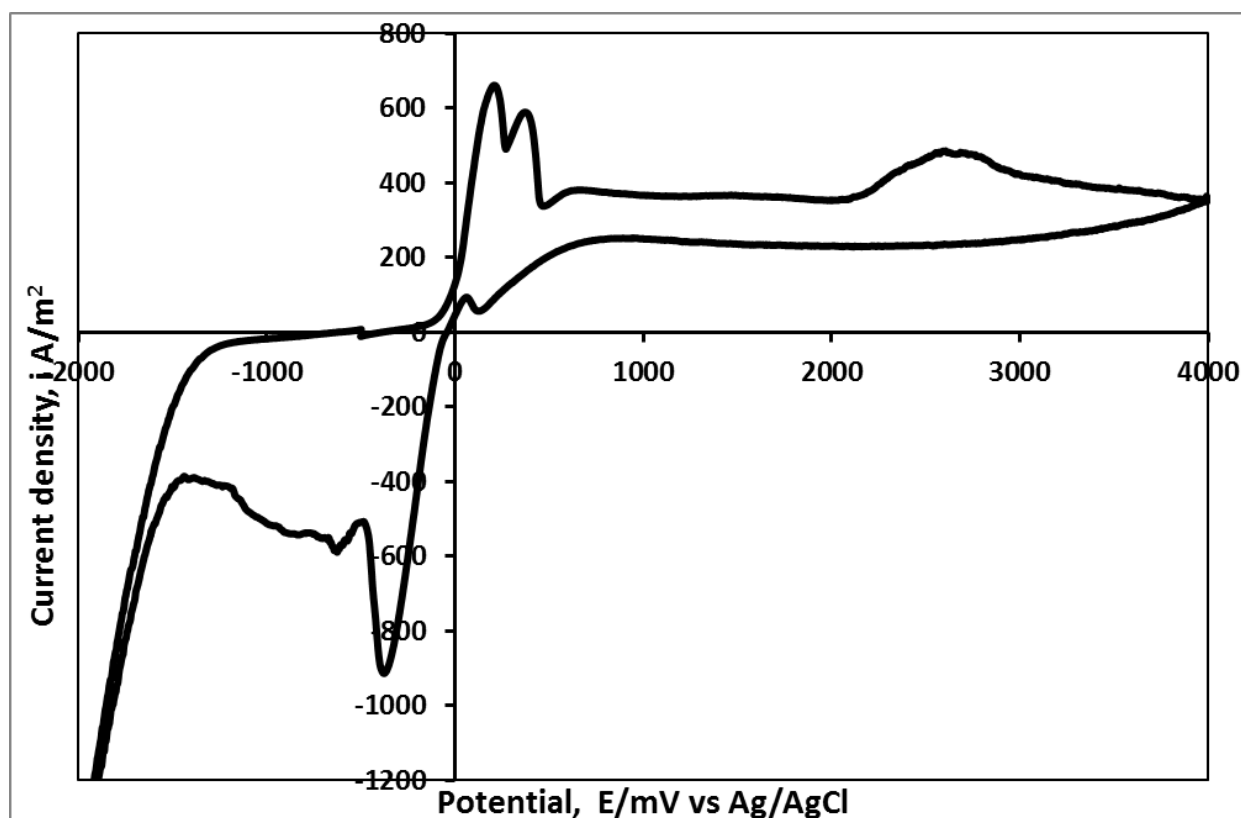


Figure 1. Cyclic voltammetry at Cu-ZrO₂ electrode in 0.5 M NaCl. 19 °C. Scan rate 25 mV/s.

The reported study was funded by the RFBR according to the research project № 16-08-00133a.

[1] Samoilova O. V., Mikhailov G. G., Trofimov E. A., Makrovets L. A., Russian Metallurgy (Metally), 9, 64–868



ABOUT SYSTEM ETHYLENE GLYCOL - DIMETHYLSULFOXID

Solonina I.A.¹, Kononova E.G.², Volkov V.V.³, Rodnikova M.N.¹

¹ N.S.Kurnakova Institute of General and Inorganic Chemistry RAS, Moscow, Russia

² A.N.Nesmeyanov Institute of Organoelement Compounds RAS, Moscow, Russia

³ A.V.Shubnikov Institute of Crystallography RAS, Moscow, Russia

E-mail: rodnikova@igic.ras.ru

Aqueous solutions of dimethyl sulfoxide (DMSO) are widely used in cryobiology due to strong supercooling and easy vitrification. They have been widely studied. At phase diagram H₂O - DMSO three compounds were registered: DMSO·3H₂O and two incongruent melting compounds - DMSO·2H₂O and DMSO·H₂O [1]. DMSO·2H₂O is the most stable in the liquid system [2]. Solvophobic effects of DMSO in H₂O solutions were found out only in the volume properties [3]. Microheterogeneous of low concentrations was marked by light scattering [4].

In the present study the system of ethylene glycol (EG) – DMSO was investigated. Selection is linked to the similarity of the EG with H₂O - both solvent have a spatial network of hydrogen bonds. It was interesting to compare the results of research. Methods of research were: DSC, infrared spectroscopy and X-ray scattering at small angles. System EG - DMSO was characterized by a strong supercooling, vitrification and the metastable region in the concentration range of 30 - 50 mol% DMSO, in which the formation of crystal solvates composition of ~35 mol% DMSO was taken place. It was very difficult to identify because of the high viscosity of the liquid phase. In the field of low-concentration solutions studied by X-ray scattering at small angles, microheterogeneous was not detected. Only volume properties indicated the presence in this system the solvophobic effects as in the DMSO-H₂O system [5].

1. Rasmussen D.H., Maskenzie A.R. // Nature (London) 1968. 220. P.1315
2. Luzar A., Chander D. // J.Chem.Phys. 1993. V.98(10). P.8160
3. Egorov G.I., Makarov D.M. // Russian Journal of Physical Chemistry A. 2009. T. 83. № 5. C. 693
4. Rodnikova M. N., Zakharova Yu. A., Solonina I. A., Sirotkin D.B. // Russian Journal of Physical Chemistry A. 2009. T. 83. № 5. C. 892
5. Egorov G.I., Makarov D.M. // Chemistry and him.tehnologiya. (Rus.) 2011. T.54 (11) P.65

This work was performed as part of a State Task of the Russian Academy of Sciences' Institute of General and Inorganic Chemistry in the field of basic research. It was supported by the Russian Foundation for Basic Research, project № 16-03-00897.

THERMODYNAMIC MODELLING OF PHASE EQUILIBRIA IN THE FERRITE CONTAINING OXIDE SYSTEMS

Trofimov E.A., Vinnik D.A., Zaiceva O.V., Chernukha A.S., Sudarikov M.V., Zhivulin V.E., Zherebtsov D.A.

South Ural State University, 454080 Chelyabinsk, Russia
E-mail: tea7510@gmail.com

The oxide systems including various ferrites (such as barium, strontium and lead hexaferrites) are of great interest. This can be explained by the fact that the phase diagrams of the ferrite systems are theoretical framework of melt-growth techniques used in magnetic materials manufacturing processes. At the present time the ferrite materials are required in many branches of industry such as ICT (terrestrial and satellite communications, radiolocation and radionavigation systems), magnetic recorders and storage devices production, development of general and special purpose radio photonics and microwave devices (microwave filters, phase shifters, isolators, generators, attenuators), etc.

Use of oxide flux in crystal growth of hexaferrites makes it possible to reduce the growth temperature to about 1300-1400 °C. That simplifies procedure conditions and makes it possible to make incongruent compounds. The multicomponent oxide systems like $\text{MeO-Fe}_2\text{O}_3\text{-R}_n\text{O-...}$ underlie crystal growth techniques and are of practical interest. However these systems are insufficiently explored.

Shortage of reference information about multicomponent oxide systems stimulated us to conduct research to determine model parameters for thermodynamic assessment of the phase diagrams. Phase equilibria have been investigated by differential thermal analysis, electron probe microanalysis and X-ray powder diffraction. The samples of oxide melts with different composition and temperature were quenched and prepared for further analysis. Nonvolatile compounds were studied using derivatograph MOM Q-1500 Paulik-Paulik-Erdey. Heat effects were investigated from 20 to 1500 °C by DTA measurements. Melting temperatures of the samples containing lead oxides were determined by precise temperature measurements below 1400 °C using calibrated thermocouple. The phase composition and crystal structure of each sample was checked by powder X-ray diffraction (XRD) using Rigaku Ultima-IV diffractometer with Cu K α emission.

Analysis of our own and literature experimental data led to making the thermodynamic database for assessment equilibria in the studied systems. Using these results and FactSage Thermochemical Software, coexistence curves of the phase diagrams $\text{BaO-Fe}_2\text{O}_3$ (Fig. 1), $\text{SrO-Fe}_2\text{O}_3$, BaO-FeO , $\text{BaO-B}_2\text{O}_3$, $\text{Fe}_2\text{O}_3\text{-Na}_2\text{O}$, BaO-PbO , $\text{Fe}_2\text{O}_3\text{-PbO}$, $\text{BaO-Fe}_2\text{O}_3\text{-Na}_2\text{O}$, $\text{BaO-Fe}_2\text{O}_3\text{-PbO}$, $\text{BaO-Fe}_2\text{O}_3\text{-B}_2\text{O}_3$ were calculated. The results are shown as temperature-composition diagrams and liquidus surfaces. Received data will be used for analysis more complex systems and improvement melt-growth techniques of hexaferrites.

The work was supported by Act 211 Government of the Russian Federation, contract № 02.A03.21.0011. Additionally it was supported by the Russian Foundation for Basic Research (project 16-08-01043) and by the Ministry of Education and Science of the Russian Federation (project code 4.1346.2017/PP).

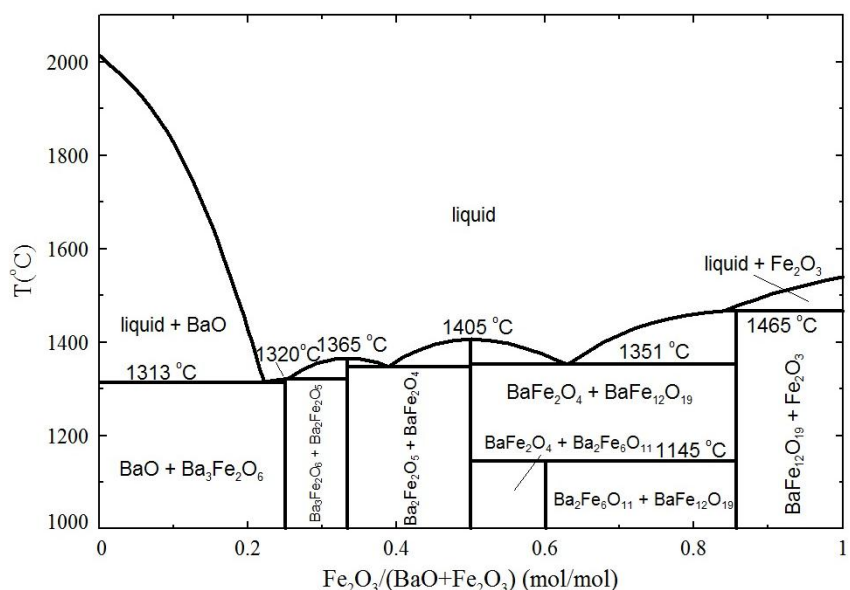


Figure 1. Phase diagram of the $\text{BaO-Fe}_2\text{O}_3$ system.

THERMODYNAMIC ANALYSIS OF THE TERNARY Cu-Cr-C AND Cu-Mo-C SYSTEMS

Trofimov E.A.¹, Samoylova O.V.², Galkina D.P.¹

¹ Zlatoust Branch of South Ural State University, 456209 Zlatoust, Russia

² South Ural State University, 454080 Chelyabinsk, Russia

E-mail: tea7510@gmail.com

Phase equilibria in the Cu–Mo–C and Cu–Cr–C systems represent some interest for analysis of copper alloys hardening technology, which are recommended using carbides particles for increase hardening and wear resistance. Interactions in the Cu–Mo–C and Cu–Cr–C systems are studied not enough yet. Therefore the aim of this work is theoretical and experimental investigation of phase equilibriums of the Cu–Mo–C and Cu–Cr–C systems.

The software FactSage (version 7.1) was used for modeling and plotting of phase diagrams. Databases SGTE2014 and SGPS (data for compounds: MoC, Cr₃C₂, Cr₇C₃, Cr₂₃C₆) are used for modeling Cu–Mo, Cu–Cr, Cu–C, Mo–C, Cr–C, Cu–Mo–C and Cu–Cr–C systems. Results of these calculations were compared with literature data. As a result, phase diagrams of the investigated systems were plotted. Projections of phase regions on the liquidus surface of copper melt were plotted as well. Such diagram for the Cu–Mo–C system is shown in Figure 1.

Experimental investigation consists mainly in electron microscopy study of shape and size of inclusions and its electron probe microanalysis. Inclusions were formed in the fast crystallization metal melts processes for the Cu–Mo–C and Cu–Cr–C systems (copper is a main element). Obtained in the investigation process results allowed to approach efficiently to selection of copper alloys hardening mode using molybdenum carbide and chromium carbide particles.

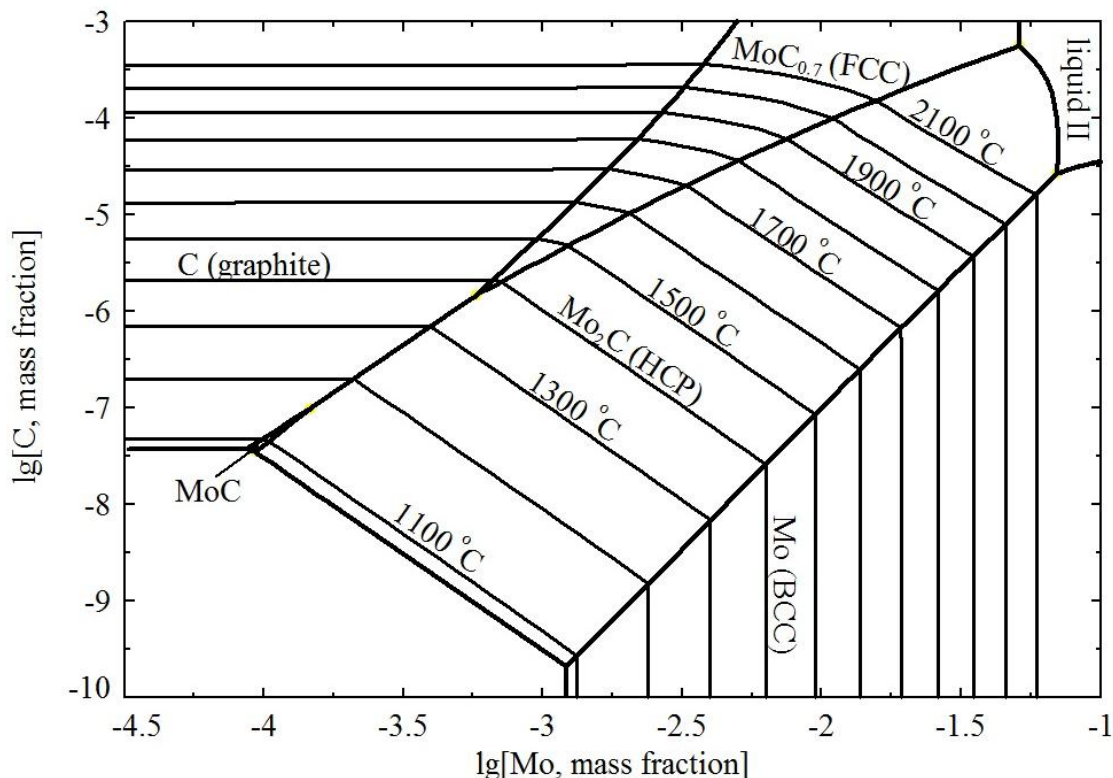
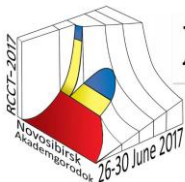


Figure 1. Projection of phase regions on the liquidus surface of copper melt for the Cu–Mo–C system.

The reported study was funded by the Russian Foundation for Basic Research according to the research project № 16-08-00133 a.



Section 3.

Thermodynamics of solutions and heterogeneous systems

Virtual presentations

STUDY OF THE EVOLUTION OF THREE PHASE SPLITTING REGION IN QUATERNARY SYSTEMS

Akishina A.A., Frolkova A.V., Frolkova A.K., Illarionova E.V.

Moscow Technological University, Institute of Fine Chemical Technology, 119571, Moscow, Russia

e-mail: anna.neudahina@mail.ru

Mathematical modeling is the most effective and widely used method of splitting system studying. Availability and quickness are advantages of this method compared to the experimental procedures. But there are some difficulties connected with mathematical modeling due to the limited experimental data of phase equilibrium (liquid-liquid and liquid-liquid-liquid).

In article [1] the method of study of liquid-liquid-liquid equilibrium in quaternary system with one region of three-phase splitting was proposed. It is based on the study of scan of tetrahedron, determination of composition of coexisting liquid phases in ternary constituents, choice of conjugate composition and analysis of compositions of three liquid phases at adding conjugate composition.

This work is devoted to study of two quaternary systems with different types of three liquid phases region: water-aniline-heptane-benzene and water-aniline-hexane-heptane (fig.1). There is only one region of three-phase splitting in first system, so an increase of the 4-th component (benzene) can be used as a direction of conjugate composition change. System of water-aniline-hexane-heptane contains two ternary constituents with LLE region and we consider the line that corresponds to the intersection of two section planes ($x_1=\text{const}$ and $x_2=\text{const}$) [2].

As can be seen from fig. 1 in the system with benzene the three-phase splitting region degenerates through critical tie-line (the addition of benzene to the ternary mixture results in a decrease in the mutual solubility of aniline and heptane and convergence of the compositions of the aniline and heptane layers). Coordinates of critical tie-line were determined: $x_1=0,042$; $x_2=0,33$; $x_3=0,32$; $x_4=0,308$ mole frac., it corresponds to gross-concentration of benzene of 0,33 mole frac.

In system (b) fig. 1 there is no degeneration of three liquid phase region. With adding of conjugated composition hydrocarbon layer are depleted by hexane and enriched by heptanes.

The study of evolution of three-phase splitting region allows determining geometric features of mutual location of regions with different number of liquid phases and separatric manifolds inside the composition tetrahedron and consequently to evaluate the possibility of using the combination of distillation process and splitting for the separation of azeotropic mixtures.

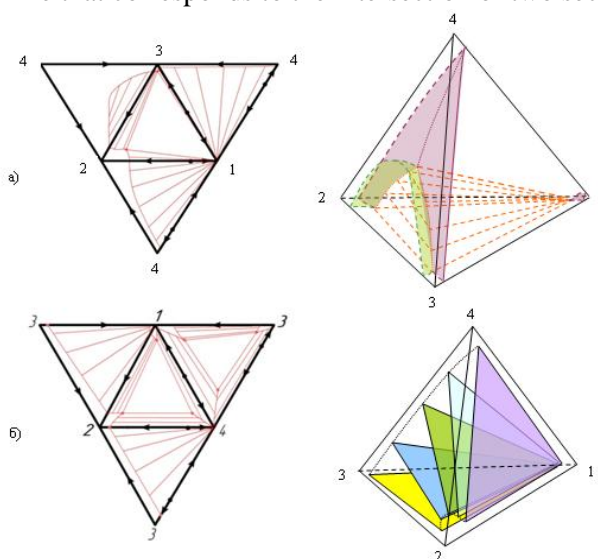


Figure 1. The scan and structure of splitting diagrams of quaternary systems

- a) water (1) – aniline (2) – heptane (3) – benzene (4)
 b) water (1) – aniline (2) – hexane (3) – heptane (4).

The work was carried out under support of Russian Science Foundation 16-19-10632.

[1] Frolkova A.V., Balbenov S.A., Frolkova A.K., Akishina A.A. Russ. Chem. Bull, 2015, 64 (10), pp. 2330-2336.

[2] Frolkova A.V., Akishina A.A., Frolkova A.K., Illarionova E.V. J. Chem. Eng. Data, 2017, 62 (4), pp. 1348-1354.

PHASE DIAGRAMS OF THE SYSTEMS FROM DICARBOXYLIC ACIDS

Alenova S.M., Kolyado A.V., Garkushin I.K.
 Samara State Technical University, 443100 Samara, Russia
 E-mail: saule-alenova@mail.ru

Abstract: The method of differential thermal analysis of phase equilibria in the ternary system were studied dibasic acids: pentanedioic, hexanedioic, nonanedioic. Revealed the eutectic composition of the ternary eutectic containing pentanedioic acid - 48.0 wt. % (53.7 mol. %), hexanedioic acid - 20.0 wt. % (20.9 mol. %), nonanedioic acid - 32.0 wt. % (25.4 mol.%) and a melting temperature of 70 °C.

Study of phase equilibria in binary systems was carried out by differential scanning calorimetry (DSC) using a medium-based heat flux scanning calorimeter (DSC microcalorimeter-500). Heating the sample rate was 8 K·min⁻¹. Temperatures are measured with an accuracy ±0.25°C. The Al₂O₃ qualification «analytical grade» is used as an indifferent matter. Concentrations of all components are expressed in weight percent, phase transformation temperature - degrees Celsius. To prepare the compositions of matter used prefabricated. Results of the study of eutectic compositions are given in tabl.1 and tabl.2.

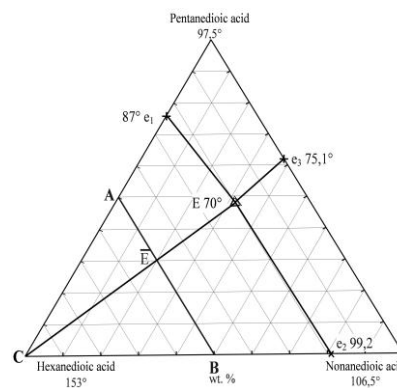


Figure 1. The concentration triangle of the system pentanedioic acid - hexanedioic acid - nonanedioic acid

Table 1. The melting temperature of the eutectic alloy in two-component systems

System	Composition, wt. %			Melting temperature, °C
	pentanedioic acid	hexanedioic acid	nonanedioic acid	
pentanedioic acid – hexanedioic acid	76.5	23.5	–	87.0±0.2 (e ₁)
hexanedioic acid – nonanedioic acid	–	18.5	81.5	99.2±0.2 (e ₂)
pentanedioic acid – nonanedioic acid	61.9	–	38.1	75.1±0.2 (e ₃)
pentanedioic acid – hexanedioic acid – nonanedioic acid	48.0	20.0	32.0	70±0.2 (E)

Table 2. Melting enthalpy and entropy of eutectic alloy compositions in the studied systems

System	$\Delta_{fus}H_{экен}$, (kJ/mol)	$\Delta_{fus}S_{экен}$, (J/(mol·K))
pentanedioic acid – nonanedioic acid	13.12±1.73	40.4
pentanedioic acid – hexanedioic acid	12.17±0.77	33.7
hexanedioic acid – nonanedioic acid	14.48±1.07	38.9
pentanedioic acid – hexanedioic acid – nonanedioic acid	13.44±0.25	42.8

PHASE EQUILIBRIA AND THERMODYNAMIC PROPERTIES IN $\text{Ca}(\text{NO}_3)_2$ - $\text{Zn}(\text{NO}_3)_2$ - H_2O SYSTEM: EXPERIMENT AND CALCULATION

Belova E.V.¹, Gorbachev A.V.², Voskov A.L.¹, Uspenskaya I.A.¹

¹Lomonosov Moscow State University, Chemistry Department, Physical Chemistry Division, Laboratory of Chemical Thermodynamics, 119991, Moscow, Russia

²Lomonosov Moscow State University, Department of Material Science, 119991, Moscow, Russia
E-mail: catrine2@mail.ru

Homogenous heavy fluids are widely used to stop oil flow during workover. Some oil deposits are situated in North regions where the outdoor temperature can reach -50°C and storehouses are not heated. Phase diagrams of heavy brine systems at subzero temperatures are very useful to estimate workover fluid compositions at which the brine stays liquid at the storage conditions. Calcium and zinc salts due to their high density and rather low cost are widely used to prepare such fluids. One of systems in interest is $\text{Zn}(\text{NO}_3)_2$ - $\text{Ca}(\text{NO}_3)_2$ - H_2O .

The experimental cross-sections of equilibrium phase diagram of $\text{Zn}(\text{NO}_3)_2$ - $\text{Ca}(\text{NO}_3)_2$ - H_2O system at 251.85 K, 262.35 K and 288.15 K were achieved by method of isothermal solution saturation and wet residues analysis. Densities of ternary $\text{Zn}(\text{NO}_3)_2$ - $\text{Ca}(\text{NO}_3)_2$ - H_2O solutions were measured at 298.15-321.35 K. Prepared mixtures were held in a refrigerator camera at fixed temperature. For additional stabilization of temperature regime in the refrigerator camera, samples were held in bathes with $\text{KCl-H}_2\text{O}$ and $\text{NaCl-H}_2\text{O}$ eutectic mixtures for $-10.8^\circ\text{C}/262.35\text{ K}$ and $-21.3^\circ\text{C}/251.85\text{ K}$ respectively. As for $15^\circ\text{C}/288.15\text{ K}$, the samples were held in a water thermostat, where the standard uncertainty of temperature registered was 0.1°C . The standard uncertainty of temperature registered during the experiment in refrigerator camera was 0.2°C for $-10.8^\circ\text{C}/262.35\text{ K}$ and 0.5°C for $-21.3^\circ\text{C}/251.85\text{ K}$. Special procedures were performed to prove an achievement of equilibrium state; we checked the influence of stirring and addition of a seed.

The sum of Ca^{2+} and Zn^{2+} ion concentrations was analyzed by the complexometric titration method with 0.0500 M EDTA and eriochrome black. The Ca^{2+} concentration was determined in the same way with ZnS precipitated by Na_2S saturated solution prepared from fresh $\text{Na}_2\text{S}\cdot 9\text{H}_2\text{O}$ (p.a., >98%). The quality of such a masking was checked on a set of solutions with known concentrations of calcium and zinc prepared from the stock solutions. Amounts found matched within error of determination the amounts added. Diluted probes were titrated with addition of diluted HNO_3 (reagent grade) to prevent hydrolysis. Thermodynamic modeling of $\text{Zn}(\text{NO}_3)_2$ - $\text{Ca}(\text{NO}_3)_2$ - H_2O system were performed with Pitzer model. As was shown by comparing results of own experiment and calculation, it is necessary to take into account both binary and ternary parameters for adequate description of available data. Stability parameters for solid phases were derived from the binary systems and SLE experimental data for the ternary system.

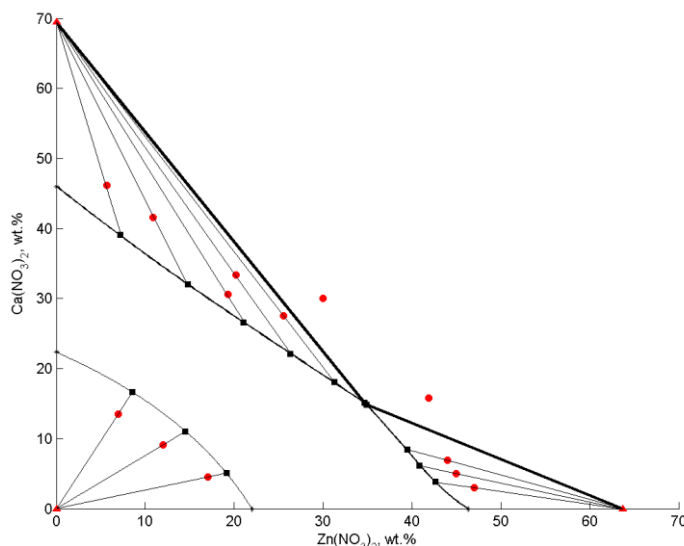


Figure 1 Cross-section of the ternary system $\text{Ca}(\text{NO}_3)_2$ - $\text{Zn}(\text{NO}_3)_2$ - H_2O at 262.35 K



EXPERIMENTAL DETERMINATION OF BINODAL CURVES IN THE SYSTEM CYCLOHEXANONE - CYCLOHEXENE - 1-BUTYL - 3-METILIMIDAZOLIUM HEXAPHLUOROPHOSPHATE

Zhuchkov V.I., Bovyryna E.A., Frolkova A.K.

Moscow Technological University, Institute of Fine Chemical Technologies, 119571 Moscow, Russia

E-mail: lena.bovyryna@yandex.ru

The aim of the present research is to determine the possibility of using ionic liquids with a limited mutual solubility with cyclohexene as a reaction medium for the synthesis of cyclohexene to cyclohexanone. Reagent and product redistribution between equilibrium liquid phases, which contain ionic liquid (lower layer) or organic components (higher level), is important for the effective chemical transformation. 1-butyl -3- metilimidazolium hexaphluorophosphate was used as ionic liquid. Compositions belonging to binodal variety (Table 1, Items 2-11) as well as liquid-liquid tie-lines position (Table 2, Items 13-20) in the ternary system cyclohexene (CYHE) – cyclohexanone (CYHAONE) – ionic liquid (IL) were experimentally determined. The experiment of titration of splitting binary mixtures CYHE - IL using CYHAONE was made at normal conditions. Transition of the system into a homogeneous phase was fixed based on visual observations: the composition became transparent when (CYHAONE) was added. Quantitative determination of the equilibrium compositions of liquid layers was made using refractometric analysis (ATAGO NAR-1T LUQUID). A calibration curve of refractive index n_D^{20} vs. ionic liquid concentration was drawn for points on binodal curve corresponding to the lower levels compositions. This calibration curve was used to draw liquid-liquid tie-lines. Experimental data are given in Tables 1 and 2.

Table 1. Compositions (W %), that lie on binodal curve in the ternary system

#	(CYHAONE)	IL	n_D^{20}	#	(CYHAONE)	IL	n_D^{20}
1	-	100,0	1,4120	7	50,0	21,3	1,4445
2	20,5	70,2	1,4280	8	46,5	12,5	1,4460
3	35,6	47,3	1,4350	9	45,5	8,4	1,4470
4	40,9	39,1	1,4390	10	40,6	5,6	1,4472
5	48,1	27,8	1,4420	11	35,8	2,7	1,4282
6	49,5	23,9	1,4425	12	-	-	1,4460

Table 2. Compositions (W %) of equilibrium liquid layers

#	Gross composition		Lower layer composition		n_D^{20}	Higher layer composition	
	CYHAONE	IL	CYHAONE	IL		CYHAONE	IL
13	41,9	26,0	31,6	53,4	1,4350	47,5	10,0
14	37,9	25,7	24,5	64,0	1,4310	44,0	7,0
15	35,2	25,1	19,6	71,2	1,4278	41,5	6,0
16	31,8	24,0	18,0	74,0	1,4265	36,0	3,5
17	25,3	23,1	6,0	91,2	1,4180	30,5	2,5
18	18,1	24,0	5,2	92,8	1,4170	23,0	2,0
19	9,9	39,9	3,8	94,6	1,4160	14,0	1,5
20	6,2	22,2	2,0	97,0	1,4145	7,5	1,0

The obtained data allows recommending using 1-butyl-3-metilimidazolium hexaphluorophosphate as a reaction medium for synthesis of cyclohexene to cyclohexanone.

The work was carried out under support of Russian Science Foundation 16-19-10632.



THE EXCEED MOLAR PROPERTIES OF BINARY SYSTEM PROPYLENE CARBONATE - ACETONITRILE

Chekunova M.D.¹, Tyunina E.Yu.²

¹*Ivanovo State Polytechnic University, 153037 Ivanovo, Russia*

²*G.A. Krestov Institute of Solution Chemistry, Russian Academy of Science, 153045 Ivanovo, Russia*

E-mail: marchekunova@mail.ru

The creation of new compounds, materials and goods implies the wide use of non-aqueous solvents including mixed ones, which may be models for study of solutions' structure. The examined system propylene carbonate – acetonitrile is of interest for application in lithium and lithium-ion batteries. This work is a logical continuation of the research of physico-chemical properties of electrolytes based on aprotic solvents [1, 2]. Density, viscosity and relative permittivity of system propylene carbonate – acetonitrile have been measured throughout the composition of mixed solvent at 253.15, 273.15, 293.15 and 313.15 K. The densities (ρ) of the solutions were measured using a digital precision vibrating-tube densimeter DMA 602 (Anton Paar, Austria). The estimated precision in the density was $\pm 0.02 \text{ kg} \cdot \text{m}^{-3}$. The kinematic viscosities ($\nu = \eta/\rho$) of the solutions were measured using an Ubbelohde suspended level capillary viscometer and an automatic digital measuring stand (LAUDA Viscotimer S, model S/2, Germany) at different temperatures and atmospheric pressure. The Viscotimer S determines the liquid level in capillary photoelectrically. The uncertainty in the viscometer measurement was 0.1%. The measurements of relative permittivity (ϵ) were carried out at 3 MHz, using a bridge of the type OH-301 (Hungary). The cell was calibrated with standard pure liquids, such as acetone, N,N-dimethylformamide, dimethylsulphoxide, propylene carbonate. The measurements accuracy of the relative permittivity was ± 0.02 . In all measurements of density, kinematic viscosity and relative permittivity the temperature was maintained with accuracy 0.005 K. Molar volume, molar viscosity, molar capacity and their exceed values of system propylene carbonate - acetonitrile are defined. The values of molar volume, molar viscosity, molar capacity droningly diminished with growth of concentration of acetonitrile in binary system. While the concentration dependences of exceed molar volume, exceed molar viscosity, exceed molar capacity are characterized by the points of extremum at mole fraction of acetonitrile equals $x_2=0.5$. The application of rational parameters method [3, 4] and using of exceed molar volume, exceed molar viscosity, exceed molar capacity allowed to find the coordinated results and to discover the formation of molecular complex between propylene carbonate and acetonitrile in the ratio 1:1 in region of mole fraction of acetonitrile equals $x_2=0.5$. The stability of this molecular complex is determined by intermolecular interaction and geometric factor (size and form of molecule). The discovered isoconcentration linear dependences of molar fluidity and molar capacity from solution's molar volume allow to forecast coefficient values of internal friction and dielectric permittivity based on density with error (0.06-3.1)% and (0.72-1.82)% in investigated temperature interval.

- [1]. Tyunina, E.Yu.; Afanasiev, V.N.; Chekunova M. D. J. Chem. Eng. Data, 2011, 56, 3222-3226.
- [2]. Tyunina, E.Yu.; Chekunova M.D. J. Mol. Liq., 2013, 187, 332-336.
- [3]. Afanas`ev, V.N.; Krestov, G.A. Dokl. Akad. Nauk SSSR, 1983, 269, 620-623.
- [4]. Afanas`ev, V.N.; Chekunova M. D.; Tyunina, E.Yu. Russ. J. Phys. Chem. A. 2006, 80, 1929-1933.



POLYTHERMAL STUDY OF LIQUID-LIQUID AND LIQUID-LIQUID-SOLID EQUILIBRIA IN THE QUATERNARY POTASSIUM NITRATE + WATER + PYRIDINE + BUTYRIC ACID SYSTEM

Cherkasov D.G., Chepurina Z.V., Smotrov M.P., and Il'in K.K.

Saratov State University named after N.G.Chernyshevsky, 410012 Saratov, Russian Federation

E-mail: ilinkk@info.sgu.ru

Introduction of salts can decrease (salting-out) or increase (salting-in) the solubility of organic compounds of various classes in water. Various processes involving salting-out electrolytes find wide application in the chemical industry for producing pigments, solvents, soaps, and medicines. Ternary fluid systems with a closed delamination region without volatile and combustible organic solvents are promising for extraction processes. Besides, salts with the salting-out effect, which can expand the region of two liquid phases in such fluid systems, find ample application in practice. Previously [1–3] phase equilibria and critical phenomena were studied in component mixtures of three cuts of the composition tetrahedron of the quaternary potassium chloride + water + pyridine + butyric acid system. No papers devoted to such studies of quaternary systems with other salts have been found in the literature.

Phase equilibria and critical phenomena in component mixtures corresponding to eleven sections of the cut triangle of the composition tetrahedron of the quaternary potassium nitrate + water + pyridine + butyric acid system whose ternary liquid subsystem has a closed delamination region were studied by means of the visual-polythermal method within 5–60°C. The cut was drawn through the composition tetrahedron pyridine – butyric acid edge and the point (25.00 wt. % of potassium nitrate) on the potassium nitrate – water edge so as to intersect the regions of liquid-phase equilibria and phase states with the presence of a solid phase. Besides, this cut intersects the critical tie line of monotectic state and the line of critical solubility points of the liquid–liquid equilibrium, which enables revealing the topological transformation of these states with temperature changes. The polytherms of phase states for all sections of the cut were plotted. Four phase states were observed in the component mixtures, namely, a monotectic state, a two-phase liquid one, saturated solutions of the salt, and a homogeneous-liquid state.

The temperature dependences of the composition of critical solubility points of the delamination region and the critical points of the monotectic critical tie line were found. It has been found that within 5.5–43.6°C the studied cut intersects the surface that occurs when the critical tie line of monotectics moves in the 4D temperature-concentration prism of the quaternary system. The surface of liquid–liquid critical solubility points formed in this prism will be crossed by the cut within 43.6–63.2°C. Consequently, at 43.6°C the plane of the cut passes through the end point of the critical tie line of monotectics. The plotted dependences have allowed us to find the composition of the liquid phase (end point) of the critical tie line of monotectic state and the temperature of its occurrence in the cut studied. Therefore, we first proposed a method to find the coordinates of the end point of the critical tie line of monotectic state in quaternary systems.

The results of our polythermal studies were used to plot the phase state isotherms on the cut triangle at twelve temperatures (5.0, 18.0, 25.0, 26.2, 30.0, 35.0, 40.0, 43.6, 47.2, 50.0, 52.0, and 60.0°C), which have shown the topological transformation of the phase diagram of the cut of the composition tetrahedron with temperature changes. Within 5–18°C a closed field of monotectic state exists on the cut triangle. Within 18–52°C the fields of two-liquid-phase and monotectic states are adjacent to the sides of the triangle of the (potassium nitrate + water) – pyridine and (potassium nitrate + water) – butyric acid cut. At 52.0°C the fields of monotectic states contact by merging the points corresponding to the composition of their liquid phases. The salting-out effect of pyridine and butyric acid from their aqueous solutions by potassium nitrate increases with an increase of temperature.

- [1] Cherkasov, D.G. *Izv. Saratovsk. Univ., Ser. Khim. Biol. Ekol.*, 2008, 8 (2), 28-36.
- [2] Cherkasov, D.G. *Izv. Saratovsk. Univ., Ser. Khim. Biol. Ekol.*, 2009, 9 (2), 36-40.
- [3] Cherkasov, D.G. *Izv. Saratovsk. Univ., Ser. Khim. Biol. Ekol.*, 2010, 10 (2), 14-19.



SALTING-OUT EFFECT AND CRITICAL PHENOMENA IN THE TERNARY SYSTEM POTASSIUM BROMIDE + WATER + PYRIDINE

Cherkasov D.G., Smotrov M.P., Danilina V.V., and Il'in K.K.

Saratov State University named after N.G. Chernyshevsky, 410012 Saratov, Russia

E-mail: ilinkk@info.sgu.ru

Studying of the influence of the salt nature and temperature on the liquid-liquid equilibrium in the ternary salt + water + organic solvent systems is of great importance for further development of the salting-in–salting-out theory and giving practical recommendations on the selection of salts for effective processes of selective extraction of organic solvents from aqueous solutions, and the choice of solvents for extractive crystallization of salts. The present paper is devoted to our polythermal study of the phase behaviour of the ternary potassium bromide + water + pyridine system to reveal the topological transformation pattern of the phase diagram of the system as temperature changes, to determine the formation temperature of the critical tie line of the monotectic state and the pyridine distribution coefficients between the equilibrium liquid phases of the monotectic state. There are no practically data on the solubility of components, phase equilibria and critical phenomena for this ternary system in the literature. The binary water + pyridine subsystem is homogeneous over the entire temperature range of its liquid state.

Phase equilibria and critical phenomena in component mixtures of the ternary system were studied by means of the visual polythermal and liquid phase–volume ratio methods under saturation pressure within 10–90°C. The following phase states are realized in the system (by nine sections of the composition triangle): unsaturated solutions, saturated solutions, delamination and monotectic state. The solid phase in each saturated solution at any temperature was pure salt. The temperature dependence of the mixture composition corresponding to the critical solubility point in the delamination field has been established within 50.6–90.0°C. The procedure for treating of the results from polythermal studies and plotting the isothermal phase diagrams of the ternary systems was described in [1].

Phase state isotherms were drawn at 10.0, 25.0, 40.0, 50.6, 55.0, 70.0, 90.0°C and enabled the topological transformation of the ternary system's phase diagram with temperature to be revealed. Within 10.0–50.6°C the phase diagram is characterized by the presence of a solubility line to separate the fields of unsaturated and saturated solutions. At 50.6°C on the field of saturated solutions a critical tie line of the monotectic state corresponding to equilibrium between the critical liquid phase and salt crystals appears; the critical end point composition has been estimated graphically. 50.6°C is the delamination onset temperature in the ternary system. As temperature increases, the critical tie line transforms into a monotectic triangle with an adjoining delamination field and saturated solutions fields. As temperature increases further, no qualitative changes on the isothermal phase diagrams of the system are observed, but the fields of monotectics and delamination expand while the fields of saturated solutions shrink.

The distribution coefficients of pyridine between the organic and aqueous phases in the monotectic state at 55.0, 70.0 and 90.0°C were calculated. The salting-out effect of potassium bromide relative to pyridine from aqueous solutions increases with temperature. On the basis of our results, we conclude that the water + pyridine system behaves as a system with a highly located lower critical solution temperature (LCST), since introduction of potassium bromide therein leads to lowering of the critical solution temperature down to 50.6°C. Analysis of the isothermal phase diagrams of studied system confirmed the corresponding fragment of a variant of our scheme of topological transformation of the phase diagrams of the ternary salt + binary solvent systems with salting-in–salting-out as temperature changes [2].

[1] Il'in, K.K.; Cherkasov, D.G. *J. Chem. Eng. Commun.*, 2016, 203, 642-648.

[2] Cherkasov, D.G.; Il'in K.K. *Proceedings of the 10th International Kurnakov's Meeting on Physicochemical Analysis*, in 2 vols., Samarsk. Gos. Tekhn. Univ., Samara, Russia, 2013, vol. 1, 57-61.



NEW INSIGHT ON PROLINE HYDRATION

Dmitrieva O.A.¹, Fedotova M.V.¹, Buchner R.²

¹*Institute of Solution Chemistry of RAS, 153045 Ivanovo, Russia*

²*Institut für Physikalische und Theoretische Chemie, Universität Regensburg, 93040 Regensburg, Germany,*

E-mail: dmitrievao.a@yandex.ru

Understanding of the refolding mechanism for denatured polypeptide chains into functional native structures in vitro and reasons affecting on this process is actual fundamental problem in biochemistry and biology [1]. It has been shown that osmolytes in the cells of living organisms under abiotic stresses promote the stabilization of improperly folded proteins, the reduction of aggregation, the prevention of nonproductive interactions with other resident proteins [2]. Therefore the effect of osmolytes on protein folding is under great interest. Proline (Pro) is the most common compatible osmolyte accumulating in many plants in the response to osmotic stress, thus, it may have a specific protective role in the adaptation of plant cells to dehydration. Despite this known biological role of Pro, the details of its interaction with surrounding water are still far from being fully understood.

Here we present the results of our study for aqueous Pro solution in the wide concentration range from infinite dilution to 6M at $T = 25^\circ\text{C}$ by using the dielectric relaxation spectroscopy (DRS) in a wide frequency range ($0.05 < \nu / \text{GHz} < 89$) and by the 1D-RISM (Reference Interaction Site Model) integral equation method.

The spectra were described by a superposition of three Debye (3D) modes. From the analysis of spectra we have determined the relaxation time of pure water (~ 8.3 ps) and found an increase in relaxation time with Pro concentration increase in the solution in comparison with pure water. The reorientation time of Pro was found in the range from 51.2 ps for infinitely diluted solution to 417.8 ps for 6 M solution. At the lowest Pro concentration the intermediate relaxation process is located at ~ 17.0 ps and assigned to the hydrated water molecules with the reduced dynamics («slow water»). This value increases up to ~ 81.8 ps at the highest Pro concentration. The obtained effective hydration number of Pro is 9 for the infinitely diluted solution and 3 for 6 M solution. The effective dipole moments, μ_{eff}^- , and orientational correlation factor, g^- , of Pro were estimated from the amplitude of the lowest frequency process. Both μ_{eff}^- and g^- values decrease strongly with solute concentration increase. The last suggests the strong dehydration of Pro in aqueous media with parallel orientation of water and Pro.

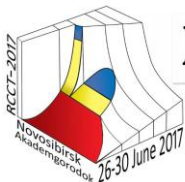
The results of the 1D-RISM calculations indicate the significant changes in hydration structure of Pro with Pro concentration increase. Under concentration growth from 0 to 6 M, the amount of water molecules in the nearest environment of carboxyl group is reduced from ~ 8.5 to ~ 4 . But the number of H-bonds of $-\text{COO}^-$ group at infinite dilution and in 6 M solution is ~ 4 and ~ 3 correspondingly. The results of calculations do not show a formation of H-bonds by nitrogen atom of $-\text{NH}_2^+$ group with water in the whole concentration range. At the lowest Pro concentration the hydration number of $-\text{NH}_2^+$ group is ~ 4.5 . At the same time, at the highest Pro concentration (6 M) this hydration number is 2.8 (a decrease is 36.6%). Hydrogen atoms of $-\text{NH}_2^+$ group form ~ 1.7 H-bonds and ~ 1.2 H-bonds with water at infinite dilution and 6 M respectively. It means a decrease of these H-bonds by 29.5%.

Thus, the data of both methods show strong dehydration of Pro under solute concentration growth. Moreover, under Pro concentration growth we have observed a significant decrease for dipole moment of Pro provoked by the changes in the nearest environment of Pro that is indicated by the RISM results.

This work was partly supported by DAAD № 57130104 and supported by the Russian Foundation for Basic Research (grant No. 15-43-03004-r_centre_a).

[1] Jaenicke, R. *Biol. Chem.*, 1998, 3, 237-244.

[2] Perlmutter, D. H. *Pediatric research.*, 2002, 6, 832-836.



THERMODYNAMIC PROPERTIES OF WATER + METHYLUREA MIXTURE OVER THE WIDE RANGE OF STATE PARAMETERS

Egorov G.I., Makarov D.M.

G.A. Krestov Institute of Solution Chemistry of the Russian Academy of Sciences, Ivanovo, Russia

E-mail: gie@isc-ras.ru

Alkyl urea derivatives are important for biological processes and the investigation of the mechanism of their interactions in aqueous solutions promotes the better understanding of the processes which occur in living biological systems. For example the urea and its alkyl-derivatives are considered to be destabilizers of the protein structure and the alkyl-derivatives are more efficient for refolding of denaturated proteins at that. Therefore the determination of structure-sensitive parameters for the above aqueous solutions allows clarifying the mechanism of urea action in the processes of proteins denaturation.

The investigation of dependences of the volume of water+methylurea binary liquid mixture on composition, temperature, and pressure is an important source of information on the interactions between the mixture components. The presence of both hydrophilic and hydrophobic groups in methylurea molecule causes the particular interest to the study of its intermolecular interactions.

Using the experimental values of density, ρ , measured at atmospheric pressure, and compressibility coefficients, $k = (V_0 - V)/V_0$, the molar isothermal compressions, $K_{T,m}$, molar isobaric expansions, $E_{p,m}$, molar isochoric elasticities, β , internal pressure, p_{int} , apparent molar volumes, $V_{\phi,i}$, and partial molar volumes, \bar{V}_i , as well as their limiting values, \bar{V}_i^∞ , were calculated over the temperature range of 278.15-323.15 K and at pressures from 1 to 100 MPa.

It was shown that the concentration dependences of the density of water + methylurea mixture were almost linear whereas the similar dependences of the mixture molar isothermal compression had weak minima at $x_2 \approx 0.03 \div 0.05$. The molar isobaric expansibilities and isochoric thermal coefficients of the mixture increased with growth of both methylurea concentration and pressure. The limiting partial molar volume of methylurea in water decreased with the pressure increase but went up with the temperature rising.

The work was financially supported by the Russian Foundation for Basic Researches (grant №15-43-03092 r_center_a)

THE APPLICATION OF ELECTRONEGATIVITY ELEMENTS VALUES FOR CALCULATION OF REAL ACTIVITY COEFFICIENTS OF IONS

Fedorova A.A., Sharonov N. Yu.

Ivanovo State University of Chemistry and Technology, 153000 Ivanovo, Russia

E-mail: fedorova@isuct.ru

For the description of the processes in real solutions the values of the activity coefficients are required. For these purposes are usually used middle values for ions mixture. However, it is obviously, that the values of the thermodynamic characteristics of individual ions can differ considerably. In this regard, it is actually the creation of calculation methods of the individual ionic activity coefficients. However, modern structural theories of electrolyte solutions, in particular the theory of Debye – Hückel, consider the energy of ions interaction to each other and to solvent in the bulk, but they do not consider the energy of ion transfer through the phase boundary, that is they can be used only for calculating of the chemical coefficients. This approach does not allow to obtain exact values of the real thermodynamic characteristics of individual ions and carry out a comparative analysis of the energy state of the ion in different solvents. In the present work, the proposed equation for calculation of the real ionic activity coefficients in aqueous electrolyte solutions:

$$\lg \gamma_i = -\frac{z_i^2 \cdot 0,5107 \cdot m^{1/2}}{1 + 1,101 \cdot m^{1/2}} - \lg(1 + 0,018 m) \pm \frac{\Delta G_{tr}^\circ}{2,303 \cdot R \cdot T} \cdot m + \frac{z_i \cdot F \cdot \chi}{2,303 \cdot R \cdot T} \cdot m, \quad (1)$$

where z_i - the charge of an ion taking into account the sign, m - the solutions molality; χ - the solutions surface potential of a given concentration, it is calculated from the data [1]; ΔG_{tr}° - change of the Gibbs energy of charged particle transfer through the surface, the sign of the third term is determined by the particle charge and the direction of charge transfer.

$$\Delta G_{tr}^\circ = (E_2 - E_1) \cdot F - T \Delta S_{tr}^\circ, \quad (2)$$

where E_1 and E_2 – the energy of ion interaction with a solvent molecule on the interface and in the bulk respectively, ΔS_{tr}° - the transfer entropy of a charged particle from the interface in the faze volume, it is calculated from the data [2].

The electronegativity of an element depends on its valence state and the environment of its atoms in different molecules. Therefore, to evaluate the energy for the process of charge transfer through the surface is proposed to use values of electronegativity. The value of the electronegativity is estimated according to the method described in work [3]. The calculation was performed at one water molecule as for weakly hydrated chlorine ion and for hydrogen ion, suggesting that the most significant charge redistribution is occurred between the ion and the first water molecule. The calculations on the example

of H^+ ions, Cl^- in aqueous solution HCl (Fig.1) showed that the proposed equation reproduces the character of the concentration dependence of the activity coefficient for the anion and cation.

The obtained results allow to conclude about the possibility of using values of electronegativity in the evaluation of the energy of charge transfer through the surface.

[1]. Rabinovich, V.A., Alekseeva, T.E. // *Electrochemistry*. 1973, 9, 10, 1434 –1436.

[2]. Sokolov, V.N., Kobenin, V.A., Gorelov, V.N. // *J. Phys. Chem.*, 2005, 79, 2, 228-232.

[3]. Hinze, J., Jaffe, H.H. *J. Am. Chem. Soc.*, 1962, 84, 540.

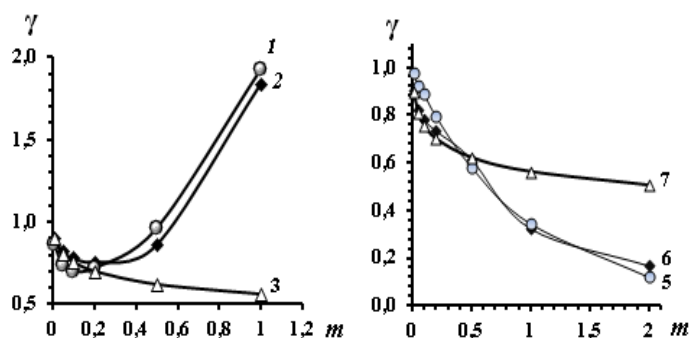


Figure 1. The real activity coefficients of H^+ -1, 2, 3 and Cl^- - 5, 6, 7 in aqueous solution of HCl: 1, 5 - calculation of the equation (1); 2, 6 - experimental data [1]; 3, 7 - calculation according to the equation 2-nd approximation of Debye-Hückel.

**STABILITY OF SCHIFF BASES DERIVED FROM PYRIDOXAL 5'-PHOSPHATE AND SOME PYRAZOLES IN AQUEOUS SOLUTION AT DIFFERENT PH VALUES**Gamov G.A.¹, Zavalishin M.N.¹, Khokhlova A.Yu.¹, Sharnin V.A.^{1,2}¹Ivanovo State University of Chemistry and Technology, 153000 Ivanovo, Russia²G.A. Krestov Institute of Solution Chemistry, Russian Academy of Sciences, 153045 Ivanovo, Russia

E-mail: georgegamov38@gmail.com

Pyridoxal 5'-phosphate (PLP) plays a key role in a number of biochemical processes including metabolism of amino acids, lipids, carbohydrates and biosynthesis of hormones, neurotransmitters and heme. PLP derivatives cover *ca.* 4% of all classified biochemical activities. PLP interaction with active site of specific enzyme (lysine residue) forming the Schiff base (internal aldimine) is the first step along the metabolic pathway of PLP. The aldehyde substituent of PLP is involved on this stage. Preliminary binding of PLP into Schiff base using another amine prevents the internal aldimine formation and, thus, could be used as a possible way of ceasing the vital functions of undesirable cells. Present contribution reports on our evaluation of two pyrazoles (2-(3,5-dimethyl-1H-pyrazole-4-yl)acetohydrazide (**I**), 3-methyl-1H-pyrazole-5-carbohydrazide (**II**)) ability to bind PLP in aqueous solution with pH value corresponding to that of healthy living tissue and some kind of tumors.

The stability constants of Schiff base of PLP-**I**, **II** were determined using spectrophotometry. The sets of 9-10 solutions with PLP:**I**, **II** concentrations ratio of 10:1÷1:1 were prepared and allowed to stay during 24h to reach the equilibrium state. Optical densities at 3-4 wavelengths corresponding to the absorbance maxima of reagents and product were measured and set as input data into FTMT [1] software together with initial concentrations of the reagents. Molar extinction coefficients of reagents required for stability constant (Table 1) calculation were determined preliminary using calibrating plots.

Table 1. Stability constants $\lg K$ of Schiff bases derived from PLP and **I**, **II**

Compound	pH 6.66	pH 7.02	pH 7.44
PLP- I	4.62±0.14	4.81±0.10	5.13±0.12
PLP- II	5.11±0.16	5.10±0.13	5.79±0.18

The stability constants values allow calculating the equilibrium compositions of PLP-**I**, **II** mixtures with initial reagents concentrations corresponding to the physiological ones (Tables 2). The mean content of PLP in the human blood serum is 51.4 nmol l⁻¹. The **I**, **II** concentrations were set to be 33 μmol l⁻¹.

Table 2. Calculated equilibrium compositions of PLP-**I**, **II**. Initial concentrations are given in the text above

Pyrazole	pH	[PLP], mol l ⁻¹	[pyrazole], mol l ⁻¹	[Schiff base], mol l ⁻¹	conversion of PLP, %
I	7.44	9.4·10 ⁻⁹	3.3·10 ⁻⁵	4.2·10 ⁻⁸	81.64
	6.66	2.2·10 ⁻⁸	3.3·10 ⁻⁵	3.0·10 ⁻⁸	57.88
II	7.44	2.4·10 ⁻⁹	3.3·10 ⁻⁵	4.9·10 ⁻⁸	95.31
	6.66	9.8·10 ⁻⁹	3.3·10 ⁻⁵	4.2·10 ⁻⁸	80.93

Table 2 data show even small quantity of **I**, **II** to bind efficiently PLP under conditions mimicking physiological ones. The drawback of **I**, **II** using is more complete reaction passing in the medium with pH of 7.4, which imitates healthy tissue.

The study was carried out in Research Institute of Thermodynamics and Kinetics of Chemical Processes of Ivanovo State University of Chemistry and Technology as a part of State Task of the Ministry of Education and Science of the Russian Federation with financial support of Russian Foundation of Basic Research (project 16-33-60017) and under grant of Council on grants of the President of the Russian Federation (project 14.Z56.16.5118-MK).

[1] Gridchin, S.N.; Kochergina, L.A.; Konovalov, P.G. Russ. J. Coord. Chem., 2003, 29(12), 868-870.

VISCOSITY AND VOLUMETRIC PROPERTIES OF ACRYLONITRILE+ DIMETHYLSULFOXIDE BINARY MIXTURES AT T= (298.15-318.15)K

Ghazoyan H.H., Grigoryan Z.L., Markarian S.A.

Department of Chemistry, Yerevan State University, 0025 Yerevan, Armenia

E-mail: heghine@ysu.am

The study of volumetric properties and viscosities of acrylonitrile (AN)-dimethylsulfoxide (DMSO) binary mixture has fundamental and practical interests. AN is a monomer of the widely used polyacrylonitrile (PAN), which has long been used as apparel and industrial fiber. DMSO has a wide application as solvent and important fine chemical in biology and medicine [1]. Moreover, the solvent of the greatest interest for the production of PAN fibers is DMSO [2].

Fundamental importance is caused by the fact that the components of this system are capable both to self-association, and to interact with each other. Obviously, that the presence of such competing interactions considerably influence on the thermodynamic properties of this system.

The densities of binary AN-DMSO mixture have been measured on a DMA 4500 vibrating-tube density meter over the (298.15–313.15)K temperature range at the atmospheric pressure.

Viscosity measurements were carried out with an Ubbelohde-type suspended-level viscometer at temperatures from (298.15-318.15) K.

Excess molar thermodynamic quantities such as excess molar volumes, V_m^E , and viscosities, $\Delta\eta$, were calculated and described by the Redlich–Kister equation. Correlation parameters and standard deviations were calculated as well.

It was found that the above mentioned excess molar thermodynamic quantities are negative over the whole range of composition of this system (Fig.). The negative deviation from ideality testifies that very strong molecular interactions take place between AN and DMSO.

In the concentration range where a minimum appears, the interaction of AN with DMSO is presumably attributed to dipole-dipole interaction between nitrile group of AN and sulfonyl group of DMSO.

Values of Gibbs energy, enthalpy and entropy of activation of viscous flow for the AN-DMSO binary mixtures at different temperatures were calculated as well and are reported in Table.

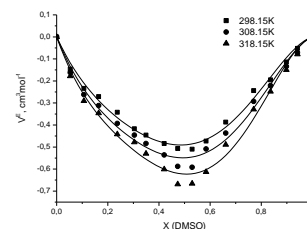


Figure. Excess molar volumes plotted against $x(\text{DMSO})$ for AN-DMSO mixture at different temperatures.

Table. Values of Gibbs energy, enthalpy and entropy of activation of viscous flow for the AN-DMSO binary mixtures at T=(298.15; 308.15 and 318.15K).

X(DMSO)	ΔG^* (kJ/mol)			ΔH^* (kJ/mol)	$-\Delta S^*$ (J/(mol · K))
	298.15K	308.15K	318.15K		
0.0000	61.339	63.247	65.142	4.648	190
0.1224	61.881	63.797	65.666	5.464	189
0.2389	62.326	64.366	66.129	5.679	190
0.3507	62.796	64.625	66.723	4.209	196
0.4579	63.273	65.113	67.159	5.308	194
0.5567	63.743	65.560	67.571	6.645	191
0.6501	64.185	66.011	68.000	7.286	191
0.7438	64.645	66.445	68.476	7.496	192
0.8377	65.109	66.903	68.839	9.480	187
0.9207	65.520	67.289	69.232	10.154	186
1.0000	65.927	67.688	69.511	12.488	179

[1] Jacob, S.; Herschler, R. Cryobiology, 1986, 24, 4-27.

[2] Eom, Y.; Kim, B.C. Polymer, 2014, 55, 2570-2577.



THERMODYNAMIC PARAMETERS OF ADSORPTION OF AMINO ACIDS ON HYDROXYAPATITE AT VARYING PH

Golovchenko K.K.¹, Chikanova E.S.¹, Golovanova O.A.¹

¹F.M. Dostoevsky State University, 644077 Omsk, Russia

E-mail: apulong@gmail.com

Interaction of inorganic and organic substances essential in the processes of physiogenic and pathogenic mineralization in human body. Of particular interest in this area is the study of reactions of free amino acids (AA) and hydroxyapatite (HA). Therefore, in a study of the adsorption interaction AA, such as Gly, Ala, Asp, Glu, Arg with hydroxyapatite (HA, Ssp = 93 m²/g, size 13 μm, particle charge in aqueous solution - positive) at pH 5,00-8,00 and concentration C = 0.030 mol/l.

It is found that the adsorption isotherm is described the Langmuir model for HA (Table. 1,2). As can be seen from Table. 1, maximum adsorption of AA on HA are variable (Gly = 7,50, Ala = 6,00, Asp = 8,00, Glu = 5,00, Arg = 5,00-6,00). calculated Gibbs energy values indicate a mechanism of physical adsorption AA as a brushite and hydroxyapatite, because it surfaces charged in an aqueous solution at a selected pH. As can be seen from Table. 2, calculated Gibbs energy values indicate a mechanism of physical adsorption of AA on hydroxyapatite, because it surfaces charged in an aqueous solution at a selected pH.

Table 1. Effect of solution pH on the adsorption of AA on HA

AA		pH					
		5,00	5,50	6,00	7,00	7,50	8,00
Gly	A, mol/kg	0,400	0,350	0,400	0,400	0,450	0,400
Ala		0,150	0,150	0,200	0,150	0,150	0,150
Asp		0,150	0,150	0,200	0,200	0,250	0,300
Glu		0,300	0,250	0,250	0,200	0,200	0,200
Arg		0,200	0,200	0,200	0,150	0,150	0,150

Table 2. Effect of solution pH on the Parameters of adsorption of AA on HA

AA		pH					
		5,00	5,50	6,00	7,00	7,50	8,00
Gly	ΔG (298°K), kJ/mol	-8,95	-8,87	-9,08	-9,08	-9,51	-8,80
Ala		-6,47	-7,42	-6,03	-6,47	-7,42	-7,42
Asp		-8,53	-8,53	-8,50	-8,50	-8,56	-8,70
Glu		-8,67	-8,53	-8,53	-8,46	-8,46	-8,46
Arg		-6,37	-6,37	-6,37	-7,42	-7,42	-7,42

Adsorption fact corroborated by FTIR spectroscopy and analysis of specific surface area (BET) for HA - Gly 52 m²/g (↓ 44 %), Ser and Glu 60 m²/g (↓ 35%), Ala and Asp 72 m²/g (↓ 22%). XRD shows that the phase transition does not occur in these adsorption conditions. Thus, a large value of the adsorption characteristic of the simplest amino acid - glycine.

The research was supported by RFBR, project mol_a No. 16-33-00684



THE EXPERIMENTAL DETERMINATION SPEED OF SOUND IN BINARY LIQUID MIXTURE TOLUENE + *n*-DODECANE AT TEMPERATURES 298.15-433.15 K AND PRESSURES UP TO 100 MPa

Golubeva N.V., Khasanshin T.S., Samuilov V.S., Shchamialiou A.P.

Mogilev State Foodstuffs University, 212027 Mogilev, Belarus

E-mail: vandnstar@yandex.ru

The study of multicomponent hydrocarbon mixtures of petroleum origin, which mostly consist of paraffinic, naphthenic and aromatic hydrocarbons is of great scientific and practical interest nowadays. These multi-component hydrocarbon mixtures composed mainly of paraffinic, naphthenic and aromatic hydrocarbons. The modern theory of the liquid state does not allow to calculate the thermodynamic properties of multicomponent liquid mixtures, which contain hydrocarbons of various classes over a wide range of parameter states within their direct experimental determination. In this case, for the study of the thermodynamic properties of multicomponent mixtures, as one of the approaches can be used the model mixes, consisting of a finite number of components. It is known that the mixtures consisting of three components exhibit the basic properties of multicomponent mixtures. The behavior of ternary mixtures can be explained with the help of a mixture of binary components. This research on the study of the acoustic and thermodynamic properties of binary liquid mixtures of toluene + *n*-dodecane is just an intermediate stage of our more complex multicomponent hydrocarbon mixture investigation.

n-Dodecane and toluene were selected as the main components of the binary model mixture. *n*-Dodecane is the component of diesel and rocket fuel, which is used in the petrochemical industry for analytical purposes. Toluene is widely used in various industries. It is used as additive to motor fuel, also as a part of various solvents, varnishes and paints and for the production of various organic substances.

The main method of binary liquid mixture of toluene + *n*-dodecane research was the acoustic one. The speed of sound was measured with the help of direct measurement of the transit time of the acoustic pulse through the test binary mixture in the temperature ranges from 298 to 433 K, pressures of up to 100.1 MPa at the molar concentration of the toluene in the mixture of $x_1 = 0.25, 0.50$ and 0.75 . An acoustic cell is the main element of measurement system. The acoustic cell is a stainless steel tube of 1Kh18N9T mark with the piezoelectric transducer and reflector disposed on its ends. As piezoelectric transducer was used a PZT-19 plate of 0.02 m diameter and 3 MHz resonance, which is covered on both sides with the thin layer of silver. As the reflector applied cylindrical surface with longitudinal triangular grooves on the back of the end surface. The length of the acoustic base was determined with the use of calibration of precise data on the speed of sound in water.

The speed of sound measurement was made using the multifunctional measuring complex UNIPRO, which consists of the pulse generator of arbitrary waveform and digital oscilloscope. The pressure was measured with the MP-2500 deadweight tester of class 0.05. The temperature was measured with the use of the precision multichannel MIT-8 temperature meter along with the exemplary 1st discharge PTS-10M resistance platinum thermometer. The control of the temperature was carried out in the automatic mode with the use of the RTP-8.1 precision temperature regulator. The accuracy of the temperature measurement is 0.02 K. The error of the experimental data do not exceed 0.1%.

The mixture was prepared using the weight method. The chromatographic analysis was performed before and after measurements. In the research we used the toluene of «ECOS-1» production with the purity of the main product by the weight for more than 99.5%, the *n*-dodecane was used of «Sigma-Aldrich» production with the purity of over 99%. The experimental data of the speed of sound was received for the first time.

The results of the speed of sound were approximated in the equation depending on temperature and pressure.



THE DETERMINATION OF THERMODYNAMIC PROPERTIES OF BINARY LIQUID MIXTURE CYCLOHEXANE + *n*-DODECANE USING ACOUSTIC METHOD

Golubeva N.V., Khasanshin T.S., Samuilov V.S., Shchamialiou A.P.

Mogilev State Foodstuffs University, Schmidt Avenue 3, 212027 Mogilev, Belarus

E-mail: vandnstar@yandex.ru

In this research work we carried out the experimental study of the speed of sound in the binary liquid mixture of cyclohexane + *n*-dodecane at temperatures from 298 to 433 K, pressures of 0.1–100.1 MPa and molar concentrations of cyclohexane, 0.25, 0.50 and 0.75. To determine the speed of sound we choose the method of direct measurement of the acoustic pulse in its time travel through the known distance in the test fluid. According to our results the error of determining the speed of sound is 0.1%. The veracity of the error is confirmed with the results of the control measurements in water and cyclohexane. As test samples we used cyclohexane and *n*-dodecane of «Sigma Aldrich» production with the purity of the main product by the weight for more than 99%, which were not cleaned further. The mixtures were prepared with the help of weighing at the atmospheric pressure and room temperature, so as to obtain the molar concentration of cyclohexane in it which will be equal to 0.25, 0.50 and 0.75.

While calculating the thermodynamic properties as inputs were used our own sound speed measures at atmospheric and elevated pressure, as well as the analytical temperature dependence of the density and isobaric heat capacity at the atmospheric pressure. To determine the temperature dependence of the density and isobaric heat capacity at the atmospheric pressure the literature data have been used for its density and the calculated values with the use of experimental data on the excess heat capacity found by linear extrapolation were used for the research of its specific heat. According to our results, the accuracy of input data of the density and sound speed in the calculation of the thermodynamic properties, does not exceed 0.1%, for the isobaric heat capacity – 1.5%.

The calculation of the thermodynamic properties was carried out by the relations linking the acoustic and thermodynamic quantities.

$$\rho = \rho_0 + \int_{p_0}^p \frac{1}{W^2} dp + T \int_{p_0}^p \frac{\alpha_p^2}{c_p} dp,$$

$$c_p = c_{p_0} - \int_{p_0}^p \frac{T}{\rho} \left[\alpha_p^2 + \left(\frac{\partial \alpha_p}{\partial T} \right)_p \right] dp,$$

$$c_v = \frac{c_p}{\left(1 + \frac{T \alpha_p^2 W^2}{c_p} \right)},$$

$$\beta_T = \frac{1}{\rho} \left(\frac{1}{W^2} + \frac{T \alpha_p^2}{c_p} \right),$$

where ρ и ρ_0 – denote the density at the increased p and atmospheric p_0 pressures; c_p и c_{p0} – denote the isobaric heat capacity at the increased and atmospheric pressures; W – denotes the speed of sound; c_v – means the isochoric heat at the increased pressure; β_T – is the isothermal compressibility at the increased pressure; $\alpha_p = -(\partial \rho / \partial T)_p / \rho$ – the coefficient of isobaric extension.

In the research we calculated the values of density, isochoric and isobaric heat capacity, the coefficient of isobaric expansion and the isothermal compressibility. The values of excess functions were also calculated. We analyzed the dependence of the thermodynamic and the excess properties of the temperature, pressure and composition. The calculated data of the density depending on the temperature, pressure and concentration were generalized in the Tate type equation.

**ENTHALPIES OF NICOTINAMIDE PROTOLYTIC EQUILIBRIA IN AQUEOUS DIMETHYLSULFOXIDE**

Grazhdan K.V., Dushina S.V., Sharnin V.A.

Ivanovo State University of Chemistry and Technology, 153000, Ivanovo, Russia

E-mail: grakonst@gmail.com

Heat effects of nicotinamide (NicNH₂) protonation in aqueous dimethylsulphoxide (DMSO) at 25.00 ± 0.01 °C and ionic strength 0.25 (NaClO₄) in range X_{DMSO} = 0 – 0.75 mole fraction were determined by means of calorimetric technique. The obtained values were extrapolated to zero ionic strength in separate experiment, thus we present the heat effects as a standard enthalpies.

Early we determined constants of nicotinamide protolytic equilibria [1].

Table 1. The enthalpies of nicotinamide protonation in water – DMSO solvents.

X _{DMSO} , mol. f.	0	0,1	0,3	0,5	0,75
Δ _r H ^o , kJ/mol	-13,75 ± 0,20	-15,88 ± 0,41	-12,45 ± 0,50	-9,70 ± 0,45	-12,05 ± 0,16

From Table 1 we can see that the change of protonation enthalpy has two extremums, when DMSO concentration increasing. In early increase of the organic component content increases absolute value of Δ_rH^o. Further, there is a decrease of reaction heat effects with a minimum at 0.5 mol. f. DMSO.

For results discussion we use the solvation-thermodynamic approach [2], based on analysis of reagents contribution to reaction enthalpy.

The authors [3] defined enthalpies of proton transfer from water to aqueous dimethylsulfoxide by means of calorimetric method from enthalpy of HCl dissolution. They used extrathermodynamic assumption about equality of thermodynamic characteristics of tetraphenylphosphonium and tetraphenylborate ions transfer.

S-shaped Δ_rH change is the result of reagents resolution dynamics at DMSO concentration increasing. The enthalpic contribution of nicotinamide predominate. A slight change of reaction heat effect at transfer from water to aqueous DMSO is caused by slight change of nicotinamide transfer enthalpy and compensation of contributions for proton and protonated nicotinamide.

A significant difference in transfer enthalpies of NicNH₂ and NicNH₃⁺ we can explain by increasing of interaction of positively charged particles with donor centers of DMSO molecules compared with water.

The earlier data on the nicotinamide protonation enthalpies in water – ethanol solvent [4] indicate that changes in these solvents composition has a similar effect on the heat effect of HL⁺ formation. This fact, however, does not mean the same effect of these solvents on the enthalpy of reagents transfer from water to binary solvents. This effect naturally has different character [4].

Acknowledgement: the research was carried out in Research Institute of Thermodynamics and Kinetics of Chemical Processes of Ivanovo State University of Chemistry and Technology in the framework of State Assignment of Ministry of Education and Science of Russian Federation.

[1] Sharnin, V. A.; Dushina, S. V.; Zevakin, M. A.; Gushchina, A. S.; Grazhdan, K. V. *Inorganica Chimica Acta*, 2009, 362, 437-442.

[2] Sharnin, V. A. *Izv. Vyssh. Uchebn. Zaved. Khim. Khim. Tekhnol.*, 2005, 48, 44-53.

[3] Hefter, G.; Marcus, Y.; Waghorne, W. A. *Chem. Rev.*, 2002, 102, 2773–2836.

[4] Grazhdan, K. V.; Dushina, S. V.; Sharnin, V. A. *Russ. J. Phys. Chem. A*, 2009, 83, 1734-1736.

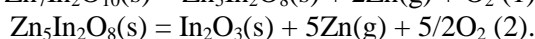
THE STANDARD ENTHALPIES OF FORMATION OF MIXED INDIUM AND ZINC OXIDES

Gribchenkova N.A., Alikhanyan A.S.

Kurnakov Institute of General and Inorganic Chemistry, Russian Academy of Sciences,
119991 Moscow, Russia
E-mail: gribchenkova@igic.ras.ru

Samples of the In_2O_3 – ZnO quasi-binary system were synthesized from mixtures of In_2O_3 and ZnO by solid-state synthesis at 1323 K in air.

The heterogeneous phase regions $[\text{ZnO} + \text{Zn}_7\text{In}_2\text{O}_{10}]$ (I), $[\text{Zn}_7\text{In}_2\text{O}_{10} + \text{Zn}_5\text{In}_2\text{O}_8]$ (II), $[\text{Zn}_5\text{In}_2\text{O}_8 + \text{In}_2\text{O}_3]$ (III) and the individual mixed oxides were studied by the Knudsen effusion technique with mass spectrometric analysis of the gas phase in the temperature range 1380 K to 1460 K. An MS-1301 high-temperature mass spectrometer was used in the experiments. Quartz effusion cells with the cell cross section area-to-effusion orifice area ratio of about 640 were employed. The vapor above the system consists almost only of $\text{Zn}(\text{g})$ and O_2 in the whole composition range except the solid solution adjacent to In_2O_3 . This fact indicates the incongruent character of vaporization in the system. The system figurative point moves toward less volatile In_2O_3 during the effusion experiments and the mixed oxides sublime by the reactions: $\text{Zn}_7\text{In}_2\text{O}_{10}(\text{s}) = \text{Zn}_5\text{In}_2\text{O}_8(\text{s}) + 2\text{Zn}(\text{g}) + \text{O}_2$ (1) and



The obtained values of the partial pressures were published previously [1]. On their basis a p - x -section of the system phase diagram was constructed (figure). The total pressure decreases when the figurative point passes through the solid solution of In_2O_3 in ZnO , the $\text{Zn}_7\text{In}_2\text{O}_{10}$ and $\text{Zn}_5\text{In}_2\text{O}_8$ homogeneity regions, the solid solution of ZnO in In_2O_3 and reaches its minimum at pure In_2O_3 .

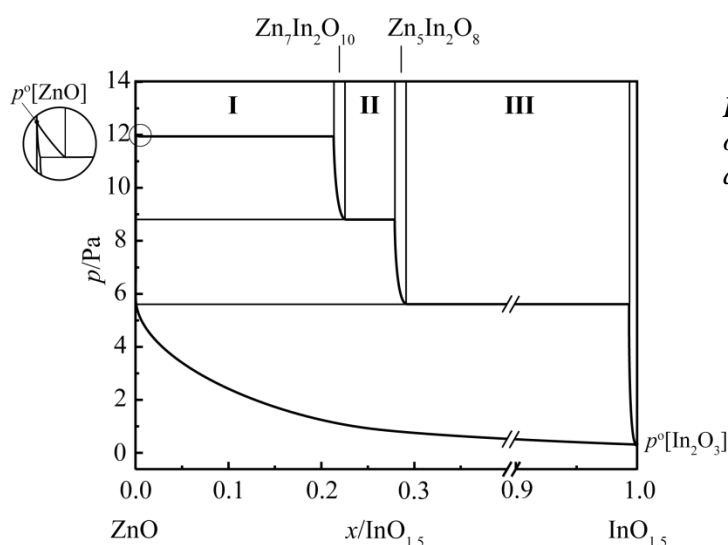


Figure. Schematic p - x -section of the system phase diagram at 1428K.

The enthalpies of sublimation reactions (1) and (2) were obtained by the modified third law calculations. The formation enthalpies of the mixed oxides were calculated (Table).

Table. Enthalpies of sublimation and formation of mixed oxides $\text{Zn}_7\text{In}_2\text{O}_{10}$ and $\text{Zn}_5\text{In}_2\text{O}_8$

Compound	$\Delta_s H^\circ(1428/\text{K})$	$\Delta_s H^\circ(298/\text{K})$	$\Delta_f H^\circ(298/\text{K})$
	kJ/mol		
$\text{Zn}_7\text{In}_2\text{O}_{10}$	935 ± 24	965 ± 30	-3390 ± 31
$\text{Zn}_5\text{In}_2\text{O}_8$	2339 ± 36	2413 ± 41	-2686 ± 42

[1] Gribchenkova, N.A.; Steblevsky, A.V.; Alikhanyan, A.S. XX International conference on chemical thermodynamics in Russia, June 22-26, 2015, Nizhni Novgorod. P. 237.


 VAPORIZATION THERMODYNAMICS OF THE Al_2O_3 - MgO SYSTEM

Gribchenkova N.A., Smorchkov K.G., Alikhanyan A.S.

 Kurnakov Institute of General and Inorganic Chemistry, Russian Academy of Sciences,
 119991 Moscow, Russia

E-mail: gribchenkova@igic.ras.ru

Samples of the $[\text{MgO} + \text{MgAl}_2\text{O}_4]$ (I) and $[\text{MgAl}_2\text{O}_4 + \text{Al}_2\text{O}_3]$ (II) heterogeneous phase regions and the MgAl_2O_4 spinel individual phase were obtained by solid-state synthesis at 1373 K in air.

Vaporization processes in the Al_2O_3 - MgO quasi-binary system were studied by the Knudsen effusion technique with mass spectrometric analysis of the gas phase in the temperature range 1750 K to 1930 K. An MS-1301 high-temperature mass spectrometer was used in the experiments. Tungsten effusion cells covered inside with iridium were employed. The cell cross sectional area-to-effusion orifice area ratio was about 800.

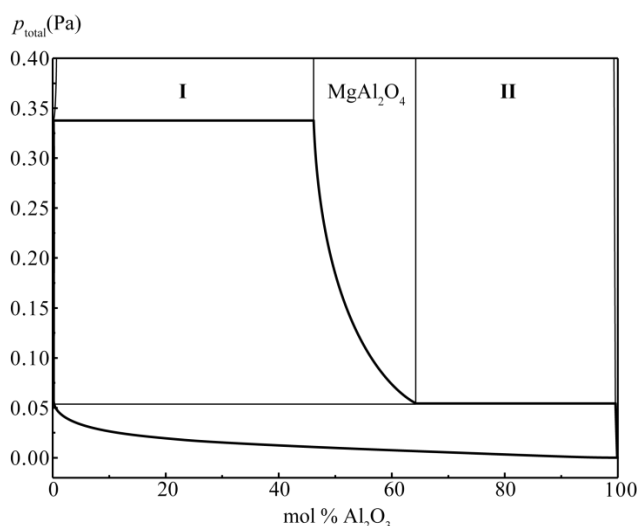
In the vapor above the system only $\text{Mg}(\text{g})$, O_2 and O were detected in the whole composition range. The nonvolatile residue in the evaporation experiments was only Al_2O_3 . That means that the MgAl_2O_4 spinel sublimes incongruently by the reaction $\text{MgAl}_2\text{O}_4(\text{s}) = \text{Mg}(\text{g}) + x\text{O}_2 + (1-2x)\text{O} + \text{Al}_2\text{O}_3(\text{s})$.

The determined partial and total pressures above the system phase fields are given in the Table. The results were summarized in a p - x -section of the system phase diagram (Figure).

Table. Partial and total pressures of the Al_2O_3 - MgO system in the effusion conditions.

Condensed phase composition	p^* (Pa)			
	Mg	O_2	O	total
MgO	0.209	0.099	0.030	0.337
MgO + MgAl_2O_4	0.209	0.099	0.030	0.337
$\text{MgAl}_2\text{O}_4 + \text{Al}_2\text{O}_3$	0.032	0.011	0.010	0.054

* The pressures are given with the precision required for a correct calculation of equilibrium constants. The O_2 and O partial pressures could not be accurately measured in the experiments and were computed from $p(\text{Mg})$.



The obtained partial pressures temperature dependences contain the dimensionless values normalized to the standard pressure of 101325 Pa. MgO, I (1750—1930 K):

$$\lg[p(\text{Mg})] = -(25242 \pm 1315)/T + (7.43 \pm 0.71),$$

$$\lg[p(\text{O}_2)] = -(25098 \pm 1797)/T + (7.01 \pm 0.80),$$

$$\lg[p(\text{O})] = -(25869 \pm 735)/T + (6.99 \pm 0.40).$$

II (1900—2100 K):

$$\lg[p(\text{Mg})] = -(26226 \pm 2784)/T + (6.72 \pm 1.40),$$

$$\lg[p(\text{O}_2)] = -(26185 \pm 4023)/T + (6.05 \pm 2.02),$$

$$\lg[p(\text{O})] = -(26413 \pm 2011)/T + (6.51 \pm 1.01).$$

Figure. Schematic p - x -section of the system phase diagram at 1900 K.

The standard enthalpy of formation of the MgAl_2O_4 spinel from the oxides was calculated by the third law calculations: $\Delta_f H^\circ(1900/\text{K}) = -14.52 \pm 10.92$ kJ/mol, $\Delta_f H^\circ(289/\text{K}) = -24.68 \pm 10.92$ kJ/mol. The standard enthalpy of formation of MgAl_2O_4 from the simple substances at 289/K was found to be -2301.61 ± 11.00 kJ/mol.

The work was supported by the Russian Foundation for Basic Research (grant 16-08-00815 A).



THE DEPENDENCE OF PARAMETERS OF THE MELTING AND CRYSTALLIZATION PROCESSES OF WATER NANOCLUSTERS IN A BIOPOLYMER MATRIX ON THEIR SIZES

Grunina N.A.* , Belopolskaya T.V., Tseretely G.I., Smirnova O.I.
Saint-Petersburg State University, Saint-Petersburg, Peterhoff 198504, Russia
* State University of Civil Aviation, Saint-Petersburg, 196210, Russia
e-mail: nagrunina@mail.ru

This work is a part of the researches of thermal properties of water structures (clusters) in various starches spent by us recently [1, 2]. As it was shown in different studies, water in starches with low hydration degree as well as in other biopolymers can be found in the dispersed state, which manifests itself by the values of its melting temperature below 0°C. Thus the starch granule that consists of starch molecules and unfrozen water (UFW), which is their closest surrounding, can be viewed as a unique flexible biopolymer matrix, in which water clusters can be formed in the pores. Importantly, changing the hydration degree of starch granule in the same original matrix can yield systems with different distributions of water clusters' sizes.

The phase transitions of frozen water (FW) dispersed in the native and amorphous potato starch with humidity 27 ÷ 45% has been studied by means of DSC. The results obtained have allowed to establish the relationship between the thermodynamic parameters of the melting and crystallization of FW and the size of water clusters in the starch matrix. We believe that peak temperature of the melting curve (T_m) reflects the average size of the water clusters formed in the starch and heat (Q_m) – their number. As for crystallization curves of FW, then, due to a more complex nature of this process, to connect directly the crystallization temperature (T_{cr}) with the size of water clusters it is not possible. However, to follow the relative change of water clusters' sizes based on the observed changes in temperature and heat of crystallization of FW depending on its content in starch, in our opinion, it is quite possible.

The size effect in the dependences of the temperatures of these processes (T_m and T_{cr}) has been detected only for the native starch: both T_m and T_{cr} of the water clusters decrease with the decrease of humidity of the native starch. The sizes of the water clusters formed in these conditions have been estimated (5 ÷ 35 nm). In contrast, in amorphous starch with low humidity the size effect for the T_m and T_{cr} of water clusters has not been observed. The various reasons for the lack of the size effect during melting and crystallization of FW for the amorphous starch are suggested. Since the process of amorphization of starch with low humidity requires heating of the sample to a high temperature, the additional FW appears in the system, that increases the average size of water clusters. This, in turn, leads to an increase of T_m . In the case of crystallization of FW in the amorphous starch with low humidity the size effect is masked by glassification of the biopolymer itself. So, the role of a cluster size is secondary. In contrast, in the native state at a relatively rigid internal structure of the granule, the water clusters' sizes play the main role at the crystallization.

A manifestation of the size effect in the dependences of the heats of the melting and crystallization of FW has been established for both native and amorphous starch. The heat values of both transitions of FW in the starch with low humidity are significantly smaller than that for the bulk water.

Importantly, the hysteresis at the melting and crystallization of FW, which is characteristic to small particles, has been found for both states of the potato starch with the fixed humidity. A manifestation of the observed hysteresis is strongly different for the native and amorphous biopolymer.

Analysis of the melting and crystallization curves of FW in the starch with different humidity has shown that the redistribution of water clusters' sizes can occur when the temperature changes, both above and below 0°C. At $T < 0^\circ\text{C}$ during cooling and heating the reorganization of the initial distribution of water clusters' sizes, which is characteristic for room temperature, is possible. Such changes may lead to an increase of an average cluster size at the crystallization and melting. The intensity of such a transformation depends on the water content in a starch and the different scan rates and differs for the native and amorphous states of the starch.

The information presented in this work concerning the thermodynamic parameters of the melting and crystallization of dispersed supercooled water in the starch matrix is very important for both theory and application, in particular, for understanding of physical processes at freezing/thawing of starch-containing substances.

[1] Grunina N.A., Tsereteli G.I., Belopolskaya T.V., Smirnova O.I. / *Carbohydr.Pol.*, **132**, 499-508 (2015).

[2] Tsereteli G.I., Belopolskaya T.V., Grunina N.A., Smirnova O.I. / *Biofizika*, **62** (1), 53-64 (2017).

EFFECT OF MEDIUM ON THE CONSTANTS OF ACID-BASE EQUILIBRIA OF NICOTINIC ACID

Guschina A.S., Kuranova N.N., Chesnokova N.A., Dushina S.V., Sharnin V.A.

Ivanovo State University of Chemistry and Technology

E-mail: kax504@isuct.ru

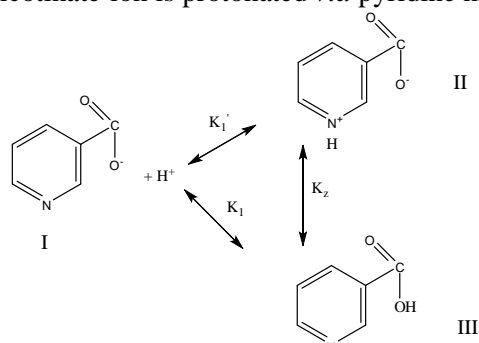
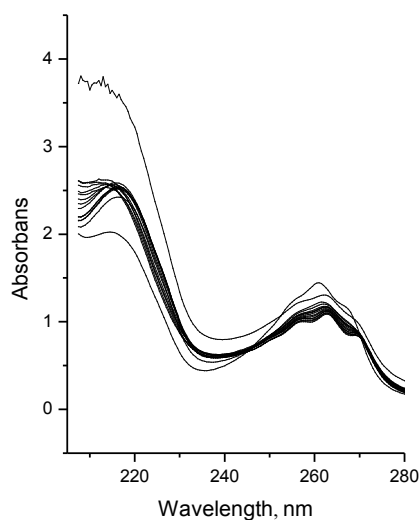
Protolytic equilibria of nicotinic acid is a biochemically relevant, especially applying toward cell-membrane transport activity. The solvent is important factor of influence on the chemical processes. One of the main problems of chemical thermodynamics is studying the solvent influence (its nature and concentration) on the reagents solvation and protolytic and coordination equilibria in solutions.

The present paper reports on the study of protonation constants nicotinate-ion (K_1') and nicotinic acid (K_2) as dependent on composition of aqueous ethanol by spectrophotometric method.

The studies have been carried out in aqueous ethanol (concentration range is 0.1 – 0.75 mol. fractions) at 298.15 K and ionic strength of $I = 0.25$ (NaClO_4). Absorption spectra were obtained using a double-beam Shimadzu UV-1800 UV/Vis scanning spectrophotometer with standard 1 cm quartz cells. UV/Vis bandwidth, scan speed and data interval used are 0.1 nm, 100 nm min^{-1} and 0.5 nm, respectively. The concentration of nicotinic-ion and perchloric acid was 0.20 – 0.47 mmol $\cdot\text{dm}^{-3}$ and 0.02 – 30 mmol $\cdot\text{dm}^{-3}$, respectively. Absorption spectra for nicotinic acid ($C = 0.40$ mmole $\cdot\text{dm}^{-3}$) at different pH (6.54-1.88) is presented (Fig). All collected spectra were processed by FTMT computer program [1].

The protonation constants of nicotinate-ion and nicotinic acid identified in this work are below than ones obtained previously [2] (within the error of determination). The increasing ethanol content in the mixed solvent in general increases the acid-base constants. We observe an extreme variation in the first-step protonation constant of nicotinate-ion. $\log K$ has a minimum in the solvent composition range where the ethanol mole fraction is ~ 0.1 , which is usually assigned to the structure strengthening of the solvent containing low content of the organic component.

The zwitterionic-ionic form (II) of nicotinic acid predominates over molecular form (III) in solution [3]. In this regard, nicotinate-ion is protonated *via* pyridine nitrogen atom.



Using the ratio of particles (II) and (III) [3] we can estimate the protonation constants of nicotinate-ion *via* pyridine nitrogen atom (K_1') and its carboxyl group (K_1), and constants of zwitterionic-ionic equilibrium (K_2).

Low value K_2 leads to a shift of equilibrium toward the formation of zwitterionic-ionic form (II) in aqueous solution. The increasing ethanol concentration in the solvent leads to an increase of constant K_2 and quantity of molecular forms of nicotinic acid (III) in solutions.

[1] Borodin V.A., Vasiliev V.P., Kozlovskii E.V., Kokovin ed, Nauka, Novosibirsk, 1985.

[2] Kuranova N.N., Dushina S.V., Sharnin V.A. Russ. J. Inorg. Chem, 2008, 53, 12, 1943-1947.

[3] Grazhdan K.V., Gamov G.A., Dushina S.V., Sharnin V.A. Russ. J. Phys. Chem. A, 2012, 86, 11, 1679-1681.



THERMODYNAMIC INVESTIGATION OF Al-N and Ga-N SYSTEMS

Ilinykh N.I., Malkova I.A., Volgarev E.A.

¹ Ural Technical Institute of Telecommunications and Informatics, 15, Repin Str., Ekaterinburg, 620109, Russia
E-mail: ninail@bk.ru

Metal nitrides of 3-th group (AlN, GaN, BN, InN) have a great scientific and practical interest because they are perspective materials for semiconductor electronics, in particular, for the use in the semiconductor radiation sources in the short-wave region of the visible range and the near ultraviolet. Many of these compounds have high refractoriness and chemical resistance in different aggressive media, dielectric and semiconductor properties, capability to pass for superconductivity at relatively high temperatures, wear resistance, low melting points and low values of hardness [1].

Despite the fact that the experimental study of these materials is given enough attention, many of their properties and characteristics are investigated insufficiently. Therefore the theoretical investigation metal nitrides of 3-th group is important.

Presented work is devoted to the investigation of Al-N and Ga-N systems. The study was carried with the use of thermodynamic modelling methods [2]. As the software the program set TERRA was used [3].

The temperature and concentration dependences of composition and thermodynamic characteristics (enthalpy, entropy and Gibbs energy) of Al-N alloys and partial pressures of the components of the gas phase above these alloys were obtained in wide range of temperatures (300 – 3000 K) at the common pressure 10^5 Pa.

It was established, that the activities of the components have big negative deviations from Raoult's law. Concentration dependencies of integral excess Gibbs energies, entropies and enthalpies are not monotonous. These facts justify, that strong interaction between atoms of different sorts takes place.

It was shown that the partial pressures of the gas phase components can be describe by linear equations $\ln P = A+B/T$, where A and B are constant coefficients, T - temperature, K.

[1] G.V. Samsonov. *Nitrides*. Kiev, Naukova Dumka, 1969, 380 p. (in Russian).

[2] N.A. Vatolin, G.K. Moiseev, B.G. Trusov. *Thermodynamic modelling in high - temperature inorganic systems*. Metallurgia, Moscow, 1994 (in Russian).

[3] B.G. Trusov. Vestnik of Bauman Moscow State Technological University, **2** (special Issue), 240-249 (2012) (in Russian).



THERMODYNAMIC MODELING OF Ni-C-Cr-Si-B ALLOYS

Krivorogova A.S.¹, Ilinykh N.I.^{1,2}

¹ Ural Institute of the State fire service EMERCOM of Russia, 22 Mira Str., Ekaterinburg, Russia

² Ural Technical Institute of Telecommunications and Informatics, 15, Repin Str., Ekaterinburg, 620109, Russia

E-mail: ninail@bk.ru

Thermal spray processes have been widely used in the different engineering industry sectors for component protection and reclamation. Thus, thermal spray coatings are used for surface hardening, protection from exposure to high temperatures, thermal erosion and abrasive wear, corrosion protection in a variety of environments and so on. Besides that, thermal spray coatings used for restoring of geometrical dimensions and form of surface of the worn details [1-3]. As the materials for thermal spray coatings self-fluxing alloys are used [4-5]. In general, there are nickel-base or cobalt-base alloys that use boron, phosphorus, or silicon, either singly or in combination, as melting-point depressants and fluxing agents. These materials have relatively low melting points and, as a rule, require post-spray heat treatment.

For designing and optimizing processes of creation of thermal spray coatings it is necessary to improve our notions about structure of liquid alloys because heat treatment of the melt can influence greatly on properties of solidified materials. The preliminary thermodynamic estimation is necessary to predict and check the multifunctional structures of complex composition and to create the flexible coating technologies.

Present work is devoted to investigation of equilibrium composition and thermodynamic characteristics of Ni-C-Cr-Si-B alloys. Investigations were carried out using the thermodynamic modeling method [6, 8]. As a software the program complex TERRA was used [7]. The structure of solid and liquid alloys was described by the model of ideal solutions (IS) and by the model of ideal solutions of interaction products (ISIP) [6, 8]. Modeling was executed in the wide range of temperatures (300 – 2000 K) at the common pressure of $P = 10^5$ Pa in argon. Initial content of modeling systems (mass. %): 1) Ni - 79.3, C - 0.5, Cr - 15, Si - 3.2, B - 2, Ar - 1; 2) Ni - 74.3, C - 1, Cr - 17, Si - 4.1, B - 3.6, Ar - 1. According to ISIP model liquid alloy (melt) consists of Ni, C, Cr, Si, B atoms and associates corresponding to the binary compositions of Ni-C-Cr-Si-B system: Ni₃C, NiB, Ni₃B, Ni₂B, Ni₄B₃, NiSi, NiSi₂, Ni₂Si, Ni₇Si₁₃, SiC, SiB₁₄, B₄Si, B₆Si, B₄C, CrB, CrB₂, Cr₃B₄, Cr₅B₃, Cr₃C₂, Cr₇C₃, Cr₂₃C₆, CrSi, CrSi₂, Cr₃Si, Cr₅Si₃.

The temperature dependences of the integral and partial excess thermodynamic characteristics (enthalpy, entropy and Gibbs energy) and equilibrium composition of alloys were obtained.

Comparison of temperature dependences of content of alloy's components with temperature dependences of thermodynamic properties shows that there is correlation between the graphs: "fractures" on the curves are observed at the same temperatures. It can be assumed that these fractures are caused by phase transformations.

1. A. Khasui, O. Morigaki, Hard Facing and Sputtering. (Mashinostroenie, Moscow. 1985) (in Russian)
2. V.V. Kudinov, Plasma coatings (Nauka, Moscow, 1977) (in Russian)
3. R. Knight and R.W. Smith, *ASM Handbook*, 7, 408 (1998)
4. R.C. Tucker, Jr. *ASM Handbook*, 5, 497 (1994)
5. Frolov V.A., Poklad V.A. *Svarochnoe proizvodstvo* **11**, 38 (2006) (in Russian)
6. N.A. Vatolin, G.K. Moiseev, B.G. Trusov, Thermodynamic modeling in high temperature inorganic systems (Metallurgia, Moscow, 1994) (in Russian).
7. B.G. Trusov, *Vestnik of Bauman Moscow State Technological University*, 2 (special Issue), 240 (2012) (in Russian).
8. N.I. Ilinykh, T.V. Kulikova, G.K. Moiseev, Composition and equilibrium characteristics of metallic melts of binary systems on the basis of iron, nickel and aluminum (Publ. UB of RAS, Ekaterinburg, 2006) (in Russian).

**LIGAND SOLVATION INFLUENCE ON THERMODYNAMIC PARAMETERS OF Ni²⁺ – GLYCYLGLYCINATE COMPLEXATION IN AQUEOUS ORGANIC SOLVENTS**

Isaeva V.A., Sharnin V.A.

Ivanovo State University of Chemistry and Technology, 153000, Ivanovo, Russia

E-mail: kvol1969@gmail.com

Enthalpies of glycyglycinate-ion (GG⁻) resolution in aqueous ethanol (EtOH) and dimethylsulfoxide (DMSO), and enthalpies of mono-, bis- and tris-glycyglycinate nickel(II) complexes formation at ionic strength 0.1 (NaClO₄) in aqueous dimethylsulphoxide were determined by means of calorimetric method at 298 K (Table 1).

Table 1. The enthalpies of GG⁻ resolution and [NiGG]⁺ complexation in water – organic solvents.

$\Delta_{tr}H$, kJ/mol	Solvent	Solvent composition, mol. f.									
		0.05	0.1	0.2	0.3	0.4	0.5	0.6	0.7	0.8	0.99
$\Delta_{tr}H_{r1} \pm 0.6$	Water + DMSO	–	-6.0	-13.0	-22.3	-27.0	-29.5	-27.5	–	–	–
$\Delta_{tr}H^{\circ}_L \pm 0.6$	Water + DMSO	0.03	0.7	16.8	36.5	47.3	56.4	62.7	–	69.6	72.5
$\Delta_{tr}H^{\circ}_L \pm 0.6$	Water + EtOH	1.9	2.8	5.9	12.1	14.4	16.1	18.9	18.1	21.1	–

Estimation of participation degree of ligands (L) resolution in the complexation process allows to predict the change in thermodynamic parameters of complexation. Quantitative assessment of thermodynamic parameters of complexation by means of thermodynamic characteristics of ligands resolution can be obtained by difference coefficient α_{dif} [1]:

$$\Delta_{tr}Y^{\circ}_r = (\alpha_{dif} - 1) \cdot \Delta_{tr}Y^{\circ}_L,$$

where $\Delta_{tr}Y^{\circ}_r$ – change of complexation ΔH° or ΔG° in aqueous organic solvents, $\Delta_{tr}Y^{\circ}_L$ – ΔH° or ΔG° of ligand resolution.

The difference coefficient α_{dif} for carboxylate ligands complexation with transition metals ions lies in the range 0.7 – 0.8, for amine ligands complexation with *d*-metals $\alpha_{dif} < 0.6$ [1]. For Ni²⁺ complexation with glycyglycinate-ion in aqueous DMSO the difference coefficient α_{dif} , calculated by enthalpic characteristics, is equal to 0.48 ($X_{DMSO} = 0.5$ mol. f.). This value is lower than range, established for acidoligands, and more close to α_{dif} value for amine-type ligands. For [NiGG]⁺ formation reaction in water – DMSO solvents α_{dif} , calculated from the change of reaction ΔG° [2] and from the ligand resolution ΔG° [3], is equal to 0.54, which is also less than the set values. Therefore, α_{dif} range should be expanded to 0.5 – 0.8, when the heat effect of glycyglycinate-ion complexation with *d*-metals ions is evaluated. For this reason on the basis of $\Delta_{tr}H^{\circ}(GG^{-})$ values we can assume that the value of complexation $\Delta_{tr}H^{\circ}$ in water – ethanol solvents will be between 3 and 8 kJ/mol. Based on the obtained range of $\Delta_{tr}H^{\circ}_{r1}$ and $\Delta H^{\circ}_{r1} = -16.72$ kJ/mol in the aqueous solution [3], we expect the heat effect of [NiGG]⁺ formation reaction in range 20 – 25 kJ/mol at water – ethanol solvent with 0.5 mol. f. of ethanol.

Acknowledgement: the research was carried out in Research Institute of Thermodynamics and Kinetics of Chemical Processes of Ivanovo State University of Chemistry and Technology in the framework of State Assignment of Ministry of Education and Science of Russian Federation.

[1] Sharnin, V. A. *Izv. Vyssh. Uchebn. Zaved. Khim. Khim. Tekhnol.*, 2005, 48, 44-53.

[2] Naumov, V. V.; Isaeva V. A.; Kovaleva, Yu. A.; Sharnin, V. A. *Russ. J. Phys. Chem. A*, 2013, 87, 1135-1137.

[3] Naumov, V. V.; Isaeva V. A.; Kuzina, E. N.; Sharnin, V. A. *Russ. J. Phys. Chem. A*, 2012, 86, 1773-1775.



EXPERIMENTAL DETERMINATION OF SPEED OF SOUND AND DENSITY OF LIQUID *ISO*-PROYLBENZENE AND *TERT*-BUTYLBENZENE AT TEMPERATURES 298.15-433.15 K AND PRESSURES UP TO 100 MPA

Khasanshin T.S.¹, Shchamialiou A.P.¹, Samuilov V.S.¹, Mosbakh F.M.¹, Drăgoescu D.², Sîrbu F.².

¹ Mogilev State University of Food Technologies, 212027 Mogilev, Belarus

² „Ilie Murgulescu” Institute of Physical Chemistry, Romanian Academy, 060021 Bucharest, Romania

E-mail: khasanshin@tut.by

At present experimental data on thermodynamic properties for liquid *iso*-proylbenzene and *tert*-butylbenzene are scarce. At the same time, these compounds are widely used in industry. Knowledge of a large number of thermodynamic properties over a wide range of state parameters is essential for designing appropriate processes and equipments in which they are used.

For a further investigation of the thermodynamic properties of the abovementioned substances and mixtures thereof, speed of sound and density of the liquid *iso*-propylbenzene and *tert*-butylbenzene in the temperature range 298.15-433.15 K at pressures up to 100 MPa have been measured. The *iso*-proylbenzene and *tert*-butylbenzene samples were obtained from Aldrich with a stated minimum purity of 98 and 99%, respectively.

Density has been measured with a new apparatus using a Anton Paar DMA HPM vibration-tube densimeter. Temperature has been measured with a platinum resistance thermometer Hart Scientific (model: 5608) with an uncertainty of 0.02 K. The pressure has been measured with an MP-2500 dead-weight pressure gage with an uncertainty of 0.05%. Densitometer has been calibrated using the model proposed by Bouchot and Richon [1]. The overall uncertainty in density measurements is estimated to be 0.03%.

Comparison of measurements of *iso*-proylbenzene and *tert*-butylbenzene densities with available experimental data has been performed. The most reliable data on the density of *iso*-proylbenzene and *tert*-butylbenzene agree with the results of measurements within 0.3 and 0.09%, respectively.

The experimental investigation of the speed of sound in liquid *iso*-proylbenzene and *tert*-butylbenzene has been done using the apparatus previously described in [2]. The ultrasonic apparatus, used for the measurement of speed of sound, is based on direct chronometry of the transfer times of pulses within the cell containing the sample at the working frequency 3 MHz. The measurement of time intervals was performed using a digital oscilloscope, which is a part of multifunctional measuring complex UNIPRO. The temperature has been measured with a PTS-10M first-class platinum resistance thermometer with an uncertainty of 0.02 K. The pressure has been measured with an MP-2500 dead-weight pressure gage with an uncertainty of 0.05%. The precision of the speed of sound measurements was estimated to be 0.1%.

A comparison of the measured values for the speed of sound in liquid *iso*-proylbenzene and *tert*-butylbenzene with available experimental data showed them to agree within 0.3 and 0.2%, respectively.

Research has been carried out in the framework of the joint project T16RA-004, with the financial support of the Belarusian Republican Foundation for Fundamental Research and the Romanian Academy. The Romanian authors want to express their acknowledgement to the Romanian Academy, for the financing the research programme “Chemical thermodynamics and kinetics. Quantum chemistry” of the “Ilie Murgulescu” Institute of Physical Chemistry. The financial support of the EU (ERDF) and Romanian Government, which allowed for the acquisition of the research infrastructure under POS-CCE O 2.2.1 Project INFRANANOCHEM - Nr. 19/01.03.2009, is also acknowledged.

[1] Bouchot, C.; Richon, D.; Fluid Phase Equilib., 2001, 191, 189-208.

[2] Khasanshin, T.S.; Samuilov, V.S.; Shchemelev, A.P. J. Eng. Phys. Thermophys., 2008, 81, 760-765.



EXPERIMENTAL DETERMINATION OF DENSITY AND SPEED OF SOUND IN THE BINARY LIQUID MIXTURE OF *ISO*-PROPYLBENZENE + *n*-HEXADECANE

Khasanshin T.S.¹, Samuilov V.S.¹, Shchemialiou A.P.¹, Paddubski A.G.¹, Drăgoescu D.², Sîrbu F.²

¹Mogilev State University of Food Technologies, 212027 Mogilev, Republic of Belarus

²„Ilie Murgulescu” Institute of Physical Chemistry, Romanian Academy, 060021 Bucharest, Romania

E-mail: khasanshin@tut.by

The present paper deals with experimental determination of density and speed of sound in the binary liquid mixture of *iso*-propylbenzene (cumene) + *n*-hexadecane at temperatures from 298 to 433 K, at pressures from 0,1 to 100 MPa and at mole fractions of cumene in mixture of 0,25, 0,50 and 0,75. The cumene and hexadecane used in this study were supplied from Sigma-Aldrich with a specified minimum purity of 98 and 99 %, respectively. The chemicals were used without any further purification.

An Anton Paar DMA HPM vibration U-tube densimeter has been used in order to measure the density as function of temperature and pressure. Densimeter has been calibrated using the method proposed by Bouchot and Richon [1] on the basis of vacuum and water data. The temperature dependencies of the oscillation period of U-tube were obtained both under vacuum and in the water. The temperature was measured by a platinum resistance thermometer Hart Scientific (model: 5608) with inaccuracy less than 0.02 K. The pressure was measured by a deadweight gauge manometer MP-2500 with a grade of accuracy of 0.05%. The overall uncertainty in density measurements is estimated to be 0.03%.

The ultrasonic apparatus, used for the measurement of speed of sound, is based on direct chronometry of the transfer times of pulses within the cell containing the sample. The apparatus and procedure of measurement have been described in detail in [2]. The measurements of speed of sound were carried out using multifunctional measuring complex UNIPRO, which consists of arbitrary waveform oscillator and digital oscilloscope. The temperature was measured by a platinum resistance thermometer PTS-10M with inaccuracy less than 0.02 K. The pressure was measured by a deadweight gauge manometer MP-2500 with a grade of accuracy of 0.05%. The precision of the speed of sound measurements was estimated to be 0.1%.

The density and the speed of sound measurements were performed along isotherms with increasing and then decreasing pressure, whereas the difference between repetitive measurements was less than 0.01%. After having carried out a measurement at all isotherms, a repeated measurement was done at first temperature. The agreement between the results of repeated measurements of speed of sound and density, in this case, was within 0.03% and 0.01%, respectively. Repeated measurements results showed that the mixture composition change during experimental work did not take place.

The experimental data for the investigated mixture have been obtained for the first time. The results of measurements have been represented both in tabular and analytical form. The standard and maximum deviations of fitted and initial experimental values do not exceed 0.02 and 0.05%, respectively.

Research has been carried out in the framework of the joint project T16RA-004, with the financial support of the Belarusian Republican Foundation for Fundamental Research and the Romanian Academy. The Romanian authors want to express their acknowledgement to the Romanian Academy, for the financing the research programme “Chemical thermodynamics and kinetics. Quantum chemistry” of the “Ilie Murgulescu” Institute of Physical Chemistry. The financial support of the EU (ERDF) and Romanian Government, which allowed for the acquisition of the research infrastructure under POS-CCE O 2.2.1 Project INFRANANOCHEM - Nr. 19/01.03.2009, is also acknowledged.

[1] Bouchot, C.; Richon, D.; Fluid Phase Equilib., 2001, 191, 189-208.

[2] Khasanshin, T.S.; Samuilov, V.S.; Shchemelev, A.P. J. Eng. Phys. Thermophys., 2008, 81, 760-765.

THERMODYNAMIC DESCRIPTION OF THE Cu–Al–Cr–O SYSTEM IN THE TEMPERATURE RANGE 1100–1300°C

Makrovets L.A.¹, Samoilova O.V.¹

¹South Ural State University, 454080 Chelyabinsk, Russia

E-mail: makrovetcla@susu.ru

Cu–Al–Cr–O system has an interest for the production technology of chromium bronze because aluminum is a major component of deoxidizing ligatures in the smelting of this type of bronze.

Thermodynamic description of the interaction processes occurring in the system Cu–Al–Cr–O in the temperature range 1100–1300°C was performed using the method of constructing a surface of components solubility in a metal melt. This diagram relates the compositions of the metal melt to the type and composition of the reaction products in the investigated system.

The data on equilibrium constants of the reactions taking place in the metal melt; the interaction parameters of the first order (Wagner); data on oxide melt, which may be in equilibrium with the molten metal of the investigated system were used for the surface simulation of the components solubility in a metal melt.

Cu₂O–Al₂O₃, Cu₂O–Cr₂O₃, Al₂O₃–Cr₂O₃ and Cu₂O–Al₂O₃–Cr₂O₃ phase diagrams thermodynamic description was previously held. Thermodynamic characteristics of compounds CuAlO₂ and CuCrO₂, as well as of the solid solution |Al₂O₃, Cr₂O₃|_{ss} were evaluated.

By results of the surface simulation of the components solubility in a metal melt (the calculation results shown in Fig. 1 at the temperature of 1100°C) it is possible to conclusion that in the system Cu–Al–Cr–O formation of copper oxide as a product of components reaction is thermodynamically unlikely. The area of the metal melt equilibrium with the pure solid oxide copper (area I) is displaced aside the minimum concentrations of aluminum and chromium, as well as the high oxygen chart area. CuAlO₂ (area II) and CuCrO₂ (area III) compounds have a same dependence. As the main reaction product will be a solid solution |Al₂O₃, Cr₂O₃|_{ss} (area IV).

The reported study was funded by the Russian Foundation for Basic Research according to the research project № 16-08-00133 a.

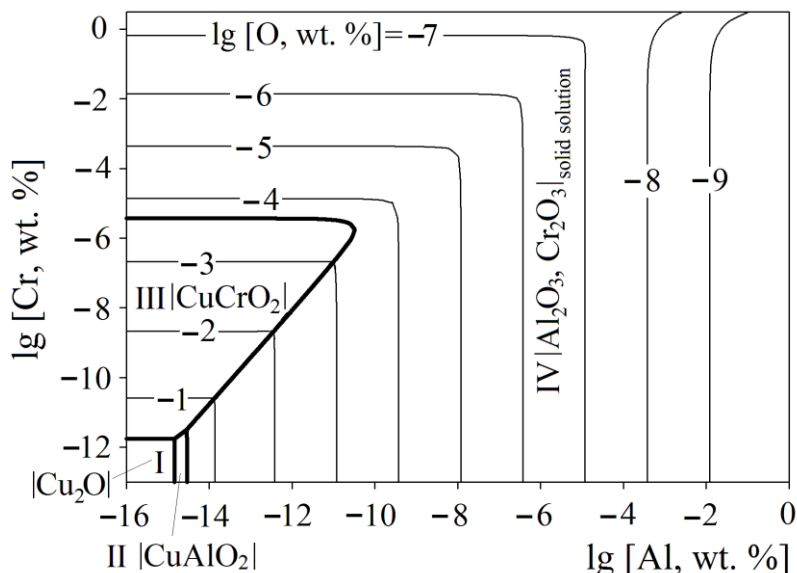


Figure 1. The surface of components solubility in a metal melt for the Cu–Al–Cr–O system at the temperature of 1100°C.

THERMODYNAMIC CALCULATION AND 3D MODELING OF THE P-T-X DIAGRAM Ag-Pb-X(S,Se,Te) SYSTEMS

Mamedov A.N.¹, Ibragimova F.S.¹, Babanly N.B.², Yusibov Yu.A.²

¹Nagiyev Institute of Catalysis and Inorganic Chemistry ANAS, AZ 1134, Baku, Azerbaijan,

E-mail: asif.mammadov.47@mail.ru

²Ganja State University, Ganja, Shah Ismail Khatai avenue 10,

E-mail: nagiyev.elsever@bk.ru

Data for P-T-X diagrams of ternary chalcogenide systems is significantly less than T-X-Y phase diagrams for condensed state. In this work from the concepts thermodynamics of heterogeneous systems the equations for calculation of the partial pressures in the ternary system on the basis of thermodynamic functions of formation of compounds and liquidus coordinates were obtained. From the condition of equality of chemical potential components of AmBn in the equilibrium liquid and solid phases following relations was received:

$$\Delta G_T^{ex,l} = \Delta H_T^{0,s} - T(\Delta S_T^{0,s} + R \ln x_A^m x_B^n) \quad (1)$$

Where $\Delta G_T^{ex,l} = m\bar{G}_A^{ex,l} + n\bar{G}_B^{ex,l}$;

$\bar{G}_A^{ex,l}, \bar{G}_B^{ex,l}$ -are the partial excess free energy of A and B in liquid solution, saturated by A_mB_n ; $\Delta H_T^{0,s}, \Delta S_T^{0,s}$ -are enthalpy and entropy formation of A_mB_n from liquid components; T, x_A, x_B -are temperature and mole fractions for liquidus. Based on the positions of the first degree homogeneous functions for calculation $\bar{G}_A^{ex,l}, \bar{G}_B^{ex,l}$ based on the values $\Delta G_T^{ex,l}$ in Eq (1) are obtained:

$$\bar{G}_A^{ex,l} = \left[\Delta G_T^{ex,l} + x_A \left(\frac{\partial \Delta G_T^{ex,l}}{\partial x_B} \right) \right] \frac{x_B}{m};$$

$$\bar{G}_B^{ex,l} = \left[\Delta G_T^{ex,l} + x_B \left(\frac{\partial \Delta G_T^{ex,l}}{\partial x_A} \right) \right] \frac{x_A}{n}$$

From the known the thermodynamics relationships of solutions we have:

$\ln p_i = \Delta G_i^{ex,l} / RT + \ln(x_i p_i^0) = \ln(x_i p_i^0 \gamma_i)$, where γ_i is thermodynamic activity coefficient. To approximate and 3D visualization of the information received for the liquidus surface AmBn compounds in the ternary system A-B-C, in particular PbSe compound in the system Ag-Pb-Se, the following equation has been used:

$$\ln p_{Se_2} (Ag - Pb - Se) = f_{Pb-Se} (10^3 / T) + \Delta \ln p_{Se_2} x_{Ag}^k.$$

The first term is an analytical expression of $\ln p_{Se_2}$ on $10^3 / T$ along to curve of PbSe liquidus in the binary system Pb-Se, the second term takes into account the change $\ln p_{Se_2}$ depending on the content of Ag. For the areas of liquidus PbSe-Se and PbSe-Pb the following relationships, respectively, were obtained:

$$\lg p_{Se_2} = [-1281+5624(1000/T)-9190(1000/T)^2+6648(1000/T)^3-1797(1000/T)^4]-12 x_{Ag}^2 \quad (2)$$

$$\lg p_{Se_2} = [2026-8778(1000/T)+14247(1000/T)^2-10259(1000/T)^3+2759(1000/T)^4]-10 x_{Ag}^2 \quad (3)$$

The calculations and 3D visualization of the P-T-x diagram for the partial pressure of Se_2 on the PbSe liquidus surface in the ternary Ag-Pb-Se were performed by using OriginLab2015,software.

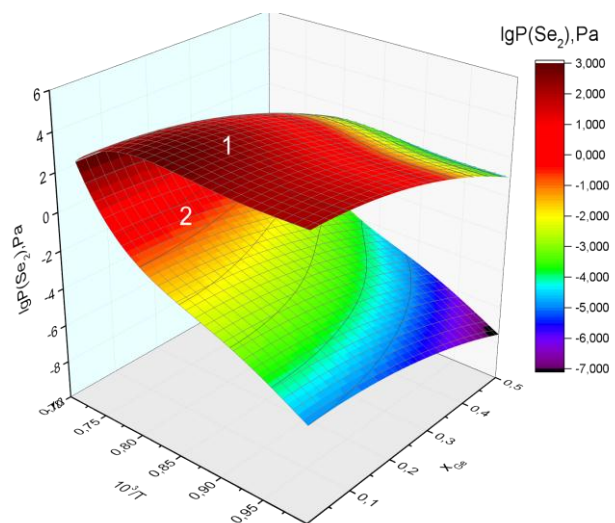


Figure 1. 3D model of the P-T-x diagram for the partial pressure of Se_2 on the PbSe liquidus surface in the ternary Ag-Pb-Se system. 1- area PbSe-Se (ed.2); 2- area PbSe-Pb (ed.3).

INTERACTIONS BETWEEN IONIC SURFACTANT AND AMINO ACID/PEPTIDE IN AQUEOUS SOLUTIONS BY CALORIMETRIC AND VOLUME METHODS

Mezhevoi I.N., Tyunina E.Yu., Badelin V.G.,

G.A. Krestov Institute of Solution Chemistry, Russian academy of Sciences, 153045 Ivanovo, Russia

E-mail: inm@isc-ras.ru

Most industrial, biological, pharmaceutical and cosmetic systems contain surfactants and proteins/amino acids as their major ingredient. The interplay between amino acid and surfactants thus received much attention in recent years. We have decided to examine interactions which contain certain bioactive molecules, glycine (Gly) and glycyglycine (GlyGly), with industrially important anionic surfactants, sodium dodecyl sulphate (SDS), at concentrations (0.00097–0.0199) mol/kg at different temperatures, $T = 293.15, 298.15, 303.15, 308.15$ and 313.15 K by volume method and at $T=298.15$ K by calorimetry. The densities of SDS-water, Gly/GlyGly-water, and Gly/GlyGly-SDS-water mixtures were determined. The density of solution was measured using a digital precision vibrating densimeter DMA-5000 M (Anton Paar, Austria). The uncertainty in density measurements was within $\pm 2 \times 10^{-3} \text{ kg} \cdot \text{m}^{-3}$. The enthalpy of solution measurements were performed using a four-ampoule “isoperibol” calorimeter of own design. Stability of the thermo stating system is ± 0.001 K. The resolutions of temperature and energy measurements are $2 \cdot 10^{-4}$ K and $1 \cdot 10^{-3}$ J per mm of the measuring device’s reading scale, respectively.

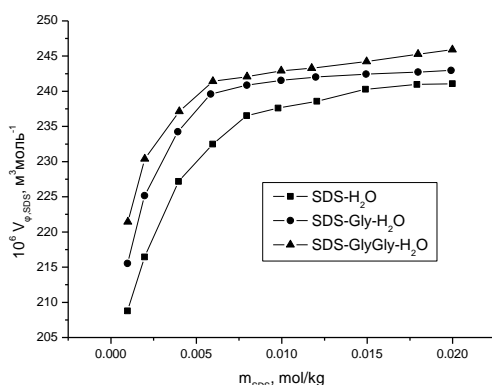


Figure 1. Apparent molar volumes of SDS in water, aqueous solutions of Gly and GlyGly

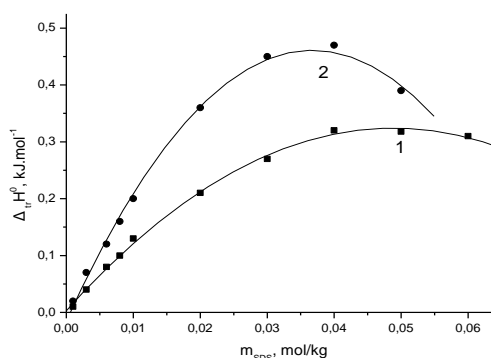


Figure 2. Enthalpies of transfer from water to SDS solutions for Gly (1) and GlyGly (2)

The apparent molar volumes (V_{ϕ}) of SDS in water and in $0.0120 \text{ mol} \cdot \text{kg}^{-1}$ amino acid/peptide solutions were evaluated. The function $V_{\phi} = f(m_{\text{SDS}})$ shows a typical surfactant behavior (Fig.1), namely, the V_{ϕ} values increase as the SDS concentration increases, reaching marked changing points after which the V_{ϕ} values remains roughly constant. A break point in the plot indicates the CMC of the SDS. The CMC values were observed near $m_{\text{SDS}} = 0.008 \text{ mol} \cdot \text{kg}^{-1}$ in water at 298.15 K and near $m_{\text{SDS}} = 0.006 \text{ mol} \cdot \text{kg}^{-1}$ in aqueous solutions of Gly and GlyGly. The limiting values of apparent molar volumes at infinite dilution (V_{ϕ}^0) were determined for premicellar and postmicellar regions. The transfer volumes (ΔV_{tr}^0) were obtained. The positive volume changes suggest that in the ternary solution (SDS–Gly/GlyGly– H_2O) hydrogen bonds and electrostatic interactions predominate over ion-hydrophobic and hydrophobic-hydrophobic groups interactions at infinite dilution. This conclusion is found to be in agreement with the enthalpies of transfer of amino acid/peptide from water to aqueous SDS solutions (Fig.2). In the systems electrostatic interactions and hydrogen bonding promote hydrophobic interactions, making the dissolution process more endothermic with increasing of SDS concentration from (0.003 to 0.062) mol/kg.

The authors are grateful for financial supports from the Russian Foundation for Basic Research (No. projects 15-43-03003-p_center_a).



PHASE TRANSITIONS IN THE BINARY SYSTEM OF N-ALKANE-WATER

Mirskaya V.A., Iभावov N.V., Nazarevich D.A.

*Amirkhanov Institute of Physics, Dagestan Scientific Center, Russian Academy of Sciences,
367003, Makhachkala, Russia
E-mail: veronika_mir@mail.ru*

An occurrence of hydrocarbon systems under ambient conditions, where basic components are alkanes, the contact of them with water is unavoidable. This significantly affects on the regularity of component properties.

There are a lot of papers reporting the studies of such systems using of PVT methods, however, an important property like isochoric heat capacity is remains poorly known.

In this work we investigated the system of n-heptane-water at broad parameters of state in three/two/single-phase areas based on isochoric heat capacity and PVT measurements.

The studied system n-heptane-water is a typical system of water-hydrocarbon, consisting of non-polar and polar molecules. Under ambient conditions, the components are mutually insoluble, and the system consists three phases: liquid 1 - liquid 2 - vapor. Depending on the composition of components these have separation phases areas. In such systems, different phase equilibria, and hence phase transitions are observed.

It was shown that, unlike to one-component systems (n-alkanes, water, etc.) on isochors of specific heat capacity and pressure of the system, the phase transitions liquid - liquid and liquid-vapor are observed. During a comparative study of the complex thermophysical properties as temperature dependence isochoric heat capacity, density and pressure of the system $[(1-x) S7N16 + xH_2O]$ in the temperature range of 300 K ÷ 527 K and pressures up to 6 MPa in the areas of three-phase state (a liquid - liquid - vapor) two phase (liquid - vapor) and homogeneous region, the phase transitions parameters are determined. The measurement were carried out on the experimental setup based on automated digital measuring and control devices with a PC.

It is shown that the parameters of the phase separation region are dependent from number of quantitative component of the system.



CALCULATION OF THE COORDINATES OF EUTECTIC POINT MnS – BaS SYSTEM

Vasilyeva I.I., Monina L.N., Ignatyeva A.A., Filippova A.A.

Tyumen State University, 625003 Tyumen, Russia

E-mail: monina83@yandex.ru

MnS - BaS system are formed 2 complex sulfide at a ratio of the initial components 1MnS: 1BaS and 1MnS: 2BaS. The Complex phases is melt incongruently at temperatures approximate below 1400 K [1, 2]. According to microstructural analysis MnS - BaMnS₂ (1MnS: 1BaS) two-phase area is eutectic type. 70 mol. % MnS - 30 mol. % BaS composition much as possible approached to the eutectic [1, 2]. In this paper, we use the equation Schroeder (eq.1) for the descending branch of the liquidus of MnS for the calculation of the melting temperature of eutectic crystals. Equations Efimova-Vozdvizhensky, Cordes and the equation changes the properties of the system (proposed in [3]) are not used, because the presence at systems of two complex sulfides (incongruent melting), significantly affects on the position of the descending branch of the liquidus from BaS. At [4] were used Schroeder and Van Laar equation for calculating of the melting temperature of eutectic crystals in the system with the formation of a complex sulfide by solid-phase reaction, and close to the values obtained by the experiment.

$$T_E = \frac{1}{\left[\frac{1}{T_m^A} - \frac{R}{\Delta H_m^A} \ln x_A^E \right]} \quad (1)$$

where is x_A^E the mole fraction of component A in eutectic (70 мол. % MnS); ΔH_m^A is the heat of melting of component A, J/mol (26100 J/mol for MnS); T_m^A is the melting temperature of component A, K (1883 K for MnS); and R is the gas constant (8.31 J/mol K).

Calculated melting point eutectic crystals was 1566 K, which is much higher than the experimental data of thermal analysis. According to the synchronic thermal analysis (STA 449 F3 Jupiter, Netzsch) of the sample composition 70 mol. % MnS - 30 mol. % BaS registered nonvariant of phase transition of melting eutectic crystals at 1346 K. This effect is manifested on thermal dependence of the samples other compositions from the field of two-phase MnS - BaMnS₂. Significant decrease the experimental temperature due to the influence of low temperature decomposition BaMnS₂ and Ba₂MnS₃ phases. Impact of the high melting component BaS on eutectic melting point is also not significant. To apply the calculation methods coordinate the eutectic point is suitable for eutectic systems and systems with the formation of complex phases by solid-phase reactions and eutectic reaction at subsolidus temperatures (eg, MnS-Tb₂S₃ system [4]).

[1] Monina, L.N. Potapov, A.G., Chelnokova, O.A., Yurkova, O.S. Mat. VI Russian Conference "Physical and chemical processes in condensed matter and at interfaces", 2012, p.345.

[2] Monina, L.N. Mat. XX Mendeleev Congress on general and applied chemistry, 2016, 2a, 413.

[3] Ganeev, A.A., Khalikov, A.R., Kabirov, R.R. Herald Ufa State Aviation technical university, 2008, 11, 2(29), 116-122.

Monina, L.N., Minikaeva, G.F., Burkhanova, T.M. Herald Tyumen State University, 2013, 5, 88-95.

[4] Monina, L.N. XX Int. Conf. Chem. Thermodyn. In Russia, Nizhni Novgorod, 2015, 275.

Andreev, O.V., Monina, L. N. Russian J. of Inorganic Chem., 2010, 55, 4, 607–610.

CALCULATION OF THE COORDINATES OF EUTECTIC POINT MnS – MnF₂ SYSTEM

Monina L.N., Ignatyeva A.A., Vasilyeva I.I.

Tyumen State University, 625003 Tyumen, Russia

E-mail: monina83@yandex.ru

Reported [1] the phase diagram of the system MnS - MnF₂ in subsolidus part relates to the eutectic type. Solid solutions based on initial components were not found. The following equation can apply to calculate the coordinates of the eutectic point in system: Schroeder, Vozdvizhensky -Efimova, Cordes and the equation changes the properties of the system proposed in work [2]. An important condition for the adequate application of the equation - the lack of solid solutions on the basis of initial components or minimum homogeneity region, and ions forming a solid solution must be isomorphic. Equations Schroeder, Efimov-Vozdvizhensky, Cordes is possible to apply only on the condition experimental data on the melting temperature or the composition of the eutectic crystals. In this study, was interested the calculation of the melting point of eutectic crystals. Because this would allow to choose the necessary range and the heating rate at the experimental determination of the melting temperature of the eutectic. According to microstructural analysis established the composition of eutectic crystals 10 mol. % MnS - 90 mol. % MnF₂ [1]. Equation [2] allows to calculate the coordinates of the eutectic point without the experiment, only on the basis of the melting temperature initial components.

Table 1. Calculated data for the melting temperature of eutectic crystals in the system MnS - MnF₂.

Equations	Calculated melting temperature of eutectic, K
Schroeder	792
Efimov-Vozdvizhensky	1050
The equation changes the properties of the system [2]	972
Cordes	1080

The calculation according to equations of Efimov-Vozdvizhensky and Cordes gave similar values, but significantly different from the other equations Schroeder and the equation changes the properties of the system (table 1). The calculations according to the equation [2] shows good agreement precisely in the melting point of eutectic crystals with the experimental values for the system MnS - SrS [3]. Also, the calculations of the eutectic melting temperatures in other sulfide systems by equations Schroeder, Efimov-Vozdvizhensky, Cordes and showed good agreement with experiment [4, 5, 6]. Since the eutectic consists 90 mol. % of crystals phase MnF₂ (melting point is approximately 1130 K), then we should expect a strong drop in temperature (liquidus line decrease) melting eutectic than it should be calculated from the data by equations Efimov-Vozdvizhensky and Cordes. Therefore, it must be assumed that the melting point of eutectic crystals in the system MnS - MnF₂ should be in the range 940-980 K.

[1] Monina, L.N., Ozerova, D.N. Fluorine notes, 4(107), 2016.

[2] Ganeev, A.A., Khalikov, A.R., Kabirov, R.R. Herald Ufa State Aviation technical university, 2008, 11, 2(29), 116-122.

[3] Monina, L.N., Minikaeva, G.F., Burkhanova, T.M. Herald Tyumen State University, 2013, 5, 88-95.

[4] Andreev, O.V., Monina, L. N. Russian J. of Inorganic Chem., 2010, 55, 4, 607–610.

[5] Solovyova, A.V. Abstract dis. ... Cand. Chem. Sciences: 02.00.04. Tyumen, 2012.

[6] Monina, L.N. XX Int. Conf. Chem. Thermodyn. In Russia, Nizhni Novgorod, 2015, 275.



THE DETERMINATION OF EQUILIBRIUM CONSTANT OF THE REACTION BETWEEN FERRIC AND IODIDE IONS IN A SOLUTION BY THE COMPLEXOMETRIC TITRATION

Soboleva Yu. O., Nikolaychuk P. A.

Kafedra analitičeskoj i fizičeskoj himii, Čelâbinskij gosudarstvennyj universitet, 454001, Chelyabinsk, Russian Federation
E-mail: npa@csu.ru

The reaction between ferric and iodide ions in a solution is well suited to demonstrate the chemical equilibrium to the undergraduate students and, therefore, is widely used in the laboratory practices of physical chemistry in various Russian universities. The original method of determination of the equilibrium constant is based on the titration of iodine, forming in the reaction, by the sodium thiosulphate. However, this approach contains a serious methodological error, since sodium thiosulphate reacts not only with free iodine, but also with ferric ions [1]. Previously, the new method of determination of the equilibrium constant, based on the argentometric titration of iodides, was proposed [1]. In this study, another method, based on the complexometric titration of ferric ions with visual and conductometric end-point detection, is reported.

The equilibrium mixture was prepared from the equal volumes of 0.015 M iron (III) sulphate and 0.03 M potassium iodide. The mixture was held in a dark place during one week before the usage in order to reach the equilibrium state and prevent the photochemical degradation of iodine. Then, the aliquots of 10 ml were taken from the mixture, a 0.5% solution of indicator was added, and the solutions were titrated by 0.05 M EDTA both with visual and conductometric end-point detection. The various indicators, namely, the potassium rhodanide, the salicylic and sulphosalicylic acids, the xylenol orange and the variamine blue, were employed. A typical conductometric titration curves are presented in Figure 1. The equivalence point, associated with the first change of the curve slope, is observed at the volume of titrant, added to the mixture, equal to 0.7 ml. The equilibrium concentration of the ferric ions was calculated according to the equivalence law, the equilibrium concentrations of the other reaction participants were calculated by the mass balance equations. The difference between the experimentally measured equilibrium constant value and those, calculated from the reference thermodynamic data, do not exceed 15%. This implies that complexometric titration can also be used in this laboratory exercise.

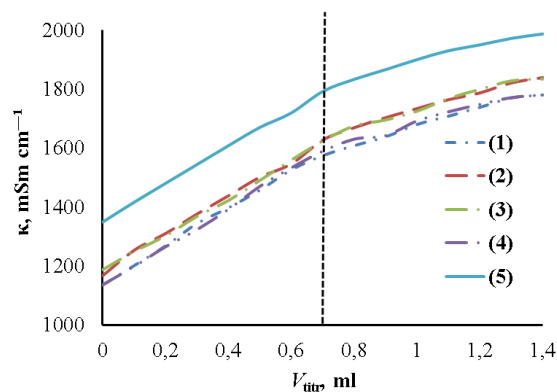


Figure 1. The titration of the equilibrium mixture by EDTA with the conductometric end-point detection: (1) – potassium rhodanide; (2) – salicylic acid; (3) – sulphosalicylic acid; (4) – xylenol orange; (5) – variamine blue.

[1] Nikolaychuk P. A., Kuvaeva A. O., J. Chem. Educ., 2016, 93(7), 1267–1269.

CONDUCTIVITIES OF AQUEOUS SOLUTIONS OF AMINO ACID IONIC LIQUIDS BASED ON 1-OCTYL-3-METHYLIMIDAZOLIUM

Nikonorova A.A.¹, Alopina E.V.², Dobryakov Yu. G.², Smirnova N.A.²

¹ State Institute of Technology Saint-Petersburg, 190013 Saint-Petersburg, Russia

² St. Petersburg State University, 199034 Saint-Petersburg, Russia

E-mail: anna.nikonorova@gmail.com

Imidazolium-based Ionic Liquids (ILs) form a class of compounds with a number of specific physicochemical properties – such as the thermal stability, negligible vapor pressure, non-flammability. They are widely used in «green chemistry» as solvents in synthesis and as catalysts (they can combine these two properties), in electrochemical and extraction methods. In aqueous solutions imidazolium-based ILs behave as surfactants when the alkyl group, attached to the imidazolium ring, is the octyl radical or a longer one. Such ILs form micelles and monolayers [1]. Numerous review articles deal with the micelle formation of imidazolium-based ILs in general [2, 3]. It is not well known how the amino acid structure affects the aggregation behavior of the amino acid ionic liquid (AAIL) in aqueous solutions.

In the present work a number of AAILs having 1-octyl-3-methylimidazolium [C_8mim] as a cation were synthesized. These are 1-octyl-3-methylimidazolium valinate [C_8mim][Val], lysinate [C_8mim][Lys], leucinate [C_8mim][Leu], alaninate [C_8mim][Ala] and 1-octyl-3-methylimidazolium serinate [C_8mim][Ser]. These AAILs were synthesized and characterized by 1H NMR and ^{13}C NMR spectroscopies. The electrical conductivities of aqueous [C_8mim][AA] solutions were measured at 298.15

K. From the experimental data on the concentration dependence of the conductivity several characteristics of the micellization process were determined. These are the critical micelle concentration (cmc), the degree of counterion binding (β), the standard Gibbs energy of micellization (ΔG_m°) for the AAILs. The dependence of the cmc, β and ΔG_m° , on the effects of anions was studied. The effects of anions on the studied properties were analyzed.

The critical micelle concentration values obtained for [C_8mim]Cl and [C_8mim]Br in the present study are in a good agreement with those reported in literature [2-4]. The comparison of the cmc values for [C_8mim]Cl, [C_8mim]Br and [C_8mim][AA] (AA = Val, Lys, Leu, Ala, Ser) solutions shows the effect of [AA]⁻ anions on the IL micellization. The cmc value increase in the following order: [C_8mim]Br < [C_8mim][Ser] < [C_8mim][Ala] < [C_8mim][Leu] < [C_8mim][Lys] < [C_8mim]Cl < [C_8mim][Val]. The highest cmc value for [C_8mim][Val] is a result of the lower electrostatic interactions (attraction) between the IL head groups and [Val]⁻ counterions in comparison with other anions. The values of the counterion binding parameter β increase in the following sequence: [C_8mim][Val] < [C_8mim][Lys] < [C_8mim][Leu] < [C_8mim][Ala] < [C_8mim][Ser]. The data obtained indicate that the anion nature of [C_8mim][Ser] results in a higher ability of micelle formation.

[1] Smirnova, N; Safonova, E, J. Phys. Chem. A, 2010, 84, 1695–1704.

[2] Baltazar, Q; Chandawalla, J; Sawyer, K; Anderson, JL, Colloids Surf. A, 2007, 302, 150-156.

[3] Bai, G; Lopes, A; Bastos, M, J. Chem. Thermodyn., 2008, 40, 1509-1516.

[4] Jungnickel, C; Łuczak, J; Ranke, J; Fernández, JF; Müller, A; Thöming, J, Colloids Surf. A, 2008, 316, 278–284.

Acknowledgements. The work was financially supported by Russian Science Foundation (grant 16-13-10042) and by the Russian Foundation for Basic Research (grant 16-03-00723). The NMR measurements were carried out at the Center for Magnetic Resonance, St. Petersburg State.

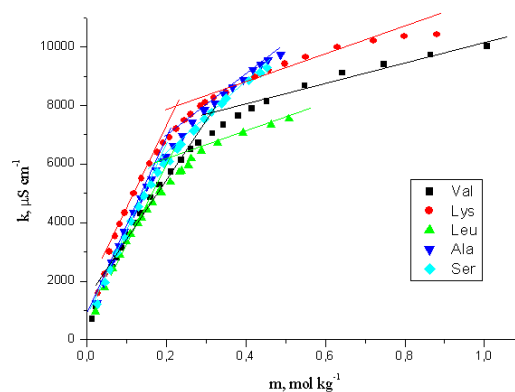


Figure 1. Specific conductivity values (χ) for aqueous solutions of [C_8mim][Val] (■), [C_8mim][Lys] (●), [C_8mim][Leu] (▲), [C_8mim][Ala] (▼) and [C_8mim][Ser] (◆) at various AAIL molar concentrations; T = 298.15 K.



THERMODYNAMICAL PROPERTIES OF MULTICOMPONENT SOLUTIONS OF ALKALI METAL IODIDES IN N-METHYLPYRROLIDONE AT 298.15 K

Novikov A.N.¹, Rassokhina L.Yu.¹, Dorokhin S.V.¹, Belikova D.V.¹, Vasilyov V.A.², Solovyov S.N.²

¹Mendeleev University of Chemical Technology, Institute in Novomoskovsk, 301665 Novomoskovsk, Russia

²Mendeleev University of Chemical Technology, 125047 Moscow, Russia

E-mail: anngic@yandex.ru

Multicomponent systems are generally of interest because of their practical applications. In this study, we experimentally investigated the volume properties of the ternary solutions of iodides alkali metals in N-methylpyrrolidone (MP). For measurement of density (ρ) the precision picnometric installation (error $\pm 1 \cdot 10^{-5} \text{ g} \cdot \text{cm}^{-3}$) were used.

To explain the character of changes in the volume of the ternary solutions of electrolytes in MP during the mixing of the isomolal binary solutions, the additivity coefficients δ_v were calculated by the equations 1:

$$\delta_v = \frac{V_{\text{exp.}} - V_{\text{add}}}{V_{\text{add}}} 100\% \quad (1) \quad V_{\text{add}} = \frac{V_1 g_1 + V_2 g_2}{g_1 + g_2} \quad (2)$$

Here, $V_{\text{exp.}}$, V_{add} are the experimental and additive values of V of the ternary solutions, V_{add} calculated by the equations 2, using the literature data on the properties of the binary solutions; V and g are the specific volumes and masses of the binary solutions, respectively.

Table 1. Additivity coefficients of the ternary solutions of electrolytes in MP at 298.15 K

m	δ_v			
	NaI-KI-MP	NaI-RbI-MP	KI-RbI-MP	KI-BaI ₂ -MP
0,10	0,09	0,10	0,02	0,01
0,20	0,18	0,19	0,02	0,04
0,30	0,27	0,28	0,02	0,04
0,40	0,38	0,37	0,01	0,04
0,50	0,44	0,47	0,00	0,04
0,60	0,52	0,55	0,00	0,05
0,75	0,66	0,69	0,00	0,06
1,00	0,90	0,90	0,04	0,06
1,25	1,16	1,09	-	-

m is the total molal concentration of the solution $(m_1 + m_2)/2$.

An analysis of the δ_v values revealed several tendencies of their variation in relation to the m : $\delta_v > 0$, which corresponds to a increase in V during the mixing. This character of the dependence probably corresponds to predominant ion interactions. These processes are favored by the lower dielectric constant of the aprotic dipolar solvents (compared with that of water) and lower solvation of anions in these solvents, which lead to considerable ion association already at low concentrations. Ion interactions, which cause the destruction of the solvation shells of ions and partial or complete desolvation increase the volume of the system. The liberation of MP molecules from the solvates is also accompanied by a decrease in electrostriction, leading to an increase in the volume. According to the electrostatic analysis, the sodium ion exhibits greater liability to ion association than potassium and rubidium ions. Therefore, considerable deviations from additivity are observed in systems containing the Na^+ ion. At the same time, for systems with electrolytes of the same valence type, the redistribution of solvent molecules among the cations, which leads to a decrease in V , does not produce a pronounced effect because the differences in the solvation enthalpies ($\Delta_{\text{solv}}H^o$) of the Na^+ and especially K^+ and Rb^+ cations in MP are insignificant. In the KI-BaI₂-MP system with electrolytes of different valence types and larger differences in solvation enthalpies ($\Delta_{\text{solv}}H^o_{\text{Ba}^{2+}} = -1477 \text{ kJ/mol}$, $\Delta_{\text{solv}}H^o_{\text{K}^+} = -389 \text{ kJ/mol}$ [1]), however, the solvation shells of Ba^{2+} ions are enriched with MP molecules due to the desolvation of K^+ ions, compensating the ion interaction and leading to small deviations from additivity.

[1] Achievements and Problems of Solvation, Ed. by A. M. Kutepov. Nauka, Moscow, 1998, 247 p.

ANALYSIS OF THE PHASE DIAGRAM AND DETERMINATION OF STRUCTURES OF SEPARATRIX SURFACES OF THE FIVE-COMPONENT SYSTEM ALLYL CHLORIDE-ETHANOL-WATER-EPICHLOROHYDRIN-HIGH BOILING FRACTION

Okhlopkova E.A., Serafimov L.A., Frolkova A.V.

Moscow Technological University (Institute of Fine Chemical Technologies), 119571 Moscow, Russia

E-mail: ea.okhl@ya.ru

One promising direction of epichlorohydrin production is the liquid-phase epoxidation of allyl chloride with an aqueous solution of hydrogen peroxide in organic solvent medium in the presence of a heterogeneous catalyst. As the solvent can be used ethanol. Here we have studied the structure of the phase equilibrium diagram of the five-component mixture of epichlorohydrin production according to this method.

In this work the thermodynamic topological analysis of the phase diagram of allyl chloride – ethanol – water – epichlorohydrin – high boiling fraction system was performed. This system comprises three binary azeotropes and one ternary azeotrope. It is shown that there is no three-dimensional separatrix manifold on the basis of two-dimensional pentahedron net (fig. 1). Thus only one distillation region exist in this system, wherein unstable node is ternary azeotrope allyl chloride-ethanol-water and stable node is high-boiling fraction.

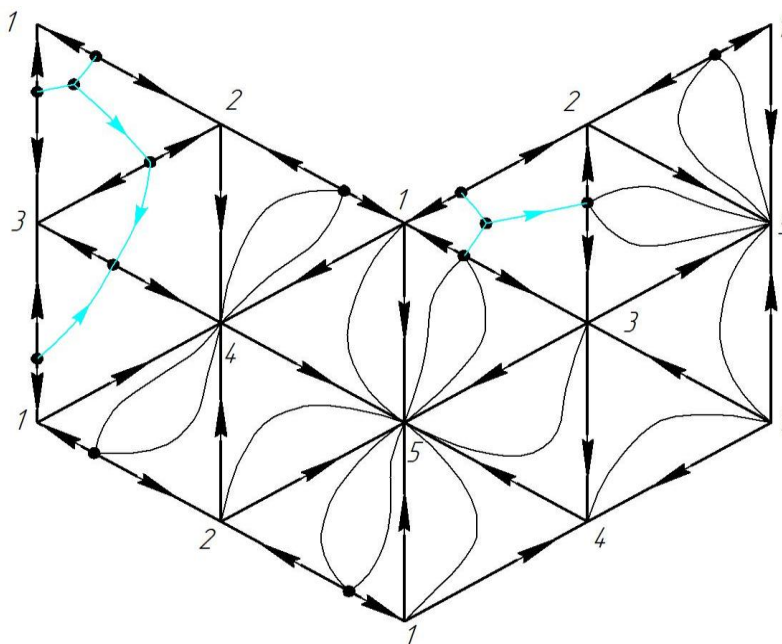


Figure 1. Two-dimensional pentahedron net of allyl chloride (1) – ethanol (2) – water (3) – epichlorohydrin (4) – high boiling fraction (5) system.



THE Na,K,Cs||F,Cl FOUR-COMPONENT RECIPROCAL SYSTEM CHEMICAL INTERACTION DESCRIPTION BY THE CONVERSION METHOD

Ragina M. S., Sukharenko M.A., Garkushin I.K.

Samara State Technical University

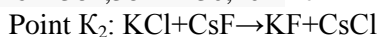
maruska-r@yandex.ru

To order to describe a chemical interaction of reciprocal systems, V.P. Radishchev introduced the concept of the conversion elements for the first time [1]. In three-component reciprocal systems of the Na,K,Cs||F,Cl four-component system, the following exchange reactions of the full conversion points are present:



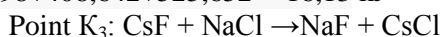
$$\Delta_f H^\circ_{298} = \Delta_f H^\circ_{298}(\text{NaF}) + \Delta_f H^\circ_{298}(\text{KCl}) - \Delta_f H^\circ_{298}(\text{KF}) + \Delta_f H^\circ_{298}(\text{NaCl}) = -572,831 - 436,558 + 566,095 + 411,412 = -31,882 \text{ kJ}$$

$$\Delta_f G^\circ_{298} = \Delta_f G^\circ_{298}(\text{NaF}) + \Delta_f G^\circ_{298}(\text{KCl}) - \Delta_f G^\circ_{298}(\text{KF}) + \Delta_f G^\circ_{298}(\text{NaCl}) = -542,572 - 408,642 + 536,426 + 384,384 = -30,404 \text{ kJ}$$



$$\Delta_f H^\circ_{298} = \Delta_f H^\circ_{298}(\text{KF}) + \Delta_f H^\circ_{298}(\text{CsCl}) - \Delta_f H^\circ_{298}(\text{KCl}) + \Delta_f H^\circ_{298}(\text{CsF}) = -566,095 - 442,437 + 436,558 + 553,501 = -18,473 \text{ kJ}$$

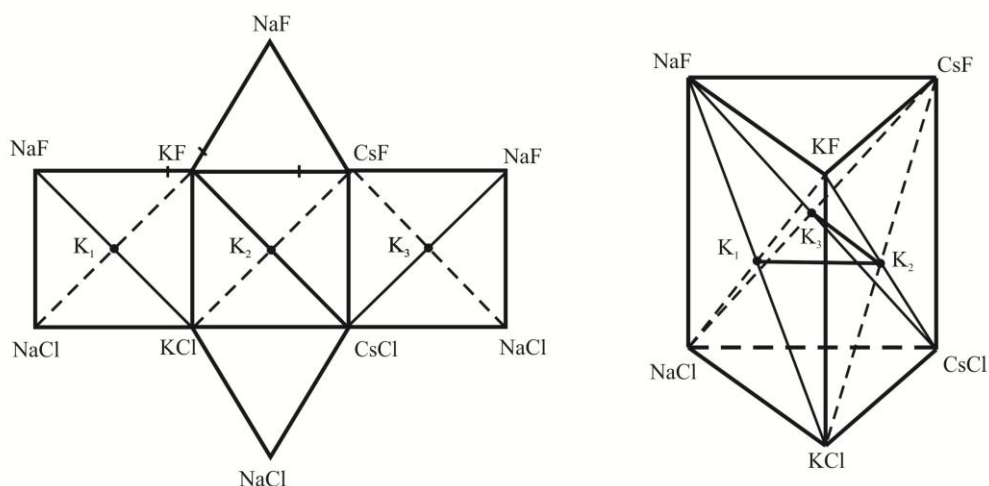
$$\Delta_f G^\circ_{298} = \Delta_f G^\circ_{298}(\text{KF}) + \Delta_f G^\circ_{298}(\text{CsCl}) - \Delta_f G^\circ_{298}(\text{KCl}) + \Delta_f G^\circ_{298}(\text{CsF}) = -536,426 - 413,998 + 408,642 + 525,652 = -16,13 \text{ kJ}$$



$$\Delta_f H^\circ_{298} = \Delta_f H^\circ_{298}(\text{NaF}) + \Delta_f H^\circ_{298}(\text{CsCl}) - \Delta_f H^\circ_{298}(\text{CsF}) + \Delta_f H^\circ_{298}(\text{NaCl}) = -572,831 - 442,43 + 553,501 + 411,412 = -50,348 \text{ kJ}$$

$$\Delta_f G^\circ_{298} = \Delta_f G^\circ_{298}(\text{NaF}) + \Delta_f G^\circ_{298}(\text{CsCl}) - \Delta_f G^\circ_{298}(\text{CsF}) + \Delta_f G^\circ_{298}(\text{NaCl}) = -542,572 - 413,998 + 525,652 + 384,384 = -46,534 \text{ kJ}$$

In the Na,K,Cs||F,Cl four-component reciprocal system, two conversion lines K_1K_2 and K_2K_3 are formed.



1. Garkushin I. K., Kondratyuk I. M., Egortsev G. E., Istomova M. A. Theoretical and experimental methods for multicomponent systems investigation. Samara: Samara State. Tech. university, 2012. 125 p.

PHASE-TRANSITION THERMODYNAMICS OF Cu_2S - SrCeCuS_3 SYSTEM

Ruseikina A.V., Grigoriev M.V., Nikitin V.E.

Institute of chemistry, Tyumen State University, 625003, Tyumen, Russia
E-mail: adeschina@mail.ru

The results of the samples study by the methods of microstructural, x-ray phase analysis, differential scanning calorimetry were basis to construct the equilibrium diagram of the system Cu_2S - SrCeCuS_3 of eutectic type with the formation of a solid solution (SS) based on Cu_2S (Fig.1). The system is partially quasi-binary section of the ternary system Cu_2S - Ce_2S_3 - SrS . Below the temperature of incongruent melting of compound SrCeCuS_3 (1486 K) the boundary SS structure based on polymorphic modifications and the compound Cu_2S SrCeCuS_3 are in equilibrium.

In thermal analysis of samples of 3.5-7.5 mol. % SrCeCuS_3 the change in the value of the peak area of incongruent dissolution of SS on the basis of β - Cu_2S : 3.53 J/g (3.5%) \rightarrow 5.16 J/g (4.5%) \rightarrow 2.97 J/g (6%) \rightarrow 0.09 J/g (7.5%) was recorded. According to DSC, formation of SS Tamman triangle β - Cu_2S dissolves incongruent with 1236 ± 5 K, 4.5 mol. % SrCeCuS_3 . Balance equation for the phase transformation was made:

$\text{SS } \beta\text{-Cu}_2\text{S} (0.045 \text{ SrCeCuS}_3; 0.955 \text{ Cu}_2\text{S}) \leftrightarrow 0.667 \text{ SS } \gamma\text{-Cu}_2\text{S} (0.030 \text{ SrCeCuS}_3; 0.970 \text{ Cu}_2\text{S}) + 0.333 \text{ L} (0.075 \text{ SrCeCuS}_3; 0.925 \text{ Cu}_2\text{S}); \Delta H = 5.2 \pm 0.5 \text{ J/g}$.

On the thermograms of samples containing 7.5-99 mol. % SrCeCuS_3 , there is a melting peak of eutectic mixture of crystals, the average temperature of the start of development for 7 samples of various compositions is 1109 ± 5 K. A change in the value of the peak area 13.3 J/g (11.9%) \rightarrow 13.9 J/g (13.9%) \rightarrow 23.1 J/g (14.7%) \rightarrow 17.8 J/g (17.1%) \rightarrow 3.2 J/g (66.6%) can be seen. The composition of the eutectic according to the MSA, DSC, formation of Tamman triangle and the extrapolation of the branches of the liquidus curve for the eutectic horizontal - 16 mol. % SrCeCuS_3 . Balance equation of eutectic crystals melting was made:

$0.90 \text{ SS } \beta\text{-Cu}_2\text{S} (\text{SrCeCuS}_3 \text{ } 0.07; 0.93 \text{ Cu}_2\text{S}) + 0.10 \text{ SrCeCuS}_{3\text{fp}} \leftrightarrow \text{L} (\text{SrCeCuS}_3 \text{ } 0.16; 0.84 \text{ Cu}_2\text{S}); \Delta H = 24.5 \pm 2.5 \text{ J/g}$.

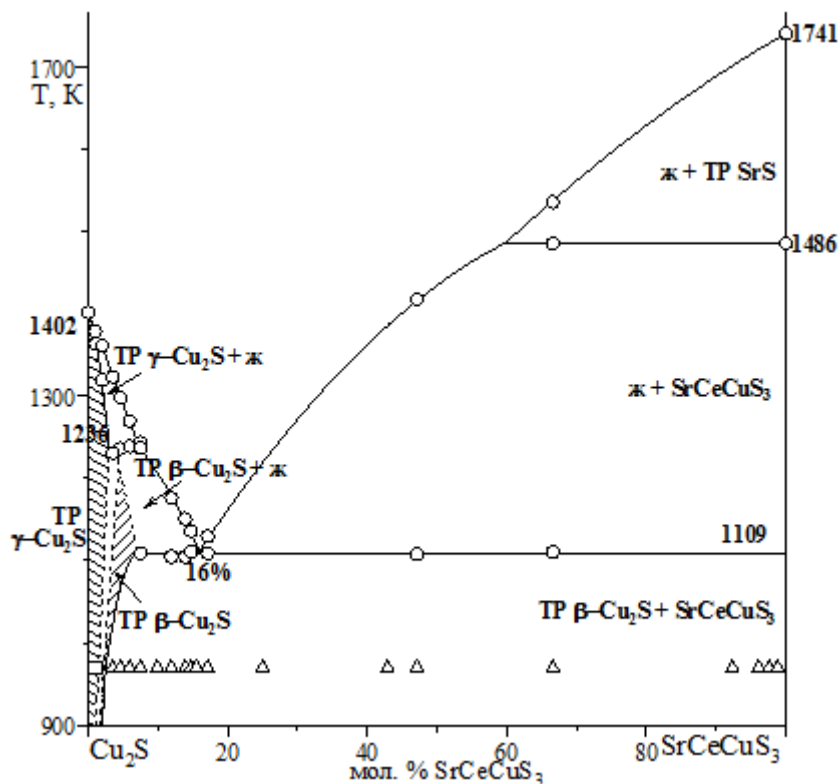


Figure 1. Equilibrium diagram of the system Cu_2S - SrCeCuS_3 : o-DSC data. State of samples based on the results of X-ray fluorescence analysis and MSA methods: □-single-phase, Δ- two-phase.

SEPARATION OF N-HEXANE - ETHANOL MIXTURE VIA EXTRACTION USING DEEP EUTECTIC SOLVENTS

Samarov A.A., Sokolova M.P., Smirnov M.A., Toikka A.M.

Institute of Chemistry, St. Petersburg University, 199034 St. Petersburg, Russia

E-mail: samarov@yandex.ru

Ionic liquids (ILs) are well known as promising materials for separation of different types of azeotropic liquid organic mixtures via extraction. At the same time, ILs has such disadvantages as high cost and toxicity that hampers their practical application. Deep eutectic solvents (DES) attract much attention during last years as green and cheap alternative for ILs. DES demonstrate all benefits of ILs and, additionally, can be prepared from biocompatible and cheap components. DES is formed during the interaction of hydrogen-bond acceptor and a hydrogen-bond donor.

In this work DES based on choline chloride as hydrogen bond donor (HBD) and simplest dibasic acids (oxalic (DES1) and malonic (DES2)) as hydrogen bond acceptors (HBA) were investigated as an extractors for separation of n-hexane - ethanol azeotropic mixtures. DESs were prepared by mixing of HBD with HBAs with molar ratio 1:1 in screw-capped bottles. The liquid-liquid equilibrium and the structure of phase diagrams of ternary systems n-hexane + ethanol + DES were studied at atmospheric pressure and 293.15 K (Figure 1) or 313.15 K. The reliability of experimental tie-line data was validated by the Othmer–Tobias and Hand correlations. The distribution coefficients of solutes and selectivity respectively to ethanol for both systems were calculated. In Figure 2 selectivities of investigated DES are compared with properties of Ionic Liquids [1,2].

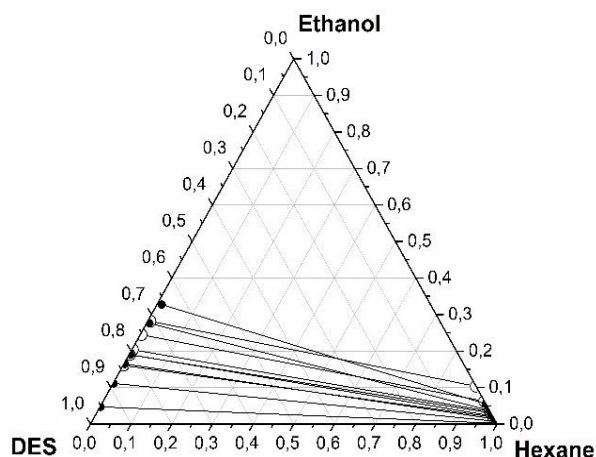


Figure 1. Ternary diagram and tie-lines for the systems n-hexane + ethanol + DES1 (○—○) and n-hexane + ethanol + DES2 (●—●) at 293.15 K.

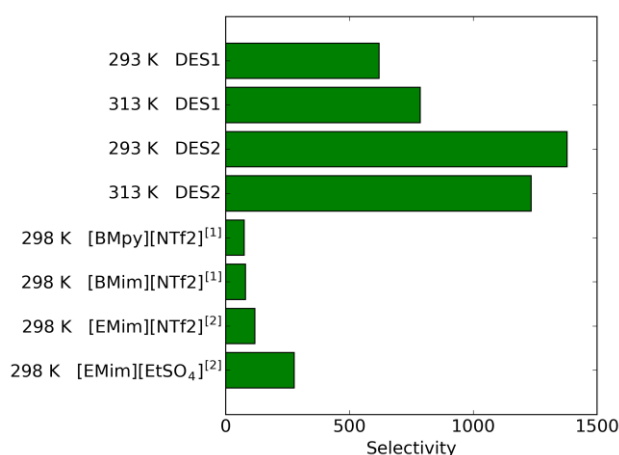


Figure 2. Selectivities of the extractive systems in the separation of ethanol - n-hexane mixture, at an ethanol mass fraction of 5 wt% in hexane-rich phase.

The results show that deep eutectic solvents based on choline chloride and both dibasic acids are very effective extracting agent for separation of ethanol from n-hexane. Obtained selectivity and distribution coefficients are higher than the values reported for ionic liquids. Experimental results were simulated according to NRTL model and energy parameters for binary interactions between components were calculated.

Acknowledgements.

The reported study was funded by RFBR, according to the research project No. 16-31-60128 mol_a_dk. Maria Sokolova is grateful to St. Petersburg State University for the postdoctoral fellowship (grant 12.50.1195.2014). The experimental work was facilitated by the equipment of the Magnetic Resonance Research Centre at St. Petersburg State University.

[1] Pereiro A.B., Deive F.J., Esperança J.M.S.S., Rodríguez A., Fluid Phase Equilib., 2010, 294, 49–53.

[2] Corderí S., González B., J. Chem. Thermodyn., 2012, 55, 138–143.



SORPTION OF SOME BENZIMIDAZOLE FROM AQUEOUS-ORGANIC SOLUTIONS ON OCTADECYL SILICA GEL

Shafigulin R.V., Bulanova A.V.

Samara National Research University, Moskovskoye shosse, 34, Samara, 443086, Russia

E-mail: shafiro@mail.ru

Studies of the chromatographic behavior of organic compounds under the conditions of reversed phase high performance liquid chromatography (RP HPLC) permits the development of the theoretical aspects of sorption from liquid multicomponent solutions. Determining the relationship between the mechanism of sorption and the physicochemical parameters of sorbate molecules allows us to expand our knowledge of the selectivity of the sorption of organic compounds from multicomponent liquid solutions, and to predict the pharmacokinetics of biologically active compounds being synthesized for the first time. Nitrogen-containing heterocyclic compounds, in particular, benzimidazoles are interesting objects of investigation. Benzimidazoles exhibit various types of biological activity and are widely used as pharmaceutical substances.

The aim of this work was thus to study the thermodynamics of the sorption of benzimidazoles on octadecyl silica gel from water–organic solutions by means of high-performance liquid chromatography (HPLC).

A chromatographic study of benzimidazoles was performed under the conditions of reversed-phase high-performance liquid chromatography on a Milichrom A-02 microcolumn liquid chromatograph using an UV spectrophotometric detector. Detection was performed at wavelengths of 210, 254, and 300 nm. A chromatographic column filled with the ProntoSil 120-5-C18 AQ sorbent (75 × 2 mm) was used. The sorbent grain size was 5 μm. The column temperature was maintained with an electrical solid-state thermostat.

The retention factors, enthalpy, entropy and differences in the Gibbs energy of adsorption from infinite diluted water-acetonitrile and water-methanol solutions were calculated, and the applicability of the Snyder–Soczewinski and Scott–Kucera models for describing the chromatographic retention of benzimidazoles on a octadecyl silica gel was shown. It is shown that with increasing molecular volume enthalpy generally increases. The influence of the composition and nature of the organic solution to the enthalpy and entropy component of the sorption process on octadecyl silica gel. The enthalpy-entropy compensation relationship was analyzed. One- and many-parameter correlation equations were obtained by linear regression analysis, and their prognostic potential in determining the retention factors of benzimidazoles under study was analyzed.

This work was supported by RFBR grant №16-33-00707 мол_a

PHASE DIAGRAMS OF QUATERNARY HOMOLOGOUS SYSTEMS OF COMPLEX PHYSICO-CHEMICAL NATURE

Shashkova Yu., Stoyakina I., Frolkova A.V., Frolkova A.K.

Moscow Technological University, Institute of Fine Chemical Technologies, 119571 Moscow, Russia

A study of homologous systems, namely their physico-chemical properties, is an important task because it allows predicting the structure of phase diagrams of new systems containing component-homolog and planning experimental research. It is especially important for the study of multicomponent systems experimental data of which are limited.

The object of the present research is quaternary systems containing ethanol (E) – benzene (B) – water (W) – hydrocarbon (HC) ($C_6H_{14} - C_{10}H_{22}$). Phase equilibrium of systems mentioned have been studied using mathematic modeling in AspenPlus and NRTL model. The relative standard uncertainty of description of phase equilibrium (VLE, LLE) is less than 5%. Analyzing the change of azeotrope composition (available experimental data [1-2]) in dependence on the number of carbons in HC the composition of azeotropes in systems _____ were predicted and compared with calculated data. Predicted and calculated results were found to be in a good agreement (relative standard uncertainty is less than 5%).

The structure of vapor-liquid diagram of five quaternary systems were studied (Figure 1).

Main characteristics of vapor-liquid diagrams of quaternary systems studied are given in table 1.

It was found that the disappearance of binary azeotropes benzene – hydrocarbon, ethanol – hydrocarbon and ternary azeotrope water – ethanol – hydrocarbon is observed with increase of the number of carbons in hydrocarbon, besides the structure of separatrix manifolds of second dimension as well as the whole structure of composition tetrahedron is simplified. The evolution of phase diagram and the changes in the structure of separatrix manifolds are thermodynamically correct (the transitions between diagrams are allowed from the point of view of the theory of tangential azeotropy).

When assessing the development of mixtures separation flowsheets for the first three members of homologous series (a-c Fig.1) we cannot recommend the use of a method based on the combination of rectification in splitting process due to the adverse location of separatrix manifolds, while for the systems (g and d of figure 1) it is quite feasible.

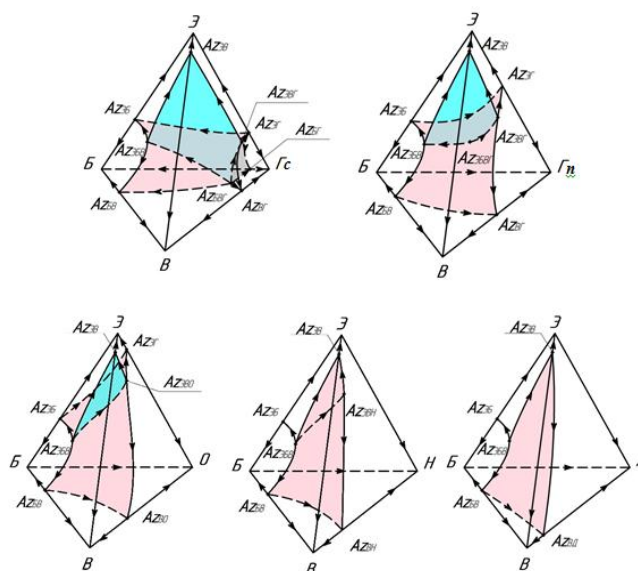


Figure 1. Phase diagrams of quaternary systems

Table 1. Main characteristics of vapor-liquid equilibrium diagrams of quaternary systems E-B-W-HC

System	C_6H_{14}	C_7H_{16}	C_8H_{18}	C_9H_{20}	$C_{10}H_{22}$
The number of azeotropes	9	8	7	6	5
The number of separatrix manifolds	3	2	2	1	1
The number of distillation regions	4	3	3	2	2

The work was carried out under support of Russian Science Foundation 16-19-10632.

[1] Ogorodnikov S.K.; Lesteva T.M.; Kogan V.B. Azeotropniye smesi., 1971, 848 p. (in Russian)

THERMODYNAMIC ASSESSMENT OF $\text{Cu}_{1.99}\text{Se}-\text{Bi}_2\text{Se}_3$ SYSTEM PHASE DIAGRAM

Shtykova M.A.¹, Kamaev D.N.², Andreev O.V.¹, Sadyihov G.A.¹, Polkovnikov A.A.¹

¹Institute of Chemistry, Chair of Inorganic and Physical Chemistry, FSAEI HE «Tyumen state university», Volodarsky Str. 6, 625003 Tyumen, Russian Federation

²Faculty of Natural Sciences, Chair of Physical and Applied Chemistry, FSBEI HPE «Kurgan state university», Gogol Str. 25, 640669 Kurgan, Russian Federation
E-mail: margarita.shurova@list.ru

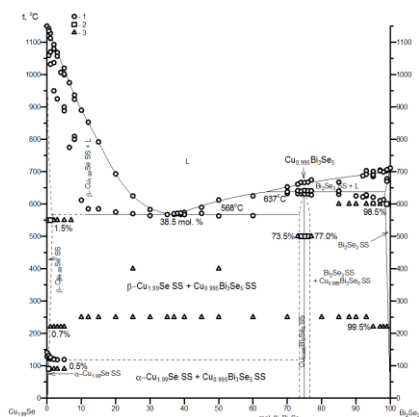


Figure 1. Experimental phase diagram

Legend: 1 – DSC data; Condition of the samples according to X-ray analysis and microstructural analysis (compositions and the annealing temperature of the samples are denoted); 2 – homogeneous sample; 3 – heterogeneous sample

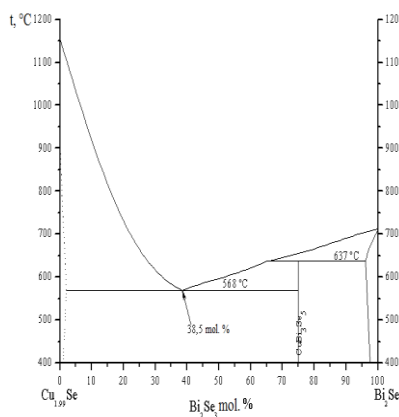


Figure 2. Calculated phase diagram

$\text{Cu}_{1.99}\text{Se}-\text{Bi}_2\text{Se}_3$ is a system with a incongruently melting compound, eutectic, and initial components ($\text{Cu}_{1.99}\text{Se}$ and Bi_2Se_3) based limited solid solutions. The incongruently melting compound $\text{Cu}_{0.995}\text{Bi}_3\text{Se}_5$ was found, its melting temperature was 637°C (910 K) and its melting enthalpy was 25.3 kJ/mol. The eutectic point with the composition 38,5 mol. % Bi_2Se_3 was found, its melting temperature was 568°C (841 K) and, its melting enthalpy was 24.1 kJ/mol. Thermodynamic data for congruently melting initial compound were obtained. Bismuth selenide's Bi_2Se_3 melting temperature was

711.73°C (984.73 K) and bismuth selenide's melting enthalpy was 51.1 kJ/mol. Copper selenide's $\text{Cu}_{1.99}\text{Se}$ melting temperature was 1154.32°C (1427.32 K) and copper selenide's melting enthalpy was 7.2 kJ/mol. The purpose of the present paper is to assess the $\text{Cu}_{1.99}\text{Se}-\text{Bi}_2\text{Se}_3$ phase diagram and comparison between the experimental data (fig.1) and calculated phase diagram (fig. 2). All samples with a particular mole fraction of each of chalcogenides were obtained by weighing the proper amount of each element on an analytical balance, the melting them together in a evacuated and sealed quartz ampoule and heating it in a muffle furnace at a temperature well above the melting temperature of the alloy. Number of samples were annealed. The samples containing from 92 to 99 mol. % Bi_2Se_3 were annealed at 220°C during 750 hours and at 600°C during 750 hours. The samples containing from 0.5 to 5 mol. % Bi_2Se_3 were annealed at $90-100^\circ\text{C}$ during 2250 hours, at 220°C during 750 hours and at 550°C during 750 hours. Lines on experimental phase diagram were obtained by differential scanning calorimetry (DSC), for which the high-technology modern equipment were employed: differential scanning calorimeter Setsys Evolution 1750 (TGA – DSC 1600) manufactured by SETARAM Instrumentation (France) with software package SETSOFT 2000 and Pt/PtRh (10%) thermocouple, and simultaneous thermal analyzer STA 449 F3 Jupiter manufactured by NETZSCH-Gerätebau GmbH (Germany) with software package NETZSCH Proteus 6.1 and thermocouple (90% Pt + 10% Rh)/Pt. all the DSC-curves for samples were obtained in evacuated silica glass ampoules and heating rate $5^\circ\text{C}/\text{min}$. For solidus and liquidus lines on experimental phase diagram the characteristic points on DSC-curves were used. Thermodynamic calculations were performed using Redlich-Kister formalism. Redlich-Kister polynomials describe temperature and composition dependent for excess Gibbs energy and activity coefficients of components. For calculation equation for equilibrium processes in fixed points were made up. A number of points of the experimental phase diagram, includes eutectic point, were used as fixed points. Numerical coefficients of polynomial model were obtained: for melt $L_0 = 4176$, $L_1 = 2077$, $L_2 = -6798$; for solid solutions $L_0 = 1,27 \cdot 10^7$, $L_1 = -6659$, $L_2 = -3,944 \cdot 10^6$. Temperature dependence for $\text{Cu}_{0.995}\text{Bi}_3\text{Se}_5$ melting constant were obtained:

$$\ln K = -\frac{3048}{T} + 1,167$$

MOLECULAR DYNAMICS SIMULATION OF ION SPUTTERING OF THE ELECTROLYTE CATHODE AND ANALYSIS OF THE COMPOSITION OF THE SPRAYED WATER CLUSTERS

Sirotkin N.A., Titov V.A.

G.A. Krestov Institute of Solution Chemistry RAS, 1, Akademicheskaja st., Ivanovo, 153045, Russia

E-mail: alexsad8@yandex.ru

The surface of the cathode electrolyte is bombarded by positive ions, which cause the appearance of chemical and physical processes, such as in liquid and gas phases. The mass transfer of water and ions of dissolving salts is due to of ion bombardment. Experimental results showed that the transfer coefficients for water are 300 - 500 molecule/ion [1]. High values of transfer coefficients allow supposing that a significant part of molecules leaves the solution in clusters or microdrops. Experimentally determine the distribution of water cluster at size is not possible. However, it is an important problem in the transfer of large water clusters into the plasma leads to additional energy consumption for their thermal destruction. In turn, it can effect on the temperature of the gas in the plasma.

The process of liquid electrolyte cathode sputtering can be studied by molecular dynamics simulation. In addition, the composition of the sputtered water clusters can be analyzed. The plasma sputtering of sodium chloride solution is studied by classical molecular dynamics method, implemented in a software package Gromacs-4.5.4, according to the algorithms described in [2]. The number of ions was 1-20, the energy of ions was varied in the range of 50-500 eV.

Sputtering both the solvent (water) and the solute is observed under the bombardment of the solution by the incident ions. It should be noted that the process of sputtering of the solution surface significantly depends on a number of the bombardment ions and energy of ions. Water molecules are preferably transferred to the gas phase at dissipated energy 0.5-9 kJ /mol. Dimers, trimers and larger clusters are transferred to the gas phase at increasing the number of the bombarding ions and ions energy. Water clusters of 5 or more molecules begin to prevail in the gas phase at the dissipated energy of about 30 kJ / mol (Figure 1).

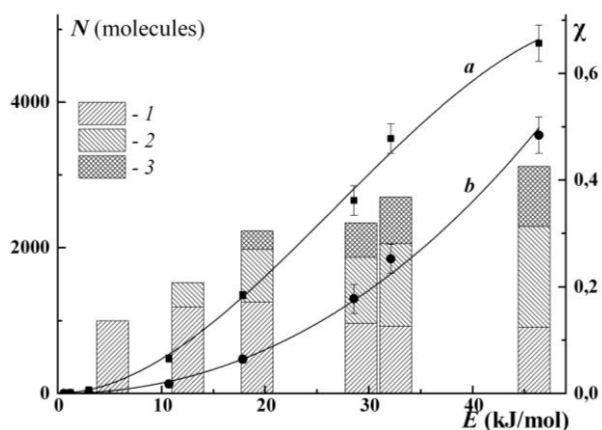


Figure 1. The number of sprayed water molecules to the gas phase (a), the number of hydrogen-bonded water molecules in the gas phase (b) and the molar fraction (χ) of the water molecules in clusters:

1 - 3-4 molecules in cluster,

2 - 5-7 molecules in cluster,

3 - more than 7 molecules in cluster.

The values of the transfer coefficients obtained by means of molecular dynamics simulation are in a good agreement with experimental data. According to the results of computer simulation, the solvent and the solute ions are transferred to the gas phase under the ion bombardment. Ions of dissolved salts are preferably sprayed as ion pairs in the water clusters.

The reported study was funded by Russian Foundation for Basic Research according to the research project No.16 – 33 – 60061 mol_a_dk.

[1]. Khlyustova A. V., Sirotkin N. A., Maximov A. I. High Energy Chem, 2010, v. 44, pp. 75-77

[2]. Titov V.A., Sirotkin N.A. in Proc. VII International Symposium on Theoretical and Applied Plasma Chemistry (September 3 – 7, 2014. Plios, Russia). published by Ivanovo State University of Chemistry and Technology, Ivanovo, Russia, 2014, pp. 160 – 163.

THERMOCHEMISTRY OF 4-OH-L-PROLINE DISSOLUTION IN SOME (WATER+AMIDE) MIXTURES AT T=298.15 K.

Smirnov V.I., Badelin V.G.

G.A. Krestov Institute of Solution Chemistry, Russian academy of Sciences, 153045 Ivanovo, Russia

E-mail: vis@isc-ras.ru

4-hydroxyproline (4-OH-L-proline) has the structure of L-proline molecule in which the OH-group is attached to the gamma carbon atom in the pyrrolidine ring. 4-hydroxyproline and L-proline are the major components of collagen. Collagen is one of the main building blocks of connective tissue such as skin, bone, and cartilage. Thus, when these tissues are damaged, 4-hydroxyproline is able to recover the damaged area. The problem of collagen stability is an area of active research that is far from being completely solved. In this sense, the study of the thermochemical properties of 4-hydroxyproline in aqueous solutions of different organic solvents can help to understand the structural bases of larger molecules which support life. The main aims of this study are: a) to study intermolecular interactions between the molecules of 4-hydroxyproline and amide molecules (FA, MFA, DMF and DMA) in aqueous solutions depending on their concentration ($x_2 = 0 - 0.3$); b) to assess the influence of different physico-chemical properties of organic co-solvents on the energy of their interaction with the molecules of 4-hydroxyproline; c) to find out distinctions and similar properties in the processes of the interaction of L-proline and 4-hydroxyproline molecules with components of similar mixtures; to compare the results with the earlier obtained data for L-proline in the same mixed solvent at $T=298.15$ K. The changes in $\Delta_{tr}H^\circ$ of 4-hydroxyproline relative to the amide content are shown in Fig.1.

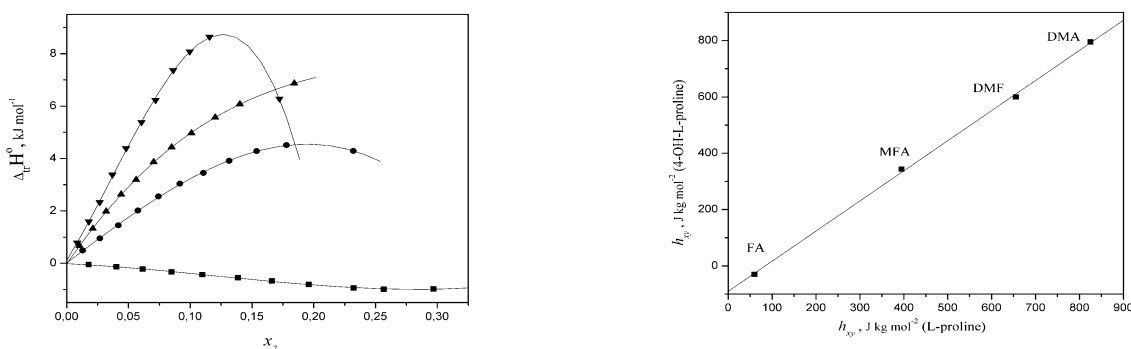


Fig.1. The transfer enthalpies, $\Delta_{tr}H^\circ$, of 4-hydroxyproline from H₂O into H₂O + FA (-■-), H₂O + MFA (-●-), H₂O + DMF (-▲-) and DMA (-▼-) mixed solvents as a function of amide mole fraction (x_2) at $T=298.15$ K.

Fig.2. Correlation between the enthalpy coefficients of pairwise interactions (h_{xy}) of 4-hydroxyproline and the enthalpy coefficients of pairwise interactions (h_{xy}) of L-proline in (H₂O + amide) mixed solvents.

We have ascertained that the energy of pairwise interactions of 4-hydroxyproline with the amide molecules in aqueous solution depends on the mixture composition. Increasing the concentration of FA in aqueous solution maximizes 4-hydroxyproline solvation in all concentration range studied. The dependencies $\Delta_{tr}H^\circ = f(x_2)$ for MFA, DMF and DMA are extreme in character, at first weakening the solvation of 4-hydroxyproline and then maximizing it. The weak intermolecular interactions in (H₂O+FA) mixture contribute to the solvation of 4-hydroxyproline; strong intermolecular interactions in (H₂O+MFA), (H₂O+DMF) and (H₂O+DMA) mixtures result in weakening the solvation of 4-hydroxyproline. The increase in the polarity, polarizability and acidity of the organic co-solvent maximizes its intermolecular interactions with the molecules of 4-hydroxyproline. The increase in the cohesion energy density, the molar volume, and basicity of the organic co-solvent causes the energy of pairwise interactions between 4-hydroxyproline and organic co-solvent to become weaker.

INTERACTION OF SOME DIPEPTIDES WITH THE SODIUM DODECYLSULFATE IN AQUEOUS SOLUTIONS AT $T=298.15$ K.

Smirnov V.I., Badelin V.G.

G.A. Krestov Institute of Solution Chemistry, Russian academy of Sciences, 153045 Ivanovo, Russia

E-mail: vis@isc-ras.ru

The present study is a continuation of our investigations of the processes of dissolution and solvation of amino acids and peptides in aqueous-organic mixtures. In this work, we report the enthalpies of dissolution and the transfer enthalpies of DL- α -alanyl-DL- α -alanine (AlaAla), DL- α -alanyl-DL- α -valine (AlaVal) and glycylglycylglycine (GlyGlyGly) from water to aqueous surfactant (sodium dodecyl sulfate (SDS)) solutions have been determined at $T=298.15$ K by isothermal calorimetry. The purpose of the real work consists in assessment of the influence of SDS concentration on the thermochemical parameters of AlaAla, AlaVal and GlyGlyGly dissolution in water solutions. The analysis of the obtained data shows that the enthalpies of dissolution and transfer of peptides from water in water solutions of surfactant depend both on their structure, and on the concentration of SDS. The effects of peptide structures and SDS dehydration are important at low concentrations of the surfactant (up to $m = 0.03$ mol kg⁻¹ of SDS). Ion - ion interactions predominate at the surfactant concentrations (up to $m = 0.08$ mol kg⁻¹ of SDS). Further, the endothermic contribution from hydrophobic - hydrophobic interactions between molecules of peptides and SDS to the total enthalpic effect of interaction becomes determinative.

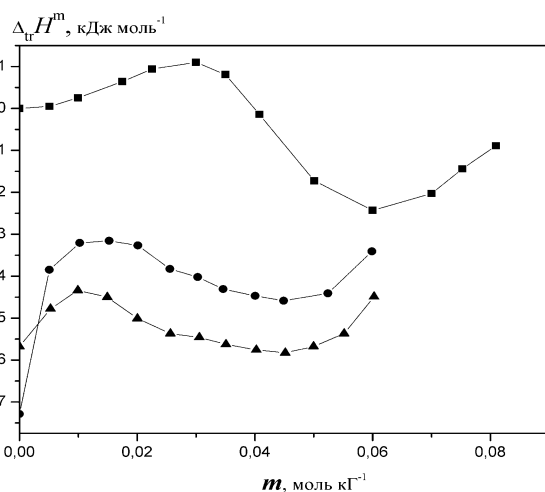


Fig.1. The transfer enthalpies, $\Delta_{tr}H^\circ$, of GlyGlyGly (-■-), AlaAla (-●-) and AlaVal (-▲-) from H₂O into H₂O + SDS mixtures as a function of SDS molality (m) at $T=298.15$ K.

The change of the energy of intermolecular interactions of AlaAla, AlaVal and GlyGlyGly molecules with the molecules of SDS in the water solution have the similar character. However, situation and size of endothermic and exothermic maximum on the dependencies of

$\Delta_{tr}H^\circ = f(m)$ depends on the composition of (H₂O + SDS) mixture, structures of peptides and energy of intermolecular interactions peptide-SDS will be defined:

a) concentration of SDS (increase in concentration of SDS from $m = 0$ to 0.03 (mol kg⁻¹) for GlyGlyGly and $m = 0$ to 0.01 (mol kg⁻¹) for AlaAla and AlaVal increases endothermicity of dissolution of peptides due to prevalence of effects of partial dehydration of molecules of the interacting substances over enthalpy effects of direct interactions; then energy of intermolecular interactions will be defined by structure of micellar solution, namely, availability of various functional SDS groups (which depends on a form of micelles) at interaction with molecules of peptides (at the same time, the dependence course $\Delta_{tr}H^\circ = f(m)$ can change on opposite);

b) hydrophobic properties of the peptide molecules.

This work is executed at financial support by the Russian Foundation for Basic Researches (Grant № 15-43-03003_r_center_a).



LIQUID-LIQUID EQUILIBRIUM IN THE QUATERNARY SYSTEM WATER + BUTYRIC ACID + *i*-BUTYRIC ACID + PYRIDINE WITHIN 30–80°C

Smotrov M.P., Shtab R.V. and Cherkasov D.G.

Saratov State University named after N.G. Chernyshevsky, 410012 Saratov, Russian Federation

E-mail: ilinkk@info.sgu.ru

Ternary systems with a closed delamination range are increasingly used in extraction practice. Chemical interaction between any two components, leading to the formation of a chemical compound in the liquid phase with a limited solubility in the third component, is one cause of delamination. The introduction of a fourth component, either liquid or solid, may help to optimize the extraction separation process. Meanwhile, the influence of this component on the phase behavior of such systems and the topological transformation of the phase diagram of the arising quaternary system with temperature changes remain little studied.

This work is devoted to our experimental study of the liquid-liquid equilibrium in few component mixtures of a cut of the composition tetrahedron of the quaternary system water + pyridine + butyric acid + isobutyric acid within 30–80°C in order to reveal topological transformation patterns of the region of two liquid phases. The constituent ternary systems water + pyridine + butyric acid and water + pyridine + *i*-butyric acid are characterized by closed delamination ranges. As temperature increases, the component solubility in these systems increases and becomes infinite at 52.0°C [1] and 79.5°C [2], respectively.

The cut was passed through points of the water–butyric acid and water–isobutyric acid edges and the pyridine top of the tetrahedron. Our selection of the cut position was determined by the condition that it should pass near the points corresponding to the mixtures with the maximum temperature of two-liquid-phases existence in the constituent ternary systems pyridine + water + butyric acid [1] and pyridine + water + isobutyric acid [2]. The weight ratio of water–butyric acid and water–isobutyric acid was 72.5 : 27.5 and 63.3 : 36.7, respectively.

Phase equilibria in the component mixtures of ten sections of the cut triangle were studied by means of the visual polythermal method. The component mixtures of sections I–V were characterized by a varying mass ratio in the mixtures water + butyric acid and water + isobutyric acid and a constant (for each section) pyridine content, namely: 12.5% (I), 15% (II), 18% (III), 23.5% (IV), and 27.5% (V). The phase state polytherms of sections I–IV are similar. They are smooth lines that separate the fields of two-liquid-phase state (I_1+I_2) and homogeneous liquid solutions (I). These lines start at the points corresponding to the mixtures with no isobutyric acid, i.e. those belonging to the ternary system water + pyridine + butyric acid; and end at the points corresponding to the mixtures with no butyric acid, i.e. those belonging to the ternary system water + pyridine + isobutyric acid. The component mixtures of sections VI–X are characterized by a constant mass ratio in the mixtures water + butyric acid and water + isobutyric acid (8:92 (VI), 32:68 (VII), 52:48 (VIII), 79:21 (IX), and 92:8 (X)) and a varying pyridine content. The polytherms of sections VI–X are similar, being smooth curves with a maximum, separating the I_1+I_2 and I fields.

The phase state polytherms were used for graphical determining the composition of the mixtures corresponding to the phase transition points at the selected temperatures and for plotting isothermal phase diagrams of the cut. The plotted isotherms show that at relatively low temperatures (30–52°C) the composition tetrahedron of the quaternary system has a single region of two liquid phases, extending from the water–pyridine–butyric acid side to the water–pyridine–isobutyric acid side. As temperature increases, the region of two liquid phases reduces and leaves the water–pyridine–butyric acid side at 52.0°C [1]. Within 52.0–79.5°C, there is clearly a region of two liquid phases adjacent to the water–pyridine–isobutyric acid side of the composition tetrahedron with a single line of critical points passing on its surface. At a temperature of 79.5°C, this region shrinks to a point and disappears on the water–pyridine–isobutyric acid side over a noncritical point.

[1] Cherkasov, D. G.; Smotrov, M. P.; Il'in, K. K. *Russ. J. of Appl. Chem.*, 2008, 81, 218-222.

[2] Sergeeva, V.F.; Matyushinskaya, L.B. *Zhurn. obsch. khimii*, 1977, 47, 1215-1218.

THE ANALYSIS OF CHANGE OF GIBBS ENERGY ΔG OF AT A CRYSTALLIZATION $Na_2S_2O_3 \cdot 5H_2O$ AND $Na_2SO_4 \cdot 10H_2O$

Sobol O.V.

Donbas National Academy of Civil Engineering and Architecture, 286123, Makeyevka, Donetsk region
E-mail: cluck@mail.ru

Taking into account dislocation and H_2O – vacant lattice site structure of germs of hydrates the general change of Gibbs energy ΔG when forming a firm phase from water solution can be written down in a look $\Delta G = -\Delta G_V + \Delta G_S - \Delta G_d - \Delta G_{H_2O}$, (1)

Where ΔG_V - a volume component, ΔG_S - a surface component, ΔG_d - additional energy which needs to be spent when forming a frame of hydrate from of the symmetric clusters for formation of a steady germ in which some number of n_d of dislocations by length of l stretching through all germ, ΔG_{H_2O} - the additional item which appeared in case of insufficient hydration of a frame of a germ water

molecules "slammed". $\Delta G = -\frac{l^3 \rho RT \Delta c}{Mc_0} + 6l^2 \sigma - W_l n_d l \pm W_g n_{H_2O}$. (2)

As a result we receive $\Delta G_{\max} = -\Delta \mu l_1^3 + 6l_1^2 \sigma - W_l n_d l_1 - W_g n_{H_2O}$, (3)

$\Delta G_{\min} = -\Delta \mu l_2^3 + 6l_2^2 \sigma - W_l n_d l_2 - W_g n_{H_2O}$. (4)

Here $\Delta G_{\max} = A_1$ - the work of formation of a steady nucleus of crystalhydrate of the critical l_1 size. $\Delta G_{\min} = A_2$ - the work of formation of a steady cluster on any reason of crystalhydrate of this structure, not capable to education.

On process of a nucleation and a mass crystallization significant effect is had thermal history of a liquid phase (an overheat, thermo temporary processing, cooling rate, external influences, etc.) While the formed crystals grow freely, they have the more or less exact geometrical form. However at collision of the growing crystals their exact form is broken as in these sites body height of sides stops. Body height continues only in those directions where there is free access of the "feeding" liquid. As a result the growing crystals having at first geometrically the regular shape after hardening receive the irregular exterior form.

So, at a crystallization in various conditions of $Na_2S_2O_3 \cdot 5H_2O$ of nuclei fluctuate within 10-15 microns (fig. 1 a,b), and when nucleating $Na_2SO_4 \cdot 10H_2O$ of aqueous solutions the critical sizes make 1-5 microns (fig. 2 a,b).

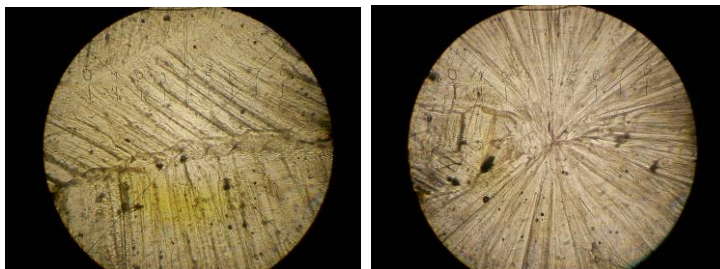


Figure 1 a, b. $Na_2S_2O_3 \cdot 5H_2O$
($T_0 = 16^\circ C$).

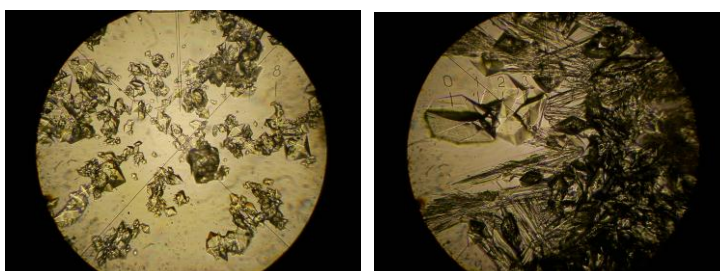


Figure 2 a, b. $Na_2SO_4 \cdot 10H_2O$
($T_0 = 16^\circ C$).



NEW METHOD OF PREDICTING THE THERMODYNAMIC PROPERTIES OF SOLUTIONS

Suntsov Y.K.

¹ Voronezh Institute of State Firefighting Service of Emercom of Russia, 394052 Voronezh, Russia

E-mail: jsyntsov@mail.ru

Thermodynamic properties of solutions are a basis for calculations of the technological parameters, defining a direction and speed of technological processes. Calculation of thermodynamic properties of solutions in full volume is practically realizable only on the basis of experimental data about phase equilibriums of various types. However, research of phase equilibriums is connected with the big experimental difficulties. In connection with this, the authors understand the importance of prediction of thermodynamic properties of solutions, based on the minimum number of experimental data. The solution to this problem is connected with the establishment of relationships between thermodynamic properties of solutions and properties forming their components. Further development of the thermodynamics of solutions is associated with the consideration of molecular concepts [1]. In this work, an attempt was made to determine the relation between to the thermodynamic functions of binary solutions and the molecular weights (structure) of solution components. As object of research binary systems formed by *n*-alcohols (a common solvent) and difficult esters of organic acids (the second components), benzene and *n*-alkyl benzenes, fluoroarene and haloarenes are chosen. We studied liquid–vapor phase equilibria and volume properties of binary systems formed by specified components. Concentration and temperature dependences of the solution properties are indicative of a complex character of molecular interactions in the solutions, which manifests itself in deviations of binary systems from ideality[2-4]. The chief disadvantage of calculations by the Lewis-Randal method is that thermodynamic functions of solutions are not related directly to molecular characteristics of components of mixtures. To achieve the assigned tasks the following algorithm of research was used: (1) Thermodynamic properties of liquid substances in homologous series were investigated; (2) Properties of solutions of the binary liquid systems formed by the common solvent and substances of these homologous series were investigated; (3) An ideal gas at the temperature (*T*), volume (*V*) and composition (*x*) of the real liquid, which obeyed the statistics of the real liquid, was used as a standard for calculating the contributions of intermolecular interactions to the thermodynamic functions of solutions; (4) For the solutions at a constants molar concentration (at *T*, *V* = const.), the functional relationship between the thermodynamic properties of solutions and the molar mass (structure) of the components forming solutions was attempted to be determined [2-4]. It is established, that for the solutions of constant molar concentrations, the Helmholtz energy (A^T , J/mol) was found to depend linearly on the molecular weight of second component of solutions. The results obtained allowed us to suggest the equation:

$$A^T = (k_1 * x + b_1) * M + k_2 * x + b_2 \quad (1)$$

where x_1 is the mole fraction of a common solvent in solution and *M* is the molecular weight the second solution component, k_1 , k_2 , b_1 , b_2 – factors. Equation (1) describes the Helmholtz energy of solutions with an accuracy of < 1%. We believe that this law is general in character and can be used to predict the thermodynamic properties of binary system solutions formed by a common solvent and representatives of homologous series of organic substances. The technique allowing with high accuracy to predict of thermodynamic properties of solutions of binary systems is offered, using properties of two pure components and two solutions constant molar concentrations. An accuracy prediction thermodynamic property of solutions depends only on the accuracy of the experimental data. Proposed a method speeds up the process of researching the thermodynamic properties of binary systems ~ 340 times.

[1] E. S. Rudakov, *Molecular, Quantum, and Evolutional Thermodynamics* (Inst. Fiz.-Org. Khim. i Uglekhim. im. M. Litvinenko, Donetsk, 1998) [in Russian].

[2]. J. Suntsov . *Legitimacies change of properties of binary systems on an example of solutions formed by aliphatic alcohol and complex ethers of organic acids. XVIII international conference "THERMODYNAMICS - 2003"*, University of Cambridge (U. K.).

[3] Y. K. Suntsov, *Zh. Fiz. Khim.* 82 (3), 410 (2008) [*Russ. J. Phys. Chem.* 82 (3), 410 (2008)].

[4] Y. K. Suntsov, *Zh. Fiz. Khim.* 82 (4), 625 (2008) [*Russ. J. Phys. Chem.* 82 (4), 625 (2008)].

[5] Y. K. Suntsov, New method of predicting the thermodynamic properties of solutions. *Journal of Chemistry and Chemical Engineering*, 2014, vol. 8, no. 3, pp. 306–314. DOI: 10.17265/1934-7375/2014.03.013.



IMPACT OF STRUCTURAL MODIFICATION OF 1,2,4-THIA DIAZOLE DERIVATIVES ON THERMODYNAMICS OF SOLUBILITY AND HYDRATION PROCESSES

Surov A.O., Perlovich G.L.

G.A. Krestov Institute of Solution Chemistry, Russian Academy of Sciences, 153045, Ivanovo, Russia

E-mail: aos@isc-ras.ru

Heterocyclic compounds having 1,2,4-thiadiazole moiety in the structure are of a great interest to the pharmaceutical and medicinal chemistry because of their high specific activity within a wide concentration range. Synthesis of new heterocyclic derivatives of 1,2,4-thiadiazole continues to be the most important area in the field of highly effective neuroprotective drugs for medicine. One of the key problems of creating the effective drugs is poor solubility, so the physicochemical study of newly synthesized drug-like compound includes, first and foremost, the elucidating of solubility behavior. Poor solubility of a potential drug compound significantly reduces the bioavailability, leads to the growth of therapeutic doses and, as a consequence, to the appearance of side effects. Solubility of the compounds is determined by the difference between the Gibbs energies of the crystal lattice (sublimation process) and that of solvation / hydration. The understanding of the relationship of the thermodynamic characteristics of these processes depending on the structural modification of the studied compounds makes possible the targeted design of the drug molecules with the required properties. The present study is a continuation of our investigations into the crystal structures [1] and biological activity [2] of 1,2,4-thiadiazole derivatives. The aim of the present investigation is to measure the thermodynamic parameters of the solubility and hydration processes of the compounds of 12 novel 1,2,4-thiadiazole drug-like compounds and elucidate the influence of the molecular structure features on the solubility behavior in the phosphate buffer solution pH 7.4 modeling the blood plasma medium.

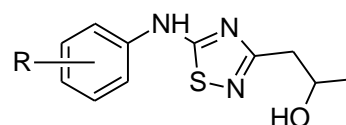


Figure 1. Basic molecular structure of the 1,2,4-thiadiazole derivatives

It was found that the introduction of any substituent in the phenyl ring of the 1,2,4-thiadiazole molecule reduces the solubility of the substance. For the most of the compounds this process is accompanied by significant decrease of the dissolution entropy, whereas the change of solution enthalpy is not considerable or not enough to balance the entropy contribution. In order to rationalize the relationships between the structure of 1,2,4-thiadiazoles and their solubility, the latter was considered in terms of two fundamental processes: sublimation and hydration. As in the dissolution process, the insertion of terminal substituents in the phenyl ring of the molecule affects the entropic term of the hydration process to a larger extent. Analysis of the hydration Gibbs energy revealed that only four substituents (R = 4-Me, 4-iso-EtOH, 4-OMe and 4-Cl) enhances the hydration of the corresponding compounds in comparison with the unsubstituted 1,2,4-thiadiazole. However, this gain of the hydration term does not compensate the increase of the sublimation contribution (interactions of the molecules in the crystal) induced by the introduction of the substituents in the phenyl fragment, which leads to consequent solubility decrease. The correlation analysis of the thermodynamic functions of hydration with HYBOT physicochemical descriptors demonstrated that the Gibbs energy of the process can be estimated using the sum of donor and acceptor ability of the atoms in the molecule to form hydrogen bonds normalized by the polarizability.

[1] Surov, A. O.; Trinh Bui, C.; Proshin, A. N.; Roussel, P.; Idrissi A.; Perlovich G. L. *J. Phys. Chem. B*, 2013, 117, 10414–10429.

[2] Perlovich, G. L.; Proshin, A. N.; Volkova, T. V.; Petrova, L. N.; Bachurin S. O. *Mol. Pharm.*, 2012, 9, 2156–2167.



IMPACT OF BIORELEVANT MEDIA COMPOSITION ON THERMODYNAMICS OF INCLUSION COMPLEX FORMATION OF 1,2,4-THIADIAZOLE DERIVATIVE WITH HYDROXYPROPYL- β -CYCLODEXTRIN

Brusnikina M.A.¹, Chislov M.V.¹, Silyukov O.I.¹, Volkova T.V.¹, Proshin A.N.², Terekhova I.V.¹

¹G.A. Krestov Institute of Solution Chemistry of the Russian Academy of Sciences, 153045 Ivanovo, Russia

²Institute of Physiologically Active Compounds of the Russian Academy of Sciences, 142432 Chernogolovka, Russia

E-mail: ivt@isc-ras.ru

Novel 1,2,4-thiadiazole derivatives are claimed as medically important since they display antioxidant and neuroprotective activity. It has been shown that these compounds are effective in the treatment of neurodegenerative diseases. However, their poor solubility in aqueous media can significantly decrease bioavailability and therapeutic action. This problem can be eliminated by use of cyclodextrins, which are able to form water-soluble inclusion complexes with a wide variety of drug molecules. Inclusion complexes are formed via non-covalent interactions and can be also considered as drug delivery systems. Generally, inclusion complex formation is studied in water or buffer solutions imitating the pH of the internal environment. However, biological liquids are more complicate and contain surfactants, enzymes and etc., which can influence the drug behaviour. In this connection, impact of biological liquids should be investigated and taken into account.

The aim of present work was to reveal the influence of buffer composition on thermodynamics of complex formation of hydroxypropyl- β -cyclodextrin (HP- β -CD) with 1-[5-(3-chlorophenylamino)-1,2,4-thiadiazol-3-yl]-propan-2-ol, which is proposed for the treatment of Alzheimer's disease. Complex formation was studied in buffer solutions pH 1.2 imitating the gastric fluid. Composition of the buffers used is given in Table.

Table 1. Composition of the media to simulate the gastric fluid

Component	Blank (HCl)	SGF	FaSSGF
Sodium dodecyl sulfate (%w)	–	0.25	–
Pepsin (mg/ml)	–	–	0.1
Sodium taurocholate (μ M)	–	–	80
Lecithin (μ M)	–	–	20
NaCl (mM)	34.2	34.2	34.2
pH	1.2	1.2	1.6

It was found that rather stable inclusion complexes of 1:1 stoichiometric ratio are formed between HP- β -CD and 1,2,4-thiadiazole derivative in blank buffer. Presence of SDS in SFG buffer prevents the inclusion complex formation. This can be caused by incorporation of 1,2,4-thiadiazole derivative into SDS micelles. Binding affinity of thiadiazole to surfactant was additionally demonstrated. Influence of the components of FaSSGF buffer is insignificant, only minor decrease of the stability constant of the inclusion complexes was observed. In this case, micelles of thaurcholic acid and lecithin are not formed due to very low concentration of these compounds in solution. Therefore, the effect of FaSSGF is determined by weak intermolecular interactions of 1,2,4-thiadiazole derivative with buffer additives.

This work was supported by Russian Science Foundation (project №15-13-10017).



INTERACTIONS OF SULFASALAZINE WITH CYCLODEXTRINS AND BIOPOLYMERS: THERMODYNAMIC STUDY

Chibunova E.S., Brusnikina M.A., Volkova T.V., Kumeev R.S., Terekhova I.V.

G.A. Krestov Institute of Solution Chemistry of the Russian Academy of Sciences, 153045 Ivanovo, Russia

E-mail: ivt@isc-ras.ru

Sulfasalazine is antirheumatic, anti-inflammatory and bacteriostatic agent, but poor solubility and low membrane permeability of this drug led to significant decrease of its bioactivity and effectiveness. Improvement of biopharmaceutical properties of sulfasalazine can be achieved by the introduction of different solubilizing agents into drug formulation.

In this work, biopolymers and cyclodextrins, which are widely used in pharmacy due to their capability to complex formation with drug molecules, are proposed as solubilizing agents for sulfasalazine. Using the isothermal saturation method, it was demonstrated that solubility of sulfasalazine in buffered solutions pH 1.2 and 7.4 containing α -, β -, γ -cyclodextrins, polyvinylpyrrolidone (PVP) and polyethylene glycol (PEG-1000) increases. β -Cyclodextrins and PVP were found as more effective solubilizers.

Interactions of sulfasalazine with biopolymers and cyclodextrins were studied by means of ^1H NMR. It was revealed that sulfasalazine forms with cyclodextrins stable inclusion complexes of 1:1 stoichiometry, while the interactions with polymers are weak and caused mainly by the hydrogen bonding. Inclusion complexes are more stable in slightly alkaline medium (pH 7.4) in comparison with an acidic buffered solution (pH 1.2). It was shown that sulfasalazine phenyl ring is inserted into the cyclodextrin cavity, thus, isolating from the aqueous environment. This causes an increase in aqueous solubility of the drug. On the basis of a comparative study of the calculated thermodynamic parameters of complex formation the influence of the structure of cyclodextrins and polymers on the binding with sulfasalazine in an aqueous solution was analyzed.

This work was supported by Russian Foundation for Basic Research (project №15-43-03017).

PECULIARITIES OF PHASE AND CHEMICAL EQUILIBRIUM IN LIQUID-LIQUID MULTICOMPONENT SYSTEMS

Toikka M.A.¹, Toikka A.M.¹, Sadaeva A.A.¹

¹Institute of Chemistry, Saint Petersburg State University, 198504 Saint Petersburg, Russia

E-mail: m.toikka@spbu.ru

This work deals with the discussion of some peculiarities of multicomponent heterogeneous systems with chemical interactions. Thermodynamic analysis of the features of liquid-liquid phase diagrams of the systems with non-equilibrium and equilibrium chemical reaction in solution is the main task. Particular attention is paid to the critical phenomena that are poorly investigated nowadays despite the significant contribution to the development of thermodynamics. The main objects of the study are the systems with the esterification reaction under polythermal conditions and atmospheric pressure. The development of new physical and chemical approaches to the study of critical phenomena in such systems (e.g. with ethyl acetate, ethyl and n-butyl propionate, amyl and butyl acetate (Figure 1.), methyl and ethyl oleate synthesis reactions) includes a complex experimental study of solubility, liquid-liquid and chemical equilibrium [1], [2], [3], [4], [5].

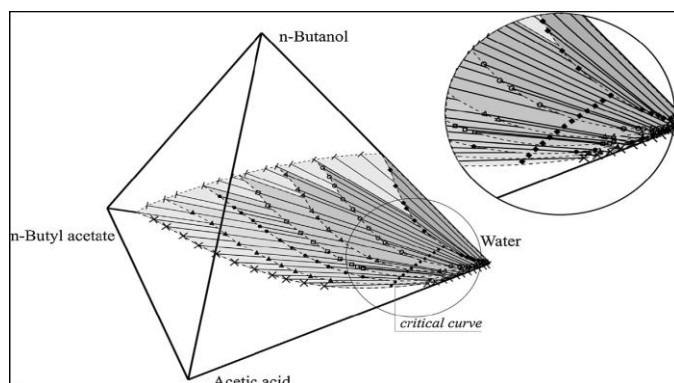


Figure 1. The qualitative view of binodal surface of acetic acid – n-butanol – n-butyl acetate – water system at 308.15 K. Tie-lines in ternary systems: acetic acid – n-butyl acetate– water (x-x), n-butanol–n-butyl acetate–water (|-|) and acetic acid–n-butanol–water (■-■); ▲-▲, ●-●, □-□, Δ-Δ and ○-○ – tie-lines in quaternary system. The bold solid line – the run of critical curve of LLE in quaternary system [5].

It should be noted that the thermodynamic analysis of the transformation of phase diagrams for the quaternary reacting systems with liquid phase splitting is really important from the theoretical point of view. At the same time the practical significance of the delamination problem of reacting mixtures is obvious: such effect changes the technological process of the synthesis. This work presents new experimental data on phase and chemical equilibrium of liquid-liquid quaternary reactive systems, including critical phenomena, in particular, critical curves, critical surfaces and unique reactive critical points.

Acknowledgements: The research is supported by the Russian President's Scholarships (SP-2140.2016.1). Authors are grateful to Russian Foundation for Basic Research for the support of this study (RFBR project 16-33-00129).

- [1] Artemiy Samarov, Maria Toikka, Maya Trofimova, Alexander Toikka. Fluid Phase Equilib., 2016, 425, 183-187.
- [2] A.A. Samarov, M.A. Toikka, P.V. Naumkin, and A.M. Toikka. Theor. Found. Chem. Eng., 2016, 50 (5), 739-745.
- [3] A.M. Toikka, A.A. Samarov, M.A. Toikka. Russian Chem. Rev., 2015, 84 (4), 378-392.
- [4] Maria Toikka, Alexander Toikka. Pure Appl. Chem., 2013, 85 (1), 277-288.
- [5] Artemiy Samarov, Maria Toikka, Alexander Toikka. Fluid Phase Equilib., 2015, 385, 129-133.

HEAT CAPACITIES AND VOLUME PROPERTIES OF NICOTINIC ACID AND L-PHENYLALANINE BUFFER SOLUTIONS

Tyunina E.Yu.¹, Badelin V.G.¹, Egorkina V.S.², Mezhevoi I.N.¹

¹ G.A. Krestov Institute of Solution Chemistry, Russian Academy of Sciences, 153045 Ivanovo, Russia

² Ivanovo State University of Chemistry and Technology, 153000 Ivanovo, Russia

E-mail: tey@isc-ras.ru

Thermodynamic and physicochemical properties of multicomponent aqueous solutions containing biologically active solutes are important in various areas of applied chemistry and are essential for understanding the binding of various molecular drugs with the biomacromolecules through specific or non-specific interactions. Nicotinic acid is a member of the B-vitamin family. Amino acids are building blocks of proteins. Interactions between nicotinic acid (NA) and L-phenylalanine (Phe), as models drug and protein, were studied in aqueous phosphate buffer solutions (pH=7.35) by differential scanning calorimetry and volume methods. Heat capacities and densities of NA-buffer, Phe-buffer, and NA-Phe-buffer mixtures were determined at T=(288.15, 298.15, 308.15, 318.15 and 323.15) K. The specific heat capacity (C_p) measurements of NA-buffer, Phe-buffer and NA-Phe-buffer mixtures were performed in a differential scanning microcalorimeter SCAL-1 (SCAL Co. Ltd., Pushchino, Russia) in glass cells of 0.337 cm³ capacity relative to buffer solvent at the scanning rate of 1.0 K/min with accuracy $\pm 0.03\%$. The density (ρ) of solution was measured using a digital precision vibrating densimeter DMA-5000 M (Anton Paar, Austria). The uncertainty in density measurements was within $\pm 2 \times 10^{-3}$ kg·m⁻³.

The apparent molar heat capacities (${}^\phi C_p$) and apparent molar volumes ($V_{\phi,NA}$) of nicotinic acid in buffer solution and in buffer 0.0120 mol·kg⁻¹ amino acid solutions were evaluated from experimental data. The concentration of NA was varied from (0.0079 to 0.036) mol·kg⁻¹. The shape of curves for apparent molar parameters of NA on NA concentration shows that Phe undergoes the binding with NA. The function $V_{\phi,NA}=f(m_{NA})$ has a maximum corresponding to the stoichiometry of complex. The maximal values of

$V_{\phi,NA}$ were observed near $m_{NA}=0.0249$ mol·kg⁻¹ at 298.15 K and near $m_{NA}=0.0219$ mol·kg⁻¹ at 288.15, 308.15 and 318.15 K, which correspond to the ~ 1:2 and 1:1.7 Phe / NA molar ratios, respectively. The maximal values of ${}^\phi C_p$ were observed near $m_{NA}=0.0199$ mol·kg⁻¹, which correspond to the ~1:1.7 Phe / NA molar ratios at the temperatures studied. The stoichiometry of the complex obtained was found to weakly depend on temperature.

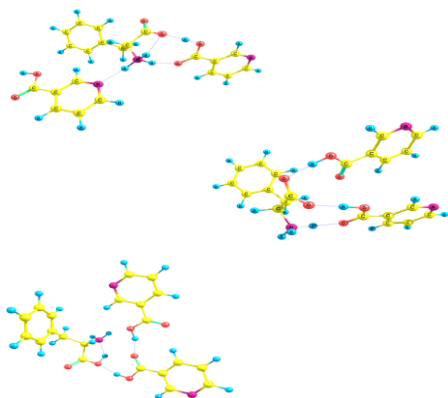


Figure 1. Structures of complexes for 1:2 Phe / NA molar ratios.

The interactions between the NA and Phe were also investigated by means of DFT/B3LYP/6-31**G calculations. The most stable complexes correspond to bidentate structures in which the terminated charge groups of Phe zwitterions interact with the COOH group of two molecules of NA (Fig.1).

The increase of ${}^\phi C_p^o$ and $V_{\phi,NA}^o$ values with increase in temperature indicates that interactions between solutes molecules are stronger than intermolecular hydrogen bonding between water molecules. The higher positive ${}^\phi C_p^o$ and $V_{\phi,NA}^o$ values for NA in 0.0120 mol·kg⁻¹ Phe compared to the aqueous buffer solution at each temperature generally suggest that the interactions between Phe zwitterions and NA molecules are predominant. The first $(\partial Y^o_\phi / \partial T)_p$ and second $(\partial^2 Y^o_\phi / \partial T^2)_p$ differentials were determined for NA in aqueous buffer solution and for NA in aqueous amino acid buffer solution. If the NA molecules in aqueous buffer solution are water structure breakers, then the structure breaking effects of NA decrease as a result of hydrogen bonding, coulombic and hydrophobic interactions between NA and Phe molecules during the complex formation in aqueous amino acid buffer solutions.



THERMODYNAMICS OF MOLECULAR COMPLEX FORMATION REACTIONS OF CROWN – ETHERS AND CRYPTANDS WITH AMINO ACIDS AND PEPTIDES IN AQUEOUS – ORGANIC SOLVENTS

Usacheva T.R.

Ivanovo State University of Chemistry and Technology, General Chemical Technology Department, 153000 Ivanovo, Russia
E-mail: oxt@isuct.ru

The problems of “host - guest” molecular complex formation reactions in systems containing solvated biomolecules and macrocyclic ligands are of current interest for fundamental studies and their solutions are of considerable importance for applications. Molecular complex formation reactions occur in many biochemical processes such as enzymatic catalysis, membrane transport, and antigen-antibody interactions, which take place in solutions. Studies on the complexing properties of synthetic macrocycles such as crown ethers and cryptand capable of recognizing other species make it possible to simulate molecular recognition processes occurring in biological systems, as well as to design various molecular devices for modern science and technology. Our finding on the effect of H₂O-EtOH, H₂O-DMSO and H₂O-Me₂CO solvents on the enthalpy and entropy of molecular complexations of 18-crown-6 (18C6) and cryptand [2.2.2] (L) with glycine (Gly), D,L-alanine (Ala), L-phenylalanine (Phe) and glycyl-glycyl-glycine (3Gly) on the stability of the resulting complexes and the literature data for related systems were reviewed. The relationships between the thermodynamic parameters of the complex formation reactions and the reactant solvation were analyzed to reveal the key factors that are crucial for the increasing stability of the complexes and the increasing exothermicity of the processes under study in water- organic solvents. The solvation contributions of the reagents to the Gibbs energy changes ($\Delta_{tr}G_r^0$) in the formation of the molecular complexes [Gly18C6], [Ala18C6], and [Phe18C6] show the same trends for all the systems under study: -replacement of water by non aqueous solvents diminishes the solvation of both amino acids (AA) and 18C6, which is evident from the increasing positive $\Delta_{tr}G^0(\text{AA})$ and $\Delta_{tr}G^0(18\text{C}6)$ values with an increase in X_2 ; -the changes in the solvated state of the complexes [AA18C6] ($\Delta_{tr}G^0[\text{AA}18\text{C}6]$) are identical with $\Delta_{tr}G^0(18\text{C}6)$, which is indicative of the key role of the solvated state of 18C6 in the formation of the solvation shell of the complex; -the contributions from $\Delta_{tr}G^0(18\text{C}6)$ and $\Delta_{tr}G^0([\text{AA}18\text{C}6])$ are outweighed by the contribution from the desolvation of the amino acids ($\Delta_{tr}G^0(\text{AA})$); -the $\Delta_{tr}G_r^0$ values correlate with but are opposite in sign to $\Delta_{tr}G^0(\text{AA})$, thus suggesting that the diminution of the AA solvation is decisive for the changes in the stability of [AA18C6] complexes. Apparently, this criterion can be employed as a basic thermodynamic parameter for estimating the changes in the stability of crown-ethers complexes with peptides and ammonium – type cations upon the replacement of water by organic solvents. The most characteristic distinction between the thermodynamic contributions of the reagents to the changes in the enthalpies and Gibbs energies of the complexations reactions is that the endothermicity of transfer of AA increase insignificantly compares to the endothermicity of transfer of 18C6. In all cases, the positive enthalpies of transfer of 18C6 and [AA18C6] increase with the content of the organic cosolvent. Note that the enthalpies of transfer of 18C6 increase more rapidly than $\Delta_{tr}H^0([\text{AA}18\text{C}6])$, and the $\Delta_{tr}H^0(\text{AA})$ values are nearly zero. Because of this, the complexations in the binary solvent enriched with the organic component is more exothermic. Apparently, the considerable energy changes due to the breakdown of the solvation shell of 18C6 are completely compensated by the increasing entropy component of the Gibbs energy of solvation of 18C6. Because of this compensating effect, the Gibbs energy change in the transfer of 18C6 is nearly zero. In contrary, the solvation enthalpy term of AA prevails on the entropy one and it results in the superiority of $\Delta_{tr}G^0(\text{AA})$ values upon $\Delta_{tr}G^0(18\text{C}6)$. This phenomenon explains the difference in key solvation contributions to the complexes stability and reaction enthalpies. Similar trends of the $\Delta_{tr}G^0$ solvation characteristics of reagents and reactions of [3GlyL], [3Gly18C6] and [Gly18C6] complex formations in H₂O–DMSO were observed. However, the relation $\Delta_{tr}G^0(\text{L}) > \Delta_{tr}G^0(18\text{C}6)$ in H₂O–DMSO solvent indicate a stronger solvation shell of 18C6 compared with that of cryptand [2.2.2]. This may explain the greater stability of the complex [3GlyL] in comparison with stability of [3Gly18C6] and [Gly18C6].

Acknowledgement. This work was performed at the Research Institute of Thermodynamics and Kinetics of Chemical Processes of the ISUCT and was carried out under grant of Council on grants of the President of the Russian Federation (project 14.Z56.16.5118-MK).

**COMPLEX FORMATION OF SILVER(I) WITH 18-CROWN-6
IN ETHANOL-DIMETHYL SULFOXIDE BINARY MIXTURES**Volkova M.A.¹, Kuz'mina I.A.¹, Usacheva T.R.¹, Sharnin V.A.^{1,2}, Arena G.³,¹Ivanovo State University of Chemistry and Technology, General Chemical Technology Department, 153000 Ivanovo, Russia²G.A. Krestov Institute of Solution Chemistry of the Russian Academy of Sciences, 153045 Ivanovo, Russia³University of Catania, Department of Chemistry, I-95125 Catania, Italy

E-mail: oxt703@isuct.ru

The effect of composition of the mixed ethanol (EtOH)-dimethyl sulfoxide (DMSO) solvents ($\chi_{\text{DMSO}} = 0.0 \div 1.0$ mol. fr.) on the stability of silver(I) (Ag^+) complexes with 18-crown-6 ether (18C6) was studied potentiometrically at 298.15 K. The corresponding stability constants of $[\text{Ag}18\text{C}6]^+$ in EtOH-DMSO mixtures are presented in Table. Errors in the values $\lg K^0$ were calculated as the standard mean square deflection with the consideration of Student criterion [1,2] at the confidence probability 0.95 for the series of experiments (3-4 measurements) in every range of composition of the mixed solvent.

It was found that the transfer from the amphoteric ethanol to the aprotic dimethyl sulfoxide causes a sharp decrease in the stability of the coordination compound formed. The authors [3] pointed out that a low stability of $[\text{Ag}18\text{C}6]^+$ observed in many aprotic solvents especially where the donor numbers of the solvents are high ($\text{DN} > 25$).

The variation in Gibbs energy of reagents were calculated from the $\lg K^0$ $[\text{Ag}18\text{C}6]^+$ values at the variation in composition of the mixed solvent $\text{EtOH} \rightarrow (\text{EtOH-DMSO})$. On the basis of equation $[-RT \ln(K^{\circ}_{(\text{S}_1+\text{S}_2)}/K^{\circ}_{\text{S}_1}) = \Delta_{\text{r}}G^{\circ}_{\text{r}} = \Delta_{\text{r}}G^{\circ}(\text{ML})^{z+} - \Delta_{\text{r}}G^{\circ}(\text{M})^{z+} - \Delta_{\text{r}}G^{\circ}(\text{L})$; where $\Delta_{\text{r}}G^{\circ}_{\text{r}}$, $\Delta_{\text{r}}G^{\circ}(\text{ML})^{z+}$, $\Delta_{\text{r}}G^{\circ}(\text{M})^{z+}$ and $\Delta_{\text{r}}G^{\circ}(\text{L})$ – are standard Gibbs energies of transfer of the reaction, complex ion, metal ion and ligand from the individual solvent (S_1) to the binary ($\text{S}_1 + \text{S}_2$), respectively], the difference between the Gibbs energy transfer $[\text{Ag}18\text{C}6]^+$ and ligand by replacing ethanol to dimethyl sulfoxide was determined. The data of $\Delta_{\text{r}}G^{\circ}(\text{Ag}^+)_{\text{EtOH} \rightarrow \text{DMSO}}$ are taken from the literature [4]. Analysis of solvation contributions of the reagents to the change of the $[\text{Ag}18\text{C}6]^+$ stability showed that the effect of solvation of the central ion plays the main part in the stability variation of $[\text{Ag}18\text{C}6]^+$. A similar ratio of solvation contributions of the reactants into a change of $\Delta_{\text{r}}G^{\circ}$ complexation reaction Ag^+ with 18C6 observed in mixed solvents MeOH-DMF [5] and AN-DMSO [6]. This is a distinctive feature of the results from the previously established laws for water and organic solvents, which determines the role in the displacement of equilibrium complexation played by the change in the solvation state of the ligand with the water is replaced by water-organic solvent [7,8].

Table. The stability constants of silver(I) complexes with 18-crown-6 ether in ethanol-dimethylsulfoxide solvents at 298.15 K.

χ_{DMSO} , mol. fr.	0.0	0.2	0.4	0.6	0.8	1.0
$\lg K^0$	4.29 ± 0.01	2.84 ± 0.01	1.98 ± 0.03	1.78 ± 0.03	1.68 ± 0.06	1.60 ± 0.03

[1] Скуг, Д. Основы аналитической химии. М.: Мир, 1979, 1, 89.

[2] Деффель, К. Статистика в аналитической химии. М.: Мир, 1994, 268.

[3] Kalidas, S; Balaji, S. Indian J. Chem., 1999, 38A, 6, 618-620.

[4] Buschmann, HJ; Schollmeyer, E. Inorg. Chim. Acta, 2000, 298, 1, 120-122.

[5] Кузьмина, ИА; Шарнин, ВА; Голиков, АН. ЖОХ, 2009, 79, 12, 1965-1968.

[6] Голиков, АН; Кузьмина, ИА; Шарнин, ВА. ЖНХ, 2007, 52, 11, 1849-1851.

[7] Усачева, ТР; Леденков, СФ; Гжейдзяк, А и др. Изв. ВУЗов. Хим. и хим. техн. 2000, 43, 5, 87-89.

[8] Усачева, ТР; Шарнин, ВА; Леденков, СФ. ЖОХ, 2001, 71, 5, 754-758.

**PHASE EQUILIBRIA, CRYSTAL STRUCTURE AND PROPERTIES OF THE COMPLEX OXIDES IN THE LN–SR–FE–CO–O (LN = SM, GD) SYSTEM**

Volkova N.E., Zubatkina L.V., Maklakova A.V., Cherepanov V.A.

Ural Federal University named after the first President of Russia B.N. Yeltsin, Mira st. 19, 620002 Yekaterinburg, Russia

E-mail: nadezhda.volkova@urfu.ru

Mixed rare earth and strontium cobaltates or ferrites attract significant attention as promising electrode materials for intermediate-temperature solid oxide fuel cells. The present work is devoted to a study of the phase equilibria in the Ln–Sr–Co–O and Ln–Sr–Fe–O (Ln = Sm, Gd) systems in air at 1100°C and determination of the crystal structure and properties of intermediate phases.

The samples were synthesized by solid-state and glycerin nitrate techniques. The changes of oxygen content in the single phase complex oxides were measured by TGA method within the temperature range 25–1100°C. The absolute value of the oxygen content was determined using direct reduction of the sample in a hydrogen flow. Moreover the value of the oxygen content was defined by red-ox titration. Thermal expansion of the ceramic samples was measured using a dilatometer in air. The total electrical conductivity was studied by the 4-probe DC method within 25–1100°C under atmospheric air.

According to the results of XRD analysis four types of solid solutions: $\text{Sr}_{1-x}\text{Ln}_x(\text{Fe},\text{Co})\text{O}_{3-\delta}$, $\text{Sr}_{2-y}\text{Ln}_y(\text{Fe},\text{Co})\text{O}_{4\pm\delta}$, $\text{Sr}_{3-z}\text{Ln}_z\text{Fe}_3\text{O}_{7-\delta}$ and $\text{Sr}_{4-r}\text{Ln}_r\text{Fe}_3\text{O}_{10-\delta}$ exist in the systems.

It was found, that single-phase Sm-substituted solid solutions formed within the range $0.05 \leq x \leq 0.50$. Gd-substituted samples were exist at $x = 0.05-0.3$ and $x = 0.1-0.4$ for ferrites and cobaltates respectively. XRD patterns of the single phase samples were refined by Rietveld method within the cubic structure ($Pm\bar{3}m$ sp. gr.) for $\text{Sr}_{1-x}\text{Ln}_x\text{FeO}_{3-\delta}$ or within the tetragonal structure ($I4/mmm$ sp. gr.) for $\text{Sr}_{1-x}\text{Ln}_x\text{CoO}_{3-\delta}$. On the other hand Sr-substitution for Sm in $\text{Sr}_{1-x}\text{Ln}_x\text{FeO}_{3-\delta}$ is also possible within the range $0.85 \leq x \leq 1.00$. These solid solutions, like unsubstituted $\text{LnFeO}_{3-\delta}$, were indexed in the orthorhombic structure ($Pbnm$ space group). Gradual substitution of strontium by samarium or gadolinium leads to the decrease of unit cell parameters and unit cell volume that can be explained by the relative cation, since the ionic radii of lanthanides are smaller than the ionic radius of strontium. An introduction of lanthanide into the strontium cobaltate and strontium ferrite increases the oxygen content. But, values of oxygen nonstoichiometry for the Sm-substituted oxides some higher than for the Gd-substituted samples with the same dopant concentration. The temperature dependencies of the total conductivity of samples possess maxima at approximately 200-350°C. At higher temperature the total conductivity of material decreases with temperature rise. It should be noted, that the values of conductivity for strontium cobaltate higher than for samples based on strontium ferrite at all studied temperatures. Seebeck coefficient for all compounds reveals positive values within the entire temperature and oxygen partial pressure ranges that indicate predominant p -type conductivity. It was shown, that the average TECs values are decreasing with an increase of dopant content in solid solutions.

According to the results of XRD analysis single phase samples $\text{Sr}_{2-y}\text{Ln}_y\text{MO}_{4\pm\delta}$ were formed within the range $0.7 \leq y \leq 1.1$ for $M = \text{Co}$ and $0.7 \leq y \leq 0.8$ for $M = \text{Fe}$. Gd-substituted solid solutions were exist at $y = 0.8-1.2$ and $y = 0.85$ for cobaltates and ferrites respectively. X-ray diffraction patterns obtained for all single phase samples were indexed in the orthorhombic structure, sp. gr $I4/mmm$. The values of oxygen content in the $\text{Sr}_{2-x}\text{Ln}_x\text{MeO}_{4\pm\delta}$ solid solutions recalculated to the room temperature were nearly equal to 4.0. Oxygen content for all samples remains practically unchanged from 25°C up to 400°C and then slightly decrease with temperature rise. The miscibility gap was found in the row with the general formula $\text{Sr}_{3-z}\text{Ln}_z\text{Fe}_2\text{O}_{7\pm\delta}$. The formation of solid solutions was found within the range $0.0 \leq z \leq 0.3$ and single phase sample was also obtained for $z=1.2$ and 1.1 for Ln = Sm and Gd respectively. The solid solutions based on strontium ferrite ($0.0 \leq z \leq 0.3$) possess tetragonal structure, $I4/mmm$ space group whereas $\text{Sr}_{1.8}\text{Sm}_{1.2}\text{Fe}_2\text{O}_{7\pm\delta}$ and $\text{Sr}_{1.9}\text{Gd}_{1.1}\text{Fe}_2\text{O}_{7\pm\delta}$ were described in $P4_2/mmm$ space group. The value of oxygen content in the $\text{Sr}_{1.8}\text{Sm}_{1.2}\text{Fe}_2\text{O}_{7\pm\delta}$ was nearly equal to 6.96 at room temperature. Crystal structure of $\text{Sr}_{3.1}\text{Sm}_{0.9}\text{Fe}_3\text{O}_{10-\delta}$ and $\text{Sr}_{3.2}\text{Gd}_{0.8}\text{Fe}_3\text{O}_{10-\delta}$ oxides were described by the orthorhombic cell.

The projections of isothermal–isobaric phase diagrams for the Ln – Sr – Co – O, Ln – Sr – Fe – (Ln = Sm, Gd) systems to the compositional triangle of metallic components were presented.

This work was financially supported by the Russian Foundation for Basic Research (project №. 16-53-45010 IND_a)



Section 4.

Thermodynamics of surface phenomena and self-organization phenomena in fluid systems

Oral presentations



K⁺ AND Na⁺ ION EXCHANGE IN MICROEMULSION FORMED BY TERGITOL NP-4 + NaAOT REVERSE MICELLES UNDER KNO₃ CRYSTALLIZATION

Beketova D.I.¹, Demidova M.G.¹, Podlipskaya T.Yu.¹ Bulavchenko A.I.¹

¹*Nikolaev Institute of Inorganic Chemistry, Siberian Branch of the Russian Academy of Sciences, 630090 Novosibirsk, Russia*

E-mail: mc_beketova8888@mail.ru

To study the crystallization mechanisms of ultrafine powders in limiting volume of nanoreactor and templates is an important issue. Earlier we studied microemulsion crystallization of KNO₃ in simple and mixed reverse micelles formed with anionic surfactant – sodium bis(2-ethylhexyl)sulfosuccinate (NaAOT) and nonionic one – oxethylnonilphenol with oxiethylation degree 4 (Tergitol NP-4). It is possible to increase a dispersion of KNO₃ powders only in mixed micelles (Tergitol NP-4+NaAOT). It was marked as a surprising thing that means that KNO₃ was always crystallized in mixed micelles, though molecules of NaAOT contain sodium cations, which can exchange with potassium ions and transfer to polar core of micelle and form solution of nitrate salt NaNO₃: NaAOT_s+KNO₃×nH₂O→KAOT_s+NaNO₃×nH₂O.

The aim of this work was to study ion exchange processes between the surface layer and polar micelle core during the potassium nitrate crystallization. Using microdrop probing as special developed technique and flame photometry it was showed that in mixed micelles at the onset of crystallization a significant part of KNO₃ is indeed replaced by NaNO₃. It was established that NaNO₃/KNO₃ concentration ration does not change during evaporation. According to the ternary phase diagram KNO₃-NaNO₃-H₂O in “normal” water systems the mixture of NaNO₃ and KNO₃ should be crystallized. Special experiments showed that salt mixture was also crystallized in simple Tergitol NP-4 micelles, since a content was the same as initial one.

Thus, mixed microemulsions of Tergitol NP-4+NaAOT are unique nanoreactors, that provide selective KNO₃ crystallization from the salt mixture. Since the crystallization begins a growth of KNO₃ particles is due to KNO₃ “reserves” in micelle cores. As they decrease and water content becomes lower the reverse exchange of K⁺ cations bound with AOT⁻ and Na⁺ cations located in a polar core appears, but crystallization continues.

The possibility of reverse cation exchange is confirmed by numerical simulation of ion electrostatic interactions by direct optimization. At the onset when the water content is high the difference of hydration energy of ion exchange exceeds the difference of Coulomb energy interaction. Gibbs energy in exchange reaction is negative, and ions Na⁺ pass into the micelle core, and ions K⁺ pass into the surface layer. However, with the decreasing content of water molecules in micelles during evaporation the difference in Coulomb interaction becomes determinative. Gibbs energy becomes positive (Na⁺ ions might approach closer to AOT⁻ ions than K⁺) and a reverse transition takes place.

The role of the surfactant ion AOT⁻ at the exchange process is to bind and hold K⁺ cation in the surface layer and to release it into the micelle core at the right time. It can be said that in studied systems ion AOT⁻ determines whether the selective KNO₃ crystallization from salt mixture KNO₃+NaNO₃ takes place. It is worth to note that Na⁺ cations have no effect on dispersion of the salts obtained. AOT⁻ influence on the morphology and dispersion of powders was not investigated in detail in this work. It might be noted that exchange processes involving AOT⁻ slightly prolong the start of crystallization in comparison with simple micelles. As a result time of water evaporation increases and smaller cores are formed, and nuclei sizes also decrease. However the main factor that determines dispersion and morphology of powders crystallized may be AOT⁻ adsorption.



THERMODYNAMIC PARAMETERS OF ADSORPTION OF AMINO ACIDS ON CALCIUM PHOSPHATES

Chikanova E.S.¹, Golovchenko K.K.¹, Golovanova O.A.¹

¹ F.M. Dostoevsky State University, 55A Prospekt Mira, 644077 Omsk, Russia

E-mail: chikanova_es@mail.ru

Interaction of inorganic and organic substances essential in the processes of physiogenic and pathogenic mineralization in human body. Of particular interest in this area is the study of reactions of free amino acids (AA) and calcium phosphate (PC). Therefore, in a study of the adsorption interaction AA, such as Gly, Ser, Ala, Asp, Glu with dihydrate calcium hydrogen phosphate (DCHP, $S_{sp} = 12 \text{ m}^2/\text{g}$, size $50 \mu\text{m}$, particle charge in aqueous solution - positive) and hydroxyapatite (HA, $S_{sp} = 93 \text{ m}^2/\text{g}$, size $13 \mu\text{m}$, particle charge in aqueous solution - positive and negative) at pH 6.5 and ionic strength of the solution $I = 0.040 \text{ mol/l}$.

It is found that the adsorption isotherm is described the Langmuir model for two calcium phosphates (Table. 1). As can be seen from Table. 1, calculated Gibbs energy values indicate a mechanism of physical adsorption AA as a brushite and hydroxyapatite, because it surfaces charged in an aqueous solution at a selected pH.

Table 1. Parameters of adsorption of AA on calcium phosphates

AA	DCHP		HA	
	Langmuir equation	ΔG (298 K), J/mol	Langmuir equation	ΔG (298 K), J/mol
Gly	$A = 0.597 \cdot \frac{49.95 \cdot C}{1 + 49.95 \cdot C}$	-9689.8	$A = 0.668 \cdot \frac{41.23 \cdot C}{1 + 41.23 \cdot C}$	-9214.5
Glu	$A = 0.371 \cdot \frac{18.01 \cdot C}{1 + 18.01 \cdot C}$	-7162.5	$A = 0.357 \cdot \frac{37.98 \cdot C}{1 + 37.98 \cdot C}$	-9011.1
Asp	$A = 0.291 \cdot \frac{8.06 \cdot C}{1 + 8.06 \cdot C}$	-5170.8	$A = 0.188 \cdot \frac{8.79 \cdot C}{1 + 8.79 \cdot C}$	-5383.9
Ser	$A = 0.197 \cdot \frac{6.55 \cdot C}{1 + 6.55 \cdot C}$	-4654.6	$A = 0.378 \cdot \frac{11.59 \cdot C}{1 + 11.59 \cdot C}$	-6071.5
Ala	$A = 0.226 \cdot \frac{17.25 \cdot C}{1 + 17.25 \cdot C}$	-7055.7	$A = 0.221 \cdot \frac{21.05 \cdot C}{1 + 21.05 \cdot C}$	-7544.2

Adsorption fact corroborated by FTIR spectroscopy and analysis of specific surface area (BET): for DCHP value S_{sp} decreased by 75% and reached $3 \text{ m}^2/\text{g}$ (regardless of the nature of the amino acid), for HA - Gly $52 \text{ m}^2/\text{g}$ ($\downarrow 44 \%$), Ser and Glu $60 \text{ m}^2/\text{g}$ ($\downarrow 35\%$), Ala and Asp $72 \text{ m}^2/\text{g}$ ($\downarrow 22\%$). XRD shows that the phase transition does not occur in these adsorption conditions.

Thus, the number obtained by an increase in the Gibbs free energy: for DCHP - Gly <Glu <Ala <Asp <Ser; for HA - Gly <Glu <Ala <Ser <Asp. In both cases, a large value of the adsorption characteristic of the simplest amino acid - glycine.

The research was supported by RFBR, project mol_a No. 16-33-00684

MOLECULAR THERMODYNAMIC MODELING OF SURFACTANT AGGREGATES OF COMPLEX SHAPE: IONIC CONTRIBUTION TO THE FREE ENERGY

Emelyanova K.A., Victorov A.I

Institute of Chemistry, St. Petersburg State University, 198504 St. Petersburg, Russia

E-mail: noctua94@gmail.com

Aggregates of complex shape are encountered in a variety of systems, including solutions of surfactants, block copolymers and lipids [1-3]. Examples are perforated bilayers and bicontinuous structures, both of great importance in bioengineering and in the design of 'smart' materials. In the classical molecular thermodynamic models, the aggregation free energy of a complex structure is estimated as a sum of the free energies of the aggregate's constituent elements (e.g., for wormlike micelles such elements are the cylindrical portions and spherical endcaps). A perforation in a bilayer has been modeled as a hole with a toroidal rim [4-5]. In a densely perforated bilayer these holes are located close to each other forming an element called a junction. The aggregation free energy of a junction is estimated as a sum of its toroidal and planar parts [4]. For ionic surfactants, the aggregation free energy is controlled by the changes of the electrostatic term. In this work we study the electrostatic contribution by numerical solution of the linearized PB equation using Comsol Multiphysics 4.3b simulation package. We show that the additivity rule for the aggregation free energy is not suitable for large holes: charged planar parts have strong effect on the surface potential inside the hole, fig. 1. For small holes, we propose an analytical approximation for the electrostatic term taking into account the interpenetration of electrical double layers. Small holes give a deep minimum in the aggregation free energy resulting in stabilization of the perforated bilayer structure.

Using accurate analytical approximation for the electrostatic contribution we illustrate the stabilization mechanism and describe the sequence of shape transitions induced by adding salt, changing temperature, tail length and head cross-sectional area of the surfactant. Calculations have been performed for ionic surfactants C_xTAB ($x = 10-16$) in aqueous solution of salt. Current work is directed toward extending the model to mixed surfactant solutions. **Acknowledgement:** we thank the Russian Science Foundation (project # 16-13-10042) for financial support. Calculations have been performed at St.Petersburg State University computational resource center.

- [1] Almgren M. *Soft Matter*, 2010, 6, 1383-1390.
- [2] Danino D. *Current Opinion in Colloid and Interface Science*, 2012, 17, 316-329.
- [3] Bergström M.; Skoglund S. et al. *Langmuir*, 2014, 30, 3928-3938.
- [4] Andreev V.; Victorov A. *Langmuir*, 2006, 22, 8298-8310.
- [5] Emelyanova K.; Gotlib I. et al. *J. Chem. Eng. Data*, 2016, 61, (12), 4013-4022.

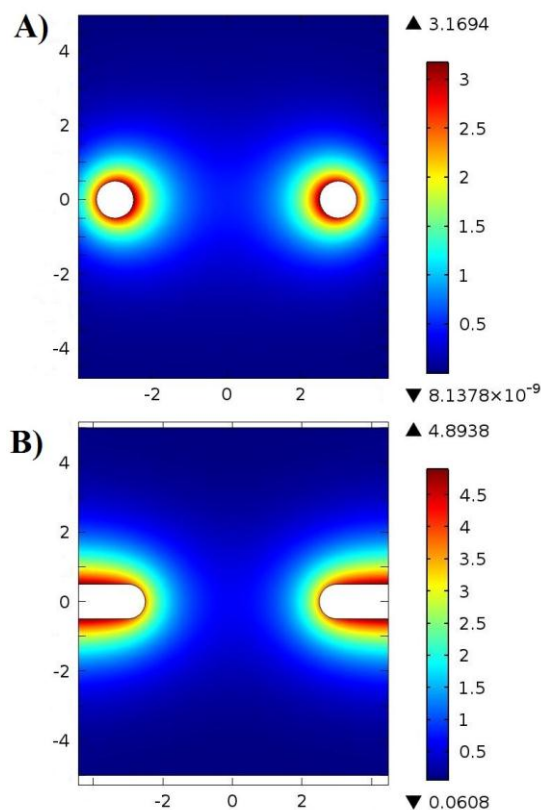


Figure 1. Electrostatic potential in a planar cross-section that contains the symmetry axis of the charged aggregate. White is the aggregate core. A) a charged toroid; B) a hole in a charged planar bilayer. $c/b=6$, $b=0.5\kappa$, $t=5$, where b and c are the minor and the major toroid radii, respectively, κ is the inverse Debye length, t is the reduced charge density.

PHASE TRANSITION- AND CATALYTIC CHEMICAL REACTION-INDUCED THERMAL MANIFESTATIONS IN GAS-SOLID HETEROGENEOUS SYSTEMS MONITORED IN REAL TIME USING FAST INFRARED THERMOGRAPHY

Boris G. Vainer^{1,2}, Semen S. Fast², Pavel A. Pyrjaev³, Boris L. Moroz^{2,3},

¹Rzhanov Institute of Semiconductor Physics, Siberian Branch of the Russian Academy of Sciences, 630090 Novosibirsk, Russia

²Novosibirsk State University, 630090 Novosibirsk, Russia

³Boriskov Institute of Catalysis, Siberian Branch of the Russian Academy of Sciences, 630090 Novosibirsk, Russia

E-mail: BGV@isp.nsc.ru; fast416@gmail.com

Infrared thermography (IRT) is a precise non-contact research instrument aimed at monitoring and qualitative/quantitative characterization of different physical, chemical, biomedical and industrial fast processes. Modern focal plane array (FPA) IR detector-based methods have some incontrovertible advantages over conventional ones for the studies of exo- and endothermal reactions, including those associated with phase transition heat, progressing at heterogeneous gas-solid interfaces. The main advantage here is the IRT-assisted ability to observe continuously the thermal processes development on a whole visible surface at once and to record the thermal characteristics in real time. A modern FPA-based IR camera makes high spatial, time (~ 0.01 s) and temperature (~ 0.01 °C) resolutions available.

In recent papers [1, 2], a series of experiments aimed at proving the IRT to study the adsorption/desorption processes on thin solid films and meshy-structured solid surfaces were successfully conducted. The temperature signal magnitude was dependent on the amount of released/absorbed phase transition heat. At the same time, it is apparent that the thin layers comprised of fine-grained solid particles may facilitate more gas molecules to attack the surface than the flat ones. That is why the research devoted to FPA-based IRT abilities for this case is a prospective issue.

One of the experiments performed in this work is illustrated in Fig. 1. Eight samples of different nature were distributed among 4 Teflon cells and placed into the box covered by the CaF_2 window transparent in the 2.5-3.05 μm IR camera spectral range. A slow flow of the gas mixture consisting of O_2 (20%), N_2 (79%) and CO (1%) was supplied to the camera for 20-60 s under IRT monitoring. A small amount of saturated water vapor at different temperatures was added to the above-mentioned mixture that slightly influenced the initial gas composition. Thermograms were continuously recorded with the frame rate of 100 fps until the thermodynamic equilibrium of the samples with the environment was reached. A typical thermogram presented in Fig. 1 clearly demonstrates the diverse thermal manifestations of different organic and inorganic materials in response to the inflow of the reactive gas mixture.

By analyzing the temperature time dependencies obtained for various solid samples and different reactive gases, a series of pronounced thermodynamic phenomena is revealed. In particular, it was directly verified that the observed thermal manifestations were caused by both physical adsorption/desorption and catalytic chemical reactions (CO oxidation on Au nanoparticles). The conclusion is made that different thermodynamic processes progressing on the surfaces of organic and inorganic solids when they interact with reactive gases may be successfully investigated using the remote-sensing non-contact IRT method.

This work was supported by the Russian Foundation for Basic Research (Grant No. 15-02-07680).

[1] Mel'gunov, M.S.; Ayupov, A.B.; Fenelonov V.B.; Vainer B.G. Adsorption, 2013, 19, 835-840.

[2] Vainer, B.G.; Guzev, A.A.; Mogilnikov, K.P.; Romanov, S.I.; Shvets, V.A. Proc. QIRT-2014 Conf.

Available at QIRT Open Archives: <http://qirt.gel.ulaval.ca/archives/qirt2014/QIRT2014.html>.

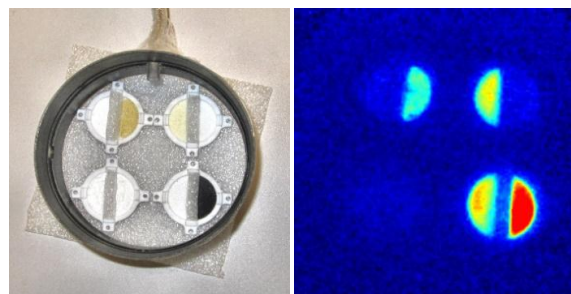


Figure 1. A set of 8 fine-grained solid reagents prepared for the IRT-based investigation of their sorptive and catalytic properties. Left panel: a photo; a round shallow cell in the bottom right corner contains small (0.25-0.5 mm) grains of porous Al_2O_3 (left) and the same grains containing deposited Au nanoparticles (right). Right panel: the thermogram measured during the inflow of the gas mixture (1% CO in synthetic air) into the camera.

ROLE OF THE PHASE TRANSITION AT GaN QDS FORMATION ON (0001)AlN SURFACE BY AMMONIA MOLECULAR BEAM EPITAXY

K.A. Konfederatova, V.G. Mansurov, T.V. Malin, Yu.G. Galitsyn, I.A. Aleksandrov, V.I. Vdovin, K.S. Zhuravlev

A.V.Rzhanov Institute of Semiconductor Physics, Siberian Branch of Russian Academy of Sciences, 630090 Novosibirsk, Russia
E-mail: kseniya.konfederatova@isp.nsc.ru

Group-III nitride semiconductors (GaN, AlN, InN) are important materials for development of modern power and microwave electronics, as well as for optoelectronics in visible and UV ranges. Formation of low-density GaN quantum dots (QDs) in AlGaIn and AlN matrices is the key point for fabrication of single electron transistors, single and entangled photons sources. The GaN QDs formation on the (0001)AlN surface is usually implemented by using the Stranski-Krastanov growth mode, or by the droplet epitaxy technique. Normally, the density of QDs is quite high as 10^{10} cm^{-2} . We have developed a new method for formation of low-density GaN QDs using incongruent decomposition and phase transition of the GaN wetting layer on the (0001)AlN surface.

In the present work for the correct description of the GaN QDs statistical ensemble we have used, so-called, lattice gas model on the surface [1]. In the model single QD is considered as lattice gas cell characterized by certain thermodynamic parameters: temperature, pressure and appropriate chemical potential. There is effective interaction between QDs, that result in the phase transitions of the first or second order. The order parameter in ensemble of QDs is directly connected with density of QDs on surface. Thus the phase transition is the transition from low density of QDs (gas branch of the phase transition isotherm) to high density of QDs (condensed state branch of the phase transition isotherm). From the viewpoint of obtaining low density of QDs it is necessary that the chemical potential of the quantum dot does not exceed the critical value at which the phase transition occurs, or in other words: the system of QDs remained on the gas branch. The QDs formation has been investigated *in situ* by RHEED technique. In process of the QDs formation was accompanied by changing of two dimensional (2D) RHEED pattern from GaN surface to three-dimensional RHEED pattern that confirm the QDs formation (Fig.1). An experimental curve of the QDs formation is shown in Fig.2. Reasonable agreement between calculated phase transition isotherm and experimental curve is achieved. GaN QDs formation have been confirmed by high-resolution transmission electron microscopy and micro-photoluminescence measurements.

The authors gratefully acknowledge the support of this work by RFBR (grants 17-52-04023, 17-52-45108, 17-32-80019, 17-02-00947).

[1] A. Zangwill, Physics at Surfaces, Cambridge University Press 1988, p. 278.

[2] Yu. G. Galitsyn; A. A. Lyamkina; S. P. Moshchenko et al., in: Self-assembly of Nanostructures, edited by S. Belucci, The INFN Lectures, Springer, 2012, 3, chap. 3.

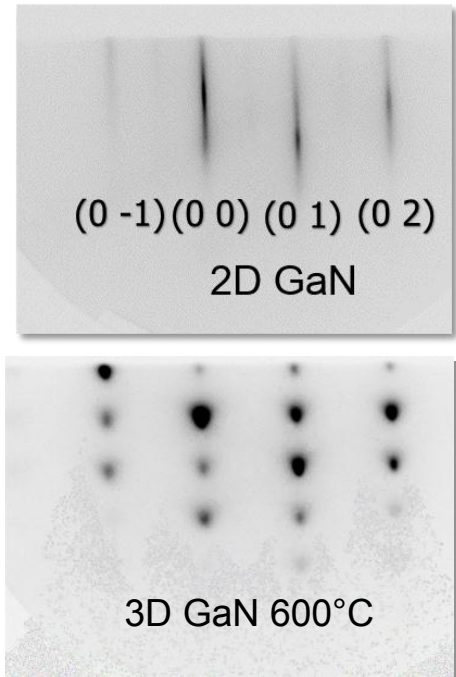


Figure 1. RHEED patterns of 2D GaN surface and 3D GaN QDs.

Figure 1. RHEED patterns of 2D GaN surface and 3D GaN QDs.

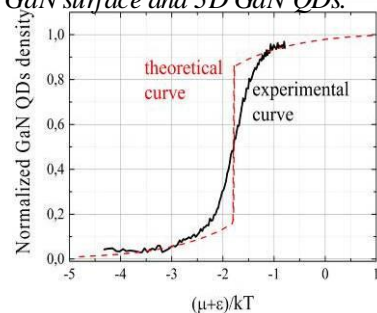


Figure 2. RHEED pattern from 2D GaN surface and from QDs.

MOLECULAR DYNAMICS SIMULATIONS OF REVERSE MICROEMULSIONS STABILIZED BY NONIONIC SURFACTANTS

Kopanichuk I. V. *, Sizov V. V., Vedenchuk E. A., Vanin A. A.

St. Petersburg State University, St. Petersburg, Russia

E-mail: kopan239@gmail.com

Water-in-Oil (W/O) microemulsions are stable dispersions of water in continuous oil phase. The microemulsions containing surfactant mixtures are of special interest because they can be more effective for the special tasks than the individual surfactants. Reverse micelles (RMs) are most common studied structural units of microemulsions. It is important to know the shape and the inner structure of the RM in details due to its applications in drug delivery, enzymatic catalysis, organic and bio-organic reactions, and synthesis of nanoparticles. However, the parameters of the RM depend on the water-to-surfactants ratio, the water solubilization capacity, and the ratio between the surfactants. Properties of the RM are individual for the system. [1]

In this work the reverse micelles stabilized by the mixture of nonionic surfactants were considered. The shape and the atomic structure of the RMs were described. The effect of variations of ratio between the surfactants on the properties of the RM was also studied. The multi-component system of Tween 80, Span 80, water, and *n*-decane was investigated using molecular dynamics simulations for the NVT-ensemble ($T = 298.15$ K) in a cubic box. All calculations were performed using GROMACS. United-atom GROMOS96 force field was used for the surfactants and oil, except atomic partial charges which were derived from the CHELPG technique. [2] SPC model was used for water. All simulations started from different random configurations to allow RMs to be self-assembled.

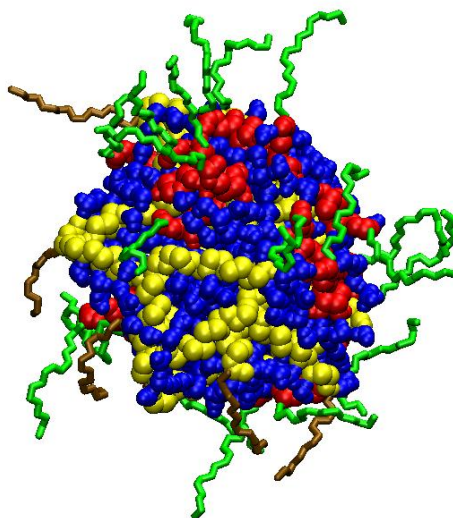


Fig. 1. The reverse micelle in *n*-decane stabilized by Tween 80 (brown tail, yellow heads) and Span 80 (green tail, red head) at the weight ratio 1:1.

Acknowledgement

This work was supported by the grant of RSCF № 16-13-10042.

References

- [1] A.S. Koneva, E.A. Safonova, P.S. Kondrakhina, M.A. Vovk, A.A. Lezov, Yu. S. Chernyshev, N.A. Smirnova, *Colloids and Surfaces A: Physicochem. Eng. Aspects*, 2017, 518, 273–282.
- [2] A. Ritwiset, S. Kongsuk, J. Johns, *J. Mol. Liq.*, 2014, 195, 157-164.



CHEMICAL THERMODYNAMICS OF THE POINT DEFECTS ADSORPTION AT THE INTERFACE OF ADJOINED MATERIALS: MAIN RELATIONS AND SOME MODELING RESULTS

Makhviladze T. M., Sarychev M. E.

Institute of Physics and Technology, Russian Academy of Sciences, 117218 Moscow, Russia

E_mail: tarielmakh@mail.ru

The development of the adequate model of point defects adsorption from the volumes of adjoined material layers at the interface between them is one of the most urgent problems [1-3]. The progress in this field is necessary for understanding and calculating the electrical and strength properties of the multilayer thin-film structures. Adhesion forces play a decisive role in the strength characteristics of layered solid-state structures and the adhesive strength has a profound effect on the reliability and lifetime of nano- and microelectronics elements.

A general thermodynamic approach to describe the adhesion properties of interfaces and especially to obtain and study their strength characteristics such as interfacial surface tension and separation work of material layers forming the interface is proposed and developed. The theory allows us to investigate these strength characteristics as functions of microscopic parameters and defectiveness of adjoined materials as well as of microstructural interfacial parameters and temperature. This analysis is based on the complete system of kinetic equations describing the adsorption processes in interfacial layered structures, initially discussed in the works [1-3], and on the use of the Gibbs-Duhem equations. The theory has been applied to the cases when lattice defects are vacancies, vacancy clusters, and impurity atoms (both substitutional and interstitial ones). For all types of defects, we have obtained and analyzed the dependences of the interfacial surface tension and separation work on the defect concentrations.

The effects of interface strengthening or strength loss as well as the effect of adhesive incompatibility of layers are predicted for various types of defects, and the range of parameters and defect concentrations where these effects could be realized and be of practical significance are found. In addition, a microscopic approach to obtain the surface tension coefficients of both free surfaces and interfaces of crystalline solids is developed, taking into account crystalline solids orientation relative to the material crystallographic axes. The dependence of the adhesion strength on microscopic parameters of the materials is studied.

It should be particularly emphasized that the model developed takes into account the following important extension. Usually it is thought that the defects of the adjoined layers are distributed in the interface independently of one another. Now the more realistic model is developed as it includes the cross correlation mechanism of the relative positions of the defects from different layers in the interface. In other words the mechanism of influence of the one of the adjoined material layers on the adsorption rate of the other layer defects is considered. This effect takes place if the defects are considered to be able with certain probability to jump from one interfacial sublattice in free sites in the second one. It is shown that the effect can lead to phenomena of great practical importance for many applications of multilayered coatings and structures.

The numerical modeling of the dependence of the interfacial separation work on concentrations of atomic impurities being contained in adjoined solid material layers at different temperatures and over a wide range of parameters has been performed. The obtained results show that the interface strengthening or strength loss effects may take place over a certain range of parameters. Moreover the multilayer interface may fall into the thermodynamically unstable state, for that the spontaneous separation is more preferable. It means that under specific conditions the layers are devoid of adhesive compatibility. These effects can be applied in practice to control the adhesion properties of multilayer systems.

[1] Goldstein, R.V.; Makhviladze, T.M.; Sarychev, M.E. Proc. SPIE, 2010, 7521, 7521B (12).

[2] Goldstein, R.V.; Makhviladze, T.M.; Sarychev, M.E. J. Surf. Invest., 2011, 5, 4. 712-717.

[3] Alekseev, I. M.; Makhviladze, T. M.; Minushev, A. Kh.; Sarychev, M. E. Russ. Microelectronics, 2011, 40, 5, 302-308.

UNUSUAL KINETICS OF SiN LAYER FORMATION ON THE Si(111) SURFACE BY AMMONIA MOLECULAR BEAM EPITAXY

Mansurov V.G., Galitsyn Yu.G., Malin T.V., Zhuravlev K.S.

Rzhanov Institute of Semiconductor Physics, Siberian Branch of the Russian Academy of Sciences, 630090 Novosibirsk, Russia

E-mail: mansurov@isp.nsc.ru

Silicon nitride (Si_3N_4) films widely used for microelectronic applications and as passivation layer due to their unique properties, including the high resistivity (10^{16} Ohm cm) and the electrical breakdown limit (10 MV/cm) which is higher than that of most other dielectric. Experiments were carried out in a Riber CBE-32 machine. Si(111) substrates were chemically pretreated to remove native oxide and protect surface before loading into growth system. The atomically clean and smooth Si(111) surface with the well-ordered (7×7) reconstruction was prepared by annealing at 1200°C under ultrahigh vacuum conditions. The sample surface was exposed to the ammonia flux of 10 sccm at different temperatures (750 - 1150°C). Reflection High Energy Electron Diffraction (RHEED) was used for *in situ* studying of the nitridation process. The entire RHEED pattern during the ammonia treatment of the samples was monitored by a CCD-based system. The intensity evolution of RHEED spots from Si and silicon nitride was measured and analyzed.

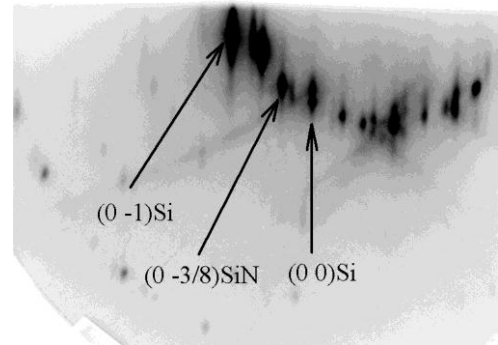


Figure 1. RHEED pattern of (8×8) structure.

Two different stages of the silicon nitridation were distinguished using RHEED during each experimental run: namely, the fast stage of an (8×8) phase formation and the following slow process of amorphous Si_3N_4 phase appearance while the growth parameters (ammonia flux and substrate temperature) were kept constant. The ordered (8×8) structure (Figure 1) appears within a few seconds under ammonia flux for the all used temperatures. The amorphous phase formation was accompanied by the total disappearance of diffraction spots in the RHEED pattern within several minutes.

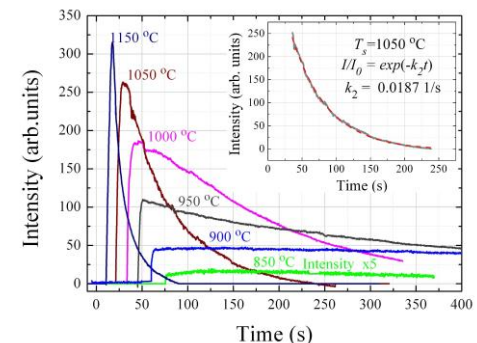


Figure 2. Fractional ($0\ 3/8$) spot intensity evolution at different temperatures.

Behavior of intensity of the fractional ($0\ 3/8$) diffraction spot as a function of time (i.e. kinetic curves) at different substrate temperatures is shown in Figure 2. It clearly demonstrates the fast rise of the fractional ($0\ 3/8$) spot intensity (corresponding to the SiN -(8×8) phase formation) and its further decay.

The rates of the SiN -(8×8) phase formation and amorphous Si_3N_4 formation were estimated by procedure where the experimental curves was fitted by exponential functions. It is found that the nitridation rate at the initial stage decreases from 0.165 to $0.035\ \text{s}^{-1}$, as the temperature increases from 900 to 1150°C . This unusual dependence does not correspond to a normal chemical thermally activated process and chemical reactions do not limit the process of the SiN -(8×8) phase formation. Such unusual temperature dependence for the formation rate is a characteristic feature for the surface order-disorder phase transitions in lattice gases with effective lateral attractive interactions. The second stage corresponds to a normal chemical process, i.e. increasing of temperature increases the reaction rate.

To describe the experimental results we have developed a kinetic model of chemical processes and performed numerical calculations of the two-step Si(111) nitridation process. The first step consists in fast reaction between Si-adatoms available on the surface and chemisorbed ammonia forming SiN cells. Phase transition in lattice gas of SiN cells results in the (8×8) phase formation. The second step is a slow reaction involving Si atoms incorporated into lattice of substrate and ammonia forming amorphous Si_3N_4 . Good agreement between calculated and experimental kinetics curves is achieved.

This work was supported by RFBR (grants 17-52-45108, 17-02-00947).

MOLECULAR DYNAMICS AND THERMODYNAMIC SIMULATIONS OF SEGREGATION PHENOMENA IN BINARY METAL NANOPARTICLES

Bembel A.G., Samsonov V.M., Kartoshkin A.Yu.

Tver State University, 170002 Tver, Russia

E-mail: samsonoff@inbox.ru

Usually both free metal nanoparticles and nanosized units of nanostructured metal materials do not adequately correspond to their one-component models. In other words, one or several additional components usually present as some impurities or specially inserted dopants improving properties of nanosized units or nanostructured materials. In particular, nanostructured polycrystalline metals are meant. For example, according to [1], Cu dopants to nanostructured Ni, make it possible to stabilize its polycrystalline nanostructure thanks to segregation of Cu to the grain boundaries. To predict the grain boundary segregation, in [1] an approach was proposed based on an equation proposed by Butler in 30-th. It is worth to mention that Butler's approach was criticized by A.I. Rusanov [2], and his objections seem to be quite reasonable. However, G. Kaptay proposed in [1] new derivation and justification of this equation.

In [2] evaluations were performed of Cu grain boundary segregation in Ni-Cu polycrystalline metals under an assumption that grains are not smaller than 100nm in size that allows to consider their cores as infinite reservoirs of the segregating component. We have extended the approach [1] to free binary nanoparticles of arbitrary size. In Fig. 1 our molecular dynamics (MD) results for Ni-Cu particles consisting of 2000 atoms are compared to the results of thermodynamic simulation. One can see that when the infinite nature of the segregating component source is not assumed, they well agree with our MD results. Moreover, Butler's equation reasonably predicts segregation in other binary metal particles as well.

This work was performed at Tver State University and was supported by Russian Foundation for Basic Research (No 16-33-60171) and by the Ministry of Education and Science of the Russian Federation (state assignment in the field of scientific activity).

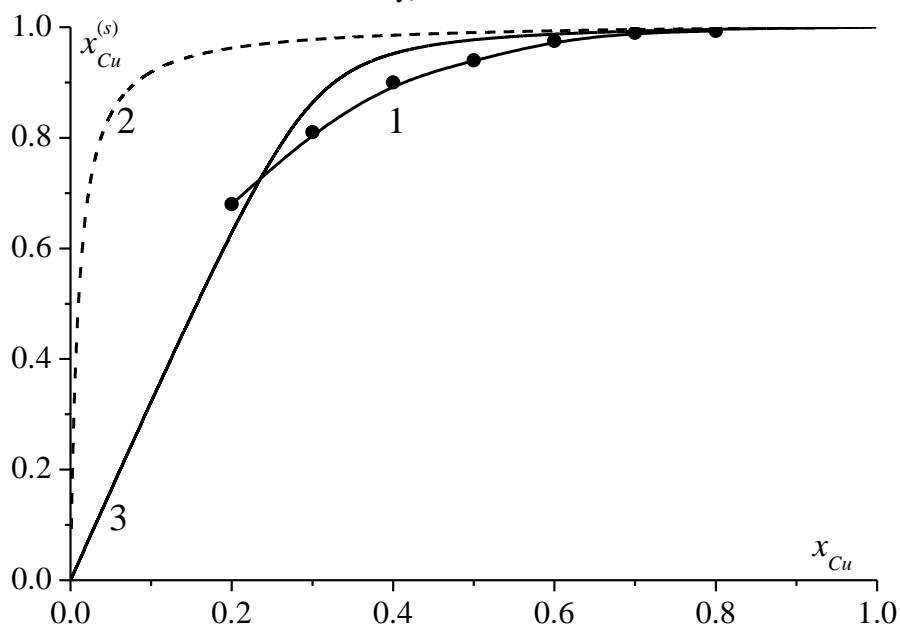


Figure 1. Dependencies of the Cu atomic fraction $x_{Cu}^{(s)}$ in the particle surface layer of binary Ni-Cu nanoparticles, consisting of 2000 atoms, on the Cu fraction x_{Cu} in the initial configuration with the uniform distribution of components: (1) MD; (2) thermodynamic simulation under an assumption that the particle core is an infinite reservoir of the segregating component; (3) thermodynamic results taken into account finite nature of the source of Cu atoms.

[1] Kaptay, G. J. Mater. Sci., 2016, 51, 1738-1755.

[2] Rusanov, A I. Colloid J., 2007, 69, 131-143.

ROLE OF SURFACE ENERGY IN DEHYDRATION OF MAGNESIUM AND CALCIUM HYDROXIDES

Shkatulov A. I.¹, Aristov Yu. I.²

¹Boriskov Institute of Catalysis, Siberian Branch of the Russian Academy of Sciences, 630090 Novosibirsk, Russia

E-mail: shkatulov@catalysis.ru

Magnesium and calcium hydroxides are materials with multiple applications. The hydroxides and corresponding oxides may be used as catalysts and sorbents as well as heat storage media in thermochemical systems. Thermal decomposition (dehydration) of these hydroxides yields high-dispersed oxides and was studied in numerous works with little attention paid to the role of surface state of the dehydration products on the dehydration temperature T_d . This temperature calculated at $P(\text{H}_2\text{O}) = 1$ bar from the thermodynamic data of bulk MgO and $\text{Mg}(\text{OH})_2$ is 536 K. However, in order for the $\text{Mg}(\text{OH})_2$ dehydration to start even *in vacuo* one has to supply heat at $T > 573$ K. Similar effect was found for $\text{Ca}(\text{OH})_2/\text{CaO}$.

Recently, it was found that the dehydration temperature of $\text{Mg}(\text{OH})_2$ may be controllably reduced by its modification with sodium nitrate [1]. The nitrate additives to the hydroxides dramatically decrease the surface area of the product (oxide). The specific surface area of the calcines is in a good correlation with the dehydration peak temperature (Figure 1a) determined by Differential Scanning Calorimetry (DSC).

In this work, a model linking the surface state of dehydration product to the hydroxides dehydration temperature is analyzed. It explains the mentioned “overheating” and the nitrate effect by the contribution of the oxide surface energy to the free Gibbs energy of the decomposition reaction. For the bulk phases, the equilibrium is determined by equality of the Gibbs formation energy of the reagents and products (point A on Figure 1b). If one accounts for contribution of the surface energy $\Delta_s G^\circ$, the equilibrium shifts towards higher temperature (point B), if $\Delta_s G^\circ(\text{product}) > \Delta_s G^\circ(\text{reagent})$.

Using literature data on the surface energy [2], the dehydration temperature for $\text{LiNO}_3/\text{Mg}(\text{OH})_2$, $\text{NaNO}_3/\text{Mg}(\text{OH})_2$ as well as for $\text{KNO}_3/\text{Ca}(\text{OH})_2$ was calculated. Its values were in good agreement with those obtained by our DSC tests.

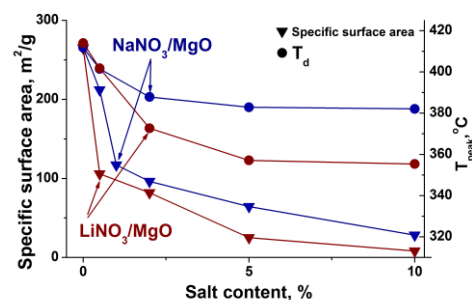
The hydroxide modification with salts may be a powerful tool of varying the oxide texture and its surface energy as well as the hydroxides’ decomposition temperature.

To summarize, the surface energy of the initial reagent and, especially, the product can strongly affect the dehydration temperature of magnesium and calcium hydroxides. The salt additives reduce the specific surface area of appropriate oxides, thus depressing the T_d -value. This opens an exciting opportunity to manage the hydroxide decomposition process.

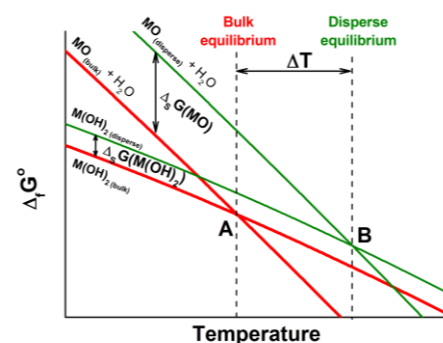
Acknowledgement One of the authors thanks RFBR grant mol_a 16-38-00503 for financial support.

[1] Shkatulov, A; Krieger, T; Zaikovskii, V; Chesalov, Y.; Aristov, Yu. ACS Appl. Mater. Inter., 2014, 6(22), 19966-19977.

[2] Hayun, S; Tien, T; Ushakov S.; Thron A.; Klaus B; Navrotsky A; Castro R. J. Phys. Chem. C., 2011, 115, 23929-23935.



a



b

Figure 1. Dehydration peak temperature of the hydroxides and specific surface areas of their calcines (a), and illustration of the surface energy effect on the dehydration temperature (b).

MOF-801 AS A PROMISING MATERIAL FOR ADSORPTIVE COOLING: WATER ADSORPTION EQUILIBRIUM

Solovyeva M.V.^{1,2}, Gordeeva L.G.^{1,2}, Aristov, Yu.I.^{1,2}

¹Boreskov Institute of Catalysis, Ac. Lavrentiev av. 5, Novosibirsk, 630090, Russia

²Novosibirsk State University, Pirogova str. 2, Novosibirsk 630090, Russia

E-mail: mvl.solovyeva@gmail.ru

Metal – Organic Frameworks (MOFs) are a novel family of supra-molecular porous compounds in which the metal-oxygen units are bonded through organic linkers. Due to the high porosity and the extensive surface containing both the hydrophilic and hydrophobic functional groups, a number MOFs possess unique adsorption properties and are of great interest for adsorption technologies. One of the most promising applications of the MOFs is the Adsorption Heat Transformation (AHT) that is an emerging technology for heat/cold production [1]. Due to their high energy saving potential and using the environmentally benign working fluids, AHT is considered as a promising alternative to common vapor compression. Several MOFs with water as working fluid demonstrate enhanced adsorption capacity and higher thermodynamic efficiency in comparison with common adsorbents suggested for AHT. In particular, adsorption of typical working fluids (water, methanol) used for AHT on these MOFs is characterized by step-wise isotherms, which were shown to be beneficial for AHT from the thermodynamic point of view [2].

This work addresses the study of water adsorption on MOF-801, which is expected to be one of the most promising for AHT, particularly for cooling cycles. MOF-801 is microcrystalline porous compound whose structure belongs to the cubic space group and consists of basic units of $Zr_6O_4(OH)_4(\text{fumarate})_6$ [3]. MOF-801 was synthesized by solvothermal method described in [3]. The MOF-801 porous texture was studied by low temperature nitrogen adsorption. Water vapor adsorption equilibrium was explored by thermogravimetric method at temperature range of 20 to 100 °C and water pressure range of 0.9 to 4.3 kPa. The mechanism of water adsorption on MOF-801 was studied by powder XRD-in situ and FT-IR spectroscopy. The hydrothermal stability of the material was analyzed under typical conditions of adsorption chillers.

Water adsorption isobars, presented as function of relative pressure P/P_0 , are S-shaped curves (Fig. 1) showing the abrupt water uptake in the P/P_0 range of 0.1 to 0.2. It has been shown previously, that step-wise adsorption isobars are the most beneficial for AHT because they a) allow the adsorbent regeneration at the lowest theoretically possible temperature T_{reg} ; and b) ensure the smallest entropy generation and, hence, the highest efficiency of the cycle that can approach the Carnot efficiency [2]. For real adsorbents, more realistic are S-shaped adsorption isobars with large uptake variation under conditions of the specific AHT cycle. Based on the data obtained, the amount of water cycled under conditions of a typical refrigeration cycle utilizing MOF-801 was estimated as 0.19 g/g that exceeds the appropriate value for other adsorbents suggested for AHT (Fig. 2). The isosteric heat Q_{ads} of water adsorption at the water uptake $w = 0.03 - 0.40$ g/g is 55–60 kJ/mol. Thus the data obtained illustrate a high potential of MOF-801 as water adsorbent for AHT cycles.

This work was supported by the Russian Foundation for Basic Researches (project № 16-03-00089).

[1] Meunier, F., Appl. Therm. Eng., 2013, 61, 830-836.

[2] Aristov, Yu.I. Int. J. Refrig., 2009, 32, 675-686.

[3] Furukawa, H; Gándara, F; Zhang, Y.-B. et al. J. Am. Chem. Soc., 2014, 136, 4369 – 4381.

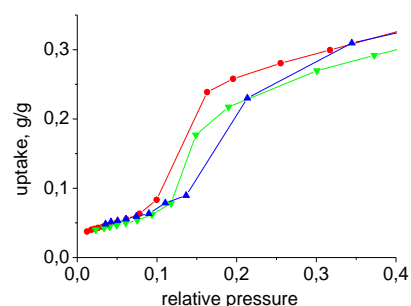


Figure 1. Isobars of water adsorption on MOF-801.

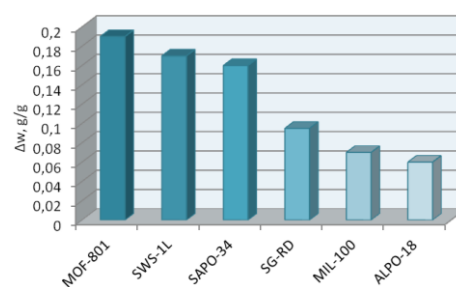
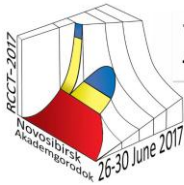


Figure 2. The amount of water exchanged in the typical chilling cycle ($T_{\text{ev}} = 278$ K, $T_{\text{ads}} = 303$ K, $T_{\text{des}} = 358$ K).



THERMODYNAMICS OF NUCLEATION ON A PARTIALLY WETTABLE SUBSTRATE: MACROSCOPIC PHENOMENOLOGY WITH LINE TENSION VS INTERFACE DISPLACEMENT MODEL

Tatyanenko D.V., Shchekin A.K.

St. Petersburg State University, 7/9 Universitetskaya nab., St. Petersburg, 199034 Russia

E-mail: d.tatyanenko@spbu.ru

We consider thermodynamics of nucleation of sessile liquid droplets from a one-component supersaturated vapor on a flat partially wettable solid substrate. In order to find shape and work of formation of critical droplet at a given chemical potential, we employ an interface displacement model [1,2] using a description of the grand thermodynamic potential of the system as a functional of the interface displacement (i.e. local film thickness) profile $l(\mathbf{x})$:

$$\Omega^{(ID)} [l(\mathbf{x})] = \int d\mathbf{x} \left[-n^\alpha \Delta\mu l(\mathbf{x}) + \sigma_0^{\alpha\gamma} + \sigma_0^{\alpha\beta} \sqrt{1 + (\nabla l(\mathbf{x}))^2} + U(l(\mathbf{x})) \right] \quad (1)$$

with n^α the number density of molecules in the liquid phase, $\Delta\mu$ the vapor/condensate chemical potential (per molecule) shift from its value at the binodal, $\sigma_0^{\alpha\gamma}$ and $\sigma_0^{\alpha\beta}$ the constant solid–liquid and liquid–vapor thermodynamic surface tensions. The interface potential $U(h) = \int_h^\infty \Pi(\tilde{h}) d\tilde{h}$ related to the disjoining pressure isotherm $\Pi(h)$ describes a specific thin-film contribution due to the thickness-dependent work of wetting. For interface potentials typical for partial wetting, two stationary profiles for the functional (1) have been found: a metastable precursor wetting film of a constant thickness f : $\Pi(f) = -n^\alpha \Delta\mu$ and a hump-shaped sessile critical droplet on top of the above-mentioned film. At $\Delta\mu \rightarrow +0$, the main part of the sessile droplet profile becomes almost spherical-segment-shaped.

The latter spherical-segment shape is rendered in another popular description of sessile droplets that we refer to as the macroscopic phenomenology: the curvature radius of the sessile droplet is given by the Laplace equation, and the contact angle θ is given by the modified Young equation

$$\sigma_0^{\alpha\beta} \cos \theta = \sigma_0^{\beta\gamma} - \sigma_0^{\alpha\gamma} - \kappa_0 / r, \quad (2)$$

an approximate form of the exact generalized Young equation [3]

$$\sigma^{\alpha\beta} \cos \theta = \sigma^{\beta\gamma} - \sigma^{\alpha\gamma} - \kappa / r - \partial\kappa / \partial r. \quad (3)$$

Here κ is the thermodynamic three-phase-line tension, the specific line excess of the grand thermodynamic potential. Approximate equation (2) uses the constant (size and chemical potential independent) values of all the tensions σ and κ corresponding to their values at the binodal (marked with “0” subscript). Such a simplified description is still often used to describe nucleation on partially wettable substrates [4] and demonstrates peculiar effects (especially at $\kappa_0 < 0$) contributed to the line tension [5].

In our work, we analyze the dependences of the condensate chemical potential and the activation barrier to nucleation as functions of the number of molecules in the critical droplet within the interface displacement model (1) for a model interface potential. Calculating the line tension κ_0 of a straight contact line [2] for our model system, we compare the results with the ones within the approximate macroscopic phenomenology with line tension based on use of Eq. (2). We found both qualitative and quantitative differences between the results of the “exact” model and “approximate” macroscopic phenomenological descriptions. Comparing Eqs. (2) and (3), we can attribute them to the effects of *size-dependent* line tension κ and the adsorption of the vapor on the solid substrate forming the precursor wetting film, that makes $\sigma^{\beta\gamma}$ depending on the chemical potential (vapor supersaturation).

This work was supported by the Russian Foundation for Basic Research, grant 16-03-01140-a.

[1] de Gennes, P.G. Rev. Mod. Phys., 1985, 57, 827–863.

[2] Dobbs, H.T., Indekeu, J.O., Physica A, 1993, 201, 457–481.

[3] Rusanov, A.I., Shchekin, A.K., Tatyanenko, D.V., Colloids Surf. A, 2004, 250, 263–268.

[4] Singha, S.K., Dasa, P.K., Maiti, B., J. Chem. Phys., 2015, 142, 104706.

[5] Navascués, G., Tarazona, P., J. Chem. Phys., 1981, 75, 2441–2446.

SURFACE FREE ENERGY AND SOME OTHER PROPERTIES OF A CRYSTAL-GAS INTERFACE

Bidakov V.G., Tipeev A.O., Protsenko K.R.

Institute of Thermal Physics, Ural Branch of the Russian Academy of Sciences, 620016 Yekaterinburg, Russia

E-mail: baidakov@itp.uran.ru

The surface of a solid is responsible for the progress of many practically important processes, such as adsorption, catalysis, flotation, etc. For their description it is necessary to know the surface free energy of a solid σ , which cannot be directly measured in an experiment. In this connection, computer simulation of a crystal-gas interface becomes topical.

The present paper gives the results of a molecular dynamics study of the properties and the structure of a plane crystal-gas interface in a system of Lennard-Jones particles. The system under investigation contained $N = 108\ 000$, $64\ 000$ and $54\ 000$ particles depending on the orientation of the (100), (110) and (111) planes of an FCC crystal. The surface free energy was determined by the method of thermodynamic integration from the values of the surface energy \bar{u} and the surface tension γ calculated in molecular dynamics experiments. Integration was carried out from a temperature $T = 0$. The surface entropy \bar{s} at $T = 0$ was obtained in the harmonic approximation of the classical dynamical theory of a crystal lattice. Calculations were made to the triple-point temperature $T_t = 0.692$ (in units of ε/k_B , where ε is a parameter of the Lennard-Jones potential and k_B is the Boltzmann constant) for three crystallographic orientations. The surface tension was calculated by the Bakker formula through the components of the Kirkwood-Buff pressure tensor, the surface energy through the internal energy of a two-phase system and the energy of bulk phases. In the range from $T = 0$ to $0.7T_t$, the surface energy, entropy and tension depend only slightly on the temperature. Anisotropy shows up most markedly on the surface tension. At the face (111), as distinct from the faces (100) and (110), the value of γ is negative. At the approach to the triple-point temperature the values of \bar{u} , γ and \bar{s} increase. This is connected with the phenomenon of premelting – at the crystal surface forms a liquid layer, whose thickness increases with increasing temperature.

The results of calculation of the surface free energy are presented in Fig. 1. As distinct from \bar{u} , γ and \bar{s} , the value of σ is a decreasing function of the temperature. The anisotropy of σ does not exceed 11 %.

At $T = 0$ we have: $\sigma(100) = 3.20$, $\sigma(110) = 3.36$, $\sigma(111) = 3.03$ (in units of ε/d^2 , where d is a parameter of the Lennard-Jones potential). When $T = 0.8T_t$, the value of σ averaged over the orientations is 2.45. The surface free energy at a liquid-gas interface $\sigma_{LV} = 1.44$ [1], and at a crystal-liquid interface $\sigma_{SL} = 0.37$ [2]. Thus, $\sigma_{SL} + \sigma_{LV} < \sigma$, and all the required and sufficient conditions for premelting are observed.

The work has been performed with a financial support of the Russian Science Foundation (project No. 14-19-00567).

[1] Bidakov, V.G.; Protsenko, S.P.; Kozlova Z.R.; Chernykh G.G. *J.Chem.Phys.*, 2007, 126, 214505(9).

[2] Bidakov, V.G.; Protsenko, S.P.; Tipeev A.O. *JETP Letters*, 2013, 98(12), 801-804.

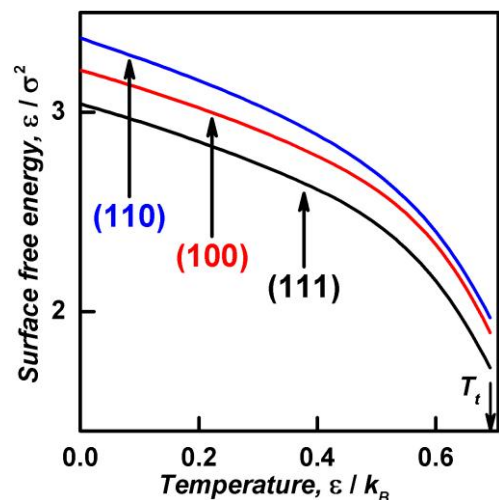


Figure 1. Temperature dependence of surface free energy.

NON-ZEOLITIC PROPERTIES OF THE DIPEPTIDE *L*-LEUCYL-*L*-LEUCINE AS A RESULT OF THE SPECIFIC NANOSTRUCTURES FORMATION

Ziganshin M.A.¹, Safiullina A.S.¹, Ziganshina S.A.², Gerasimov A.V.¹, Gorbachuk V.V.¹

¹ Butlerov Institute of Chemistry, Kazan Federal University, Kazan, 420008 Russia

² Zavoisky Physical-Technical Institute, Kazan Scientific Center, Russian Academy of Sciences, Kazan, 420029 Russia

E-mail: Marat.Ziganshin@kpfu.ru

Short-chain oligopeptides which are capable to self-organize in solutions and in solid phase are attractive building blocks for the design of new nanostructured materials with complex, hierarchical architectures. Such materials can have specific properties, such as piezoelectric activity, specific electrochemical behavior, high optical nonlinearity and nanoscale wettability, as well as magnetic susceptibility and luminescence. Some short-chain oligopeptides can form porous crystals with hydrophobic or hydrophilic layers or channels. As a result, such crystals exhibit zeolite-like properties, and can selectively bind some gases or separate mixtures of gases.

The present work is the first reported comprehensive study of the sorption properties of *L*-leucyl-*L*-leucine toward a wide range of organic compounds. Different experimental methods are used to investigate and explain the specific sorption properties of the dipeptide. The sorption of organic vapors or water by a dipeptide layer was studied on a quartz crystal microbalance. The thermal stabilities of the products of the interaction of *L*-leucyl-*L*-leucine with vapors were studied using thermogravimetric analysis with simultaneous differential scanning calorimetry, and mass-spectrometry detection of the evolved vapors. The self-organization of the dipeptide in solutions, and effect of vapors on the surface morphologies of thin dipeptide films were observed by atomic force microscopy. Changes in the crystal packing of *L*-leucyl-*L*-leucine were characterized by X-ray powder diffraction.

The non-zeolitic behavior of *L*-leucyl-*L*-leucine and its self-organization in solid phase and from solutions with formation of different nanostructures are reported. The unusual sorption properties of *L*-leucyl-*L*-leucine were observed as an increase in the sorption volume of the dipeptide phase with increasing sorbate molecular size, Figure 1. The specific sorption properties of *L*-leucyl-*L*-leucine result

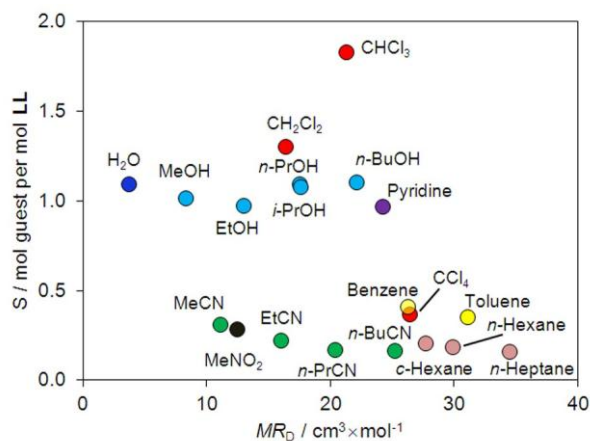
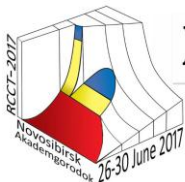


Figure 1. Correlation of the sorbate (guest) content S in *L*-leucyl-*L*-leucine with guest molar refraction MR_D .

from change in its crystal packing from channel-type to layered-type, when binding strong proton acceptors or proton donors of molecular size are greater than 18-20 cm³/mol. The high sorption capacity of *L*-leucyl-*L*-leucine toward dichloromethane results from the self-organization of the dipeptide, by forming nanofiber or web-like structures. The low thermal stability of clathrates of the dipeptide containing large guest molecules and

the selectivity of *L*-leucyl-*L*-leucine toward alcohols over nitriles can be used to separate organic mixtures, for example, methanol/*n*-butanol and methanol/acetonitrile.

Acknowledgement. This study was by grant №14.Y26.31.0019 from Ministry of Education and Science of Russian Federation.



Section 4.

Thermodynamics of surface phenomena and self-organization phenomena in fluid systems

Poster presentations



RESEARCH OF NUCLEATION OF HYDRATE FORMATION IN THE TWO-LAYER WATER-DECANE SYSTEM

Adamova¹ T., Manakov¹ A.

¹*Nikolaev Institute of Inorganic Chemistry, Siberian Branch of the Russian Academy of Sciences, 630090 Novosibirsk, Russia*

E-mail: adamova@niic.nsc.ru

Gas hydrates are formed when the gas molecules (guest molecules) include into hydrogen-bonded water molecules (host framework) without formation of chemical bonds between molecules of guests and host. Studies of clathrate hydrates allows to use these inclusion compounds as unique molecular containers of natural gas (mostly methane) for practical application.

The aim of the work is investigation of nucleation mechanism on contact surface of pure water-methane and two-layer system of water-decane and methane. The study was conducted the contact surface area r and $3,5r$. Water and decane were additionally purified from impurity particles by filtration twice ($0.2 \mu\text{m}$). Nucleation of methane hydrate have been studied with the use of isothermal method at -5°C and 12 MPa. It was shown that the nucleation rates tend to increase in the two-layer system of water-decane.

THERMAL PROPERTIES OF THE POLYMETHYLMETHACRYLATE FILMS FILLED WITH FULLERENE

Alekseeva O.V., Noskov A.V., Guseynov S.S.

G.A. Krestov Institute of Solution Chemistry, Russian Academy of Sciences

Akademicheskaya str., 1; Ivanovo, 153045, Russia

E-mail: ova@isc-ras.ru

In recent years, fullerene-containing composites are becoming more interesting for several research areas, such as polymer materials science, as well due to the perspective using of these materials in electronics, optics, medicine, and pharmaceuticals. Insertion of these fillers results to modify the original polymer matrix, which can lead to the creation of materials with improved physicochemical properties. Polymethylmethacrylate (PMMA) is well-known film-forming polymer often used for different modifications with low molecular compounds of special properties, including fullerenes. In the current study, the samples of the PMMA/fullerene composite films were fabricated. Also an effect of the filler content on the glass transition temperature of composite and its thermal degradation parameters was researched.

To production of the film composites, polymethylmethacrylate ("Aldrich", US; $M=1.2 \cdot 10^5$) and fullerenes C_{60} ("NeoTechProduct", Russia) were used. A solvent casting of perspective components from solutions was employed for preparing the mixtures of C_{60} with polymer. PMMA/fullerene composite films were produced as follows. Fullerene batches were dissolved in toluene in the required concentrations. Then PMMA batches were dissolved in all obtained solutions, and the mixed solutions were stirred for about 1 day before being cast into thin films. After casting the solvent was slowly evaporated over several days to produce the composite films.

Thermal behavior of the PMMA/ C_{60} composites was studied by the DSC and TG techniques. It was found the DSC curve mode to be depended on the composite composition. For films containing up to 0.1 wt. % of C_{60} , one glass transition temperature (T_g^{soft}) is observed, whereas in the case of films with a higher concentration of the filler, two glass transition temperatures (T_g^{soft} and T_g^{solid}) are observed (**Figure 1**). The dependence of the T_g^{soft} value on the fullerene content is non-monotonic with a minimum at 0.5 wt. % of C_{60} .

The thermograms of pure PMMA and PMMA/ C_{60} composite have presented that these film materials decomposed in three stages. The first stage of PMMA decomposition (from 140 °C to 190 °C) is due to the loss of solvent. The second stage decomposition of polymer begins at about 260 C. It is due to depolymerization initiated at unsaturated chain ends. In the third stage, peak of DTG is situated about 360 C and the weight loss is associated with random scission of the backbone chains. The thermograms of PMMA/ C_{60} composites have clearly indicated that the second and third stages of decomposition of the composite were shift to higher temperature as compared to pure PMMA. It means that the incorporation of fullerene enhances the thermal degradation of PMMA.

The study was supported by the Russian Foundation for Basic Research (project no. 15-43-03034-a).

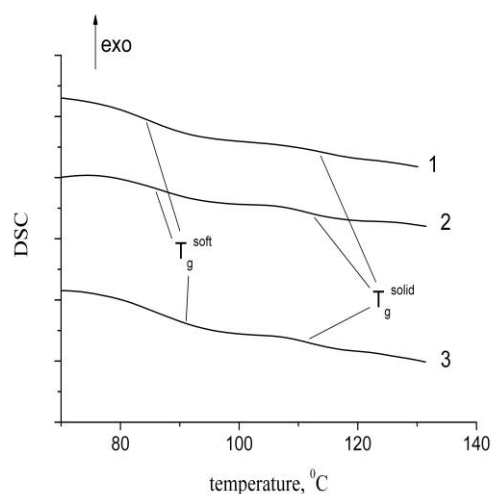


Figure 1 DSC curves of the PMMA/ C_{60} composites films with various filler content, wt. %: 0.5 (1); 1 (2); 3 (3).



THERMODYNAMIC DESCRIPTION OF CONCENTRATION OF LANTHANUM (III) ION ON THE CHELATE-CONTAINING SORBENTS

Amerkhanova Sh.K., Uali A.S, Shlyapov R.M., Imankulova A.Ye.

Buketov Karaganda State University, 100028, Karaganda, Kazakhstan

E-mail: amerkhanova_sh@mail.ru

One of the most important indicators of the economy of any country is the consumption of rare earth elements (REE) in various fields. These materials change completely the properties of the products manufactured. Relevance of these researches is due to the need to study the thermodynamics of sorption of lanthanum (III) ions on the modified sorbents that allows choosing selective sorbents for extraction and concentration of REE from dilute solutions and improving the efficiency of chelate-containing sorbents in the processing of low-conditioned rare earth raw materials.

It has been investigated sorption concentration of lanthanum (III) ions on active charcoals (BAU) and silica (SiO₂) modified by CDTA (trans-1,2-diaminocyclohexane- N,N,N',N'- tetraacetic acid). Sorption concentration was carried out in a static mode. Experiments on the adsorption of lanthanum (III) ions were performed by the method of mathematical planning. The generalized equations describing the impact of pH, the initial concentration of a sorbate, and the temperature have been obtained.

The comparative study of the applicability of the adsorption model of Langmuir, Freundlich, BET, the theory of volume fill of micropores (TVFM), Aranovich and GAB (Guggenheim, Anderson, de Boer) to describe the experimental adsorption isotherms of lanthanum (III) ion has been carried out [1]. The establishment of equilibrium adsorption characteristics according to the GAB model allows following the changes in the chemical nature of the sorbents surface after their chemical modification.

Sorption of lanthanum (III) ion on chelate-containing sorbents increases with increasing pH, the optimal value for the isolation of lanthanum (III) ions is pH=8.0±0.5. Basic sorption thermodynamic parameters are calculated from the data of GAB model and shown in Table 1.

Table 1. Thermodynamic parameters of sorption of lanthanum (III) ions on the BAU and silica modified by CDTA at pH = 8

Chelate-containing sorbent	T, K				
	298	303	308	313	318
SiO ₂	-ΔG (kJ/mole)				
	14.92	14.68	14.56	14.47	14.40
	ΔS (J/(mole·K))				
	4.04	-8.81	-22.01	-35.34	-48.74
Active charcoals	-ΔG (kJ/mole)				
	16.91	17.09	17.24	17.36	17.45
	ΔS, (J/(mole·K))				
	-95.25	-90.79	-86.24	-81.59	-76.84

The table shows that the Gibbs energy of adsorption of lanthanum (III) ions on the activated charcoals has the highest values. Also, the surface of sorbents was characterized by FT-IR spectra and SEM pictures.

[1] Kamalyan, O.A., Kamalyan, T.O., Stepanyan, A.V., Avetisyan, A.E. Scien.Notes of the Yerevan St.Univ., 2009, 3, 13-17.

INVESTIGATION OF RELAXATION TIMES OF MICELLAR SYSTEMS FOR QUASI-DROP MODEL OF SPHERICAL MICELLE

Babintsev I.A.^{1,2}, Adzhemyan L.Ts.¹, Shchekin A.K.¹

¹Department of Statistical Physics, St. Petersburg State University, St. Petersburg, 199034, Russia

²NRC "Kurchatov Institute", Petersburg Nuclear Physics Institute, Gatchina, 188300, Russia

E-mail: il2b@rambler.ru

Valuable information about the physical and chemical properties of micellar systems can be obtained from a study of the kinetics of aggregation and relaxation. The kinetics of aggregation and relaxation in micellar solutions of surfactants in the case of molecular aggregation mechanism, in which the change in the size of the unit is done by joining or emission of only one surfactant molecule, described by a system of difference equations Becker-Döring.

The role of the molecular mechanism has been widely discussed [1-7]. In [8] were found relaxation times micellar system with non-ionic surfactants with spherical micelles for a wide range of concentrations from the first critical concentration (CMC) to 30CMC by solving the linearized Becker-Döring equations. Becker-Döring equations

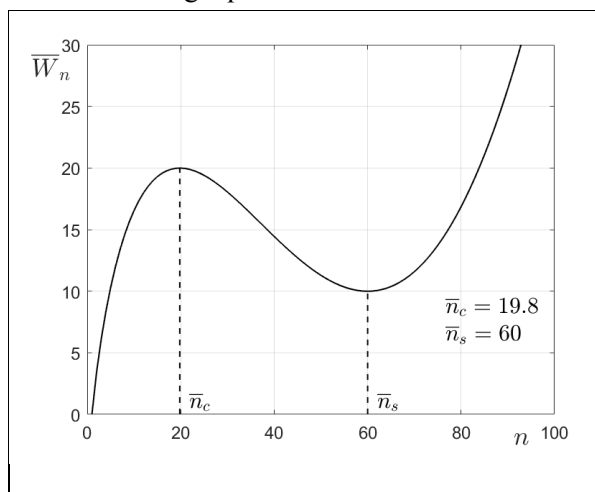


Рис.1. Aggregation work \bar{W}_n as function of aggregation number n for quasi-drop model of spherical micelle.

$$\frac{\partial c_n}{\partial t} = -(J_n - J_{n-1}), \quad n = 2, 3, \dots, \quad (1)$$

where $J_n \equiv a_n c_1 c_n - b_{n+1} c_{n+1}$ flow of aggregates in the space of aggregation numbers, c_n - concentration aggregates with aggregation number n , a_n - monomer addition rates to the aggregation with the number of aggregation n , a b_n - ratio of monomer emission from the aggregate to the number of aggregation n . Since the equilibrium flow $\tilde{J}_n = 0$, due to detailed balance flow

$$J_n \equiv a_n \left(c_1 c_n - \frac{\tilde{c}_n \tilde{c}_1}{\tilde{c}_{n+1}} c_{n+1} \right), \quad \text{where } \tilde{c}_n = \tilde{c}_1^n \exp(-\bar{W}_n)$$

- equilibrium concentration of aggregates. We used aggregation work for drop model of spherical micelle [8]. Now we use a quasi-drop model (Fig.1)

$$\bar{W}_n = \omega_1 (n-1)^2 + \omega_2 (n-1)^{3/2} + \omega_3 (n-1)$$

(2)

at the same total surfactant concentration and compare the obtained results.

[1] E. A. G. Aniansson and S. N. Wall, J. Phys. Chem. 78, 1024 (1974).
 [2] S. N. Wall and E. A. G. Aniansson, J. Phys. Chem. 84, 727 (1980).
 [3] M. Almgren, E. A. G. Aniansson, and K. Holmaker, Chem. Phys 19, 1 (1977).
 [4] M. Kahlweit and M. Teubner, Adv. Colloid Interface Sci. 13, 1 (1980).
 [5] R. Zana, «Dynamics in micellar solutions of surfactants», Chap. 3, p. 75. (2005)
 [6] A. K. Shchekin, F. M. Kuni, A. P. Grinin, and A. I. Rusanov, «Nucleation in micellization processes», Chap. 9, p. 312. (2005)
 [7] F. M. Kuni, A. I. Rusanov, A. K. Shchekin, and A. P. Grinin, Russ. J. Phys.Chem. 79, 833 (2005).
 [8] I. A. Babintsev, L. T. Adzhemyan, A. K. Shchekin, J. Chem. Phys. 137, 044902 (2012)

SURFACE TENSION OF GAS-SATURATED CRYOGENIC AND LOW-BOILING LIQUIDS

Baidakov V.G., Kaverin A.M., Khotienkova M.N., Grishina K.A.

Institute of Thermal Physics, Ural Branch of the Russian Academy of Sciences, 620016 Yekaterinburg, Russia

E-mail: baidakov@itp.uran.ru

Gas-saturated liquids are solutions in which the substance being dissolved is usually a surface active component. We have investigated the surface tension of cryogenic (nitrogen, oxygen, argon, methane) and low-boiling (ethane, propane, xenon) liquids saturated with helium and nitrogen. Such mixtures are used as a motor fuel, in the dispersion of liquid jets, etc.

The capillary constant a^2 has been measured in experiments by the differential capillary method, and the surface tension σ has been calculated with the use of literature data on the liquid and vapor density. Measurements were conducted in the temperature range from the triple point temperature to that close to the critical one and the pressure range from that of the saturated vapors of a pure solvent to 4 MPa. The composition of solutions was determined through phase-equilibrium parameters. Experimental data on a^2 and σ , as functions of the temperature, pressure and concentration, are presented by analytical dependences. The concentration dependence of the surface tension for a methane-hydrogen solution is shown in Fig.1.

The results of measurements are discussed in the framework of thermodynamic models and the van der Waals theory of capillarity. The composition of the surface layer of a gas-saturated liquid has been determined. It has been shown that for all systems under investigation a dissolved substance concentrates at the interface, which leads to a decrease in the surface tension. The adsorption has been determined. Figure 2 presents the adsorption isotherms of a methane–helium system.

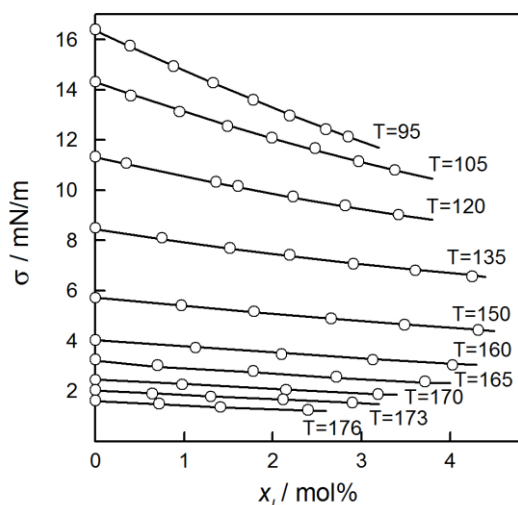


Figure 1. Surface tension of a methane–hydrogen solution as a function of the hydrogen concentration.

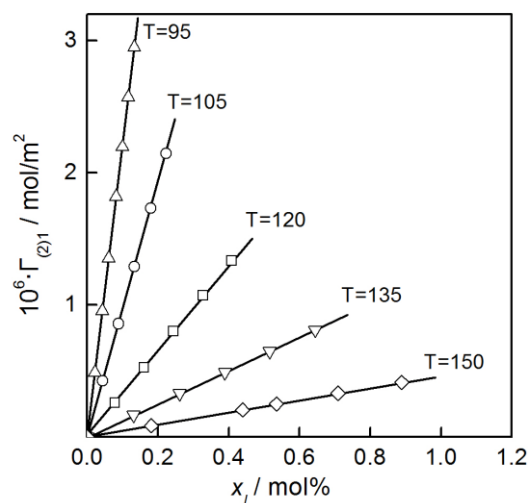


Figure 2. Isotherms of relative adsorption for a methane–helium system

The functional of an inhomogeneous liquid–gas system with a flat interface has been built up with the use of a one-liquid solution model and the van der Waals theory of capillarity. The functional obtained has been minimized to determine the distributions of the partial densities of the solution components in the interfacial layer, the positions of the interfaces, the surface tension, and the Tolman length. A good agreement has been noted between the calculated values of the surface tension and the results of experimental investigations. A means of generalization of data on the surface tension of gas-saturated solutions in the framework of the theory of thermodynamic similarity has been suggested.

The work has been performed with a financial support of the Russian Foundation for Basic Research (project № 15-08-03399) and the Complex Programme of Fundamental Investigations of the Ural Branch of RAS (project № 15-1-2-6).

COMPARISON BETWEEN PYROLYSIS, GASIFICATION AND OXIDATION OF OIL ASPHALTENES

Boytsova A.A., Kondrasheva N.K.

Saint Petersburg Mining University, 199106 Saint Petersburg, Russia

E-mail: cadaga@mail.ru

Crude oil (unprocessed petroleum) is a complex fluid containing many components ranging from low to high molecular weight. Most of them are kept soluble in the fluid under reservoir conditions but may precipitate as solid materials such as asphaltenes at some stage in upstream, transportation, and downstream processes of crude oil. Mostly, the asphaltenes are responsible for plugging surface facilities and flow lines, catalyst deactivation and equipment fouling in hydroprocessing.

Thermal analysis of extracted asphaltenes from Yarega heavy crude oil experimental measurements were made for better understanding behavior of the asphaltenes during pyrolysis (nitrogen), gasification (steam) and oxidation (air) processes. Scanning electron microscope (SEM) and second law of thermodynamics were also used. Figure 1 shows TG curve of the asphaltenes behavior during different processes. The higher amount of coke yield was obtained as a result of gasification. It should be noted that this process has the highest temperature range of weight loss and the temperatures of the beginning and the end of process, which are shown in Table 1. The energy activation of this process is 248.7 kJ/mol.

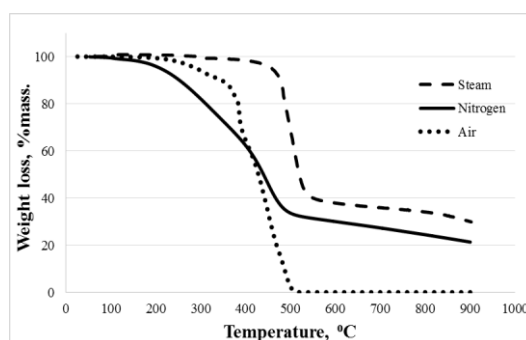


Figure 1. TG curve of asphaltenes in steam, nitrogen and air condition

Coke yield during pyrolysis composes 21% wt. The weight loss occurs in temperature range from 154°C to 511°C. The pyrolysis has the lowest process temperature (from 380°C to 444°C) and has the lowest energy activation (42.9 kJ/mol).

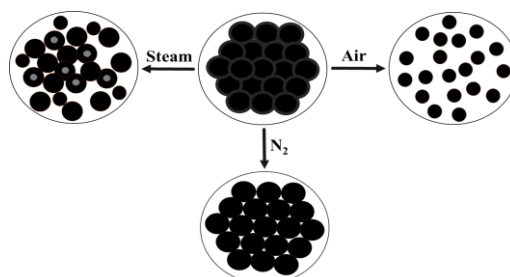


Figure 2. Difference between asphaltene decomposition during processes

The oxidation process has no coke yield, but occurs in the highest temperature rate (from 485°C to 521°C) and has the highest energy activation (294.2 kJ/mol).

Based on thermodynamic calculations and photos of coke yields, which were made by SEM, difference between asphaltenes during oxidation, gasification and pyrolysis were obtained (Fig. 2).

The asphaltenes have the lower strong and well-ordered structure as a result of oxidation process. It could be the reason of absence of coke yield. During pyrolysis the most strong and well-ordered structure occurs. But the highest amount of coke yield is produced during gasification. It could be explained of new pattern formation as a result of interaction between hydrocarbon components and steam. This result could be proved by previous research [1].

Table 1. The main parameters of TG under different condition.

Condition	Temperature range of weight loss, °C	Coke yield, % mass.	Temperature range of process, (°C)	Ea, (kJ/mol)	R
Steam	353-556	30	426-483	248.7	0.969
Nitrogen	154-511	21	380-444	42.9	0.983
Air	220-518	0	485-521	294.2	0.951

[1] Yarranton, H.W.; Hussein, H.; Masliyah, J.H. Water-in-hydrocarbon emulsions stabilized by asphaltenes at low concentrations. J. Colloid Interface Science, 2000, 228(1), 52–63



DIFFERENTIAL THERMAL ANALYSIS OF THE TITANIUM OXIDE AND OXYNITRIDE FILMS

Boytsova E.L., Leonova L.A.

Tomsk Polytechnic University, Lenin av. 30, Tomsk, 634050, Russia

E-mail: boi5@list.ru

The thin-film titanium dioxide coatings are widely used in technological application. This coatings are deposited on the metal, semiconductor, dielectric surface for use in the microelectronics industry, atomic engineering, tool production, and for medical applications. Doping of the films by nitrogen atoms is the most affordable and reasonable way to improve TiO₂ features: a significant change of the refractive index, increase of the hardness, electrical conductivity and elasticity modulus. The nitrogen atoms are generally incorporated into the TiO₂ structure in the oxygen position or in the interstice of crystal lattice [1].

To increase corrosion resistance and extend the lifetime of hardware, they are annealed at the temperature 600–900°C [2]. In this work we present the results of thermal stability evaluation of the Ti-O and Ti-O-N films, formed on silicon substrates by reactive magnetron sputtering [3]. We investigated films using differential thermal analysis (DTA). The temperature range was 20–1300°C at a heating rate of 10°C/min under argon at termoanalizatore SDT Q600 (TG, DTA, DSC), TA Instruments (USA). The experimentally obtained thermogravimetric curves, which allow detecting of the samples weight changes with temperature, show a small weight increase (less than 0.2% of total weight) in the temperature interval 1150 ± 35°C. In a temperature range 1150–1250°C we observed exothermic effect on the DTA curves for film TiO₂ and TiO₂(N). Stretch gently sloping shape and asymmetry of exothermic effect indicates some slow, gradual process, which depends mostly on the environment oxidative capacity, as well as non-isometric of the sample grains; usually this effect is due to the processes of oxidation and burning [4]. However, in an inert atmosphere - it is impossible. We can assume that this is due to the small destruction of the films, as evidenced by the samples weight reduction at the temperature more than 1150°C in the TG curves; and/or the transition from the nonequilibrium forms to equilibrium (transition from the amorphous to the crystalline state), since the film deposition by magnetron sputtering lead to the formation of amorphous phases TiO₂ island at the surface [3].

Thus, studying the properties of coatings by DTA we found that titanium oxide and oxynitride coatings are thermally stable in a wide temperature range, have high corrosion properties, and are prospective for practical application.

References

- [1] Gnedenkova S.V., Khrisanova O.A., Volkova L.M., Kaydalova T.A., Gordienko P.S. Synthesis films of chemical compounds on titanium in a microplasma discharges // *Journal of Inorganic Chemistry*. 1995. T. 40. №. 4, pp 558-562.
- [2] Molodechkina T.W., Vasiukov A.V., Bor A.V., Molodechkin M.O. The study of the properties of titanium dioxide films formed by various methods// *New materials and technologies in mechanical engineering: materials of the 7th Int. scientific and engineering. Internet Conf. Bryansk – 2007*
- [3] Leonova L.A., Boytsova E.L., Pustovalova A.A. The study of titanium oxynitride coatings solubility deposited by reactive magnetron sputtering// *IOP Conference Series: Materials Science and Engineering*. 2016. Vol. 135 (1) [012026, 5 p.]
- [4] Dharmaraj N., Park H. C., Kim C. K., Kim H. Y., Lee D. R.//*Materials Chemistry and Physics* 2004.– V. 87, Iss.1.– P. 5

DETERMINATION OF DNA MELTING TEMPERATURE WITH THE HELP OF QCM

 Kurus N.N.¹, Dultsev F.N.^{1,3}, Shevelev G.Y.², Lomzov A.A.^{2,3}, Pyshnyi D.V.^{2,3}
¹Institute of Semiconductor Physics, Siberian Branch of the Russian Academy of Sciences, 630090 Novosibirsk, Russia

²Institute of Chemical Biology and Fundamental Medicine, SB RAS, 630090 Novosibirsk, Russia

³Novosibirsk State University, Russia

E-mail: fdultsev@isp.nsc.ru

DNA denaturation, namely helix unwinding (which is the transition from dsDNA to ssDNA) is usually carried out by rising the temperature, and this is the major method of DNA unwinding during PCR. The temperature at which denaturation occurs is called melting temperature; it is one of the basic parameters for oligonucleotide design. Melting temperature depends on base sequence, as well as on oligonucleotide concentration and on the presence of cations in the buffer, both monovalent (Na⁺) and divalent ones (Mg²⁺).

Thermal denaturation studies. Hybridization analysis was performed to confirm that the designed oligonucleotides can form intermolecular complexes; determination of thermodynamic parameters of duplex formation was carried out.

The melting temperatures, enthalpies and Gibbs free energy changes are summarized in Table 1.

M2 – 5'-NH₂-(CH₂)₆-p-GATCATAGCTTCGAAAGATC-3';

N2-1 – 5'-GATCTTTCGAAGCTATGATC-3'; N2-3 – 5'-GACCTTTCGAAGCTATGATC-3';

N2-4 – 5'-GATCTTTCGAAGCTATGCTC-3';

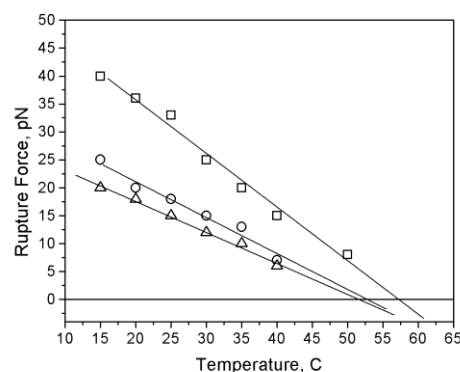


Figure 1. Dependence of rupture force on temperature for different complexes.

Table 1. Thermodynamic parameters of the DNA duplex formation obtained using UV melting technique

Complex	[Na ⁺], M	S ^o (298 K) cal/(mol×K)	ΔH ^o , kcal/mol	ΔG ^o (37 °C), kcal/mol	T _m , °C	T _m , °C QCM
M2/N2-1	0.1	-318 ± 1	-114.3 ± 0.3	-15.7 ± 0.1	58.4 ± 0.1	57
M2/N2-3	0.1	-295 ± 0	-105.2 ± 0.0	-13.8 ± 0.1	53.8 ± 0.1	53
M2/N2-4	0.1	-313 ± 11	-110.9 ± 3.6	-13.8 ± 0.2	52.8 ± 0.1	51
M2/N2-1	2.0	-340 ± 21	-125.4 ± 7.3	-20 ± 0.8	68.7 ± 0.2	-

T_m calculated at 5*10⁻⁶ M total oligonucleotide concentration.

Using the QCM-based method to determine the rupture force [1], we carried out the measurements at different temperatures indicated in Fig. 1; relying on the data obtained, we plotted the dependences which were used to determine T_m (the right column in Table 1).

Acknowledgement This study was supported by the Ministry of Education and Science of the Russian Federation (Agreement No. 14.607.21.0125 from 27.10.2015). Unique identifier of the project - RFMEFI60715X0125.

[1] F.N. Dultsev, V.P. Ostanin, D. Klenerman, Hearing the bond breakage. Langmuir, 2000, 16 5036–5040.



THERMODYNAMIC OF DISSOLUTION OF SOLID DISPERSIONS OF HYDROPHOBIC DRUGS

Gerasimov A.V., Usmanova L.S., Boldyrev A.E.

Kazan Federal University, 420088 Kazan, Russia

E-mail: alexander.gerasimov@kpfu.ru

One of the important stages defining the bioavailability in case of oral administration of drugs is their dissolution in water. It is well-known fact, that hydrophobic drugs are only partially soluble in aqueous media, resulting in a significant reduction in their effectiveness. Usage of solid dispersions of such drugs as dosage forms for pharmaceutical applications can significantly improve their solubility.

In the last few years, neutral polymeric materials capable of forming solid dispersions with various drugs attract the attention of scientists. Most effective among such polymers are Pluronic i.e. block copolymers of polyoxyethylene (PEO) and polyoxypropylene (PPO), as well as polyethylene glycol (PEG) with different molecular mass.

In this work enthalpies of dissolution in water of polyethylene glycols (PEG) having an average molecular weight of 1000 and 1400, Pluronic-F127, phenacetin as well as the composites prepared from them were measured using solution calorimetry method at 298.15 K. Intermolecular interaction energies of polymer-phenacetin were calculated on the basis of an additive scheme proposed. It was shown that for mixtures with high content of polymer (more than 90 wt %) Pluronic F127 has the highest solubilizing effect, while for mixtures with (4-6):1 polymer:phenacetin ratio the best solubilizing agent is PEG-1400. IR spectroscopy recorded a decrease in the number of self-associated molecules of phenacetin with increasing polymer content in the composites. The results obtained enabled us to identify the features of intermolecular interactions of polymers with a model hydrophobic drug – phenacetin to optimize the conditions for preparing solid dispersions based on hydrophilic polymers.

This work has been performed according to the Russian Government Program of Competitive Growth of Kazan Federal University. The work of Gerasimov A.V. was supported by Scholarship of the President of the Russian Federation (SP-1423.2016.4). The work of Usmanova L.S. was supported by grant №14.Y26.31.0019 from Ministry of Education and Science of Russian Federation.



THERMODYNAMIC ASPECTS OF THE FORMATION OF SOLID DISPERSIONS BASED ON POLYMERS AND PROTEINS WITH THE ABILITY TO INHALATION ADMINISTRATION

Gerasimov A.V., Usmanova L.S., Boldyrev A.E.

Kazan Federal University, 4200088 Kazan, Russia

E-mail: alexander.gerasimov@kpfu.ru

Inhalation therapy is one of the methods of express administration of drugs into the human body. Thanks to the extremely abundant capillary network and huge surface of lung alveoli drugs may be absorbed very fast. With this method of administration of inhaled substances do not undergo changes similar to those observed when administered via the gastrointestinal tract. The substances introduced into the lungs by inhalation have a 10-200 fold greater bioavailability than nasal and gastrointestinal administration. Furthermore, inhalation administration in aerosol form of the drug with controlled parameters can serve as a non-invasive alternative to injecting drugs.

Therapeutically useful particulate limited range in diameter from 1 to 5 microns. Particles with a diameter higher than 10 μm are deposited in the oropharynx, those measuring between 5 and 10 μm in the central airways and those from 0.5 to 5 μm in the small airways and alveoli. In order to target the alveolar region specifically, the aerosol droplet diameter should not be more than 3 μm .

In this paper, the complex of physical and chemical methods have been optimized composition of the solid dispersion of polyvinylpyrrolidone and sodium caseinate with a well-established as a model hydrophobic drug compound - phenacetin. The optimum concentrations of the components in solution to produce spherical microparticles with an average diameter of 1.3 microns, which can be used for inhalation delivery of drugs and have increased solubility, are determined. The thermodynamic parameters of the dissolution for produced microspheres were obtained. Preliminary minimum set of methods needed for preparing solid dispersions by spray dried are: differential scanning calorimetry, X-ray powder diffraction, the study of the rheological characteristics of the solution and determination of quantitative characteristics of the dissolution process.

This work has been performed according to the Russian Government Program of Competitive Growth of Kazan Federal University. The work of Gerasimov A.V. was supported by Scholarship of the President of the Russian Federation (SP-1423.2016.4). The work of Usmanova L.S. was supported by grant №14.Y26.31.0019 from Ministry of Education and Science of Russian Federation.

CHARACTERIZATION OF FERROGELS AND MAGNETIC COMPOSITES BASED ON POLYACRYLAMIDE WITH EMBEDDED IRON AND NICKEL NANOPARTICLES

Mikhnevich E.A., Safronov A.P.

Ural Federal University named after B.N.Yeltzin, 620002 Yekaterinburg, Russia

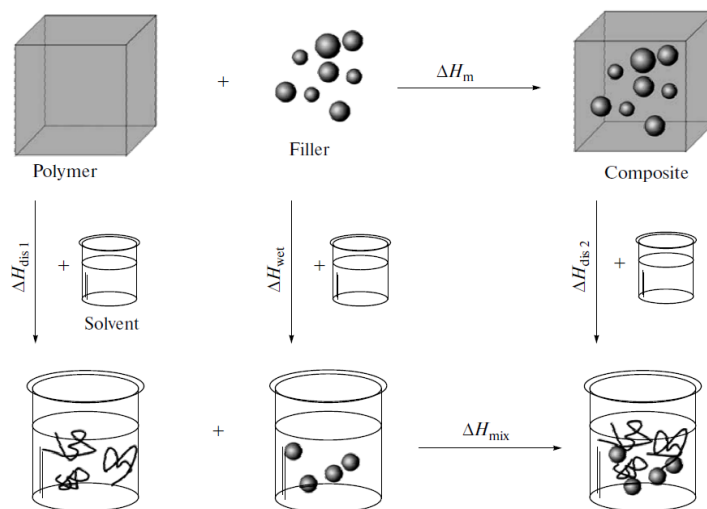
E-mail: emikhnevich93@gmail.com

Biocompatible ferrogels are the advanced materials, they gain attention both from the theory and from the viewpoint of prospective bio-medical application in the magneto-sensitive sensors and biosensors. The ferrogel contains the polymeric network of a water-soluble polymer, which provides its mechanical elasticity and the magnetic particles embedded in the network, which give the sensitivity of the material to the external magnetic field.

The objective of the present research was to study the interactions in the ferrogel based on polyacrylamide (PAAm) with embedded iron (Fe) and nickel (Ni) nanoparticles (MNPs).

The iron and nickel magnetic nanoparticles (MNP) with mean diameters 80 – 90 nm were synthesized by one of the highly productive techniques – the electrical explosion of metal wire [1,2]. To estimate the interaction between PAAm and MNPs in composites, calorimetric measurements were performed.

The mixing enthalpy (ΔH_m) for the composites PAAm filled with iron and nickel MNPs has to be calculated, because it is not measurable directly. For the calculation the thermochemical cycle is used. It follows the depicted scheme (figure 1).



The thermal cycle is based on **Figure 1. Scheme of thermochemical** the fact that a change in enthalpy of a system is independent from the path the components undergo. It enables the calculation of ΔH_m by considering the enthalpy change of the polymer and the solvent (ΔH_{dis1}), of the filler and the solvent (ΔH_{wet}), of the polymer solution and the filler solution (ΔH_{mix}) and of the composite and the solvent (ΔH_{dis2}). Hence ΔH_m can be expressed by the following equation:

$$\Delta H_m = \omega_{fil} * \Delta H_{wet} + \omega_{pol} * \Delta H_{dis1} - \Delta H_{dis2} + \Delta H_{mix}$$

[1] Beketov, I.V.; Safronov, A.P.; Medvedev, A.I.; Alonso, J.; Kurlyandskaya, G.V.; Bhagat, S.M. AIP, 2012, 2, 022154.

[2] Safronov, A.P.; Kurlyandskaya, G.V.; Chlenova, A.A.; Kuznetsov, M.V.; Bazhin, D.N.; Beketov, I.V. et al., Langmuir, 2014, 30, 3243–3253.



DIFFUSION OF SURFACTANTS IN AQUEOUS MICELLAR SOLUTIONS

Movchan T.G.¹, Rusanov A.I.^{1,2}, Plotnikova E.V.¹

¹The A.N. Frumkin Institute of Physical Chemistry and Electrochemistry, Russian Academy of Sciences, 119071 Moscow, Russia; ²St. Petersburg State University, 199034 St. Petersburg, Russia

E-mail: movchan_tamara@mail.ru

The problem of electrolyte diffusion in aqueous solutions had, to a substantial extent, been studied already by the mid-20th century [1]. An important event was the discovery of the relation between transport properties and thermodynamic parameters of solutions. Beginning from the 1980s, diffusion of ionic surfactants in micellar systems has attracted an increasing attention [2–5]. The passage from nonionic to ionic surfactants immediately encounters a complication associated with the fact that, for the former, the diffusion coefficient always decreases with increasing concentration whereas, for the latter, a drastic decrease at the critical micelle concentration (CMC) is followed by a growth, which continues until a rise in viscosity hinders it.

Leaist [4] proposed an idea that the increase in the diffusion coefficient is related to the transport properties of micelles. When constructing in terms of mobility, the theory [6] predicts micellization to enhance the mobility for any surfactant. The difference in behavior between nonionics and ionics arises when passing from the mobility to the diffusion coefficient. The aggregation number of micelles increases with the length of hydrocarbon radicals in a homologous series; hence, the average mobility of surfactants must increase in the homologous series as well. Since, for ionic surfactants, the mobility and diffusion coefficient vary symbatically, the growth of the diffusion coefficient must be enhanced with the length of the hydrocarbon tail. Such dependence has been just experimentally found for alkyltrimethylammonium bromides [7]. On the basis of theories [4,5], the calculations of non-ionic (oligooxyethylene n-alkyl ethers $C_8(EO)_4$ and $C_{12}(EO)_5$) and of ionic alkyl (decyl-, dodecyl-, tetradecyl-, cetyl-) trimethylammonium bromides and sodium dodecylsulfate) surfactant diffusion coefficients were performed with used data on the aggregation numbers, the degree of counterion binding as well as the diffusion coefficients of monomers and micelles. A method has been analyzed for calculating diffusion coefficients of surfactants as functions of their micellar solution concentrations within the framework of the quasi-chemical variant of the mass action law. The methods for introducing initial calculation parameters and the computational scheme for an ideal mixture of monomeric ions and micelles, as well as the correction for a deviation from ideality and a change in solution viscosity, have been considered. The combined correction for the activity and viscosity widens the range of agreement between the theory [3–5] and experimental data [7,9].

This work was supported by the Russian Science Foundation, grant 14–13–00112.

- [1] Robinson, R. and Stokes, R. *Electrolyte Solutions*, London, 1959.
- [2] Weinheimer, R.M.; Evans D.F.; Cussler E.L. *J. of Coll. Inter. Sci.*, 1981, 80, 357–368.
- [3] Evans, D.F.; Mukherjee, S.; Mitchell, D.J.; Ninham, B.W. *J. of Coll. and Inter. Sci.*, 1983, 93, 184–204.
- [4] Leaist, D.G. *J. of Coll. Inter. Sci.*, 1986, 111, 230–239.
- [5] Sutherland, E.; Mercer, S.; Everist, M.; Leaist, D. *J. Chem. Eng. Data*, 2009, 54, 272–277.
- [6] Rusanov, A.I., *Colloid J.*, 2016, 78, 102–108.
- [7] Movchan, T.G.; Shchekin, A.K.; Soboleva, I.V.; Khlebunova, N.R.; Plotnikova, E.V.; Rusanov, A.I. *Colloid J.*, 2015, 77, 179–185.
- [8] Rusanov, A.I. *Colloid J.*, 2016, 78, 669–732.
- [9] Movchan, T.G.; Rusanov, A.I.; Plotnikova, E.V. *Colloid J.*, 2016, 78, 785–794.

ON SIZE DEPENDENCES OF MELTING AND CRYSTALLIZATION ENTROPIES OF METAL NANOPARTICLES

N.Yu. Sdobnyakov, A.D. Veselov, P.M. Ershov, D.N. Sokolov, V.M. Samsonov, S.A. Vasilyev,

V.S. Myasnichenko

Tver State University, Sadovii per., 35, 170002 Tver, Russia

E-mail: nsdobnyakov@mail.ru

Investigation of melting and crystallization of nanoclusters, including size dependences of melting and crystallization entropies, makes it possible to predict the nominal size and temperature ranges for nanosized working units. Size dependences for melting $\Delta S_m = H_m(N^{1/3})/T_m(N^{1/3})$ and crystallization $\Delta S_c = H_c(N^{1/3})/T_c(N^{1/3})$ entropies are presented in Fig. 1.

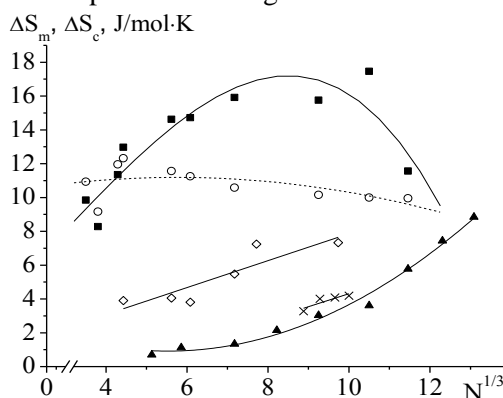


Figure 1. Size dependences of the melting entropy (■) and crystallization entropy (○) for copper nanoclusters (Monte-Carlo simulation data) [1], × – values of the melting entropy calculated using values of H_m and T_m taken from [2], ▲ – results taken from [3], ◇ – molecular dynamics results obtained using program [4]. The bulk value $\Delta S_m^{(\infty)} = 9.6$ J/mol·K [5].

Analysis of the size dependences for ΔS_m and ΔS_c shows that for the entropy of crystallization ΔS_c it is much less pronounced than for the entropy of melting. Really a value obtained in molecular dynamics experiments corresponds to 44% of the bulk value whereas Monte-Carlo (MC) results for copper nanoclusters, containing up to 1500 atoms, are a bit higher than the macroscopic value. It is noted in [3] that the melting and crystallization temperatures are linear functions of $N^{-1/3}$. However, the heat and entropy of melting vary by a more complex way. In particular in [3] the value $\Delta S_m = 9.2$ J/mol·K was obtained for nanoclusters consisting of $N = 2243$ atoms that practically coincides with the bulk value. At the same time, for nanoclusters consisting of $N = 10005$ atoms the obtained value 5 times exceeds the bulk value that, in our opinion, needs an additional justifications (data from [6] predict for this size the value $\Delta S_m = 8.7$ J/mol·K but for $N > 2 \cdot 10^5$ and even in the macroscopic limit – the value $\Delta S_m^{(\infty)} < \Delta S_m = 10.1$ J/mol·K). Besides, theoretical results for the size dependences in question as well as MC results demonstrate a trend to their merging for small particle sizes. However, it remains unclear why theoretical results predict $\Delta S_c(r) > \Delta S_m(r)$ whereas MC results give $\Delta S_c(r) < \Delta S_m(r)$.

The work was supported by RFBR (grant No 16-33-00742) and by Ministry of education and science of Russia.

[1] Sdobnyakov, N.Y. et al. // Clusters, Nanostructures, and Nanomaterials: Physicochemical Research. Collection of Scientific Papers, 2014, 6, 342-348.

[2] Samsonov, V.M. et al. Bull. Russ. Acad. Sci.: Phys., 2016, 80, 547-550.

[3] Gafner, S.L. et al. // Journ. Exp. and Theor. Phys., 2009, 135, 899-916.

[4] Myasnichenko, V.S. Certificate for computer programs № 2011615692, 20.01.2011 [in Russian].

[5] Physical values, The Handbook (Energiya, Moscow, 1991) [in Russian].

[6] Delogu, F. Physical Review B, 2005, 72, 205418.

GIANT SHIFT OF THE NEMATIC–ISOTROPIC PHASE TRANSITION TEMPERATURE IN LAYER OF A METALLOMESOGENIC COMPLEX

Polushin S.G., Lezova I.E., Polushina G.E.

St. Petersburg State University, 199164 St. Petersburg, Russia

E-mail: s.g.polushin@mail.ru

The successful synthesis of *nematic* metallomesogens [1] opened up the possibility to obtain and study macroscopically ordered liquid-crystalline phases in metallomesogen. Systematic studies of metallomesogens revealed one more feature, which has not been deliberately investigated so far and is analyzed in this work. In particular, the first-order phase transition from the liquid-crystalline to isotropic phases can take place within a temperature range of one to several degrees [2]. This should give rise to coexistence of the anisotropic and isotropic phases and to effective anisotropy of physical properties being lower in this range than the anisotropy of the proper liquid-crystalline phase.

The liquid-crystalline complex studied in this work was tris[1-(4-(4-propylcyclohexyl)phenyl)octane-1,3-diono]-[5,5'-di(heptadecyl)-2,2'-bipyridine]terbium. It has both smectic A and nematic phases [1]. We compared the electro-optical properties of the metallomesogen in isotropic (I) phase with the optical and dielectric anisotropy of the metallomesogen determined in the nematic (N) phase on the basis of the Landau–de Gennes theory. The anisotropy measured experimentally near the transition proved to be many times lower than the calculated value.

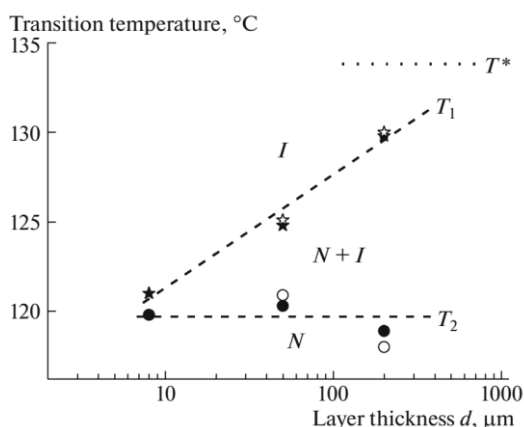


Figure 1. Phase diagram of a metallomesogen obtained using three samples with different layer thicknesses: 8, 50, and 200 μm . The nematic and isotropic phase regions and the coexistence region are designated. The temperature T^* was determined by using the Kerr effect. During cooling (dark dots), the nematic–isotropic phase transition starts at the temperature T_1 and ends at T_2 . During heating (light dots), melting of the nematic starts at the temperature T_2 and ends at T_1 .

The cause for phase coexistence was determined by monitoring the phase transition by polarization microscopy. According to polarization microscopy data, the phase transition temperature decreases by more than 10°C as the metallomesogen layer thickness is reduced from 200 to 5 μm . This is the effect of boundaries of the cell containing the sample on the N–I phase transition temperature, i.e., the confinement effect. In the case of classical liquid crystals placed into a thin cell or porous matrix, this effect is manifested if the cell (pore) characteristic dimension is less than a micrometer. The confinement effect found in metallomesogens for order of magnitude greater layer thicknesses was a new and unexpected finding.

Thus, for the first time it was shown that in metallomesogen complexes exist very strong confinement effect. The reason seems to lie in the physical-chemical nature of the complexes, namely in the presence of coordination bonds.

[1] Dzhabarov, V.I.; Knyazev, A.A.; Strelkov, M.V.; Molostova, E.Yu.; Schustov, V.A.; Haase, W.; and Galyametdinov, Y.G. *Liq. Cryst.*, 2010, 37, no. 3, 285–291.

[2] Polushin, S.G.; Rogozhin, V.B.; Polushina, G.E.; Lezova, I.E.; et al. *Doklady Physical Chemistry*, 2016, 471, Part 2, 197–200.

**EVALUATION OF THE PROPORTIONALITY COEFFICIENT IN RUSANOV'S FORMULA FOR SURFACE TENSION OF NANOPARTICLES**

N.Yu. Sdobnyakov, V.M. Samsonov, A.N. Bazulev, D.A. Novozhilova
Tver State University, Sadovii per., 35, 170002 Tver, Russia
E-mail: nsdobnyakov@mail.ru

The problem of size dependence of the surface tension σ and surface energy ε was analyzed in details by A.I. Rusanov [1]. In particular, he proposed an asymptotic linear dependence

$$\sigma = Kr \quad (1)$$

between σ and the particle radius r . For a long time Rusanov's formula (1) was overlooked. Therefore, paper [2] by E.N. Vitol' seems to be of special interest, where parameter K was evaluated for solid metal particles and metal nanodroplets using experimental data on the particle evaporation and vacancy pore shrinkage rates. So, paper [2] may be treated as a single experimental confirmation of the linear dependence (1).

Evaluation of the K parameter from kinetics of the particles evaporation.

On the basis of an equation [3] for the particle evaporation rate dr/dt [3], the next formula can be derived for the K parameter

$$K = \left(\frac{kT}{2V_r} \right) \ln \left(\frac{(2\pi kTm)^{1/2} \left[\frac{dr}{dt} \right]}{\alpha P V_r} \right), \quad (2)$$

where α is the evaporation coefficient ($\alpha = 1$ for liquids and $\alpha \in (0.2; 1.0)$ for solids), m is the atomic mass, k is the Boltzmann constant, P is the pressure of the saturated vapor above the flat surface at temperature T and V_r is the atomic volume in a microparticle (in what follows we assume that $V_r \approx V$ where V is the atomic volume in the bulk sample).

Evaluation of the K parameter via the pore shrinkage rate.

Using an equation [4] for the vacancy pore shrinkage rate dr/dt , the next formula can be written:

$$K = \left(\frac{kT}{2V_r} \right) \ln \left(1 - \frac{r}{D} \left[\frac{dr}{dt} \right] \right). \quad (3)$$

Here D is the self-diffusion coefficient.

An analysis of the calculation results for the K parameter (including those for silver particles) shows that usage of different values of parameters controlling kinetics of evaporation gives the range $(10.9 - 148.6) \cdot 10^{10}$ mJ/m³ for the K parameter that agrees with [2] in an order of magnitude only. At the same time, using different values of the input parameters for nanopores in aluminum we have found a wider interval $(2.2 - 160.8) \cdot 10^{10}$ mJ/m³ for K parameter that also agrees with [2] in the order of magnitude only. A more detailed analysis is presented in [5].

The work was supported by Russian Foundation for Basic Research (grant No 17-52-18035) and by Ministry of Education and Science of Russian Federation.

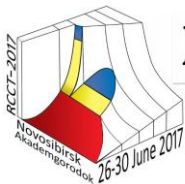
[1] Rusanov, A.I. Thermodynamics of Surface Phenomena (Leningr. Univ., Leningrad, 1960) [in Russian].

[2] Vitol', E.N. Kolloidn. Zhurn. Journal, 1992, 54, 21-22.

[3] Sambles, J.R. et al. Proceedings of the Royal Society A, 1970, 318, 507-522.

[4] Westmacott, K.H. et al. Metals Science Journal, 1968, 2, 177-181.

[5] Sdobnyakov, N.Y. et al. Physico-chemical aspects of the study of clusters, nanostructures and nanomaterials, 2016, 8, 337-344.



THERMODYNAMICS OF SORPTION EQUILIBRIUMS AT THE PHASE INTERFACE SULFIDE ORE - SOLUTION OF A COLLECTING REAGENTS' MIXTURE

Shlyapov R.M., Amerkhanova Sh.K., Uali A.S.

Buketov Karaganda State University, 100028, Karaganda, Kazakhstan

E-mail: amerkhanova_sh@mail.ru

Analysis of sorption capacity of different collecting reagents in relation to the samples of polymetallic ores has showed that the majority of sulfur-containing flotation reagents are adsorbed to form a mono-layer, and the equilibrium sorption characteristics are described by the equations of Langmuir and Freundlich. However, the interpretation of sorption processes using only these equations is incomplete since xanthate-ions form disulfides during the oxidation on the sphalerite surface, and diisobutyldithiophosphate-ions are adsorbed on several centers in the case of pyrite ores [1].

The aim of this research is to identify the nature of sorption processes of collecting reagents mixture on Cu-Pb sulphide ore based on the thermodynamic characteristics. Therefore, sorption isotherms were constructed on the basis of experimental data, the values of the Gibbs energy characterizing the Langmuir model ($-\Delta G_L$), Freundlich ($-\Delta G_F$), Temkin ($-G_T$), Frumkin ($-\Delta G_F'$), and the micropore volume filling theory (TVFM) were calculated.

It is shown that high values of Gibbs energy of sorption process for homogeneous surfaces ($-\Delta G_L=25.79$ kJ/mole) are observed for a mixture of sodium dibutyldithiophosphate and ammonium dibutyldithiophosphate in the ratio 1:1 with the concentration of components that equals to 10^{-4} M. The Gibbs energy takes lower values ($-\Delta G_L=19.34$ kJ/mole) in the case of sorption of a mixture of sodium oleate, sodium diisooctyldithiophosphate and ammonium diisooctyldithiophosphate. Therefore, in these cases the formation of a monomolecular layer from anions of dibutyldithiophosphoric and oleic acids at the centers formed by copper (II) ions are observed. Formation of two or more layers of sorbates due to the interaction between the molecules of the sorbate is possible for sulfur- and oxygen-containing collecting reagents. This fact is confirmed by the positive values of the attraction constant (2.61) and (1.1).

The changes in Gibbs energy according to Frumkin are equal to ($-\Delta G_F'=23.62$ kJ/mole), ($-\Delta G_F'=3.20$ kJ/mole), and ($-\Delta G_F'=0.15$ kJ/mole) for mixtures consisting of ammonium dibutyldithiophosphate, sodium diisooctyldithiophosphate and ammonium diisooctyldithiophosphate with sodium oleate, respectively.

The first layer is firmly bound to the surface of the ore via a sulfur atom according to the heat of activation of sorption for a mixture of sodium and ammonium dibutyldithiophosphates, which is equal to 21.08 kJ/mole. However, mixtures of sodium oleate with ammonium dibutyldithiophosphate, sodium diisooctyldithiophosphate and ammonium diisooctyldithiophosphate are characterized by high negative values of Gibbs energy that are equal to 61.00, 72.35, 78.57 kJ/mole, respectively, and low values of heat of activation of sorption by the TVFM model that are equal to 7.92, 7.68, 7.68 kJ/mole, respectively, which indicates a predominance of the physical nature of the sorption. At the same time for testing mixtures $-\Delta G_T=24.77$ kJ/mole, which indicates an increase of sorption on the active centers of Cu-Pb ore. Thus, according to the researches it has been found that sorption of sodium dibutyldithiophosphate on Cu-Pb ore samples can be described by models of Freundlich, Langmuir, Frumkin, and TVFM for mixtures of sodium dibutyldithiophosphate and ammonium dibutyldithiophosphate, sodium oleate and ammonium dibutyldithiophosphate, sodium and ammonium diisooctyldithiophosphates in a (1:1) ratio. The formation of primary mono-layer by chemical and van-der-Waals bonds with copper ions, that is also the basis for the formation of subsequent molecular layers, is typical for these collecting reagents.

[1] Ignatkina, V.A., Bocharov, V.A., Khachatryan, L.S. On the question of the development of selective flotation reagent modes of refractory sulfide ores. Innovative processes are complex and deep processing of mineral raw materials. The international conference "Plaksin readings-2013". Tomsk, 2013, 199-202.



SMALL AGGREGATES OF NONIONIC SURFACTANTS IN SOLUTIONS. MOLECULAR DYNAMICS SIMULATION

Vanin A.A., Brodskaya E.N.

Institute of Chemistry, St. Petersburg State University, 198504 St. Petersburg, Russia

E-mail: alexvanin@yandex.ru

The structure of spherical micelles of nonionic ($n\text{-C}_n\text{H}_{2n+1}\text{-}\{\text{OCH}_2\text{CH}_2\}_m\text{-OH}$) surfactants in aqueous solution of sodium chloride and in pure water has been studied. The molecular dynamics method has been used to self-assembling of aggregates from initially homogeneous mixture of water and surfactant molecules.

It has been found that the addition of salt to the system influences significantly on the structure and size of the micelles. In the salt solutions, the polar heads leave the center of the micelle and concentrate in the micellar corona while the hydrocarbon tails predominantly accumulate in the central region. This redistribution is accompanied by a contraction of the micelles. Aggregate radius decreases from 2.0 nm (nonionic micelle in water without salt) to 1.8 nm (with salt). This compression is, however, not change the thickness of the surface layer.

Data on the structure of solution near the micellar corona and the micelle itself allowed us to calculate the various contributions to the local electric potential. The comparison of water molecules contribution with the contribution of the polar heads and ions showed a significant difference in the behavior of the micelles of ionic and non-ionic surfactant. However, for all the systems considered the conclusion about substantial compensation of the ion-micellar contribution to the electric double layer by water molecules is valid.

The work was supported by Russian Science Foundation (Grant No. 14-13-00112).



Section 4.

Thermodynamics of surface phenomena and self-organization phenomena in fluid systems

Virtual presentations



Thermodynamic Characteristics of Sorption of Some Ions on a Mono- and Bifunctional Sorbents from Aqueous Solutions

Abbasov A.D., Mamedova F.S., Jafarli M.M.,
Institute of Natural Resources, Nakhchivan branch, Azerbaijan;
E-mail: ada.nat.res@mail.ru

This report presents the results of equilibrium, kinetics and thermodynamics of sorption Cu^{2+} , Zn^{2+} , Cd^{2+} , Pb^{2+} ions weakly acidic polyacrylate cationites Amberlite IRC-748 (iminodiacetate), Duolite C 467 (aminophosphonic) in Na^+ -form, Dowex MAC-3 (carboxyl functional group) in the H^+ -form cationites and a strongly acidic polystyrene cationites Amberlite IR-120 H^+ -form. The change of parameters, such as energy and entropy of activation, free energy of sorption and diffusion coefficients change on various factors. Thermodynamic description of exchange of studied ions by exchangers was conducted on the assumption of ideality of the solid phase, i.e. without taking into account the activity coefficients of ions in the absorbed state. Analysis of the kinetic curves methods by G.Boyd, Yu.A.Kokotov and V.A.Pasechnik and interruption methods revealed that at a concentration of about 1.0 g of sorbates $\text{E} \cdot \text{L}^{-1}$ is controlled intradiffusion kinetics. The value of the entropy of activation was calculated from the equation proposed by R.M.Barrer and his collaborators: $D_0 = d^2 (ekT/h) \exp(\Delta S^*/R)$.

For the mathematical processing of sorption isotherms were used Langmuir, Freundlich and Redlich-Peterson sorption models. Sorption of ions across the study area on the concentrations of these ion exchangers primarily occurs by the mechanism of Langmuir, i. e. ion exchangers is formed on the surface of a monomolecular layer and a sorption all active centers are mainly of equal energy and enthalpy of absorption. We offer relevant equations describing isotherms similar to the equations of Langmuir and Freundlich.

Kinetic studies have shown that the sorption equilibrium when removing the metal ions is well established within 2.5-3.0 hours. Changing the conditions of the experiment (with and without interruption) significantly affects the rate of sorption of ions of sorbents. At low degrees of reaching equilibrium depending $-\log(1-F)$ on the deviate from a straight line, and the high-gain a straightforward character, while the F from $t^{1/2}$ values for F are to 0.4-0.45 lines emanating from the origin. According to the kinetic ability the study of ions of sorbents is arranged in series: Dowex MAC 3 > Duolite C 467 > Amberlite IRC 748 > Amberlite IR-120.

The calculated value of the entropy of activation in all cases have a negative value. Experimental data confirm the tendency to reduce the entropy of sorption with increasing selectivity in the considered systems. The enthalpy of the studied processes is determined by the ratio of quantity of released heat to the amount of adsorbed ions. The selectivity of ion exchangers to the study of ions increases with decreasing temperature, i. e. ion absorption of ion exchangers - exothermic and accompanied by heat. Increasing the selectivity of ion exchangers to the study of ions is correlated with the change in enthalpy of the parameter in the system. Reducing the enthalpy and entropy of the system indicates a strong binding between ions and sorbents. Hibbs energies with increasing concentrations of sorbents in sorption complexions Duolite C 467 ion exchangers and the Amberlite IRC-748 fall, which is not unexpected for the sorption process, complicated by complication. Increasing temperatures more pronounced effect when the sorption of lead and cadmium ions with sorbents Amberlite IRC 748, i. e. higher than the activation energy, the more the sorption rate varies with temperature. Experimental data confirm the tendency to reduce the entropy of sorption with increasing selectivity. The values of the entropy multipliers, calculated according to the formula S.Glasstone: $[D = e \lambda^2 kT/h \cdot \exp(\Delta S/R) \cdot \exp(-E_{\text{act}}/RT)]$ for copper ions is less than for other ions. Hibbs energy studied by us in all cases is maximal for sodium and minimal for protonated forms of ion exchangers.

This suggests a more rapid establishment of sorption equilibrium, which is confirmed by experimental data. For example, the sorption of copper ion through polyampholytes Duolite C 467 values of the diffusion coefficient, activation energy, activation entropy, enthalpy, free energy and entropy factor have been calculated: $2.64 \cdot 10^{-7} \text{ cm}^2 / \text{sec}$, $14.5 \text{ kC} / \text{mol}$, $-51 \text{ C} / \text{mol} \cdot \text{K}$, $-21.5 \text{ kC} / \text{mol}$, $-6.3 \text{ kC} / \text{mol}$ and $5.44 \cdot 10^{-18} \text{ cm}^2$. One of the most important theoretical and practical results of this work is the proof of the relationship of selective sorption and kinetic ion exchanger capacity: increase of the kinetic constant of ion exchangers is accompanied by increased selectivity of sorption.

Quantitative values of diffusion coefficients, pre-exponential factors, the exchange constants, energies of activation and entropy, Hibbs free energies, enthalpies and entropy multipliers are given in the report.



EXPERIMENTAL STUDY OF THERMODYNAMIC PROPERTIES AND PHASE TRANSITIONS IN THE BINARY SYSTEM N-HEXANE + WATER

Bezgomonova E.I., Saidov S.M.

H.I. Amirkhanov Institute of Physics, Dagestan Scientific Center of the RAS, 367000 Makhachkala, Russia

E-mail: bezgomonova_lena@mail.ru

The investigation of the thermodynamic properties of the hydrocarbon + water systems is the deal of great interest both for the oil and oil-chemical industry. Experimental investigation of the C_v , V , T properties in the n-hexane + water system with the different compositions (x) 0.120; 0.200; 0.247 and 0.256 molar fraction (m.f.) H_2O were made with the high-temperature adiabatic calorimeter designed by Kh.I. Amirkhanov [1].

For our investigations we used adiabatic calorimeter with the volume $432.611 \pm 0.2 \text{ cm}^3$ at temperature $T = 298.15 \text{ K}$ and atmosphere pressure 0.1 MPa. Isochoric heat capacity measurement error was 2% to 3% in the near-critical and supercritical regions, 0.5% to 1.0 % in the liquid phase and 3% to 4% for the vapor phase.

The moment of the phase transition identifies itself by the jump of isochoric heat capacity, which can be accurately noticed by the measuring vehicle. All of the measured isochores displays two features in the heat capacity as a function of temperature: first peak when one of the liquid phases disappears (transition from liquid-liquid-vapor to liquid-vapor); and second peak when vapor or liquid phase disappears (from liquid-vapor to liquid or vapor, depending on filling factor). The heat capacity C_v at the first peak changes smoothly in the wide temperature interval. The second peak is characterized by the sharp jump of the isochoric heat capacity.

The Krichevskii parameter plays a great role in determining the thermodynamic behavior of dilute solutions near the solvent's critical point. The value of the Krichevskii parameter was calculated for the pure solvent (n-hexane) [2]. The Krichevskii parameter can be estimated from the initial slopes (at $x=0$), (dT_c/dx) and (dP_c/dx) , of the $T_c(x)$ and $P_c(x)$ critical lines of the mixture and the value of the vapor-pressure curve slope $(dP_s/dT)_{CXC}^C$ of pure n-hexane (pure solvent) at the critical point.

The thermodynamic: partial molar volume \bar{V}_2^∞ and partial molar enthalpy \bar{H}_2^∞ at infinite dilution, vapor-liquid distribution coefficient K_D , cross virial coefficient B_{12} and structural: excess number of solvent molecules surrounding molecule of the solute N_{exc}^∞ , direct C_{12} and total H_{12} correlation integrals properties of dilute n-hexane + water mixture near the critical point of pure solvent (n-hexane) were calculated using the Krichevskii parameter principle.

[1] Amirkhanov, Kh.I.; Stepanov, G.V.; Alibekov, B.G. Isochornaya teploemcost vody I vodyanogo para, Makhachkala, 1969, 39-47.

[2] Bezgomonova, E.I.; Abdulagatov, I.M.; Stepanov, G.V. Journal of Molecular Liquids, 2012, 175, 12-23.



NOVEL INSIGHT ON C₆₀ FULLERENE AGGREGATION

Buchelnikov A.S.¹, Voronin D.P.², Wyrzykowski D.³, Piosik J.⁴, Prylutskyi Yu.I.⁵, Evstigneev M.P.^{1,2}

¹Laboratory of Organic Synthesis and NMR Spectroscopy, Belgorod State University, 308015 Belgorod, Russia

²Department of Physics, Sevastopol State University, 299053 Sevastopol, Russia

³Faculty of Chemistry, University of Gdańsk, 80-308 Gdańsk, Poland

⁴Laboratory of Biophysics, Intercollegiate Faculty of Biotechnology, 80-308 Gdańsk, Poland

⁵Department of Biophysics. ESC "Institute of Biology", Taras Shevchenko National University of Kyiv, 01601 Kyiv, Ukraine

E-mail: buchelnikov@bsu.edu.ru

An increasing importance is being attached to the investigation of C₆₀ fullerenes behaviour in aqueous solution. It has been previously confirmed by means of dynamic light scattering that C₆₀ fullerenes are able to form clusters [1]. The authors of Ref. [1] have provided a statistical-thermodynamic model of the aggregation process and have calculated the value of association constant ($K = 56000 \text{ M}^{-1}$). However, the knowledge of physical factors governing this process is still quite limited and is mainly based on the results of computer simulations. As a consequence, the overall thermodynamic picture of C₆₀ fullerene aggregation in aqueous solution remains unclear. The aim of the present work was to provide the experimental evidence suggesting that C₆₀ fullerene aggregation in aqueous solution is a predominantly entropically driven process with negligible net enthalpic contribution.

For this purpose, we applied dynamic light scattering (DLS) and isothermal titration calorimetry (ITC) methods to study the aggregation of pristine C₆₀ fullerene aqueous colloid solution prepared according to Ref. [2]. The DLS study resulted in temperature dependence of mean hydrodynamic diameter, d_z , demonstrating the absence of any statistically meaningful trend of d_z in the temperature range studied (288-333 K). Taking into account the well-known Van't Hoff equation as the dependency of equilibrium constant, K , on temperature, T , we have shown that the DLS data obtained suggest close to zero enthalpy change of fullerene aggregation [3].

To directly verify this conclusion we measured thermal effects of C₆₀ fullerene aggregation in ITC study. Thermograms representing titration of water with water (control) and water with C₆₀ fullerene solution shown no essential differences between magnitudes of recorded peaks. Determined thermal effects of titration of water with water and water with C₆₀ fullerene solution also did not exhibit significant differences. All determined values of experimental points as well as heat difference obtained by subtraction heat effects mentioned above did not differ and oscillated near zero. The performed ITC analysis indicates no enthalpy changes on aggregation of C₆₀ particles [3].

The principal result obtained from analysis of DLS and ITC data, viz., $\Delta H \approx 0$, enables one to conclude that the observed independence of the particles' diameters in C₆₀ fullerene aqueous solution on temperature is likely due the fact that C₆₀ particle aggregation in solution is an entropically driven process with negligible contribution from enthalpy change [3]. These results deepen our understanding of the nature of factors stabilizing fullerene clusters in aqueous solution.

[1] Prylutskyi, Yu.I.; Buchelnikov, A.S.; Voronin, D.P.; Kostjukov, V.V.; Ritter, U.; Parkinson, J.A.; Evstigneev, M.P. *Phys. Chem. Chem. Phys.*, 2013, 15, 9351.

[2] Scharff, P.; Risch, K.; Carta-Abelmann, L.; Dmytruk, I.M.; Bilyi, M.M.; Golub, O.A.; Khavryuchenko, A.V.; Buzaneva, E.V.; Aksenov, V.L.; Avdeev, M.V.; Prylutskyi, Yu.I.; Durov, S.S. *Carbon* 2004, 42, 1203.

[3] Voronin, D.P.; Buchelnikov, A.S.; Kostjukov, V.V.; Khrapaty, S.V.; Wyrzykowski, D.; Piosik, J.; Prylutskyi, Yu.I.; Ritter, U.; Evstigneev, M.P. *J. Chem. Phys.*, 2014, 140, 104909.

THE SURFACE LAYERS STATE IN SYSTEMS OF AQUEOUS POLYCHLOROPHENOLS SOLUTION – MAGNETIC MICROPOROUS POLYMER

Sharonov N.Yu., Fedorova A.A., Filippov D.V.

Ivanovo State University of Chemistry and Technology, Sheremetevski pr.7, Ivanovo, 153000 Russia

E-mail: sharonov@isuct.ru

The thermodynamic study of various physico-chemical systems and processes are both theoretical and practical interest. Thus, the thermodynamic characteristics of surface phenomena can be successfully used for various types of modeling heterogeneous systems and interfacial processes.

In this work we studied the state of the surface layers in the system poly(styrene-divinylbenzene) (hereinafter StDVB) – aqueous solutions of 2,4-dichlorophenol and 2,4,6-trichlorophenol at 298 K on the basis of experimental data [1]. For imparting magnetic properties StDVB on its surface it was formed of iron particles. Using the method of scanning electron microscopy revealed that the polymer beads have a diameter of 4–5 microns, and the low-temperature nitrogen adsorption – a specific surface area 429 m²/g due to pores with a prevalence of 1–2 nm [1].

Status substances in the interfacial layer can be characterized by a two-dimensional phase diagrams [2], similar to the diagrams of surface films [3]. Fig. 1 and 2 are two-dimensional layers phase diagrams in interfacial adsorption chlorophenols from water solutions StDVB microsphere polymer magnetic particles. Dependence of the two-dimensional surface pressure on the value of the molar area of the adsorbate obtained with the assistance of numerical methods from experimental adsorption isotherms [1]. Fractures to the above dependence is characterized by changes in the state of the interfacial layer when a certain amount of adsorbed chlorophenol. These changes are similar to the two-dimensional phase transitions occurring at the surface films compression [3]. The essence of these transitions are in surface films restructure, and for interfacial layers – and even in a partial or complete desolvation adsorption solution [2].

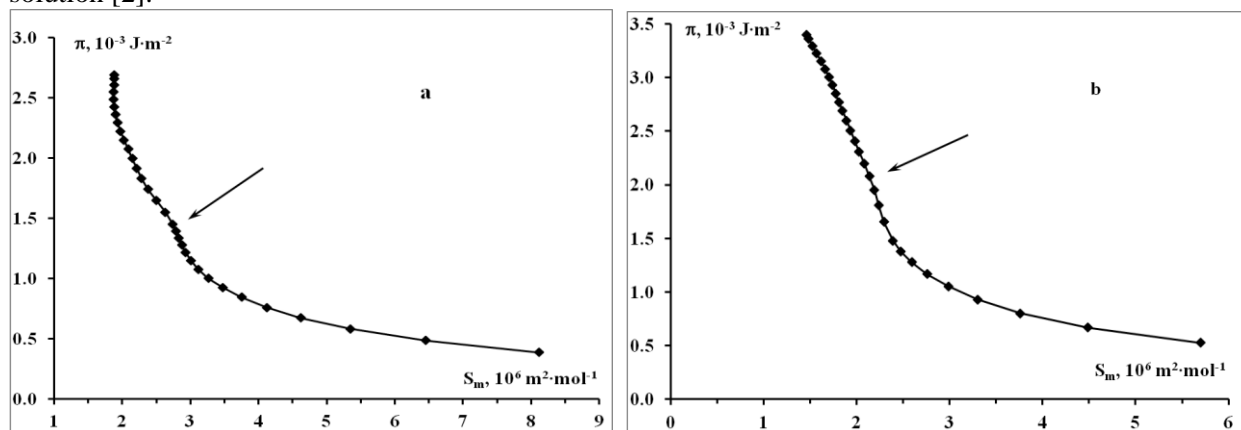


Fig.1. The surface layer state diagram of a polystyrene-divinylbenzene-chlorophenol aqueous solutions at 298 K: 2,4-dichlorophenol (a) and 2,4,6-trichlorophenol (b).

The obtained data suggest that a high specific surface area, small pore size and the presence in polymer the magnetic inclusions determines the high value of the adsorption potential in the pores of the polymer StDVB, which, in turn, influence the state of matter in the surface layer and are able to determine their condition.

[1] Ping Yu, Qilong Sun, Jianfeng Li, Jianming Pan, Zhenjiang Tan, Yongsheng Yan. Desalination and Water Treatment. 2015, 56 (1), 1610-1621. doi:10.1080/19443994.2014.950988.

[2] Sharonov N. Y., Ulitin M. C., Budanov M. A., Izv. Vyssh. Uchebn. Zaved. Khim. Khim. Tekhnol. 2009. V. 52, № 4, S. 11-14.

[3] Shchukin E.D., Pertsov A.V., Amelina E.A. Colloid chemistry. M.: Higher. school. 2004. 445 p.



SELF-ASSEMBLY REACTION OF ORGANIC COMPOUNDS BY SORPTION ON NANOCOMPOSITE SORBENT AND ITS PHYSICO-CHEMICAL ASPECTS

Kibalnikova O.V.

Saratov State University named after N.G. Chernyshevsky, 83 Astrakhanskaya St., Saratov 410012, Russia

e-mail:kib.o@list.ru

The work is devoted to investigation of physic-chemical characteristics of molecular complex, metallocene and dimer of pyridine, toluene and benzene, the be formed in resulting sorption and process self-assembly on the nanocomposite (10% threenitrlpropanamin on colorchrom, fr. 0,14÷0,25 mm). Reaction self-assembly study of gas chromatography method. The especially of these reactions is the participation a large number of components, multistage, big dependence on the nature of the solvent, pressure and temperature.

Intermolecular [1] interaction, contributing to the passage of the reactions of self-assembly can be of different nature and therefore different energy.

The sorbent is represents the electrochemically active heteroboundary «proton conductor- hydride metal». One of factors affecting the speed of chemical reactions depends on the presence of surface-active substances (PAV) and their aggregates on the surface of the sorbent. The rate limiting reaction in the catalytic micelle is the reaction of binding the substrate micelles (effect of concentration).

Earlier show [2], that mechanism division in method gas chromatograph is isoelectric point.

Using thermodynamic equation calculate chemical potentials of supramolecular and dimer compounds of pyridine, toluene and benzene. In forming the compounds observen diamagnetic effect [3,4], which affects the calculated data of the chemical potential. Below are the values of the enthalpy of formation, chemical potentials of theses compound.

Data for Cr (C₅H₅N)₂ by the temperature sorbent 120÷190°C $\Delta H = 1,738 \cdot 10^4$ J/mol, $\mu = -2,175 \cdot 10^5$ J/mol; $s = 1$. Data [CrH](C₆H₅CH₃)₂ $\mu_1 = -2,06 \cdot 10^5$ J/mol; $s = 0$;

Cr(C₆H₅CH₃)₂ $\mu_2 = -1,8 \cdot 10^5$ J/mol; $s = 0$; $\mu_3 = -2,34 \cdot 10^5$ J/mol; $s = 1$; $\Delta H = 1,79 \cdot 10^4$ J/mol;

Data for Cr(C₆H₆)₂ by the temperature sorbent 80÷160°C $\Delta H = 1,269 \cdot 10^4$ J/mol; $s = 1$; $\mu = -1,876 \cdot 10^5$ J/mol .

The energy disparity of active sites on the surface of the nanosorbent leads to solvation effects of heterogeneous catalytic reactions of self-assembly. The solvent can be used not only as medium but also as an effective means to study the nature of chemical interaction and reactivity of substances. Result this reaction be formed dimmers.

Data for dimer pyridine: $\Delta H = 1,78 \cdot 10^3$ J/mol; $\mu = -1,303 \cdot 10^5$ J/mol; $s = 1$;

$\mu = -1,206 \cdot 10^5$ J/mol; $s = 0$.

Data for dimer toluene: $\Delta H = -21,187 \cdot 10^4$ J/mol; $\mu_1 = -1,185 \cdot 10^5$ J/mol; $s = 1$;

$\mu_2 = -1,264 \cdot 10^5$ J/mol; $s = 0$.

References

1. O.V. Kibalnikova. Synergistic inhibition effect electrocatalytic reaction self-assemble /10thInternational symposium on Electrochemistry 2015.-p.137. Moscow, Russia.
2. O.V. Kibalnikova. Fractal skeling of reactions self-assembly on the nanocomposite sorbent with quantum points./ International conference on chemical thermodynamic in Russia. RCCT-2015. Abstract. Lower Novgorod. 252 p.
3. O.V. Kibalnikova. Modeling catalytic process of Method Functional Density. J. Chem. Eng. Chem Res. Vol.2. N8. 2015.- pp. 755-761.
4. I. Maier. Selected chapter quantum chemistry. M.: Laboratory knowledge. 2006.-384 c.



COMPLEXATION OF ORGANIC COMPOUNDS WITH ADSORPTION ON A SILICA SUBSTRATE MODIFIED BY β -CYCLODEXTRIN

Kopytin K.A., Maximova A.A., Kuraeva Yu.G., Pariychuk M.Yu.

Samara University, 443086 Samara, Russia

E-mail: kirko87@inbox.ru

At present, supramolecular chemistry is one of the most important and rapidly developing fields of chemistry. The objects of supramolecular chemistry are the systems formed by non-covalent bonds and inclusion “host – guest” complexes are one of well-known classes of such systems. Cyclodextrins (CD) are among the most important molecular “hosts” studied in supramolecular chemistry. Experimental study of CDs and development of theory of their “host-guest” complexes are mainly based on the investigations of non-valence interactions in condensed phases. Variation of the free energy, when cavities are being formed in CD solutions, includes the terms that depend not only on the “host – guest” interactions but also on solvation of guest, host molecules, or their complex as well as on changes of the solvate structure due to dissolved molecules. Such effects result in difficulties and unambiguity in treatment of the experimental data. It is convenient to study the “host – guest” complexation at adsorption on the “gas – solid” interface as the influence of solvent can be excluded in this case. Out of all CDs the best studied are β -CD complexes. Earlier, we applied inverse gas chromatography to explore the influence of composition and size of substituents in the β -CD derivatives on behavior of organic molecules in the adsorption layer on a flat homogeneous surface of graphite adsorbents. Our analysis of thermodynamic characteristic of the adsorption showed that the “host-guest” complexes of the unsubstituted β -CD and β -CD derivatives can form in the two-dimensional adsorption layer. At the same time, similar investigations with adsorbent of another nature have not yet been performed.

The aim of this work is to evaluate the adsorption properties of adsorbent SIL/ β -CD obtained by depositing unsubstituted β -CD on a surface of silica substrate against the non-modified silica adsorbent.

The experiments were performed with gas chromatograph Kristall 5000.2 with flame ionization detector. For modification, we chose the silica adsorbent Silohrom C-80 with a surface of $\approx 80 \text{ m}^2/\text{g}$. As adsorbates used organic compounds of different classes: normal alkanes, aromatics, alcohols, normal and branched chain, saturated and unsaturated cyclic compounds, including those containing heteroatoms, and enantiomers. Henry constants of adsorption $K_{1,c}$ (cm^3/m^2) were determined at different temperatures.

They were used to calculate differential molar heat of adsorption and the difference between the standard differential molar entropy of the adsorbed substance and standard molar entropy of an ideal gas (the change in entropy during adsorption).

It was found that modification a surface of silica substrate by β -CD showed an increase of the Henry constants of adsorption for polar substances (alcohols, ketones). At the same time, there is a slight variation Henry adsorption constants for non-polar compounds. Substances with a cyclic and bicyclic structure of the molecules were the exception. For these compounds modifying also led to an increase in the Henry constants. The deposition of a macrocyclic modifier enhanced the “adsorbate – adsorbent” intermolecular interactions, increasing the adsorption heats. The change in entropy during adsorption on the modified adsorbent was larger in absolute value than for the starting adsorbent. The values of change in entropy during adsorption found for SIL/ β -CD adsorbent can be interpreted as indications to the adsorption localization. These data suggest that in the case of adsorbent SIL/ β -CD cavity of unsubstituted β -CD are open and available to interact with the molecules of the “guest”.

Thus, the analysis of the thermodynamic properties can be concluded that complexation of β -CD with a wide range of organic compounds can take place in the case of monolayer adsorbent when the molecular size commensurate with the volume of macrocyclic cavity unsubstituted β -CD.

**THERMODYNAMICS COMPLEXATION VOC WITH PERMETHYLATED CYCLODEXTRIN IN POLYMER SOLVENTS BY GC**

Kuraeva Yu.G., Onuchak L.A., Evdokimova M.A.
Samara National Research University, 443086 Samara, Russia
E-mail: kuraeva81@mail.ru

Chiral gas chromatography with cyclodextrin-containing stationary phases (SPs) is now widely used to separate and determine the enantiomers of volatile organic compounds. Capillary columns for chiral separations are usually manufactured using cyclodextrin derivatives dissolved in such low-polar SPs as polydimethylsiloxane and polymethylphenylsiloxane, or are grafted to polymer chains. The aim of this work is was to establish the thermodynamics of the sorption and the complexation of organic compounds of different classes from the gas phase on polymer – permethylated β -cyclodextrin SP, and to determine the effect the nature of sorbate molecules have on the possibility of their bonding to the macrocycle.

Polydimethylsiloxane oil $\text{CH}_3[-\text{SiO}(\text{CH}_3)_2-]_n\text{CH}_3$ (PMS-100, ~5000g/mol) and polyethylene glycol $\text{H}[-\text{OCH}_2\text{CH}_2-]_n\text{OH}$ (PEG-400, ~400g/mol) was used as the main component of SPs. Permethylated β -cyclodextrin such as *heptakis*(2,3,6-tri-*O*-methyl)- β -cyclodextrin (Me- β -CD, $M_r = 1429.6$, Sigma-Aldrich) (10 wt %) was added to PMS-100 and PEG-400. The stability constants K_1 of the the 1:1 sorbate-cyclodextrin inclusion complex were determined using the equation $K_C = K_C^0(1 + K_1 C_{cd})$, where K_C and K_C^0 are the partition coefficients of a sorbate in the polymer–Me- β -CD and polymer stationary phases, respectively, and C_{cd} is the cyclodextrin concentration.

In contrast to the rest of the investigated compounds, the distribution coefficient and heat of sorption values of C_6 – C_{10} alkanes diminished adding Me- β -CD to PMS-100. The increased solubility of alkanes in the low polarity polydimethylsiloxane matrix relative to the binary PMS–Me- β -CD system presumably caused the observed changes. In turn, the increased chemical potential of the cyclic hydrocarbons and polar compounds in PMS promotes the formation of their complexes with cyclodextrin. Evidently, the size, shape, polarity, and chirality of the sorbate molecules play an important role in this process. The PMS-100 – Me- β -CD stationary phase proved to be enantioselective towards optical isomers of limonene ($\alpha_{+/-} = 1.07$), camphene ($\alpha_{+/-} = 1.05$), and menthol ($\alpha_{+/-} = 1.12$, 120°C). It was assumed that the structure of a polymeric matrix remains unchanged by the addition of the solutes. The observed athermal and endothermic enthalpies of formation of host-guest complexes in the PMS–Me- β -CD system were presumably due to the lower polarity of the polymeric matrix and permethylated cyclodextrin, and to the partial blocking of cavity entrances by polymer chains.

Adding Me- β -CD to PEG-400 results reduces the K_C distribution constants of C_7 – C_9 *n*-alkanes and cyclohexane, while they increase in the case of other studied compounds with linear or cyclic molecular structure. The K_C/K_C^0 ratio proportional to the complex formation constant depends more on the geometrical structure of molecules (volume and anisometry) than on their polarity. The distribution constants of optical isomers of limonene and camphene selectively grow, indicating the enantioselectivity of the sorbent. The separation factors ($\alpha_{+/-}$) of limonene and camphene isomers determined at 90°C were 1.09 and 1.07, respectively.

The data obtained in this work confirm the conclusion that the formation of guest–host complexes in polymer solvents with additives of cyclodextrin and its derivatives is largely determined by the entropy factor.



THE SORPTION OF ORGANIC COMPOUNDS ON A SILICA GEL MODIFIED NICKEL NANOPARTICLES

E.G. Shubina¹, N.S. Filimonov¹, R.V. Shafigulin¹, A.V. Bulanova¹,
I.V. Shishkovskiy², Y.G. Morozov³

¹ Samara National Research University, Moskovskoye shosse, 34, Samara, 443086, Russia

² Samara Branch of the Lebedev Physical Institute, Russian Academy of Sciences Novo-Sadovaya Str. 221, 443011 Samara, Russia

³ Institute of Structural Macrokinetics and Materials Science of the Russian Academy of Sciences Acad. Osipyan Str. 8, 142432 Chernogolovka, Moscow Region, Russia
E-mail: ktyfvbn@mail.ru

Nickel nanoparticles deposited on the silica gel, are often used as catalysts in various industrial chemical processes including hydrogenation of unsaturated hydrocarbons. Thermodynamics of adsorption of unsaturated hydrocarbons on silica gel modified by nickel nanoparticles was investigated in this work.

Test nanoparticles were obtained levitation-jet method. According to the transmission electron microscopy nickel nanoparticles have a spherical shape and average size is 50-200 nm. Nickel nanoparticles were deposited on Silochrome C-120 (15 wt. % of Ni) from solution in hexane. Characteristics of the pore structure were examined by low-temperature nitrogen adsorption-desorption apparatus by ASAP 2010N (Micromeritics, USA). The specific surface area was 103,3 m²/g.

The adsorption properties of the composite (Ni/silohrom C-120) were tested by inverse gas chromatography, as the carrier gas was helium. As sorbates were taken various linear and cyclic hydrocarbons: hexane, 1-hexene, 1-hexyne, 1,5-hexadiene, cyclohexane, cyclohexene, 1,3-cyclohexadiene (1,3-CHD), 1,4-cyclohexadiene (1,4-CHD), and benzene. Study of the adsorption process carried out at temperatures of 383 K, 393 K, 403 K, 413 K and 423 K.

On the basis of experimental data, we calculated the specific retention volumes, the heat of adsorption and adsorption entropy.

These data indicate that the heat of adsorption increases with increasing multiplicity-C-bonds in the molecule. 1-hexyne is characterized by the highest heat of absorption, and hexane and cyclohexane have lowest heat of adsorption. Sorbate with double bonds have intermediate values of the heat of sorption.

This work was supported by grant RFBR № 15-43-02115 r_povolzhe_a



**THERMODYNAMICS OF SORPTION AND ENANTIOSELECTIVITY OF SYSTEM
"SUPRAMOLECULAR LIQUID CRYSTAL - ACETYLATED β -CYCLODEXTRIN" IN
GAS CHROMATOGRAPHY**

Tugaryova D.A., Kapralova T.S., Kuraeva Yu.G., Onuchak L.A.

Samara National Research University, 443086 Samara, Russia

E-mail: tugaryova_da@mail.ru

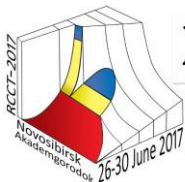
Development of universal sorbents for separation of structural and optical isomers is a perspective trend of modern gas chromatography. The solution to this problem is possible through a combination of selective properties of supramolecular (associate) liquid crystals (LC) and chiral macrocyclic compounds. β -CD and its various derivatives is used as chiral additives to LC. Purposeful change of mesomorphic, selective and sorption properties of composite sorbents LC can be achieved by varying the nature of the substituent and the degree of substitution in the β -CD molecule.

The aim of this study was to establish the influence of the degree of substitution of hydroxyl groups in β -CD on the Sorption and selective properties of supramolecular composite sorbents. Supramolecular smectic-nematic LC – 4-(3-hydroxypropyloxy)-4'-formylazobenzene (HPOFAB) was used as a matrix. Chiral macrocyclic components were acetylated β -CD derivatives having a degree of substitution of 87% ($\text{Ac}_{87\%}\text{-}\beta\text{-CD}$) and 100% ($\text{Ac-}\beta\text{-CD}$). The degree of substitution of β -CD was established by NMR.

The thermodynamic functions of adsorption from the gas phase of organic compounds of different classes on composite sorbents "HPOFAB – $\text{Ac}_{87\%}\text{-}\beta\text{-CD}$ " and "HPOFAB – $\text{Ac-}\beta\text{-CD}$ " were determined by inverse gas chromatography. The addition of the acetylated β -CD derivatives irrespective of the degree of substitution results in a better dissolution of most of sorbates in mixed S_A phases. Analysis of thermodynamic functions of sorption showed that an increase in the retention of sorbates while adding macrocycle due to the influence of the entropy factor ($\Delta(\Delta_{sp}\bar{S}_i^0) > 0$). This indicates that the molecular mobility of sorbates in mixed smectic A phase is higher than in the original HPOFAB. In turn, the weakening of the interaction "sorbate – sorbent" ($\Delta(\Delta_{sp}\bar{H}_i^0) > 0$) is offset by an increase in the number of possible conformations and increase freedom of rotational movement in S_A phases mixed sorbents.

The work also studied and compared the selective properties of the studied LC sorbents. It is shown that the binary sorbents "HPOFAB – $\text{Ac-}\beta\text{-CD}$ " and "HPOFAB – $\text{Ac}_{87\%}\text{-}\beta\text{-CD}$ " have about the same moderate structural selectivity to xylene isomers. The degree substitution of the hydroxyl groups in β -CD have more influence on enantioselective properties of composite sorbents "LC – macrocycle". Partial substitution of hydroxyl groups in the molecule acetyl β -CD leads to less shielding cavity of the macrocycle and makes it more accessible to the formation of complexes "guest - host" with sorbates. Thus, the sorbent "HPOFAB – $\text{Ac}_{87\%}\text{-}\beta\text{-CD}$ " has pronounced enantioselectivity towards optical isomers of camphene ($\alpha_{+/-} = 1,076$, 90 °C), α -pinene ($\alpha_{+/-} = 1,124$, 125 °C), limonene ($\alpha_{+/-} = 1,071$, 100 °C) and a polar optical isomers of menthol ($\alpha_{+/-} = 1,043$, 95 °C). Sorbent with additive of peracetylated $\text{Ac-}\beta\text{-CD}$ showed lower values of separation factors of low polarity optical isomers, and does not show selective activity towards polar enantiomers.

Thus, in this paper determined that for the creation of universal isomeraselective sorbents it is preferable to use supramolecular LC with additives of partially substituted β -CD. In this case, the β -CD cavity is more accessible for the formation of inclusion complexes "sorbate – macrocycle" due to the smaller shielding substituents located at the entrance to the cavity.



Section 5.

Applied aspects of chemical thermodynamics

Oral presentations



EVALUATION OF THE PROCESS EFFICIENCY OF THE EXTRACTION OF AROMATIC COMPOUNDS USING IONIC LIQUIDS FROM BIOMASS MATERIALS

Cesari L., Mutelet F.

Laboratoire Réactions et Génie des Procédés, 54000 Nancy, France

E-mail : laetitia.cesari1@gmail.com

The ligno-cellulosic biomass is the most abundant renewable resource in the world. It was referred as a waste and burned for energy for decades. It has only been recently, with the increase of global warming and the depletion of fossil fuels that lignocellulosic biomass could be considered as a promising feedstock for the production of fuels and chemicals. Equal to 25 wt% of the biomass, lignin could be a new source of aromatics compounds[1]. A particular attention was made on phenolic compounds because of their antioxidant or antimicrobial properties.

This presentation is devoted to the extraction of high value compounds from biomass materials using water and one ammonium based ionic liquid [choline][NTf₂]. Focus is made on four phenolic compounds (phenol, guaiacol, syringol and pyrocatechol). The presentation is divided into three parts.

First, the diagrams of the ternary systems {water + [choline][NTf₂] + phenolic compound} at 298K under atmospheric pressure are presented. Experimental data were used to regress the parameters of the NRTL[2] and UNIQUAC[3] thermodynamic models.

Secondly, the capacity of [choline][NTf₂] to extract phenolic compounds from aqueous solutions has been evaluated. The influence of several factors (time, temperature, amount of [choline][NTf₂]) have been investigated.

Finally, a process is proposed for the extraction and the recovery of the compounds of interest. Process sizing was designed using the thermodynamic parameters determined previously. Results show that this design is simpler and economically competitive compared to classical process using organic solvent.[4]

In conclusion, [choline][NTf₂] is appears to be an excellent media for liquid-liquid extraction of high value aromatics compounds from lignin.

[1] A. V. Bridgwater, D. Meier, and D. Radlein, "An overview of fast pyrolysis of biomass," *Org. Geochem.*, vol. 30, no. 12, pp. 1479–1493, Dec. 1999.

[2] H. Renon and J. M. Prausnitz, "Local compositions in thermodynamic excess functions for liquid mixtures," *AIChE J.*, vol. 14, no. 1, pp. 135–144, Jan. 1968.

[3] D. S. Abrams and J. M. Prausnitz, "Statistical thermodynamics of liquid mixtures: A new expression for the excess Gibbs energy of partly or completely miscible systems," *AIChE J.*, vol. 21, no. 1, pp. 116–128, Jan. 1975.

[4] X. Li, S. R. A. Kersten, and B. Schuur, "Extraction of Guaiacol from Model Pyrolytic Sugar Stream with Ionic Liquids," *Ind. Eng. Chem. Res.*, vol. 55, no. 16, pp. 4703–4710, Apr. 2016.

COMPOSITE “LiCl/VERMICULITE” AS WATER SORBENT FOR THERMAL ENERGY STORAGE

Grekova A.D.^{1,2}, Aristov Y.I.^{1,2}, Gordeeva L.G.^{1,2}

¹Boreshkov Institute of Catalysis, Siberian Branch of the Russian Academy of Sciences, 630090 Novosibirsk, Russia

²Novosibirsk State University, 630090 Novosibirsk, Russia

E-mail: grekova@catalysis.ru

A large barrier to successful utilization of renewable energy sources for heating/cooling is a mismatch between the production of and demand for the heat. For this reason the development of reliable thermal energy storage systems may promote the broader dissemination of energy saving technologies. Sorption heat storage (SHS) has gained large interest during the last decades due to its high heat storage density. SHS is based on reversible sorption (heat releasing) and desorption (heat storing) processes. The development of new advanced adsorbents is a prerequisite for successful SHS implementation. Among adsorbents suggested for SHS, the composites "salt in porous matrix" (CSPM) are considered promising due to their high Heat Storage Capacity (HSC) and tunable sorption behavior [1, 2]. This paper addresses the intent synthesis of novel CSPM, adapted for two SHS cycles: seasonal (SS), and daily (DS) heat storage.

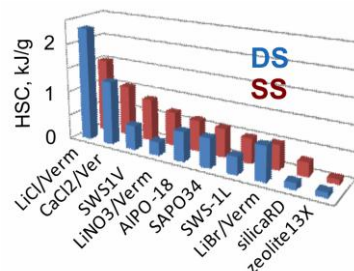


Figure 1. The HSC for different sorbents under SS and DS cycles conditions (working fluid - water).

Expanded vermiculite was used as a host matrix with large pore volume ($V_p = 2.7 \text{ cm}^3/\text{g}$), and LiCl as an active salt. The aims of this work are: 1) preparation of new composite specified for the abovementioned cycles; 2) investigation of its texture and phase composition; 3) study of equilibrium and dynamics of water sorption on the prepared material, and 4) evaluation of composite potential for SHS.

The XRD pattern of LiCl/vermiculite shows that LiCl forms well-crystallized phase (cubic lattice Fm-3m) in the vermiculite pores with the coherently scattering domains of 100 nm size. Isobars of water sorption on the composite are step-wise curves. At high temperature, the sorption is minor; at decreasing temperature the sorption steeply rises indicating the formation of $\text{LiCl} \cdot n\text{H}_2\text{O}$ ($n = 1, 2$). The new composites exchange 0.75 and 0.60 g/g of water under conditions of DS and SS cycles, respectively.

The isosteric heats of water sorption are evaluated as $(56 - 61) \pm 3 \text{ kJ/mol}$ at different uptake. The working pair LiCl(59 wt.)/vermiculite possesses HSC equal to 1.8 and 2.3 kJ/g under conditions of SS and DS cycles, respectively. These values are superior to appropriate HSCs (0.1 – 0.9 kJ/g) reported for the common and innovative adsorbents proposed for SHS [3].

The data on water sorption dynamics allows the estimation of the Specific Power (SP) of SHS unit, which can be reached utilizing the "LiCl/vermiculite - water" working pair with loose grains configuration of the adsorbent bed. The conversion was restricted by $q = 0.8$ in order to avoid strong falling down the power at approaching to the equilibrium. For the SS cycle and the studied configurations, the $\text{SP} = 3.4\text{-}15.6 \text{ kW/kg}$ are obtained. For the DS cycle, the SP for discharging and charging stages is essentially lower: 1.6-2.4 kW/kg, respectively. However, even under conditions of the DS cycle one needs only 0.5-1.3 kg or 1.5-3.5 dm^3 of the new sorbent to realize a 2 kW heating power that is very promising.

Thus, owing to their high HSC and SP values the new composite holds great promise for realization of the SHS cycles.

This work was conducted within the framework of budget project No. 0303-2016-0013 for Boreshkov Institute of Catalysis. Grekova A.D. thanks the Ministry of Education and Science of the Russian Federation (the Russian President's Scholarship SP-3769.2016.1)

1. Gordeeva, L; Aristov, Y, Int. J. Low Carbon Technol., 2012,7,288-302.
2. D. Aydin, S.P. Casey, S. Riffat, Renew. Sustain. Energy Rev. 2015,41,356-367.
3. Yu, N; Wang, R; Wang, L, Prog. Energy Comb. Sci., 2013,39,489-514.

PREDICTIVE THERMODYNAMIC MODELING – A POWERFUL TOOL FOR THE PROCESS DEVELOPMENT IN THE CHEMICAL INDUSTRY

Grütznert Th.¹, Lorenz H.-M.¹, Seyfang B. C.²

¹Lonza AG, Research & Development, Center of Excellence – Technology, 3930 Visp, Switzerland

²Lonza AG, Front End Development, 3930 Visp, Switzerland

E-mail: thomas.gruetzner@lonza.com

During the past years cost pressure on the European chemical companies grew dramatically by increased competition from low-labor-cost countries on the one side and the U.S., favored by decreased energy costs due to shale gas exploitation, on the other side. Raising costs for energy consumption and wages come on top. In order to maintain competitiveness, time-to-market is a crucial factor and many initiatives rose in the past years in both, chemical industry as well as academia, to accelerate development cycles. Within the procedure of process development, thermo-physical modeling is a very time and money consuming step. Very often data is not available for the relevant substances in the system to be modeled. Experimental determination is often not possible due to time and money related constraints or issues with toxicity or thermal process safety, especially in an early stage of process development. Predictive modeling for pure component and mixture data is an approach to overcome this problem. In combination with very specific lab trials this is a very powerful tool to build reliable thermodynamic models which can be applied for process simulation.

Using a real and complex example of developing an extractive dividing wall column (Figure 1) the above mentioned approach is explained in greater detail. The entrainer selection for the separation task as well as the entire process development and equipment design was carried out based on predictive models, e.g. COSMO-RS and modified UNIFAC. The model predictions have been verified by simple batch distillation experiments. Subsequently the model was implemented in a process simulator where all the optimization work was conducted. A pilot scale step has been skipped and the column was directly build and operated in the plant. A comparison of real plant data with the simulation results confirms the reliability of our approach.

As a result the time-to-market can be considerably reduced – a great step towards reducing cost and time for process development.

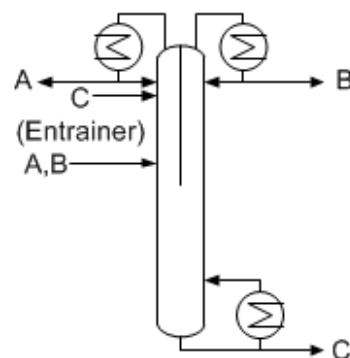


Figure 1. Extractive dividing wall column with a partitioning wall extended to the upper end of the equipment.



THERMODYNAMIC MODELING OF REAL MULTICOMPONENT PROCESS SOLUTIONS - SUCCESSFUL PROCESS OPTIMIZATION IN CHEMICAL INDUSTRY

Lorenz H.-M.¹, Staak D.¹, Grützner Th.¹, Seyfang B. C.²

¹Lonza AG, Research & Development, Process Technologies & Innovation, 3930 Visp, Switzerland

²Lonza AG, Front End Development, 3930 Visp, Switzerland

E-mail: hilke.lorenz@lonza.com

Due to an increasing energy demand and to the shortage of fossil resources, sustainable and efficient processes in the chemical industry become more and more important. The continuous improvement and development of existing industrial processes offer a high potential to increase the efficiency. Since it is still a major challenge to make changes in a running plant, in particular if the process comprises a large number of components, unit operations and internal recycle streams, effective process analysis and optimization is crucial.

An established way for optimization of processes in the chemical industry is the simulation in a flow sheet simulation tool (e. g. Aspen Plus, Chemcad). A wide range of different unit operations and thermodynamic models are implemented in these programs. In industry, the assumption of thermodynamic equilibrium is the most common way to describe the important vapor-liquid equilibria found in distillation columns. Thus, interaction parameters for all binary component groups are required for a representative simulation. In real process solutions this number is often very high due to side products and impurities in raw materials.

Lonza uses a combination of different approaches to describe the thermodynamic behavior of such complex mixtures. A special accuracy-significance-matrix is developed in order to prioritize binary systems. Thus, even for multicomponent mixtures, an efficient and reliable prediction of boiling behaviors is possible.

The contribution presents an industrially applied example of a modeling approach described above. The process solution contains more than 20 known and numerous unknown components. Based on the different approaches such as predictive methods, lab experiments or a combination of both, a detailed model can be developed. Additionally, unknown components can be represented by pseudo components. This model is then successfully verified with data received from a world-scale plant under full capacity production. Thus, the reliable and detailed model is used for a reduction of production costs, for improvement in efficiency and for securing competitiveness.

EVALUATION ADSORPTION HEAT AMMINE PLATINUM COMPLEX (II) AND (IV) ON THE OXIDATION OF THE NANOPOROUS CARBON MATERIALS

Mikheev A.N.^{1,2}, Levchenko L.M.¹, Matskevich N.I.¹, Pishchur D.P.¹, Kerzhentseva V.E.¹, Gelfond N.V.¹

¹Federal State Budget Institution of Science Institute of Inorganic Chemistry. AV Nikolaev SB RAS, Novosibirsk

²National Research Novosibirsk State University, Russia

E-mail: man@niic.nsc.ru

In this work, the thermodynamic characteristics of the interaction of cis- [Pt (NH₃)₂Cl₂] and cis-[Pt (NH₃)₂Cl₂(OH)₂] with the oxidized nanoporous carbon material were determined. The oxidized nanoporous carbon material (NUMS₇₀₋₃₀), (a specific surface area 330 m²/g, amount of carboxyl groups – 3,5 ± 0,2%, hydroxyl – 1.17 ± 0.10) was used as a container for complexes of platinum (II) and (IV).

The heat capacity of the samples of cis-[Pt (NH₃)₂Cl₂], cis-[Pt(NH₃)₂Cl₂(OH)₂] and carbon materials NUMS₇₀₋₃₀ platinum complexes was measured with a differential scanning calorimeter NETZSCH DSC 204 F1 Phoenix in the temperature range of 173–373 K.

To quantify the effect of the interaction of platinum complexes with the oxidized surface carbon the heat curves in the temperature range of 170÷370 K were obtained (Figure 1). All the experimental data are characterized by a bend at ~ 270 K, which is obviously due to the melting of ice in the samples due to the humidity of the analyzed samples.

The specimens contain moisture in the range of 0.2–0.3%. To assess the effects of thermal interaction of the carbon material and platinum compounds is used the temperature range from 280 to 370 K. The thermal effects of obtained values are shown in Table 1.

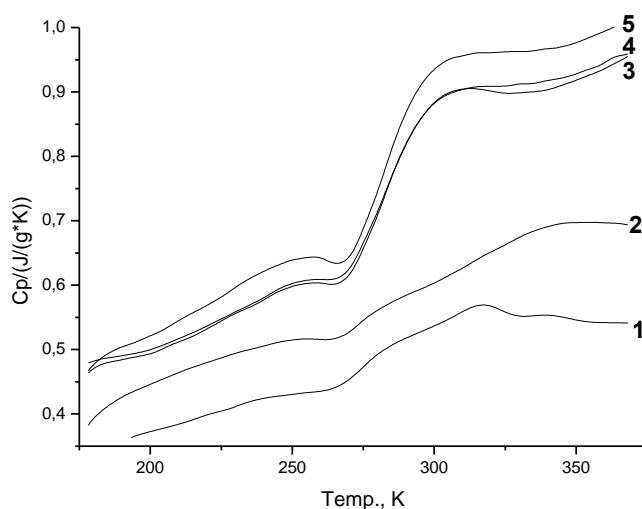


Figure 1. The temperature dependence of the heat capacity of the samples:
 1 - cis-[Pt(NH₃)₂Cl₂];
 2 - cis- [Pt (NH₃)₂Cl₂ (OH)₂];
 3- NUMS₇₀₋₃₀ sorbent;
 4 - cis- [Pt (NH₃)₂Cl₂] on NUMS₇₀₋₃₀;
 5 - cis- [Pt (NH₃)₂Cl₂ (OH)₂] on NUMS₇₀₋₃₀.

Table 1. Values of the thermal effects of interaction between the platinum salt and NUMS₇₀₋₃₀

Sample	ΔJ , J/g	ΔJ_k , J/mol
NUMS ₇₀₋₃₀ + cis- [Pt(NH ₃) ₂ Cl ₂]	88,2	24,46
NUMS ₇₀₋₃₀ + cis- [Pt(NH ₃) ₂ Cl ₂ (OH) ₂]	82,2	27,46

Values of the thermal effects favor the physical adsorption mechanism, since this process characterized by low heat of adsorption values – from 8 to 34 kJ/mol. However, taking into account the data obtained by other physical and chemical methods, namely the formation of a hydrogen bond between the carboxyl groups and ammine groups of platinum complexes, in this case adsorption should be regarded as an intermediate case between physical and chemical adsorption.



SYNTHESIS AND CONCENTRATION OF BIMETALLIC Cu/Ag NANOPARTICLES STABILIZED BY AOT

Popovetskiy P.S., Arymbaeva A.T., Demidova M.G., Bulavchenko A.I.

Nikolaev Institute of Inorganic Chemistry, Siberian Branch of the Russian Academy of Sciences, 630090, Novosibirsk, Russia

E-mail: popovetskiy@niic.nsc.ru

The printing electronics is one of the most promising areas of modern high-tech manufacturing. This area of electronics allows you to create conductive electronic circuits using printing equipment. Researches in the field of new inks for printed electronics recipes creation is carried out worldwide. Silver and gold nanoparticles are the most widely used as the main component of such inks because of the high corrosion resistance and electrical conductivity of silver and gold. High cost of silver and gold prevents the spread of this technology, because metal content in the inks should be tens of percent by weight. Partial or complete replacement of silver and gold by copper is actual scientific and technical task. Copper exceeds gold and almost as good as silver by electrical conductivity but it has a much lower cost.

We obtained nanoparticles containing silver and copper in various proportions (copper content was varied from 0 to 100%) using oil-soluble surfactant sodium bis-(2-ethylhexyl)sulfosuccinate (AOT) as stabilizer and n-decane as solvent. Using the authors' non-aqueous electrophoretic technique [1] concentrated organosols were separated. Metal ratio in concentrate corresponds to that in the initial organosol before concentration according to the atomic absorption analysis. This technique allows separating AOT reverse micelles containing nanoparticle in the polar cavities from micelles containing only reaction by-products and water. We use chloroform additives (more polar solvent than the n-decane) for increase the surface potential of nanoparticles and for more complete separation [2]. The particle dispersity was controlled using spectrophotometry by changes in position and intensity of plasmon resonance peaks. Nanoparticles hydrodynamic diameter at various AOT concentrations (including concentration below the critical micelle concentration) was evaluated by dynamic light scattering. Increasing of the nanoparticles hydrodynamic diameter is observed at high concentrations of AOT for all metal ratios investigated. The increase of the hydrodynamic diameter is due to AOT micelles adsorption [3]. Concentrated organosols were also tested for producing of conductive coatings using thermal and chemical treatment.

Acknowledgement: This work was supported by the Russian Science Foundation (project № 15-13-00080). Authors wish to thank Ph.D. Petrova N.S.

[1] Bulavchenko, A; Popovetskiy, P. *Langmuir.*, 2010, 26, 736-742.

[2] Popovetskiy, P; Bulavchenko, A; Demidova, M; Podlipskaya, T. *Colloid. J.*, 2015, 77, 58-64.

[3] Bulavchenko, A; Popovetskiy, P. *Langmuir.*, 2014, 30, 12729-12735.

SALT EFFECT ON LLE OF WATER–1-BUTANOL–LACTIC ACID SYSTEM AND ITS APPLICATION IN LACTIC ACID EXTRACTION

Chawong K., Rattanaphanee P.

School of Chemical Engineering, Institute of Engineering, Suranaree University of Technology,
30000, Nakhon Ratchasima Thailand
E-mail: panarat@sut.ac.th

Lactic acid is widely used in many industries including food additives, cosmetic, pharmaceuticals, as well as lactic-based biodegradable polymer production. The acid is preferentially produced by bacterial fermentation and has to be isolate and purified from the fermentation broth after the production is terminated. The broth normally contains various kinds of impurities including hydrophilic salts and ions, which can lead to high production cost of this acid due mostly to the complicated and multistep separation processes needed.

Numerous separation and purification techniques have been proposed for recovery of lactic acid from the fermentation media, and solvent extraction is one among them. In this research, extraction of lactic acid from its aqueous solution using 1-butanol of 303.15 K was studied. Liquid-liquid equilibrium (LLE) of water–1-butanol–lactic acid mixture was first studied. The experimental data was correlated by UNIQUAC model and satisfactory agreement was achieved with the average root mean square absolute deviation of 0.3417%. It appeared in this study that 1-butanol could extract lactic acid and extraction efficiency increased with initial acid concentration in the starting solution.

$$D = \frac{[LA]_{org} V_{org}}{[LA]_{aq} V_{aq}} \quad (1)$$

Effect of salt types and concentrations on the LLE behavior of this mixture in the presence of different inorganic salts, i.e. NaCl, Na₂SO₄, NH₄Cl and (NH₄)₂SO₄ was then investigated. Distribution of lactic acid among each phase was expressed by the distribution coefficient (K_D) of lactic acid in each

system. Since water and 1-butanol are partially miscible, volumes of the aqueous (V_{aq}) and organic (V_{org}) phase the extraction was differed from their initial volumes. These variables are, therefore, incorporated in the calculation in addition to equilibrium lactic acid concentration in the organic ($[LA]_{org}$) and aqueous ($[LA]_{aq}$) phase as shown in Eq.(1).

Figure 1. shows relationship between K_D and the ionic strength, which reflects the salt concentration in each system. In the system with NaCl and NH₄Cl, K_D slightly decreases with increasing of the salt content in the system. This can be considered as salting-in where lactic acid becomes more soluble in the aqueous phase when these salts are added. Na₂SO₄ and (NH₄)₂SO₄ produces opposite effect, salting out, as K_D substantially increased upon the addition of the salts. It is concluded in this study that types and concentration of inorganic salts in the aqueous solution, hence fermentation broth, do effect efficiency of lactic acid extraction using 1-butanol. This result could be a guidance for selection of either the neutralizing base or mineral salts to be added during fermentation. It can also be useful in choosing a particular salt as an extraction aid in lactic acid, or other organic acid, recovery by solvent extraction.

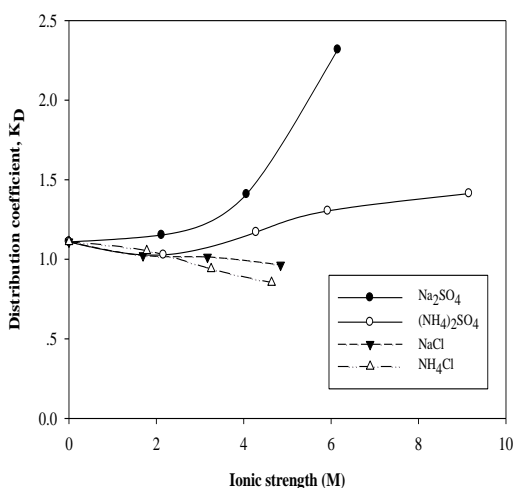


Figure 1. Effect of ionic strength on distribution of lactic acid for extraction with initial acid concentration 1 M

It can also be useful in choosing a particular salt as an extraction aid in lactic acid, or other organic acid, recovery by solvent extraction.

THE THERMAL PROPERTIES OF DONOR-ACCEPTOR CHROMOPHORE-POLYMER COMPOSITES FOR NONLINEAR OPTICAL APPLICATION

V.V. Shelkovnikov¹, G. A. Selivanova¹, S.V. Korotaev¹, I.K. Shundrina¹, I.Yu. Kargapolova¹, N.A. Orlova¹, D.I. Derevyanko¹, A.I. Plekhanov², S. L. Mikerin², A.E. Simanchuk²

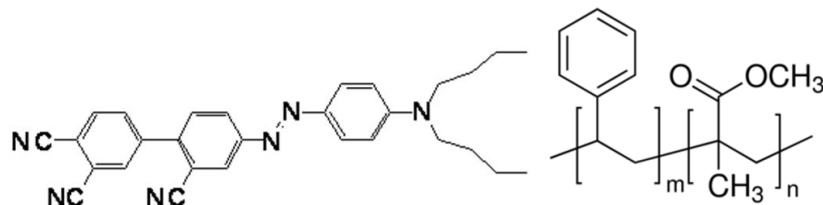
¹ N.N. Vorozhtzov Novosibirsk Institute of Organic Chemistry, Siberian Branch of the Russian Academy of Sciences, 630090, Novosibirsk, pr. Lavrentjeva, 9, Russia

² Institute of Automation and Electrometry, Siberian Branch of the Russian Academy of Sciences, 630090, Novosibirsk, pr. Koptyuga 1, Russia

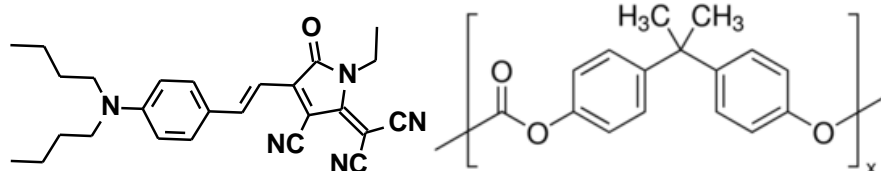
E-mail: vice@nioch.nsc.ru

The nonlinear optical properties of the donor-acceptor chromophores in polymer matrix attract the great interest being connected with the material searching for radiophotonics application. That material has to poses the high thermal stability apart from the second order optical nonlinearity itself. There are two reasons why the material has to poses the high thermal stability: the first for one is the burning of the spin-coated chromophore-polymer films to remove the high-boiling organic solvent at the temperature higher 100 °C; the second one is the poling of the chromophore-polymer films at the action of the electrical field at the temperature higher the glass-transition temperature of the polymer matrix.

The chromophore-polymer films containing the synthesized donor-acceptor GAS1 chromophore structure and copolymer polystyrole-methylmetacrylate (PSMMA), hybrid organic-inorganic photopolymer matrix and tricyanopyrroline styryle (TPCS) chromophore in Poly(Bisphenol-A carbonate - PBC) matrix (the structures are shown below) were obtained and investigated by the thermal analysis methods. The determination of the nonlinear optical properties of guest-host chromophore-polymer films were carried out also.



GAS1 chromophore structure in copolymer (PSMMA) matrix



TPCS chromophore structure in PBC matrix

The features of the thermal behavior of the polymer films with the synthesized chromophores and the comparison of the thermal and nonlinear optical properties of the some chromophores in the poled polymers are discussed in the report. In particular, it is shown that introduction the GAS1 chromophore 10 wt.% to the photopolymer hybrid composition leads to the photopolymerisation difficulty and to the lowering of the photopolymer film glass transition temperature more than 60 °C.

Acknowledgement. The authors are grateful to the RSF (grant N 16-13-10156) for the financial support.

EVIDENCE OF CARBIDE PHASES $\text{Ni}_x\text{Pd}_{1-x}\text{C}_\delta$ FORMATION IN THE PROCESS OF CHLORINATED HYDROCARBONS DECOMPOSITION ON Ni-Pd CATALYSTS

Shorstkaya Yu.V.¹, Bauman Yu.I.², Shubin Yu.V.^{1,3}, Plyusnin P.E.^{1,3}, Mishakov I.V.^{2,4}

¹Nikolaev Institute of Inorganic Chemistry, Siberian Branch of the Russian Academy of Sciences, 630090 Novosibirsk, Russia

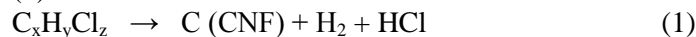
²Boreskov Institute of Catalysis, Siberian Branch, Russian Academy of Sciences, pr. Lavrentieva 5, Novosibirsk, 630090

³Novosibirsk State University, 2 Pirogova Str., Novosibirsk, 630090

⁴National Research Tomsk Polytechnic University, Lenin Avenue 30, Tomsk, 634050

E-mail: shorstkaya@niic.nsc.ru

In present work we consider in detail the carbide phases $\text{Ni}_x\text{Pd}_{1-x}\text{C}_\delta$ formation in the process of chlorinated hydrocarbons decomposition at 600 °C over $\text{Ni}_{0.95}\text{Pd}_{0.05}$ catalyst. A number of specimens, reacted with 1,2-dichloroethane for 6, 12, 18, 30, 60 min were investigated. The powder X-ray diffraction analysis (XRD) of these specimens confirms the formation of carbide phases $\text{Ni}_x\text{Pd}_{1-x}\text{C}_\delta$ for all samples. Via calculating of the lattice parameters for all samples the carbide phases $\text{Ni}_x\text{Pd}_{1-x}\text{C}_\delta$ formation is proved. The recycling of Cl-containing organic wastes, including variety of chlorinated hydrocarbons, is known to be rather difficult and important ecological problem. One of the actively used recycling methods is catalytic decomposition of chlorinated hydrocarbons on Ni, Co, Fe metals. It results in formation of carbon nanomaterial (CNF) – a developed surface nanofibers [1]. Depending on reaction's conditions the decomposition of chlorinated hydrocarbons can proceed in several directions [2]. At $T < 500$ °C the process occurs as hydrogenolysis of C-Cl bond, which results in generation of hydrocarbons without chlorine in their composition. If the temperature is higher than 500 °C, catalytic decomposition of Cl-containing hydrocarbons occurs and carbon nanomaterial is formed (1).



For this research 1,2-dichloroethane (DCE) was selected as a model chlorinated hydrocarbon to be processed via catalytic decomposition over $\text{Ni}_x\text{Pd}_{1-x}$ alloy [3]. To investigate the process of formation of catalyst's active particles (sites) and initial stages of generation of carbon fibers we carried out the ex-situ powder X-ray diffraction analysis (XRD) of $\text{Ni}_{0.95}\text{Pd}_{0.05}$ alloy after 6, 18, 30, 60 min reaction with 1,2-dichloroethane decomposition at 600 °C. XRD pattern of $\text{Ni}_x\text{Pd}_{1-x}\text{C}_\delta$ specimen (far angles reflex – 331), reacted with DCE for 6 min, demonstrates a shift of the peak to the low-angle region (Fig. 1).

The lattice parameters for $\text{Ni}_{0.95}\text{Pd}_{0.05}$ kept under catalytic experiment conditions were found to be increased by 0.003-0.004 in comparison with initial catalyst. This lattice parameter increase is explained by the entry of carbon into the alloy's crystal lattice with formation of interstitial solid solution phase $\text{Ni}_x\text{Pd}_{1-x}\text{C}_\delta$. Formation of nonstoichiometric carbide correspond to carbon solubility in Ni and Pd known data [4,5].

[1] V.V. Chesnokov, R.A. Buyanov. Uspekhi Khimii (in Russian). Vol. 69. № 7 (2000) P. 675–692.

[2] I.V. Mishakov, V.V. Chesnokov, R.A. Buyanov, N.A. Pakhomov. Kinet. Catal. 42 (2001) 598–603.

[3] Yu.I. Bauman, Yu.V. Shorstkaya, I.V. Mishakov, P.E. Plyusnin, Yu.V. Shubin, D.V. Korneev, V.O. Stoyanovskii, A.A. Vedyagin. Catalysis Today, 2016. doi: 10.1016/j.cattod.2016.11.020.

[4] Lander J.J., Kern H.E., Beach A.L. J. Appl. Phys. 1952. Vol. 23, № 12. P. 1305.

[5] Massalski T.B. Binary Alloy Phase Diagrams. 2nd ed. ASM International, 1990. P. 1100.

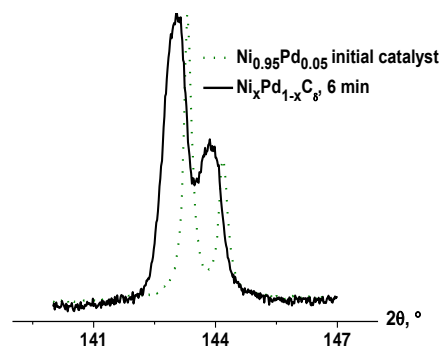


Figure 1. X-ray diffraction reflexes (331) in far angles for $\text{Ni}_{0.95}\text{Pd}_{0.05}$ alloy and $\text{Ni}_x\text{Pd}_{1-x}\text{C}_\delta$ specimen, reacted with DCE for 6 min.

NEW Pd(II) AND Cu(II) β -KETOIMINATES' THERMAL BEHAVIOR AS A CLUE FOR SUCCESSFUL DEPOSITION OF Pd_{1-x}Cu_x SYSTEMS BY MOCVD

Shushanyan A.D.^{1,2}, Nikolaeva N.S.¹, Zelenina L.N.^{1,2}, Dorovskikh S.I.^{1,2}, Sysoev S.V.¹, Trubin S.V.¹, Morozova N.B.¹

¹Nikolaev Institute of Inorganic Chemistry, Siberian Branch of the Russian Academy of Sciences, 630090 Novosibirsk, Russia

²Novosibirsk State University, 630090 Novosibirsk, Russia

E-mail: shushart@yandex.ru

For hydrogen separation and purification (>99.9999%) from gas mixtures inorganic membranes based on different metals and alloys [1] are widely used. Palladium-based ones (e. g. Pd-Au, Pd-Ag, Pd-Ru, Pd-Y etc.) are the most popular due to their high permeability and hydrogen selectivity. However pure palladium-based membranes suffer from phase transition and H₂S, CO₂ and O₂ impacts. Within this study our attention is focused on Pd-Cu systems by reason of their high permeability, reaction resistance and low cost. To obtain Pd-Cu layers on different geometrically complicated formed substrates metal-organic chemical vapor deposition (MOCVD) can be used. MOCVD process requires application of precursors which are volatile, thermally stable etc. β -diketonate derivatives of Pd(II) and Cu(II), particularly their β -ketoiminates, are extremely demanded as MOCVD-precursors.

Our goal within this work is to investigate thermal behavior of new Pd(II) and Cu(II) and find the pair of precursors with compatible thermal properties for single process codeposition of Pd-Cu films by means of MOCVD method.

Three new β -ketoiminates of Pd(II) and Cu(II) with common formula (fig. 1) M(CF₃C(O)CHC(NY)CH₃)₂, Y = N(CH₃)₂ (dmht), Y = CH₃ (Mei-tfac) were synthesized and identified by elemental analysis, IR-, NMR- and mass-spectrometry and X-ray analysis. Thermal behavior of Pd(dmht)₂ and Cu(dmht)₂ in condensed state was investigated by TG-DTA method. Those complexes transfer into the gaseous phase with a partial decomposition (Δm (%): Pd(dmht)₂ (90), Cu(dmht)₂ (85)). Endo-effects on DTA-curves indicate on melting points of samples (T_{melt}, (°C): Pd(dmht)₂ (140), Cu(dmht)₂ (120)). By means of DSC method the thermodynamic parameters of Cu(dmht)₂ melting were defined (T_{melt} = 122.65 C, $\Delta_{melt}H = (27.2 \pm 0.5) \text{ kJ}\cdot\text{mol}^{-1}$, $\Delta_{melt}S^\circ = (68.7 \pm 0.6) \text{ J}\cdot\text{mol}^{-1}\cdot\text{K}^{-1}$). Using Knudsen's effusion method and the flow method for Cu(dmht)₂ and Pd(dmht)₂ complexes the temperature dependencies of saturated vapor were investigated and thermodynamic parameters of sublimation process were calculated (table 1).

Using new Pd(II) and Cu(II) complexes as MOCVD precursors Pd-Cu films have been obtained. Varying the experiment conditions we have obtained PdCu-containing films with different composition, microstructure and thickness in a single process.



Figure 1. Common formula of new β -ketoiminates

Table 1. Thermodynamic parameters of Pd(dmht)₂ and Cu(dmht)₂ vaporization processes

Compound	Method	Process	ln(p, Pa) = A -		$-\Delta H_{T^*}$, kJ/mol	$\Delta S_{T^*}^\circ$, J/mol·K	Temperature range, K
			A	B			
Pd(dmht) ₂	flow	subl.	39.1	14128	117.5±1.5	229.6±4.0	343-388
Cu(dmht) ₂	K. effusion	subl.	39.6	13936	115.8±3.6	234.0±10.7	321-351
Cu(dmht) ₂	*	evap.	31.4	10664	88.6±4.1	165.3±11.3	—

* calculated with DSC data

[1] Ockwig N., Nenoff T. Chemical Reviews. 2007, 10 (107), 4078–4110.

CONTINUOUS PREFERENTIAL CRYSTALLIZATION OF A CHIRAL API

 Temmel E.¹, Bartz A.¹, Lorenz H.¹, Seidel-Morgenstern A.^{1,2}
¹ Max Planck Institute for Dynamics Complex Technical Systems, 39106 Magdeburg, Germany

² Otto von Guericke University, Chair of chemical process engineering, 39106 Magdeburg, Germany

E-mail: temmel@mpi-magdeburg.mpg.de

Guaifenesin (3-(2-Methoxyphenoxy)-propane-1,2-diol) is a chiral active pharmaceutical ingredient (API) that was successfully applied against respiratory diseases with an expectorant and decongestant effect. Furthermore it is utilized as a precursor of muscle relaxants and tranquilizers which are synthesized from the enantiomers of this substance. Commonly guaifenesin is produced with a racemic composition and thus requires a subsequent separation of the stereoisomers. Preferential crystallization can be applied for this purpose as a cost efficient technique to provide enantiopure substances.

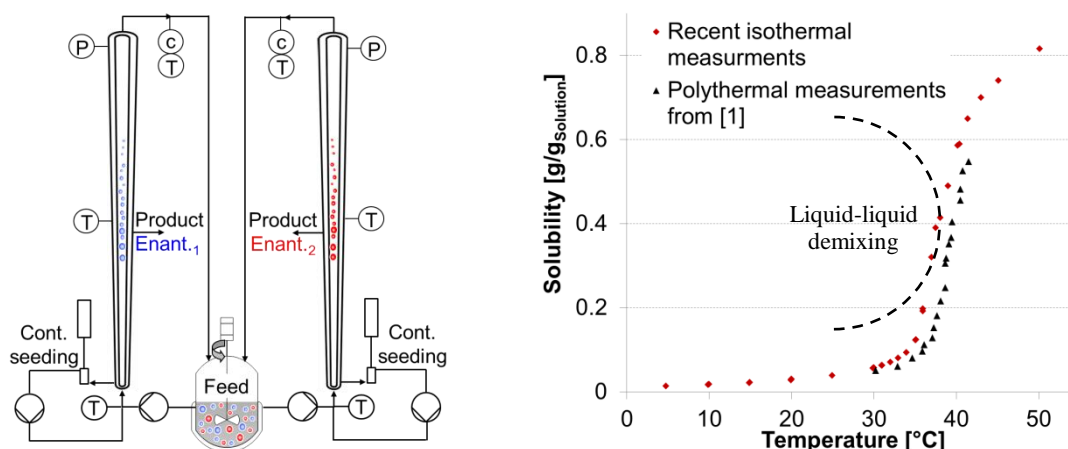


Figure 1: left: scheme of the continuous preferential crystallization in fluidized beds. Right: Solubility curve of the racemic guaifenesin with suspected liquid-liquid demixing in the supersaturated zone.

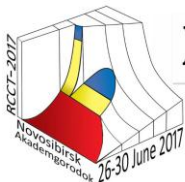
A fluidized bed process is utilized to perform a continuous preferential crystallization (Fig. 1, left) of guaifenesin. Therefore, two coupled tubular crystallizers with a conical shape are fed with a racemic solution and seeded with crystalline material of one of the enantiomers. Hence, the stereoisomers are selectively removed from the solution. The depleted mother liquors are enriched again in the feed tank where a suspension of the liquid phase and solid racemic guaifenesin is present. This ensures that always a solution saturated at feed temperature with a 50:50 composition is transported into the columns. Additionally, permanent seeding is necessary to operate the process continuously since secondary nuclei are transported out of the columns by the liquid stream. Therefore, large particles located at the bottom of the columns are withdrawn and crushed in a bypass. The fragments are transported back to the crystallization to serve as new seeds.

In the contribution, the design and operation of this process will be discussed based on the measured solid-liquid equilibrium (Fig. 1, right). Here, the strong increase in solubility of the guaifenesin probably caused by a metastable liquid-liquid demixing is of special interest. Such a phase separation can lead to unexpected and massive primary nucleation during the process and needs to be investigated in detail to produce pure components.

Furthermore, the initial seed generation utilizing a coupled batch process for preferential crystallization will be explained as well as the experimental procedure and setup of the continuous fluidized bed crystallization. Finally, the results of the actual separation process will be presented.

References

[1] Fayzullin, R. R.; Lorenz, H.; Bredikhina, Z. A.; Bredikhin, A. A.; Seidel-Morgenstern, A. J. *Pharm. Sciences*, 2014, 103, 3176-3182.



Section 5.

Applied aspects of chemical thermodynamics

Poster presentations



NONIONIC OXYETHELATED SURFACTANT SALTING-OUT BY INORGANIC SALTS

Elokhov A.M.^{1,2}, Stankova A.V.², Kudryashova O.S.³, Lesnov A.E.¹

¹*Institute of Technical Chemistry UB RAS. 3, Akademik Korolev St., Perm, 614013*

²*Perm State University. 4, Bukirev St., Perm, 614990*

³*Institute of Natural Science, Perm State University. 4, Genkel St., Perm, 614990.*

E-mail: elhalex@yandex.ru

There has been transition from traditional extraction systems containing organic solvent to systems including surfactants and water soluble polymers in recent years. Stratification in this case is a result of salting-out or heating of aqueous solutions above cloud point temperature. The main problem of similar systems development is salting-out agent selection and optimization of temperature and concentration extraction parameters. Phase diagram investigation of salting-out agent – surfactant – water systems allows to determine temperature of delamination area existence, to estimate the salts salting-out ability with temperature increase and to select optimal extraction parameters by analysis of system isothermal diagram at optimal temperature.

This work summarizes results of inorganic salts salting-out ability study in relation to technical oxyethelated nonionic surfactants – monoalkyl polyethylene glycols ($C_nH_{2n-1}O(C_2H_4O)_{10}H$, $n = 10-18$ for Synthanol DS-10, $n = 10-12$ for Synthanol ALM-10) and oxyethelated nonylphenols ($C_9H_{19}(C_6H_4O)(CH_2CH_2O)_nH$, $n = 12$ for Neonol AF 9-12 and $n = 25$ for Neonol AF 9-25).

Inorganic salts salting-out ability was determined by plotting of sections polytherms containing fixed amount of surfactant (5.0 wt% for the Sinthanol DS-10, Synthanol ALM-10 and Neonol AF 9-12; 4.3 wt% Neonol AF-9-25). Polytherm constructed in temperature versus salting-out ion molality concentration coordinates allows tracking changes inorganic salts salting-out ability depending on salts nature, surfactants structure and temperature.

It is shown that anions possess salting-out action and cations – salting-in action in relation to oxyethelated nonionic surfactant which is correlated with ion hydration energy. The formation of stratification region in salting-out agent - oxyethelated surfactant - water systems is determined by several interactions.

1. Surfactant micelles partial dehydration with increasing temperature due to conformational changes of surfactant molecules oxyethylene fragments. This effect is observed at temperature close to cloud point of aqueous surfactant solutions without salting-out agent, which leads to leveling influence ions nature on salting-out process with increasing temperature.

2. Hydration salt ions associated with dehydration or hydration of surfactant micelles, depending on the cation and anion nature.

3. Possibility of adsorption of low hydrated and easily polarizable anions on surfactant micelles surface and lowering salt salting-out ability.

4. Possibility of ion-dipole interaction between salting-out agent cation and oxygen atoms of surfactant molecules oxyethylene fragments, which is accompanied by decrease of salt salting-out ability.

Contribution of each factor into observable temperature and concentration boundaries of stratification region is determined by temperature, nature and concentration of salts in mixtures.

The obtained data allowed establishing influence surfactant structure on ability to salting-out by inorganic salts. It was shown that dominant role in salting-out process is playing surfactant molecule hydrophilic moiety - increase of surfactant degree oxyethylation reduces its ability to salting-out by inorganic salts. At the same time hydrophobic moieties structure almost has no influence on ability to salting-out by inorganic salts.

Established regularities of oxyethylated nonionic surfactant salting-out by inorganic salts can be used for targeted selection of salting-out agent in extraction systems development.



LIQUID-LIQUID EQUILIBRIA IN THE $\text{H}_2\text{O} - \text{HNO}_3 - (\text{C}_4\text{H}_9\text{O})_3\text{PO} - \text{Nd}(\text{NO}_3)_3 - \text{Sm}(\text{NO}_3)_3 - \text{Eu}(\text{NO}_3)_3$ SYSTEM

Dement'ev P.D.¹, Arkhipin A.S.², Kovalenko N.A.¹

¹Chemistry Department, Lomonosov Moscow State University
119991, GSP-1, 1-3 Leninskie Gory, Moscow, Russia

²Department of Materials Science, Lomonosov Moscow State University
119991, GSP-1, 1-73 Leninskie Gory, Laboratory Building B, Moscow, Russia
E-mail: pd.dementev@yandex.ru, arkhipinmsu@gmail.com

The continuously increasing world market demand for rare earth elements (REE) forces the intense development of new technologies of processing REE, as well as improvement of existing technologies. Usually pure rare earth elements are obtained by liquid extraction. As an example, research and collection of the data on phase equilibria in the lanthanides – nitric acid – organic extractant (in our case – tributyl phosphate, TBP) systems are necessary to construct an accurate model of extraction cascades. Available publications on the similar subject give a very limited knowledge on the distribution coefficients in the multi-component system, and lack the information on the complete composition of the equilibrium phases. For closing this gap new experimental data are needed.

The purpose of the current research was to obtain new experimental data in the extraction system water – nitric acid – tributyl phosphate – neodymium nitrate – samarium nitrate – europium nitrate. The work consisted of two parts: extraction experiments and determination of the equilibrium phases composition.

Extraction experiments were conducted at 298 K. For preparing initial mixtures for extraction experiments lanthanide nitrate hydrates, TBP, water and nitric acid were used. Our research covered a wide range of concentration of REE nitrates and nitric acid. The mixtures under study were placed in separating funnels, then the content of funnels was mixed using shaker for 1 hour and the mixtures were left in the air thermostat for at least ten hours. After separating by decantation liquid phases were analyzed. The content of lanthanides in the aqueous phase was determined by ICP-AES. For determination of REE in the organic phase multistage re-extraction was used with further analysis of the extract. The content of nitric acid in the aqueous and organic phases was determined by acid-base potentiometric titration.

As a result liquid-liquid equilibria data in the REE nitrates – nitric acid – water – tributyl phosphate system were obtained and REE partition coefficients and separation factor between aqueous and organic phases have been calculated. The current research is a part of the project devoted to the thermodynamic investigation of liquid extraction which is realized at the Laboratory of Chemical Thermodynamics, Lomonosov Moscow State University. And obtained liquid-liquid equilibria data in the next step of the work will be used for construction of the thermodynamic model of the water – nitric acid – lanthanide (Nd, Sm, Eu) nitrates – TBP systems.

The work was financially supported by RFBR according to the research project No. 16-33-01038 mol_a and by the URALCHEM Holding.



SULFUR INDUCED BREAKAWAY OXIDATION OF AUSTENITIC STAINLESS STEELS: EXPERIMENTAL AND THERMODYNAMIC STUDIES

E. Fedorova^{1,2}, M. Mantel^{3,4}, C. Pascal³, V. Parry³, M. Braccini³, Y. Wouters³, D. Oquab⁵, D. Monceau⁵

¹Siberian Federal University, 660041, Krasnoyarsk, Russia

²Institute of Computational Technologies SB RAS, SKTB "Nauka, 660049, Krasnoyarsk, Russia

³Univ. Grenoble Alpes, CNRS, SIMaP, F-38000 Grenoble, France

⁴UGITECH SA, Ugine, France

⁵Univ. Toulouse, Institut Carnot CIRIMAT, ENSIACET, F-31030 Toulouse, France

E-mail: efedorova@sfu-kras.ru

Negative effect of sulfur on the protective behavior of oxide layers grown on alumina or chromia forming alloys during high temperature isothermal or cyclic oxidation is known and has been widely studied.

The present work focuses on the effect of alloyed sulfur as MnS inclusions in chromia forming austenitic stainless steels under severe experimental conditions. AISI 304L and AISI 303, with close compositions except their sulfur content (0.025 and 0.249 wt.% S respectively), were oxidized at 1000 °C for 50 hours in synthetic air flow. Although the chemical compositions and the initial microstructure of AISI 304L and AISI 303 are very close, the oxidation behavior of the two alloys differs strongly. Under experimental conditions indicated above, the high sulfur grade, AISI 303, presents catastrophic oxidation behavior with a high oxidation rate, a high net mass gain and severe spalling events during cooling [1].

Thermodynamic calculations were used to explain the observed differences in oxidation behavior of two steels focusing on the effect of alloyed sulfur as MnS inclusions and the amount of free S, i.e. which is not tied up with sulfide former elements such as Mn, Ca, Cr or Ti in the alloys. This S is in solid solution and is free to diffuse towards metal/oxide interface where it can segregate and possibly lead to formation of non-protective oxide (high oxidation rate) with poor interfacial adhesion.

Free S content was estimated using Thermo-Calc with TCFE6 database [2, 3] and the home-built model describing metallic phases in equilibrium with oxide and sulfide inclusions CEQCSI (Chemical Equilibrium Calculations for the Steel Industry) [4]. TCFE6 database only takes into account MnS and FeS when CEQCSI is upgraded with CaS, CrS, TiS and oxysulfide that may precipitate in the liquid, therefore gives much less free S than CEQCSI calculations. Thermodynamic calculations concerning the high S grade, AISI 303, were also carried out using Thermo-Calc with TCFE6 database and FactSage [5] to determine the most stable phase containing sulfur.

It was shown that the free S amount cannot explain the observed differences of oxidation behavior and the poor mechanical properties of the oxide scale grown on AISI 303 are not related to free S segregation at the metal/oxide interface. Sulfur seems to decrease the toughness of the oxide scale through an indirect mechanism involving a change in composition of the oxide scale. The local decrease of the Cr concentration trapped in the form of oxide-sulfide aggregates in the underneath substrate promotes the formation of non-protective and porous Fe-rich oxide.

Based on experimental results and thermodynamic calculations, the scenario has been proposed to explain the breakaway oxidation of AISI 303.

This work was realized in the framework of a PICS project supported by National Centre for Scientific Research (CNRS, France) Ref n° 6095 and Russian Foundation for Basic Research (RFBR, Russia) Ref n° 13-08-91053-CNRS_a.

[1] C. Pascal et al., *Corros. Sci.*, 2015, 93, 100-108.

[2] Thermo-Calc TCCS Version S, ThermoCalc Software AB, Stockholm, Sweden
<http://www.thermocalc.com>

[3] TCFE6 – TCS steels/Fe-alloys database, version 6.2, Thermo-Calc Software AB, Stockholm, Sweden, 2009.

[4] J. Lehmann, *Rev. Metall.*, 2008, 105, 539–550.

[5] FactSage 6.2 Thermochemical Software, Thermfact and GTT-Technologies, Center for Research in Computational Thermochemistry, Montreal, Canada, 2009.

KINETIC AND ENERGETIC PARAMETERS OF BASIC COPPER CARBONATES FORMATION IN THE LACTATE CONTAINING SOLUTION

Fomin V.N.^{1,3}, Gogol D.B.^{2,3}, Rozhkovoy I.E.³, Ponomarev D.L.³

¹Academician E.A. Buketov Karaganda State University, 100028 Karaganda, Kazakhstan

²Institute of Problems of Complex Development of Mineral Resources, 100019 Karaganda, Kazakhstan

³Public Association "Grazhdane Kazakhstan", 100008 Karaganda, Kazakhstan

E-mail: nauka@grazhdane.kz

The basic copper carbonates, malachite and azurite, are not only semiprecious stones but also important ore-forming minerals. The formation of these minerals at natural conditions can take place with participation of organic ligands. To evaluate kinetic parameters of such kind reactions, the number of experiments for determination of formation velocity of basic copper carbonates from simple salts and from complex organic compounds was carried out.

The studied system consisted of temperature-controlled solution with specified concentration, where the cube from natural marble with known size was placed. Such approach allows to consider the mineral formation reaction on marble surface as heterogeneous interaction and allow to apply some aspects adsorption theory. The change of initial compound concentration in solution was measured daily by photometric method with use of sodium diethyldithiocarbamate [1].

The kinetic curve for copper chloride solution at 40°C show strong increase of reaction velocity after 6 days of process passing. On the curve for copper chloride at 40°C the corresponding region can be also identified. Probably, such behavior can be explained by parallel formation of insoluble copper compounds on carbonate collector surface and in bulk solution. The transition of colloidal particles of copper compounds onto substrate take place after formation of sufficient number of crystallization centers on the marble surface. Besides that, the copper concentration in solution at higher temperature is staying more higher on initial stage. This fact show comparable stability of the particles of copper compounds at this conditions and show lower primary adsorption on marble. The reaction rate constants of mineral formation from copper chloride are: $7.24 \cdot 10^{-6} \text{ s}^{-1}$ at 20°C and $5.40 \cdot 10^{-6} \text{ s}^{-1}$ at 40°C at initial stage; $1.66 \cdot 10^{-5} \text{ s}^{-1}$ at 20°C and $8.01 \cdot 10^{-5} \text{ s}^{-1}$ at 40°C at final stage.

For the solutions with copper lactate, in opposition, the mineral formation at 40°C is faster a little than at 20°C. The dependencies are linear in studied range, indicating that microcrystalline precipitate is formed gradually. The reaction rate constants in this case are $4.19 \cdot 10^{-6} \text{ s}^{-1}$ at 20°C and $5.86 \cdot 10^{-6} \text{ s}^{-1}$ at 40°C.

Relatively low velocity of the processes in these systems allow to characterize them by an effective diffusion coefficient. For the system with copper chloride D_e is $1.36 \cdot 10^{-13} \text{ m}^2/\text{s}$ at 20°C and $7.54 \cdot 10^{-14} \text{ m}^2/\text{s}$ at 40°C; for the system with copper lactate D_e is $1.43 \cdot 10^{-14} \text{ m}^2/\text{s}$ at 20°C and $6.15 \cdot 10^{-14} \text{ m}^2/\text{s}$ at 40°C. The order of obtained values is characteristic for processes occurring in solids. The activation energy for reaction with copper lactate are equal to 12.8 kJ/mol; in the system with copper chloride the activation energy is 60.1 kJ/mol at final stage, and at initial stage it has imaginary quantity in -11.2 kJ/mol. It correlates with the fact that the diffusion coefficient in this system has a higher value at lower temperature.

In accordance with the obtained reaction rate constants, the time of growth of precipitate layer with 1 mm thickness is about 300-400 days in case of copper chloride and 400-500 days in case of copper lactate, that confirms the theoretical calculations performed earlier [2].

[1] Marczenko, Z. Kolorymetryczne oznaczanie pierwiastków. Warszawa, 1968.

[2] Fomin, V; Rozhkovoy, I; Gogol, D; Ponomarev, D. Bull. Karaganda State University, 2015, No.4(80), 22-26.

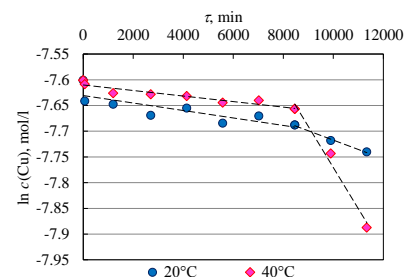


Figure 1. Kinetic curves for copper (II) chloride solutions.

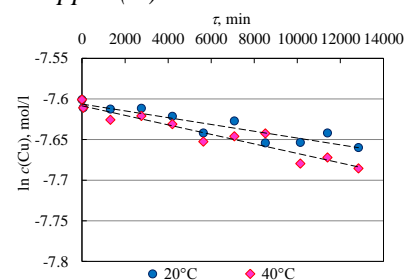


Figure 2. Kinetic curves for copper (II) lactate solutions.



HIGHLY CHARGED GALLIUM CLUSTER CATIONS AND WEAKLY COORDINATING ANIONS. IS NATURE TEASING US?

Himmel D., Gloetz K., Kratzert D., and Krossing I.

Albert-Ludwigs-Universität Freiburg

daniel.himmel@ac.uni-freiburg.de

From the reaction of $[\text{Ga}^{\text{I}}(\text{o-DFB})_2]^+[\text{PF}]^-$ (*o*-DFB: *ortho*-difluorbenzene, $[\text{PF}]^-: [\text{Al}(\text{OC}(\text{CF}_3)_3)_4]^-$)^[1] with aromatic nitrogen bases, salts with amazingly highly charged cations (up to +5!) were obtained. Similar observations were already reported from indium chemistry.^[2]

The formation of such highly charged cations seemingly is in contradiction to electrostatic laws (Coulomb explosion!) and shatters our anterior belief that large, lowly charged weakly coordinating anions (WCAs) promote the formation of lowly charged cations in the crystal lattice.

What makes these clusters stable?

Considerations outgoing from periodic point charge lattices result in internal repulsion energies of up to several thousand kJ per mole within the cations which are balanced by Madelung energies of the same magnitude in combination with charge delocalisation.

Supported by quantumchemical calculations, first attempts to explain the stability of such highly charged cations are presented. Furthermore, some other interesting aspects of these compounds are highlighted.



COLLISIONAL QUENCHING OF METASTABLE $^3P_{1,2}$ AND 1D_2 LEAD ATOMS BY SEVERAL MOLECULES

P. A. Bokhan, N. V. Fateev, V. A. Kim, and Dm. E. Zakrevskii

*Rzhanov Institute of Semiconductor Physics, Siberian Branch of the Russian Academy of Sciences, 13, Lavrentieva av.,
Novosibirsk 630090, Russia*

e-mail: kim@isp.nsc.ru

Rate constants for the quenching of metastable $^3P_{1,2}$ lead atoms by H_2O , NH_3 , CH_3COCH_3 , C_2H_5OH , C_3H_8 , $(C_2H_5)_2O$, SF_6 , CO_2 , $C_4H_{10}O$, C_6H_6 , CH_3OH , N_2O , C_2H_5Br , CH_2Cl_2 , $CuBr$ have been measured using time-resolved light-induced fluorescence spectroscopy at 930° K. $Pb(^3P_{1,2})$ atoms were produced by the pulse glow discharge in the flow of the lead atoms, added molecules and a carrier gas Ar. The quenching cross sections varied from 0.16 to 580 Å². The quenching mechanisms for the different type of molecules are discussed.

AQUEOUS BIPHASIC SYSTEMS BASED ON TRITON X-114 AS BIOCATALYTIC REACTION MEDIUM. SALTING AND SUGARING OUT EFFECTS

Koneva A.S.¹, Kondrakhina P.S.¹, Safonova E.A.¹, Smirnova I.V.²

¹St. Petersburg State University, 7/9 Universitetskaya nab., St. Petersburg, 199034 Russia

²Institute of Thermal Separation Processes, TUHH, Eißendorfer Straße 38, 21073 Hamburg, Germany

E-mail: alina.s.koneva@gmail.com

Aqueous biphasic systems based on nonionic surfactants are an alternative of traditional water-organic solvent biphasic systems in a separation field. Due to its aqueous environment and biocompatibility of most of nonionic surfactants, these systems are of interest in particular for separation processes with biomolecules [1]. Micellar solution of a nonionic surfactant separates into two phases, micellar or surfactant rich and aqueous or surfactant poor phases, at a certain temperature, so called cloud point temperature (CP). The extraction process based on this phenomenon (cloud point extraction, CPE) is carried out at the temperature above the CP or at the presence of certain additives limiting solubility of the surfactant. CPE has been successfully applied for the extraction of hazardous compounds or high valued products [2].

A number of the nonionic surfactants has a low CP and exhibits no effect on the bioactivity of enzymes or proteins, what makes CP systems a suitable medium for a biocatalytic extractive process. Thus, Triton X-114 aqueous biphasic solution has been studied as a potential eco-friendly system for the extractive enzymatic hydrolysis of PenG (penicillin G) [1]. A scheme of the process is presented in **Figure 1**. Different additives such as salts or organic molecules allow varying the CP values and affect the partitioning of some solutes [3]. This helps one to choose mild but effective conditions for the extractive process.

In the present work, aqueous biphasic systems containing nonionic surfactant Triton X-114 with different additives (salt or sugars) are considered as an improved medium for a biocatalytic extractive hydrolysis of penicillin G to 6-aminopenicillanic acid (APA) and phenylacetic acid (PAA) [1]. The partition coefficients ($\lg P^{ob}$) of the solutes (PAA and APA) between micellar and aqueous phases at the presents of salts (NaCl or K_2HPO_4/KH_2PO_4), sugars (glucose or arabinose) have been investigated. The solute concentrations in the both phases were determined by means of HPLC analysis.

The influence of additives and component concentrations on the phase behavior, physicochemical properties of coexisting phases (density and viscosity) is also discussed. The most promising systems have been applied to perform the extractive enzymatic hydrolysis of PenG.

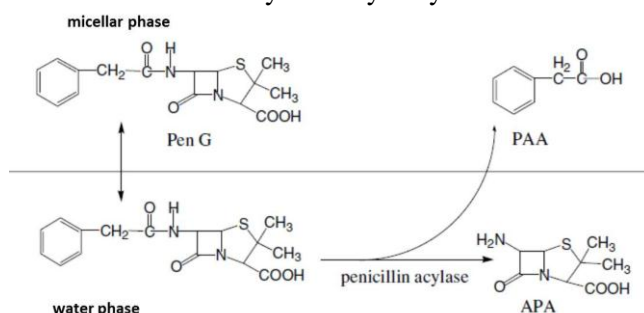


Figure 1. A scheme of enzymatic hydrolysis of Pen G to produce APA and PAA with penicillin G acylase in cloud point system [1].

Chromatographic analysis was carried out on the equipment of the Research park of St. Petersburg State University, Center for Chemical Analysis and Materials Research.

This study was financially supported by RFBR according to the research project # 16-53-12029 ННЮ_а and by DFG the research project # SM82/14-1.

References

- [1] Z. Wang, Appl. Microbiol. Biotechnol. 2007, 75, 1-10.
- [2] P. Mukherjee et al. Adv. Colloid Interf. Sci. 2011, 162, 59.
- [3] E.A. Safonova et al., Chem. Eng. Res. Des. 2014, 92, 1840-1850.



**PHASE BEHAVIOR OF AQUEOUS-SALT SOLUTIONS CONTAINING
DIALKYLIMIDAZOLIUM IONIC LIQUIDS WITH HALIDE OR
AMINOACID ANIONS AND L-TRYPTOPHAN AS SOLUTE**

Safonova E.A., Korchak P.A., Pukinsky I.B., Koneva A.S., Alopina E.V., Smirnova N.A.

St. Petersburg State University, 7/9 Universitetskaya nab., St. Petersburg, 199034 Russia

E-mail: alina.s.koneva@gmail.com

Aqueous-salt biphasic systems containing water miscible Ionic Liquids (IL) are considered as a very perspective media for liquid-liquid extraction (LLE) of bioactive materials (incl. proteins, enzymes, antibiotics, DNA), metal ions, nanoparticles, radioisotopes etc. [1]. One of the important advantages of ILs is great possibility of the modification of their chemical structure and properties, i.e. their multifunctionality. Among the modified ILs amino acid ILs (AAILs) attract particular attention [2]. Thus, chiral AAILs have high potential in the chiral ligand-exchange separation, e.g. in the separation of the amino acid enantiomers [3]. Most of the AAILs are non-toxic and biodegradable materials.

The main aim of this work is an evaluation of the effect of ILs structure on the system phase behavior [4] and on the partitioning of L-tryptophan between the liquid phases. The systems under investigation are the aqueous-salt solutions containing dialkylimidazolium ILs with halide or amino acid anions. AAILs (1-octyl-3-methylimidazolium valinate [C₈mim][Val], 1-octyl-3-methylimidazolium lysinate [C₈mim][Lys], 1-octyl-3-methylimidazolium leucinate [C₈mim][Leu]) were synthesized and characterized by ¹H NMR and ¹³C NMR spectroscopies.

The liquid-liquid equilibrium at 298.15 K was studied for ternary systems, [C₈mim][AA] ([AA] = [Val], [Lys], [Leu]) + water + salt (K₂CO₃ or K₃PO₄), and for quasi-ternary systems, [C_nmim][Hal] (n = 4, 6, 8; [Hal] = Br⁻ or Cl⁻) or [C₈mim][AA] + water + salt (K₂HPO₄ or K₃PO₄) + L-tryptophan, by the isothermal titration method. The binodal curve data were correlated by the Merchuk' equation [5]. The tie lines were obtained by using the data on the binodal curve and on the water concentrations in the coexisting liquid phases (from Karl Fischer titration, modified for the systems with K₂CO₃). The binodal curve and the tie lines data obtained for the systems [C₈mim]Cl + salt + water are in a satisfactory agreement with the literature data [6].

The two phase formation abilities for all of the investigated systems are discussed. Additionally, the effects of the length of the hydrocarbon tale of [C_nmim][X] (for n = 4, 6, 8) and anions nature on the partition coefficients of L-tryptophan are considered.

The obtained results are helpful to understand how anionic structures of the ILs affect the phase behavior and the relative extractive capacities of the IL-rich liquid phase taking into account its hydrophobicity and possible specific IL-solute interactions. These data provide new information on the design of such aqueous-salt biphasic systems containing water miscible ILs towards their application in LLE of the bioorganic compounds.

The NMR and spectrophotometric measurements were carried out on the equipment of the Research park of St. Petersburg State University (Center for Magnetic Resonance, Center for Chemical Analysis and Materials Research).

This study was financially supported by RFBR according to the research project # 16-03-00723 a.

References

- [1] Freire, M G; et al. *Chem. Soc. Rev.*, 2012, 41, 4966-4995.
- [2] Dagade, D H; et al. *J. Phys. Chem. B*, 2013, 117, 1031-1043.
- [3] Tang, F; Zhang, Q; Ren, D; et al. *J. Chromatogr. A*, 2010, 1217, 4669-4674.
- [4] Alopina, E V; et al. *J. Chem. Eng. Data*, 2016, 61, 6, 2013-2019.
- [5] Merchuk, J; Andrews, B; Asenjo J. J. *J. Chromatogr. B*, 1998, 711, 285-293.
- [6] Pei, Y; et al. *J. Chem. Eng. Data*, 2007, 52, 2026-2031.



EFFECTS OF pH AND COMPOSITION OF AQUEOUS BIPHASIC SYSTEMS CONTAINING NONIONIC SURFACTANT TRITON X-114 ON PARTITION BEHAVIOR OF THE BIOCOMPOUNDS

Kondrakhina P.S., Koneva A.S., Safonova E.A.

St. Petersburg State University, 7/9 Universitetskaya nab., St. Petersburg, 199034 Russia

E-mail: polina_kond95@mail.ru

Aqueous biphasic systems are applied in liquid-liquid extraction (LLE) of organic and bioactive compounds, ions of metals [1], [2]. One of the techniques of biphasic partitioning is a cloud point extraction (CPE) based on nonionic surfactant (NIS). The extract (i.e. micellar or surfactant rich) and raffinate (i.e. aqueous or surfactant poor) phases in NIS system are formed at the cloud point temperature (CPT). The CPE method is carried out at the temperature above the CPT or in the presence of certain additives limiting solubility of NIS in aqueous solution. In comparison with the traditional organic solvents for LLE, NISs are biocompatible and provide mild conditions, which are especially important for extraction processes of biomolecules sensitive to the organic media and to the high temperatures. The CPE has been successfully applied to provide the biocatalytic reaction by a continuous mode [3].

It is known that an addition of some additives (salt or other surfactant) impact on CPT and on the partition coefficient ($\lg P^{ab}$) of some solutes in biphasic micellar system [4]. Furthermore, some additives affect the density and the viscosity of both liquid phases what determines velocity of the phase separation. Hence, density and viscosity data of both phases are particularly important for a design of the extraction process.

In the present work, the aqueous solutions of NIS Triton X-114 with salt additives (NaCl and K_2HPO_4/KH_2PO_4) were considered as the systems for CPE of the compounds of penicillin G hydrolysis i.e. penicillin G (PenG), 6-aminopenicillanic (APA) acid and phenylacetic acid (PAA) [3]. The effects of pH, salt additives and component concentrations on phase behavior, physicochemical properties of coexisting phases (density and viscosity) and partitioning of the solutes are under study. The temperature of the measurements (310.2 K) was chosen as provided the highest velocity of the bioreaction. The $\lg P^{ab}$ values of the solutes were determined by phase separation followed by HPLC analysis.

The study of the phase behavior shows that the CPT of Triton X-114 micellar systems without solutes do not sensitive to a change in pH value from 6.8 to 2.7. An addition of NaCl or K_2HPO_4/KH_2PO_4 reduces expectably the CPT of the Triton X-114 solutions with and without solutes. An addition of APA has no effect on CPT, while the presence of PAA leads to a significant decrease of the CPT.

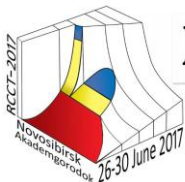
Moreover, it was found, that an addition of the organic compounds has almost no effect on density of both phases. The viscosity of micellar phase containing APA is close to that of surfactant-rich phase of Triton X-114 system without any additives. The additive of PAA highly decreases the viscosity of the micellar phase. The viscosity values of the aqueous phases are practically the same for all the systems and are close to the viscosity of the pure water. The $\lg P^{ab}$ data show that NaCl as additive or decrease of pH improves the extraction of PAA.

Chromatographic researches were carried out on the equipment of the Research park of St. Petersburg State University, Center for Chemical Analysis and Materials Research.

This study was financially supported by RFBR according to the research project # 16-53-12029 НННО_a.

References

- [1] F.H. Quina, W.L. Hinze, *Ind. Eng. Chem. Res.* 1999, 38, 4150-4168.
- [2] K. Holmberg, D. O. Shah, M. J. Schwuger, *Handbook of applied surface and colloid chemistry* 2002.
- [3] Z. Wang, *Appl. Microbiol. Biotechnol.* 2007, 75, 1-10.
- [4] E.A. Safonova et al., *Chem. Eng. Res. Des.* 2014, 92, 1840-1850.



MODEL OF Ni-Al COMPOSITE SYNTHESIS UNDER ELECTRON-BEAM CONTROLLING

Knyazeva A.G.^{1,2}, Kryukova O.N.²

¹Tomsk Polytechnic University (TPU), 634050, Tomsk, Russia

²Institute of Strength Physics and Materials Science of Siberian Branch of Russian Academy of Sciences (ISPMS SB RAS), 634055, Tomsk, Russia

E-mail: anna-knyazeva@mail.ru, okruk@ispms.tsc.ru

Methods of powder metallurgy together with the use of concentrated energy fluxes have special capabilities for the materials and compositions creation with given properties. The complex method of the electron-beam treatment of material with a preliminary deposited layer allows combining the advantages of electron beam treatment and conversions in the condensed phase. However the substrate consuming the heat from the heated zone can affect essentially the regimes of the reaction initiation and propagation especially the regime of layer-by-layer reaction propagation in the condensed phase. This paper describes the mathematical model of the process of Ni-Al layer synthesis under electron-beam treatment. The model takes into account the main physical and chemical phenomena and the porosity evolution in the powder layer. The synthesis is carried out on the iron substrate of given thickness. The study takes into account the difference in the thermal physical properties of the substrate and reacting layer, chemical reaction heat release and change of the phase composition in the intermixing materials. Powder layer shrinkage and change of the thermal physical properties happen due to the porosity reduction. The formulated problem is solved numerically. The paper discusses some additional mechanism of convective heat transfer connected with the evolution of powder layer thickness. The composition and the final porosity of the layer depend on the technological parameters.

The study was supported by the Russian Foundation for Basic Research (grant No. 16-58-00116 BeI_a).



POLYCOMPONENT WATER-SALT SYSTEMS WITH METAL FORMATES

Kudryashova O.S.¹, Gordenchuk A.D.¹, Elokhov A.M.²

¹*Institute of Natural Science, Perm State University, 614990 Perm, Russia*

²*Institute of Technical Chemistry, Ural Branch of the Russian Academy of Sciences, 614013 Perm, Russia*

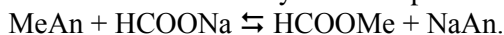
E-mail: oskudr@psu.ru

Sodium formate is widely used as an antifreezing and plasticizing additive in the production of the building constructions, in the leather industry as an agent in pre-tanning activities, raw materials in the production of formic acid and as a component of the ice-melting compositions. Sodium formate received in the solution form as a by-product in a number of productions is in high demand only in winter time due to its no additional processing. Crystalline sodium formate which is in constant demand in the market significantly increases the price for the product and makes it less competitive. This provides the interest in processing the sodium formate into the formates of other heavily demanded metals.

Potassium formates is used as an antifreezing additive component for concrete, a component of organic salts and ice-melting reagents based coolants, an additive for reinforced and unreinforced concrete, floors, plaster and brick glue. Calcium formate is used as a promoter for concrete setting and for making it more durable in construction, as a component for the ice-melting reagents, as an additive - E238 preservative - in food industry, as a mineral fertilizer in agricultural industry. Formates of the transition and rare-earth metals are used as the primary components in the production of the high-temperature superconductors, highly-dispersive and nanosized oxides, hydrogenation catalysts and oxidation of the organic substances. Conversion method to receive the salts is the most eco-friendly and the easiest one. Despite the evident advantages of this process in the world practices there are no technologies to receive the formates based on salt conversion in aqueous systems. The advantages of the proposed technology are as follows:

- Versatility. The same technological equipment can be used to receive a wide range of metal formates provided the appropriate raw materials and technological modes with the temperature concentration parameters of the process are exploited.
- Possibility to process both the crystalline salts and their water solutions;
- Usage of the technogenic wastes as the raw materials;
- Cost of the obtained formates (for example, calcium or potassium formates) is significantly higher than the primary sodium formate.

Metal formates can be received from sodium formate by double replacement in the water solutions:



Water-soluble salts of the alkali, alkali-earth and transition metals or technogenic raw materials can be used as the second raw component.

Physical chemical grounds for the conversion processes to receive the formates of the alkali, alkali-earth and transition obtain:

- experimental data in solubility in four-component mutual systems with the formates of the metals;
- temperature and concentration parameters to receive the metal formates by the double replacement of salts;
- theoretical grounds for the technological process scheme based on the data in salt joint solubility;
- results of the large-sized laboratory experiments with pure salts and technogenic raw materials.



COMPUTER SIMULATION OF QUERCETIN-CARBOHYDRATE AND QUERCETIN-SILICON OXIDE REACTION PRODUCT. SITES OF INTERACTION.

Mamylov S.G., Lomovsky O.I

*Institute of Solid State Chemistry and Mechanochemistry, Siberian Branch of the Russian Academy of Sciences, 630128
Novosibirsk, Russia*

E-mail: mamyllov@solid.nsc.ru

Natural polyphenols act as the transport agent of substances necessary for a living plant, they may be used as chelate reagents for heavy metals, and as nutritional dietary supplements. Problems of formation of fertility of the soil are also connected with reactions of humin polyphenols with silicon dioxide surface. Biologically active antioxidants of a class of flavonoids (quercetin, catechins) include in structure hydroxyl groups. Polyphenols can react through various sites of a molecule, forming isomers with the different properties. Change of system energy defines the formation of various isomers.

The aim of the work is a computer simulation of system energy changing in reactions "quercetin - carbohydrate" and "quercetin - silicon oxide".

Simulation was carried out in molecular editor Avogadro.

Carbohydrates are alpha- and beta-anomers of D-glucopyranose in "chair" conformation 4c1. Chemical formula is $C_6H_{12}O_6$, molar weight is 180. Model silica particle has a tridymite structure. It allows to reach hydroxyl groups above the surface and to provide silanol and silandiol bondings of polyphenol reagents. Silica particle chemical formula is $Si_{48}O_{120}H_{48}$, molar weight is 3316.

Quercetin, 3,3',4',5,7-pentahydroxyflavon, $C_{15}H_{10}O_7$. Molar weight is 302.

Quercetin molecule has 5 hydroxyl groups. In various compounds quercetin can react both one or several hydroxyl groups. At interaction with carbohydrates it acts as aglycon. It is considered that carbohydrate bonding with aglycon through glycoside atom of carbon meets more often. Any of five hydroxyl atoms of oxygen can be a bonding site on the aglycon (quercetin), but for different types of compounds they change. Carbohydrates connect hydroxyls of a quercetin in 3,5,7 positions more often. We have received in computer simulation that silica preferably forms the isomers bonded with 3', 4' sites of a quercetin.

Energy of reaction at interaction of a quercetin with carbohydrate is in range $-10 - +60$ kJ/mol depending upon type of saccharide anomer and the site of carbohydrate to quercetin bonding. Alpha anomer connects preferably in the 3 and 5 sites of a quercetin, beta anomer – in 3 and 3' sites. Reaction with a molecule of silicon oxide is preferable in sites 3', 4' and 7.

The situation considerably changes by consideration of interaction of quercetin with a model silica particle. Silanol type bonding of polyphenol to a particle is most probable for sites 3' and 4' at interaction with a particle surface (the ring B). Reaction energy value is in the range of $-10 - +60$ kJ/mol. Interaction with side atoms of silicon underlines the main role of quercetin ring A, sites 5 and 7 are preferable.

At silandiol type of bonding, when two hydroxyl groups of quercetin participate, sites 3' and 4' (a ring B) become dominating. In this case energy of reaction is about 80 kJ/mol, the maximum value is about 320 kJ/mol (sites 5 and 7).

APPLICATIONS OF FAST SCANNING CALORIMETRY

Schubnell M., Schawe Jü.

Mettler-Toledo AG, Sonnenbergstrasse 74, CH-8603 Schwerzenbach, Switzerland

E-mail: markus.schubnell@mt.com

For the thermal analysis of meta-stable materials, such as e.g. semi-crystalline polymers, availability of a wide range of heating and cooling rates is crucial. Also, to mimic process conditions of materials such as polymers, active pharmaceutical ingredients or alloys high cooling rates are required. With conventional differential scanning calorimetry maximum cooling rates of several 100 K/min can be achieved. This is far away from cooling rates applied in real processes. To realize process relevant cooling rates of up to several 1000 K/s fast scanning calorimeters have to be used.

We present applications of fast scanning calorimetry from different fields (polymers, alloys, pharmaceuticals). As an example Figure 1 (left side) shows the crystallization behavior of iPP during cooling. The crystallization temperature of iPP decreases with increasing cooling rate. Above 100 K/s the mesomorphic phase crystallizes below 40 °C. At cooling rates faster than 2000 K/s the material becomes amorphous. The isothermal crystallization of iPP, measured after cooling at 2000 K/s from the melt, is shown at various temperatures on the the right side in Figure 1. The curves show the temperature dependence of the crystallization kinetics. One clearly can confirm the two crystallization regimes also identified from the cooling experiments. The mesomorphic phase is formed only with large supercooling.

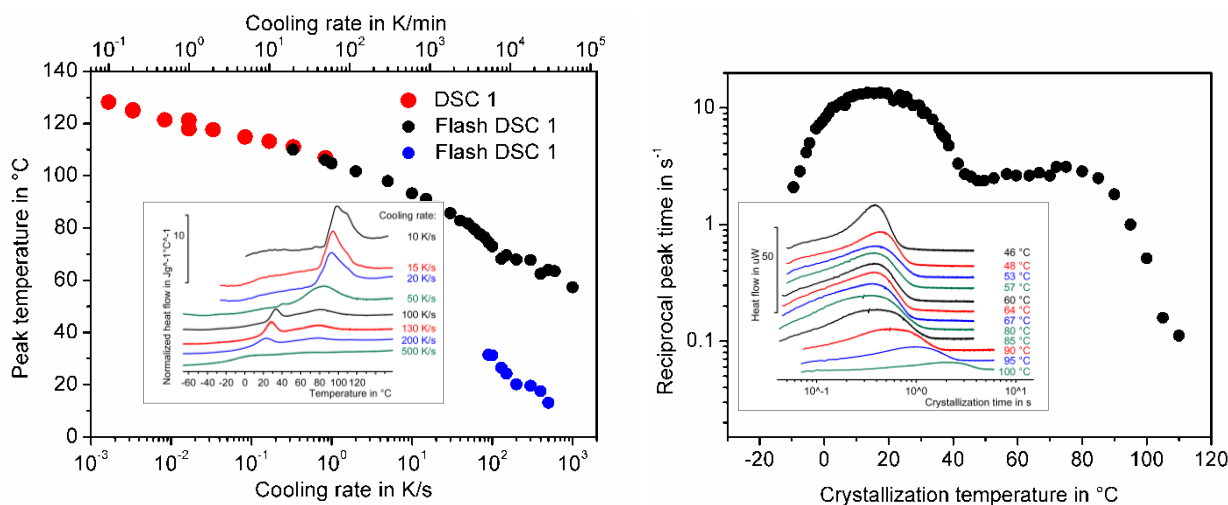


Figure 1. Left: Peak temperature of the crystallization peaks of iPP as a function of the cooling rate. Insert: Collection of DSC cooling curves. Right: Reciprocal peak time of the iPP crystallization peaks versus the crystallization temperature. The reciprocal crystallization time is proportional to the crystallization speed. Insert: Collection of isothermal DSC curves.

PULSE MICROCALORIMETRY STUDY OF Ni/CeZrO₂ CATALYST IN DRY REFORMING OF METHANE

Simonov M.N., Rogov V.A., Sadykov V.A.

Boreskov Institute of Catalysis, Siberian Branch of the Russian Academy of Sciences, 630090 Novosibirsk, Russia

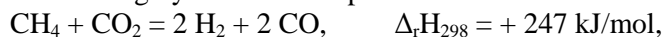
Novosibirsk State University, 630090 Novosibirsk, Russia

E-mail: smike@catalysis.ru

Investigation of reaction mechanism plays a crucial role for the design and development of highly efficient processes of transformation of different types of fuels such as natural gas, biogas, biofuels into syngas and hydrogen. Catalysts comprised of Ni-based alloys supported on perovskite or fluorite-like oxides with a high oxygen mobility and reactivity demonstrate a high activity and coking stability in methane dry reforming (MDR) [1,2,3]. However, features of reaction mechanism and CH₄ and CO₂ activation as well as factors controlling oxygen mobility/reactivity known to be important for stable performance of these catalysts remain to be clarified. This work presents results of pulse microcalorimetric studies aimed at elucidating specificity of MDR mechanism for catalysts of Ni/Ce_{1-x}Zr_xO₂ composition.

A continuous preparation method in supercritical alcohol medium was used for the preparation of Ni/ceria-zirconia catalysts with tunable particle size of the mixed oxide support and nickel dispersion. Rates and heats of the catalysts reduction/reoxidation by pulses of CH₄ or CO₂ in He for catalysts after different pretreatment were estimated using a Setaram Sensys DSC TG calorimeter and a pulse kinetic installation equipped with GC, MS and gas sensors.

MDR is highly endothermic process which can be described by the following equation:



including a side reverse water-gas shift reaction:



The strength of oxygen bonding with the steady-state surface corresponds to bridging M₂O forms since measured heat of O₂ adsorption is about 630-670 kJ/mol. Methane transformation in absence of CO₂ in pulses fed to the steady-state surface proceeds with conversion and products selectivities (H₂/CO) close to those in reaction mixture (CH₄+CO₂) pulses. The heat effects (figure 1) correspond to CH₄ oxidation by bridging oxygen forms. Reoxidation of the steady-state surface by CO₂ yielding CO (fast reversible step) proceeds with nearly constant heats of reaction (from - 69 to - 47 kJ/mol CO₂) corresponding to replenishing of bridging oxygen forms. Hence, for fluorite-like oxide supported catalysts with a high oxygen mobility, steady-state reaction of CH₄ dry reforming is described by a simple redox scheme with independent stages of CH₄ and CO₂ activation. This is provided by easy CO₂ dissociation on reduced sites of oxide supports followed by a fast oxygen transfer along the surface/domain boundaries to metal nickel sites where CH₄ molecules are transformed to CO and H₂.

In summary, the catalytic properties of Ni/ceria-zirconia nanoparticles synthesized via continuous preparation technique in supercritical alcohol medium are studied for the first time. Microcalorimetry data revealed that the mechanism of MDR reaction is step-like with independent activation of the methane on the metal sites and oxygen on the oxide support sites.

Financial support by NICE project of ERA Net Rus Plus Call and Ministry of Education and Science of Russian Federation under grant agreement 14.616.21.0036 is gratefully acknowledged.

[1] Sadykov, V, Gubanova, E, Mirodatos C, et al. *Catal. Today*, 2011, 171, 140-149.

[2] Kapokova, L, Pavlova, S, Sadykov, V, et al. *Catal. Today*, 2011, 164, 227-233.

[3] Sadykov, V, Simonov, M., Mezentseva, N., et al. *Open Chem.*, 2016, 14, 363-376.

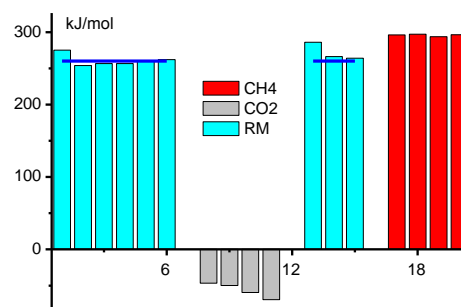


Figure 1. Measured heat effects in consecutive pulses of reaction mixture (RM, 5% CH₄ + 5%CO₂), 5% CO₂, RM, 5% CH₄ supplied at 550°C on the steady-state catalyst. Blue line is a theoretical heat effect of MDR reaction at 550°C.

**THERMODYNAMIC ANALYSIS OF ZrB₂ FILM SYNTHESIS FROM Zr(BH₄)₄ + H₂/NH₃ GAS MIXTURES**

Sulyaeva V.S., Shestakov V.A., Rumyantsev Yu.M., Kosinova M.L.

Nikolaev Institute of Inorganic Chemistry, Siberian Branch of the Russian Academy of Sciences, 630090 Novosibirsk, Russia

E-mail: veronica@niic.nsc.ru

Zirconium diboride (ZrB₂) is known as a high-melting point ceramic with high hardness, high thermal and electrical conductivities, chemical inertness, and great thermal shock resistance in the bulk form [1]. These properties are potentially useful for the thin film applications [2]. At present, both physical and chemical deposition processes can produce ZrB₂ films. Application of the CVD method allows the use of single source precursor, which in this case is a zirconium tetrahydroborate Zr(BH₄)₄. The thermodynamic modeling is important for studying the CVD process. It allows calculating the change in the chemical and phase composition of the film depending on such parameters as the deposition temperature and composition of synthesis starting gas mixture fed to the reactor.

The purpose of this work was to examine the possibility of using Zr(BH₄)₄ + H₂ and Zr(BH₄)₄ + NH₃ mixtures for the forming ZrB₂ films by chemical vapor deposition and to assess the effect of oxygen impurities on the composition of the deposits.

Thermodynamic modeling of deposition processes in the Zr-B-(N)-H and Zr-B-(N)-H-O systems in a wide temperature range of 100-2500 °C and at various ratios of the partial pressures of p(H₂)/p(Zr(BH₄)₄) or p(NH₃)/p(Zr(BH₄)₄) the initial mixtures in the range from 0 to 20 was carried out. Considering the residual pressure in the system during the experiment, the calculations for oxygen-containing systems were taken p(O₂)/p(Zr(BH₄)₄) = 0.02.

Zr(BH₄)₄ + H₂ (+ O₂) mixture. Calculations have shown that, depending on the conditions of CVD process in Zr-B-H system ZrB₂ either biphasic composition ZrB₂ + B can be deposited. In a similar process in Zr-B-H-O system single-phase ZrB₂, biphasic composition ZrB₂ + B, and three-phase composition ZrB₂ + B + B₂O₃ can be prepared. A small content of oxygen in the system does not affect the boundary ZrB₂ + B|ZrB₂ position on the CVD diagram. In Zr-B-H system at 400 and 1300 °C in equilibrium with the phase complex ZrB₂ + B is a gas phase consisting essentially of only hydrogen. At temperatures above the interface ZrB₂ + B | ZrB₂ the boron excess goes into the gas phase, which contains primarily in atomic form. In the case of Zr-B-H-O system, the gas phase at 400 °C also represents hydrogen in equilibrium with the three-phase complex. At 1300 °C, in the equilibrium with two-phase region with complex ZrB₂ + B, almost all of the oxygen and partially the boron contained in the gas mainly in the form of H₃B₃O₃. At 2200 °C in equilibrium between the gas and ZrB₂, boron contained in the gas is generally in atomic form and oxygen in the form of BO.

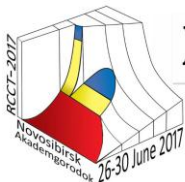
Zr(BH₄)₄ + NH₃ (+ O₂) mixture. In the case of Zr-B-N-H system there are single-, bi-, and three-phase composition fields of condensed phases can be prepared: ZrN + BN | ZrB₂ + ZrN + BN | ZrB₂ + BN | ZrB₂ + B + BN | ZrB₂ + B | ZrB₂ with increasing deposition temperature. The temperature boundary between these phase fields almost independent on ratio of p(NH₃)/p(Zr(BH₄)₄). A similar pattern was observed in the Zr-B-N-H-O system except in the presence of oxygen as oxide phases. In this case ZrN + BN + ZrO₂ | ZrB₂ + ZrO₂ + BN + ZrN | ZrB₂ + ZrO₂ + BN | ZrB₂ + BN | ZrB₂ + B + BN | ZrB₂ + B | ZrB₂ can be prepared.

In this paper ZrB₂ CVD synthesis by decomposition of Zr(BH₄)₄ was developed. During these experiments the ratio of p(H₂)/p(Zr(BH₄)₄), p(NH₃)/p(Zr(BH₄)₄), and deposition temperature were varied. With increasing film deposition temperature the increase in growth rate was observed in the range of 1-3 nm/min, which is typical for LPCVD processes. Wherein the refractive index varied in the range of 1,57-2,89. The film surface morphology synthesized at low temperature was featureless, smooth. While the films deposited at higher temperature synthesis, had a grainy surface with a grain size of about 150 nm. According to EDX, atomic content was Zr 5-18 at.%, B 78-89 at.%, O 1-3 at.% and N 5-8 at.% in case of adding ammonia. In the FTIR absorption spectra of the films the bands corresponding to the νZrB (400-500 cm⁻¹), δBH₂ (1150-1290 cm⁻¹), νBH (2530-2600 cm⁻¹) and νBN (1380-1400 cm⁻¹), νNH₂ (3400 cm⁻¹) in case of adding ammonia were recorded.

[1] Guo, S.-Q. J. Eur. Ceram Soc., 2009, 29, 995–1011.

[2] Broitman, E.; Tengdelius, L.; Hangen, et. al. Scripta Materialia, 2016, 124, 117–120.

This work was supported by the RFBR (project No 16-33-00448 мол_a).



EXPLANATION OF DEXTRAN 40 SIDE EFFECTS BY THERMODYNAMICS

Wenjian Sun

WenJian Bioresearch Institute of Heping District, Shenyang, China

E-mail: wenjians@live.com

Dextran 40 is used in patients for expanding and maintaining blood volume by intravenous infusion. It can cause patients pruritus by over dosage or long time in use. This symptom can be hugely influenced by outside temperature change and body's activity (work). Clinical investigation and vitro experiments support this viewpoint because human body is an open system. Energy plays an important role in Dextran 40 absorption, distribution and metabolism. This paper is trying to explain the reason that produces pruritus symptom, caused by intravenous infusion of Dextran 40, with the help of thermodynamics. By thermodynamics principle, patients can understand how to prevent the appearance of pruritus.



THERMODYNAMICS OF COMPONENTS INTERACTION IN CRYSTALLIZING ROTARY STEEL MELTS

Tanklevskaya N.M. Mikhailov G.G.

South Ural State University, Lenin avenue, 76, Chelyabinsk, 454080, Russia

E-mail: tanklevskaianm@susu.ru

The problem of producing the alloys with the given properties is directly connected with deep understanding the characters of alloy components interaction with an atmosphere, present impurity elements, and also refining mixes. At the same time the thermodynamic analysis of reactions of heterogeneous phases formation from metal melt components allows to establish precise dependence between modification of the metal structure and the change of chemical and component contents of forming condensed and gas non-metal phases.

In this research a thermodynamic analysis of the phase equilibria in the Fe–Mn–Cr–Si–Al–V–S–C–O system at the temperatures of molten metal existence and within the crystallization temperatures was performed. The concentrations of some elements were fixed ([Mn]=0.4; [Cr]=1.5; [V]=0.1; [S]=0.01; [C]=0.25 wt %).

It is found that at the casting temperature ($T = 1823$ K) in equilibrium with the liquid metal, similar in composition 25KHN3MFA rotary steel, may be an oxide melt containing traces of sulfur, the solid oxide solution based on corundum, spinel solid solution based galaxite, cristobalite, and the gas phase consisting mainly of CO. When the silicon content in the molten metal at the level tenths of a percent the equilibrium oxide melt occurs the delamination on enriched and depleted silicon oxide phases. Sulphide crystalline phases in equilibrium with the examined liquid metal compositions cannot exist.

The nonmetallic phases formation upon cooling and crystallization of various composition liquid metal solutions was studied. It was established how the aluminum, silicon, manganese, carbon and sulphur content in the liquid metal solution affects the composition and amount of the separated excess phases.

Calculations have indicated that oxide melt contain mainly SiO_2 , MnO and Al_2O_3 can be in equilibrium with the molten metal at $T=1823$ K. Cooling and solidification the molten metal is also accompanied by release variable composition oxide melt inclusions. Already at the crystallization beginning, the Al_2O_3 content in the equilibrium liquid silicate falls to zero. After the crystallization starts formation of these inclusions continues and the content of the manganese oxide in these inclusions increases. The equilibrium sulfur content in the inclusions is also increasing, reaching almost 1 wt. %. At the end of the crystallization a large amount of sulfides (MnS, FeS) is formed.

Calculations indicate that in the case of increasing aluminium content the main equilibrium phase becomes corundum. In addition, the aluminum reduces the solubility of sulfur in a metal melt, which leads to the release of larger amounts excess phase (MnS, FeS).

Increase of silicon concentration in the liquid metal prevents the risk of spinel formation as a phase equilibrium with the liquid metal. However, leads to an increase in the mass of the sulphides formed during solidification because silicon to a greater extent than aluminium affects of the sulfur solubility in the metallic melt.

Manganese and carbon mainly affect the process of sulfide inclusions (MnS, FeS) formation. Low (up to 0.2 wt. %) manganese content ensures the absence of these inclusions in the metal at the end of crystallization. The increase of manganese concentration up to 0.4 wt. % significantly intensifies process of these inclusions formation. Increasing the carbon concentration leads to the opposite effect.

The work was supported by Act 211 Government of the Russian Federation, contract № 02.A03.21.0011.

**THERMOCHEMICAL INVESTIGATION OF IRIIDIUM (I) VOLATILE PRECURSORS FOR MOCVD PROCESSES**Vikulova E.S.¹, Karakovskaya K.I.^{1,2}, Ilyin I.Yu.¹, Zelenina L.N.^{1,2}, Turgambaeva A.E.¹, Sysoev S.V.¹, Morozova N.B.¹¹Nikolaev Institute of Inorganic Chemistry, Siberian Branch of the Russian Academy of Sciences, 630090 Novosibirsk, Russia²Novosibirsk State University, 630090 Novosibirsk, Russia

E-mail: lazorevka@mail.ru

Iridium volatile complexes are caused the growing interest as potential precursors for Meta-Organic Chemical Vapor Deposition (MOCVD) of functional Ir-containing coatings for protective, medical and other applications. The systematic investigations of thermal properties for such complexes are needed to the most success of their MOCVD application, *i.e.* to distinctly determine the evaporator and substrate temperature intervals, the type of the gas-reagent and the concentration of the precursors' vapours in the reactor. In general, such thermochemical investigations will provide the opportunity to create the platform to choose the best precursor for material with specified characteristics.

The present work is summarize our investigation of thermochemical properties of volatile iridium (I) complexes of [Ir(Q)_n(L)] type. The 1,5-cyclooctadiene (cod, n = 1) or carbolyls (n = 2) were chosen as neutral ligands Q. A number of β-diketonate derivatives R¹C(X¹)CHC(X²)R² were used as anionic ligand L in order to explore the influence of the donor group and terminal substituent types on the thermal properties of complexes: X¹ = X² = O : R¹ = R² = Me (*acac*), ^tBu (*thd*), CF₃ (*hfac*); R¹ = CF₃, R² = Me (*tfac*); ^tBu (*ptac*), Ph (*btfac*), R¹ = ^tBu, R² = Me₂OMe (*zis*); X¹ = NR³, X² = O: R¹ = Me, R² = Me, R³ = H (*i-acac*), R³ = Me (*Mei-acac*), R¹ = CF₃, R³ = Me (*Mei-tfac*).

The thermal properties of the complexes in condensed phase were investigated by thermogravimetry and differential scanning calorimetry. The thermal stability, relative volatility orders and thermodynamic parameters of melting were determined. The temperature dependencies of saturated vapor pressure over solid compounds were measured by flow (transmission) method and the corresponding thermodynamic parameters of melting were calculated. Some results concerning cyclooctadiene complexes are presented in Table 1. The volatility row of the complexes is following: L = *hfac* > *tfac* > *ptac* > *acac* > *thd* > *i-acac* > *Mei-acac* > *btfac*. The thermal stabilities of the compounds' vapors on the heated surface were investigated by *in situ* high temperature mass-spectrometry. The thermal interval and the main gaseous products of the thermodestruction of vapors of complexes [Ir(cod)(L)] (L = *hfac*, *acac*) and [Ir(CO)₂(*hfac*)] in vacuum and in presence of hydrogen were determined.

The usage of the obtained thermochemical data in MOCVD experiments to deposit the high capacitive metal Ir, iridium oxide and composite Ir-IrO₂ coatings with fractal-like morphology onto the working surfaces of endocardial electrode pole tips will be also presented.

Table 1. Thermodynamic parameters of sublimation of iridium (I) cyclooctadiene complexes [Ir(cod)(L)] normalized to the mean temperature (T*) of the examined interval (ΔT).

L	ΔT, K	N	ln(p/p ₀) = A - B/T		Δ _{sub} H _{T*} , kJ·mol ⁻¹	Δ _{sub} S ^o _{T*} , J·(mol·K) ⁻¹
			A	B		
<i>hfac</i>	353 – 387	12	22.16	11039	92 ± 2	184 ± 6
<i>tfac</i>	343 – 385	19	23.18	12129	101 ± 2	192 ± 7
<i>ptac</i>	363 – 397	14	23.64	12643	105 ± 2	197 ± 5
<i>thd</i>	373 – 438	14	22.74	13055	109 ± 2	189 ± 4
<i>acac</i>	363 – 423	13	23.02	12817	106.6 ± 0.7	191 ± 2
<i>i-acac</i>	383 – 431	9	25.30	14312	119 ± 2	210 ± 5
<i>Mei-acac</i>	383 – 423	9	22.47	13360	111 ± 2	187 ± 6

The work was partially financially supported by the Council on the Grants from the President of the Russian Federation (SP-3215.2016.4).



INVESTIGATION OF STABILITY OF LAYERED PEROVSKITE-LIKE TITANATE $K_2Nd_2Ti_3O_{10}$ IN WATER AND HUMID ATMOSPHERE BY METHODS OF THERMAL ANALYSIS

Utkina T.D., Chislov M.V., Rodionov I.A., Zvereva I.A.

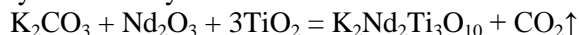
Saint Petersburg State University, Institute of Chemistry, 198504 Saint Petersburg, Russia

E-mail: utkina.td7@gmail.com

Layered perovskite-like titanates are known as promising catalysts and photocatalysts in the reaction of water splitting with using sunlight energy. The stability of these substances in water solution and humid atmosphere is very important because the processes occurring in such conditions can affect their properties. Previously it has been found that intercalation of water into the interlayer space and ion exchange of alkali cations to protons are typically observed for layered perovskite-like titanates, in particular, for $K_2Nd_2Ti_3O_{10}$ during the interaction with liquid water [1, 2].

At the same time the composition of $K_2Nd_2Ti_3O_{10}$ can also change in a humid atmosphere and that also can significantly influence on the physicochemical properties of the oxide and such investigation should not be neglected.

The perovskite-like titanate was synthesized by the solid-state reaction at 1100°C during 6h in air:



Then $K_2Nd_2Ti_3O_{10}$ was investigated by sorption analysis (TA Instruments TGA Q5000SA) in humid atmosphere at 100% RH and in alterable conditions of humidity (0 – 95 – 0%) Moreover stable hydrated protonated oxides $H_xK_{2-x}Nd_2Ti_3O_{10} \cdot yH_2O$ were obtained by continuous water flushing of the initial substance.

The phase composition of the investigated compounds was monitored using XRD analysis (Rigaku MiniFlex II). To determine the degree of protonation and the amount of intercalated water thermogravimetric analysis (Netzsch TG 209 F1 Libra) was used.

As a result, the study of stability of the layered perovskite-type oxide $K_2Nd_2Ti_3O_{10}$ in water and humid atmosphere with the obtaining of protonated hydrated $H_xK_{2-x}Nd_2Ti_3O_{10} \cdot yH_2O$ and hydrated $K_2Nd_2Ti_3O_{10} \cdot yH_2O$ compounds was carried out. The composition of the investigated forms was determined.

It was found that there are two stable phases after water flushing of $K_2Nd_2Ti_3O_{10}$. While the initial layered oxide crystallizes in a tetragonal I4/mmm space group and its hydrated form - in a P4/mmm space group, it was found that the crystal symmetry lowers upon protonation during water flushing. Thus, two stable partially protonated and hydrated compounds with orthorhombic symmetry (suggested space group - C222) were obtained. The 2nd phase, which was exposed to water for a longer time, has a higher protonation degree and a lower interlayer distance compared to the 1st phase.

Investigation of both phases in humid atmosphere demonstrated that these compounds are resistant to intercalation and protonation processes and are exposed to sorption process only.

The results of X-ray and TG analysis have shown that the initial $K_2Nd_2Ti_3O_{10}$ titanate exposed at 100% RH during 1 day is regenerated to the initial composition after the heating of sample.

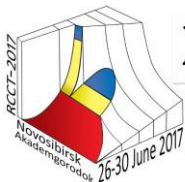
Sorption analysis of $K_2Nd_2Ti_3O_{10}$ under alterable conditions of humidity has presented that the sorption-desorption process is not-reversible. Therefore, this behavior is characterized by sorption, intercalation and protonation processes.

Scientific research were performed at the Research park of St.Petersburg State University Center for X-ray Diffraction Methods and Center for Thermogravimetric and Calorimetric Research.

This work was supported by the Russian Foundation for Basic Research (grants №15-03-05981 and №16-33-60044).

[1] I. A. Rodionov, O. I. Silyukov, T. D. Utkina, M. V. Chislov, Yu. P. Sokolova, and I. A. Zvereva. *Russian J. of General Chemistry*. 2012, 82 (7), 1191–1196.

[2] T. Utkina, M. Chislov, O. Silyukov, A. Burovikhina, I. Zvereva. *J. Thermal Analysis and Calorimetry*. 2016, 125 (1), 281–287.



Section 5.

Applied aspects of chemical thermodynamics

Virtual presentations

THERMODYNAMIC MODELING OF THE BEHAVIOR OF EUROPIUM WHILE HEATING RADIOACTIVE GRAPHITE IN INERT ATMOSPHERE

TS Kolbin,¹ NM Barbin,^{1,2} DI Terentev,¹ SG Alekseev¹

¹Ural Institute of the State Fire Service Emergency Russia, Mira st. 22, 620062, Ekaterinburg, Russia

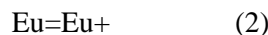
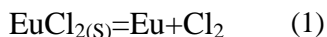
²Ural Agrarian State University, Karl Liebknecht st., 42, 620075, Ekaterinburg, Russia

E-mail: NMBarbin@mail.ru

Nowadays it is become a promising high-temperature treatment of radioactive waste. To date, there are several ways of high-temperature utilization of radioactive graphite [1,2,3]. The criterion for successful recycling is acceptable emissions of radioactive elements to the environment. Investigations were carried out by means of the thermodynamic modeling.

Distribution of Eu in the system while radioactive graphite is heated in an argon atmosphere is shown in Fig. 1. The basic elements to a temperature of 1300 K is condensed EuCl_2 . Increasing of the temperature to 1500 K leads to higher content of gas Eu to 98 mol. %. Further heating system reduces the amount of gas Eu and an increase in the content of Eu^+ ions up to 60mol. %.

The minimum basic set of reactions (equilibrium) and in the individual phases at the interface might be written.



The dependence of the equilibrium constants of reactions (1) - (7) of the temperature is described by the equation of the form:

$$\ln k_i = A + B/T$$

Table 1. The coefficients in equation constants reaction.

Reaction	Temperature range ΔT_i , K	A	B	The value of the approximation R^2
1	1073-1473	-98556	36,107	0,978
2	2073-3273	-35078	12,291	0,995

[1]Kolbin TS Terentev DI, Barbin NM, Alekseev SG. Technosphere safety, **1**, 30 (2013). <http://uigps.ru/content/nauchnyy-zhurnal/povedenie-eu-pu-am-pri-gorennii-radioaktivnogo-grafita-v-srede-kislороda-pri-razlichnyh>

[2]Kolbin TS Terentev DI, Barbin NM, Alekseev SG. Technosphere safety, **2**, 40 (2013). <http://uigps.ru/content/nauchnyy-zhurnal/povedenie-eu-pu-u-pri-nagreve-radioaktivnogo-grafita-v-srede-argona-pri-razlichnyh>

[3] Kolbin TS Terentev DI, Barbin NM, Alekseev SG. EPJ Web of Conferences **82**, 01013 (2015) DOI: <http://dx.doi.org/10.1051/epjconf/20158201013>

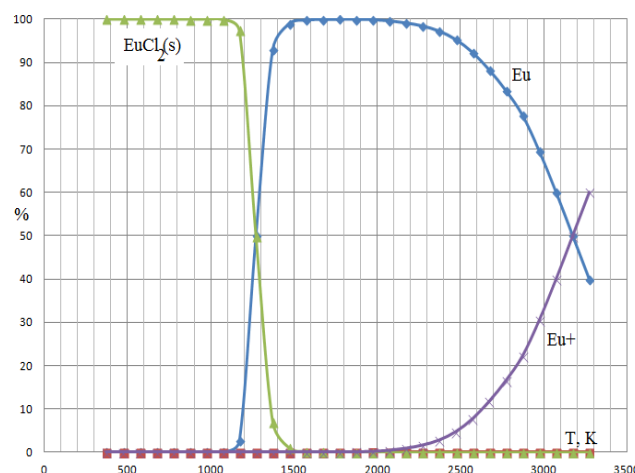


Figure 1: Distribution of Eu in the system

FORMATION OF THE CERAMIC PRECURSOR BASED ON TITANIUM OXIDE AND ALUMINA DURING ELECTROLYSIS WITH COMBINED SOLUBLE ANOD

Khayrullina L.R., Grigoryeva I.O., Dresvyannikov A.F.
 Kazan National Research Technological University, Kazan, Russia
 Leniza_rinatovna@mail.ru

At present, the complex systems based on alumina and titanium oxides are used to create new ceramic and composite materials with improved functional properties. Such materials are widely used as efficient catalysts, heat-resistant catalyst supports, highly selective sorbents, in technologies for producing special ceramics, including medical biomaterials.

An electrochemical synthesis of oxide systems is the most efficient method [1], which allows to obtain high-purity dispersed products with definite predetermined characteristics and controlled properties (morphology, particle shape and size range, phase and chemical composition).

In this work dispersed oxide system Al_2O_3 - TiO_2 has been formed by means of joint anodic dissolution of aluminum and titanium in aqueous solutions containing chloride and fluoride ions with the subsequent thermal treatment. The phase and elemental composition and structural characteristics of the samples have been studied using X-ray phase analysis and scanning electron microscopy. It is shown that by changing the electrolysis mode (total anode current density, solution composition), the ratio of aluminum and titanium working surfaces and thermal treatment conditions can be controlled phase and elemental composition of the products of anode oxidation of combined electrode.

As a result of electrochemical synthesis in an aqueous solution of sodium chloride (1.0 mol/l) with the addition of hydrofluoric acid (0.05 mol/l) at a ratio of the working metals surfaces $S(\text{Al}) : S(\text{Ti}) = 2:1$, current density of 100 mA/cm^2 , the hydrolysis of the ionization products and subsequent thermal treatment (80°C , 8 h) aluminum hydroxide is formed with a structure of boehmite (73.6%), and titanium oxide is formed in anatase form (26.4%). After calcination of the sample at 550°C (2 h) boehmite is thermally decomposed to form $\gamma\text{-Al}_2\text{O}_3$ (3.8%). In the same time the modification of titanium oxide remains unchanged, but its amount in the precipitate increases from 26 to 96%. Further thermal treatment (1100°C) leads to the appearance in the XRD pattern of the synthesized product (Figure 1a) the phases of corundum (20.8%) and rutile (79.2%). At lower concentrations of hydrofluoric acid (0.025 mol/l) only aluminum actively dissolves with the formation of the precipitate, which contains after filtration and drying (80°C) aluminum hydroxide with the structure of boehmite and bayerite, which are moving into a phase of corundum during the subsequent thermal treatment (1100°C).

According to SEM photographs (Figure 1b) it is observed that synthesized sample consist of irregular shaped aggregates, preferably of elongated hexagonal shape (Al_2O_3 particles) with edge dimensions of $\sim 650\text{-}700 \text{ nm}$, and needle-shaped (TiO_2 particles) with width of $90\text{-}150 \text{ nm}$ and a length of $1.5\text{-}2.0 \mu\text{m}$ and above.

Thus, the synthesized mixed titanium oxide-alumina systems may be used as precursors in the process of producing ceramics and composite materials. It is found that the particle size and phase composition of the samples can be controlled by varying the electrolysis conditions.

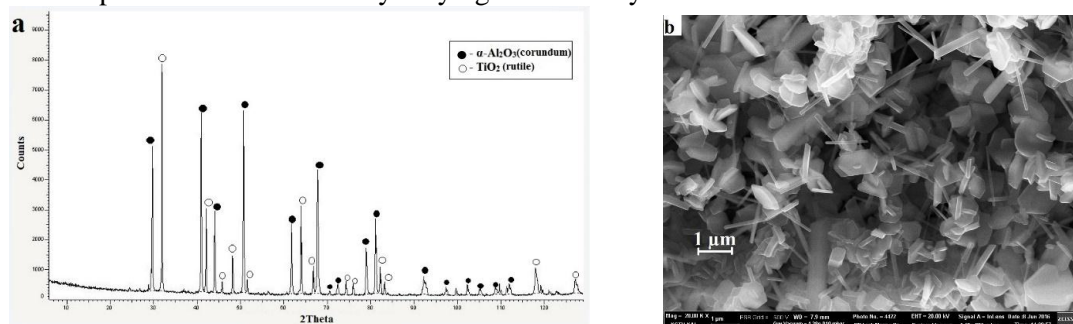
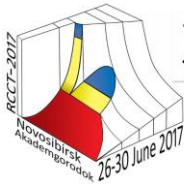


Figure 1. XRD pattern (a) and SEM image (b) of the sample obtained by means electrolysis (solution – 1.0 M $\text{NaCl} + 0.05\text{M HF}$, current density – 100 mA/cm^2 , temperature – 25°C , duration of electrolysis – 80 min) and subsequent calcined at 1100°C

References

1. M. Starowicz, P. Starowicz, B. Stypula Alumina-based nanoparticles obtained by anodic dissolution of Al in electrolytes with alcohol solvents. *J. Solid State Electrochem.* 2014, 18, 3065-3071.



THE PHASES RULE FOR PHOTONS AS WORKING BODY OF AN ENGINE

Laptev V.I.

Russian New University, 105005 Moscow, Russia

E-mail: viktor.laptev@yahoo.com

A **photon gas** (Einstein, 1905) in equilibrium is black body radiation which has temperature T (Golitzyn, 1893), pressure p (Lebedev, 1899) and entropy S . In solar energy technique, solar chemical engine-reactors the photon gas as working body of an engine was recently described [1].

The photon phases rule. The number of thermodynamic degrees of freedom for the photon gas is equal to one. The determinant of the stability of thermodynamic system with internal energy U [2]

$$D = (\partial^2 U / \partial^2 S)_{\nu} (\partial^2 U / \partial^2 V)_{S} - \partial^2 U / (\partial S \partial V)$$

for an equilibrium radiation in volume V is equal to zero because $U(S, V) = \sigma V(3S/4\sigma V)^{4/3}$, where σ is the Stefan-Boltzmann constant. While the zero determinants are related to the limit of stability, there are no thermodynamic restrictions for phase equilibrium [2].

Let us assume that an equilibrium photon system consist of the phase 1 and 2. Description of a thermodynamic phase in equilibrium requires temperature, pressure and chemical potentials of every component in all phases. To fix the equilibrium of two photonic phases it is necessary and sufficiently to have validity of the following equations: $p_1 = p_2$, $T_1 = T_2$ and $m_1 = m_2$, when $V_1 = V_2$.

The pressure of equilibrium radiation is fixed by temperature. Then the one-component system of photons can consist of no more than two phases in equilibrium and the phases rule for the equilibrium is in order written as $n \leq k+1$, where n is number of phases, k is number of components. In our case $n=1$ or 2 , $k=1$ and the number of thermodynamic degrees of freedom for the photon two phase system is $(k+1-n) = 0$. Then the three phase photon system does not exist. It means that: 1) the equilibrium curve of photonic phases has no triple point and critical point; 2) the ratio of photonic phase masses remains constant under fixed p and T .

The photonic bodies. The thermodynamics of radiation (Kirchhoff, 1859) knows the ratio [3]

$$\alpha + \rho + \tau = 1,$$

where α is absorbance coefficient, ρ is reflectance coefficient, and τ is transmission coefficient. We suppose that there are no principal restrictions for validity of this ratio for photonic bodies 1 and 2. There are three cases: 1) the photonic bodies are absolutely black with the coefficients $\alpha = 1$ and $\rho = \tau = 0$; 2) the photonic bodies are absolutely transparent with the coefficients $\tau = 1$ and $\alpha = \rho = 0$; 3) the photonic body can reflect and refract light beams: reflectance coefficient $\rho \neq 0$.

For our cases the condition of mechanical equilibrium of photonic bodies 1 and 2 is expressed by the equation $p_1 dV_1 + p_2 dV_2 = 0$.

If photonic body can reflect and refract light beams it is localized and has a phase surface. The total volume is equal to the sum $V_1 + V_2$. Fixing volume V , we find that the pressures of photonic bodies are the same due to $dV_1 = -dV_2$, i.e. $p_1 = p_2$. In this case the photonic bodies 1 and 2 are not absolutely black: the body 1 is radiation, the body 2 is the photon Bose-condensate which can be obtained.

The absolutely black photon bodies 1 and 2 are identical: $p_1 = p_2 = p$, $n = 1$ and $(k+1-n) = 1$.

If photonic body 1 is absolutely transparent for photonic body 2, than $V = V_1 = V_2$ and $dV_1 = dV_2$. In this case the condition of their mechanical equilibrium means that the pressure p_1 is not equal to the pressure p_2 : by they are connected $p_1 = -p_2 = \sigma T^4/3$ and the total pressure $(p_1 + p_2)$ is equal to zero by any temperature.

The working bodies of solar reactor-engine consist of photons and atoms. The positive and negative pressure of the photonic and matter bodies means that phase 1 and 2 are compression and tension phases. Actions of tension and compression forces are compared by the effect of reversing sign of the enthalpy change. In solar engine-reactor components of the photon-matter medium are getting chemical active due to $\Delta H_1 = -\Delta H_2$ and $\Delta S_1 = -\Delta S_2$. Gibbs' energy change of supposed chemical reaction is $\Delta G_{\text{reac}} = \Delta H_{\text{reac}} - T\Delta S_{\text{reac}}$: if the sign is positive, the term ΔG_{reac} changes the sign during the transition $p_1 = -p_2$ [1].

[1] Laptev, V.I., Khlyap, H. Technological Prerequisites for the Energy and Raw Materials Independence of State and Corporate Economies. N-Y: Nova Science Publishers, 2014. ISBN: 978-1-63117-703-3.

[2] Semenchko, V.K. Izbrannie glavi of theoretical physics, Prosvezhenie: Moscow, 1966.

[3] Bazarov, I.P. Thermodynamic; Pergamon Press: Oxford 1964.



THERMODYNAMIC EQUILIBRIUM BETWEEN TWO ABSOLUTE TRANSPARENT PHOTONIC BODIES

Laptev V.I.

Russian New University, 105005 Moscow, Russia

E-mail: viktor.laptev@yahoo.com

The amount of heat Q that must be added to photon system with $T=\text{const}$ to create the gas is in order $Q=U - W = H$, where U is the internal energy, W is the total work done to create this photon gas at volume V and H is the enthalpy. It is seen that the enthalpy is the energy needed to create the photon gas. As an example of a thermodynamic process involving a photon gas, consider a cylinder with a movable piston by coordinate 1 and 2. The photonic body is absolutely black with the absorbance coefficient, equal to one. The total volume is equal to the sum V_1 of photonic body 1 and V_2 of photonic body 2. Entropy S_V of the volume V , where photonic gases 1 and 2 are located is equal to the sum S_1+S_2 . The condition of entropy variation $\delta S_V = \delta S_1 + \delta S_2 = 0$ is a general condition of thermodynamic equilibrium of photon gases 1 and 2 in the volume V of cylinder with a movable piston. Defining δS_1 and δS_2 from the equation $T\delta S = \delta U + p\delta V$, we obtain

$$(\delta U_1 + p_1 \delta V)/T_1 + (\delta U_2 + p_2 \delta V)/T_2 = 0.$$

The condition of internal energy variation $\delta U_V = \delta U_1 + \delta U_2 = 0$ will be completed by the expression $T\delta S$, and then we get an equation $(1/T_2 - 1/T_1)\delta U_2 + (p_2/T_2)\delta V_2 + (p_1/T_1)\delta V_1 = 0$.

$\delta V_1 = -\delta V_2$ in case of a cylinder with a movable piston when $V = V_1 + V_2 = \text{const}$. Then for any values of variations δU_2 and δV_2 we find $T_1 = T_2 = T$, $p_1 = p_2 = p$ as the equilibrium conditions. Photonic bodies 1 and 2 are not segregated: they are homogeneous photon gas, bodies 1 and 2 are not distinguished.

As a second example of a thermodynamic equilibrium involving a photon gas only, consider two absolutely transparent photonic bodies 1 and 2. In this case $V = V_1 = V_2$, $dV_1 = dV_2$ and the condition of their mechanical equilibrium means that the pressure p_1 of photonic body 1 is not equal to the pressure p_2 of the transparent photonic body 2: they are connected as follows:

$$p_1 = -p_2.$$

We don't know any analysis of the stability of the sign-alternative pressure medium. Let us examine their by stability related to the initial medium by using the Gibbs' stability criterion. The initial medium with constant mass is homogeneous and isotropic. Indexing its entropy $S_0 = S_1 + S_2$ we write

$$U_0 - T_0 S_0 + p_0 V_0 = 0.$$

We have to find out which of signs $=$, $>$ or $<$ appears between the internal energy U_0 of the initial medium and the sum $U_1 + U_2$ of the phase energies under the sign variation of the pressures p_1 , p_2 and the pressure p_0 of the initial medium. In this case, according to eq. $p_1 = -p_2$,

$$U_0 + p_0 V_0 = U_1 + U_2. \quad (1)$$

Now we investigate the phase equilibrium condition relating to the initial medium under variation of the pressure of initial medium p_0 in three cases below. To visualize our description we denote the internal energy \bar{U} when the pressure is negative.

Scenario 1. When $p_0 = 0$, instead of eq. (1) we have $U_0 = U_1 + \bar{U}_2$. The sign " $=$ " means that under $p_0 = 0$ the phases 1 and 2 may be in equilibrium with the initial medium without segregation.

Scenario 2. If $p_0 > 0$, instead of eq. (1) we have $U_0 < U_1 + \bar{U}_2$. The sign " $<$ " means that the phases 1 and 2 are unstable relating to the initial medium with a positive pressure without segregation.

Scenario 3. When $p_0 < 0$, instead of eq. (1) we have $\bar{U}_0 > U_1 + \bar{U}_2$. The sign " $>$ " means that the initial medium with a negative pressure is unstable relating to the equilibrium of the absolute transparent phases 1 and 2 without segregation.

Pressures p_1 and p_2 in scenarios 1-3 have opposite signs. Then the photonic bodies 1 and 2 as absolutely transparent photon systems condensate combine unusual media. Actually, we reduce the function $U = TS - pV$ to the expression $\omega \equiv p/u = \alpha T - 1$, that is obtained by substitutions $u \equiv U/V$, $s \equiv S/V$ and $\alpha \equiv s/u$. If $\omega = 0$, then $p = 0$ at $T = 1/\alpha$. While ω does not fix the energy density u at $p=0$, the temperature $1/\alpha$ may have any values at any volume, i.e. unusual media $p_1 = -p_2$ is stable at any temperature, volume and consequently can be used in solar chemical reactor [1].

[1] Laptev, V.I., Khlyap, H. Technological Prerequisites for the Energy and Raw Materials Independence of State and Corporate Economies. N-Y: Nova Science Publishers, 2014. ISBN: 978-1-63117-703-3.

THERMODYNAMIC ANALYSIS OF THE CONJUGATED RECOVERY REACTIONS THE GRANULES TITANOMAGNETITE CONCENTRATE WITH NATURAL GAS

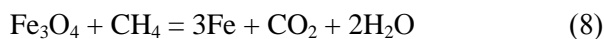
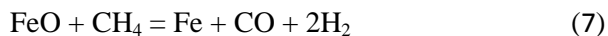
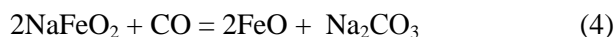
Mamedov A.N., Qasimova A.M., Samedzade Q.M.

Nagiyev Institute of Catalysis and Inorganic Chemistry ANAS, G.Javid av.,113, AZ 1134, Baku, Azerbaijan, E-mail: asif.mammadov.47@mail.ru

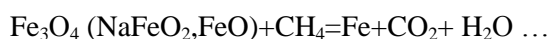
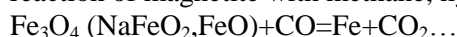
Temperature dependences of the Gibbs free energy of the reduction reactions of titanomagnetite concentrate granules [1] have been calculated (according to the equation

$$\Delta G_T^0 = \Delta H_{298}^0 - T\Delta S_{298}^0 - \Delta c_{p,298}^0 T \left[\ln(T/298) + (298/T) \right] - RT \left[x \ln f(x) + (1-x) \ln f(1-x) \right]$$

where ΔG_T^0 , ΔH_{298}^0 , ΔS_{298}^0 – the standard free energy, enthalpy, entropy of reactions (1-8). x – mole fraction in solid solution $\text{Fe}_{3-2x}\text{Ti}_{2x}\text{O}_4$. $f(x)$ – functions for the configurational entropy of solid solutions. When recovering granules of titanomagnetite concentrate with natural gas generally the following reactions mainly took place:



From figure 1 it follows that the magnetite starts to interact with soda with obtaining ferrite (III) sodium (reaction 1) at 500-550K. The sodium titanate produced by the reaction (2) proceeds in a non-magnetic phase. The basic reactions of magnetite recovery (reactions 6-8) through wustite at the temperature range 500-800K occur weakly. The equilibrium of reactions (6-8) is shifted to the right side, only from the 1010K ($\Delta G_T^0 < 0$) are displaced. At the same time a negative value of the Gibbs free energy of ferrite reduction reactions (III) and the sodium hydrogen carbon monoxide (3-5) are observed in a relatively low temperatures. However, this does not mean that we should use hydrogen and carbon monoxide instead of reducing agent is very cheap methane. At the same time a negative value of the Gibbs free energy for reduction reactions (3-5) of ferrite (III) sodium with hydrogen and carbon monoxide are observed in a relatively low temperature. However, this does not mean that we should use hydrogen and carbon monoxide of reducing agent instead of very cheap methane. We found that the use of methane in admixture with no more than 10% by volume of hydrogen and carbon monoxide, recovery reaction (6-8) of magnetite, FeO and NaFeO₂ till metal occur with high productivity. This is because the reduction reaction of magnetite with methane, hydrogen and carbon monoxide are conjugated:



In these reactions, the CO and H₂, are inducers and CH₄ is an acceptor. The first two reactions initiated the recovery of magnetite with methane till metal.

[1] Gudret I. Kelbaliyev, Asif N. Mamedov et al. Modelling of granule formation process of titanomagnetite powdered materials by the method of rolling // Elixir International Journal. Materials Science 2016, 96, p. 41434-41442

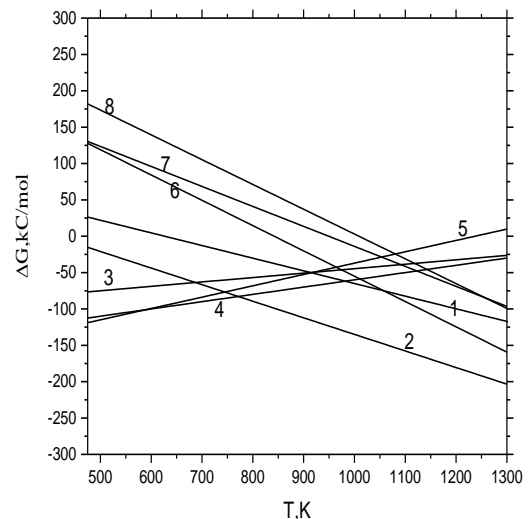
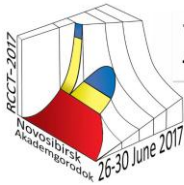


Figure 1. Temperature dependences of the Gibbs free energy for reactions (1-8)



THE POSSIBILITY OF USING THERMODYNAMIC MODELING IN STEELMAKING TECHNOLOGY

Myalkin I.V.¹, Safonov V.M.¹, Morov D.V.², Korzun E.L.³, Smirnova N.N.⁴

¹ Vyksa branch NUST «MISIS»,

² JSC "VSW" Vyksa, Russia

³ JSC "Ruspolimet" Kulebaki, 607030 Russia

⁴ Chemistry Research Institute of N.I.Lobachevsky State University, Nizhni Novgorod, 603950, Russia

E-mail: i.v.myalkin@gmail.com

The Furnace (EAF) is the most powerful and high-efficiency unit for the production of steel. Generally in DSP is loaded metal charge, a main part of which is scrap steel of different chemical composition, size, and pollution [1]. The aim of this study was to test the possibility of industrial sufficiently deep decarburization of the metal in the final stage of melting steel in an electric arc furnace-staleplavil for the carbon content in the metal before the release of lower than 0.05% pa mass parallel to reduce oxidation by stirring the melt with an inert gas. In the first stage of the work we examined the degree of deviation from equilibrium "slag-metal" system in the electric arc furnace after blowing oxygen and before release. Evaluation of equilibrium composition of metal and slag were performed using the software complex «GIBBS», which is designed to calculate the molten state and the gaseous phase in plavilleneuve metallurgical units. The basis of the complex is a thermodynamic calculation unit, which is based on the implementation of the method Gibbs A description of the chemical processes in any system without preliminary submission in the form of stoichiometric reactions. This method is based on the axiom, according to which in the equilibrium state of any material system is completely characterized by the equation of state:

$$f(S, V, m_1, m_2, \dots, m_k) = 0,$$

where S - entropy V - volume and m_j - the mass of the chemical elements of the 1 st to k (M the total mass of the masses replaced k components). Included expression $k + 2$ values represent a complete set of independent variables, sufficient to describe all the properties of the system. In particular, the free energy of the metal-slag-gas system (G) is a function of these variables:

$$G = G(T, P, m_1, m_2, \dots, m_k)$$

This expression is called the equation of state. The specific form of the equations of state are determined in the theory of solutions. For a description of the three-phase system of metal-slag-gas three equations need to know the status: $G = G_{mem} + G_{uvl} + G_{gaz}$.

Table 1 As an example, data in industrial melting CPD given below

System "Slag-metal"	The composition of the metal, %			Mass metal, τ	The slag composition, %			Mass slag, τ	T, K
	C	Mn	O		CaO	FeO	MnO		
Try 1	0,061	0,053	0,176	162,3	27,71	35,59	6,25	8,0	1976
Calculation	0,018	0,058	0,143	162,4	28,69	32,75	6,30	7,7	1947
Try 2	0,027	0,048	0,125		28,57	36,58	5,35		1947

The table below shows some of the parameters of the system after the purge oxygen (sample 1); estimated system state "slag - metal" in the transition state of equilibrium in the post purge after mixing oxygen and an inert gas into the bath for 6 minutes (sample 2). The studies found that after the oxygen blowing, there sufficiently high degree of removal of system "slag - metal" from equilibrium. Thus, carbon and oxygen in a metal (sample 1) differs from the calculated equilibrium at 70 and 19% respectively. At the second stage of the work we examined the fundamental possibility of bias "slag - metal" system in the direction of approach to equilibrium by mixing an inert gas into the bath chipboard. It is found that the mixing of the inert gas in the bath for 6 minutes (without any external influence) reduced the oxidation and carbon concentration in the metal to a predetermined. Thus established in principle the possibility of a sufficiently deep decarburization of the metal in the electric arc furnace with a parallel reduction of oxidation by stirring the melt with an inert gas.

1. Safonov VM, Smirnov AN modern electric arc furnace: the basic parameters and conceptual solutions // Electrometallurgy. - 2005. - №6. - S. 2-13.



THERMODYNAMIC ASSESSMENT OF THE CALCULATED AND ACTUAL SULFUR PARTITION COEFFICIENT BETWEEN THE METAL AND SLAG LADLE-FURNACE

Myalkin I.V.¹, Safonov V.M.¹, Smirnov A.N.², Proskurenko D.V.², K.E. Pismarev K.E.³, Smirnova N.N.⁴

¹ Vyksa branch NUST «MISIS», Vyksa, 607030 Russia

² Donetsk National Technical University, Donetsk, 83020, Ukraine

³ PJSC «Alchevsk Iron & Steel Works», Alchevsk, 94201, Ukraine

⁴ Chemistry Research Institute of N.I.Lobachevsky State University, Nizhni Novgorod, 603950, Russia

E-mail: i.v.myalkin@gmail.com

The research is aimed at clarifying the sulfur distribution coefficient between slag and metal in a secondary oxidation while stirring the molten bath in the ladle furnace (AKP) [1, 2]. The equilibrium sulphur distribution coefficient between the metal and slag could be calculated due to Equation (1):

$$\lg \frac{(S)}{[a_S]} = \frac{21920 - 54640\Lambda}{T} + 43,6\Lambda - 23,9 - \lg[a_O] \quad (1)$$

where $a_{[S]}$ - an activity of sulphur in molten steel; $a_{[O]}$ - an activity of oxygen in molten metal; Λ - an optical basity of slag; T - the temperature of molten bath, K.

According to the Equation 1 the coefficient depends from the $a_{[O]}$. The results of calculation for the sulphur distribution coefficient are introduced in the Table 1. It is seen from the Table 1 that the calculated values in the "slag-metal" system for LF essential exceed factual data.

Table 1. The results of evaluation of the thermodynamic distribution coefficient of sulfur between slag and metal

The probe	The optical basity of slag Λ	The factual value of the sulphur distribution coefficient (S)/ $a_{[S]}$	The calculated value	
			Equilibrium concentration of dissolved in steel oxygen, [O] _{eq} wt (with Al in steel)	The sulphur distribution coefficient (S)/ $a_{[S]}$
AKP	0,7662	64	0,00074	243

The studies found that a satisfactory result of the calculation of the equilibrium sulfur distribution ratio between slag and metal in a secondary oxidation melt oxygen furnace working space atmosphere can be obtained by using the actual value of the oxygen concentration in the steel at the interface "slag-metal" (variant calculation used, Table. 2) or by using the calculated value of the equilibrium oxygen concentration with the aluminum content of which is defined at the interface (with the option of calculating, see Table. 2). The results of calculation using an average oxygen concentration in the steel are shown in Table. 2 (options).

Table 2. Actual and estimated sulfur distribution ratio

The variant of calculation	The temperature of the steel T, °C	The concentration of the aluminium in the steel [Al], %	The concentration of the oxygen in the steel [O], %	The optical basity of the slag Λ	The calculated activity of the sulphur in the steel $a_{[S]}$, %	The factual concentration of the sulphur in the steel [S], %	The calculated sulphur distribution coefficient	The factual sulphur distribution coefficient
a	1569	0.005	0.00058	0.7749	0.0090	0.009	129	55
b	1569	0.002	0.00106	0.7749	0.0079	0.008	68	62
c	1569	0.002	0.00130	0.7749	0.0090	0.009	56	56

Similar values calculated and the actual sulfur distribution coefficient confirms the position that the oxygen concentration at the interface is defined as the oxidation refining slag, and the aluminum content in the molten metal and is determined by the ratio of oxygen flow and aluminum to this border.

[1] To problem of steel desulfurization in ladle furnace unit and chamber vacuum degassing plant Safonov, V.M.; Smirnov, A.N.; Pismarev, K.E.; Proskurenko, D.V., *Elektrometallurgiya*, №11, 2009, p.14-32

[2] Smirnov A.N., Safonov V.M., Proskurenko D.V., Pismarev K.E. Investigation of the nature of metal particle distribution in the slag melt by blowing argon into the ladle *Elektrometallurgiya*, №7, 2009, p.17-22



THERMODYNAMIC ASPECTS OF FREEZE DRYING: A CASE STUDY OF AN “ORGANIC SOLVENT-WATER” SYSTEM

A.G. Ogienko^{1,2,3}, V.A. Drebuschak^{2,4}, E.G. Bogdanova², A.S. Yunoshev^{2,5}, A.A. Ogienko⁶,
E.V. Boldyreva^{1,7}, A.Yu. Manakov^{1,2}

¹*Nikolaev Institute of Inorganic Chemistry, Siberian Branch of the Russian Academy of Sciences, 630090 Novosibirsk, Russia*

²*Novosibirsk State University, 630090, Novosibirsk, Russia*

³*Novosibirsk State Medical University, 630091, Novosibirsk, Russia*

⁴*Sobolev Institute of Geology and Mineralogy, Siberian Branch of the Russian Academy of Sciences, 630090 Novosibirsk, Russia*

⁵*Lavrentiev Institute of Hydrodynamics, Siberian Branch of the Russian Academy of Sciences, 630090 Novosibirsk, Russia*

⁶*Institute of Cytology and Genetics, Siberian Branch of the Russian Academy of Sciences, 630090 Novosibirsk, Russia*

⁷*Institute of Solid State Chemistry and Mechanochemistry, Siberian Branch of the Russian Academy of Sciences, 630090
Novosibirsk, Russia*

E-mail: andreyogienko@gmail.com

Aqueous solutions of glycine and tetrahydrofuran (THF) were frozen under variable conditions and subsequently annealed. The phases that resulted from this process were studied by X-ray diffraction, DSC and cryotemperature SEM. Under conditions achieved in common laboratory freeze-dryers, the THF clathrate hydrate of cubic structure II was formed in near-quantitative yields. The temperature-composition state diagram for the THF – water - β -glycine systems suggests that the critical temperature of the primary drying stage is the temperature of the four-phase peritectic reaction (269 K), and not the temperature of the congruent melting of the THF hydrate in the THF-water system (278 K). Freeze-drying is shown to go much faster if aqueous solutions are substituted for THF-water solutions. This finding is of great importance for practical applications, including pharmaceutical drug formulation.

THE EFFECT OF SOLUTE ON STABILITY OF THF CLATHRATE HYDRATE IN TERNARY SYSTEMS

A.G. Ogienko^{1,2}, A.S. Yunoshev^{2,3}, A.Yu. Manakov^{1,2}

¹Nikolaev Institute of Inorganic Chemistry, Siberian Branch of the Russian Academy of Sciences, 630090 Novosibirsk, Russia

²Novosibirsk State University, 630090, Novosibirsk, Russia

³Lavrentiev Institute of Hydrodynamics, Siberian Branch of the Russian Academy of Sciences, 630090 Novosibirsk, Russia

E-mail: andreyogienko@gmail.com

Formation and stability of cubic structure II THF clathrate hydrate have been studied for aqueous solutions (frozen under variable conditions) of THF and some inorganic compounds with use of X-ray diffraction and thermal analysis. Recently it has been shown that the addition of the third component changes the melting behavior of the THF hydrate [1]. On the base on the experimental data and the suggested model (Figure 1) we conclude that the incongruent melting temperature of the THF hydrate is determined by the eutectic melting temperatures in respective binary systems (in the case of hydrate formation: “hydrohalite-water” eutectic; hydrate is not formed: “NH₄NO₃-water” eutectic)). Fine powders of NH₄NO₃ / NaCl / KCl were prepared by freeze-drying using THF-water co-solvent system. It has been shown that using a mixed solvent giving a clathrate on freezing is beneficial in terms of the significant shortening of the primary drying stage and significant reduction of the particle size of powders.

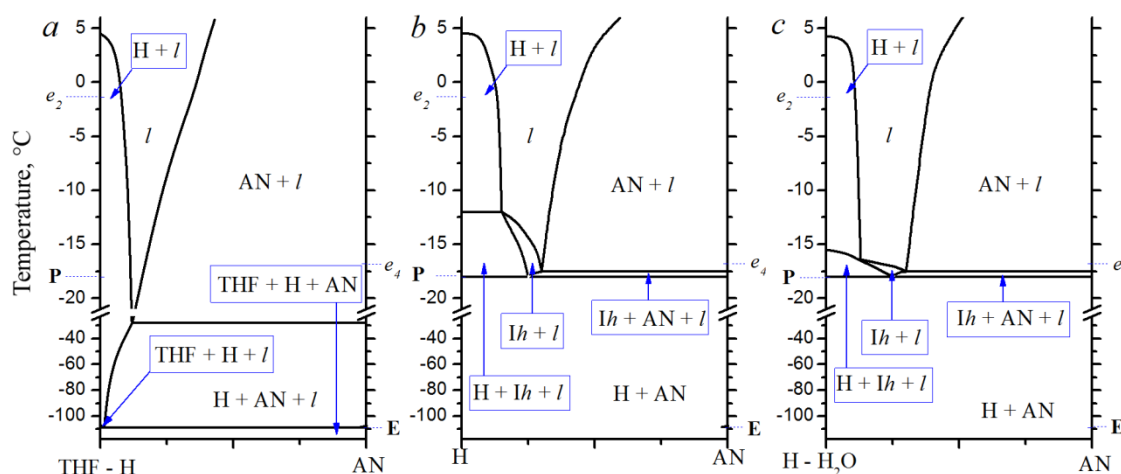


Figure 1. Polythermal sections of the suggested model of the state diagram of the ‘THF – water – NH₄NO₃’ ternary system (*a* – “THF – H subsystem” - AN; *b* – ‘H - AN’; *c* - “H - water subsystem” - AN’. Designations: H – THF clathrate hydrate; *Ih* – ice *Ih*; AN – NH₄NO₃; *l* - solution; *e*₁, *e*₂, *e*₃, *e*₄ – binary eutectics; E, P – ternary eutectics and ternary peritectic, respectively.

[1] Ogienko A.G., Drebuschak V.A., Bogdanova E.G., Yunoshev A.S., Ogienko A.A., Boldyreva E.V., Manakov A.Yu. *J. Therm. Anal. Calorim.*, 2017, 127, 1593-1604.

This study was supported by RFBR (№ 17-03-00784-A).

KINETICS OF EUTECTOID TRANSFORMATION IN HIGH-CHROMIUM HIGH-CARBON IRON ALLOYS

Okishev K.Yu., Vasyukova E.S., Grebenschikova A.G., Sozykina A.S., Mirzaev D.A.
South Ural State University, 454080 Chelyabinsk, Russian Federation
E-mail: okishevki@susu.ru

Ternary alloys of the Fe–Cr–C system are widely used in industry as wear-resistant and tool materials. When not subjected to special heat treatment, their final structure is formed by the eutectoid transformation of the high-temperature gamma solid solution (austenite) to a mixture of alpha solution and (Cr, Fe)₇C₃ carbides. The paper presents a model describing kinetics of this transformation as a function of alloy composition and austenitization mode.

Experimental data for analysis were taken from [1]. Experimental TTT diagrams were treated using conventional Avrami equation $f(t)=1-\exp(-Kt^n)$ with the following temperature dependence of the K

coefficient: $K^{1/n}=C\left(\frac{T_s-T}{T}\right)^m \exp\left(-\frac{U}{RT}\right)$, where T_s is the upper limit of the transformation temperature

range (actually, the upper asymptote of the C-curve), U is activation energy, and C is constant that determines the time scale of the transformation [2]. Exponent m was accepted $m=3$ in accordance with theoretical models, and other parameters were determined from experimental TTT diagrams. The following dependences of these parameters on C and Cr content in the gamma phase (in wt. %) were adjusted:

$$T_s = 760 \text{ }^\circ\text{C};$$

$$n = 9.50 - 0.91 \cdot \text{Cr} - 2.85 \cdot \text{C} + 0.50 \cdot \text{Cr} \cdot \text{C};$$

$$U = 289 + 11 \cdot \text{Cr} - 87 \cdot \text{C} + 5 \cdot \text{Cr} \cdot \text{C}, \text{ kJ/mole};$$

$$\ln C = 39.74 + 0.86 \cdot \text{Cr} - 9.58 \cdot \text{C} + 0.69 \cdot \text{Cr} \cdot \text{C} \text{ [sec}^{-1}\text{]}.$$

Examples of calculated isothermal (TTT) diagrams of eutectoid transformation are presented in Fig. 1. They are in sufficient correspondence with experiment.

The authors kindly acknowledge the support from the Ministry of Education and Science of the Russian Federation.

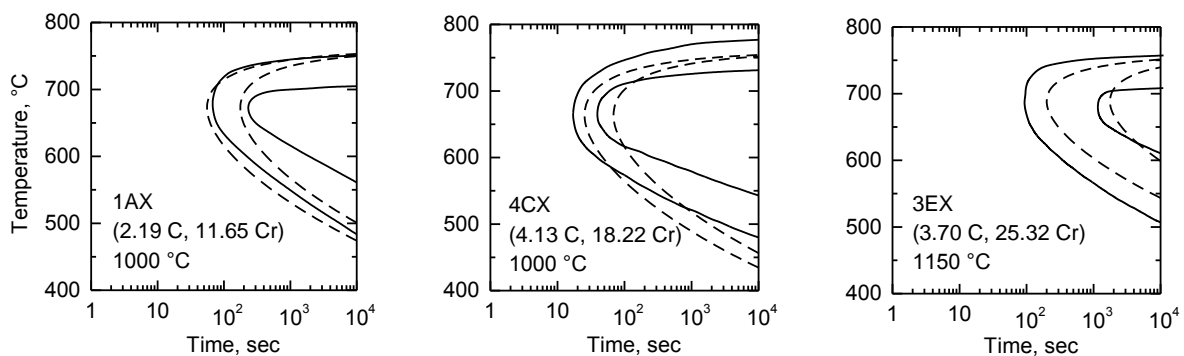


Figure 1. Examples of calculated isothermal eutectoid transformation C-curves (dashed lines) compared with experiment [1] (solid lines).

[1] Maratray, F.; Usseglio-Nanot, R. Atlas: courbes de tranformation de fontes blanches au chrome et au chrome-molybdène. Climax Molybdenum S.A., Paris, 1970.

[2] Mirzaev, D.A.; Okishev, K.Yu.; Mirzaeva, K.D. Materials Performance and Characterization, 2013, 2, 134–152. DOI: 10.1520/MPC20120023



CORRELATION BETWEEN PHASE COMPOSITION AND CATALYTIC PROPERTIES OF COMPLEX OXIDES

O.V. Russkikh, A.A. Ostroushko

Ural federal University named after the first president of Russia B.N. Yeltsin, 620000 Ekaterinburg, Russia

E-mail: O.V.Russkikh@urfu.ru

Atmosphere protection from transport and industrial gas emissions is one of the actual problems nowadays. Catalytic systems on the basis of complex oxides are among the prospective methods for its solving. They can be used both in mobile sources (such as road, rail or water transport) and for stationary pollutants: various manufacturing processes and devices, for example heat power engineering. Gas emissions may contain a wide range of harmful substance, such as carbon monoxide, remnants of unburned methane and other hydrocarbons (including carcinogenic), nitrogen oxides and soot the solid component, which consists from carbon and adsorbed toxic compounds on it.

In this respect complex oxide systems based on cerium oxide with the fluorite structure and perovskite-like complex oxides, in particular, on the basis of lanthanum manganite are of practical interest. Properties of such complex oxide catalysts could be controlled by the introduction of dopants with different nature. Alkaline and transition metals (as copper, silver, iron, nickel, etc.) can significantly change characteristics of the complex oxides on the basis of cerium oxide and lanthanum manganite when doping their structure. It should be noted that properties control of such systems is not limited to chemical composition's change. Homogeneous system due to the occurrence of solid solutions or heterogeneous, containing additional phases could be formed during the synthesis of complex oxides depending on the nature of the dopant. And heterogeneous systems often possess higher catalytic activity.

This work is the part of systematic studies of the correlation between synthesis of complex oxide systems and their properties, such as chemical and phase composition, morphology, and catalytic activity in the reaction of carbonaceous substances' oxidation. Complex oxide systems based on ceria oxide $Ce_{1-x}M_xO_{2-\delta}$ ($M=Cs, K, Ag, Fe, Ni, Cu$) and lanthanum manganite $La_{1-x}Me_xMnO_{3-y}$ ($Me=Sr, Ag$) were investigated. Complex oxides were synthesized by pyrolysis of polymer-salt compositions [1]. This method allows obtaining nanosized complex oxides. It based on combustion of compositions consisting from the nitrates of the appropriate metals and organic components (polyvinyl alcohol, glycine, glycerin etc).

Phase analysis was examined by x-ray method using diffractometer D8 Advance (Bruker; $Cu_{K\alpha}$ irradiation, $\lambda = 1,5418 \text{ \AA}$, $2\Theta=20^\circ-70^\circ$). Thus the introduction of alkaline metals and Fe leads to the formation of solid solutions (up to $x=0.3$). The smooth change of the lattice parameter of the basic compound was observed. Doping with Ag, Ni, Cu leads to the formation of heterogeneous systems. Metallic silver or oxides of nickel and copper, respectively, were detected in addition to the main phase (perovskite or fluorite). By scanning electron microscopy it was shown that second phase is evenly distributed over the surface of complex oxide.

It was shown that doping leads to increasing of catalytic activity in the reactions of CO, CH₄ and soot oxidation by oxygen in comparison with pure $CeO_{2-\delta}$ and $LaMnO_{3-y}$.

Model (Degussa) and «real» soot were taken for experiments. Four-fold excess of oxide materials and soot were carefully grinded to achieve tight contact between particles. Soot oxidation was performed in air, in an open reactor under isothermal or polythermal conditions. Methane and carbon monoxide oxidation was performed in a flow reactor at step temperature rise (350-650°C, with step 50°).

It was found that $CeO_{2-\delta}$ and $LaMnO_{3-y}$ doped with alkaline metals possess the highest catalytic activity in the reaction of soot oxidation. Doping with transition metals which possess several stable oxidation states led to the growth of catalytic activity in the reactions of CO and CH₄ oxidation.

The research has been performed within the State Task from the Ministry of Education and Science of Russian Federation (project 4.6653.2017/BP) and the program of competitiveness' increase (project 14.594.21.0011).

[1] Ostroushko A.A. Polymer-salt composites based on nonionic water-soluble polymers and preparation of oxide materials from them // Mendeleev Chemical Journal. V.42. No.1–2. 1998. pp. 153-168.

ASSESSMENT OF SECONDARY CARBIDE PRECIPITATION KINETICS IN HIGH-CHROMIUM HIGH-CARBON IRON ALLOYS

Vasyukova E.S., Okishev K.Yu., Sozykina A.S., Karlikov A.M., Mirzaev D.A.

South Ural State University, 454080 Chelyabinsk, Russian Federation

E-mail: kapitan225@mail.ru

Alloys of the Fe–Cr–C system with high contents of Cr and C are widely used as wear-resistant and tool materials. When they are cooled from high temperature, either in the casting mold or during heat treatment, eutectoid or martensitic transformations in them may be preceded by precipitation of disperse secondary carbides $(Cr, Fe)_7C_3$ from the gamma solid solution (austenite), which affects the chemical composition of the matrix and properties of alloys. The model describing the kinetics of this process is presented in the work.

Isothermal precipitation was assumed to have an Avrami-type kinetics, and to obey conventional diffusion-controlled growth equations. Assuming for simplicity that equilibrium solubility is a linear function of temperature and approximating the C-curve of precipitation with a parabola, one may use the Scheil–Steinberg integral for passing to continuous cooling conditions and bind cooling rate to the amount of precipitated carbides.

Experimental data used [1] showed the increase of the martensitic point (reflecting intensity of precipitation) in a number of alloys containing 2–3 C and 15–25 Cr (wt. %) as a function of cooling rate after holding for 20 min at 1000 °C. Method of calculation of the kinetics of carbide dissolution on heating was developed previously [2], which allowed to determine the composition of austenite by the start of cooling.

After determining kinetic parameters for each alloy, concentration dependences of all of them were found, and both isothermal and continuous cooling (TTT and CCT) precipitation diagrams could have been drawn for an arbitrary alloy composition and austenitization mode. An example is shown in Fig. 1; the model provides sufficient correspondence with experimental data.

The authors kindly acknowledge the support from the Ministry of Education and Science of the Russian Federation.

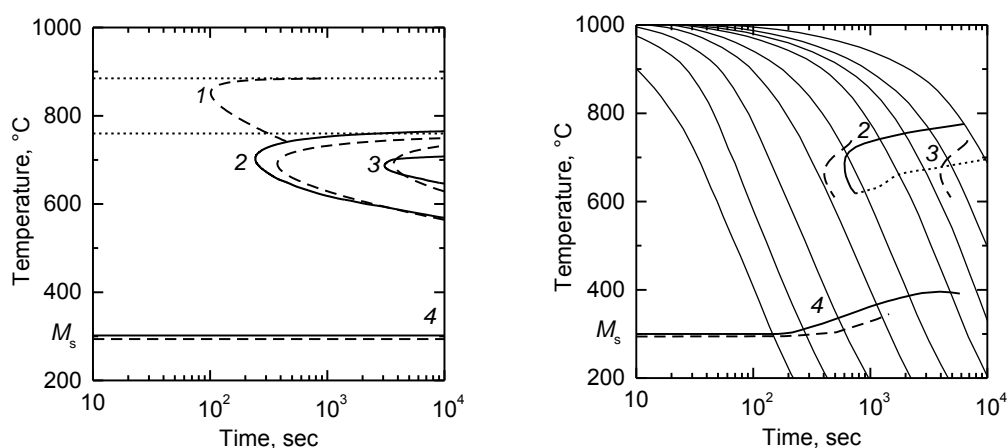


Figure 1. An example of calculated isothermal and continuous cooling diagrams (dashed lines) compared with experiment [1] (solid lines). 1 – carbide precipitation start; 2, 3 – eutectoid transformation start and finish; 4 – martensitic transformation start, M_s (pay attention to the rise of M_s due to carbide precipitation at low cooling rates). Alloy composition: 2.95 C, 25.82 Cr (wt. %). Austenitization 1000 °C, 20 min

[1] Maratray, F.; Usseglio-Nanot, R. Atlas: courbes de tranformation de fontes blanches au chrome et au chrome-molybdène. Climax Molybdenum S.A., Paris, 1970.

[2] Sozykina, A.S.; Okishev, K.Yu.; Grebenshchikova, A.G.; Mirzaev, D.A. *Materials Science Forum*, 2016, 870, 409–415. DOI: 10.4028/www.scientific.net/MSF.870.409